

**Leveraging Lewis Acids and Visible Light for Method Development and Total Synthesis**

by

Alistair D. Richardson

A dissertation submitted in partial fulfillment  
of the requirements for the degree of  
Doctor of Philosophy  
(Chemistry)  
in the University of Michigan  
2022

Doctoral Committee:

Professor Corinna S. Schindler, Chair  
Professor Anna K. Mapp  
Professor Pavel Nagorny  
Professor Corey R. J. Stephenson

Alistair D. Richardson

[adrich@umich.edu](mailto:adrich@umich.edu)

ORCID iD: [0000-0002-7894-1682](https://orcid.org/0000-0002-7894-1682)

© Alistair D. Richardson 2022

## **Dedication**

To Nikki, Amy, Stewart, and Victoria.

## **Acknowledgements**

As I reflect on this journey, I am overwhelmed with gratitude for the people that have helped make this possible. Most stories are defined by the people in them, and this story was no different. Words are rarely enough, but for what it's worth I want to say thank you and that I will be forever grateful.

First, I would like to thank my advisor Professor Corinna Schindler. Corinna is an ambitious, enthusiastic, and dedicated individual who was taught me a lot about being a better scientist. Her confidence in me kept me going during some difficult times in my research. I greatly appreciated her trust and the freedom she granted me to try new ideas. She has been a constant source of mentorship, guidance, and advice, and for that I am thankful. I would also like to thank my committee, Professor Corey Stephenson, Professor Pavel Nagorny, and Professor Anna Mapp, for their help navigating through this process. Special thanks to Corey for allowing me to spend a semester in his lab and for his help in the job application process.

Next, I would like to thank all the scientists that I have worked with during my time at Michigan. As a member of Corinna's fifth class, I have had the pleasure of watching a young research group establish a culture based on hard work and acceptance. The Schindler Lab is the perfect place for a young scientist. I am a better chemist and person because of the challenging and nurturing environment I was a part of. I have truly enjoyed working with every person that I have overlapped with over these past five years, thank you all for everything. I would like to extend that thanks to members of the Stephenson lab, as well as the department as a whole. I want to specifically thank the people that worked on the research described in this thesis: Dr. Paul Riehl, Dr. Marc Becker, Professor Jolene Reid, Trenton Vogel, Emily Traficante, Kason Glover, Rob King, Stephen Chamness, and Tatsuhiro Sakamoto. Paul and Marc were both excellent mentors, thank you both for your patience and understanding in the early stages of my graduate studies. Thank you to Trenton, Emily, Kason, Rob, and Stephen for your hard work and time. Special thanks to Professor Jolene Reid, our collaborator at the University of British Columbia, for her expertise in computational analysis. None of this work would have been possible without these people, I will always be indebted to them.

I also want to thank all my mentors and friends from Clark University. In particular, I want to thank Professor Mark Turnbull. His relentless positivity and curiosity are inspiring. His dedication to mentorship and his students is unmatched. He is someone who I aspire to be like as a scientist and person.

Next, I would like to thank my mom, Amy, my dad, Stewart, and my sister, Victoria. My parents understand this grueling process more than most. As accomplished scientists themselves, they have been an invaluable source of wisdom and encouragement. However, I am most grateful for their lessons in humility, perseverance, kindness, patience, and positivity. Being an older brother has always been one of my favorite things, and I want to thank my sister for her support. I feel blessed to have such an incredible family.

Finally, I want to thank my wife, Nikki. She is a never-ending source of positivity and energy. She is fiercely loyal and amazingly kind. She provided constant encouragement even in difficult times. Our time in Michigan has been filled with unforgettable adventures. It's hard to put into words just how much she means to me. All I can say is thank you, and I love you.

## Table of Contents

Dedication .....	ii
Acknowledgements .....	iii
List of Tables .....	ix
List of Figures .....	xi
List of Equations .....	xvii
Abstract .....	xviii
Chapter 1 Enantiodivergent Total Synthesis of (+) and (-)-Lingzhiol .....	1
1.1 Introduction .....	1
1.2 Results and Discussion .....	6
1.3 Conclusion .....	12
1.4 Experimental .....	12
1.4.1 General Information .....	12
1.4.2 Experimental Procedures .....	13
1.4.3 X-Ray Crystallographic Data .....	25
1.5 References .....	29
Chapter 2 Origin of Enantioselectivity Reversal in Lewis Acid-Catalyzed Michael Additions ..	32
2.1 Introduction .....	32
2.2 Results and Discussion .....	35
2.2.1 Reaction Optimization .....	35
2.2.2 Metal Ionic Radii vs. Enantiomeric Excess Correlations .....	38
2.2.3 Nonlinear Effect Studies .....	38

2.2.4 Kinetic Studies.....	39
2.2.5 Ligand Structure Analysis .....	40
2.2.6 Substrate Structure Evaluation .....	41
2.2.7 Computational Analysis .....	43
2.3 Conclusion.....	48
2.4 Experimental .....	49
2.4.1 General Information .....	49
2.4.2 Experimental Procedures .....	50
2.4.3 Mechanistic Experiments .....	60
2.4.4 Computational Investigation .....	71
2.5 References .....	72
Chapter 3 Synthesis of Functionalized Azetidines using Visible Light-Mediated [2+2] Cycloaddition Reactions .....	77
3.1 Introduction .....	77
3.2 Results and Discussion .....	85
3.2.1 Reaction Design and Optimization.....	85
3.2.2 Substrate Scope .....	87
3.2.3 Mechanistic Studies.....	90
3.2.4 Synthetic Applications.....	92
3.3 Conclusion.....	93
3.4 Experimental .....	93
3.4.1 General Information .....	93
3.4.2 Mechanistic Investigations .....	95
3.4.3 Experimental Procedures.....	99
3.4.4 X-Ray Crystallographic Data .....	149
3.5 References .....	152

Chapter 4 Total Synthesis of Cochlearol B.....	157
4.1 Introduction .....	157
4.2 Retrosynthesis .....	160
4.3 Results and Discussion.....	163
4.3.1 Chromanone Synthesis .....	163
4.3.2 Investigations towards enantioenriched chromanone.....	164
4.3.3 Preliminary Investigations of the Key Steps .....	169
4.3.4 Revised Approach to the Core of Cochlearol B .....	173
4.3.5 Strategies Towards the $\alpha,\beta$ -Unsaturated Aldehyde.....	174
4.3.6 Completion of the Total Synthesis of Cochlearol B.....	179
4.3.7 Total Synthesis of (+)-Cochlearol B.....	180
4.4 Conclusion.....	180
4.5 Experimental .....	182
4.5.1 General Information .....	182
4.5.2 Experimental Procedures.....	183
4.5.3 HPCL Spectra.....	205
4.5.4 X-Ray Crystallographic Data .....	207
4.6 References .....	211
Chapter 5 Progress Towards the Total Synthesis of Gelsemoxonine .....	217
5.1 Introduction .....	217
5.2 Results and Discussion.....	227
5.2.1 First Generation: Aldol/Enyne Metathesis Approach .....	227
5.2.2 Second Generation: Aldol/Achmatowicz Approach .....	231
5.2.3 Third Generation: Oxidative Rearrangement Approach .....	233
5.3 Conclusion and Outlook.....	236



5.4 References ..... 238

## List of Tables

Table 1.1 Optimization of the Lewis acid catalyzed Michael addition reveal unique enantiodivergent behavior.....	7
Table 1.2 Optimization of the allylic alcohol reduction. ....	9
Table 1.3 Optimization of the benzylic oxidation reaction.....	10
Table 1.4 Optimization of the double demethylation reaction. ....	11
Table 2.1. Catalyst and solvent optimization revealed unique enantiodivergent behavior. ....	35
Table 2.2 Reaction Optimization with Y(OTf) <sub>3</sub> as a catalyst. ....	36
Table 2.3 Catalyst screen of commercially available lanthanide(III) triflates.....	37
Table 2.4 Ligand structure evaluations. ....	41
Table 2.5 Evaluating differentially substituted aryl β-ketoester substrates. ....	42
Table 2.6 (A) Computationally analyzed complexes.(B) Lowest energy pathways for each complex relative to the pre-TS complex.....	46
Table 2.7 Ionic radii of the lanthanide(III) triflate catalysts. ....	60
Table 2.8 Yield values of <b>2.24</b> using 2.5 mol% Y(OTf) <sub>3</sub> and 5 mol% <b>2.23</b> . Determined using area of <b>2.24</b> vs. area of caffeine.....	63
Table 2.9 Yield values of <b>2.24</b> using 5 mol% Y(OTf) <sub>3</sub> and 10 mol% <b>2.23</b> . Determined using area of <b>2.24</b> vs. area of caffeine.....	64
Table 2.10 Yield values of <b>2.24</b> using 7.5 mol% Y(OTf) <sub>3</sub> and 15 mol% <b>2.23</b> . Determined using area of <b>2.24</b> vs. area of caffeine. ....	65
Table 2.11 Yield values of <b>2.24</b> using 2.5 mol% Sc(OTf) <sub>3</sub> and 5 mol% <b>2.23</b> . Determined using area of <b>2.24</b> vs. area of caffeine. ....	67
Table 2.12 Yield values of <b>2.24</b> using 5 mol% Sc(OTf) <sub>3</sub> and 10 mol% <b>2.23</b> . Determined using area of <b>2.24</b> vs. area of caffeine. ....	68
Table 2.13 Yield values of <b>2.24</b> using 7.5 mol% Sc(OTf) <sub>3</sub> and 15 mol% <b>2.23</b> . Determined using area of <b>2.24</b> vs. area of caffeine. ....	69

Table 3.1 Aza Paternò-Büchi reaction optimization. ....	86
Table 3.2 Oxime and hydrazone scope. ....	88
Table 3.3 Data from the Stern-Volmer quenching study. ....	97
Table 3.4 Data from the NMR time study. ....	98
Table 3.5 Crystallographic parameters and structure refinement for compound <b>3.80</b> . ....	150
Table 4.1 (A) Conditions evaluated for an asymmetric copper-catalyzed conjugate addition. (B) Background reactivity responsible for racemic product observation. ....	165
Table 4.2 Conditions evaluated for an asymmetric Kabbe condensation. ....	167
Table 4.3 (A) Conditions evaluated for oxidative cleavage of <b>4.88</b> to provide <b>4.89</b> . (B) Two step protocol to <b>4.89</b> through dihydroxylation followed by oxidative cleavage. ....	175
Table 4.4 Conditions evaluated for phenol demethylation. ....	179
Table 4.5 Comparing <sup>1</sup> H and <sup>13</sup> C NMR data for natural and synthetic cochlearol B. ....	203
Table 4.6 Crystal data and structure refinement for <b>4.74</b> . ....	207
Table 4.7 Crystal data and structure refinement for <b>4.70</b> . ....	209
Table 5.1 Conditions evaluated for the oxidative rearrangement reaction. ....	235

## List of Figures

Figure 1.1 Biologically active terpenes and meroterpenoids isolated from <i>Ganoderma lucidum</i> , including (-) and (+)-lingzhiol. ....	2
Figure 1.2 Different proposed biosyntheses of lingzhiol. ....	3
Figure 1.3 (A) Summary of the previous syntheses of lingzhiol. (B) Two starting points utilized in all syntheses reported to date. (C-F) Key steps in the previous syntheses of lingzhiol. ....	4
Figure 1.4 Our enantiodivergent approach to (-)- and (+)-lingzhiol. ....	5
Figure 1.5 Retrosynthetic analysis of lingzhiol highlighting the key AlEt <sub>3</sub> mediated cascade reaction. ....	5
Figure 1.6 Model studies to test the viability of the AlEt <sub>3</sub> mediated cascade reaction. ....	6
Figure 1.7 Completion of the syntheses of (+)-lingzhiol. ....	8
Figure 1.8 Lower equivalents of NaBH <sub>4</sub> leads to a retro-aldol product. ....	10
Figure 1.9 Completion of the synthesis of (-)-lingzhiol. ....	11
Figure 1.10 ORTEP diagram of (S,S)- <b>1.43</b> . ....	25
Figure 1.11 ORTEP diagram of (R)- <b>1.31</b> . ....	26
Figure 1.12 ORTEP diagram of <b>1.49</b> . ....	27
Figure 2.1 (A) Established methods for asymmetric synthesis. (B-E) selected examples of enantiodivergent reactions. ....	33
Figure 2.2 This work: Lewis acid dependent enantiodivergent Michael addition. ....	35
Figure 2.3 Plot of log(er) vs. catalysts ionic radii for each lanthanide catalyst. ....	38
Figure 2.4 Nonlinear effect studies of the scandium- and yttrium-catalyzed reactions. ....	39
Figure 2.5 Potential bidentate and tetradentate binding modes between the metal catalyst and ligand <b>2.23</b> . ....	39
Figure 2.6 Kinetic analysis of the scandium- and yttrium-catalyzed reactions. ....	40
Figure 2.7 NMR shift investigations using Eu(Fod) <sub>3</sub> and β-ketoester substrate <b>2.24</b> . ....	43

Figure 2.8 (A) Hypothesized enolate transition states and electrophile facial approach. (B) Potential activation modes of ketone <b>2.22</b> . Purple boxes denote enolate binding sites for substrate <b>2.21</b> .....	44
Figure 2.9 The lowest energy transition states leading to both enantiomers in the scandium- and yttrium-catalyzed reactions.....	47
Figure 2.10 Transition states leading to (S)- <b>2.24</b> and (R)- <b>2.24</b> using scandium and yttrium respectively.....	49
Figure 2.11 Observed shift of the methine signal in <sup>1</sup> H NMR of ligand <b>2.23</b> at different ratios of <b>2.23</b> and Sc(OTf) <sub>3</sub> in d <sub>6</sub> -benzene.....	61
Figure 2.12 Observed shift of the methine signal in <sup>1</sup> H NMR of ligand <b>2.23</b> at different ratios of <b>2.23</b> and Y(OTf) <sub>3</sub> in d <sub>4</sub> -DCE.....	61
Figure 2.13 Plot of the relative area of caffeine vs. product <b>2.24</b> .....	62
Figure 2.14 Plot of yield of <b>2.24</b> over time with 2.5 mol% Y(OTf) <sub>3</sub> and 5 mol% <b>2.23</b> .....	64
Figure 2.15 Plot of yield of <b>2.24</b> over time with 5 mol% Y(OTf) <sub>3</sub> and 10 mol% <b>2.23</b> .....	65
Figure 2.16 Plot of yield of <b>2.24</b> over time with 7.5 mol% Y(OTf) <sub>3</sub> and 15 mol% <b>2.23</b> .....	66
Figure 2.17 Plot of yield of <b>2.24</b> over time with 2.5 mol% Sc(OTf) <sub>3</sub> and 5 mol% <b>2.23</b> .....	68
Figure 2.18 Plot of yield of <b>2.24</b> over time with 5 mol% Sc(OTf) <sub>3</sub> and 10 mol% <b>2.23</b> .....	69
Figure 2.19 Plot of yield of <b>2.24</b> over time with 7.5 mol% Sc(OTf) <sub>3</sub> and 15 mol% <b>2.23</b> .....	70
Figure 3.1 (A) Distribution of Nitrogen containing heterocycles in FDA approved drugs. (B) Selected examples of nitrogen heterocycle containing drugs.....	77
Figure 3.2 Recently FDA approved, azetidines containing drugs.....	78
Figure 3.3 Azetidines featured in lead compounds.....	78
Figure 3.4 Conventional methods used to synthesize azetidines including intramolecular substitution, β-lactam reduction, and azabicyclobutane ring opening.....	79
Figure 3.5 (A) Overview of the challenges in imine photochemistry. (B) Singlet state vs. triplet state aza Paternò-Büchi reaction.....	80
Figure 3.6 (A) Summary of imines that engage in intermolecular aza Paternò-Büchi reactions. (B) Example of an intramolecular aza Paternò-Büchi reactions. (C) Single example of an acyclic imine participating in an aza Paternò-Büchi reaction via a unique singlet state exciplex.....	81
Figure 3.7 Examples of visible light mediated aza Paternò-Büchi reactions using triplet energy transfer.....	82

Figure 3.8 Intramolecular aza Paternò-Büchi reaction through selective alkene excitation using xanthone as a sensitizer.....	83
Figure 3.9 Indole dearomatization via a [2+2]-cycloaddition (left) or 1,5-H atom transfer (right) using visible light.....	83
Figure 3.10 Overview of triplet energy transfer and selected commercially available photosensitizers.....	84
Figure 3.11 Reaction design for an aza Paternò-Büchi enabled by selective alkene excitation using visible light.....	85
Figure 3.12 Evaluation of the scope of this [2+2]-cycloaddition reaction.....	89
Figure 3.13 Modification of the agrochemical herbicide safener isoxadefin ethyl.....	89
Figure 3.14 Diene substrate evaluations.....	90
Figure 3.15 (A) Stern-Volmer quenching studies. (B) Terminal alkene control reaction. (C) Styrene stereoconvergence experiments.....	91
Figure 3.16 <sup>1</sup> H NMR studies of the styrene and oxime isomer consumption and formation of the desired product.....	91
Figure 3.17 Proposed mechanism for the aza Paternò-Büchi reaction.....	92
Figure 3.18 Synthetic modifications of the azetidine products prepared through this method. ...	93
Figure 3.19 Cyclic voltammogram of compound <b>3.73</b> .....	96
Figure 3.20 UV/Vis spectra of <b>3.73</b> (blue) and <b>3.63</b> (red).....	96
Figure 3.21 NMR spectra at t = 8 min. The signals that were used to obtain the data in table 2.4 have been highlighted.....	98
Figure 3.22 Reaction set up for small and large scale [2+2]-photocycloadditions.....	130
Figure 3.23 Rationale for the observed diastereoselectivity.....	146
Figure 3.24 Selected NOE data for the azetidines synthesized herein.....	148
Figure 3.25 ORTEP diagram of <b>3.80</b> .....	149
Figure 4.1 (A) Biologically active meroterpenoids isolated from <i>Ganoderma cochlearol</i> . (B) Biologically active cyclobutane containing natural products.....	159
Figure 4.2 Sugita's synthesis of cochlearol B.....	160
Figure 4.3 Retrosynthetic analysis of cochlearol B.....	161

Figure 4.4 Yoon's synthesis of ( $\pm$ )-cannabiorcycloic acid enabled by a visible light mediated [2+2]-cycloaddition.....	162
Figure 4.5 (A) Overview of the Catellani reaction. (B) Alkenyl Catellani reaction for the synthesis of all-carbon tetrasubstituted olefins. (C) Catellani reaction design for the synthesis of cochlearol B. ....	163
Figure 4.6 (A) Conjugate addition approach to chromanone <b>4.26</b> . (B) Kabbe condensation approach to chromanone <b>4.26</b> . ....	164
Figure 4.7 Proposed mechanism for the Kabbe condensation. ....	168
Figure 4.8 Chiral resolution using Ellman's sulfinamide enables synthesis of (-)- <b>4.26</b> .....	169
Figure 4.9 Synthesis of vinyl triflate <b>4.25</b> and the unexpected formation of <b>4.68</b> , a structure found within ganocins B and C.....	169
Figure 4.10 Triflation using Comins' reagent. ....	170
Figure 4.11 Initial investigations into the alkenyl Catellani reaction. ....	170
Figure 4.12 Photochemical excitation of <b>4.24</b> using a visible light absorbing photosensitizer leads to unexpected formation of cyclopropane <b>4.74</b> .....	171
Figure 4.13 Alternative, failed substrates in the [2+2]-cycloaddition and Catellani reactions...	172
Figure 4.14 Model systems to test the role of sterics and electronics in cyclopropane formation. ....	173
Figure 4.15 Revised Catellani reaction using 5-iodo-1-pentene subsequently enables a successful [2+2]-photocycloaddition. ....	174
Figure 4.16 Strategy for $\alpha,\beta$ -unsaturated aldehyde formation. ....	175
Figure 4.17 First approach to the $\alpha,\beta$ -unsaturated aldehyde. ....	176
Figure 4.18 Second approach to the $\alpha,\beta$ -unsaturated aldehyde.....	177
Figure 4.19 Third approach to the $\alpha,\beta$ -unsaturated aldehyde.....	177
Figure 4.20 Fourth approach to the $\alpha,\beta$ -unsaturated aldehyde.....	178
Figure 4.21 3-step synthesis of $\alpha,\beta$ -unsaturated aldehyde <b>4.92</b> from ketone <b>4.89</b> . ....	178
Figure 4.22 Completion of the synthesis of cochlearol B.....	180
Figure 4.23 Total synthesis of (+)-cochlearol B. ....	181
Figure 4.24 HPLC traces of racemic (above) and enantioenriched (below) <b>4.26</b> .....	205

Figure 4.25 HPLC traces of racemic (above) and enantioenriched (below) cochlearol B. ....	206
Figure 4.26 ORTEP diagram of <b>4.74</b> . ....	207
Figure 4.27 ORTEP diagram of <b>4.70</b> . ....	209
Figure 5.1 Representative member from each of the six families of Gelsemium alkaloids. ....	217
Figure 5.2 (A) Conserved substructures of the gelsedine alkaloids. (B) Carbon numbering scheme of gelsedine. (B) Representative Gelsemium alkaloids. ....	218
Figure 5.3 EC <sub>50</sub> values for six gelsedine type alkaloids against human A431 epidermoid carcinoma cells. ....	219
Figure 5.4 Proposed biosynthesis of gelsedine. ....	220
Figure 5.5 Previously used disconnections to access the oxacyclo[3.2.2]nonane core of the gelsedine type alkaloids. ....	221
Figure 5.6 (A) Fukuyama's asymmetric total synthesis of gelsemoxonine. (B) Divergent synthesis of gelsidine, gelsenicine, 14-hydroxygelsenicine, 14,15-dihydroxygelsenicine, and gelsedilam. ....	222
Figure 5.7 (A) Carreira's total synthesis of (±)-gelsemoxonine. (B) Enantioselective approach to intermediate <b>3.35</b> . ....	223
Figure 5.8 (A) Ma's asymmetric total synthesis of gelsemoxonine. (B) Divergent total synthesis of gelsedine, gelsenicine, gelsedilam. ....	224
Figure 5.9 (A) Spirocyclic oxindoles in natural products and lead compounds. (B) Numbered oxindole. (C) Common starting materials for the synthesis of oxindoles. (D) Oxidative rearrangement approach to oxindoles. (E) Transition metal mediated approach to forming the C3-C4 bond. (F) Transition metal mediated approach to forming the C2-C3 bond. ....	226
Figure 5.10 Retrosynthetic analysis of gelsemoxonine featuring a key visible light mediated [2+2]-cycloaddition as well as an enyne metathesis reaction. ....	227
Figure 5.11 A) Envisioned aldol approach to key intermediate <b>5.74</b> . B) Enantioselective synthesis of aldehyde <b>5.82</b> . ....	228
Figure 5.12. (A) Attempted Aldol and Mukaiyama-Aldol reactions to access key intermediate <b>5.85</b> . (B) Retro-aldol reaction scheme. (C) Evidence for the influence of the nitrogen protecting group on pK <sub>a</sub> . ....	229
Figure 5.13 (A) Synthesis of <b>5.93</b> under acidic or basic conditions. B) Evaluation of different alkylation conditions. C) Aldol reaction between indole <b>5.91</b> and chiral aldehyde <b>5.82</b> . ....	230
Figure 5.14 Model systems studies on the enyne metathesis reaction. ....	231



Figure 5.15 Retrosynthetic analysis utilizing an alternative Achmatowicz reaction approach. .	231
Figure 5.16 Initial studies verifying the feasibility of the Achmatowicz reaction and the challenges that arise in the subsequent steps. ....	232
Figure 5.17 Progress towards an Achmatowicz product capable of undergoing selective lactol reduction. ....	233
Figure 5.18 Third generation retrosynthetic analysis relying on an oxidative rearrangement approach to the oxindole. ....	234
Figure 5.19 Synthesis of oxidative rearrangement substrate <b>5.130</b> . ....	234
Figure 5.20 Hypothesized mechanism for the formation of unexpected byproduct <b>5.132</b> . ....	235

### List of Equations

Equation 2.1 Formula used to determine yield based on UPLC data using caffeine as an internal standard. ....	63
Equation 2.2 Equation to determine $Y(OTf)_3$ rate order. ....	66
Equation 2.3 Equation to determine $Sc(OTf)_3$ rate order. ....	70

## Abstract

The synthesis of natural products, pharmaceuticals, and organic materials has long driven much of the organic chemistry research conducted in both academic and industrial settings. Target directed synthesis often inspires the creation of new methodologies and acts as the ultimate proving ground for existing procedures. As the targets become more complex, methods must advance to enable their syntheses. Since chirality is integral to natural products and pharmaceuticals, developing new methods in asymmetric synthesis is of utmost importance. Originally, asymmetric synthesis was accomplished through the use of chiral pool reagents, but this has limitations based on availability. This realization gave rise to the field of asymmetric catalysis in which an achiral or racemic starting material undergoes an enantioselective transformation aided by a chiral catalyst. Many of these catalysts are transition metal based with chiral ligands of natural origin. However, since the enantioselectivity is conferred by a chiral ligand, these reactions are also limited by the scope of their availability. This limitation is perhaps most apparent when both enantiomers of a target structure are desired. In these instances, both enantiomers of the chiral ligand would be needed which may not be possible. Enantiodivergent catalysis, where a single chiral source is used to obtain either product enantiomer, represents an attractive yet underdeveloped alternative. During our lab work towards the total synthesis of lingzhiol, a meroterpenoid natural product isolated as a racemic mixture, we discovered a Lewis acid dependent enantiodivergent Michael addition. We then applied this method to the total synthesis of (-)- and (+)-lingzhiol (Chapter 1), both of which show promise as a potential treatment for renal fibrosis. Subsequent studies revealed the mechanism of this enantiodivergent reactivity (Chapter 2).

In addition to asymmetric synthesis, the synthesis of heterocyclic compounds is strongly emphasized in many research programs. Nitrogen containing heterocycles are of particular importance because of their prevalence in pharmaceuticals. However, azetidines remains largely underrepresented, most likely because of the lack of efficient methods for their synthesis. While photochemical [2+2]-cycloaddition reactions between imines and alkenes, known as the aza Paternò-Büchi reaction, would potentially allow straightforward access to azetidines, this process

has been hampered by competing reactivities of excited state imines. Using the tools of visible light photocatalysis, we developed an alternative approach relying on selective excitation of the alkene-coupling partner using triplet energy transfer (Chapter 3).

This work inspired our lab's interest in other 4-membered rings, such as cyclobutanes, which are featured in a number of biologically active natural products and could be made via a [2+2]-cycloaddition. Cochlearol B is unique among them because of its highly substituted cyclobutane ring containing three quaternary and one tertiary carbon. Isolated in 2014 from *Ganoderma cochlear*, cochlearol B is a meroterpenoid with documented renoprotective activity. Herein, we report our 14-step synthesis of (+)-cochlearol B, enabled by an alkenyl Catellani reaction and visible light mediated [2+2]-photocycloaddition (Chapter 4).

Azetidines are less common in natural products, but there are examples in the literature. Gelsemoxonine is a monoterpene indole alkaloid that contains an azetidine ring. Part of the family of *Gelsemium* alkaloids, gelsemoxonine is structurally related to many biologically active natural products. We envisioned applying our aza Paternò-Büchi method to the total synthesis of gelsemoxonine. Here, we report our progress towards that goal (Chapter 5).

## Chapter 1 Enantiodivergent Total Synthesis of (+) and (–)-Lingzhiol

Portions of this chapter have been published in: Riehl, P. S.; Richardson, A. D.; Sakamoto, T.; Schindler, C. S. Eight-Step Enantiodivergent Synthesis of (+)- and (–)-Lingzhiol. *Org. Lett.* **2020**, *22*, 290-294.<sup>1</sup>

### 1.1 Introduction

Extracts from fungi within the *Ganoderma* genus have a history of use in traditional Chinese medicine for the prevention and treatment of cancer, hypertension, renal fibrosis, chronic bronchitis, and asthma.<sup>2</sup> There are 219 species of fungi within this genus found across the world. Morphologically, the species can be quite different; however, they are generally described as polypore basidiomycetous fungi having a double-walled basidiospore. *Ganoderma lucidum*, a species within the *Ganoderma* genus, is a mushroom with over 2,000 years of documented medicinal use.<sup>2</sup> The beneficial pharmacological properties are often credited to the terpenoid compounds found within these fungi. To date over 100 different terpenes have been isolated and characterized, with over 50 being unique to *Ganoderma lucidum*.<sup>2</sup> These compounds possess a variety of biological activities. For example, lucidenic acid B (**1.1**)<sup>3</sup> induces apoptosis in human leukemia cells (Figure 1.1A)<sup>4</sup> and ganoderic acid B (**1.2**)<sup>5</sup> and ganoderiol A (**1.3**)<sup>6</sup> have been studied in the treatment of HIV (Figure 1.1A).<sup>7</sup> There is a growing interest in meroterpenoids, which are simply defined as structures partially derived from terpenoid pathways, because of their unique structures and biological activities.<sup>8</sup> Generally, fungi are a rich source of meroterpenoids, and *Ganoderma lucidum* is no exception. Recently, 5 meroterpenoid enantiomeric pairs (dayaolingzhiols I-M) were isolated from *Ganoderma lucidum* and evaluated as potential treatments for diabetes and triple negative breast cancer (TNBC).<sup>9</sup> Of these compounds, (+)-dayaolingzhiol M (**1.4**) shows the most promise for diabetes management, whereas (+)- and (–)-dayaolingzhiol L (**1.5**) and (+)-dayaolingzhiol I (**1.6**) may be useful in TNBC therapy (Figure 1.1B). Two additional representative members of this family are (–)-lingzhiol (**1.7**) and (+)-lingzhiol (**1.8**), meroterpenoid natural products that were isolated as a racemic mixture from *Ganoderma lucidum* in 2013 (Figure 1.1C).<sup>10</sup> In contrast to the dayaolingzhiols, lingzhiol is much

more structurally complex yet contains fewer total carbon atoms. Lingzhiol is a rotatory door shaped molecule possessing a 5/5/6/6 tetracyclic core structure with two vicinal stereogenic quaternary carbons. Comprehensive biological activity studies demonstrated that both enantiomers of lingzhiol inhibit the generation of collagen IV, fibronectin, and reactive oxygen species (ROS).<sup>10</sup> Additionally, (-)- and (+)-lingzhiol were both shown to inhibit the Smad (Small worm phenotype, *Mothers Against Decapentaplegic*) pathway, which is implicated in chronic kidney diseases (CKD) such as renal fibrosis and diabetic nephropathy.<sup>10</sup> Both these conditions can ultimately lead to kidney failure and death. CKD affects more than 1 in 7 U.S. adults, and over 750,000 Americans are experiencing end stage renal disease (ESRD).<sup>11</sup> Apart from a healthier lifestyle, very few options for CKD amelioration exist, with dialysis and transplant being the only treatment options for people with ESRD. As a result, kidney disease represents a substantial social and economic burden on society and new treatments are highly desirable. Dysregulation of the Smad pathway can lead to accumulation of extracellular matrix,<sup>12</sup> which is the root cause of renal fibrosis and CKD.<sup>13</sup> The Smad pathway is comprised of signal transducing proteins that respond to activated TGF- $\beta$  receptors, which are themselves important for regulating cell development and growth.<sup>12</sup> Specifically, both enantiomers of lingzhiol can selectively inhibit Smad3 without inhibiting Smad2.<sup>10</sup> Smad3 is a transcriptional modulator that upregulates genes associated with differentiation and growth,<sup>14</sup> which, in turn, promotes renal fibrosis.<sup>15</sup> Recent studies showed the Smad2 knockdown epithelial cells have an increased expression of collagen, whereas Smad2 overexpression leads to attenuation of collagen expression.<sup>15</sup> These studies suggest that Smad2 has

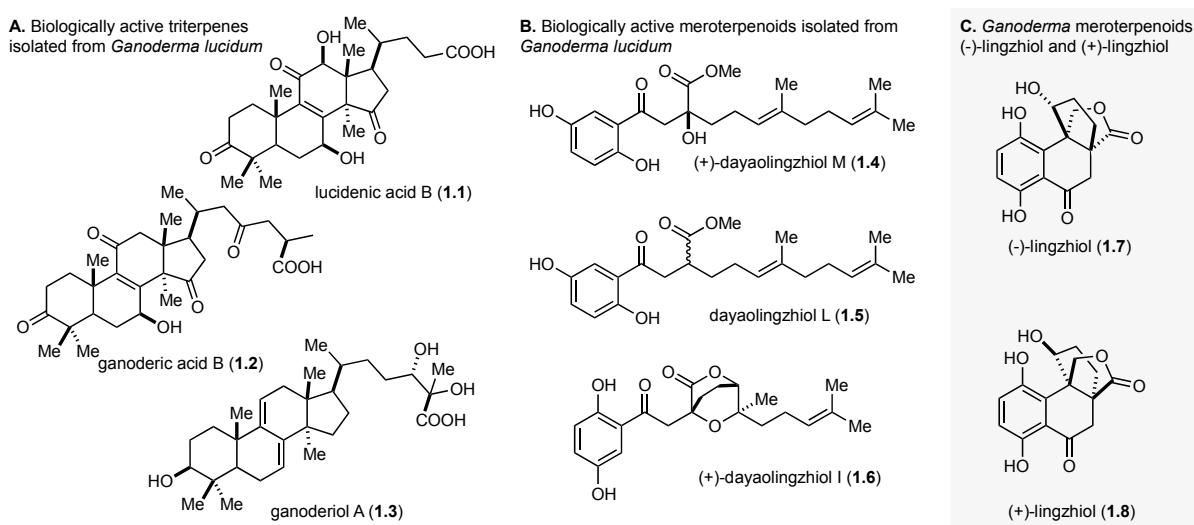
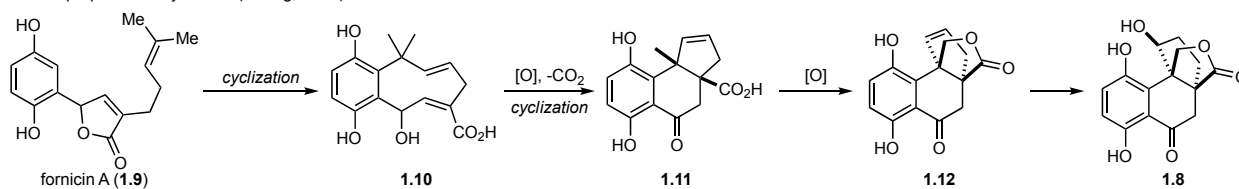


Figure 1.1 Biologically active terpenes and meroterpenoids isolated from *Ganoderma lucidum*, including (-) and (+)-lingzhiol.

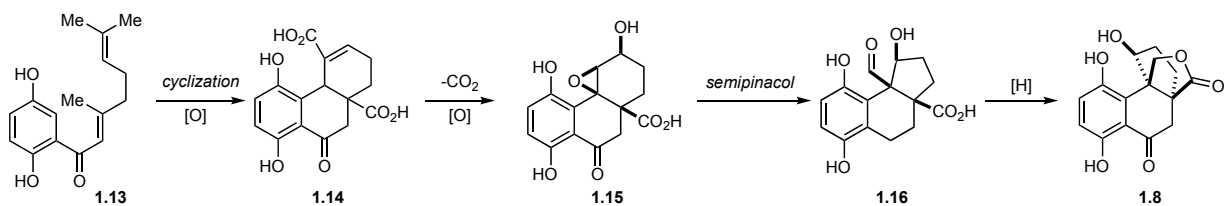
a renoprotective role. By selectively inhibiting Smad3 and not Smad2, lingzhiol may have compounding benefits for the treatment of renal fibrosis. In this capacity, (–)-lingzhiol (**1.7**) is more active than (+)-lingzhiol (**1.8**), but both can act as selective Smad3 inhibitors.<sup>10</sup>

Although the biosynthesis of lingzhiol has not been elucidated, three different routes have been proposed. In the first hypothesis, proposed by the group who reported its isolation, fornicin A (**1.9**) undergoes a series of cyclization and oxidations to arrive at lingzhiol (Figure 1.2A).<sup>10</sup> In the second, geranylated hydroquinone **1.13** undergoes a cyclization and multiple oxidations followed by a semipinacol rearrangement and reduction (Figure 1.2B).<sup>16</sup> The third proposal also starts from geranylated hydroquinone **1.13**, but instead draws inspiration from the proposed biosynthesis of a related natural product sinensilactam (**1.20**) (Figure 1.2C).<sup>17</sup>

A. First proposed biosynthesis (Cheng, 2013)



B. Second proposed biosynthesis (Birman, 2016)



C. Third proposed biosynthesis (Maier, 2017)

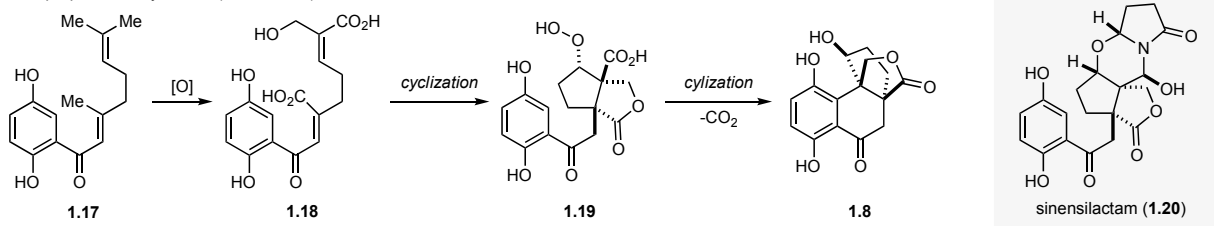


Figure 1.2 Different proposed biosyntheses of lingzhiol.

Due to its promising biological activity, low natural abundance, and unique structural features, lingzhiol has attracted substantial interest from the synthetic community. To date, seven additional syntheses have been reported, and of these seven, three were enantioselective (Figure 1.3). Including our report, five out of the eight syntheses start from dimethoxy-tetralone **1.21**, and the other three proceed via **1.22** (Figure 1.3B). The first published route was a 17-step synthesis that relied on a rhodium-catalyzed [3+2] cycloaddition to access (–)-lingzhiol (Figure 1.3C).<sup>18</sup> The Qin<sup>19,20</sup> and Maier<sup>17,21</sup> groups each reported two separate syntheses of lingzhiol. Three of those

four routes employed an epoxy-arene cyclization to access the tetracyclic core (Figure 1.3D),<sup>17,19,20</sup> and the fourth utilized a titanocene-catalyzed radical cyclization (Figure 1.3E).<sup>21</sup> In addition to the work described herein, two other groups took advantage of a semipinacol ring contraction approach to lingzhiol (Figure 1.3F).<sup>16,22</sup>

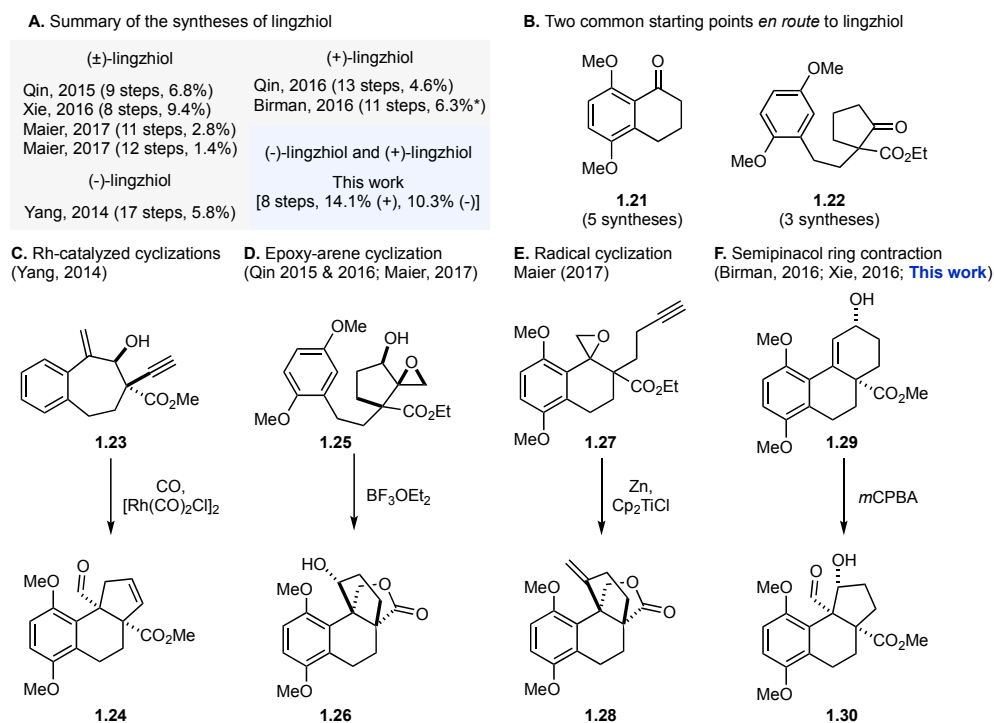


Figure 1.3 (A) Summary of the previous syntheses of lingzhiol. (B) Two starting points utilized in all syntheses reported to date. (C-F) Key steps in the previous syntheses of lingzhiol.

Despite the desirable biological activity possessed by both enantiomers, no independent synthesis of both (+)- and (-)-lingzhiol has been reported. This could be explained, in part, by the current limitation of asymmetric catalysis,<sup>23</sup> where chirality is usually conferred by optically active ligands often derived from chiral pool reagents.<sup>24</sup> As such, asymmetric transformations are limited by the availability/accessibility of one or both enantiomers of the ligand. In order to access both enantiomers of a product under a typical reaction paradigm, both enantiomers of the ligand would be required, which may not be possible or straightforward to realize.<sup>25</sup> Interestingly, concomitant studies in our lab demonstrated that a single enantiomer of a bipyridine ligand can enable enantiodivergent reactivity in Michael addition reactions when combined with different simple Lewis-acid catalysts (Figure 1.4).<sup>26</sup> This represents a rare phenomenon in asymmetric catalysis where an achiral reaction parameter dictates the stereochemical outcome of a reaction.<sup>27</sup> This enantiodivergent reaction will be discussed in detail in Chapter 2, but in the context of this chapter,



we felt this enantiodivergent method would be ideally suited to enable the synthesis of both (-)-lingzhiol (**1.7**) and (+)-lingzhiol (**1.8**).

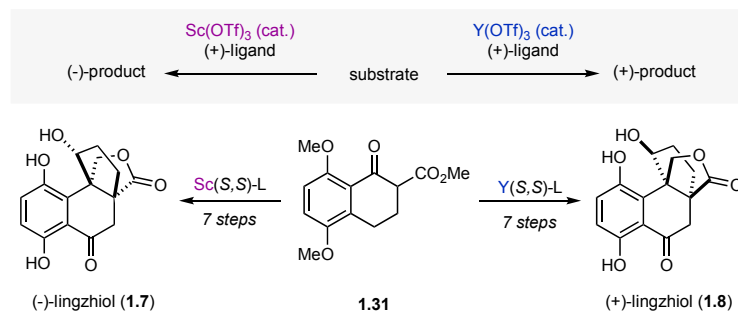
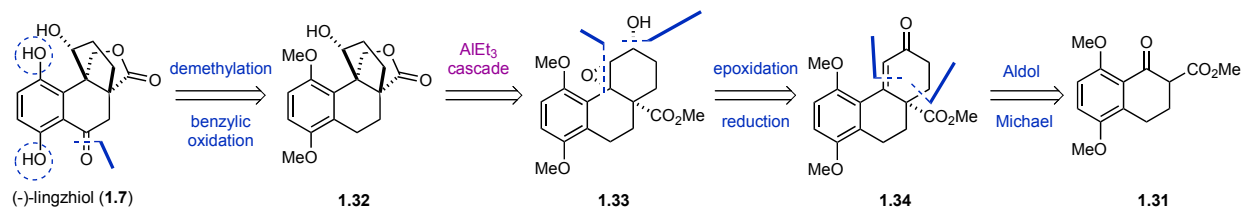


Figure 1.4 Our enantiodivergent approach to (-)- and (+)-lingzhiol.

Our approach towards lingzhiol relied on a few key carbon-carbon bond forming steps to selectively set the stereocenters and rapidly assemble the core of this natural product (Figure 1.5). Retrosynthetically, we envisioned that the phenols could be revealed through a deprotection and that the benzylic ketone could come from a benzylic oxidation reaction. We proposed to arrive at the core structure of lingzhiol (**1.32**) via a  $\text{Et}_3\text{Al}$ -mediated semipinacol-reduction-lactonization cascade<sup>28</sup> from epoxy-alcohol **1.33** (Figure 1.5B).

A. Retrosynthetic analysis of lingzhiol.



B. Key  $\text{AlEt}_3$  mediated cascade reaction.

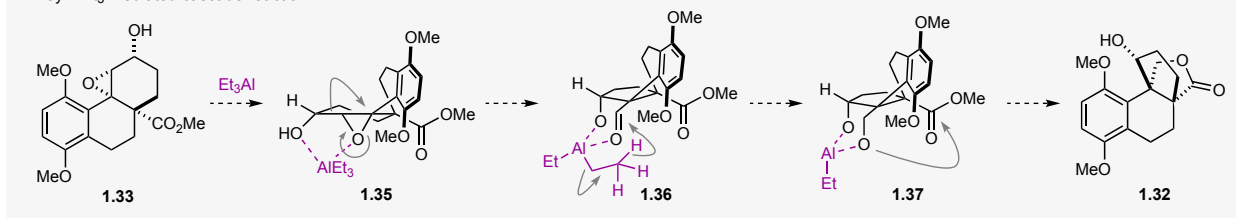


Figure 1.5 Retrosynthetic analysis of lingzhiol highlighting the key  $\text{AlEt}_3$  mediated cascade reaction.

**1.33** could come from a two-step sequence of reduction followed by epoxidation from enone **1.34**. We planned to prepare **1.34** asymmetrically via a Lewis-acid catalyzed Michael addition followed by a Robinson annulation starting from known tetralone **1.31**.<sup>29</sup> The key asymmetric Lewis-acid catalyzed Michael addition was inspired by a report from the Kobayashi group in which  $\text{Sc}(\text{OTf})_3$  catalyzed highly enantioselective Michael additions in the presence of

chiral bipyridine ligands.<sup>30</sup> This served as the starting point for our synthesis as well as the discovery of the aforementioned enantiodivergent Michael addition.

## 1.2 Results and Discussion

To test our key Et<sub>3</sub>Al cascade, model epoxy-alcohol **1.40** was prepared in two steps from known enone **1.38** (Figure 1.6).<sup>31</sup> Upon treatment with Et<sub>3</sub>Al, **1.40** was successfully converted to tetracyclic lactone **1.41** in 30% yield. Emboldened by this success, we focused our efforts on applying this transformation to the total synthesis of lingzhiol.

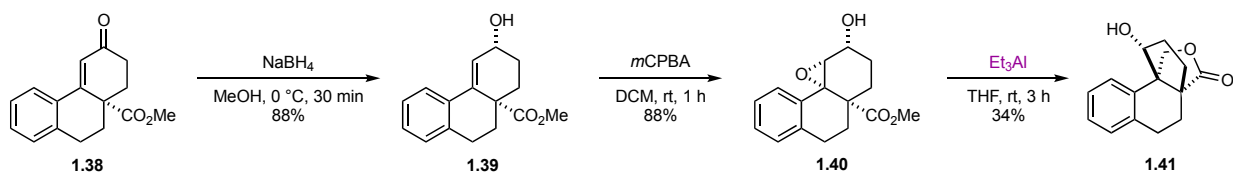


Figure 1.6 Model studies to test the viability of the AlEt<sub>3</sub> mediated cascade reaction.

Our synthesis commenced with a Michael addition between known  $\beta$ -ketoester **1.31**<sup>29</sup> and methyl vinyl ketone (MVK). To accomplish an asymmetric synthesis, we envisioned applying Kobayashi's conditions<sup>30</sup> that rely on chiral bipyridine ligand<sup>32,33</sup> **1.42** and catalytic Sc(OTf)<sub>3</sub> to effect enantioselective Michael addition. In our system, the reported conditions provided the desired product (S)-**1.44** in 31% yield and 90% ee after 4 days of reaction time (Table 1.1, entry 1). Importantly, we were able to verify the absolute stereochemistry of (S)-**1.44** by X-ray crystallographic analysis. In an effort to improve the yield, alternative metal triflate catalysts were tested in this reaction. Y(OTf)<sub>3</sub> and Dy(OTf)<sub>3</sub> proved to be more efficient catalysts affording **1.44** in higher yields (92% and 88%, respectively) and shorter reaction times (18 and 17 hours, respectively) while maintaining good enantiomeric excess (71% and 76% ee, respectively) (Table 1.1, entries 2 and 3). Interestingly, these catalysts afforded (R)-**1.44** as the major enantiomer despite using the same (S,S)-**1.42** ligand as was used the Sc(OTf)<sub>3</sub> catalyzed reaction. This represents a rare phenomenon in asymmetric catalysis where an achiral reaction parameter dictates the stereochemical outcome of a reaction and as such, we felt this result warranted further investigation.<sup>27</sup> Additionally, we believed that this enantiodivergent reactivity could provide an efficient method to access both enantiomers of lingzhiol.

Additional experimentation revealed that switching to benzene as a solvent improved the Y(OTf)<sub>3</sub> and Dy(OTf)<sub>3</sub> catalyzed reactions by maintaining high yields (91% and 83%, respectively) and improving the enantioselectivity (91% and 90% ee, respectively) (Table 1.1,

Table 1.1 Optimization of the Lewis acid catalyzed Michael addition reveal unique enantiodivergent behavior.

entry	Lewis acid	solvent	time (h)	yield (%)	ee (%)
1	Sc(OTf) <sub>3</sub>	DCE	96	31	-90
2	Dy(OTf) <sub>3</sub>	DCE	17	90	73
3	Y(OTf) <sub>3</sub>	DCE	18	92	71
4	Lu(OTf) <sub>3</sub>	benzene	42	93	82
5	Yb(OTf) <sub>3</sub>	benzene	42	89	84
6	Tm(OTf) <sub>3</sub>	benzene	22	92	86
7	Er(OTf) <sub>3</sub>	benzene	18	95	89
8	Ho(OTf) <sub>3</sub>	benzene	18	98	89
9	Y(OTf) <sub>3</sub>	benzene	18	91	91
10	Dy(OTf) <sub>3</sub>	benzene	17	83	90
11	Tb(OTf) <sub>3</sub>	benzene	17	98	90
12	Gd(OTf) <sub>3</sub>	benzene	17	97	87
13	Eu(OTf) <sub>3</sub>	benzene	17	99	83
14	Sm(OTf) <sub>3</sub>	benzene	17	96	74
15	Nd(OTf) <sub>3</sub>	benzene	17	96	13
16	Pr(OTf) <sub>3</sub>	benzene	17	94	-23
17	Ce(OTf) <sub>3</sub>	benzene	17	81	-42
18	La(OTf) <sub>3</sub>	benzene	17	97	-43
19	Sc(OTf) <sub>3</sub>	benzene	96	0	—
20 <sup>a</sup>	Y(OTf) <sub>3</sub>	benzene	17	99	94
21 <sup>b</sup>	Sc(OTf) <sub>3</sub>	DCE	96	58	-91
22 <sup>c</sup>	Y(OTf) <sub>3</sub>	benzene	4	97	91

Reactions were performed on 0.15 mmol scale at 0.02 M at 60 °C. M(OTf)<sub>3</sub> and **1.42** were pre-stirred at 60 °C for 1 hour. <sup>a</sup> Reaction performed at 80 °C and 0.04 M. <sup>b</sup> Ligand **1.43** was used instead of **1.42**. <sup>c</sup> Identical reaction conditions to entry 20 using ligand **1.43**.

entries 9 and 10). To thoroughly evaluate this reaction, all other commercially available lanthanide triflates were tested. Lu(OTf)<sub>3</sub> and Yb(OTf)<sub>3</sub> required extended reaction times (42 hours) but did provide **1.44** in high yields (93% and 89%, respectively) and good enantioselectivity (82% and 84% ee, respectively) (Table 1.1, entries 4 and 5). The reaction times shortened ( $\leq 22$  h) when moving to Tm(OTf)<sub>3</sub>, Er(OTf)<sub>3</sub>, Ho(OTf)<sub>3</sub> and Tb(OTf)<sub>3</sub> and **1.44** was isolated in high yields (92%, 95%, 98%, 98% respectively) and with high enantioselectivities (86%, 89%, 89% and 90%, respectively) (Table 1.1, entries 6–8 and 11). Gd(OTf)<sub>3</sub>, Eu(OTf)<sub>3</sub>, and Sm(OTf)<sub>3</sub> provided **1.44** in high yields (97%, 99%, and 96%, respectively); however, the enantiomeric excess began to drop incrementally (87%, 83%, and 74%, respectively) (Table 1.1, entries 12–14). Nd(OTf)<sub>3</sub> was

similarly high yielding, affording **1.44** in 96%; however it led to the lowest enantiomeric excess at 13% ee (Table 1.1, entry 15). Pr(OTf), Ce(OTf)<sub>3</sub>, and La(OTf)<sub>3</sub> were also high yielding (94%, 81%, and 97%, respectively) but did not impart high enantioselectivity (23%, 42%, and 43%, respectively) (Table 1.1, entries 16–18). Interestingly, the major enantiomer provided by these last three catalyst was (S)-**1.44**, which is opposite to all the other catalyst evaluated except Sc(OTf)<sub>3</sub>. Based on these data, the variability in enantiomeric excess can be attributed in part to the different ionic radii of the M<sup>3+</sup> catalysts.<sup>34</sup> This likely leads to different binding modes between the substrate, ligand, and catalyst. A complete picture of the underlying mechanism of this enantiodivergent transformation was the subject of a separate study and will be discussed in detail in Chapter 2.

Of the all the metals that were tested on this reaction, Y(OTf)<sub>3</sub> was selected as the optimal catalyst based on the yield, enantioselectivity, and commercial availability. Further experimentation using Y(OTf)<sub>3</sub> as a catalyst revealed that increasing the temperature from 60 °C to 80 °C improved both the yield and enantioselectivity of this reaction (Table 1.1, entry 20).

Based on the proposed mechanism of a metal-enolate formation between the metal-ligand complex and the substrate,<sup>30</sup> we hypothesized that a more electron rich ligand could increase the reactivity of the enolate thus accelerating the rate of the reaction. This would be especially useful for the slow Sc(OTf)<sub>3</sub> catalyzed reaction. To this end, methoxy substituted ligand (S,S)-**1.43** was prepared and tested. Gratifyingly, Sc(OTf)<sub>3</sub>, in combination with new electron rich ligand (S,S)-

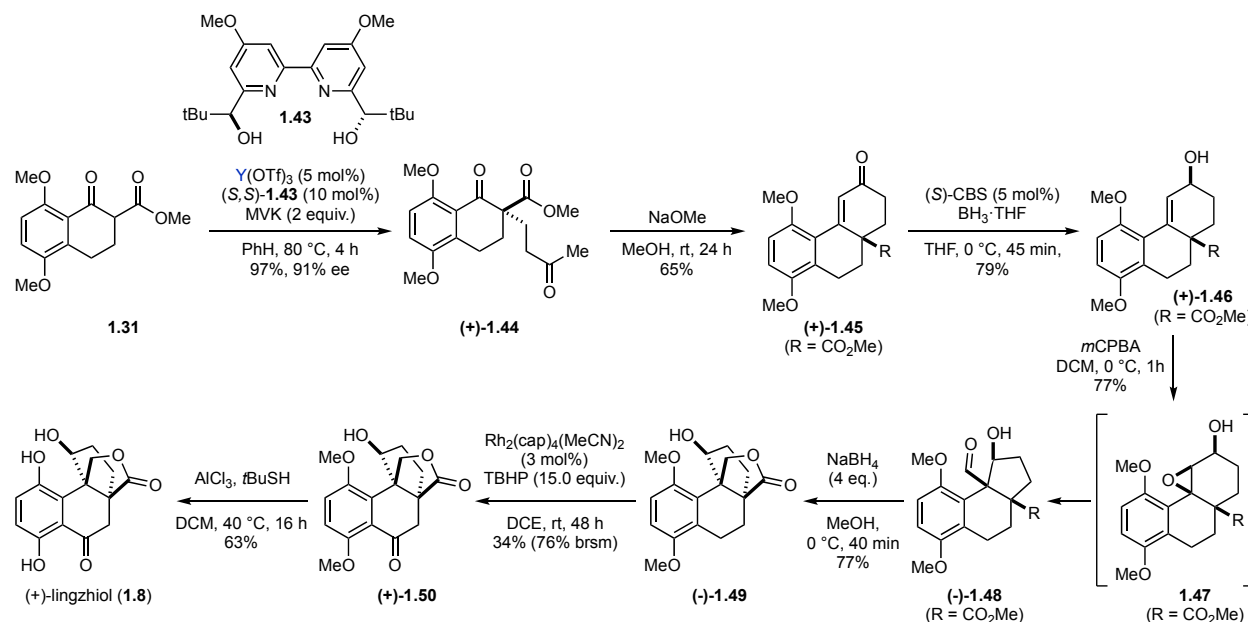
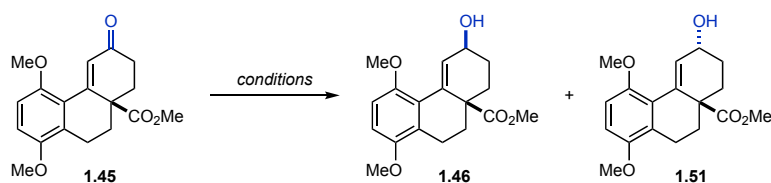


Figure 1.7 Completion of the syntheses of (+)-lingzhiol.

**1.43**, yielded 58% of **1.44** while maintaining an excellent enantiomeric excess of 91% ee (Table 1.1, entry 21). Similar acceleration was observed in the  $Y(OTf)_3$  catalyzed reaction, shortening the reaction time to 4 h while maintaining a high yield and enantiomeric excess (97% yield and 91% ee) (Table 1.1, entry 22).

With optimized conditions in hand, our focus shifted to elaborating (+)-**1.44** to (+)-lingzhiol (**1.8**) (Figure 1.7). An NaOMe mediated aldol condensation afforded enone (+)-**1.45** in 65% yield. Reduction of the ketone using  $BH_3$  in the presence of catalytic (S)-CBS provided allylic alcohol (+)-**1.46** in 79% yield (Table 1.2, entry 1) and minor diastereomer **1.51** in 9% yield.<sup>35</sup> Alternatively, both  $NaBH_4$  and (R)-CBS/ $BH_3$  were lowering yielding, with the later giving a greater amount of the minor diastereomer **1.51** (Table 1.2, entries 2 & 3).

Table 1.2 Optimization of the allylic alcohol reduction.



entry	conditions	yield <b>1.46</b> (%)	yield <b>1.51</b> (%)
1	(S)-CBS, $BH_3$ THF THF, 0 °C, 45 min	79	9
2	(R)-CBS, $BH_3$ THF THF, 0 °C, 45 min	72	11
3	$NaBH_4$ , MeOH 0 °C, 1 h	75	7

As in the model system (Figure 1.6), epoxidation with *m*CPBA was expected to yield epoxide **1.47**, the precursor for the  $Et_3Al$ -mediated semipinacol-reduction-lactonization cascade reaction (Figure 1.7). Instead, aldehyde (–)-**1.48** was isolated as the sole product in 77% yield indicating that epoxide **1.47** does form, then undergoes a spontaneous, *in situ* semipinacol rearrangement (Figure 1.7).<sup>16 22</sup> In comparison to model epoxide **1.40**, the electron-rich aromatic substituents of **1.47** decrease the stability of the epoxide under the mildly acidic reaction conditions and decrease the transition state energy for the semipinacol rearrangement. Upon treatment with  $NaBH_4$ , aldehyde (–)-**1.48** underwent reduction and lactonization to afford (–)-**1.49** in 76% yield, arriving at the core of (+)-lingzhiol in 6 steps from commercially available materials. Interestingly, lowering the equivalents of  $NaBH_4$  yielded a minor amount of **1.52** suggesting that **1.48** can undergo a retro-aldol reaction under these conditions (Figure 1.8).

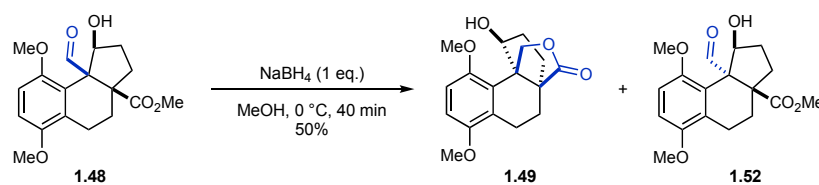


Figure 1.8 Lower equivalents of NaBH<sub>4</sub> leads to a retro-aldol product.

After arriving at the core structure, our goal became to incorporate the benzylic ketone without protecting the secondary alcohol in **1.49** to avoid additional protection and deprotection steps (Figure 1.7). To this end several conditions were evaluated (Table 1.3). A two-step approach utilizing aqueous NBS followed by MnO<sub>2</sub> did not give the desired product **1.50** (Table 1.3 entry 1).<sup>18</sup> Additional attempts using a number of oxidation conditions, including RuCl<sub>3</sub>/TBHP,<sup>36</sup> Co(OAc)<sub>2</sub>/NHPI/O<sub>2</sub>,<sup>37</sup> Pd(OH)<sub>2</sub>/TBHP,<sup>38</sup> and oxone/KBr/hν,<sup>39</sup> all failed to provide the desired benzylic ketone (Table 1.3, entries 2-5). However, conditions developed by the Doyle group relying on a Rh<sub>2</sub>cap<sub>4</sub> catalyst and T-HYDRO as a stoichiometric oxidant did successfully yield the desired benzylic ketone **1.50** in 6% yield (Table 1.3, entry 6).<sup>40</sup> Exploring other stoichiometric oxidants proved fruitful as switching to TBHP improved the yield to 38% (76% BRSM) (Table 1.3, entry 7).

Table 1.3 Optimization of the benzylic oxidation reaction.



entry	conditions	solvent	yield (%)
1	NBS/H <sub>2</sub> O then MnO <sub>2</sub>	CCl <sub>4</sub>	0
2	RuCl <sub>3</sub> , TBHP	cyclohexane	0
3	Co(OAc) <sub>2</sub> , NHPI, O <sub>2</sub>	acetone	0
4	Pd(OH) <sub>2</sub> , K <sub>2</sub> CO <sub>3</sub> , TBHP	DCM	0
5	oxone, KBr, hν	DCM/H <sub>2</sub> O	0
6	Rh <sub>2</sub> cap <sub>4</sub> , T-HYDRO	DCE	6
7	Rh <sub>2</sub> cap <sub>4</sub> , TBHP	DCE	34 (76 brsm)

To complete the synthesis of (+)-lingzhiol the hydroquinone must be revealed via a double demethylation reaction (Figure 1.7). Despite literature precedent,<sup>19</sup> extensive experimentation with BBr<sub>3</sub> did not provide any of the natural product; instead only singly demethylated product **1.53** was observed in 82% yield (Table 1.4, entry 1). Monoprotected **1.53** could not be pushed to (+)-lingzhiol upon re-subjecting it to BBr<sub>3</sub>. Alternative demethylation conditions relying on

$\text{BCl}_3/\text{TBAI}$  also exclusively yield **1.53** (Table 1.4, entry 2).<sup>41</sup> Successful double demethylation was achieved using  $\text{AlCl}_3$  and *t*BuSH at elevated temperatures,<sup>18</sup> yielding (+)-lingzhiol (**1.8**) in 63% yield.

Table 1.4 Optimization of the double demethylation reaction.

entry	Lewis acid	temperature	time (h)	yield <b>1.8</b> (%)	yield <b>1.53</b> (%)
1	$\text{BBr}_3$	0 °C	2	0	82
2	$\text{BCl}_3$ , $\text{Bu}_4\text{NI}$	-78 °C to rt	11	0	69
3	$\text{AlCl}_3$ , <i>t</i> BuSH	40 °C	16	63	0

To accomplish a synthesis of (–)-lingzhiol we employed the enantiodivergent Michael addition conditions by switching from  $\text{Y}(\text{OTf})_3$  to  $\text{Sc}(\text{OTf})_3$  to prepare (–)-**1.44**. Then, this compound was taken through the same 6-step sequence to successfully complete the synthesis of (–)-lingzhiol (**1.7**) (Figure 1.10).<sup>1</sup>

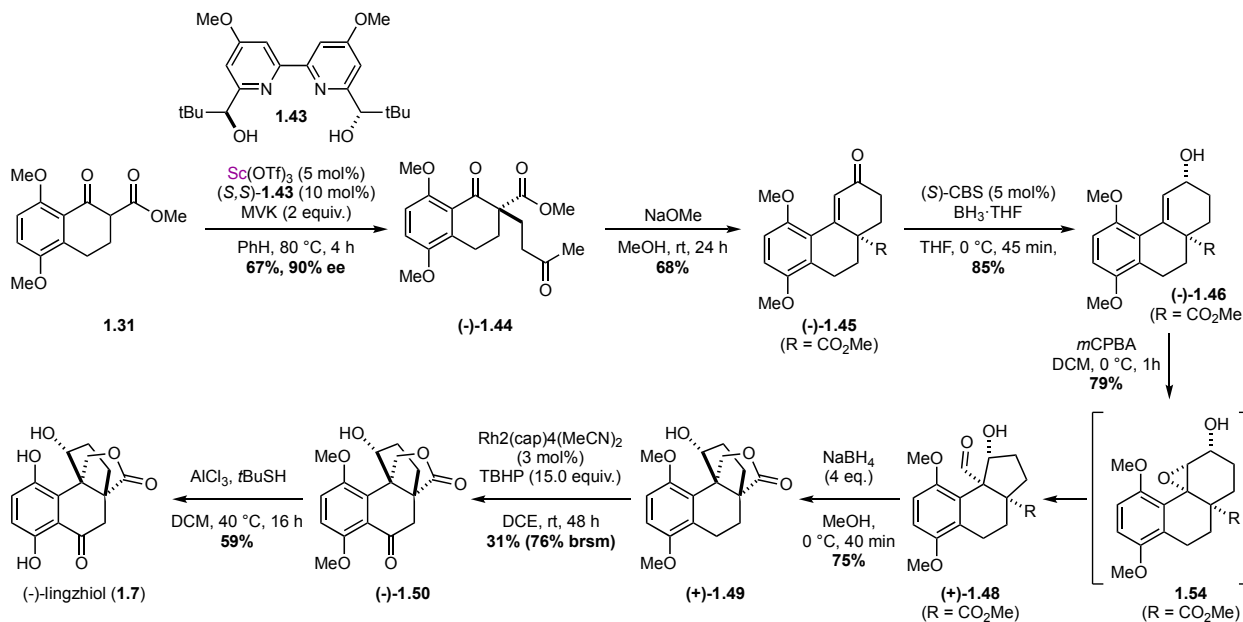


Figure 1.9 Completion of the synthesis of (–)-lingzhiol.

### 1.3 Conclusion

In our efforts towards the total syntheses of (+)- and (-)-lingzhiol, we discovered a Lewis acid dependent enantiodivergent Michael addition. In this reaction, a single enantiomer of a chiral bipyridine ligand is used to access both enantiomers of the Michael product in high selectivity. The enantiodivergence arises from the choice of Lewis acid catalyst. The mechanistic origin of this enantiodivergence could have interesting implications in asymmetric catalysis and will be discussed at length in Chapter 2. This highly selective, enantiodivergent Michael addition also served as the second step in our synthesis and enable facile access to both (+)- and (-)-lingzhiol. Our approach was also highlighted by a spontaneous semipinacol rearrangement and selective radical benzylic oxidation. Our synthesis is the shortest and highest yielding synthesis of both (+)-lingzhiol (**1.8**) and (-)-lingzhiol (**1.7**) to date.<sup>1</sup>

### 1.4 Experimental

#### 1.4.1 General Information

All moisture-sensitive reactions were performed under nitrogen in oven- or flame-dried round bottom flasks fitted with rubber septa. Dry solvents and air- and moisture- sensitive reagents were transferred via oven-dried stainless-steel needles or hypodermic needles. Flash chromatography and silica plugs were carried out using Silicycle Silia Flash<sup>®</sup> 40-63 micron (230-400 mesh) silica gel. All heated reactions were heated in Teflon/aluminum heating mantles (Chemglass). All chemicals were purchased from Sigma Aldrich, Alfa Aesar, Acros Organics, TCI America, and Ark Pharm and were used as received unless noted otherwise. Tetrahydrofuran and dichloromethane were dried by being passed through columns of activated alumina. Benzene and dichloroethane were removed from sealed bottles under nitrogen atmosphere. Chiral ligands (*S,S*)-**1.42** and **1.43** were prepared according to the procedures reported by Kobayashi.<sup>33</sup> Chiral HPLC analysis was performed on an Agilent Infinity 1260 equipped with a ChiralCel OD-H column (5  $\mu\text{m}$ ; 4.6 mm x 250 mm) unless otherwise noted. HPLC purification was performed using an Agilent 1260 Infinity II equipped with a Phenomenex Luna 5  $\mu\text{m}$  C18 column (10 mm x 250 mm). Proton nuclear magnetic resonance NMR (<sup>1</sup>H NMR) spectra and carbon nuclear magnetic resonance spectra (<sup>13</sup>C NMR) were measured on Varian MR400, Varian vnmrs 500, Varian Inova

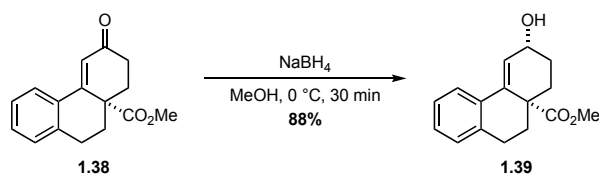


500, or Varian vnmrs 700 spectrometers. Chemical shifts for protons are reported in parts per million (ppm) and are referenced to the residual NMR solvent peak (CHCl<sub>3</sub>:  $\delta$ 7.26, acetone: 2.05). Chemical shifts for carbons are reported in parts per million and are referenced to the carbon resonances of the NMR solvent (CDCl<sub>3</sub>: 77.16, acetone-*d*<sub>6</sub>: 206.26 (C=O)). Data are described as follows: chemical shift, integration, multiplicity (br = broad, s = singlet, d = doublet, t = triplet, q = quartet, p = pentet, dd= doublet of doublets, m = multiplet), and coupling constant in Hertz (Hz). High resolution mass spectroscopic (HRMS) data were recorded at the University of Michigan Chemistry Department's mass spectrometry facility in Ann Arbor, MI on an Agilent Q-TOF HPLC-MS with ESI high resolution mass spectrometer unless otherwise noted. Infrared (IR) spectra were measured on a Thermo-Nicolet IS-50 infrared spectrometer. IR data are represented as frequency of absorption (cm<sup>-1</sup>). Optical rotations were acquired on a Jasco P-2000 digital polarimeter and are reported as *c* = g/100 mL at 589 nm (sodium D line) at 26 °C and 10 cm path length unless otherwise noted and CD spectra were acquired on a Jasco J-1500 CD spectropolarimeter.

**Abbreviations used:** Et<sub>3</sub>N = triethylamine, EtOAc = ethyl acetate, DCE = dichloroethane, DCM = dichloromethane, THF = tetrahydrofuran, MeOH = methanol, DCE = dichloroethane, OTf = trifluoromethanesulfonate (triflate), Na<sub>2</sub>SO<sub>4</sub> = sodium sulfate, MgSO<sub>4</sub> = magnesium sulfate, HCl = hydrochloric acid, NH<sub>4</sub>Cl = ammonium chloride, NaHCO<sub>3</sub> = sodium hydrogencarbonate (sodium bicarbonate), NaBH<sub>4</sub> = sodium borohydride, *m*CPBA = *m*-chloroperoxybenzoic acid, NHPI = N-hydroxy phthalimide, TLC = thin-layer chromatography.

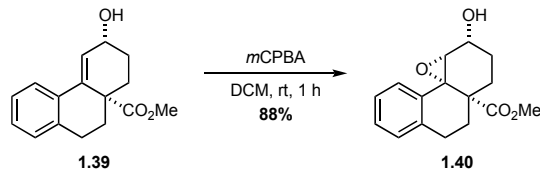
### 1.4.2 Experimental Procedures

#### Model Systems

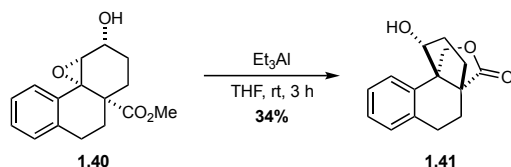


**Methyl (6*R*\*,8*aS*\*)-6-hydroxy-7,8,9,10-tetrahydrophenanthrene-8*a*(6*H*)-carboxylate (1.39):** Enone **1.38**<sup>31</sup> (1.07 g, 4.17 mmol) was dissolved in MeOH (40 mL) and cooled to 0 °C. Solid NaBH<sub>4</sub> (237 mg, 6.26 mmol, 1.5 equiv.) was added in a single portion and the reaction mixture was allowed to stir for 30 minutes. The reaction mixture was quenched with water and extracted

with three portions of ethyl acetate, dried over Na<sub>2</sub>SO<sub>4</sub>, concentrated by rotary evaporator and purified by silica gel column chromatography eluting with ethyl acetate/hexanes to afford a white solid (953 mg, 88% yield). **<sup>1</sup>H NMR** (500 MHz, CDCl<sub>3</sub>) δ 7.68 – 7.59 (m, 1H), 7.16 (dt, *J* = 9.6, 3.4 Hz, 2H), 7.08 – 7.02 (m, 1H), 6.32 (d, *J* = 1.8 Hz, 1H), 4.48 – 4.37 (m, 1H), 3.60 (s, 3H), 2.80 (dd, *J* = 9.0, 3.2 Hz, 2H), 2.40 (ddd, *J* = 13.1, 11.0, 4.2 Hz, 1H), 2.29 (ddd, *J* = 13.6, 4.0, 2.8 Hz, 1H), 2.15 – 2.08 (m, 1H), 1.73 – 1.57 (m, 3H), 1.48 (ddd, *J* = 12.0, 7.1, 2.2 Hz, 1H). **<sup>13</sup>C NMR** (126 MHz, CDCl<sub>3</sub>) δ 175.8, 137.0, 135.7, 133.9, 129.2, 127.7, 126.4, 126.2, 124.6, 68.3, 52.4, 47.3, 34.9, 34.2, 29.6, 27.1. **IR** (cm<sup>-1</sup>, neat): 1725.39, 1702.50, 1432.91, 1272.83, 1236.95, 1188.05, 1167.54, 1140.07, 1075.25, 1052.20, 1021.73, 1002.99, 977.02. **HRMS** (ESI<sup>+</sup>): Calculated for C<sub>16</sub>H<sub>18</sub>O<sub>3</sub>Na<sup>+</sup> [M+Na<sup>+</sup>]<sup>+</sup>: 281.1148 Found [M+Na<sup>+</sup>]<sup>+</sup>: 281.1149.



**Methyl (4b*S*\*,5a*R*\*,6*R*\*,8a*S*\*)-6-hydroxy-5a,6,7,8,9,10-hexahydro-8a*H*-phenanthro[4,4a-*b*]oxirene-8a-carboxylate (1.40):** Allylic alcohol **1.39** (214 mg, 0.83 mmol) was dissolved in DCM (8 mL) and cooled to 0 °C and solid *m*CPBA (75% purity; 429 mg, 2.49 mmol, 3 equiv.) was added. The reaction mixture was allowed to stir until judged complete by TLC. The reaction mixture was diluted with DCM and a saturated aqueous solution of sodium bicarbonate was poured onto the mixture, followed by a saturated aqueous solution of sodium thiosulfate. The layers were separated and the organic layer was dried over Na<sub>2</sub>SO<sub>4</sub> and concentrated by rotary evaporator. After purification by silica gel chromatography, the product was isolated as a clear, thick oil (200 mg, 88% yield). **<sup>1</sup>H NMR** (500 MHz CDCl<sub>3</sub>) δ 7.25 – 7.15 (m, 3H), 7.09 (d, *J* = 7.0 Hz, 1H), 4.13 – 4.06 (m, 1H), 3.65 (d, *J* = 4.7 Hz, 3H), 3.27 (d, *J* = 3.2 Hz, 1H), 2.86 – 2.72 (m, 2H), 2.25 – 2.13 (m, 2H), 2.09 – 2.00 (m, 2H), 1.78 (tdd, *J* = 8.5, 6.2, 3.5 Hz, 1H), 1.67 – 1.52 (m, 2H), 1.52 – 1.42 (m, 1H). **<sup>13</sup>C NMR** (126 MHz, CDCl<sub>3</sub>) δ 174.9, 138.1, 136.2, 127.7, 127.5, 127.0, 123.2, 66.8, 66.4, 63.1, 52.3, 45.8, 33.48, 29.3, 26.7, 26.2. **IR** (cm<sup>-1</sup>, neat): 2949.31, 1725.15, 1433.94, 1267.63, 1195.34, 1172.52, 1069.14, 1041.35, 990.27, 965.21, 928.00, 864.91. **HRMS** (ESI<sup>+</sup>): Calculated for C<sub>16</sub>H<sub>18</sub>O<sub>4</sub>Na<sup>+</sup> [M+Na<sup>+</sup>]<sup>+</sup>: 297.1097 Found [M+Na<sup>+</sup>]<sup>+</sup>: 297.1095.



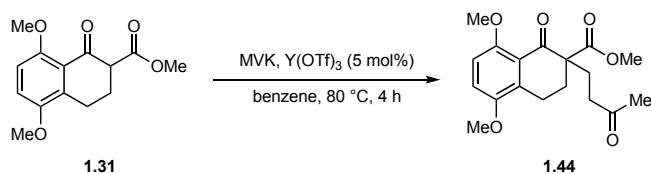
**(3a*S*\*,9b*R*\*)-1-Hydroxy-2,3,4,5-tetrahydro-1*H*-3a,9b-(methanooxymethano)cyclopenta[*a*]-**

**naphthalen-12-one (1.41):** Epoxide **1.40** (34 mg, 0.12 mmol) was dissolved in THF (1.2 mL) and a freshly prepared solution of triethylaluminum (3M in hexanes, 0.37 mL, 0.37 mmol, 3 equiv.) was added at room temperature and stirred for 3 hours, at which point another portion of triethylaluminum solution (3M in hexanes, 0.37 mL, 0.37 mmol, 3 equiv.) was added. The reaction was quenched with aqueous 1M HCl and allowed to stir until homogeneous. The mixture was then poured onto ethyl acetate and the layers were separated. The aqueous layer was extracted with two additional portions of ethyl acetate. The yield of the reaction was measured by NMR of the crude reaction mixture with dimethyl terephthalate as an internal standard (9 mg, 34%) The combined organic layers were washed with brine and dried over Na<sub>2</sub>SO<sub>4</sub>, then concentrated by rotary evaporator and purified by silica gel column chromatography eluting with hexanes/ethyl acetate and then HPLC eluting with water/acetonitrile to afford the title compound as a white solid (3 mg) for characterization. <sup>1</sup>H NMR (700 MHz, CDCl<sub>3</sub>) δ 7.30 – 7.23 (m, 3H), 7.21 – 7.12 (m, 2H), 5.02 (d, *J* = 9.6 Hz, 1H), 4.28 – 4.21 (m, 1H), 4.09 (d, *J* = 9.6 Hz, 1H), 2.81 – 2.74 (m, 1H), 2.69 (dt, *J* = 16.1, 5.0 Hz, 1H), 2.38 – 2.24 (m, 1H), 2.02 – 1.83 (m, 5H), 1.73 – 1.64 (m, 1H). <sup>13</sup>C NMR (176 MHz, CDCl<sub>3</sub>) δ 182.8, 139.8, 136.11, 128.9, 127.6, 127.0, 126.6, 82.0, 72.12, 54.2, 52.5, 33.1, 32.2, 29.5, 26.6. IR (cm<sup>-1</sup>, neat): 2935.39, 1742.94, 1490.31, 1451.16, 1377.10, 1254.78, 1168.92, 1118.50, 1083.80, 1025.83, 942.96, 925.55. HRMS (ESI<sup>+</sup>): Calculated for C<sub>15</sub>H<sub>16</sub>O<sub>3</sub>H<sup>+</sup> [M+H]<sup>+</sup>: 245.1172 Found [M+H]<sup>+</sup>: 245.1179.

**Michael Addition Reaction Optimization**

General procedure: Metal triflate (0.0075 mmol, 0.05 equiv.) and ligand (*S,S*)-**1.42** (0.015 mmol, 0.1 mmol) were dissolved in solvent (1.2 mL) and heated to 60 °C for 1 hour. The reaction mixture was diluted with solvent (5 mL) and a solution of **1.31** (40 mg, 0.15 mmol) in solvent (5 mL) was added followed by methyl vinyl ketone (25 mL, 0.2 mmol, 2equiv.). The reaction mixture was stirred for the time listed in Table 1.1. The reaction mixture was directly concentrated onto silica gel and purified by column chromatography eluting with hexanes/ethyl acetate. Deviations from this procedure are listed as footnotes in the table. Yields and enantiomeric excess for the products are listed in Table 1.1.

## Total Synthesis of Lingzhiol

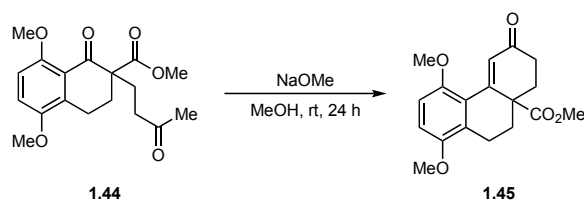


**Methyl 5,8-dimethoxy-1-oxo-2-(3-oxobutyl)-1,2,3,4-tetrahydronaphthalene-2-carboxylate (1.44).** A 100 mL round bottom flask equipped with a magnetic stir bar was charged with yttrium triflate (120 mg, .223 mmol), **1.31** (1.18 g, 4.47 mmol), and benzene (60.0 mL). The solution was heated to 80 °C and left to react for 4 hours. After cooling to room temperature, the solution was filtered through silica eluting with dichloromethane. The volatiles were removed through rotary evaporation. The crude product was purified via flash column chromatography eluting with hexanes/ethyl acetate (3:2) to give **1.44** as a yellow oil (1.40 g, 94%). <sup>1</sup>H NMR (500 MHz, CDCl<sub>3</sub>) δ 6.95 (d, *J* = 9.0 Hz, 1H), 6.79 (d, *J* = 9.0 Hz, 1H), 3.85 (s, 3H), 3.80 (s, 3H), 3.64 (s, 3H), 2.98 – 2.79 (m, 2H), 2.72 (ddd, *J* = 16.0, 10.6, 5.1 Hz, 1H), 2.53 (ddd, *J* = 19.1, 10.5, 5.2 Hz, 2H), 2.20 (ddd, *J* = 15.5, 10.6, 5.1 Hz, 1H), 2.14 (s, 3H), 2.11 – 1.94 (m, 2H). <sup>13</sup>C NMR (176 MHz, CDCl<sub>3</sub>) δ 208.1, 195.0, 172., 154.3, 150.2, 133.3, 122.7, 115.3, 110.4, 57.5, 56.6, 56.0, 52.4, 39.4, 30.6, 30.0, 27.9, 20.6. IR (cm<sup>-1</sup>): 2950.8, 2837.0, 1713.8, 1689.5, 1586.8, 1475.8, 1434.6, 1259.1, 1195.3, 1167.22, 1098.3, 1066.0, 980.4, 804.57. HRMS Calculated for C<sub>18</sub>H<sub>22</sub>O<sub>6</sub>Na<sup>+</sup> [M+Na<sup>+</sup>]<sup>+</sup>: 357.1309 Found: 357.1312.

**Asymmetric synthesis of Methyl 5,8-dimethoxy-1-oxo-2-(3-oxobutyl)-1,2,3,4-tetrahydronaphthalene-2-carboxylate ((+)-1.44).** A 100 mL round bottom flask equipped with a magnetic stir bar was charged with ligand (51.5 mg, 0.132 mmol), yttrium triflate (35.5 mg, 0.066 mmol), and benzene (7 mL). This solution was left to stir at 80 °C for 45 minutes, then diluted with 15 mL of benzene and left to stir for another 45 minutes at the same temperature. A solution of **1.31** (350 mg, 1.32 mmol) in benzene (13 mL) was added, and the reaction was left to stir for 4 hours. After cooling to room temperature, the solution was filtered through silica eluting with dichloromethane. The volatiles were removed through rotary evaporation. The crude product was purified via flash column chromatography eluting with hexanes/ethyl acetate (3:2) to give the product (+)-**1.44** as a yellow oil (430 mg, 97%) in 91% ee. HPLC (10% isopropanol/hexanes) [35.2 min (minor); 38.4 (major)]. [α]<sub>D</sub> = +23.1 (c=2.2, MeOH). The absolute configuration was assigned by comparison of the sign of optical rotation to the (+)-lingzhiol enantiomer (**1.8**) isolated by Cheng and coworkers.<sup>10</sup>

Following the same procedure, prochiral **5** (175 mg, 0.662 mmol), using scandium triflate (16.3 mg,  $3.31 \times 10^{-5}$  mol) in place of yttrium triflate and DCE at 60 °C in place of benzene at 80 °C, was converted to (-)-**1.44** (130 mg, 59%) in 90% ee in 96 hours. HPLC [31.6 (major), 39.4 (minor)].  $[\alpha]_D = -23.4$  ( $c=1.4$ , MeOH). Scaling this procedure to 291 mg (1.1 mmol) afforded 245 mg (67% yield) of product in 90% ee.

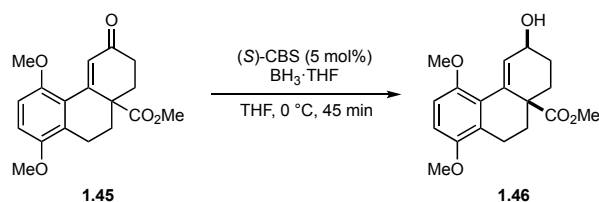
Elaboration of this compound to (-)-lingzhiol (**1.7**) enabled assignment of the absolute configuration of the product. This is in agreement with the stereochemical model proposed by Kobayashi and coworkers for the scandium-catalyzed conjugate addition reaction.<sup>30</sup>



**Methyl 1,4-dimethoxy-6-oxo-7,8,9,10-tetrahydrophenanthrene-8a(6*H*)-carboxylate (1.44).** A 100 mL round bottom flask equipped with a magnetic stir bar was charged with sodium methoxide (905 mg, 16.7 mmol) and methanol (10.0 mL). This solution was cooled in to 0 °C with an ice bath. A solution of **1.44** (1.40 g, 4.19 mmol) in 20 mL of methanol was added slowly with stirring. This solution was removed from the ice bath and left to react at room temperature for 16 hours. The volatiles were removed through rotary evaporation and the mixture was treated with water (10 mL) and diethyl ether (20 mL). The biphasic solution was separated, and the aqueous layer was extracted with diethyl ether (3 x 20 mL). The combined organic layers were washed with brine (20 mL), dried over MgSO<sub>4</sub> and concentrated through rotary evaporation. The crude product was purified via flash chromatography over silica gel eluting with hexanes/ethyl acetate (3:2) to give the product as a yellow solid (890 mg, 67%). **<sup>1</sup>H NMR** (500 MHz, CDCl<sub>3</sub>)  $\delta$  7.28 (s, 1H), 6.84 – 6.75 (m, 2H), 3.82 (s, 3H), 3.79 (s, 3H), 3.62 (s, 3H), 2.89 (ddd,  $J = 18.2, 5.6, 3.0$  Hz, 1H), 2.65 (ddd,  $J = 18.0, 11.7, 5.6$  Hz, 1H), 2.53 – 2.39 (m, 4H), 2.06 (td,  $J = 14.0, 12.9, 4.4$  Hz, 1H), 1.85 – 1.75 (m, 1H). **<sup>13</sup>C NMR** (126 MHz, CDCl<sub>3</sub>)  $\delta$  200.4, 174.2, 153.5, 151.8, 150.9, 129.1, 128.9, 123.1, 111.6, 110.0, 56.2, 55.9, 52.7, 47.8, 34.6, 34.5, 34.1, 21.5. **IR** (cm<sup>-1</sup>): 2936.1, 2837.6, 1724.9, 1670.7, 1580.5, 1473.9, 1455.1, 1441.1, 1335.4, 1262.1, 1248.7, 1194.7, 1173.9, 1165.4, 1133.5, 1111.7, 1091.3, 1079.1, 1022.4, 975.7. **HRMS** Calculated for C<sub>18</sub>H<sub>20</sub>O<sub>5</sub>Na<sup>+</sup> [M+Na]<sup>+</sup>: 339.1203 Found: 339.1205.

Following the same procedure, enantioenriched (+)-**1.44** (440 mg, 1.32 mmol) was converted to product (+)-**1.45** (270 mg, 65%) with preservation of enantiomeric excess (90%). **HPLC** [Diacel ChiralPak IA column] (10% isopropanol/hexanes) [20.2 (minor), 25.3 (major)].  $[\alpha]_D = +211.6$  (c=0.22, MeOH).

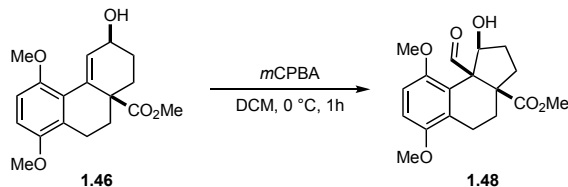
Following the same procedure, enantioenriched (-)-**1.44** (125 mg, 0.374 mmol) was converted to (-)-**1.45** (80 mg, 68%) with preservation of enantiomeric excess (90%). **HPLC** [Diacel ChiralPak IA column] (10% isopropanol/hexanes) [18.4 (major), 27.3 (minor)].  $[\alpha]_D = -211.8$  (c=0.22, MeOH).



**Methyl 6-hydroxy-1,4-dimethoxy-7,8,9,10-tetrahydrophenanthrene-8a(6H)-carboxylate (1.46).** A 100 mL round bottom flask equipped with a magnetic stir bar was charged with **1.45** (890 mg, 2.81 mmol) and THF (55.0 mL). A solution of (*S*)-CBS (39.0 mg, 0.141 mmol) in THF (5 mL) was added slowly while stirring. This solution was cooled to 0 °C with an ice bath. Borane tetrahydrofuran complex (4.22 mL, 1.0 M) was added dropwise over 5 minutes. The solution was left to react at 0 °C for 45 minutes. The volatiles were removed through rotary evaporation. The crude product was purified via flash chromatography over silica gel eluting with hexanes/ethyl acetate (1:1) to give the product as a white solid (750 mg, 84%). **<sup>1</sup>H NMR** (500 MHz, CDCl<sub>3</sub>)  $\delta$  6.89 (d, *J* = 2.5 Hz, 1H), 6.75 (d, *J* = 8.9 Hz, 1H), 6.65 (d, *J* = 8.9 Hz, 1H), 4.33 (s, 1H), 3.79 (s, 3H), 3.76 (s, 3H), 3.57 (s, 3H), 2.82 (ddd, *J* = 18.3, 6.3, 1.6 Hz, 1H), 2.59 (ddd, *J* = 18.4, 12.0, 6.3 Hz, 1H), 2.39 (ddd, *J* = 13.2, 6.3, 1.8 Hz, 1H), 2.27 (dd, *J* = 10.9, 5.3 Hz, 1H), 2.03 (dd, *J* = 10.7, 5.0 Hz, 1H), 1.76 – 1.59 (m, 4H). **<sup>13</sup>C NMR** (126 MHz, CDCl<sub>3</sub>)  $\delta$  176.0, 152.0, 151.4, 133.1, 132.3, 126.8, 125.4, 110.7, 108.5, 68.3, 56.6, 55.7, 52.3, 46.8, 34.3, 33.6, 28.9, 21.7. **IR** (cm<sup>-1</sup>): 3429.1, 2944.5, 2836.9, 1723.0, 1474.1, 1435.5, 1260.0, 1258.6, 1198.3, 1172.5, 1093.0, 1072.0, 1048.7. **HRMS** Calculated for C<sub>18</sub>H<sub>22</sub>O<sub>5</sub>Na<sup>+</sup> [*M*+Na<sup>+</sup>]<sup>+</sup>: 341.1359 Found: 341.1360.

Following the same procedure, enantioenriched (+)-**1.45** (270 mg, 0.853 mmol) was converted to product (+)-**1.46** (215 mg, 79%) with a slight increase in enantiomeric excess (94%). **HPLC** (10% isopropanol/hexanes) [11.8 (major), 14.2 (minor)].  $[\alpha]_D = +94.3$  (c=0.11, MeOH).

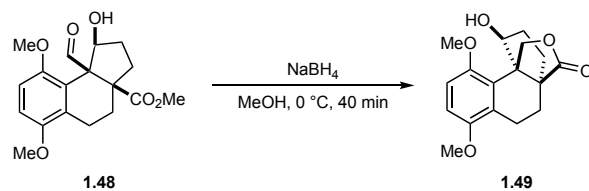
Following the same procedure, enantioenriched (-)-**1.45** (70 mg, 0.221 mmol) was converted to (-)-**1.46** (60mg, 85%) with preservation of enantiomeric excess (90%). **HPLC** (10% isopropanol/hexanes) [12.4 (minor), 14.7 (major)].  $[\alpha]_D = -97.9$  (c=0.01, MeOH).



**Methyl 9b-formyl-1-hydroxy-6,9-dimethoxy-1,2,3,4,5,9b-hexahydro-3aH-cyclopenta[*a*]naphthalene-3a-carboxylate (1.48).** A 100 mL round bottom flask equipped with a magnetic stir was charged with **1.46** (749 mg, 2.34 mmol) and dichloromethane (35 mL). This solution was cooled to 0 °C with an ice bath. *meta*-Chloroperoxybenzoic acid was added in one portion. The solution was removed from the ice bath and left to react at room temperature for one hour. The reaction was quenched with 1:1 saturated sodium thiosulfate/saturated sodium bicarbonate (20 mL). The layers were separated and the aqueous layer was extracted with dichloromethane (3 x 20 mL). The combined organic layers were washed with brine (20 mL), dried over MgSO<sub>4</sub> and concentrated through rotary evaporation. The crude product was purified via flash chromatography over silica gel eluting with hexanes/ethyl acetate (1:1) to give the product as a white solid (585 mg, 74%). **<sup>1</sup>H NMR** (500 MHz, CDCl<sub>3</sub>) δ 10.01 (s, 1H), 6.74 (t, *J* = 6.7 Hz, 2H), 4.59 (s, 1H), 3.79 (s, 6H), 3.68 (s, 3H), 2.78 – 2.63 (m, 2H), 2.57 – 2.46 (m, 1H), 2.14 – 1.96 (m, 2H), 1.89 (ddd, *J* = 13.3, 10.4, 5.8 Hz, 3H). **<sup>13</sup>C NMR** (126 MHz, CDCl<sub>3</sub>) δ 204.5, 177.6, 151.5, 150.8, 127.5, 126.7, 109.3, 108.9, 81.7, 63.0, 57.8, 56.3, 55.8, 52.7, 33.2, 32.5, 29.0, 20.0. **IR** (cm<sup>-1</sup>): 3398.4, 2957.9, 2903.5, 2838.4, 1722.1, 1695.0, 1599.8, 1470.7, 1433.6, 1252.5, 1214.4, 1117.1, 1102.9, 1087.7, 1062.1, 1022.3, 996.1, 916.5, 893.6, 802.3. **HRMS** Calculated for C<sub>18</sub>H<sub>22</sub>O<sub>6</sub>Na<sup>+</sup> [M+Na<sup>+</sup>]<sup>+</sup>: 357.1309 Found: 357.1308.

Following the same procedure, enantioenriched (+)-**1.46** (197 mg, 0.619 mmol) was converted to (-)-**1.48** (160 mg, 77%) with preservation of enantiomeric excess (91%). **HPLC** (10% isopropanol/hexanes) [19.0 (minor), 22.1 (major)].  $[\alpha]_D = -36.8$  (c=3.8, MeOH).

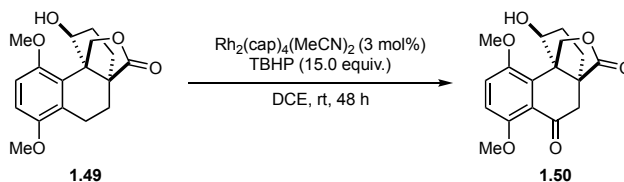
Following the same procedure, enantioenriched (-)-**1.46** (54 mg, 0.170 mmol) was converted to (+)-**1.48** (45 mg, 79%) with preservation of enantiomeric excess (91%). **HPLC** (10% isopropanol/hexanes) [18.6 (major), 22.5 (minor)].  $[\alpha]_D = +31.4$  (c=0.02, MeOH).



**1-Hydroxy-6,9-dimethoxy-2,3,4,5-tetrahydro-1*H*-3*a*,9*b*-(methanooxymethano)cyclopenta-*[a]*naphthalen-12-one (1.49).** A 25 mL round bottom flask equipped with a magnetic stir bar was charged with **1.48** (108 mg, 0.323 mmol) and methanol (5 mL). This solution was cooled to 0 °C with an ice bath. Sodium borohydride (49 mg, 1.29 mmol) was added slowly. The solution was left to react for 40 minutes. The reaction was quenched with acetone (0.5 mL) and then sat. ammonium chloride (2 mL). The volatiles were removed through rotary evaporation and the mixture was extracted with ethyl acetate (3 x 10 mL). The combined organic layers were washed with brine (10 mL), dried over MgSO<sub>4</sub> and concentrated through rotary evaporation. The crude product was purified via flash chromatography over silica gel eluting with hexanes/ethyl acetate (1:1) to give the product as a white solid (80 mg, 81%). <sup>1</sup>H NMR (500 MHz, CDCl<sub>3</sub>) δ 6.77 – 6.65 (m, 2H), 5.20 (d, *J* = 9.9 Hz, 1H), 4.20 – 4.11 (m, 1H), 4.09 (d, *J* = 9.8 Hz, 1H), 3.83 (s, 3H), 3.79 (s, 3H), 3.05 (dt, *J* = 17.4, 4.0 Hz, 1H), 2.44 (ddd, *J* = 17.4, 12.7, 4.6 Hz, 1H), 2.26 – 2.18 (m, 1H), 2.12 (dt, *J* = 13.5, 4.0 Hz, 1H), 1.98 – 1.82 (m, 2H), 1.68 (td, *J* = 13.1, 4.7 Hz, 1H), 1.61 – 1.52 (m, 1H). <sup>13</sup>C NMR (176 MHz, CDCl<sub>3</sub>) δ 182.4, 151.4, 151.4, 129.5, 126.4, 108.8, 108.4, 81.9, 71.2, 56.0, 55.9, 53.8, 52.8, 32.6, 30.2, 26.9, 18.7. IR (cm<sup>-1</sup>): 3456.1, 2953.5, 2834.9, 1748.3, 1477.6, 1437.7, 1257.5, 1114.5, 1088.4, 961.8. HRMS Calculated for C<sub>17</sub>H<sub>20</sub>O<sub>5</sub>Na<sup>+</sup> [M+Na<sup>+</sup>]<sup>+</sup>: 327.1203 Found: 327.1201.

Following the same procedure, enantioenriched (-)-**1.48** (68 mg, 0.203 mmol) was converted to (-)-**1.49** (48 mg, 77%) with preservation of enantiomeric excess (91%). HPLC (10% isopropanol/hexanes) [19.9 (minor), 27.8 (major)]. [α]<sub>D</sub> = -6.6 (c=0.27, MeOH).

Following the same procedure, enantioenriched (+)-**1.48** (44 mg, 0.132 mmol) was converted to (+)-**1.49** (30 mg, 75%) with preservation of enantiomeric excess (88%). HPLC (10% isopropanol/hexanes) [19.2 (major), 28.5 (minor)]. [α]<sub>D</sub> = +5.1 (c=0.10, MeOH).

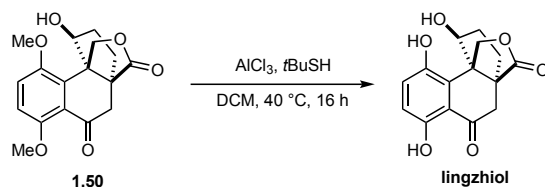




**(1*S*,3*aS*,9*bS*)-1-Hydroxy-6,9-dimethoxy-2,3-dihydro-1*H*-3*a*,9*b*-(methanooxymethano)-cyclopenta[*a*]naphthalene-5,12(4*H*)-dione (1.50)**. A 25 mL round bottom flask equipped with a magnetic stir bar was charged with, **1.49** (46 mg, 0.151 mmol), dichloroethane (4.00 mL), catalyst (1.2 mg,  $1.51 \times 10^{-6}$  mmol, 1 mol%), sodium bicarbonate (6.35 mg,  $7.56 \times 10^{-5}$  mmol, 50 mol%). The flask was sealed and an empty balloon was inserted to capture oxygen. TBHP (0.151 mL, 5 M in decane) was added in one portion while stirring. After 3 hours, catalyst (1.2 mg,  $1.51 \times 10^{-6}$  mmol, 1 mol%) and TBHP (0.151 mL, 5 M in decane) were added to the solution. After 24 hours, catalyst (1.2 mg,  $1.51 \times 10^{-6}$  mmol, 1 mol%) and TBHP (0.151 mL, 5 M in decane) were added to the solution. After 48 hours, the solution was filtered through a plug of silica eluting with dichloromethane then 80% ethyl acetate/hexanes. The volatiles were removed through rotary evaporation and the crude product was purified via flash chromatography over silica gel eluting with hexanes/ethyl acetate (1:3) to give the product as an off white solid (18 mg, 39%), as well as recovered starting material (22 mg, 85% yield BRSM). **<sup>1</sup>H NMR** (500 MHz, CDCl<sub>3</sub>)  $\delta$  7.10 (d,  $J = 9.1$  Hz, 1H), 6.89 (d,  $J = 9.1$  Hz, 1H), 5.31 (d,  $J = 9.9$  Hz, 1H), 4.31 – 4.20 (m, 2H), 3.88 (s, 3H), 3.85 (s, 3H), 2.91 – 2.76 (m, 2H), 2.38 (ddd,  $J = 13.1, 6.8, 4.2$  Hz, 1H), 1.93 (dq,  $J = 10.9, 5.7, 4.7$  Hz, 1H), 1.83 – 1.74 (m, 1H), 1.55 (ddt,  $J = 14.1, 9.8, 7.3$  Hz, 1H). **<sup>13</sup>C NMR** (100 MHz, CDCl<sub>3</sub>)  $\delta$  194.9, 179.7, 152.7, 150.3, 134.1, 122.6, 117.2, 111.7, 81.7, 70.3, 56.7, 56.5, 53.8, 53.5, 44.3, 32.4, 31.6. **IR** (cm<sup>-1</sup>): 3461.3, 2957.6, 2839.0, 1756.1, 1583.9, 1476.8, 1435.5, 1268.55, 1250.3, 1179.6, 1105.3, 1011.0, 961.6, 942.0, 812.1. **HRMS** Calculated for C<sub>17</sub>H<sub>18</sub>O<sub>6</sub>Na<sup>+</sup> [M+Na<sup>+</sup>]<sup>+</sup>: 341.0996 Found: 341.0993.

Following the same procedure, enantioenriched (-)-**1.49** (45 mg, 0.148 mmol) was converted to (+)-**1.50** (16 mg, 34%, 76% BRSM) with preservation of enantiomeric excess (94%). **HPLC** (20% isopropanol/hexanes) [17.9 (minor), 36.5 (major)].  $[\alpha]_D = +66.7$  (c=0.01, MeOH).

Following the same procedure, enantioenriched (+)-**1.49** (28 mg,  $9.20 \times 10^{-5}$  mol) was converted to (-)-**1.50** (30 mg, 31%, 76% BRSM). The recovered starting material (13 mg,  $4.27 \times 10^{-5}$  mol) was subjected to the same conditions to yield additional product (6 mg, 46%, 77% BRSM). The combined product displayed preservation of enantiomeric excess (92%). **HPLC** (20% isopropanol/hexanes) [17.0 (major), 37.9 (minor)].  $[\alpha]_D = -67.9$  (c=0.01, MeOH).

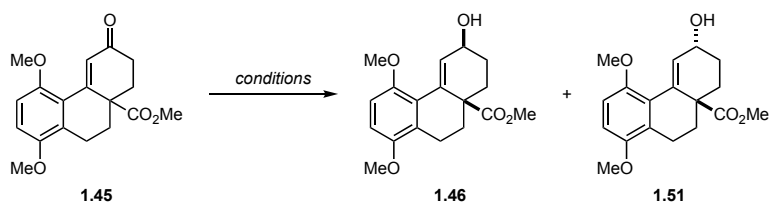


**Lingzhiol.** A 25 mL round bottom flask equipped with a magnetic stir bar was charged with aluminum trichloride (117 mg, 0.880 mmol) and *tert*-butylthiol (2 mL). This mixture was cooled to 0 °C with an ice bath. A solution of **1.50** (14 mg, 4.40x10<sup>-5</sup> mol) in dichloromethane (2 mL) was added. This solution was transferred to a heating mantle and left to react at 40 °C for 16 hours. After cooling to room temperature, the reaction was quenched with water (3 mL) and saturated sodium phosphate. The biphasic solution was separated and the aqueous layer was extracted with diethyl ether (3 x 10 mL). The combined organic layers were washed with brine (10 mL), dried over Na<sub>2</sub>SO<sub>4</sub> and concentrated through rotary evaporation. The crude product was purified via flash chromatography over silica gel eluting with dichloromethane/ethyl acetate (4:1) to give the product as a yellow (8 mg, 63%). <sup>1</sup>H NMR (700 MHz, Acetone-*d*<sub>6</sub>) δ 11.58 (s, 1H), 7.22 (d, *J* = 9.0, 1H), 6.77 (d *J* = 8.9, 1H), 5.22 (d, *J* = 9.5 Hz, 1H), 4.67 – 4.59 (m, 1H), 4.45 (d, *J* = 9.6 Hz, 1H), 3.09 (d, *J* = 16.0 Hz, 1H), 2.79 (d, *J* = 16.0 Hz, 1H), 2.45 (dt, *J* = 14.1, 7.7 Hz, 1H), 1.83 (m, 1H), 1.78 (m, 1H), 1.70 (m, 1H). <sup>13</sup>C NMR (176 MHz, Acetone-*d*<sub>6</sub>) δ 202.4, 180.1, 156.4, 148.0, 129.2, 127.6, 118.0, 116.5, 80.7, 71.0, 56.2, 52.6, 42.4, 33.8, 33.4. IR (cm<sup>-1</sup>): 3255.0, 2924.0, 1754.1, 1646.8, 1586.8, 1464.9, 1332.2, 1292.5, 1220.7, 1178.5, 1103.0, 1014.6. HRMS Calculated for C<sub>15</sub>H<sub>14</sub>O<sub>6</sub>H<sup>+</sup> [M+H]<sup>+</sup>: 291.0863 Found: 291.0864.

Following the same procedure, enantioenriched (+)-**1.50** (14 mg, 4.40x10<sup>-5</sup> mmol) was converted to (+)-lingzhiol (**1.8**) (8 mg, 63%) with preservation of enantiomeric excess (93%). HPLC (20% isopropanol/hexanes) [8.10 (minor), 11.0 (major)]. [α]<sub>D</sub> = +89.2 (c=0.01, MeOH).

Following the same procedure, enantioenriched (-)-**1.50** (13 mg, 4.08x10<sup>-5</sup> mmol) was converted to (-)-lingzhiol (**1.7**) (7 mg, 59%) with preservation of enantiomeric excess (95%). HPLC (20% isopropanol/hexanes) [8.02 (major), 11.3 (minor)]. [α]<sub>D</sub> = -87.2 (c=0.01, MeOH).

### Enone Reduction Reaction Optimization

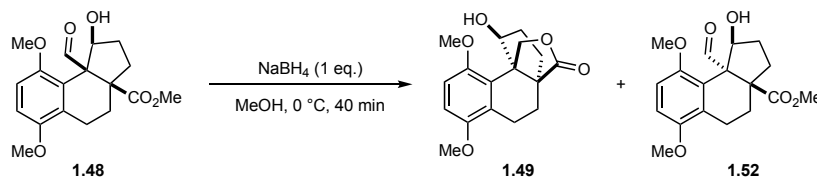


Results are tabulated in Table Table 1.2.

Reduction using sodium borohydride: Enone **1.45** (50 mg, 0.16 mmol) was dissolved in methanol (3 mL) and cooled to 0 °C on an ice bath. Sodium borohydride (9 mg, 0.24 mmol) was added as a solid and the reaction was stirred at this temperature until judged complete by TLC. The reaction mixture was quenched with saturated aqueous ammonium chloride and extracted with three portions of ethyl acetate. The combined organic layers were dried over Na<sub>2</sub>SO<sub>4</sub> and concentrated by rotary evaporator. Purification by silica gel column chromatography eluting with hexanes/EtOAc afforded first **1.51** (2 mg, 7% yield) followed closely by **1.46** (38 mg, 75% yield) as a white foam. Characterization data for **1.51**: <sup>1</sup>H NMR (700 MHz, CDCl<sub>3</sub>) δ 6.79 (d, *J* = 4.1 Hz, 1H), 6.64 (d, *J* = 8.8 Hz, 1H), 6.54 (d, *J* = 8.8 Hz, 1H), 4.43 (d, *J* = 3.3 Hz, 1H), 3.69 (d, *J* = 3.7 Hz, 3H), 3.66 (s, 3H), 3.45 (s, 3H), 2.72 (dd, *J* = 18.3, 5.7 Hz, 1H), 2.53 (ddd, *J* = 18.4, 11.6, 6.7 Hz, 1H), 2.30 (dd, *J* = 13.1, 6.4 Hz, 1H), 2.01 (dd, *J* = 16.6, 10.1 Hz, 1H), 1.85 – 1.77 (m, 2H), 1.73 (td, *J* = 12.4, 6.4 Hz, 1H), 1.67 – 1.58 (m, 1H). <sup>13</sup>C NMR (176 MHz, CDCl<sub>3</sub>) δ 175.9, 151.8, 151.3, 134.5, 130.0, 127.0, 125.9, 110.4, 108.6, 66.0, 56.6, 55.70, 52.3, 47.0, 33.5, 31.2, 28.1, 21.6. IR (cm<sup>-1</sup>): 2942.03, 1723.76, 1474.19, 1435.47, 1248.63, 1200.69, 1172.81, 1097.14, 1073.22, 1027.85, 984.65. HRMS (ESI<sup>+</sup>): Calculated for C<sub>18</sub>H<sub>22</sub>O<sub>5</sub>Na<sup>+</sup> [M+Na<sup>+</sup>]<sup>+</sup>: 341.1359 Found: 341.1355.

Reduction using Corey-Bakshi-Shibata (CBS) catalyst: Enone **1.45** (50 mg, 0.16 mmol) was dissolved in THF (3 mL) and cooled to 0 °C on an ice bath and either (*R*)- or (*S*)-CBS catalyst was added as a solid, followed by dropwise addition of borane tetrahydrofuran complex (0.19 mL, 0.19 mmol, 1.2 equiv.) via syringe. The reaction was allowed to stir for 1 hour and directly concentrated by rotary evaporator. The crude residue was purified by column chromatography. (*R*)-CBS afforded 36 mg (72% yield) of **1.46** and 5.3 mg (11% yield) of **1.46**.

### Reduction-lactonization Reaction Optimization



A 25 mL round bottom flask equipped with a magnetic stir bar was charged with **1.48** (108 mg, 0.323 mmol) and methanol (5 mL). This solution was cooled to 0 °C with an ice bath. Sodium borohydride (12 mg, 1.29 mmol) was added slowly. The solution was left to react for 40 minutes. The reaction was quenched with acetone (0.5 mL) and then sat. ammonium chloride (2 mL). The

volatiles were removed through rotary evaporation and the mixture was extracted with ethyl acetate (3 x 10 mL). The combined organic layers were washed with brine (10 mL), dried over MgSO<sub>4</sub> and concentrated through rotary evaporation. The crude product was purified via flash chromatography over silica gel eluting with hexanes/ethyl acetate (1:1) to give **1.49** as a white solid (49 mg, 50%) and **1.52** as a white solid (11 mg, 10%). Characterization data for **1.52** matched the reported data.<sup>22</sup>

### Benzylic Oxidation Reaction Optimization



Results are tabulated in Table 1.3. Lingzhiol core **1.49** (0.065 or 0.13 mmol) was dissolved in the solvent listed in Table 1.3 in the manuscript (reproduced here) and treated with catalyst, additives, and oxidant. The reactions were conducted according to procedures described in the literature.<sup>18, 36-39</sup> Only conditions relying on Rh<sub>2</sub>Cap<sub>4</sub> as catalyst afforded any desired product.

### Demethylation Reaction Optimization



Results are tabulated in table 1.4.

A 10 mL round bottom flask equipped with a magnetic stir bar was charged with **1.50** (12 mg, 3.77x10<sup>-5</sup> mmol) and DCM (2 mL). This solution was cooled to 0 °C with an ice bath. Boron tribromide (0.188 mL, 1.0 M) was added slowly. The solution was left to react for 2 h. The reaction was quenched with a saturated aqueous solution of sodium bicarbonate. The biphasic solution was separated and the aqueous layer was extracted with DCM (3 x 10 mL). The combined organic layers were washed with brine, dried over Na<sub>2</sub>SO<sub>4</sub> and concentrated through rotary evaporation. The crude product was purified via flash chromatography over silica gel eluting with hexanes/ethyl acetate (1:4) to give the product **1.53** as a yellow oil (9.4 mg, 82%).

A 5 mL round bottom flask equipped with a magnetic stir bar was charged with **1.50** (10 mg, 3.14x10<sup>-5</sup> mmol), Bu<sub>4</sub>NI (29 mg, 7.85x10<sup>-5</sup>), and DCM (2 mL). This solution was cooled to -78 °C with dry ice bath. Boron trichloride (0.157 mL, 1.0 M) was added slowly. The solution was left to

react at room temperature for 11 h. The reaction was quenched with water. The biphasic solution was separated, and the aqueous layer was extracted with DCM (3 x 10 mL). The combined organic layers were washed with brine, dried over Na<sub>2</sub>SO<sub>4</sub> and concentrated through rotary evaporation. The crude product was purified via flash chromatography over silica gel eluting with hexanes/ethyl acetate (1:4) to give the product **1.53** as a yellow oil (6.6 mg, 82%).

#### 1.4.3 X-Ray Crystallographic Data

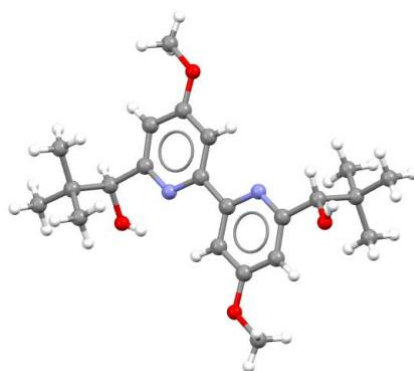


Figure 1.10 ORTEP diagram of (S,S)-**1.43**.

#### **(1*S*,1'*S*)-1,1'-(4,4'-dimethoxy-[2,2'-bipyridine]-6,6'-diyl)bis(2,2-dimethylpropan-1-ol) [(*S,S*)-**1.43**]**

CCDC 1968348. Colorless needles of (*S,S*)-**1.43** were grown from a dichloromethane/methanol solution of the compound at 22 deg. C. A crystal of dimensions 0.08 x 0.08 x 0.05 mm was mounted on a Rigaku AFC10K Saturn 944+ CCD-based X-ray diffractometer equipped with a low temperature device and Micromax- 007HF Cu-target micro-focus rotating anode ( $\lambda = 1.54187 \text{ \AA}$ ) operated at 1.2 kW power (40 kV, 30 mA). The X-ray intensities were measured at 85(1) K with the detector placed at a distance 42.00 mm from the crystal. A total of 2028 images were collected with an oscillation width of 1.0° in  $\omega$ . The exposure times were 1 sec. for the low angle images, 3 sec. for high angle. Rigaku d\*trek images were exported to CrysAlisPro for processing and corrected for absorption. The integration of the data yielded a total of 28334 reflections to a maximum  $2\theta$  value of 138.75° of which 3810 were independent and 3746 were greater than  $2\sigma(I)$ . The final cell constants were based on the xyz centroids of 5852 reflections above  $10\sigma(I)$ . Analysis of the data showed negligible decay during data collection. The structure was solved and refined with the Bruker SHELXTL (version 2018/3) software package, using the space group P1 with  $Z =$

1 for the formula  $C_{22}H_{32}N_2O_4$ . All non-hydrogen atoms were refined anisotropically with the hydrogen atoms placed in a combination of idealized and refined positions. Full matrix least-squares refinement based on  $F^2$  converged at  $R1 = 0.0396$  and  $wR2 = 0.1102$  [based on  $I > 2\sigma(I)$ ],  $R1 = 0.0400$  and  $wR2 = 0.1116$  for all data. Acknowledgement is made for funding from NSF grant CHE-0840456 for X-ray instrumentation.

G.M. Sheldrick (2015) "Crystal structure refinement with SHELXL", Acta Cryst., C71, 3-8 (Open Access).

CrystalClear Expert 2.0 r16, Rigaku Americas and Rigaku Corporation (2014), Rigaku Americas, 9009, TX, USA 77381-5209, Rigaku Tokyo, 196-8666, Japan.

CrysAlisPro 1.171.38.41 (Rigaku Oxford Diffraction, 2015).

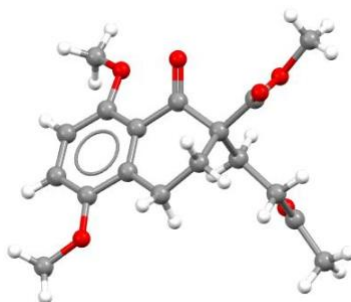


Figure 1.11 ORTEP diagram of (R)-1.31.

**(R)-5,8-dimethoxy-1-oxo-2-(3-oxobutyl)-1,2,3,4- tetrahydronaphthalene-2-carboxylate [(R)-16]**

CCDC 1968351. Colorless plates of (R)-1.31 were grown from a hexane/isopropanol solution of the compound at 23 deg. C. A crystal of dimensions 0.12 x 0.10 x 0.03 mm was mounted on a Rigaku AFC10K Saturn 944+ CCD- based X-ray diffractometer equipped with a low temperature device and Micromax-007HF Cu-target micro- focus rotating anode ( $\lambda = 1.54187 \text{ \AA}$ ) operated at 1.2 kW power (40 kV, 30 mA). The X-ray intensities were measured at 85(1) K with the detector placed at a distance 42.00 mm from the crystal. A total of 4056 images were collected with an oscillation width of  $1.0^\circ$  in  $\omega$ . The exposure times were 1 sec. for the low angle images, 3 sec. for high angle. Rigaku d\*trek images were exported to CrysAlisPro for processing and corrected for absorption. The integration of the data yielded a total of 25375 reflections to a maximum  $2\theta$  value of  $138.59^\circ$  of which 3063 were independent and 3005 were greater than  $2\sigma(I)$ . The final cell constants were based on the xyz centroids of 7093 reflections above  $10\sigma(I)$ . Analysis of the data showed negligible decay during data collection. The structure was solved and refined with the

Bruker SHELXTL (version 2018/3) software package, using the space group P2(1) with  $Z = 2$  for the formula  $C_{18}H_{22}O_6$ . All non-hydrogen atoms were refined anisotropically with the hydrogen atoms placed in idealized positions. Full matrix least-squares refinement based on  $F^2$  converged at  $R1 = 0.0334$  and  $wR2 = 0.0813$  [based on  $I > 2\sigma(I)$ ],  $R1 = 0.0344$  and  $wR2 = 0.0830$  for all data. Acknowledgement is made for funding from NSF grant CHE-0840456 for X-ray instrumentation.

G.M. Sheldrick (2015) "Crystal structure refinement with SHELXL", *Acta Cryst.*, C71, 3-8 (Open Access).

CrystalClear Expert 2.0 r16, Rigaku Americas and Rigaku Corporation (2014), Rigaku Americas, 9009, TX, USA 77381-5209, Rigaku Tokyo, 196-8666, Japan.

CrysAlisPro 1.171.38.41 (Rigaku Oxford Diffraction, 2015).



Figure 1.12 ORTEP diagram of **1.49**.

**1-hydroxy-6,9-dimethoxy-2,3,4,5-tetrahydro-1H-3a,9b-(methanooxymethano)cyclopenta-[a]naphthalen-12-one (1.49).**

CCDC 1963936. Colorless plates of **1.49** were grown from an ethyl acetate solution of the compound at 22 deg. C. A crystal of dimensions 0.26 x 0.16 x 0.14 mm was mounted on a Rigaku AFC10K Saturn 944+ CCD-based X-ray diffractometer equipped with a low temperature device and Micromax-007HF Cu-target micro-focus rotating anode ( $\lambda = 1.54187$  Å) operated at 1.2 kW power (40 kV, 30 mA). The X-ray intensities were measured at 85(1) K with the detector placed at a distance 42.00 mm from the crystal. A total of 2028 images were collected with an oscillation width of  $1.0^\circ$  in  $\omega$ . The exposure times were 1 sec. for the low angle images, 5 sec. for high angle. Rigaku d\*trek images were exported to CrysAlisPro for processing and corrected for absorption. The integration of the data yielded a total of 42748 reflections to a maximum  $2\theta$  value of  $138.91^\circ$  of which 2758 were independent and 2752 were greater than  $2\sigma(I)$ . The final cell constants were

based on the xyz centroids 34910 reflections above  $10\sigma(I)$ . Analysis of the data showed negligible decay during data collection. The structure was solved and refined with the Bruker SHELXTL (version 2014/6) software package, using the space group Pbc<sub>a</sub> with  $Z = 8$  for the formula C<sub>17</sub>H<sub>20</sub>O<sub>5</sub>. All non-hydrogen atoms were refined anisotropically with the hydrogen atoms placed in a combination of idealized and refined positions. Full matrix least-squares refinement based on  $F^2$  converged at  $R1 = 0.0439$  and  $wR2 = 0.0442$  [based on  $I > 2\sigma(I)$ ],  $R1 = 0.1082$  and  $wR2 = 0.1087$  for all data. Acknowledgement is made for funding from NSF grant CHE-0840456 for X-ray instrumentation.

Sheldrick, G.M. SHELXTL, v. 2014/6; Bruker Analytical X-ray, Madison, WI, 2014. CrystalClear Expert 2.0 r16, Rigaku Americas and Rigaku Corporation (2014), Rigaku Americas, 9009, TX, USA 77381-5209, Rigaku Tokyo, 196-8666, Japan. CrysAlisPro 1.171.38.41 (Rigaku Oxford Diffraction, 2015).



## 1.5 References

- (1) Riehl, P. S.; Richardson, A. D.; Sakamoto, T.; Schindler, C. S. Eight-Step Enantiodivergent Synthesis of (+)- and (-)-Lingzhiol. *Org. Lett.* **2020**, *22*, 290–294.
- (2) Wachtel-Galor, S.; Yuen, J.; Buswell, J. A.; Benzie, I. F. F. *Ganoderma Lucidum* (Lingzhi or Reishi): A Medicinal Mushroom. In *Herbal Medicine: Biomolecular and Clinical Aspects*; Benzie, I. F. F., Wachtel-Galor, S., Eds.; CRC Press/Taylor & Francis: Boca Raton (FL), 2011.
- (3) Nishitoba, T.; Sato, H.; Kasai, T.; Kawagishi, H.; Sakamura, S. New Bitter C27 and C30 Terpenoids from the Fungus *Ganoderma Lucidum* (Reishi). *Agric. Biol. Chem.* **1985**, *49*, 1793–1798.
- (4) Hsu, C.-L.; Yu, Y.-S.; Yen, G.-C. Lucidenic Acid B Induces Apoptosis in Human Leukemia Cells via a Mitochondria-Mediated Pathway. *J. Agric. Food Chem.* **2008**, *56*, 3973–3980.
- (5) Kubota, T.; Asaka, Y.; Miura, I.; Mori, H. Structures of Ganoderic Acid A and B, Two New Lanostane Type Bitter Triterpenes from *Ganoderma Lucidum* (FR.) KARST. *Helv. Chim. Acta.* **1982**, *65*, 611–619.
- (6) Sato, H.; Nishitoba, T.; Shirasu, S.; Oda, K.; Sakamura, S. Ganoderiol A and B, New Triterpenoids from the Fungus *Ganoderma Lucidum* (Reishi). *Agric. Biol. Chem.* **1986**, *50*, 2887–2890.
- (7) El-Mekki, S.; Meselhy, M. R.; Nakamura, N.; Tezuka, Y.; Hattori, M.; Kakiuchi, N.; Shimotohno, K.; Kawahata, T.; Otake, T. Anti-HIV-1 and Anti-HIV-1-Protease Substances From *Ganoderma Lucidum*. *Phytochem.* **1998**, *49*, 1651–1657.
- (8) Russo, D.; Milella, L. Analysis of Meroterpenoids. In *Recent Advances in Natural Products Analysis*; Elsevier, 2020.
- (9) Zhang, J.-J.; Wang, D.-W.; Cai, D.; Lu, Q.; Cheng, Y.-X. Meroterpenoids From *Ganoderma Lucidum* Mushrooms and Their Biological Roles in Insulin Resistance and Triple-Negative Breast Cancer. *Front. Chem.* **2021**, *9*, 1–11.
- (10) Yan, Y.-M.; Ai, J.; Zhou, L.; Chung, A. C. K.; Li, R.; Nie, J.; Fang, P.; Wang, X.-L.; Luo, J.; Hu, Q.; Hou, F.-F.; Cheng, Y.-X. Lingzhiols, Unprecedented Rotary Door-Shaped Meroterpenoids as Potent and Selective Inhibitors of p-Smad3 from *Ganoderma Lucidum*. *Org. Lett.* **2013**, *15*, 5488–5491.
- (11) Kidney Disease Statistics for the United States <https://www.niddk.nih.gov/health-information/health-statistics/kidney-disease>.
- (12) Derynck, R.; Zhang, Y.; Feng, X.-H. Smads: Transcriptional Activators of TGF- $\beta$  Responses. *Cell* **1998**, *95*, 737–740.
- (13) Liu, Y. Renal Fibrosis: New Insights into the Pathogenesis and Therapeutics. *Kidney Int.* **2006**, *69*, 213–217.
- (14) Zhang, Y.; Feng, X.-H.; Wu, R.-Y.; Derynck, R. Receptor-Associated Mad Homologues Synergize as Effectors of the TGF- $\beta$  Response. *Nature* **1996**, *383*, 168–172.
- (15) Meng, X. M.; Huang, X. R.; Chung, A. C. K.; Qin, W.; Shao, X.; Igarashi, P.; Ju, W.; Bottinger, E. P.; Lan, H. Y. Smad2 Protects against TGF- $\beta$ /Smad3-Mediated Renal Fibrosis. *J. Am. Soc. Nephrol.* **2010**, *21*, 1477–1487.
- (16) Sharmah Gautam, K.; Birman, V. B. Biogenetically Inspired Synthesis of Lingzhiol. *Org. Lett.* **2016**, *18*, 1499–1501.
- (17) Rengarasu, R.; Maier, M. E. Total Synthesis of Lingzhiol and Its Analogues through the Wittig Reaction of an Oxocyclopentane Carboxylate. *Asian J. Org. Chem.* **2017**, *6*, 108–117.

- (18) Long, R.; Huang, J.; Shao, W.; Liu, S.; Lan, Y.; Gong, J.; Yang, Z. Asymmetric Total Synthesis of (-)-Lingzhiol via a Rh-Catalysed [3+2] Cycloaddition. *Nat. Commun.* **2014**, *5*, 5707.
- (19) Chen, D.; Liu, H.-M.; Li, M.-M.; Yan, Y.-M.; Xu, W.-D.; Li, X.-N.; Cheng, Y.-X.; Qin, H.-B. Concise Synthesis of (±)-Lingzhiol via Epoxy-Arene Cyclization. *Chem. Commun.* **2015**, *51*, 14594–14596.
- (20) Chen, D.; Xu, W.-D.; Liu, H.-M.; Li, M.-M.; Yan, Y.-M.; Li, X.-N.; Li, Y.; Cheng, Y.-X.; Qin, H.-B. Enantioselective Total Synthesis of (+)-Lingzhiol via Tandem Semipinacol Rearrangement/Friedel–Crafts Type Cyclization. *Chem. Commun.* **2016**, *52*, 8561–8564.
- (21) Mehl, L.-M.; Maier, M. E. A Radical-Based Synthesis of Lingzhiol. *J. Org. Chem.* **2017**, *82*, 9844–9850.
- (22) Li, X.; Liu, X.; Jiao, X.; Yang, H.; Yao, Y.; Xie, P. An Approach to (±)-Lingzhiol. *Org. Lett.* **2016**, *18*, 1944–1946.
- (23) Jacobsen, E. N.; Pfaltz, A.; Yamamoto, H. *Comprehensive Asymmetric Catalysis*; Springer: London, 2003.
- (24) Paquette, L. A. *Chiral Reagents for Asymmetric Synthesis*; Wiley: Chichester, 2003; Vol. 2.
- (25) Kim, Y. H. Dual Enantioselective Control in Asymmetric Synthesis. *Acc. Chem. Res.* **2001**, *34*, 955–962.
- (26) Riehl, P. S.; Richardson, A. D.; Sakamoto, T.; Reid, J. P.; Schindler, C. S. Origin of Enantioselectivity Reversal in Lewis Acid-Catalysed Michael Additions Relying on the Same Chiral Source. *Chem. Sci.* **2021**, *12*, 14133–14142.
- (27) Cao, W.; Feng, X.; Liu, X. Reversal of Enantioselectivity in Chiral Metal Complex-Catalyzed Asymmetric Reactions. *Org. Biomol. Chem.* **2019**, *17*, 6538–6550.
- (28) Li, X.; Wu, B.; Zhao, X. Z.; Jia, Y. X.; Tu, Y. Q.; Li, D. R. An Interesting AlEt<sub>3</sub>-Promoted Stereoselective Tandem Rearrangement/Reduction of α-Hydroxy (or Amino) Heterocyclopropane. *Synlett.* **2003**, *2003*, 623–626.
- (29) Johnson, D. W.; Mander, L. N. Studies on Intramolecular Alkylation. X. The Acid-Catalysed Reactions of 5,8-Dialkoxy-1,2,3,4-Tetrahydronaphthyl Diazomethyl Ketones. *Aust. J. Chem.* **1978**, *31*, 1561–1568.
- (30) Ogawa, C.; Kizu, K.; Shimizu, H.; Takeuchi, M.; Kobayashi, S. Chiral Scandium Catalysts for Enantioselective Michael Reactions of β-Ketoesters. *Chem. Asian J.* **2006**, *1*, 121–124.
- (31) Li, W.; Zheng, S.; Higgins, M.; Morra, R. P.; Mendis, A. T.; Chien, C.-W.; Ojima, I.; Mierke, D. F.; Dinkova-Kostova, A. T.; Honda, T. New Monocyclic, Bicyclic, and Tricyclic Ethynylcyanodienones as Activators of the Keap1/Nrf2/ARE Pathway and Inhibitors of Inducible Nitric Oxide Synthase. *J. Med. Chem.* **2015**, *58*, 4738–4748.
- (32) Bolm, C.; Zehnder, M.; Bur, D. Optically Active Bipyridines in Asymmetric Catalysis. *Angew. Chem. Int. Ed.* **1990**, *29*, 205–207.
- (33) Ishikawa, S.; Hamada, T.; Manabe, K.; Kobayashi, S. New Efficient Method for the Synthesis of Chiral 2,2'-Bipyridyl Ligands. *Synthesis* **2005**, *2005*, 2176–2182.
- (34) Mikami, K.; Terada, M.; Matsuzawa, H. “Asymmetric” Catalysis by Lanthanide Complexes. *Angew. Chem. Int. Ed.* **2002**, *41*, 3554–3572.
- (35) Corey, E. J.; Bakshi, R. K.; Shibata, S. Highly Enantioselective Borane Reduction of Ketones Catalyzed by Chiral Oxazaborolidines. Mechanism and Synthetic Implications. *J. Am. Chem. Soc.* **1987**, *109*, 5551–5553.
- (36) Shingate, B. B.; Hazra, B. G.; Salunke, D. B.; Pore, V. S. RuCl<sub>3</sub>-TBHP Mediated Allylic Oxidation of Δ<sup>8</sup> (9) Lanosterol Derivatives. *Tetrahedron Lett.* **2011**, *52*, 6007–6010.

- (37) Hruszkewycz, D. P.; Miles, K. C.; Thiel, O. R.; Stahl, S. S. Co/NHPI-Mediated Aerobic Oxygenation of Benzylic C–H Bonds in Pharmaceutically Relevant Molecules. *Chem. Sci.* **2017**, *8*, 1282–1287.
- (38) Yu, J.-Q.; Corey, E. J. A Mild, Catalytic, and Highly Selective Method for the Oxidation of  $\alpha,\beta$ -Enones to 1,4-Enediones. *J. Am. Chem. Soc.* **2003**, *125*, 3232–3233.
- (39) Moriyama, K.; Takemura, M.; Togo, H. Direct and Selective Benzylic Oxidation of Alkylarenes via C–H Abstraction Using Alkali Metal Bromides. *Org. Lett.* **2012**, *14*, 2414–2417.
- (40) Catino, A. J.; Nichols, J. M.; Choi, H.; Gottipamula, S.; Doyle, M. P. Benzylic Oxidation Catalyzed by Dirhodium(II,III) Caprolactamate. *Org. Lett.* **2005**, *7*, 5167–5170.
- (41) Brooks, P. R.; Wirtz, M. C.; Vetelino, M. G.; Rescek, D. M.; Woodworth, G. F.; Morgan, B. P.; Coe, J. W. Boron Trichloride/Tetra- *n* -Butylammonium Iodide: A Mild, Selective Combination Reagent for the Cleavage of Primary Alkyl Aryl Ethers. *J. Org. Chem.* **1999**, *64*, 9719–9721.

## Chapter 2 Origin of Enantioselectivity Reversal in Lewis Acid-Catalyzed Michael Additions

Portions of this chapter have been published in: Riehl, P. S.; Richardson, A. D.; Sakamoto, T.; Reid, J. P.; Schindler, C. S. Origin of Enantioselectivity Reversal in Lewis Acid-Catalysed Michael Additions Relying on the Same Chiral Sources. *Chem. Sci.* **2021**, *12*, 14133-14142.<sup>1</sup>

### 2.1 Introduction

Chirality is integral to nature, and as such asymmetric synthesis is highly desirable because individual enantiomers can exhibit distinct biological activity. For example, (S)-naproxen is a nonsteroidal anti-inflammatory drug (NSAID) used in the treatment of arthritis, whereas (R)-naproxen has no analgesic effects and causes liver poisoning.<sup>2</sup> Additional examples of functionally different enantiomeric pairs include thalidomide,<sup>3</sup> ethambutol,<sup>4</sup> propranolol,<sup>5</sup> carvedilol,<sup>6</sup> amphetamine,<sup>7</sup> and ketamine.<sup>8</sup>

There are number of different strategies that can be used to synthesize enantiopure compounds (Figure 2.1A). One common approach is to start with a reagent from the chiral pool.<sup>9</sup> These compounds are commercially available as single enantiomers and therefore are a convenient source of chirality. However, many chiral pool reagents are only readily available in one absolute configuration,<sup>10</sup> which may or may not be the enantiomer needed for a given synthesis. Additionally, this strategy is restricted to products that are accessible from the limited number of chiral pool reagents, and there are many desirable enantiopure molecular targets outside of that scope.

A second strategy in asymmetric synthesis involves the use of chiral auxiliaries.<sup>11</sup> Chiral auxiliaries can be used to resolve a pair of enantiomers through the formation and separation of two diastereomers. Alternatively, chiral auxiliaries can be coupled with an achiral molecule to form an enantiopure compound which can then be manipulated in a diastereoselective fashion. Typically, chiral auxiliaries are removed after the diastereoselective step to provide the enantiopure product. Common chiral auxiliaries include Evans' oxazolidones<sup>12,13</sup> and Ellman's sulfonamide.<sup>14</sup> Unfortunately, chiral auxiliaries must be used in stoichiometric amounts and can be

expensive, although they can be recovered in some cases. Additionally, the use of chiral auxiliaries adds multiple steps to a synthesis.

Asymmetric synthesis can also be achieved through asymmetric catalysts.<sup>15</sup> In asymmetric catalysis, an achiral or a racemic starting material undergoes an enantioselective transformation aided by an asymmetric catalyst. Efficient, general, and scalable enantioselective catalysts are highly desirable. There are many different types of chiral catalysts including biocatalysts, organocatalysts, and transition metal-based catalysts. Biocatalysts, such as enzymes, offer several advantages including high selectivity and specificity, mild conditions, and

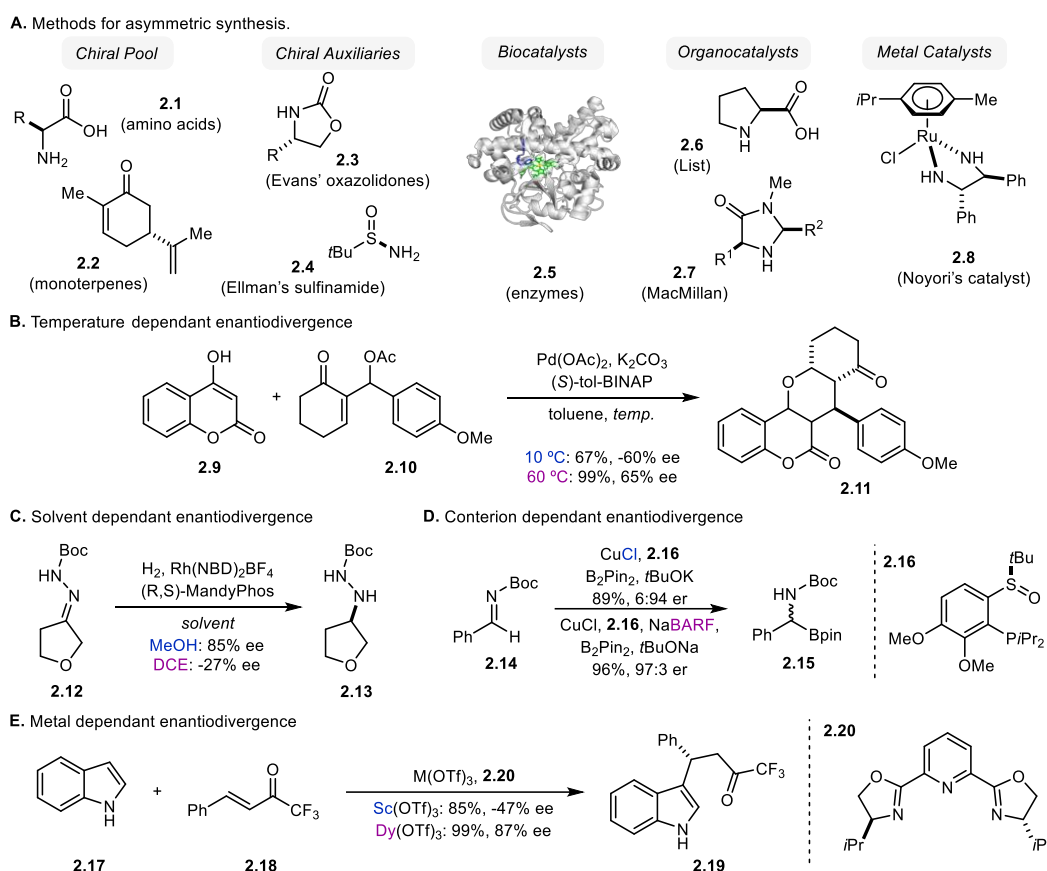


Figure 2.1 (A) Established methods for asymmetric synthesis. (B-E) selected examples of enantiodivergent reactions.

limited environmental damage.<sup>16</sup> Directed evolution has helped broaden the possibilities for biocatalysis,<sup>17,18</sup> however the substrate and transformation scope remain limited. Enantioselective organocatalysts are chiral organic molecules that have a variety of different applications.<sup>19,20</sup> Culminating in the 2021 Nobel Prize, organocatalysis has received growing recognition as an inexpensive and green alternative to transition metal catalysis.<sup>21</sup> However, efficient

enantioselective metal containing catalysts are still prevalent and widely applicable. For example, asymmetric hydrogenation catalysts, such as Noyori's catalyst,<sup>22</sup> are used on an industrial scale.<sup>23</sup> Enantioselective metal catalysts contain optically active ligands that are often derived from chiral pool reagents of natural origin.<sup>24</sup> Some of these ligands, referred to as privileged ligands, are effective for a variety of different transformations. Under this reaction paradigm, the synthesis of both enantiomers of a target structure requires the use of both enantiomers of a chiral catalyst. However, many chiral pool reagents are only available in one absolute configuration.<sup>10</sup> This makes accessing both enantiomers of a chiral target structure challenging.

Enantiodivergent catalytic strategies represent an attractive alternative when only one enantiomer of a chiral catalyst is available.<sup>25</sup> In enantiodivergent catalysis, the chirality is derived from a single chiral source that can be used to selectively obtain either enantiomer of a product depending on the other conditions of the reaction. Enantiodivergence can arise from several factors. For instance, a change in temperature<sup>26,27</sup> or solvent<sup>28,29</sup> has been shown to induce enantiodivergence (Figures 2.1B and 2.1C). However, this strategy is limited by the unpredictability and lack of understanding of how these factors induce enantiodivergence. Alternatively, changing counter ions has proven to be an effective promoter of enantiodivergent reactivity (Figure 2.1D).<sup>30,31</sup> Typically the enantiodivergence is realized by switching from a hard counterion, like a halide, to a soft counterion like tetrakis(3,5-bis(trifluoromethyl)phenyl)borate. Although this strategy has been successful, it remains limited because counterions are not involved in many reactions, and the role of counterions remains poorly understood. Finally, changing metal can enable enantioselectivity reversal (Figure 2.1E).<sup>32-35</sup> This strategy holds promise for developing more general approaches to enantiodivergent reactivity, but often in these reactions only one of the two enantiomers of the product is obtained in high enantiomeric excess (ee). This can be explained by the difficulty of inducing a large enough energetic difference between the two diastereomeric transition states that lead to the two different enantiomers of the product. Furthermore, the controlling features of metal dependent enantiodivergent catalysts remain poorly understood. As such, there remains a need for highly selective enantiodivergent catalytic strategies and insights into their underlying mechanisms. Chapter 1 described our syntheses of (+) and (-)-lingzhiol enabled by an enantiodivergent Michael addition.<sup>36</sup> This reaction was catalyzed by a complex between chiral bipyridine **2.23** and scandium triflate [Sc(OTf)<sub>3</sub>] or yttrium triflate [Y(OTf)<sub>3</sub>] (Figure 2.2). Switching between these two reversed the stereochemical outcome of the

reaction, representing a remarkable example of an achiral reaction parameter controlling the enantioselectivity of a reaction. Importantly, both enantiomers of the product (**2.24**) were accessed in  $\geq 90\%$  ee making this reaction unique when compared to other enantiodivergent transformations. Consequently, we felt that elucidating the mechanism could enable the design and development of general enantiodivergent synthetic strategies.

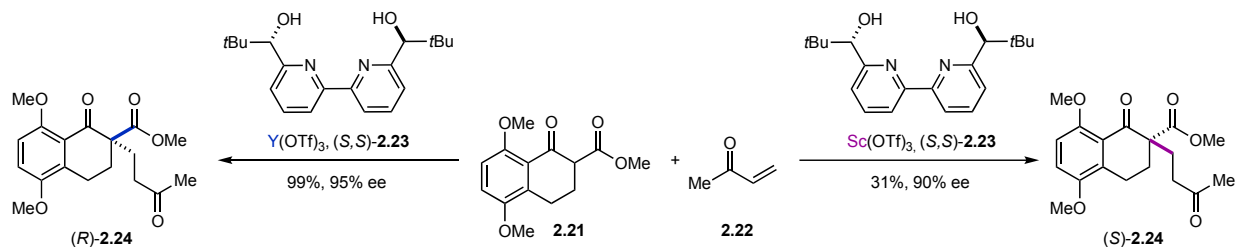
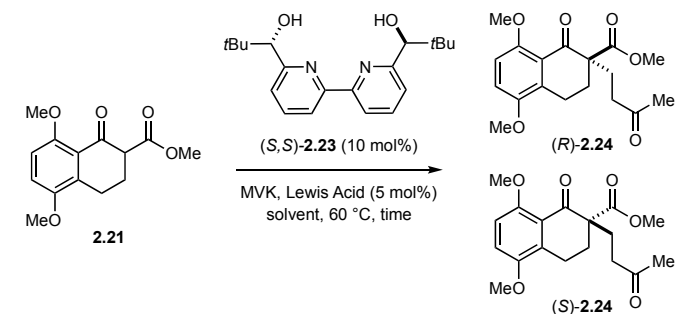


Figure 2.2 This work: Lewis acid dependent enantiodivergent Michael addition.

## 2.2 Results and Discussion

### 2.2.1 Reaction Optimization

Table 2.1. Catalyst and solvent optimization revealed unique enantiodivergent behavior.



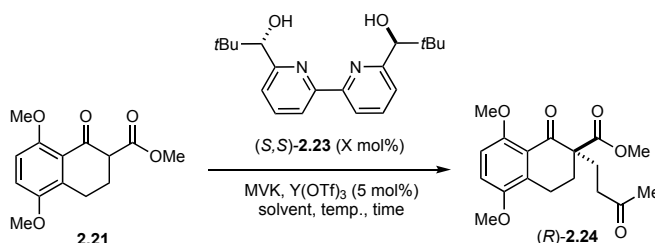
entry	metal ion	r(Å)	solvent	time (h)	yield <b>2.24</b> (%)	ee (%)
1	Sc <sup>3+</sup>	0.870	DCE	96	31	90 (S)
2			benzene	96	trace	-
3	Y <sup>3+</sup>	1.019	DCE	18	92	71 (R)
4			benzene	18	91	91 (R)
5	Dy <sup>3+</sup>	1.027	DCE	17	88	76 (R)
6			benzene	17	83	90 (R)
7	La <sup>3+</sup>	1.160	DCE	14	93	60 (S)
8			benzene	14	97	43 (S)

Reactions were performed on 0.15 mmol scale at 0.02 M at 60 °C. 5 mol% M(OTf)<sub>3</sub> and 10% mol (S,S)-**2.23** were pre-stirred at 60 °C for 1 hour.

Our strategy for the total syntheses of (+) and (-)-lingzhiol relied on an asymmetric Michael addition between  $\beta$ -ketoester **2.21** and methyl vinyl ketone (MVK, **2.22**). To accomplish this we applied conditions developed by the Kobayashi group using Sc(OTf)<sub>3</sub> as a catalyst and

bipyridine **2.23** as a chiral ligand.<sup>37</sup> In our system, we were able to isolate the desired product (*S*)-**2.24** in 90% ee (Table 2.1, entry 1) using DCE as a solvent. However, this reaction was slow, only providing 31% yield after 96 h. In an effort to improve the conversion, a number of different metal triflates were evaluated (Table 2.1). Gratifyingly, higher yields were observed with Dy(OTf)<sub>3</sub>, Y(OTf)<sub>3</sub> and La(OTf)<sub>3</sub>, in 88%, 92% and 93% yield, respectively, in shorter reaction times. Although, the ee decreased to 71%, 76%, and 60% ee, respectively (Table 2.1, entries 3, 5, and 7). Unexpectedly, the Dy(OTf)<sub>3</sub> and Y(OTf)<sub>3</sub> catalyzed reactions favored the formation of (*R*)-**2.24**, the opposite enantiomer to Sc(OTf)<sub>3</sub> despite relying on the same enantiomer of the chiral ligand (*S,S*)-**2.23**. Additional optimization showed that switching from DCE to benzene could improve the enantioselectivity of the Y(OTf)<sub>3</sub> and Dy(OTf)<sub>3</sub> catalyzed reactions to 91% and 90% ee, respectively, while maintaining high yield (Table 2.1, entries 4 and 6). No reaction was observed with Sc(OTf)<sub>3</sub> in benzene due to its low solubility (Table 2.1, entry 2). The divergent behavior of Sc(OTf)<sub>3</sub> versus Y(OTf)<sub>3</sub> and Dy(OTf)<sub>3</sub> has been observed previously.<sup>35 38</sup>

Table 2.2 Reaction Optimization with Y(OTf)<sub>3</sub> as a catalyst.



entry	X mol %	solvent	conc. (M)	temp. (°C)	time (h)	yield (%)	ee (%)
1	10	benzene	0.02	60	20	91	91
2	10	toluene	0.02	60	20	73	88
3	10	chlorobenzene	0.02	60	18	90	73
4	10	nitrobenzene	0.02	60	28	89	45
5	10	trifluorotoluene	0.02	60	41	88	53
6	10	THF	0.02	60	90	14	43
7	10	CH <sub>3</sub> CN	0.02	60	44	80	42
8	10	benzene	0.02	25	96	40	63
9	10	benzene	0.02	40	25	79	84
10	10	benzene	0.02	50	21	89	88
11	10	benzene	0.02	80	14	99	93
12	10	toluene	0.02	100	22	58	90
13	10	benzene	0.01	80	19	86	94
14	10	benzene	0.04	80	16	99	93
15	10	benzene	0.1	80	1.5	99	90
16	5	benzene	0.04	80	16	62	51
17	15	benzene	0.04	80	16	99	94

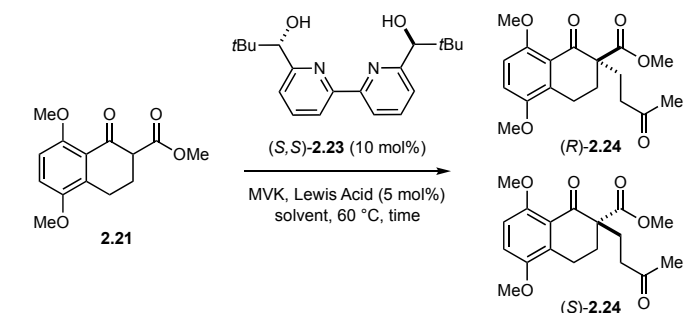
Reactions were performed on 0.15 mmol scale. 5 mol% M(OTf)<sub>3</sub> and 10% mol (*S,S*)-**2.23** were pre-stirred at 60 °C for 1 hour.



To verify that benzene was the ideal solvent, several polar and nonpolar aprotic solvents were evaluated for the yttrium-catalyzed reaction (Table 2.2, entries 1-6); however, none proved superior to benzene. Furthermore, temperature evaluations showed that the ideal reaction temperature was 80 °C (Table 2.2, entries 7-11), and concentration screening revealed that the optimal concentration was 0.04 M (Table 2.2, entries 12-14). Switching the amount of ligand to 5 mol% had a deleterious effect on the yield and ee, and switching to 15 mol% did not improve the reaction further (Table 2.2, entries 15 and 16).

As discussed in Chapter 1, all other commercially available lanthanide triflates were tested (Table 2.3). For both yield and selectivity, the optimal catalyst for the synthesis of (*S*)-**2.24** was Sc(OTf)<sub>3</sub>, whereas Y(OTf)<sub>3</sub> was the optimal catalyst for the synthesis of (*R*)-**2.24**. As such, our mechanistic experiments will focus on these two catalysts.

Table 2.3 Catalyst screen of commercially available lanthanide(III) triflates.



entry	Lewis acid	solvent	time (h)	yield (%)	ee (%)
1	Sc(OTf) <sub>3</sub>	DCE	96	31	90 ( <i>S</i> )
2	Y(OTf) <sub>3</sub>	benzene	18	91	91 ( <i>R</i> )
3	Dy(OTf) <sub>3</sub>	benzene	17	83	90 ( <i>R</i> )
4	Lu(OTf) <sub>3</sub>	benzene	42	93	82 ( <i>R</i> )
5	Yb(OTf) <sub>3</sub>	benzene	42	89	84 ( <i>R</i> )
6	Tm(OTf) <sub>3</sub>	benzene	22	92	86 ( <i>R</i> )
7	Er(OTf) <sub>3</sub>	benzene	18	95	89 ( <i>R</i> )
8	Ho(OTf) <sub>3</sub>	benzene	18	98	89 ( <i>R</i> )
9	Tb(OTf) <sub>3</sub>	benzene	17	98	90 ( <i>R</i> )
10	Gd(OTf) <sub>3</sub>	benzene	17	97	87 ( <i>R</i> )
11	Eu(OTf) <sub>3</sub>	benzene	17	99	83 ( <i>R</i> )
12	Sm(OTf) <sub>3</sub>	benzene	17	96	74 ( <i>R</i> )
13	Nd(OTf) <sub>3</sub>	benzene	17	96	13 ( <i>R</i> )
14	Pr(OTf) <sub>3</sub>	benzene	17	94	23 ( <i>S</i> )
15	Ce(OTf) <sub>3</sub>	benzene	17	81	42 ( <i>S</i> )
16	La(OTf) <sub>3</sub>	benzene	17	97	43 ( <i>S</i> )

Reactions were performed on 0.15 mmol scale at 0.02 M at 60 °C. 5 mol% M(OTf)<sub>3</sub> and 10% mol (*S,S*)-**2.23** were pre-stirred at 60 °C for 1 hour.

### 2.2.2 Metal Ionic Radii vs. Enantiomeric Excess Correlations

In previous examples of metal dependent enantiodivergence, metal ionic radius has been an important contributing factor.<sup>32</sup> To examine the role of metal ionic radius in this transformation, the log of the enantiomeric ratio was plotted against the ionic radius of all the metal catalysts (Figure 2.3).<sup>38</sup> The resulting bell-shaped curve demonstrates the correlation between ionic radius and enantiomeric ratio, which is consistent with the literature findings on the importance of ionic radius.<sup>38</sup> Interestingly, the small  $\text{Sc}(\text{OTf})_3$  catalyst strongly favors the formation of (*S*)-**2.24**, whereas larger catalysts like  $\text{Y}(\text{OTf})_3$  lead to selective formation of (*R*)-**2.24**. However, a further increase in the ionic radii to catalysts like  $\text{La}(\text{OTf})_3$  reverses this trend to favor (*S*)-**2.24**, albeit less selectively. Although these studies suggest that the ionic radius of the catalysts alters the chiral environment, it cannot be concluded how it does so. Therefore, additional experiments were conducted to try and further elucidate the mechanism.

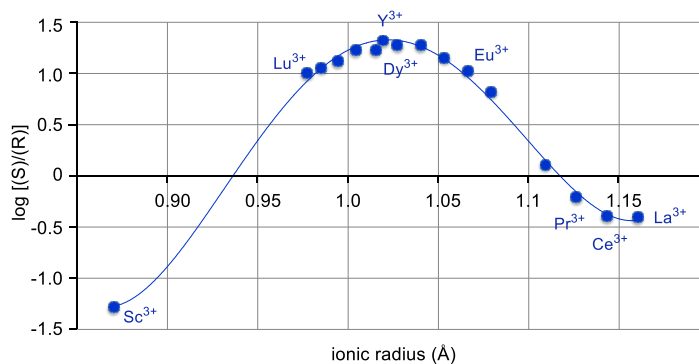


Figure 2.3 Plot of log(er) vs. catalysts ionic radii for each lanthanide catalyst.

### 2.2.3 Nonlinear Effect Studies

Given that ionic radius is influencing the enantioselectivity we hypothesized that this enantiodivergent phenomenon could be explained by the formation of metal-ligand aggregates or metal complexes varying in their metal to ligand ratio.<sup>39</sup> To test this, nonlinear effect studies were conducted with  $\text{Sc}(\text{OTf})_3$  and  $\text{Y}(\text{OTf})_3$  as catalysts.<sup>40,41</sup> To do so, (*S,S*)-**2.24** was prepared in varying degrees of enantiomeric excess then tested in the reaction. Importantly, in both the scandium- and yttrium-catalyzed reactions, a linear relationship between the ee of the ligand (**2.23**) and the ee of the product (**2.24**) was observed (Figure 2.4). This result rules out the presence of aggregate species and is consistent with one equivalent of chiral ligand **2.23** being in the catalytically active species for both the scandium- and yttrium-catalyzed reactions.

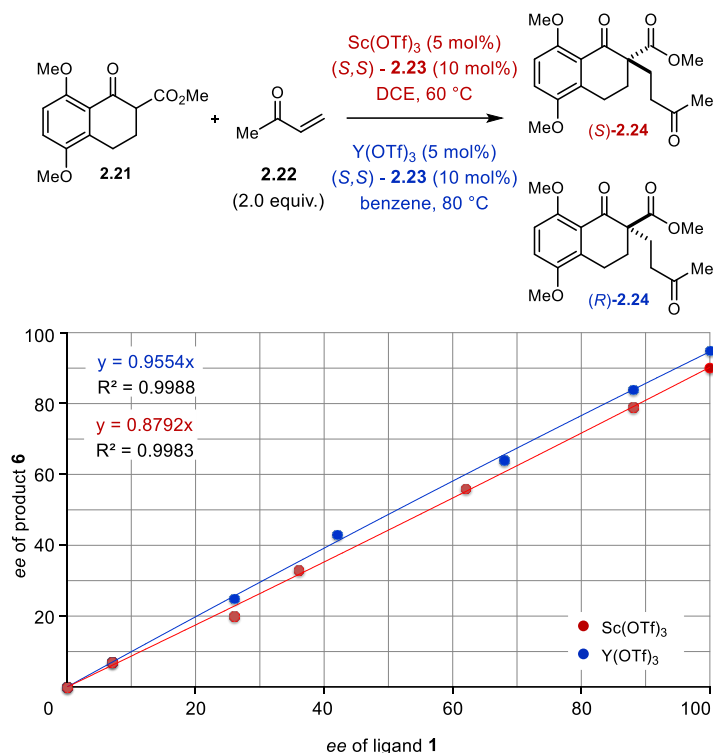


Figure 2.4 Nonlinear effect studies of the scandium- and yttrium-catalyzed reactions.

## 2.2.4 Kinetic Studies

To determine if multiple metal atoms were in the active catalysts, we conducted kinetic investigations into both the scandium- and yttrium-catalyzed reactions. This question was prompted by Kobayashi and coworkers observations that excess ligand was required to maintain high enantioselectivity in a  $\text{Bi}(\text{OTf})_3$  catalyzed Mukaiyama aldol reaction using the same chiral ligand **2.23**.<sup>42</sup> As was the case in this report, we hypothesized that a bidentate binding mode (**2.26**) could be possible in the scandium or yttrium systems as opposed to the expected tetradentate binding (**2.25**) (Figure 2.5). The Kobayashi group determined that excess ligand was essential to overcoming a competing bimetallic binding mode **2.26** that forms at lower equivalents of ligand.

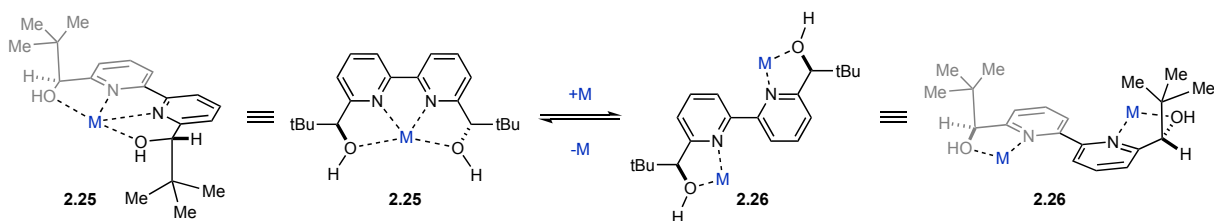


Figure 2.5 Potential bidentate and tetradentate binding modes between the metal catalyst and ligand **2.23**.

Initial  $^1\text{H-NMR}$  studies were consistent with tetradentate binding mode **2.25** between ligand **2.23** and both scandium and yttrium. In addition, kinetic investigations were conducted to further support this observation (Figure 2.6).<sup>43,44</sup> For consistency, we opted to study initial rates for both catalyst in DCE at 60 °C. Despite the deviation from optimal conditions with  $\text{Y}(\text{OTf})_3$ , the enantioselectivity reversal is still observed and these conditions would allow for a more direct comparison. The scandium-catalyzed reaction could not be adopted to the optimal yttrium conditions, as no product forms in that case. We studied initial rates at 2.5%, 5%, and 7.5% loading of metal catalyst with double the loading of ligand in each case. For the faster  $\text{Y}(\text{OTf})_3$  catalyzed reaction, the yield of **2.24** was monitored by UPLC analysis every 3 minutes for 30 total minutes. Based on this analysis, the order in  $\text{Y}(\text{OTf})_3$  was 1.02. For the slower  $\text{Sc}(\text{OTf})_3$  reaction, the yield of **2.24** was monitored in 30 minute increments for 7 hours and the order was determined to be 0.91. The first-order kinetics and  $^1\text{H-NMR}$  studies are consistent with a single catalyst atom bound in a tetradentate fashion with **2.23** for both scandium and yttrium.

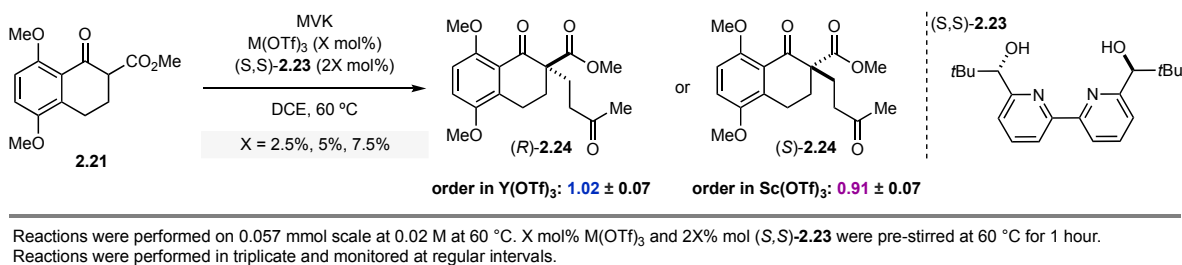


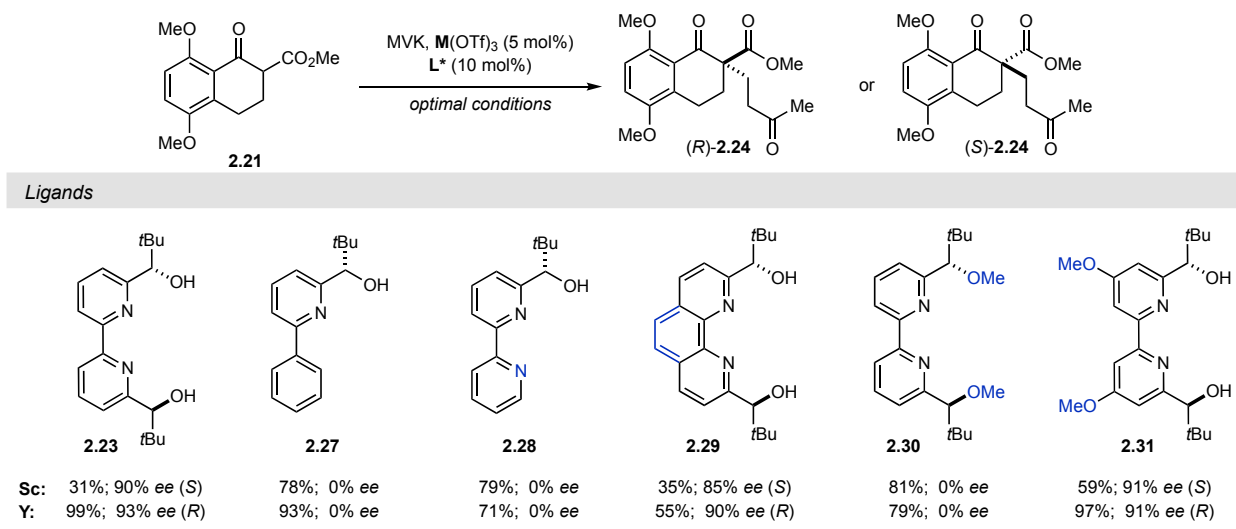
Figure 2.6 Kinetic analysis of the scandium- and yttrium-catalyzed reactions.

### 2.2.5 Ligand Structure Analysis

In order to determine what features of the ligand were essential to the enantioselectivity, a number of pyridine-derived ligands were prepared and tested in the reaction (Table 2.4). Bidentate and tridentate ligands **2.27** and **2.28** did not impart any stereoselectivity, yielding **2.24** in 0% ee. This further supports that **2.23** binds in a tetradentate fashion, and that this binding mode is important for enantioinduction. Rotationally fixed phenanthroline ligand **2.29** performed comparably well to ligand **2.23** and successfully effected enantiodivergence. This ligand would be unable to adopt the alternative bidentate binding mode discussed previously.<sup>42</sup> Interestingly, methyl ether ligand **2.30** failed to provide **2.24** with any ee. This suggests that hydrogen bonding plays an essential role in the enantioselectivity of this reaction. Electron rich methoxy-substituted ligand **2.31** was able to increase the yield of the scandium reaction and decrease the reaction time

of the yttrium reaction while maintaining excellent enantioselectivity. Since this reaction is believed to proceed via an enolate complex between the substrate-metal-ligand complex, we hypothesize that this electron rich ligand increases the reactivity of the enolate thus increasing the rate of the reaction. Taken together, the data up until this point suggests that the one ligand is bound in a tetradentate fashion to one metal for both the scandium- and yttrium-catalyzed reactions.

Table 2.4 Ligand structure evaluations.



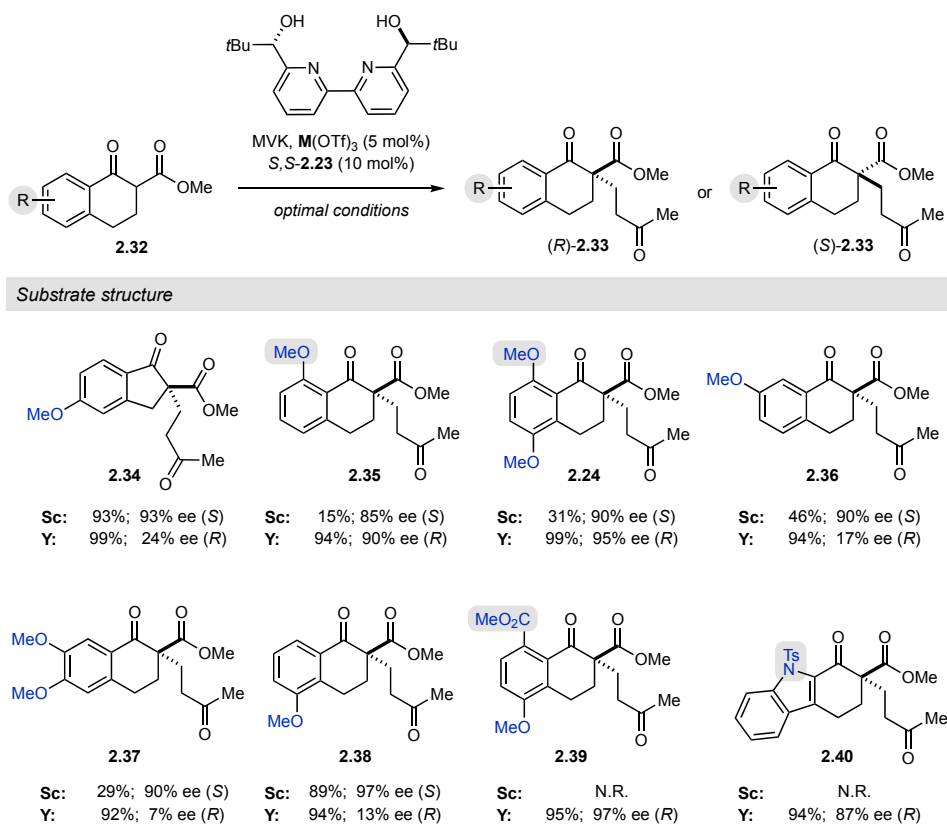
**Y(OTf)<sub>3</sub> optimal conditions:** L\* and Y(OTf)<sub>3</sub> were pre-stirred in benzene at 80 °C for 30 minutes. Reactions were performed at 0.04 M in benzene at 80 °C with monitoring at regular intervals. **Sc(OTf)<sub>3</sub> optimal conditions:** L\* and Y(OTf)<sub>3</sub> were pre-stirred in DCE and stirred at 60 °C for 30 minutes. Reactions were performed at 0.02 M in DCE at 60 °C with monitoring at regular intervals.

## 2.2.6 Substrate Structure Evaluation

We next investigated what role the substrate might play in the reversal of enantioselectivity. To do so, we prepared a number of aromatic  $\beta$ -ketoesters with differing aromatic substitution patterns and tested them with both catalysts (Table 2.5). The scandium-catalyzed reaction proved more sensitive to the substitution pattern, providing the Michael products in low yields in some cases. This appears to be a steric trend; as the methoxy substituent moves further away from the reaction site the yield increases (Table 2.5, entries **2.35**, **2.36**, **2.38**). However, despite the low yields, all products were isolated in high enantioselectivity, which is consistent with Kobayashi's initial report.<sup>37</sup> In comparison, the yttrium-catalyzed reaction provided the Michael products in high yields in all cases. Yet, high enantioselectivity was only observed in substrates that contained a Lewis basic substituent (Table 2.5, entries **2.35**, **2.24**, **2.39**,

**2.40).** Importantly, for all substrates, the major enantiomer formed under the scandium-catalyzed reaction was opposite to that formed in the yttrium-catalyzed reaction.

Table 2.5 Evaluating differentially substituted aryl  $\beta$ -ketoester substrates.



**Y(OTf)<sub>3</sub> optimal conditions:** (S,S)-**2.23** and Y(OTf)<sub>3</sub> were pre-stirred in benzene at 80 °C for 30 minutes. Reactions were performed at 0.04 M in benzene at 80 °C with monitoring at regular intervals. **Sc(OTf)<sub>3</sub> optimal conditions:** (S,S)-**2.23** and Y(OTf)<sub>3</sub> were pre-stirred in DCE and stirred at 60 °C for 30 minutes. Reactions were performed at 0.02 M in DCE at 60 °C with monitoring at regular intervals.

Based on this result, we hypothesized that the ortho methoxy group could be acting as a Lewis base and coordinating the yttrium-catalyst. To verify that this interaction was occurring we conducted <sup>1</sup>H-NMR studies using Eu(fod)<sub>3</sub>, a paramagnetic NMR shift reagent.<sup>45</sup> Importantly, Eu(OTf)<sub>3</sub> performs comparably to Y(OTf)<sub>3</sub> (Table 2.3) and has a similar ionic radius (Figure 2.3), therefore, we felt that this would provide a good model to study this potential Lewis basic interaction by NMR. Indeed, when **2.24** was treated with Eu(fod)<sub>3</sub> in *d*<sub>6</sub>-benzene, two new methoxy signals were observed by <sup>1</sup>H-NMR, one arising from the methyl ester and the other from the ortho aromatic methyl ether (Figure 2.7). This result supports the hypothesis that the ortho methoxy group is interacting with the catalyst and implies it plays an important role in the observed enantiodivergence.

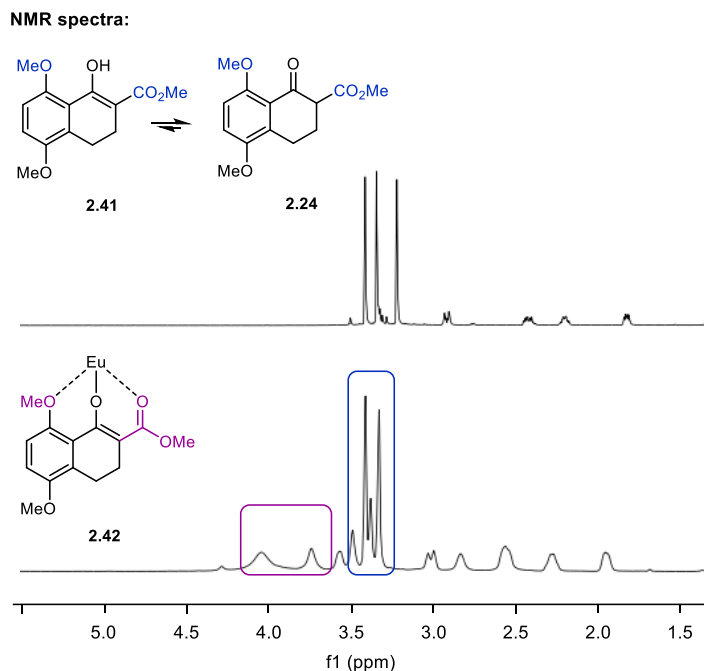


Figure 2.7 NMR shift investigations using  $\text{Eu}(\text{Fod})_3$  and  $\beta$ -ketoester substrate **2.24**.

### 2.2.7 Computational Analysis

Our experimental analysis provided a good foundation to computationally explore the precise interactions that determine the stereochemical outcome. We employed density functional theory (DFT) calculations because this technique has proven useful for mechanistic interrogation,<sup>46</sup> including Lewis acid catalyzed transformations.<sup>47</sup> However, asymmetric catalysis adds an extra layer of complexity, such as the presence of multiple catalytically competent species. Thus, we aimed to simplify the computational analysis by studying solely the enantiodetermining step. Stationary points relevant to this step were located using M06 density functional using a mixed basis set of SDD for yttrium and 6-31G(d,p) for all other atoms. For scandium, the same functional was deployed with the 6-31G(d,p) basis set. Solvation free energy corrections were computed by means of single point energy calculations at the same level of theory with the IEFPCM model.

Taking into consideration our experimental results, we identified two ways in which the enolate could orient itself with respect to the catalyst-ligand complex: 1) with the aromatic ring on the opposite face as the axial triflate (**2.43**), or 2) adjacent to the axial triflate (**2.44**). In each orientation, the electrophile could approach from either the *Re* or *Si* face of the enolate (Figure 2.8A). Furthermore, we identified two possible modes of electrophile activation, through either a

1) Lewis acid mediated mechanism, or 2) a Brønsted acid type mechanism (Figure 2.8B). In the former, the carbonyl of MVK is activated through coordination with the Lewis acid catalyst; whereas in the latter, the hydroxy proton of the ligand participates in hydrogen bonding with MVK. Additionally, given the labile nature of triflate ligands, several complexes with different triflate coordination number and ligand protonation state were considered. At 60-80 °C, Curtin-Hammett conditions should apply assuming that the ligand bound Lewis acid species are in equilibrium.<sup>48</sup> Therefore, the most favored pathway is determined by the absolute energies of the transition state.<sup>49</sup> The computed enantiomeric excess arises from comparing the lowest-energy pathways leading to the (*R*)- and (*S*)-enantiomer. Given that all species are assumed to be in solution, different binding modes, electrophile activation modes, ligand protonation state and/or triflate binding number could be operative in the transition states leading to the (*R*)- and (*S*)-enantiomers of **2.24**.

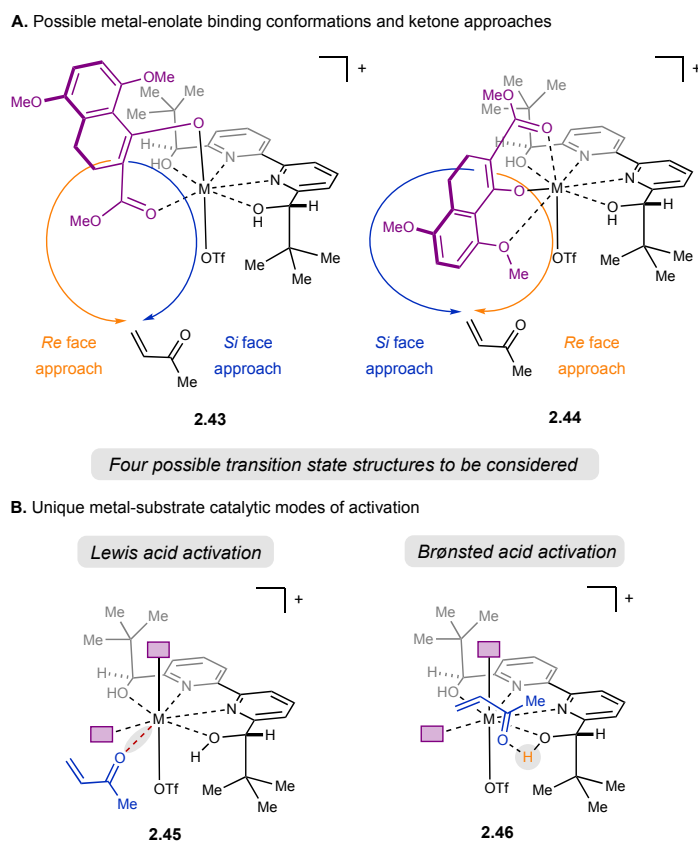


Figure 2.8 (A) Hypothesized enolate transition states and electrophile facial approach. (B) Potential activation modes of ketone **2.22**. Purple boxes denote enolate binding sites for substrate **2.21**.

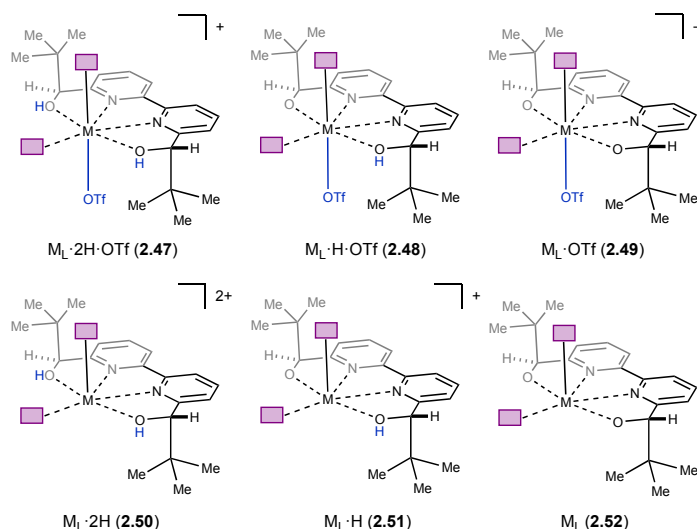
Our investigations started with complex  $M_L \cdot 2H \cdot OTf$  (**2.47**), which was initially proposed by Kobayashi.<sup>37</sup> The calculations for  $S_{CL} \cdot 2H \cdot OTf$  determined that the lowest-energy transition



state proceeded via *Si*-face attack from **Sc-2.47** on MVK having an activation free energy of 20.1 kcal mol<sup>-1</sup> (Table 2.6B, entry 1). This pathway was 0.2 kcal mol<sup>-1</sup> lower in energy than the one leading to the opposite enantiomer via **Sc-2.47-Re**. Therefore, the enantiomeric excess was computed to be -15% ee, which is significantly lower than the experimental value of -90% ee. This suggests that Sc<sub>L</sub>·2H·OTf (**Sc-2.47**) is likely not the operative transition state. This led us to consider several other catalytically active species with varied triflate coordination number and ligand protonation state. For Sc<sub>L</sub>·H·OTf, **Sc-2.48-Si** had an activation energy of 15.9 kcal mol<sup>-1</sup> whereas **Sc-2.48-Re** had an activation energy of 19.4 kcal mol<sup>-1</sup> (Table 2.6, entry 2). Although these values are already much lower than Sc<sub>L</sub>·2H·OTf (**Sc-2.47**), we considered the possibility that even lower energy transition states could exist. Therefore, we extensively evaluated the remaining complexes highlighted in Table 2.6. The lowest transition state energy was found to proceed via TS **Sc-2.51** (Table 2.6, entry 5). In both **Sc-2.51-Si** and **Sc-2.51-Re**, electrophile activation occurs via Brønsted acid type activation (Figure 2.9B). The combination of reduced steric constraints with the axial triflate and strong H-bonding interactions contribute to the low activation barriers observed in Sc<sub>L</sub>·H. The energetic difference between **Sc-2.51-Si** and **Sc-2.51-Re** can be explained by the steric clash between the *t*Butyl group of the ligand and substrate **2.21** present in **Sc-2.51-Re**. **Sc-2.51-Si** has an activation free energy of 14.1 kcal mol<sup>-1</sup> and yields (*S*)-**2.24** in agreement with our experimental result. These calculations also show that the lowest energy pathway leading to (*R*)-**2.24** is via **Sc-2.49-Re** (Table 2.6, entry 3). The energetic difference between these two transition states corresponds to a computed ee of -64%,<sup>50</sup> closer to the experimental value at 60 °C of 90% ee. Since this catalyst is fully deprotonated, this proceeds through Lewis acid activation of MVK instead. Interestingly, although the activation modes of Sc<sub>L</sub>·OTf (Table 2.6, entry 3) and Sc<sub>L</sub> (Table 2.6, entry 6) are similar, the former is considerably lower in energy. Although the axial triflate likely destabilizes the transition state of Sc<sub>L</sub>·OTf (**Sc-2.49**), this complex also has higher Lewis acidity that compensates for the steric destabilization. Additionally, these calculations suggest that Brønsted acid activation is more effective than Lewis acid activation (Figure 2.9B). No interactions between the *ortho*-methoxy substituent and the complex were observed. This suggests that the selectivity of the scandium-catalyzed transformation should not be sensitive to modifications at that position, which agrees with our experimental results.

Table 2.6 (A) Computationally analyzed complexes.(B) Lowest energy pathways for each complex relative to the pre-TS complex.

A. Metal-enolate complexes used for computational analysis.



B. Summary of lowest energy pathways for each complex relative to Pre-TS complex. All solvent corrected free energies of activation reported in kcal/mol.

Entry	Catalyst Complex	<i>Si</i> -addition DG <sup>‡</sup>	<i>Re</i> -addition DG <sup>‡</sup>	Product
1	Sc <sub>L</sub> ·2H·OTf ( <b>Sc-2.47</b> )	20.1	20.3	S
2	Sc <sub>L</sub> ·H·OTf ( <b>Sc-2.48</b> )	15.9	19.4	S
3	Sc <sub>L</sub> ·OTf ( <b>Sc-2.49</b> )	17.9	15.1	R
4	Sc <sub>L</sub> ·2H ( <b>Sc-2.50</b> )	15.9	18.5	S
5	Sc <sub>L</sub> ·H ( <b>Sc-2.51</b> )	14.1	17.6	S
6	Sc <sub>L</sub> ( <b>Sc-2.52</b> )	21.4	17.9	R
7	Y <sub>L</sub> ·2H·OTf ( <b>Y-2.47</b> )	17.0	12.6	R
8	Y <sub>L</sub> ·H·OTf ( <b>Y-2.48</b> )	17.3	19.3	S
9	Y <sub>L</sub> ·OTf ( <b>Y-2.49</b> )	13.9	16.8	S
10	Y <sub>L</sub> ·2H ( <b>Y-2.50</b> )	16.8	17.0	S
11	Y <sub>L</sub> ·H ( <b>Y-2.51</b> )	11.9	10.0	R
12	Y <sub>L</sub> ( <b>Y-2.52</b> )	12.8	15.2	S

The same possible pathways were then computed for the yttrium-catalyzed system. As with scandium, Y<sub>L</sub>·2H·OTf (**Y-2.47**) was initially investigated as the potential active catalyst species (Table 2.6, entry 7). In the larger yttrium system, Lewis acid activation of MVK is the lowest energy TS pathway. Comparing the lowest TS energies for **Y-2.47-Re** and **Y-2.47-Si** reveals that this reaction is expected to give the (*R*) product, which agrees with our experimental results. However, as with the scandium systems, we found that Y<sub>L</sub>·2H·OTf (**Y-2.47**) was not the likely catalytically active species. Subsequent investigations of the other complexes determined that the lowest energy pathways to both the major and minor enantiomer proceed through Y<sub>L</sub>·H (**Y-2.51**) (Table 2.6, entry 11). In addition, the computed enantiomeric excess closely matches the

experimental value (88% ee computed, 95% ee experimental). The reproduction of the experimental ee highlights the capabilities of computations analysis in this area. In addition, **Y-2.51** (Table 2.6, entry 11) has a lower energetic barrier than **Sc-2.51** (Table 2.6, entry 5) which is consistent with the faster reaction rate of the yttrium-catalyzed transformation. The computations reveal a key hydrogen bonding interaction between the *ortho*-methoxy substituent of **2.21** and the hydroxy group of **Y-2.51-Si** (Figure 2.9C). This interaction changes the orientation of and explains the strong preference for the formation of (*R*)-**2.24**. Additionally, this is supported by the experimental evidence of the importance of hydrogen bonding and the participations of the *ortho*-methoxy group. Furthermore, when THF is used instead of benzene the ee drops from 95% to 43% ee (Table 2.2, entry 5). This is further evidence for this type of interaction because THF can disrupt that H-bonding interaction. Using the IEFPCM solvation model, single point energy calculations in THF reduced the relative free energy difference between **Y-2.51-Re** and **Y-2.51-Si** by 0.2 kcal mol<sup>-1</sup>. This corresponds to a computed ee of 15%, and provides additional support for our hypothesis. The enantiodetermining role of the *ortho*-methoxy hydrogen-bonding contact between

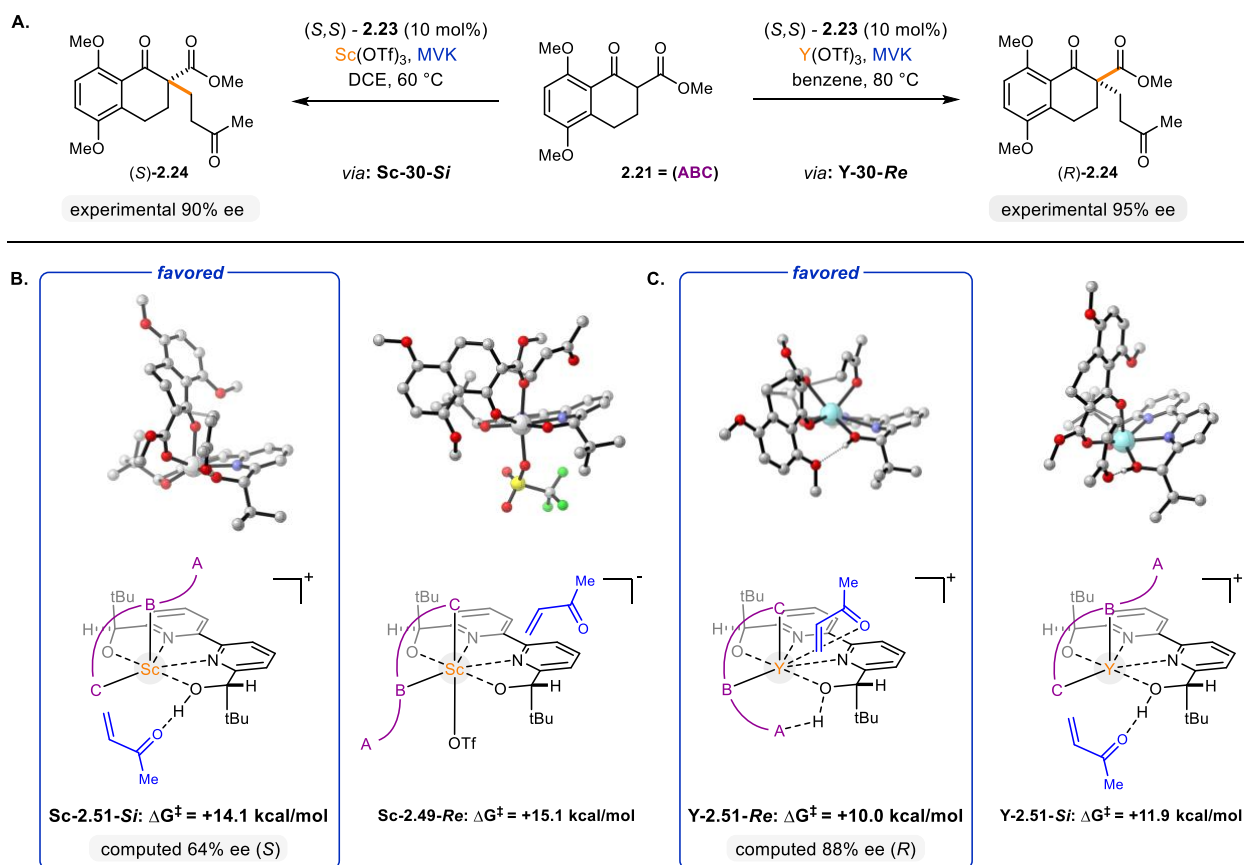


Figure 2.9 The lowest energy transition states leading to both enantiomers in the scandium- and yttrium-catalyzed reactions.

the substrate and ligand is supported by our ligand and substrate studies (Table 2.4, Table 2.5, Figure 2.7). Despite the challenges in modeling this reaction, our computational results accurately reproduced our experimental results and provided crucial insights into how enantiodivergence is achieved.

## 2.3 Conclusion

While working towards the total synthesis of lingzhiol, we observed a metal-dependent reversal of enantioselectivity in a Lewis acid catalyzed Michael addition. This enantiodivergent transformation used a single enantiomer of chiral bipyridine ligand **2.23**. Scandium and yttrium proved to be the optimal catalysts, with each providing a different enantiomer of the product in moderate to high yields and excellent enantioselectivities. A thorough mechanistic investigation enhanced our understanding of this reaction. Preliminary catalyst screening revealed the importance of the ionic radius of the catalyst. Non-linear effect and kinetic studies determined that the active catalyst species is a 1:1 ligand:metal complex for both the scandium and yttrium systems. Ligand structure analysis established the requirement for a tetradentate  $C_2$  symmetric ligand. Notably, free hydroxy groups were also a requirement for the ligand. Interestingly, substrate structure analysis showed that an ortho Lewis basic site was necessary for high enantioselectivity in the yttrium reaction but not in the scandium reaction. Subsequent NMR studies confirmed the ortho substituent was likely interacting with the yttrium catalyst. Density functional theory (DFT) calculations on the scandium system revealed that the small scandium atom can only coordinate to the ligand and enolate, so the electrophile is activated through hydrogen-bonding with the ligand. However, in the yttrium system, DFT computations indicated that the larger yttrium-catalyst could also activate the electrophile via coordination, and hydrogen bonding instead occurred between the ortho substituent and the ligand. This interaction flips the orientation of the substrate, reversing the enantioselectivity of the reaction (Figure 2.10). We believe these studies will aid the development of future enantiodivergent transformations.

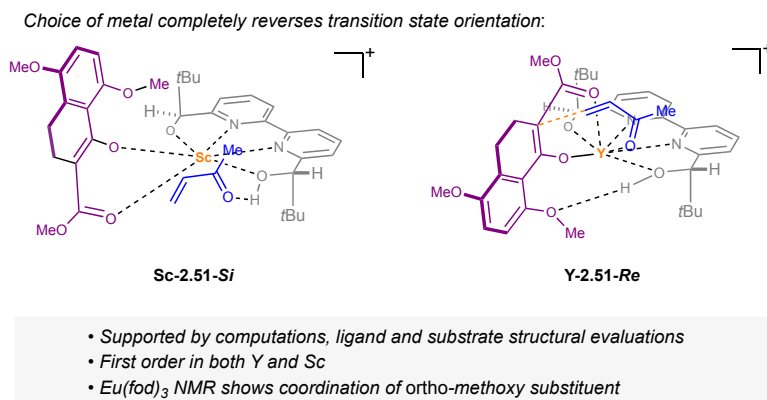


Figure 2.10 Transition states leading to (S)-2.24 and (R)-2.24 using scandium and yttrium respectively.

## 2.4 Experimental

### 2.4.1 General Information

**General Laboratory Procedures:** All moisture-sensitive reactions were performed under nitrogen in oven- or flame-dried round bottom flasks equipped with rubber septa. Dry solvents and air- and moisture-sensitive reagents were transferred via oven-dried stainless steel needles or hypodermic needles. Flash chromatography and silica plugs were carried out using Silicycle Silia Flash<sup>®</sup> 40-63 micron (230-400 mesh) silica gel. All heated reactions were heated in Teflon/aluminum heating mantles (Chemglass).

**Materials and Instrumentation:** All chemicals were purchased from Sigma Aldrich, Alfa Aesar, Acros Organics, TCI America, and Ark Pharm and were used as received unless noted otherwise. Chiral ligands were prepared in accordance with the procedures described or cited in section 3a (Ligand Synthesis). Tetrahydrofuran and dichloromethane were dried by being passed through columns of activated alumina. Benzene and dichloroethane were removed from sealed bottles under nitrogen atmosphere. Enantiomeric excess (ee) values were determined by chiral HPLC analysis, which were performed using an Agilent Infinity 1260 system eluting with hexane/isopropanol. Chiral stationary phases are described in the experimental for individual compounds (column size 4.6 mm x 250 mm). Proton nuclear magnetic resonance NMR (<sup>1</sup>H NMR) spectra and carbon nuclear magnetic resonance spectra (<sup>13</sup>C NMR) were measured on Varian MR400, Varian vnmrs 500, Varian Inova 500, or Varian vnmrs 700 spectrometers. Chemical shifts for protons are reported in parts per million (ppm) and are referenced to the residual solvent peak ( $\text{CHCl}_3$ ;  $\delta$ 7.26). Chemical shifts for carbons are reported in parts per million and are referenced to

the carbon resonances of the NMR solvent (CDCl<sub>3</sub>: 77.16). Data are described as follows: chemical shift, integration, multiplicity (br = broad, s = singlet, d = doublet, t = triplet, q = quartet, p = pentet, dd= doublet of doublets, m = multiplet), and coupling constant in Hertz (Hz). High resolution mass spectroscopic (HRMS) data were recorded using TOF HPLC-MS with ESI high resolution mass spectrometer equipped with an Agilent 1290 Infinity II UHPLC pump and multisampler unless otherwise noted. Infrared (IR) spectra were measured on a PerkinElmer Frontier MIR spectrometer. IR data are represented as frequency of absorption (cm<sup>-1</sup>). Optical rotations were acquired on a Jasco P-2000 digital polarimeter and are reported as *c* = g/100 mL at 589 nm (sodium D line) at 26 °C and 10 cm path length unless otherwise noted.

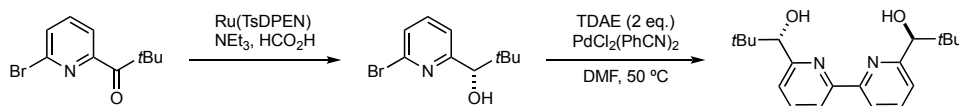
*Abbreviations used:* Et<sub>3</sub>N = triethylamine, EtOAc = ethyl acetate, DCE = dichloroethane, DCM = dichloromethane, THF = tetrahydrofuran, MeOH = methanol, DCE = dichloroethane, OTf = trifluoromethanesulfonate (triflate), Na<sub>2</sub>SO<sub>4</sub> = sodium sulfate, MgSO<sub>4</sub> = magnesium sulfate, HCl = hydrochloric acid, NH<sub>4</sub>Cl = ammonium chloride, NaHCO<sub>3</sub> = sodium hydrogencarbonate (sodium bicarbonate), TLC = thin-layer chromatography.

## 2.4.2 Experimental Procedures

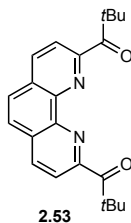
### Reaction Optimization

Reaction optimization was initially carried out as part of our studies resulting in the asymmetric total synthesis of lingzhiol (Chapter 1),<sup>36</sup> with several additional conditions evaluated here. *General procedure:* Metal triflate (0.0075 mmol, 0.05 equiv.) and ligand (*S,S*)-**1.42** (0.015 mmol, 0.1 mmol) were dissolved in solvent (1.2 mL) and heated to 60 °C for 1 hour. The reaction mixture was diluted with solvent (5 mL) and a solution of **1.31** (40 mg, 0.15 mmol) in solvent (5 mL) was added followed by methyl vinyl ketone (25 mL, 0.2 mmol, 2equiv.). The reaction mixture was stirred for the time listed in Tables 2.1 – 2.3. The reaction mixture was directly concentrated onto silica gel and purified by column chromatography eluting with hexanes/ethyl acetate. The enantiomeric excess was determined by chiral HPLC (Diacel ChiralCel OD-H column eluting with 10% isopropanol/hexane. Yields and enantiomeric excess for the products are listed in Tables 2.1 – 2.3.

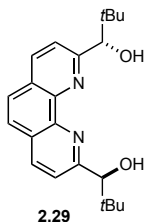
### Ligand Synthesis



Ligands **2.23**,<sup>51</sup> **2.27**,<sup>52</sup> **2.28**,<sup>51</sup> **2.30**,<sup>53</sup> and **2.31**<sup>54</sup> were prepared according to literature procedures and all characterization data matched the reported data. A general scheme for the synthesis of ligand **2.23** is shown above.



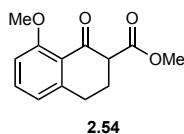
**1,1'-(1,10-Phenanthroline-2,9-diyl)bis(2,2-dimethylpropan-1-one) (2.53)**: 2,9-Dibromo-1,10-phenanthroline (2.25 g, 6.66 mmol) was dissolved in THF (70 mL) and cooled to -78 °C in a dry ice/acetone bath. *n*BuLi (2.5 M in hexane, 10.7 mL, 26.6 mmol, 4 equiv.) was added slowly via syringe. The reaction mixture was allowed to stir at -78 °C before trimethylacetonitrile (3.0 mL, 26.6 mmol, 4 equiv.) was added quickly dropwise via syringe. The reaction mixture was allowed to stir at this temperature for 1 hour before warming to room temperature and carefully quenching with aqueous 1M HCl. The mixture was stirred at room temperature for 1 hour before being poured into a separatory funnel and diluted with EtOAc. The layers were separated and the aqueous layer was washed with two additional portions of EtOAc. The combined organic layers were dried over Na<sub>2</sub>SO<sub>4</sub> and concentrated by rotary evaporator. The crude product was purified by flash column chromatography eluting with hexanes/EtOAc to afford 788 mg (34% yield) of the title compound as an orange solid. <sup>1</sup>H NMR (700 MHz, CDCl<sub>3</sub>) δ 8.40-8.31 (m, 4H), 7.90 (s, 2H), 1.72 (s, 18H). <sup>13</sup>C NMR (176 MHz, CDCl<sub>3</sub>) δ 207.0, 153.9, 144.9, 137.0, 130.3, 128.3, 122.9, 44.8, 28.1. IR (cm<sup>-1</sup>): 2947.27, 1678.71, 1549.38, 1487.29, 1390.55, 1292.74, 1087.84, 1040.53, 972.90, 890.83, 863.46. HRMS (ESI<sup>+</sup>): Calculated for C<sub>22</sub>H<sub>24</sub>N<sub>2</sub>O<sub>2</sub>Na<sup>+</sup> [M+Na<sup>+</sup>]<sup>+</sup>: 371.1730 Found [M+Na<sup>+</sup>]<sup>+</sup>: 371.1724.



**(1S,1'S)-1,1'-(1,10-Phenanthroline-2,9-diyl)bis(2,2-dimethylpropan-1-ol) (2.29)**: **2.53** (71 mg, 0.204 mmol) and (*S,S*)-RuTsDPEN (13 mg, 0.204 mmol, 0.1 equiv.) were dissolved in DCM (2 mL) and a mixture of triethylamine (1.42 mL, 10.2 mmol, 50 equiv.) and formic acid (0.6 mL,

17.5 mmol, 86 equiv.) was added and the reaction mixture heated in a capped scintillation vial to 60 °C. The DCM solvent was replenished every twelve hours (2 mL) and the reaction was cooled to room temperature, concentrated by rotary evaporator and purified by flash column chromatography eluting with DCM/MeOH to afford 30 mg (42% yield) of the title compound as a yellow-brown solid in >99% ee. The (*S,S*) configuration was assigned based on the sign of the optical rotation (opposite to that reported for a different synthetic approach to the (*R,R*) enantiomer).<sup>55</sup> **<sup>1</sup>H NMR** (700 MHz, CDCl<sub>3</sub>) δ 8.16 (d, *J* = 7.9 Hz, 2H), 7.78 (s, 2H), 7.54 (d, *J* = 8.1 Hz, 2H), 1.03 (s, 18H). **<sup>13</sup>C NMR** (176 MHz, CDCl<sub>3</sub>) δ 161.1, 143.9, 135.3, 127.7, 125.9, 122.8, 81.6, 36.7, 26.3. **IR** (cm<sup>-1</sup>): 3272.95, 2951.28, 1590.32, 1498.05, 1477.57, 1364.36, 1240.23, 1096.19, 1059.48, 1016.29, 860.69. **HRMS** (ESI<sup>+</sup>): Calculated for C<sub>22</sub>H<sub>28</sub>N<sub>2</sub>O<sub>2</sub>Na<sup>+</sup> [M+Na<sup>+</sup>]<sup>+</sup>: 353.2224 Found [M+Na<sup>+</sup>]<sup>+</sup>: 353.2222. **HPLC** [ChiralPak AD-H column] (20% isopropanol/hexanes) [14.238 (major), 16.205 (minor)]. [α]<sub>D</sub> = +252.3 (c=0.24, CHCl<sub>3</sub>).

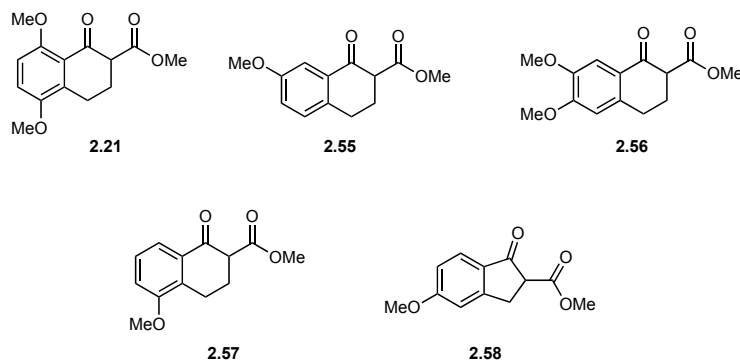
### Substrate Synthesis



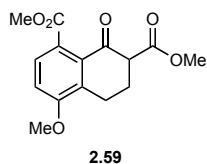
**Methyl 8-methoxy-1-oxo-1,2,3,4-tetrahydronaphthalene-2-carboxylate (2.54):** 8-Methoxy-tetralone (300 mg, 1.70 mmol) was dissolved in THF (1.7 mL) and dimethyl carbonate (1.7 mL) and sodium hydride (60% dispersion in mineral oil, 204 mg, 5.11 mmol, 3 equiv.) was added at room temperature. The reaction mixture was heated to 110 °C until judged complete by TLC. After cooling to room temperature, the reaction mixture was poured onto ice and diluted with 1M HCl and ethyl acetate. The layers were separated and the aqueous layer was washed with two additional portions of ethyl acetate. The combined organic layers were dried over Na<sub>2</sub>SO<sub>4</sub> and concentrated by rotary evaporator before being purified by flash column chromatography eluting with hexanes/EtOAc to afford 318 mg (80% yield) of the title compound as a white solid (2:1 mixture of keto/enol tautomers by NMR). **<sup>1</sup>H NMR** (500 MHz, CDCl<sub>3</sub>) δ 12.98 (s, 0.5H), 7.39 (t, *J* = 8.0 Hz, 1H), 7.25 (t, *J* = 7.9 Hz, 1H), 6.87 – 6.75 (m, 3H), 3.93 – 3.85 (m, 4.5H), 3.79 (s, 1.5H), 3.74 (s, 3H), 3.58 (dd, *J* = 10.4, 4.9 Hz 1H), 3.03 (dd, *J* = 13.7, 8.5 Hz, 1H), 2.96 (dd, *J* = 9.9, 4.8 Hz, 1H), 2.75 – 2.67 (m, 1H) 2.48 – 2.37 (m, 3H), 2.34 – 2.24 (m, 1H). **<sup>13</sup>C NMR** (keto form, 126 MHz, CDCl<sub>3</sub>) δ 192.17, 170.99, 160.95, 146.18, 134.63, 120.79, 120.37, 110.16, 56.17, 56.07, 52.31, 28.64, 26.02. **<sup>13</sup>C NMR** (enol form, 126 MHz, CDCl<sub>3</sub>) δ 173.2, 167.3, 158.5, 143.1, 131.6,



121.3, 118.7, 111.1, 97.7, 56.4, 51.7, 29.7, 20.6. **IR** (cm<sup>-1</sup>): 3002.83, 2951.12, 2845.56, 1732.57, 1673.06, 1593.79, 1577.22, 1471.79, 1457.63, 1440.20, 1370.98, 1352.37, 1318.92, 1295.18, 1269.91, 1248.44, 1223.59, 1210.15, 1194.70, 1172.74, 1104.12, 1079.17, 999.76, 939.78. **HRMS** (ESI<sup>+</sup>): Calculated for C<sub>13</sub>H<sub>14</sub>O<sub>4</sub>Na<sup>+</sup> [M+Na<sup>+</sup>]<sup>+</sup>: 257.0784 Found [M+Na<sup>+</sup>]<sup>+</sup>: 257.0780.

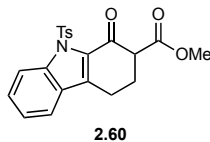


Known  $\beta$ -ketoesters **2.21**,<sup>36</sup> **2.55**,<sup>56</sup> **2.56**,<sup>57</sup> **2.57**,<sup>58</sup> and **2.58**<sup>55</sup> were prepared according to the same procedure. Their characterization data matched the reported values.



**Dimethyl 4-methoxy-8-oxo-5,6,7,8-tetrahydronaphthalene-1,7-dicarboxylate (2.59)**: Methyl 8-methoxy-4-oxo-tetralin-5-carboxylate<sup>59</sup> (325 mg, 1.39 mmol) was dissolved in THF (1 mL) and dimethyl carbonate (5 mL) and sodium hydride (60% suspension in mineral oil, 106 mg, 2 equiv.) was added at room temperature. The reaction mixture was heated to 110 °C until judged complete by TLC analysis. The reaction mixture was cooled to room temperature and was poured onto ice and diluted with 1M HCl and ethyl acetate. The layers were separated and the aqueous layer was washed with two additional portions of ethyl acetate. The combined organic layers were dried over Na<sub>2</sub>SO<sub>4</sub> and concentrated by rotary evaporator before being purified by flash column chromatography eluting with hexanes/EtOAc to afford 406 mg (59% yield) of the title compound as a white solid. **<sup>1</sup>H NMR** (500 MHz, CDCl<sub>3</sub>)  $\delta$  7.31 (d,  $J$  = 8.3 Hz, 1H), 7.00 (d,  $J$  = 8.3 Hz, 1H), 3.89 (s, 3H), 3.88 (s, 3H), 3.76 (s, 3H), 3.66 (dd,  $J$  = 10.3, 4.8 Hz, 1H), 3.10 (dt,  $J$  = 18.1, 5.3 Hz, 1H), 2.81 (ddd,  $J$  = 18.0, 9.3, 5.1 Hz, 1H), 2.49 – 2.41 (m, 1H), 2.39 – 2.30 (m, 1H). **<sup>13</sup>C NMR** (126 MHz, CDCl<sub>3</sub>)  $\delta$  192.50, 170.52, 170.20, 157.72, 133.51, 131.01, 127.02, 126.40, 113.31, 55.96, 54.05, 52.75, 52.43, 25.53, 21.35. **IR** (cm<sup>-1</sup>): 2965.61, 1742.04, 1717.16, 1693.75, 1583.09,

1428.52, 1367.43, 1264.76, 1192.40, 1034.22, 954.32. **HRMS** (ESI<sup>+</sup>): Calculated for C<sub>15</sub>H<sub>16</sub>O<sub>6</sub>Na<sup>+</sup> [M+Na<sup>+</sup>]<sup>+</sup>: 315.0845 Found [M+Na<sup>+</sup>]<sup>+</sup>: 315.0834.



**Methyl 1-oxo-9-tosyl-2,3,4,9-tetrahydro-1H-carbazole-2-carboxylate (2.60):**

Diisopropylamine (0.46 mL, 3.30 mmol, 2 equiv.) was dissolved in THF (10 mL) and cooled to -78 °C. n-Butyllithium (2.5 M in hexanes, 1.3 mL, 3.3 mmol, 2 equiv.) was added dropwise via syringe and the mixture was allowed to stir at -78 °C for 30 minutes. 9-tosyl-2,3,4,9-tetrahydro-1H-carbazol-1-one<sup>60</sup> (560 mg, 1.65 mmol, 1 equiv.) in THF (5 mL) was added dropwise via syringe and allowed to stir for 30 minutes at -78 °C. Methyl cyanofomate (0.27 mL, 3.30 mmol, 2 equiv.) was added dropwise and the reaction mixture was slowly allowed to warm to room temperature. When judged complete by TLC, the reaction was quenched with saturated aqueous ammonium chloride and diluted with ethyl acetate. The layers were separated and the aqueous layer was washed with two additional portions of EtOAc. The combined organic layers were dried over Na<sub>2</sub>SO<sub>4</sub> and concentrated by rotary evaporator before being purified by flash column chromatography eluting with hexanes/EtOAc to afford 656 mg (50% yield) of the title compound as a yellow solid. <sup>1</sup>H NMR (700 MHz, CDCl<sub>3</sub>) δ 8.34 (d, *J* = 8.6 Hz, 1H), 8.07 – 8.01 (m, 2H), 7.62 (d, *J* = 7.8 Hz, 1H), 7.59 – 7.54 (m, 1H), 7.35 (t, *J* = 7.3 Hz, 1H), 7.32 – 7.27 (m, 2H), 3.73 (s, 3H), 3.67 – 6.42 (m, 1H), 3.13 (ddd, *J* = 17.4, 7.0, 5.2 Hz, 1H), 2.96 (ddd, *J* = 17.3, 7.0, 5.3 Hz, 1H), 2.62 – 2.55 (m, 1H), 2.44 – 2.36 (m, 4H). <sup>13</sup>C NMR (176 MHz, CDCl<sub>3</sub>) δ 182.68, 170.24, 144.71, 140.03, 137.53, 137.01, 131.42, 129.70, 129.54, 127.87, 127.02, 123.91, 121.45, 116.18, 54.84, 52.68, 27.18, 26.07, 21.83, 20.10. **IR** (cm<sup>-1</sup>): 2951.44, 1737.80, 1673.85, 1598.33, 1555.91, 1360.28, 1311.67, 1264.13, 1220.34, 1141.36, 1093.28, 980.78, 958.37. **HRMS** (ESI<sup>+</sup>): Calculated for C<sub>21</sub>H<sub>19</sub>NO<sub>5</sub>SNa<sup>+</sup> [M+Na<sup>+</sup>]<sup>+</sup>: 420.0875 Found [M+Na<sup>+</sup>]<sup>+</sup>: 420.0846.

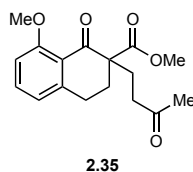
**Sc(OTf)<sub>3</sub>- and Y(OTf)<sub>3</sub>-Catalyzed Asymmetric Michael Addition**

*General Procedure A* for Y(OTf)<sub>3</sub>-catalyzed asymmetric Michael addition: Y(OTf)<sub>3</sub> (0.0075 mmol, 0.05 equiv.) and bipyridine ligand **1** (0.015 mmol, 0.1 equiv.) were combined in benzene (1.2 mL) and stirred at 80 °C for 30 minutes. The reaction mixture was diluted with benzene (2.6 mL) and starting material (0.15 mmol, 1 equiv. 0.04M) was added followed by methyl vinyl ketone (0.30 mmol, 25 μL, 2 equiv.) and the reaction was allowed to stir until complete by TLC analysis.

After cooling to room temperature, the reaction mixture was dry loaded onto silica gel and purified by flash column chromatography.

*General procedure B* for Sc(OTf)<sub>3</sub>-catalyzed asymmetric Michael addition: Sc(OTf)<sub>3</sub> (0.0075 mmol, 0.05 equiv.) and bipyridine ligand **1** (0.015 mmol, 0.1 equiv.) were combined in DCE (1.2 mL) and stirred at 60 °C for 30 minutes. The reaction mixture was diluted with DCE (6.4 mL) and starting material (0.15 mmol, 1 equiv. 0.04M) was added followed by methyl vinyl ketone (0.30 mmol, 25 μL, 2 equiv.) and the reaction was allowed to stir for 96 hours. After cooling to room temperature, the reaction mixture was loaded directly onto silica gel and purified by flash column chromatography.

Racemic standards of compounds were prepared by either general procedure with the omission of ligand.



**Methyl 8-methoxy-1-oxo-2-(3-oxobutyl)-1,2,3,4-tetrahydronaphthalene-2-carboxylate (2.35):**

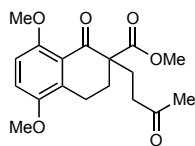
General Procedure A (35 mg, 0.15 mmol) afforded 43 mg (94% yield) of product **2.35** (90% ee).

**HPLC** [Diacel ChiralPak AS-H column] (10% isopropanol/hexanes) [22.960 (major), 25.909 (minor)]. [ $\alpha$ ]<sub>D</sub> = -37.4 (c=0.20, DCM).

General Procedure B (35 mg, 0.15 mmol) afforded 7 mg (15% yield) of product **2.35** (-85% ee).

**HPLC** [Diacel ChiralPak AS-H column] (10% isopropanol/hexanes) [22.957 (minor), 25.741 (major)]. [ $\alpha$ ]<sub>D</sub> = +43.9 (c=0.15, DCM).

**<sup>1</sup>H NMR** (400 MHz, CDCl<sub>3</sub>)  $\delta$  7.38 (t, *J* = 8.0 Hz, 1H), 6.82 (d, *J* = 8.3 Hz, 1H), 6.77 (d, *J* = 7.6 Hz, 1H), 3.91 (s, 3H), 3.67 (s, 3H), 3.11 – 2.99 (m, 1H), 2.93 (dt, *J* = 17.6, 5.1 Hz, 1H), 2.81 – 2.67 (m, 1H), 2.60 – 2.45 (m, 2H), 2.27 – 2.17 (m, 1H), 2.15 (s, 3H), 2.13 – 1.98 (m, 2H). **<sup>13</sup>C NMR** (126 MHz, CDCl<sub>3</sub>)  $\delta$  208.2, 194.6, 172.8, 161.0, 145.3, 134.3, 121.8, 120.8, 110.1, 58.0, 56.2, 52.5, 39.4, 31.3, 30.1, 28.3, 26.7. **IR** (cm<sup>-1</sup>): 2950.61, 1714.32, 1678.92, 1577.97, 1470.13, 1452.99, 1435.26, 1354.45, 1307.01, 1268.94, 1190.72, 1167.16, 1087.68, 1087.68, 1001.10, 954.19, 915.11 **HRMS** (ESI<sup>+</sup>): Calculated for C<sub>17</sub>H<sub>20</sub>O<sub>5</sub>Na<sup>+</sup> [M+Na<sup>+</sup>]<sup>+</sup>: 327.1203 Found [M+Na<sup>+</sup>]<sup>+</sup>: 327.1210.



2.24

**Methyl 5,8-dimethoxy-1-oxo-2-(3-oxobutyl)-1,2,3,4-tetrahydronaphthalene-2-carboxylate (2.24):**

General Procedure A (40 mg, 0.15 mmol) afforded 50 mg (99% yield) of product **2.24** (95% ee).

**HPLC** [Diacel ChiralPak OD-H column] (10% isopropanol/hexanes) [35.200 (minor), 38.482 (major)].  $[\alpha]_D = +23.1$  (c=2.2, MeOH).

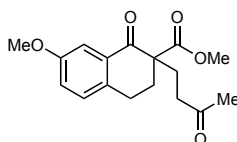
General Procedure B (40 mg, 0.15 mmol) afforded 16 mg (31% yield) of product **2.24** (-90% ee).

**HPLC** [Diacel ChiralPak OD-H column] (10% isopropanol/hexanes) [31.646(major), 39.358 (minor)].  $[\alpha]_D = -23.4$  (c=1.4, MeOH).

Characterization data reproduced from our previous report on the total synthesis of lingzhiol:<sup>36</sup> **<sup>1</sup>H**

**NMR** (500 MHz, CDCl<sub>3</sub>)  $\delta$  6.95 (d,  $J = 9.0$  Hz, 1H), 6.79 (d,  $J = 9.0$  Hz, 1H), 3.85 (s, 3H), 3.80 (s, 3H), 3.64 (s, 3H), 2.98 – 2.79 (m, 2H), 2.72 (ddd,  $J = 16.0, 10.6, 5.1$  Hz, 1H), 2.53 (ddd,  $J = 19.1, 10.5, 5.2$  Hz, 2H), 2.20 (ddd,  $J = 15.5, 10.6, 5.1$  Hz, 1H), 2.14 (s, 3H), 2.11 – 1.94 (m, 2H).

**<sup>13</sup>C NMR** (176 MHz, CDCl<sub>3</sub>)  $\delta$  208.1, 195.0, 172., 154.3, 150.2, 133.3, 122.7, 115.3, 110.4, 57.5, 56.6, 56.0, 52.4, 39.4, 30.6, 30.0, 27.9, 20.6. **IR** (cm<sup>-1</sup>): 2950.8, 2837.0, 1713.8, 1689.5, 1586.8, 1475.8, 1434.6, 1259.1, 1195.3, 1167.22, 1098.3, 1066.0, 980.4, 804.57. **HRMS** Calculated for C<sub>18</sub>H<sub>22</sub>O<sub>6</sub>Na<sup>+</sup> [M+Na<sup>+</sup>]: 357.1309 Found: 357.1312.



2.36

**Methyl 7-methoxy-1-oxo-2-(3-oxobutyl)-1,2,3,4-tetrahydronaphthalene-2-carboxylate (2.36):**

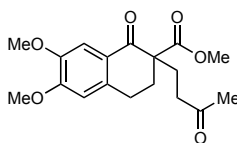
General Procedure A (35 mg, 0.15 mmol) afforded 43 mg (94% yield) of product **17** (17% ee).

**HPLC** [Diacel ChiralPak IA column] (10% isopropanol/hexanes) [12.007 (major), 14.715 (minor)].  $[\alpha]_D = +9.2$  (c=0.09, DCM).

General Procedure B (35 mg, 0.15 mmol) afforded 21 mg (46% yield) of product **17** (-90% ee).

**HPLC** [Diacel ChiralPak IA column] (10% isopropanol/hexanes) [12.062 (minor), 14.754 (major)].  $[\alpha]_D = -70.5$  (c=0.07, DCM).

**<sup>1</sup>H NMR** (400 MHz, CDCl<sub>3</sub>) δ 7.50 (s, 1H), 7.12 (d, *J* = 8.5 Hz, 1H), 7.05 (d, *J* = 8.4 Hz, 1H), 3.84 (s, 3H), 3.68 (s, 3H), 2.99 – 2.84 (m, 2H), 2.76 – 2.65 (m, 1H), 2.60 – 2.50 (m, 2H), 2.29 – 2.03 (m, 6H). **<sup>13</sup>C NMR** (126 MHz, CDCl<sub>3</sub>) δ 207.9, 195.6, 172.5, 158.6, 135.6, 132.7, 130.1, 122.4, 109.9, 56.7, 55.6, 52.6, 39.3, 32.1, 30.1, 27.8, 25.2. **IR** (cm<sup>-1</sup>): 2952.47, 1715.41, 1682.29, 1609.34, 1575.17, 1496.94, 1421.02, 1353.72, 1328.78, 1280.07, 1196.17, 1095.06, 983.31. **HRMS** (ESI<sup>+</sup>): Calculated for C<sub>17</sub>H<sub>20</sub>O<sub>5</sub>Na<sup>+</sup> [M+Na<sup>+</sup>]<sup>+</sup>: 327.1203 Found [M+Na<sup>+</sup>]<sup>+</sup>: 327.1201.



2.37

**Methyl 6,7-dimethoxy-1-oxo-2-(3-oxobutyl)-1,2,3,4-tetrahydronaphthalene-2-carboxylate (2.37):**

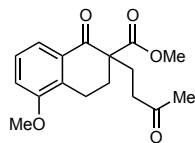
General Procedure A (40 mg, 0.15 mmol) afforded 46 mg (92% yield) of product **2.37** (7% ee).

**HPLC** [Diacel ChiralCel OD-H column] (10% isopropanol/hexanes) [24.464 (minor), 28.694 (minor)]. [α]<sub>D</sub> = +5.7 (c=0.06, DCM).

General Procedure B (40 mg, 0.15 mmol) afforded 15 mg (29% yield) of product **2.37** (-90% ee).

**HPLC** [Diacel ChiralCel OD-H column] (10% isopropanol/hexanes) [24.308 (major), 29.337 (minor)]. [α]<sub>D</sub> = -82.7 (c=0.02, DCM).

**<sup>1</sup>H NMR** (400 MHz, CDCl<sub>3</sub>) δ 7.50 (s, 1H), 6.62 (s, 1H), 3.93 (s, 3H), 3.91 (s, 3H), 3.69 (s, 3H), 2.98 – 2.86 (m, 2H), 2.71 – 2.63 (m, 1H), 2.60 – 2.51 (m, 2H), 2.32 – 1.93 (m, 6H). **<sup>13</sup>C NMR** (126 MHz, CDCl<sub>3</sub>) δ 208.0, 194.3, 172.7, 154.0, 148.3, 138.0, 125.0, 110.2, 109.2, 56.2, 56.1, 52.6, 39.3, 32.1, 30.1, 27.8, 25.8. **IR** (cm<sup>-1</sup>): 2951.22, 1716.95, 1666.86, 1597.83, 1587.82, 1511.3, 1470.68, 1444.29, 1414.16, 1371.13, 1333.16, 1307.16, 1264.03, 1179.85, 1128.40, 1094.58, 1058.78, 1015.98, 977.54, 915.98. **HRMS** (ESI<sup>+</sup>): Calculated for C<sub>18</sub>H<sub>22</sub>O<sub>6</sub>Na<sup>+</sup> [M+Na<sup>+</sup>]<sup>+</sup>: 357.1309 Found [M+Na<sup>+</sup>]<sup>+</sup>: 357.1307.



2.38

**Methyl 5-methoxy-1-oxo-2-(3-oxobutyl)-1,2,3,4-tetrahydronaphthalene-2-carboxylate (2.38):**

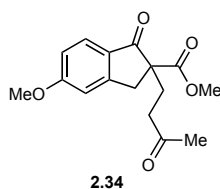
General Procedure A (35 mg, 0.15 mmol) afforded 43 mg (94% yield) of product **2.38** (13% ee).

**HPLC** [Diacel ChiralPak AD-H column] (10% isopropanol/hexanes) [14.639 (major), 19.915 (minor)].  $[\alpha]_D = +5.6$  (c=0.09, DCM).

General Procedure B (35 mg, 0.15 mmol) afforded 40 mg (89% yield) of product **2.38** (-97% ee).

**HPLC** [Diacel ChiralPak AD-H column] (10% isopropanol/hexanes) [14.619 (minor), 19.880 (major)].  $[\alpha]_D = -38.9$  (c=0.10, DCM).

**<sup>1</sup>H NMR** (400 MHz, CDCl<sub>3</sub>)  $\delta$  7.63 (d,  $J = 7.8$  Hz, 1H), 7.29 (d,  $J = 8.0$  Hz, 1H), 7.01 (d,  $J = 8.1$  Hz, 1H), 3.86 (s, 3H), 3.67 (s, 3H), 2.95 – 2.82 (m, 1H), 2.70 – 2.63 (m, 1H), 2.60 – 2.52 (m, 1H), 2.50 – 2.45 (m, 2H), 2.25 – 2.02 (m, 6H). **<sup>13</sup>C NMR** (126 MHz, CDCl<sub>3</sub>)  $\delta$  207.9, 195.9, 172.5, 156.8, 132.9, 132.00, 127.3, 119.6, 114.5, 56.4, 55.8, 52.6, 39.3, 31.0, 30.1, 27.6, 19.9. **IR** (cm<sup>-1</sup>): 2952.96, 171538, 1686.4, 1584.0, 1472.37, 1437.72, 1352.75, 1318.94, 1259.76, 1220.76, 1197.44, 1167.75, 1094.42, 1067.10, 1048.25, 978.77, 943.49. **HRMS** (ESI<sup>+</sup>): Calculated for C<sub>17</sub>H<sub>20</sub>O<sub>5</sub>Na<sup>+</sup> [M+Na<sup>+</sup>]<sup>+</sup>: 327.1203 Found [M+Na<sup>+</sup>]<sup>+</sup>: 327.1208.



**Methyl 5-methoxy-1-oxo-2-(3-oxobutyl)-2,3-dihydro-1H-indene-2-carboxylate (2.34):**

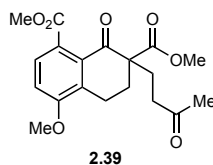
General Procedure A (33 mg, 0.15 mmol) afforded 43 mg (99% yield) of product **2.34** (24% ee).

**HPLC** [Diacel ChiralCel OD-H column] (10% isopropanol/hexanes) [18.926 (minor), 21.556 (major)].  $[\alpha]_D = -29.4$  (c=0.05, DCM).

General Procedure B (35 mg, 0.15 mmol) afforded 40 mg (93% yield) of product **2.34** (-93% ee).

**HPLC** [Diacel ChiralCel OD-H column] (10% isopropanol/hexanes) [18.823 (major), 21.783 (minor)].  $[\alpha]_D = +92.4$  (c=0.07, DCM).

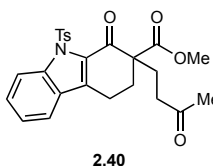
**<sup>1</sup>H NMR** (400 MHz, CDCl<sub>3</sub>)  $\delta$  7.70 (d,  $J = 8.5$  Hz, 1H), 6.93 (d,  $J = 8.5$  Hz, 1H), 6.89 (s, 1H), 3.89 (s, 3H), 3.69 (s, 3H), 3.65 (d,  $J = 17.3$  Hz, 1H), 2.97 (d,  $J = 17.4$  Hz, 1H), 2.65 – 2.43 (m, 2H), 2.28 – 2.19 (m, 2H), 2.13 (s, 3H). **<sup>13</sup>C NMR** (126 MHz, CDCl<sub>3</sub>)  $\delta$  207.7, 200.3, 171.9, 166.1, 155.8, 128.4, 126.7, 116.3, 109.6, 59.5, 55.9, 52.9, 39.0, 37.9, 30.1, 28.8. **IR** (cm<sup>-1</sup>): 2952.18, 1737.99, 1699.53, 1596.30, 1491.06, 1434.31, 1369.78, 1338.07, 1257.41, 1169.22, 1147.63, 1086.98, 1020.23, 967.36, 931.67, 912.56. **HRMS** (ESI<sup>+</sup>): Calculated for C<sub>16</sub>H<sub>18</sub>O<sub>5</sub>Na<sup>+</sup> [M+Na<sup>+</sup>]<sup>+</sup>: 313.1046 Found [M+Na<sup>+</sup>]<sup>+</sup>: 313.1053.



**Dimethyl 4-methoxy-8-oxo-7-(3-oxobutyl)-5,6,7,8-tetrahydronaphthalene-1,7-dicarboxylate (2.39):** General Procedure A (44 mg, 0.15 mmol) afforded 52 mg (95% yield) of product **2.39** (97% ee).

**HPLC** [Diacel ChiralPak AD-H column] (10% isopropanol/hexanes) [45.862 (major), 61.028 (minor)].  $[\alpha]_D = +40.9$  (c=0.57, DCM).

**<sup>1</sup>H NMR** (400 MHz, CDCl<sub>3</sub>)  $\delta$  7.34 (d,  $J = 8.3$  Hz, 1H), 2.96 (d, 8.5 Hz, 1H), 3.90 – 3.84 (m, 6H), 3.68 (s, 3H), 3.00 – 2.92 (m, 1H), 2.89 – 2.83 (m, 1H), 2.74 – 2.62 (m, 1H), 2.62 – 2.45 (m, 2H), 2.27 – 2.18 (m, 1H), 2.12 – 1.56 (m, 4H). **<sup>13</sup>C NMR** (126 MHz, CDCl<sub>3</sub>)  $\delta$  207.82, 195.19, 172.07, 170.50, 157.86, 132.66, 132.08, 127.49, 126.44, 112.80, 56.67, 55.97, 52.75, 52.63, 39.08, 31.13, 30.09, 27.66, 20.13. **IR** (cm<sup>-1</sup>): 2951.88, 1718.63, 1693.63, 1585.45, 1432.01, 1312.66, 1256.46, 1193.72, 1170.17, 1068.89, 1010.72. **HRMS** (ESI<sup>+</sup>): Calculated for C<sub>19</sub>H<sub>22</sub>O<sub>7</sub>Na<sup>+</sup> [M+Na<sup>+</sup>]<sup>+</sup>: 385.1263 Found [M+Na<sup>+</sup>]<sup>+</sup>: 385.1256.



**Methyl 1-oxo-2-(3-oxobutyl)-9-tosyl-2,3,4,9-tetrahydro-1H-carbazole-2-carboxylate (2.40):**

General Procedure A (60 mg, 0.15 mmol) afforded 66 mg (94% yield) of product **2.40** (87% ee).

**HPLC** [Diacel ChiralPak IA column] (10% isopropanol/hexanes) [9.614 (minor), 10.442 (major)].  $[\alpha]_D = +8.8$  (c=2.0, DCM).

**<sup>1</sup>H NMR** (700 MHz, CDCl<sub>3</sub>)  $\delta$  8.28 (d,  $J = 8.5$  Hz, 1H), 8.08 – 8.03 (m, 2H), 7.64 – 7.49 (m, 2H), 7.37 – 7.27 (m, 3H), 3.67 (s, 3H), 3.09 – 3.01 (m, 1H), 2.98 (d,  $J = 17.5$  Hz, 1H), 2.71 – 2.59 (m, 2H), 2.59 – 2.49 (m, 1H), 2.41 (s, 3H), 2.28 – 2.19 (m, 1H), 2.19 – 2.00 (m, 5H). **<sup>13</sup>C NMR** (176 MHz, CDCl<sub>3</sub>)  $\delta$  207.84, 185.30, 171.98, 144.66, 139.98, 137.07, 136.16, 132.09, 129.56, 129.39, 127.82, 127.06, 123.89, 121.37, 116.13, 58.03, 52.74, 39.06, 32.89, 30.12, 27.83, 21.81, 19.12. **IR** (cm<sup>-1</sup>): 2950.33, 1731.92, 1671.77, 1600.39, 1557.39, 1405.96, 1360.25, 1224.78, 1174.60, 955.78. **HRMS** (ESI<sup>+</sup>): Calculated for C<sub>25</sub>H<sub>25</sub>NO<sub>6</sub>SN<sup>+</sup> [M+Na<sup>+</sup>]<sup>+</sup>: 490.1295 Found [M+Na<sup>+</sup>]<sup>+</sup>: 490.1253.

### 2.4.3 Mechanistic Experiments

#### Ionic Radii Values

Table 2.7 Ionic radii of the lanthanide(III) triflate catalysts.

entry	Metal	<i>ir</i> (Å) <sup>a</sup>	ee
1	Sc <sup>3+</sup>	0.870	-90% ee
2	Lu <sup>3+</sup>	0.977	82% ee
3	Yb <sup>3+</sup>	0.985	84% ee
4	Tm <sup>3+</sup>	0.994	86% ee
5	Er <sup>3+</sup>	1.004	89% ee
6	Ho <sup>3+</sup>	1.015	89% ee
7	Y <sup>3+</sup>	1.019	91% ee
8	Dy <sup>3+</sup>	1.027	90% ee
9	Tb <sup>3+</sup>	1.040	90% ee
10	Gd <sup>3+</sup>	1.053	87% ee
11	Eu <sup>3+</sup>	1.066	83% ee
12	Sm <sup>3+</sup>	1.079	74% ee
13	Nd <sup>3+</sup>	1.109	13% ee
14	Pr <sup>3+</sup>	1.126	-23% ee
15	La <sup>3+</sup>	1.160	-43% ee

#### Non-Linear Effect Studies

Enantiomerically pure (>99% ee) (*R,R*)-**1** and (*S,S*)-**1** were combined in various ratios on ~20 mg scale in 1 dram scintillation vials and dissolved fully in DCM and then concentrated by rotary evaporator. HPLC analysis determined the enantiomeric excess of the five mixtures to be 7%, 26%, 42%, 68%, and 88%. Each of these was used as ligand according to *General Procedure A* and the enantiomeric excess of product **6** was determined by HPLC analysis. The ee of the ligand was plotted against the ee of product **6** to show a linear correlation between ligand ee and product ee for Y(OTf)<sub>3</sub>. The same experiment was repeated with *General Procedure B* to show a linear relationship for the Sc(OTf)<sub>3</sub> system.

This data is summarized in Figure 2.4.

#### NMR Studies

NMR samples containing varying ratios of M(OTf)<sub>3</sub> and ligand **2.23** were prepared for both Sc(OTf)<sub>3</sub> in *d*<sub>4</sub>-DCE and for Y(OTf)<sub>3</sub> in *d*<sub>6</sub>-benzene. A 2 mL stock solution of ligand in the appropriate NMR solvent (5 mg/mL) was prepared.

Five screw-top NMR tubes were each charged with 0.4 mg Sc(OTf)<sub>3</sub> and 10 μL, 50 μL, 100 μL, 200 μL, and 500 μL of the stock solution of **2.23** in *d*<sub>4</sub>-DCE was added. Enough *d*<sub>4</sub>-DCE was then added to bring the total volume in the tube to 760 μL. The tubes were sealed and heated at 60 °C



in a water bath for 30 minutes, and then the  $^1\text{H}$  NMR spectra were acquired at  $60\text{ }^\circ\text{C}$ . In accordance with a previous report by Kobayashi and coworkers,<sup>42</sup> the chemical shift of the benzylic methine peak of **2.23** changed significantly depending on the metal-to-ligand ratio, corresponding to a shift in equilibrium between monometallic complex **2.25** and bimetallic complex **2.26**, as illustrated in Figure S1 and Figure S2. The same procedure was repeated for  $\text{Y}(\text{OTf})_3$  in benzene at  $80\text{ }^\circ\text{C}$  and with final volumes of  $d_6$ -benzene of  $380\text{ }\mu\text{L}$ .

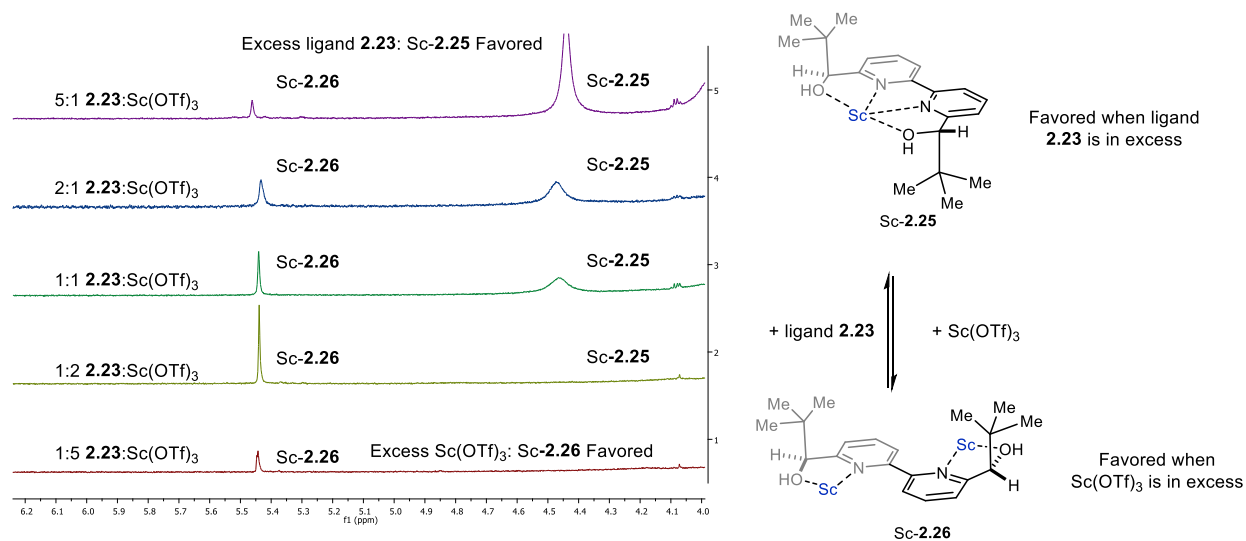


Figure 2.11 Observed shift of the methine signal in  $^1\text{H}$  NMR of ligand **2.23** at different ratios of **2.23** and  $\text{Sc}(\text{OTf})_3$  in  $d_6$ -benzene

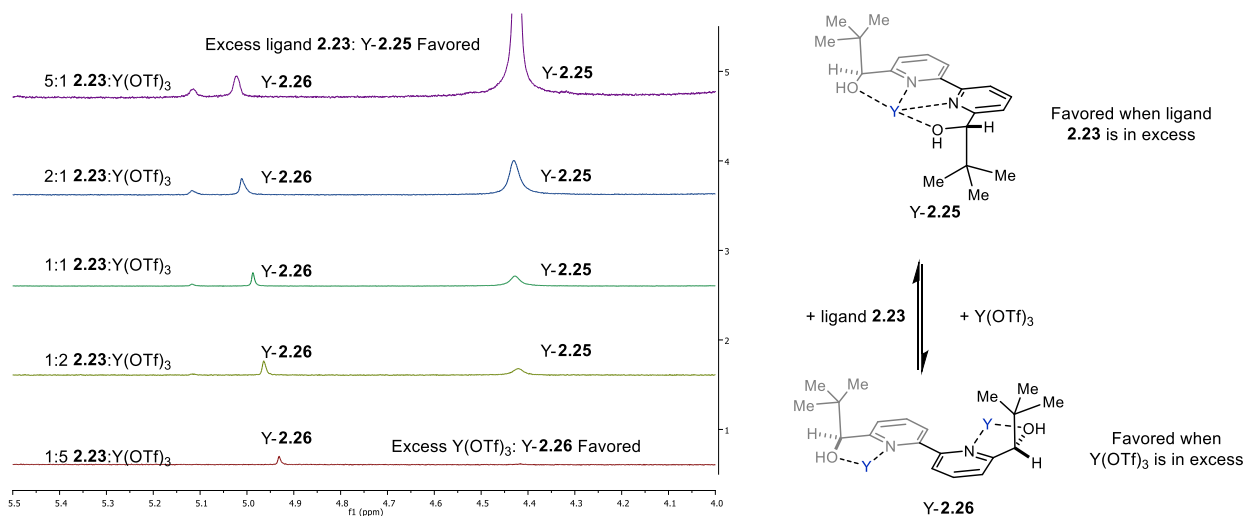


Figure 2.12 Observed shift of the methine signal in  $^1\text{H}$  NMR of ligand **2.23** at different ratios of **2.23** and  $\text{Y}(\text{OTf})_3$  in  $d_4$ -DCE.

In both cases, excess  $\text{M}(\text{OTf})_3$  shows the major species is associated with the peak at  $4.9\text{ ppm}$  (species **2.26**) while excess ligand **1** leads to a preference for the peak at  $4.4\text{ ppm}$  (species **2.25**).

This is consistent with the previous report by Kobayashi detailing a similar experiment with  $\text{Bi}(\text{OTf})_3$  and ligand **2.23**.<sup>42</sup> Under the optimized reaction conditions for both  $\text{Y}(\text{OTf})_3$  and  $\text{Sc}(\text{OTf})_3$  with excess ligand relative to  $\text{M}(\text{OTf})_3$ , species **2.25** is the major species.

### Kinetic Analysis

The results of these experiments are summarized in Figure 2.6.

Based on our optimization of these reactions, the highest enantioselectivity was achieved with a 2:1 ratio of ligand **2.23** to metal. As a result, this ratio was maintained in these kinetic experiments. The loading of both metal and ligand were varied while keeping the ratio of ligand **2.23** to metal 2:1. The optimal solvent was DCE (60°C, 0.02M) for  $\text{Sc}(\text{OTf})_3$  and benzene (80 °C, 0.04M) for  $\text{Y}(\text{OTf})_3$ , but good enantioselectivity and the reversal of enantioselectivity was observed with  $\text{Y}(\text{OTf})_3$  in DCE (60 °C, 0.02M). To maintain consistency between the two reactions, orders for both  $\text{Sc}/\mathbf{2.23}$  and  $\text{Y}/\mathbf{2.23}$  were determined in DCE at 60 °C and 0.018 M. Rates were determined based on formation of product **2.24**. The reactions were monitored by UPLC using caffeine as an internal standard. A stock solution of 2.55 mg caffeine/100 mL (0.13 mM) of acetonitrile was added to all UPLC samples to measure yield of **2.24**. The relative peak area ( $R_f$ ) between caffeine and product **2.24** was determined to be 0.997507 with an  $R^2$  of 0.99973 between 0.02 mg/mL ( $4.73 \times 10^{-8}$  mol/sample) and 0.4 mg/mL ( $1.18 \times 10^{-6}$  mol/sample) of **2.24**. This value was used in later calculations to determine UPLC yield of **2.24**.

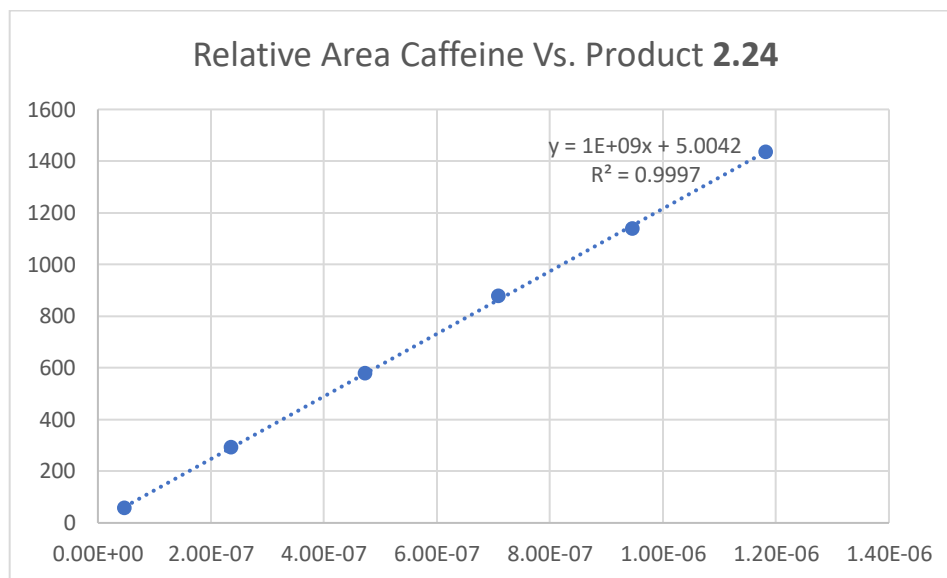


Figure 2.13 Plot of the relative area of caffeine vs. product **2.24**.

Experimental procedure for 2.5%  $\text{Y}(\text{OTf})_3$  and 5% ligand **2.23**:

A stock solution of 2:1 ligand **2.23** to Y(OTf)<sub>3</sub> was prepared by heating 2.5 mg Y(OTf)<sub>3</sub> and 3.1 mg **1** in DCE (2 mL) at 60 °C for 30 minutes. These solutions were then diluted to 10 mL and 50 mg (0.189 mmol) substrate **2.21** was added. 3 mL of this solution (corresponding to 15 mg (0.057 mmol) of **2.21**) was transferred to a vial and stirring continued at 60 °C. 10 μL (0.126 mmol, 2.2 equiv.) of MVK was added (T<sub>0</sub>). Every three minutes for a 30-minute interval, a 20 μL aliquot was taken from the reaction mixture and diluted into an HPLC vial containing 900 μL of acetonitrile and 80 μL of a 0.13 mM stock solution of caffeine in acetonitrile. The samples were then analyzed by UPLC analysis using an Agilent 1290 Infinity II system equipped with an InifinityLab Poroshell 120 C-18 column eluting with water/MeCN. This experiment was performed in triplicate and reaction rate was determined based on the average of the three replicates.

The same procedure was employed to measure reaction rates for 5% Y(OTf)<sub>3</sub> (5.1 mg) and 10% ligand **1** (6.2 mg) and for 7.5% Y(OTf)<sub>3</sub> (7.6 mg) and 15% ligand **2.23** (9.3 mg).

Rate calculations:

The rate of product formation was determined as the slope of the plot between yield of **2.24** (%) vs. time. 20 mL aliquots were calculated to have a theoretical 100% yield of 3.78x10<sup>-4</sup> mmol of **2.24** and the relative peak area between caffeine and product was calculated (above) to be 0.997507. 2.57x10<sup>-4</sup> mmol caffeine was calculated to have been added as an internal standard to each sample. The following formula was used to calculate yield of each UPLC sample:

*Equation 2.1* Formula used to determine yield based on UPLC data using caffeine as an internal standard.

$$Rf * \left( \frac{\text{area } \mathbf{2.24}}{\text{area caffeine}} \right) * \left( \frac{\text{mmol caffeine}}{\text{theoretical yield}} \right) * 100$$

Error bars are represented as the standard deviation.

Yield vs time for 2.5 mol% Y(OTf)<sub>3</sub> and 5 mol% ligand **2.23**:

Table 2.8 Yield values of **2.24** using 2.5 mol% Y(OTf)<sub>3</sub> and 5 mol% **2.23**. Determined using area of **2.24** vs. area of caffeine.

Time (min)	Area <b>2.24</b>			Area Caffeine			Yield (%)			Avg. Yield (%)
3	3.55	5.29	5.15	489.89	491.96	491.96	0.49	0.73	0.71	0.64
6	6.46	7.93	8.23	492.34	493.51	492.46	0.89	1.09	1.14	1.04
9	9.55	12.06	10	495.23	495.08	496.43	1.31	1.66	1.37	1.44
12	13.84	13.43	15.27	497.68	493.01	494.94	1.89	1.85	2.10	1.95
15	12.1	20.27	19.29	499.38	496.73	496.36	1.65	2.77	2.64	2.35
18	20.21	23.04	22.14	499.46	497.24	497.42	2.75	3.15	3.02	2.97
21	21.68	27.11	25.71	497.13	496.53	497.96	2.96	3.71	3.51	3.39

24	23.68	27.52	26.76	499.1	499.43	499.14	3.22	3.74	3.64	3.54
27	24.71	31.59	29.42	500.91	499.42	498.75	3.35	4.30	4.01	3.89
30	46.12	49.61	48.49	506.85	501.09	500.27	6.18	6.73	6.59	6.50

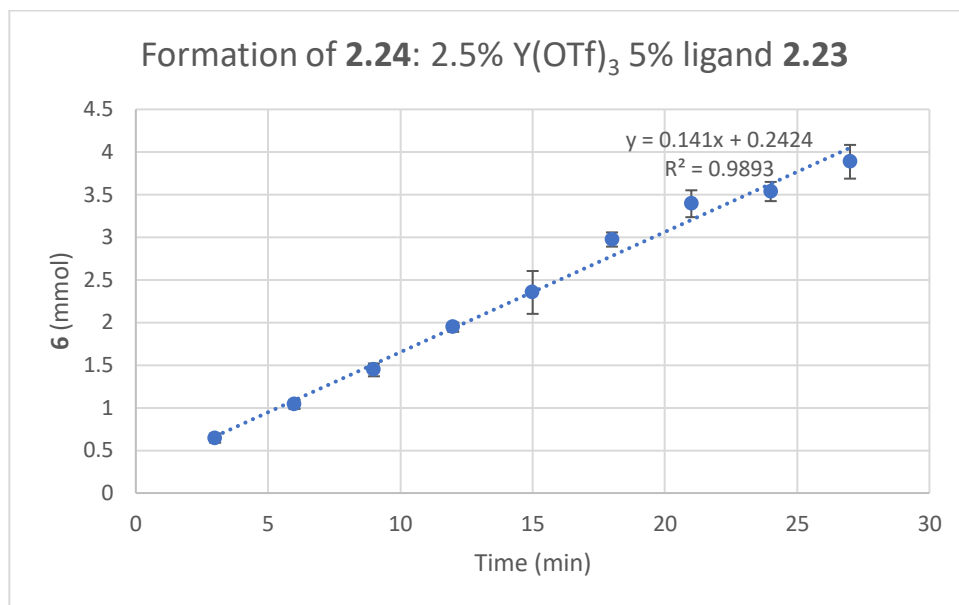


Figure 2.14 Plot of yield of **2.24** over time with 2.5 mol% Y(OTf)<sub>3</sub> and 5 mol% **2.23**.

**Rate:** 0.1410 mmol/min

Yield vs time for 5 mol% Y(OTf)<sub>3</sub> and 10 mol% ligand **2.23**:

Table 2.9 Yield values of **2.24** using 5 mol% Y(OTf)<sub>3</sub> and 10 mol% **2.23**. Determined using area of **2.24** vs. area of caffeine.

Time (min)	Area <b>2.24</b>			Area Caffeine			Yield (%)			Avg. Yield (%)
3	5.96	7.85	8.51	484.3	483.67	486.13	0.84	1.10	1.19	1.04
6	13.14	14.15	14.26	486.24	484.95	485.47	1.84	1.98	2.00	1.94
9	17.06	19.88	21.98	485.99	481.48	484.36	2.39	2.81	3.08	2.76
12	23.14	24.39	26.76	485.31	483.79	483.05	3.24	3.43	3.76	3.48
15	36.7	29.09	34.23	483.05	483.48	483.26	5.16	4.09	4.81	4.69
18	53.98	37.88	40.54	480.69	479.65	481.99	7.63	5.37	5.71	6.24
21	30.99	44.42	42.1	481.19	480.5	482.94	4.38	6.28	5.92	5.53
24	46.16	52.99	48.15	481.57	483.73	483.46	6.51	7.44	6.77	6.91
27	49.61	50.36	57.6	483.04	480.02	482.56	6.98	7.13	8.11	7.41
30	58.16	58.4	65.81	483.89	487.29	482.43	8.17	8.14	9.27	8.53

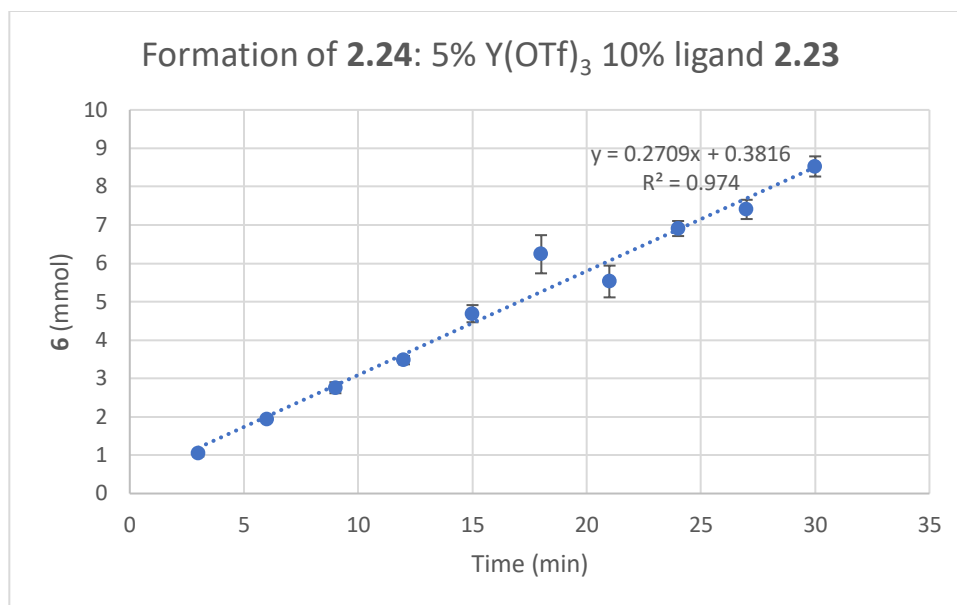


Figure 2.15 Plot of yield of **2.24** over time with 5 mol% Y(OTf)<sub>3</sub> and 10 mol% **2.23**.

**Rate:** 0.2709 mmol/min

Yield vs time for 7.5 mol% Y(OTf)<sub>3</sub> and 15 mol% ligand **2.23**:

Table 2.10 Yield values of **2.24** using 7.5 mol% Y(OTf)<sub>3</sub> and 15 mol% **2.23**. Determined using area of **2.24** vs. area of caffeine.

Time (min)	Area <b>2.24</b>			Area Caffeine			Yield (%)			Avg. Yield (%)
3	9.48	11.31	14.26	498.94	497.94	499.02	1.29	1.54	1.94	1.59
6	17.35	20.27	24.77	498.65	497.59	500.25	2.36	2.77	3.36	2.83
9	26.13	27.22	34.85	500.09	499.84	500.62	3.55	3.70	4.73	3.99
12	36.16	40.83	45.91	499.65	499.55	499.5	4.92	5.55	6.25	5.57
15	41.95	47.33	58.15	500.09	500.69	499.85	5.70	6.42	7.90	6.68
18	49.37	58.64	57.91	497.75	499.48	500.41	6.74	7.98	7.86	7.53
21	59.18	66.43	71.2	499.38	500.48	498.35	8.05	9.02	9.71	8.93
24	62.29	79.79	82.85	501.38	499.62	501.38	8.44	10.85	11.23	10.17
27	78.47	87.07	101.44	501.42	499.87	500.03	10.63	11.84	13.78	12.08
30	87.4	92.94	109.45	502.21	502.27	502.69	11.82	12.57	14.79	13.06

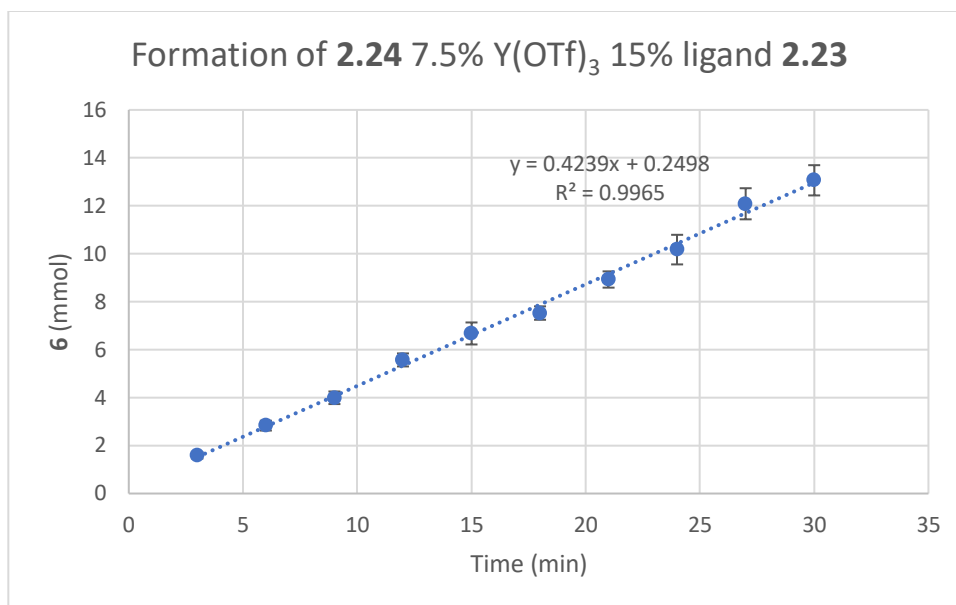


Figure 2.16 Plot of yield of **2.24** over time with 7.5 mol% Y(OTf)<sub>3</sub> and 15 mol% **2.23**.

**Rate:** 0.4239 mmol/min

Order determination for Y(OTf)<sub>3</sub>/**2.23**:

Y(OTf) <sub>3</sub> (mol%)	Rate (mmol/min)
2.5	0.1410
5.0	0.2709
7.5	0.4239

Rate order was determined according to the following equation, where  $m$  = rate and  $y$  = rate order:

Equation 2.2 Equation to determine Y(OTf)<sub>3</sub> rate order.

$$\ln\left(\frac{m_1}{m_2}\right) = y * \ln\left(\frac{\text{mol}\%_1}{\text{mol}\%_2}\right)$$

Solving for  $y$  using the following table determines an average rate order of  $1.02 \pm 0.07$ :

Loadings	Calc. order
5.0 vs. 2.5	0.942065
7.5 vs. 2.5	1.001935
7.5 vs. 5.0	1.104282
average order:	1.016094

Experimental procedure for 5% Sc(OTf)<sub>3</sub> and 10% ligand **2.23**:

A stock solution of 2:1 ligand **2.23** to Sc(OTf)<sub>3</sub> was prepared by heating 2.3 mg Sc(OTf)<sub>3</sub> and 3.1 mg **2.23** in DCE (2 mL) at 60 °C for 30 minutes. These solutions were then diluted to 10 mL and 50 mg (0.189 mmol) substrate **2.21** was added. 3 mL of this solution (corresponding to 15 mg (0.057 mmol) of **2.21**) was transferred to a vial and stirring continued at 60 °C. 10 μL (0.126 mmol, 2.2 equiv.) of MVK was added (T<sub>0</sub>). Every 30 minutes for a 420-minute interval, a 20 μL aliquot was taken from the reaction mixture and diluted into an HPLC vial containing 900 μL of acetonitrile and 80 μL of a 0.13 mM stock solution of caffeine in acetonitrile. The samples were then analyzed by UPLC analysis using an Agilent 1290 Infinity II system equipped with an InifinityLab Poroshell 120 C-18 column eluting with water/MeCN. This experiment was performed in triplicate and reaction rate was determined based on the average of the three replicates.

The same procedure was employed to measure reaction rates for for 7.5% Sc(OTf)<sub>3</sub> (7.6 mg) and 15% ligand **2.23** (9.3 mg). To ensure accurate measurement of 2.5 mol% Sc(OTf)<sub>3</sub>, the same procedure was performed on a larger scale: 5.8 mg Sc(OTf)<sub>3</sub> and 7.8 mg **1** were heated to 60 °C in DCE (5 mL) for 30 minutes before being diluted to 25 mL and 125 mg (0.473 mmol) of **2.21** was added. 3 mL of this solution (corresponding to 15 mg (0.057 mmol) of **2.21**) was transferred to a vial and heated at 60 °C before 10 mL of MVK (0.126 mmol, 2.2 equiv.) was added. UPLC sample preparation and yield calculations were unaffected by this change.

All calculations were performed using the same equations as for Y(OTf)<sub>3</sub> above.

Yield vs time for 2.5 mol% Sc(OTf)<sub>3</sub> and 5 mol% ligand **2.23**:

Table 2.11 Yield values of **2.24** using 2.5 mol% Sc(OTf)<sub>3</sub> and 5 mol% **2.23**. Determined using area of **2.24** vs. area of caffeine.

Time (min)	Area <b>2.24</b>			Area Caffeine			Yield (%)			Avg. Yield (%)
30	2.38	2.59	3.85	478.45	477.64	476.76	0.34	0.37	0.55	0.42
60	3.41	4.72	4.01	472.65	474.47	472.75	0.49	0.68	0.58	0.58
90	4.76	5.53	5.99	481.08	478	480	0.67	0.79	0.85	0.77
120	5.24	6.48	7.18	485.77	485.37	486.73	0.73	0.91	1.00	0.88
150	6.53	8.12	8.38	481.2	477.18	476.81	0.92	1.16	1.19	1.09
180	7.01	8.92	10	480.33	476.47	478.32	0.99	1.27	1.42	1.23
210	8.05	8.05	10.93	484.04	480.41	481	1.13	1.14	1.54	1.27
240	9.2	9.81	13.18	488.97	485.23	487.76	1.28	1.37	1.84	1.50
270	9.83	12.9	14.97	498.77	493.26	492.34	1.34	1.78	2.07	1.73

300	11.27	13.54	15.61	481.59	476.8	475.66	1.59	1.93	2.23	1.92
330	12.02	15.79	16.46	486.85	484.02	481.13	1.68	2.22	2.32	2.07
360	13.96	16.5	19.49	489.47	483.11	483.08	1.94	2.32	2.74	2.33
390	13.3	16.99	19.12	480.79	477.66	478.81	1.88	2.42	2.71	2.34
420	12.16	18.53	22.05	486.49	486.95	486.15	1.70	2.59	3.08	2.46

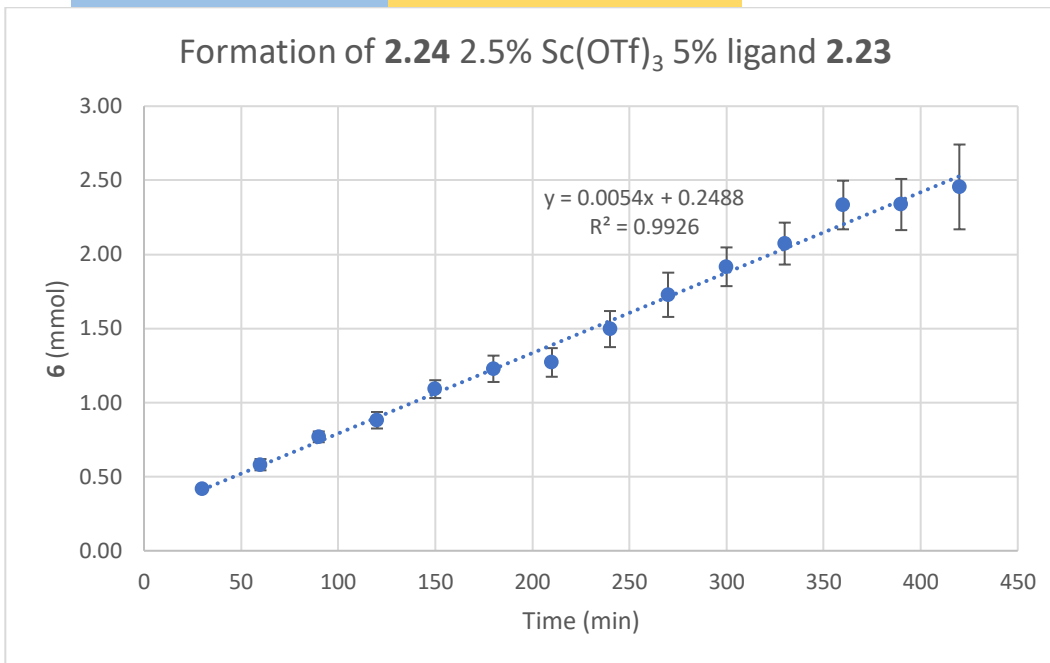


Figure 2.17 Plot of yield of **2.24** over time with 2.5 mol% Sc(OTf)<sub>3</sub> and 5 mol% **2.23**.

**Rate:** 0.00540 mmol/min

Yield vs time for 5 mol% Sc(OTf)<sub>3</sub> and 10 mol% ligand **2.23**:

Table 2.12 Yield values of **2.24** using 5 mol% Sc(OTf)<sub>3</sub> and 10 mol% **2.23**. Determined using area of **2.24** vs. area of caffeine.

Time (min)	Area <b>6</b>			Area Caffeine			Yield (%)			Avg. Yield (%)
30	4.21	3.09	2.38	487.22	488.28	489.03	0.59	0.43	0.33	0.45
60	5.25	5.29	4.84	492.67	492.02	493.29	0.72	0.73	0.67	0.71
90	7.58	7.42	6.12	492.57	492.09	492.38	1.05	1.02	0.84	0.97
120	9.8	9.39	8.24	496.89	496.66	497.42	1.34	1.28	1.13	1.25
150	11.98	11.35	9.84	493.51	494.03	494.45	1.65	1.56	1.35	1.52
180	14.19	11.87	10.7	501.48	500.54	501.5	1.92	1.61	1.45	1.66
210	15.77	14.89	11.65	504.85	504.17	504.7	2.12	2.01	1.57	1.90
240	17.42	17.64	14.25	503.12	504.47	504.44	2.35	2.38	1.92	2.22
270	19.44	18.27	13.27	477.47	475.41	473.54	2.77	2.61	1.90	2.43
300	22.91	22.23	18.13	478.36	468.99	484.94	3.25	3.22	2.54	3.01
330	24.21	23.78	20.46	474.84	480.52	477.55	3.46	3.36	2.91	3.25
360	28.51	28.34	22.19	479.95	482.36	484.3	4.04	3.99	3.11	3.71
390	27.19	29.23	23.21	475.52	478.44	478.79	3.89	4.15	3.29	3.78



420 29.86 30.62 25.93 484.34 462.94 480.98 4.19 4.49 3.66 4.12

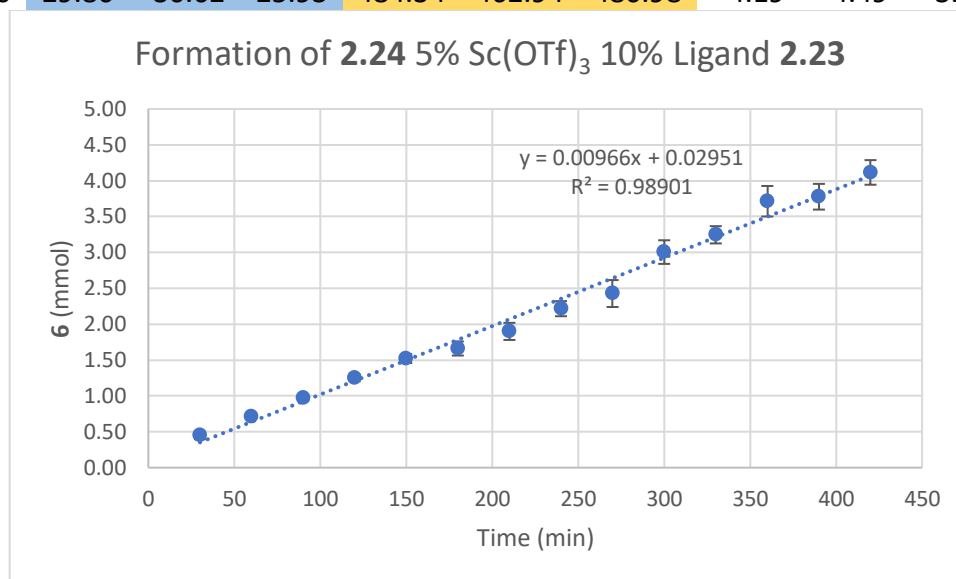


Figure 2.18 Plot of yield of **2.24** over time with 5 mol% Sc(OTf)<sub>3</sub> and 10 mol% **2.23**.

**Rate:** 0.00966 mmol/min

Yield vs time for 7.5 mol% Sc(OTf)<sub>3</sub> and 15 mol% ligand **2.23**:

Table 2.13 Yield values of **2.24** using 7.5 mol% Sc(OTf)<sub>3</sub> and 15 mol% **2.23**. Determined using area of **2.24** vs. area of caffeine.

Time (min)	Area <b>2.24</b>			Area Caffeine			Yield (%)		Avg. Yield (%)	
30	4.96	6.14	5.1	499.29	500.91	498.27	0.67	0.83	0.70	0.73
60	6.49	9.3	5.91	505.31	503.66	503.92	0.87	1.25	0.80	0.97
90	8.52	13.32	8.4	503.94	503.99	506.16	1.15	1.80	1.13	1.36
120	10.65	15.98	10.97	507.9	507.18	508.67	1.42	2.14	1.47	1.68
150	13.65	22.47	12.55	505.53	508.92	505.6	1.83	3.00	1.69	2.17
180	15.82	27.4	15.45	512.15	516.08	510.74	2.10	3.61	2.06	2.59
210	18.52	29.6	18.67	518.35	514.95	519.59	2.43	3.91	2.44	2.92
240	21.63	34.13	19.78	521.07	520.93	517.84	2.82	4.45	2.60	3.29
270	23.15	36.48	20.97	491.44	473.87	490.4	3.20	5.23	2.91	3.78
300	27.72	40.81	24.65	482.61	505.26	468.58	3.90	5.49	3.57	4.32
330	28.51	46.09	28.3	488	481.38	483.12	3.97	6.51	3.98	4.82
360	33.86	50.78	29.89	483.76	493.96	487.82	4.76	6.99	4.16	5.30
390	35.99	57.6	31.14	495.57	453.7	488.47	4.93	8.63	4.33	5.96
420	39.51	61.27	33.4	495.25	493.86	488.88	5.42	8.43	4.64	6.16

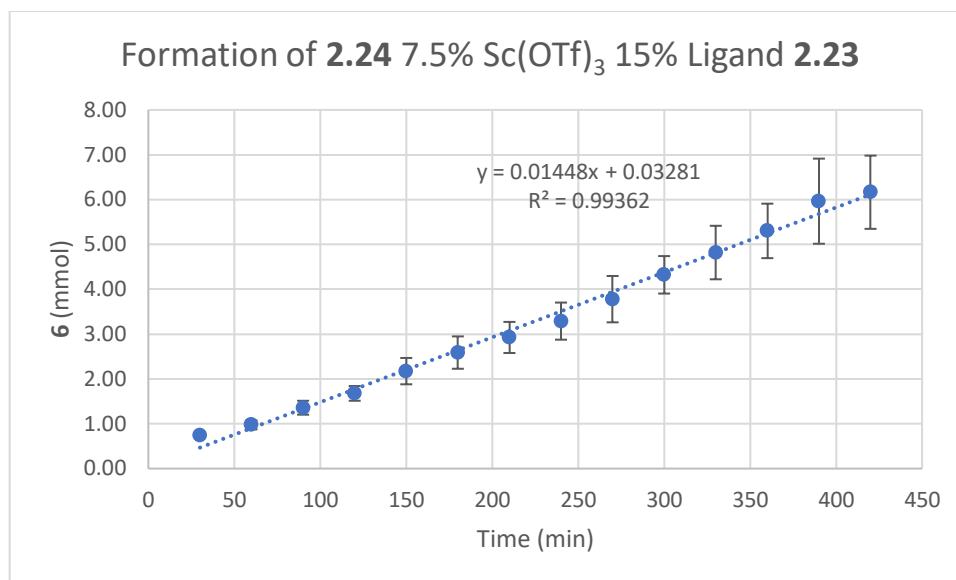


Figure 2.19 Plot of yield of **2.24** over time with 7.5 mol% Sc(OTf)<sub>3</sub> and 15 mol% **2.23**.

**Rate:** 0.01448 mmol/min

Order determination for Sc(OTf)<sub>3</sub>/**2.23**:

Y(OTf) <sub>3</sub> (mol%)	Rate (mmol/min)
2.5	0.00540
5.0	0.00966
7.5	0.01448

Rate order was determined according to the following equation, where  $m$  = rate and  $y$  = rate order:

Equation 2.3 Equation to determine Sc(OTf)<sub>3</sub> rate order.

$$\ln\left(\frac{m_1}{m_2}\right) = y * \ln\left(\frac{\text{mol}\%_1}{\text{mol}\%_2}\right)$$

Solving for  $y$  using the following table determines an average rate order of  $0.91 \pm 0.07$ :

Loadings	Calc. order
5.0 vs. 2.5	0.839064
7.5 vs. 2.5	0.897832
7.5 vs. 5.0	0.998297
average order:	<b>0.911731</b>

#### ***2.4.4 Computational Investigation***

Computational methods: Unless otherwise noted, stationary points with the catalyst systems were located using Gaussian 09 (D.01)<sup>61</sup> with the density functional,<sup>62</sup> and a mixed basis set of SDD for yttrium and 6-31G(d,p) for all other atoms.<sup>63,64</sup> For scandium the same functional was deployed with the 6-31(d,p) basis set. Free energies in solution were derived from structures optimized in the gas phase by means of a single point calculation at the same level of theory with the polarizable continuum model (IEFPCM) as implemented in Gaussian 16 (B.01).<sup>65</sup>

Conformational searches were performed with Macromodel version 11.7<sup>66</sup> and the OPLS\_2005 force field.<sup>67-69</sup>

Cartesian coordinates of all stationary point structures herein can be obtained free of charge from <https://pubs.rsc.org/en/content/articlelanding/2021/SC/D1SC03741B>.

## 2.5 References

- (1) Riehl, P. S.; Richardson, A. D.; Sakamoto, T.; Reid, J. P.; Schindler, C. S. Origin of Enantioselectivity Reversal in Lewis Acid-Catalysed Michael Additions Relying on the Same Chiral Source. *Chem. Sci.* **2021**, *12*, 14133–14142.
- (2) Valentovic, M. Naproxen. In *xPharm: The Comprehensive Pharmacology Reference*; Elsevier, 2007; pp 1–6.
- (3) Teo, S. K.; Colburn, W. A.; Tracewell, W. G.; Kook, K. A.; Stirling, D. I.; Jaworsky, M. S.; Scheffler, M. A.; Thomas, S. D.; Laskin, O. L. Clinical Pharmacokinetics of Thalidomide: *Clinical Pharmacokinetics* **2004**, *43*, 311–327.
- (4) Chhabra, N.; Aseri, M. L.; Padmanabhan, D. A Review of Drug Isomerism and Its Significance. *Int. J. Appl. Basic. Med. Res.* **2013**, *3*, 16–18.
- (5) Stark, G.; Stark, U.; Lueger, A.; Bertuch, H.; Pilger, E.; Pietsch, B.; Tritthart, H. A.; Lindner, W. The Effects of the Propranolol Enantiomers on the Intracardiac Electrophysiological Activities of Langendorff Perfused Hearts. *Basic Res. Cardiol.* **1989**, *84*, 461–468.
- (6) Bartsch, W.; Sponer, G.; Strein, K.; Muller-Beckmann, B.; Kling, L.; Böhm, E.; Martin, U.; Borbe, H. O. Pharmacological Characteristics of the Stereoisomers of Carvedilol. *Eur. J. Clin. Pharmacol.* **1990**, *38*, S104–S107.
- (7) Heal, D. J.; Smith, S. L.; Gosden, J.; Nutt, D. J. Amphetamine, Past and Present – a Pharmacological and Clinical Perspective. *J. Psychopharmacol.* **2013**, *27*, 479–496.
- (8) Vollenweider, F. X.; Leenders, K. L.; Oye, I.; Hell, D.; Angst, J. Differential Psychopathology and Patterns of Cerebral Glucose Utilisation Produced by (S)- and (R)-Ketamine in Healthy Volunteers Using Positron Emission Tomography (PET). *Eur. Neuropsychopharmacol.* **1997**, *7*, 25–38.
- (9) Brill, Z. G.; Condakes, M. L.; Ting, C. P.; Maimone, T. J. Navigating the Chiral Pool in the Total Synthesis of Complex Terpene Natural Products. *Chem. Rev.* **2017**, *117*, 11753–11795.
- (10) Paquette, L. A. *Chiral Reagents for Asymmetric Synthesis*; Wiley, 2003.
- (11) Diaz-Muñoz, G.; Miranda, I. L.; Sartori, S. K.; de Rezende, D. C.; Alves Nogueira Diaz, M. Use of Chiral Auxiliaries in the Asymmetric Synthesis of Biologically Active Compounds: A Review. *Chirality* **2019**, *31*, 776–812.
- (12) Evans, D. A.; Bartroli, J.; Shih, T. L. Enantioselective Aldol Condensations. 2. Erythro-Selective Chiral Aldol Condensations via Boron Enolates. *J. Am. Chem. Soc.* **1981**, *103*, 2127–2129.
- (13) Heravi, M. M.; Zadsirjan, V.; Farajpour, B. Applications of Oxazolidinones as Chiral Auxiliaries in the Asymmetric Alkylation Reaction Applied to Total Synthesis. *RSC Adv.* **2016**, *6*, 30498–30551.
- (14) Robak, M. T.; Herbage, M. A.; Ellman, J. A. Synthesis and Applications of *Tert* -Butanesulfinamide. *Chem. Rev.* **2010**, *110*, 3600–3740.
- (15) Jacobsen, E. N.; Pfaltz, A.; Yamamoto, H. *Comprehensive Asymmetric Catalysis*; Springer: London, 2003.
- (16) Yi, D.; Bayer, T.; Badenhorst, C. P. S.; Wu, S.; Doerr, M.; Höhne, M.; Bornscheuer, U. T. Recent Trends in Biocatalysis. *Chem. Soc. Rev.* **2021**, *50*, 8003–8049.
- (17) Arnold, F. H.; Volkov, A. A. Directed Evolution of Biocatalysis. *Curr. Opin. Chem. Biol.* **1999**, *3*, 54–59.
- (18) Turner, N. J. Directed Evolution Drives the next Generation of Biocatalysts. *Nat. Chem. Biol.* **2009**, *5*, 567–573.

- (19) MacMillan, D. W. C. The Advent and Development of Organocatalysis. *Nature* **2008**, *455*, 304–308.
- (20) List, B. Introduction: Organocatalysis. *Chem. Rev.* **2007**, *107*, 5413–5415.
- (21) Xiang, S.-H.; Tan, B. Advances in Asymmetric Organocatalysis Over the Last 10 Years. *Nat. Commun.* **2020**, *11*, 3786.
- (22) Noyori, R. Facts Are the Enemy of Truth—Reflections on Serendipitous Discovery and Unforeseen Developments in Asymmetric Catalysis. *Angew. Chem. Int. Ed.* **2013**, *52*, 79–92.
- (23) Blaser, H. U.; Schmidt, E. *Asymmetric Catalysis on Industrial Scale*; Wiley-VCH, 2007.
- (24) Pfaltz, A.; Drury, W. J. Design of Chiral Ligands for Asymmetric Catalysis: From C<sub>2</sub>-Symmetric P,P- and N,N-Ligands to Sterically and Electronically Nonsymmetrical P,N-Ligands. *Proc. Natl. Acad. Sci. U.S.A.* **2004**, *101*, 5723–5726.
- (25) Bartók, M. Unexpected Inversions in Asymmetric Reactions: Reactions with Chiral Metal Complexes, Chiral Organocatalysts, and Heterogeneous Chiral Catalysts. *Chem. Rev.* **2010**, *110*, 1663–1705.
- (26) Storch, G.; Trapp, O. Temperature-Controlled Bidirectional Enantioselectivity in a Dynamic Catalyst for Asymmetric Hydrogenation. *Angew. Chem. Int. Ed.* **2015**, *54*, 3580–3586.
- (27) Wang, S.; Xiao, J.; Li, J.; Xiang, H.; Wang, C.; Chen, X.; Carter, R. G.; Yang, H. Discovery of Temperature-Dependent, Autoinductive Reversal of Enantioselectivity: Palladium-Mediated [3+3]-Annulation of 4-Hydroxycoumarins. *Chem. Commun.* **2017**, *53*, 4441–4444.
- (28) Yu, H.; Xie, F.; Ma, Z.; Liu, Y.; Zhang, W. The Effects of Solvent on Switchable Stereoselectivity: Copper-Catalyzed Asymmetric Conjugate Additions Using D<sub>2</sub>-Symmetric Biphenyl Phosphoramidite Ligands. *Org. Biomol. Chem.* **2012**, *10*, 5137.
- (29) Haddad, N.; Qu, B.; Rodriguez, S.; van der Veen, L.; Reeves, D. C.; Gonnella, N. C.; Lee, H.; Grinberg, N.; Ma, S.; Krishnamurthy, D.; Wunberg, T.; Senanayake, C. H. Catalytic Asymmetric Hydrogenation of Heterocyclic Ketone-Derived Hydrazones, Pronounced Solvent Effect on the Inversion of Configuration. *Tetrahedron Lett.* **2011**, *52*, 2011.
- (30) Ding, Z.-Y.; Chen, F.; Qin, J.; He, Y.-M.; Fan, Q.-H. Asymmetric Hydrogenation of 2,4-Disubstituted 1,5-Benzodiazepines Using Cationic Ruthenium Diamine Catalysts: An Unusual Achiral Counteranion Induced Reversal of Enantioselectivity. *Angew. Chem. Int. Ed.* **2012**, *51*, 5706–5710.
- (31) Wang, D.; Cao, P.; Wang, B.; Jia, T.; Lou, Y.; Wang, M.; Liao, J. Copper(I)-Catalyzed Asymmetric Pinacolboron Addition of *N*-Boc-Imines Using a Chiral Sulfoxide–Phosphine Ligand. *Org. Lett.* **2015**, *17*, 2420–2423.
- (32) Cao, W.; Feng, X.; Liu, X. Reversal of Enantioselectivity in Chiral Metal Complex-Catalyzed Asymmetric Reactions. *Org. Biomol. Chem.* **2019**, *17*, 6538–6550.
- (33) Mazumder, S.; Crandell, D. W.; Lord, R. L.; Baik, M.-H. Switching the Enantioselectivity in Catalytic [4 + 1] Cycloadditions by Changing the Metal Center: Principles of Inverting the Stereochemical Preference of an Asymmetric Catalysis Revealed by DFT Calculations. *J. Am. Chem. Soc.* **2014**, *136*, 9414–9423.
- (34) Kokubo, M.; Naito, T.; Kobayashi, S. Metal-Controlled Reversal of Enantioselectivity in Catalyzed Asymmetric Ring-Opening Reactions of *Meso* -Epoxides in Water. *Chem. Lett.* **2009**, *38*, 904–905.
- (35) Sasaki, S.; Yamauchi, T.; Higashiyama, K. Dy(OTf)<sub>3</sub>/Pybox-Catalyzed Enantioselective Friedel–Crafts Alkylation of Indoles with  $\alpha,\beta$ -Unsaturated Trifluoromethyl Ketones. *Tetrahedron Lett.* **2010**, *51*, 2326–2328.

- (36) Riehl, P. S.; Richardson, A. D.; Sakamoto, T.; Schindler, C. S. Eight-Step Enantiodivergent Synthesis of (+)- and (-)-Lingzhiol. *Org. Lett.* **2020**, *22*, 290–294.
- (37) Ogawa, C.; Kizu, K.; Shimizu, H.; Takeuchi, M.; Kobayashi, S. Chiral Scandium Catalysts for Enantioselective Michael Reactions of  $\beta$ -Ketoesters. *Chem. Asian J.* **2006**, *1*, 121–124.
- (38) Desimoni, G.; Faita, G.; Guala, M.; Pratelli, C. Different Lanthanide Ions and the Pybox Substituents Induce the Reverse of the Sense of Induction in the Enantioselective Diels–Alder Reaction between Acryloyloxazolidinone and Cyclopentadiene. *J. Org. Chem.* **2003**, *68*, 7862–7866.
- (39) Lutz, F.; Igarashi, T.; Kinoshita, T.; Asahina, M.; Tsukiyama, K.; Kawasaki, T.; Soai, K. Mechanistic Insights in the Reversal of Enantioselectivity of Chiral Catalysts by Achiral Catalysts in Asymmetric Autocatalysis. *J. Am. Chem. Soc.* **2008**, *130*, 2956–2958.
- (40) Girard, C.; Kagan, H. B. Nonlinear Effects in Asymmetric Synthesis and Stereoselective Reactions: Ten Years of Investigation. *Angew. Chem. Int. Ed.* **1998**, *37*, 2922–2959.
- (41) Mai, E.; Schneider, C. Scandium–Bipyridine-Catalyzed Enantioselective Aminolysis of Meso-Epoxides. *Chem. Eur. J.* **2007**, *13* (9), 2729–2741.
- (42) Kobayashi, S.; Ogino, T.; Shimizu, H.; Ishikawa, S.; Hamada, T.; Manabe, K. Bismuth Triflate–Chiral Bipyridine Complexes as Water-Compatible Chiral Lewis Acids. *Org. Lett.* **2005**, *7*, 4729–4731.
- (43) Blackmond, D. G. Kinetic Profiling of Catalytic Organic Reactions as a Mechanistic Tool. *J. Am. Chem. Soc.* **2015**, *137*, 10852–10866.
- (44) Mukherjee, C.; Kitanosono, T.; Kobayashi, S. Kinetics Studies of the Enantioselective Hydroxymethylation of Silicon Enolates Using Aqueous Formaldehyde in the Presence of Sc(OTf)<sub>3</sub> and a Chiral 2,2'-Bipyridine Ligand. *Chem. Asian J.* **2011**, *6*, 2308–2311.
- (45) Cockerill, A. F.; Davies, G. L. O.; Harden, R. C.; Rackham, D. M. Lanthanide Shift Reagents for Nuclear Magnetic Resonance Spectroscopy. *Chem. Rev.* **1973**, *73*, 553–588.
- (46) Cheng, G.-J.; Zhang, X.; Chung, L. W.; Xu, L.; Wu, Y.-D. Computational Organic Chemistry: Bridging Theory and Experiment in Establishing the Mechanisms of Chemical Reactions. *J. Am. Chem. Soc.* **2015**, *137*, 1706–1725.
- (47) Becker, M. R.; Reid, J. P.; Rykaczewski, K. A.; Schindler, C. S. Models for Understanding Divergent Reactivity in Lewis Acid-Catalyzed Transformations of Carbonyls and Olefins. *ACS Catal.* **2020**, *10*, 4387–4397.
- (48) Seeman, J. I. Effect of Conformational Change on Reactivity in Organic Chemistry. Evaluations, Applications, and Extensions of Curtin-Hammett/Winstein-Holness Kinetics. *Chem. Rev.* **1983**, *83*, 83–134.
- (49) Reid, J. P.; Hu, M.; Ito, S.; Huang, B.; Hong, C. M.; Xiang, H.; Sigman, M. S.; Toste, F. D. Strategies for Remote Enantiocontrol in Chiral Gold(III) Complexes Applied to Catalytic Enantioselective  $\gamma,\delta$ -Diels–Alder Reactions. *Chem. Sci.* **2020**, *11*, 6450–6456.
- (50) Peng, Q.; Duarte, F.; Paton, R. S. Computing Organic Stereoselectivity – From Concepts to Quantitative Calculations and Predictions. *Chem. Soc. Rev.* **2016**, *45*, 6093–6107.
- (51) Ishikawa, S.; Hamada, T.; Manabe, K.; Kobayashi, S. New Efficient Method for the Synthesis of Chiral 2,2'-Bipyridyl Ligands. *Synthesis* **2005**, *2005*, 2176–2182.
- (52) Bolm, C.; Ewald, M.; Felder, M.; Schlingloff, G. Enantioselective Synthesis of Optically Active Pyridine Derivatives and C<sub>2</sub>-Symmetric 2,2'-Bipyridines. *Chem. Ber.* **1992**, *125*, 1169–1190.
- (53) Bolm, C.; Zehnder, M.; Bur, D. Optisch Aktive Bipyridine in Der Asymmetrischen Katalyse. *Angew. Chem.* **1990**, *102*, 206–208.

- (54) Mikami, K.; Terada, M.; Matsuzawa, H. “Asymmetric” Catalysis by Lanthanide Complexes. *Angew. Chem. Int. Ed.* **2002**, *41*, 3554–3572.
- (55) Nandakumar, M. V.; Ghosh, S.; Schneider, C. Enantioselective Synthesis of a Novel Chiral 2,9-Disubstituted 1,10-Phenanthroline and First Applications in Asymmetric Catalysis. *Eur. J. Org. Chem.* **2009**, *2009*, 6393–6398.
- (56) Ding, T.; Jiang, L.; Yang, J.; Xu, Y.; Wang, G.; Yi, W. Highly Carbon-Selective Monofluoromethylation of  $\beta$ -Ketoesters with Fluoromethyl Iodide. *Org. Lett.* **2019**, *21*, 6025–6028.
- (57) Cívicos, J. F.; Ribeiro, C. M. R.; Costa, P. R. R.; Nájera, C. Copper- Versus Palladium-Catalyzed Aromatization of 2-(Methoxycarbonyl) Tetralones: Synthesis of Methyl 1-Hydroxy-2-Naphthoates. *Tetrahedron* **2016**, *72*, 1897–1902.
- (58) Qiu, J.-S.; Wang, Y.-F.; Qi, G.-R.; Karmaker, P. G.; Yin, H.-Q.; Chen, F.-X. Highly Enantioselective  $\alpha$ -Cyanation with 4-Acetylphenyl Cyanate. *Chemistry – A European Journal* **2017**, *23*, 1775–1778.
- (59) Cabrera, E. V.; Reyes, C.; Peña, N.; Marrugo, K. P.; Bedoya, L.; Banerjee, A. K. Isopropylation of 5-Methoxy-1-Tetralone. *Org. Prep. Proced. Int.* **2015**, *47*, 379–383.
- (60) Wu, Z.; Li, Y.; Cai, Y.; Yuan, J.; Yuan, C. A Novel Necroptosis Inhibitor—Necrostatin-21 and Its SAR Study. *Bioorg. Med. Chem. Lett.* **2013**, *23*, 4903–4906.
- (61) Frisch, M. J.; Trucks, G. W.; Schlegel, H. B.; Scuseria, G. E.; Robb, M. A.; Cheeseman, J. R.; Scalmani, G.; Barone, V.; Mennucci, B.; Petersson, G. A.; Nakatsuji, H.; Caricato, M.; Li, X.; Hratchian, H. P.; Izmaylov, A. F.; Bloino, J.; Zheng, G.; Sonnenberg, J. L.; Hada, M.; Ehara, M.; Toyota, K.; Fukuda, R.; Hasegawa, J.; Ishida, M.; Nakajima, T.; Honda, Y.; Kitao, O.; Nakai, H.; Vreven, T.; Montgomery, Jr., J. A.; Peralta, J. E.; Ogliaro, F.; Bearpark, M.; Heyd, J. J.; Brothers, E.; Kudin, K. N.; Staroverov, V. N.; Keith, T.; Kobayashi, R.; Normand, J.; Raghavachari, K.; Rendell, A.; Burant, J. C.; Iyengar, S. S.; Tomasi, J.; Cossi, M.; Rega, N.; Millam, J. M.; Klene, M.; Knox, J. E.; Cross, J. B.; Bakken, V.; Adamo, C.; Jaramillo, J.; Gomperts, R.; Stratmann, R. E.; Yazyev, O.; Austin, A. J.; Cammi, R.; Pomelli, C.; Ochterski, J. W.; Martin, R. L.; Morokuma, K.; Zakrzewski, V. G.; Voth, G. A.; Salvador, P.; Dannenberg, J. J.; Dapprich, S.; Daniels, A. D.; Farkas, O.; Foresman, J. B.; Ortiz, J. V.; Cioslowski, J.; Fox, D. J. *Gaussian 09 (D.01)*; Gaussian Inc.: Wallingford CT, 2013.
- (62) Zhao, Y.; Truhlar, D. G. The M06 Suite of Density Functionals for Main Group Thermochemistry, Thermochemical Kinetics, Noncovalent Interactions, Excited States, and Transition Elements: Two New Functionals and Systematic Testing of Four M06-Class Functionals and 12 Other Functionals. *Theor. Chem. Account.* **2008**, *120*, 215–241.
- (63) Krishnan, R.; Binkley, J. S.; Seeger, R.; Pople, J. A. Self-Consistent Molecular Orbital Methods. XX. A Basis Set for Correlated Wave Functions. *J. Chem. Phys.* **1980**, *72*, 650–654.
- (64) Andrews, R. S.; Becker, J. J.; Gagné, M. R. Intermolecular Addition of Glycosyl Halides to Alkenes Mediated by Visible Light. *Angewandte Chemie* **2010**, *122*, 7432–7434.
- (65) Tomasi, J.; Mennucci, B.; Cammi, R. Quantum Mechanical Continuum Solvation Models. *Chem. Rev.* **2005**, *105*, 2999–3094.
- (66) *Schrödinger Release 2020-1*; Schrödinger, LLC: New York, NY, 2020.
- (67) Kaminski, G. A.; Friesner, R. A.; Tirado-Rives, J.; Jorgensen, W. L. Evaluation and Reparametrization of the OPLS-AA Force Field for Proteins via Comparison with Accurate Quantum Chemical Calculations on Peptides. *J. Phys. Chem. B* **2001**, *105*, 6474–6487.

- (68) Jorgensen, W. L.; Maxwell, D. S.; Tirado-Rives, J. Development and Testing of the OPLS All-Atom Force Field on Conformational Energetics and Properties of Organic Liquids. *J. Am. Chem. Soc.* **1996**, *118*, 11225–11236.
- (69) Jorgensen, W. L.; Tirado-Rives, J. The OPLS Potential Functions for Proteins. Energy Minimizations for Crystals of Cyclic Peptides and Crambin. *J. Am. Chem. Soc.* **1988**, *110*, 1657–1666.



## Chapter 3 Synthesis of Functionalized Azetidines using Visible Light-Mediated [2+2] Cycloaddition Reactions

Portions of this chapter have been published in: Becker, M. R.; Richardson, A. D.; Schindler, C. S. Functionalized Azetidines via Visible Light-Enabled Aza Paternò-Büchi Reactions. *Nat. Commun.* **2019**, *10*, 5095. DOI: 10.1038/s41467-019-13072-x.<sup>1</sup> and Richardson, A. D.; Becker, M. R.; Schindler, C. S. Synthesis of Azetidines by Aza Paternò-Büchi Reactions. *Chem. Sci.* **2020**, *11*, 7553-7561.<sup>2</sup>

### 3.1 Introduction

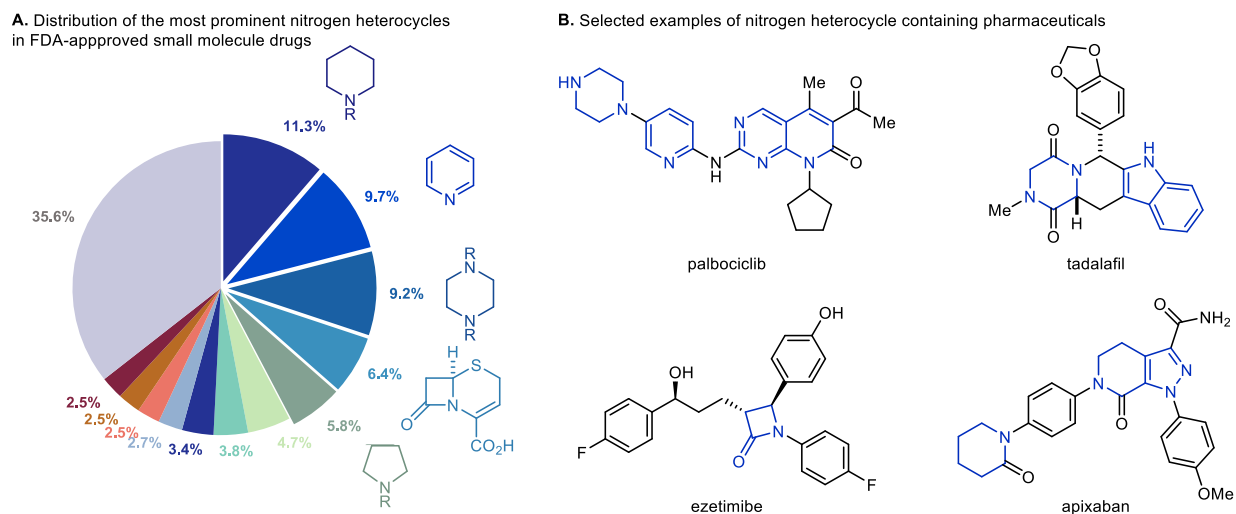


Figure 3.1 (A) Distribution of Nitrogen containing heterocycles in FDA approved drugs. (B) Selected examples of nitrogen heterocycle containing drugs.

Azetidines are saturated four-membered nitrogen-containing rings that are a part of a larger class of molecules known as nitrogen heterocycles. These are ubiquitous in modern pharmaceuticals and are also prevalent in many biologically active natural products. In fact, in 2014 Njardarson and coworkers found that 59% of all FDA approved small molecule drugs contain at least one nitrogen heterocycle.<sup>3</sup> An analysis of the different ring sizes revealed that 59% of those drugs contained a six-membered nitrogen heterocycle with piperidine, pyridine, and piperazine being the most common in that order (Figure 3.1). Five-membered rings were the second biggest

class (39%) represented primarily by pyrrolidines, thiazoles, imidazoles and indoles. Four membered rings were found to be comparatively less common although they are represented by the  $\beta$ -lactam component of cephem and penem containing drugs. Together, cephems and penems are present in 10% of the nitrogen heterocycle containing drugs. However, azetidines remain underrepresented in current pharmaceuticals.

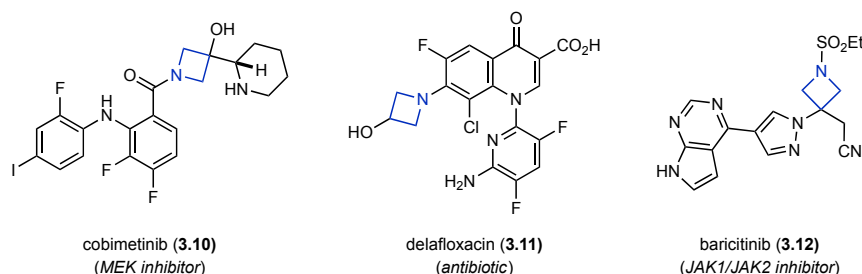
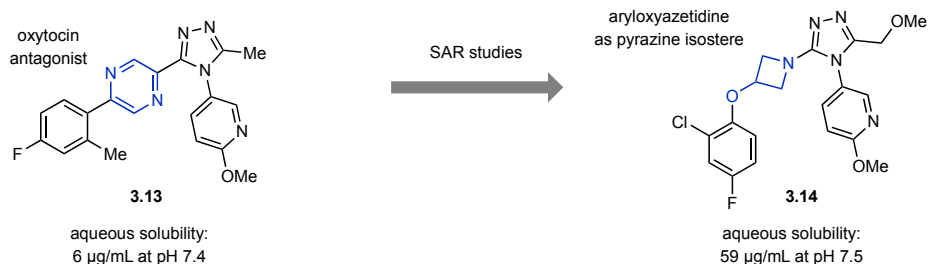


Figure 3.2 Recently FDA approved, azetidine containing drugs.

Yet, since this report was released azetidines have been featured in three new FDA approved drugs (Figure 3.2). In 2015, the kinase inhibitor cobimetinib (**3.10**) was approved for the treatment of metastatic melanoma.<sup>4</sup> In 2017, delafloxacin (**3.11**) was approved for the treatment of pneumonia as well as acute bacterial skin infections.<sup>5</sup> In 2018, another azetidine containing kinase inhibitor, baricitinib (**3.12**), was approved for the treatment of severe rheumatoid arthritis.<sup>6</sup>

A. Aryloxyazetidine as a pyrazine isostere leads to increased aqueous solubility.



B. Switching to an azetidine increases activity and metabolic stability.

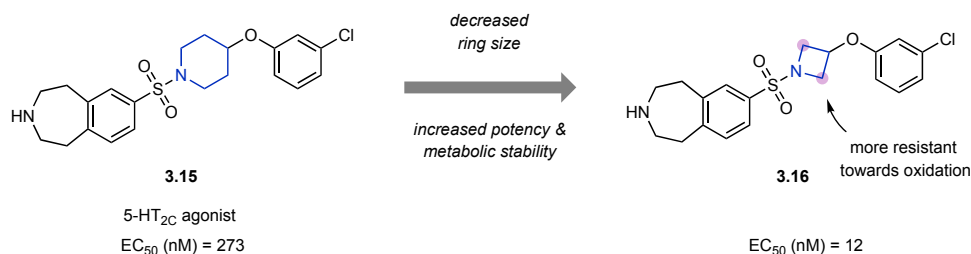


Figure 3.3 Azetidines featured in lead compounds.

Despite being underrepresented, azetidines are known to exhibit desirable physicochemical properties such as increased metabolic stability, lower lipophilicity, and increased aqueous solubility (Figure 3.3).<sup>7,8</sup> For example, Brown and coworkers found that replacing the pyrazine

ring in **3.13** with an oxyazetidone increased the aqueous solubility 10-fold while maintaining high target selectivity (Figure 3.3A).<sup>9</sup> In addition, Fish and coworkers demonstrated that an azetidine analog of piperidine **3.15** had a significantly better EC<sub>50</sub> for serotonin 2C (5-HT<sub>2C</sub>) receptors (Figure 3.3B). These 5-HT<sub>2C</sub> receptors have been linked to multiple diseases including obesity and schizophrenia.<sup>10</sup>

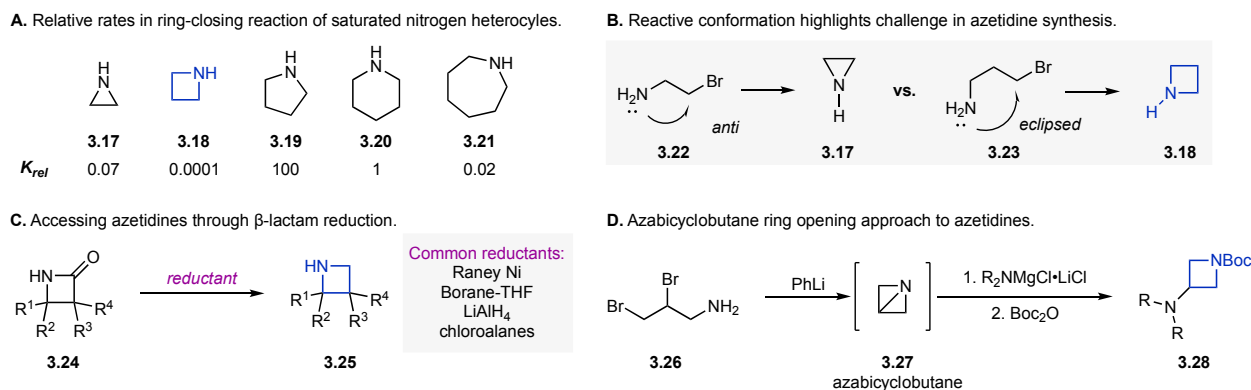


Figure 3.4 Conventional methods used to synthesize azetidines including intramolecular substitution,  $\beta$ -lactam reduction, and azabicyclobutane ring opening.

We hypothesized that azetidines continue to remain underrepresented, despite their desirable properties, because of the challenges associated with their synthesis.<sup>11,12</sup> One common method for the synthesis of azetidines is an intramolecular ring closing substitution reaction with a nitrogen nucleophile.<sup>13</sup> However, four membered rings are particularly challenging to synthesize through this method (Figure 3.4A).<sup>14</sup> The high strain in the transition state offers one explanation for the challenges of this reaction, although, a more significant contributing factor can be seen through analyzing the reactive conformation. Specifically, cyclization to form an azetidine proceeds via an unfavorable eclipsed conformation (Figure 3.4B).<sup>15</sup> Considering the reactive conformation explains why aziridine formation occurs at a rate 700-fold faster than azetidines despite having a higher overall ring strain. Consequently, elevated temperatures and activated leaving groups are typically required limiting the scope of this azetidine forming reaction. Alternatively, azetidines can be synthesized through the reduction of  $\beta$ -lactams (Figure 3.4B),<sup>13,16</sup> which can themselves be synthesized via several different methods including the Staudinger, the aza-Reformatsky, and the Kinugasa reaction.<sup>17,18</sup> Subsequent reduction to the corresponding azetidine can be accomplished with diborane, LiAlH<sub>4</sub>, DiBAL-H, chloroalanes, or Raney nickel. Although  $\beta$ -lactam reduction broadens the scope of accessible azetidines compared to intramolecular substitution reactions, the need for a strong reductant does limit the utility of this

transformation. More recently, the Baran group, has reported the synthesis of azetidines through strain-release of azabicyclobutanes using nitrogen nucleophiles (Figure 3.4D).<sup>19,20</sup> This method provides a mild way to azetidinylate many different amines, including drug scaffolds. Other groups have since developed comparable reactions using different nucleophiles.<sup>21,22</sup> However, this strategy is limited to the synthesis of 3 substituted azetidines, which is already a more readily accessible substitution pattern starting from commercially available 3-azetidinones.

Arguably the most efficient and atom economical way to access azetidines is via a [2+2] cycloaddition between an imine and alkene. Although there are a select few examples of synthesizing an azetidine through a thermal [2+2] cycloaddition,<sup>11</sup> the majority of the literature in this area is on photochemical [2+2] cycloadditions, often referred to as the aza Paternò-Büchi reaction. In fact, a photochemical [2+2] cycloaddition is a well-established tool for the synthesis of four-membered rings. This strategy works especially well when synthesizing cyclobutanes<sup>23</sup> and oxetanes.<sup>24</sup> In contrast, the aza Paternò-Büchi reaction is comparatively less developed.<sup>2</sup> This can be attributed to the differences between excited state imines versus excited state alkenes or carbonyls. Like alkenes and carbonyls, excited state imines can undergo relaxation pathways such as fragmentation, photoreduction or rearrangement.<sup>25,26</sup> However, imines are unique in that they are susceptible to radiationless decay back to the ground state via rotation around the carbon nitrogen bond followed by relaxation (Figure 3.5A).<sup>27</sup> This constant isomerization and relaxation render imines unreactive to traditional [2+2] photocycloadditions.

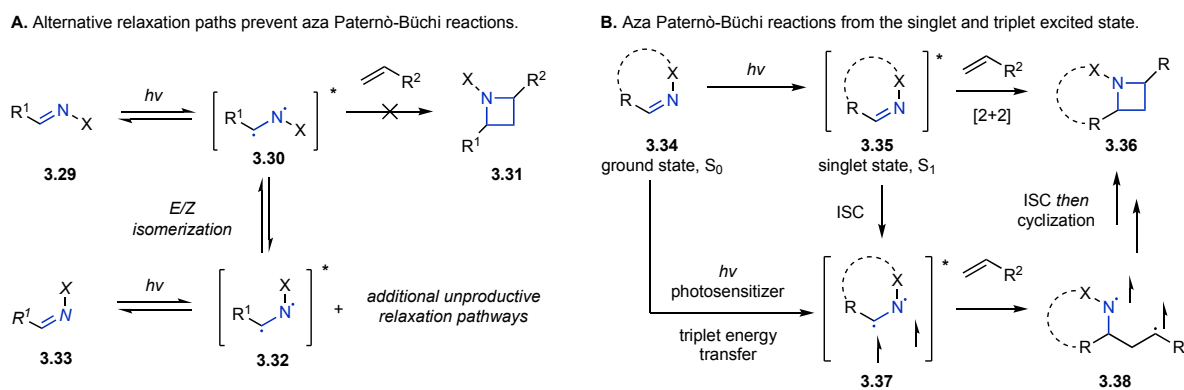


Figure 3.5 (A) Overview of the challenges in imine photochemistry. (B) Singlet state vs. triple state aza Paternò-Büchi reaction.

Despite these challenges, there are examples where imines engage in intra- and intermolecular aza Paternò-Büchi reactions to form azetidines. High energy, ultraviolet (UV) light is typically required to directly excite an imine to its excited state. Upon excitation, the imine first

arrives at a singlet excited state (Figure 3.5B). In the singlet state, imines can react with an alkene in a concerted fashion achieving high levels of stereoselectivity. Alternatively, the singlet state imine can undergo a process called intersystem crossing (ISC) and arrive at a triplet excited state. The triplet state has a longer lifetime than the singlet state as returning to the ground state is spin-forbidden.<sup>28</sup> Additionally, a cycloaddition reaction from the triplet state proceeds via a stepwise radical mechanism. The triplet state can also be accessed through a process called triplet energy transfer, or triplet sensitization, using a photosensitizer. This process will be discussed in detail later in this chapter.

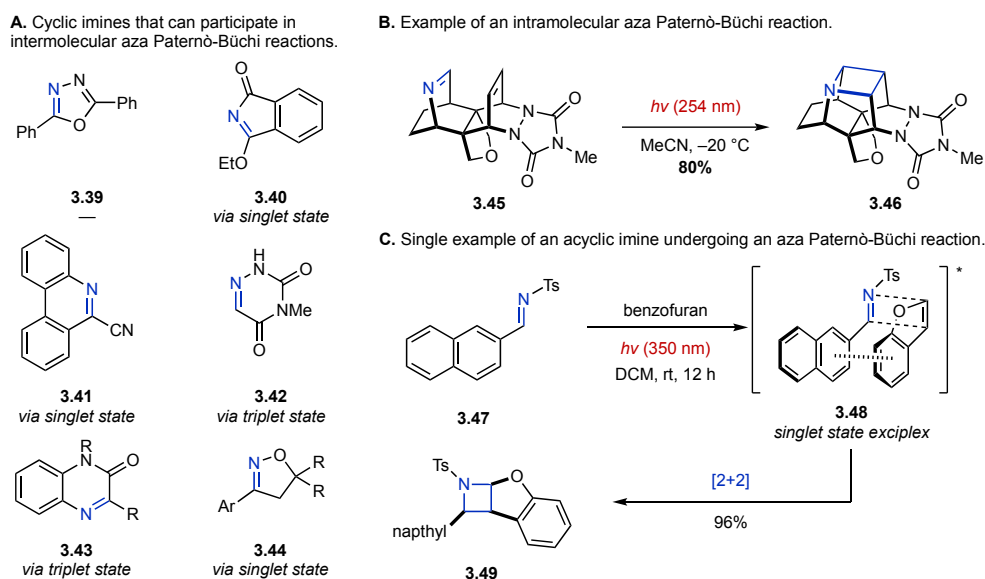
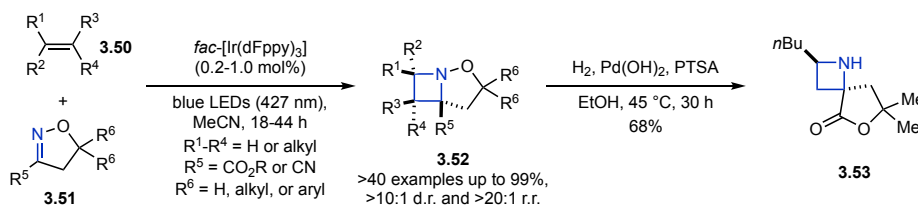


Figure 3.6 (A) Summary of imines that engage in intermolecular aza Paternò-Büchi reactions. (B) Example of an intramolecular aza Paternò-Büchi reactions. (C) Single example of an acyclic imine participating in an aza Paternò-Büchi reaction via a unique singlet state exciplex.

In order to overcome the radiationless isomerization relaxation pathway, typically the aza Paternò-Büchi reaction is limited to cyclic imines that are unable to undergo isomerization. The first report of an aza Paternò-Büchi reaction came from the Tsuge group in 1968.<sup>29</sup> They relied on 1,3,4-oxadiazoles (**3.39**) as a cyclic imine equivalents. Since then, several other imine containing molecules have been reported to undergo aza Paternò-Büchi reactions (Figure 3.6A).<sup>28,30-46</sup> It has been shown that the scaffolds can participate in intra-<sup>47</sup> and intermolecular [2+2] photocycloadditions (Figure 3.6A&B). Interestingly, these molecules are structurally different and don't all proceed via the same mechanism. To date, there is only one report of an acyclic imine undergoing an aza Paternò-Büchi reaction. Maruoka and coworkers found that *N*-

(arylsulfonyl)imines could react with styrenyl alkenes via a unique singlet state exciplex intermediate mechanism (Figure 3.6C).<sup>48</sup>

A. Visible light mediated aza Paternò-Büchi reaction using glyoxyl derived isoxazolines.



B. Enantioselective aza Paternò-Büchi reaction using quinoxalinones and a chiral photosensitizer.

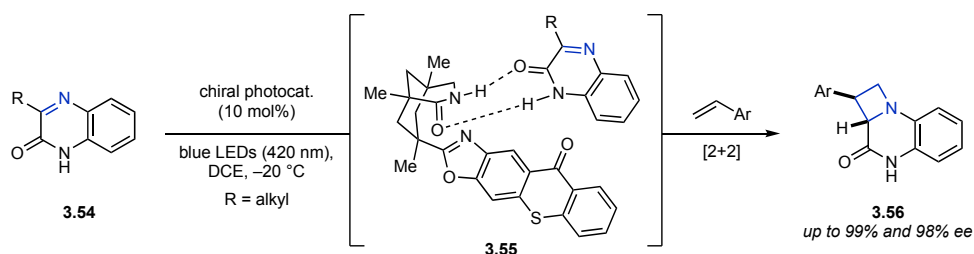


Figure 3.7 Examples of visible light mediated aza Paternò-Büchi reactions using triplet energy transfer.

The requirement for harsh UV light has limited the scope of this transformation due to poor functional group tolerance. Recently, there has been an effort to adapt the tools of modern visible light photocatalysis to the aza Paternò-Büchi reaction. In fact, many visible light absorbing photosensitizers have been developed and successfully applied to related transformations like [2+2] cycloadditions for the synthesis of cyclobutanes. In 2020, our group reported the first example of a visible light absorbing photosensitizer catalyzed intermolecular aza Paternò-Büchi reaction (Figure 3.7A).<sup>49</sup> In this paper, glyoxylate derived isoxazolines (**3.51**) were sensitized with an iridium photosensitizer and subsequently reacted with many unactivated and functionalized alkenes (**3.50**). This mild and efficient method yielded polycyclic azetidines in up to 99% yield. Additionally, the N-O bond could be cleaved to reveal the free monocyclic azetidone (**3.53**). Our group has since expanded on this method and developed visible-light mediated syntheses of azetidines<sup>50</sup> and oxetanes.<sup>51</sup> In 2021, Bach and coworkers reported the first example of an enantioselective aza Paternò-Büchi reaction using visible light (Figure 3.7B).<sup>52</sup> In this intermolecular reaction, quinoxalinones (**3.54**) were excited with a dual functioning chiral organic photosensitizer. The chiral transition state consisted of the excited state quinoxalinone hydrogen bonded to the catalyst (**3.55**), reacting with a styrene and yielding chiral azetidines (**3.56**). The azetidone products were isolated in up to 99% yield and 98% ee. Unlike the report from Schindler

and coworkers, this transformation was limited to styrenes, except for a single example of an intramolecular reaction with a pendant terminal alkene.

Selective alkene over imine activation offers an alternative method to circumvent the challenges associated with excited state imines. Alkene excitation, and subsequent [2+2] cycloaddition, is well established, and importantly modern photochemical techniques provide the potential for selective alkene excitation. The Sivaguru group tested this principle by demonstrating that cyclic enamides (**3.57**) can be sensitized by xanthone, and then react with a pendant oxime or hydrazone to form an azetidione (**3.58**) (Figure 3.8).<sup>53</sup> Xanthone is a UV light absorbing photosensitizer, and 30-100 mol% was needed for this transformation. A series of polycyclic azetidiones were isolated in 21-79% yield. Mechanistic studies were able to verify that this reaction proceeds via a triplet state enamide, rather than an excited imine, supporting the viability of this strategy for synthesizing azetidiones. Based on their experiments, the authors propose that the enamide has a triplet energy between 63-74 kcal mol<sup>-1</sup>.

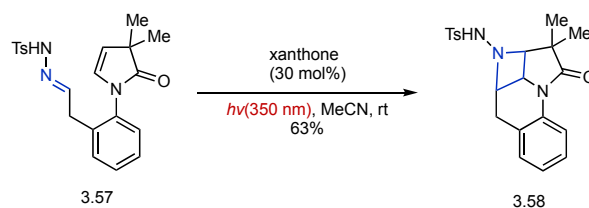


Figure 3.8 Intramolecular aza Paternò-Büchi reaction through selective alkene excitation using xanthone as a sensitizer.

You and coworkers reported a similar transformation, instead relying on indoles as the alkene partner (Figure 3.9).<sup>54</sup> Indole (**3.60**) sensitization with an iridium photosensitizer, and a subsequent [2+2] cycloaddition, yield dearomatized azetidione products in 33-99% yield. Interestingly, 3-methylindoles underwent reversible [2+2] reactions, and under prolonged reaction times this reaction funneled to the thermodynamic product **3.61**. Several related products were prepared to demonstrate the utility of this divergent reactivity.

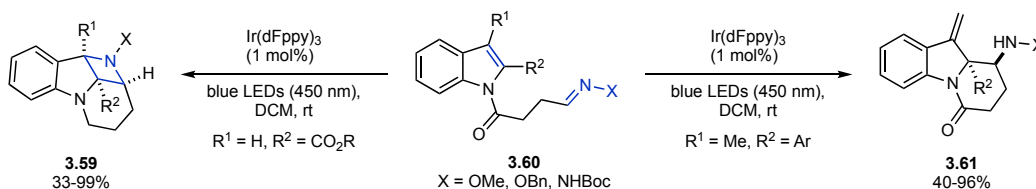


Figure 3.9 Indole dearomatization via a [2+2]-cycloaddition (left) or 1,5-H atom transfer (right) using visible light.

Many of these [2+2] photocycloaddition reactions rely on a process called triplet energy transfer. In this type of energy transfer, an excited state photosensitizer transfers its triplet excited

state energy to a ground state substrate.<sup>55,56</sup> This is an alternative strategy to direct excitation in route to an excited state substrate. Direct excitation of most organic molecules requires irradiation with UV light, whereas many photosensitizers absorb in the visible light wavelengths. Additionally, energy transfer offers an efficient way to access a substrate's triplet state, which may not be as accessible via direct excitation when inefficient intersystem crossing is required. Typical photosensitizers include ruthenium- and iridium-based complexes, as well as organic dyes (Figure 3.10C).

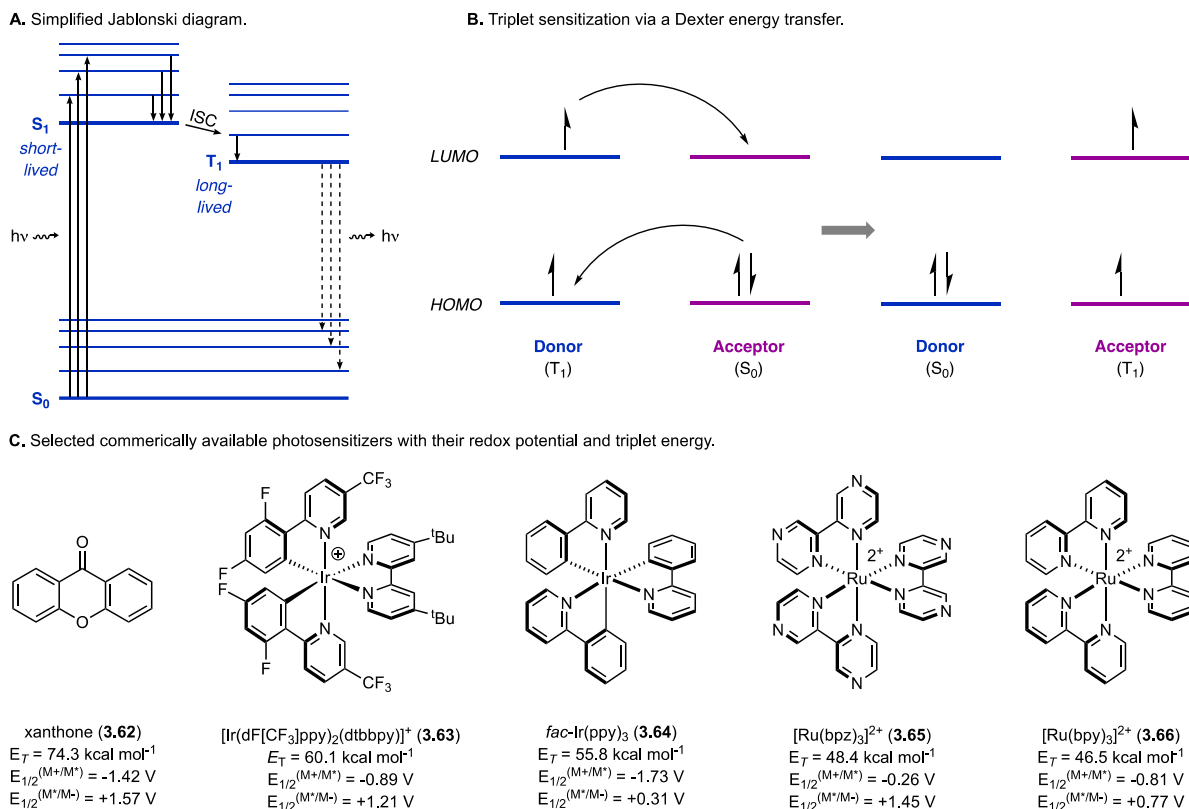


Figure 3.10 Overview of triplet energy transfer and selected commercially available photosensitizers.

As with simpler organic compounds, after absorbing light a photosensitizer is excited to its singlet excited state in which the electrons are still spin coupled (Figure 3.10A). This is a short-lived state that often just relaxes back to the ground state via fluorescence. However, the singlet state can also undergo intersystem crossing to the triplet state (Figure 3.10A). Many photosensitizer undergo ISC more efficiently than a typical substrate. In this state, the electrons are no longer spin coupled and therefore cannot relax back to the ground state without undergoing a second intersystem crossing event, which is a spin-forbidden process. Therefore, the triplet state has a longer lifetime, and can engage in reactions with a substrate. The energy transfer event



happens through a process called Dexter energy transfer (Figure 3.10B). When the substrate and excited state photocatalyst are in proximity, a simultaneous double electron transfer occurs yielding an excited state substrate and ground state photocatalyst. For this process to occur, the energy transfer must be energetically favored, which can be determined by comparing the triplet energies of the substrate and catalyst.

Given the challenges associated with excited state imines, in combination with the precedence for excited state alkene [2+2] cycloaddition reactions, we sought to develop an orthogonal approach to the traditional aza Paternò-Büchi reaction relying on selective excitation of the alkene partner using visible light.

## 3.2 Results and Discussion

### 3.2.1 Reaction Design and Optimization

In order to take advantage of a visible light absorbing photosensitizer, an alkene with an appropriate triplet energy must be selected. Styrenes and conjugated dienes have a history of use in visible light mediated [2+2] photocycloadditions<sup>57,58</sup> (Figure 3.11C) and are known to have a lower triplet energy than functionalized imines. After excitation, we hypothesized that a subsequent [2+2] cycloaddition with a C=N double bond would yield the desired azetidine product (Figure 3.11C).

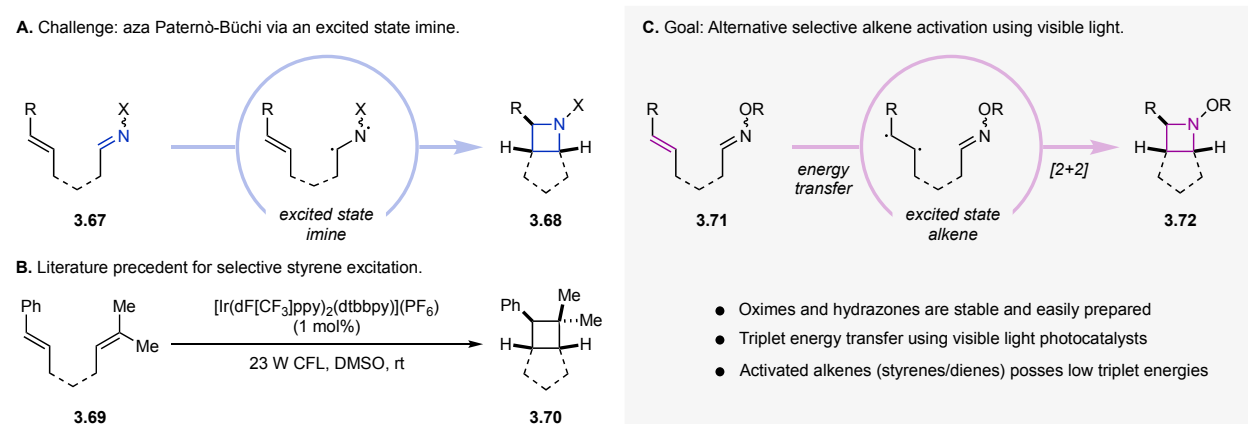
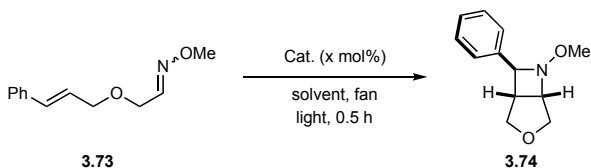


Figure 3.11 Reaction design for an aza Paternò-Büchi enabled by selective alkene excitation using visible light.

Substrate **3.73** was designed to test the potential of this reaction. We selected oximes as the C=N component because of their facile synthesis and superior stability compared to imines. In accordance with the literature, direct excitation of oxime **3.73** with UV light resulted in primarily E/Z isomerization with only trace amounts of azetidine **3.74** (Table 3.1, entry 1). Based on

Sivaguru's report, the photosensitizer xanthone was evaluated under UV irradiation resulting in full conversion of the substrate and a 43% yield of azetidine **3.74** (Table 3.1, entry 2). We hypothesized that the harsh light could explain the low yield.

Table 3.1 Aza Paternò-Büchi reaction optimization.



entry	Catalyst (mol%)	Wavelength (nm)	Solvent	Concentration (M)	yield <sup>a</sup>
1 <sup>b</sup>	—	365	DCM	0.01	6
2 <sup>c</sup>	xanthone (30)	365	MeCN	0.01	43
3	[Ru(bpy) <sub>3</sub> ](PF <sub>6</sub> ) <sub>2</sub> (2.5)	427	THF	0.01	—
4	<i>fac</i> -[Ir(ppy) <sub>3</sub> ] (2.5)	427	THF	0.01	39
5	<i>fac</i> -[Ir(dFppy) <sub>3</sub> ] (2.5)	427	THF	0.01	52
6	<i>fac</i> -[Ir(Fppy) <sub>3</sub> ] (2.5)	427	THF	0.01	30
7	[Ir(dF(CF <sub>3</sub> )ppy) <sub>2</sub> (dtbbpy)] (PF <sub>6</sub> ) (2.5)	427	THF	0.01	97
8	[Ir(dF(CF <sub>3</sub> )ppy) <sub>2</sub> (dtbbpy)] (PF <sub>6</sub> ) (2.5)	427	DCM	0.025	72
9	[Ir(dF(CF <sub>3</sub> )ppy) <sub>2</sub> (dtbbpy)] (PF <sub>6</sub> ) (2.5)	427	MeOH	0.025	87
10	[Ir(dF(CF <sub>3</sub> )ppy) <sub>2</sub> (dtbbpy)] (PF <sub>6</sub> ) (2.5)	427	EtOAc	0.025	87
11	[Ir(dF(CF <sub>3</sub> )ppy) <sub>2</sub> (dtbbpy)] (PF <sub>6</sub> ) (2.5)	427	acetone	0.025	86
12	[Ir(dF(CF <sub>3</sub> )ppy) <sub>2</sub> (dtbbpy)] (PF <sub>6</sub> ) (2.5)	427	MeCN	0.025	88
13	[Ir(dF(CF <sub>3</sub> )ppy) <sub>2</sub> (dtbbpy)] (PF <sub>6</sub> ) (2.5)	427	THF	0.025	93
14	[Ir(dF(CF <sub>3</sub> )ppy) <sub>2</sub> (dtbbpy)] (PF <sub>6</sub> ) (2.5)	427	THF	0.05	88
15	[Ir(dF(CF <sub>3</sub> )ppy) <sub>2</sub> (dtbbpy)] (PF <sub>6</sub> ) (2.5)	427	THF	0.10	90
16	[Ir(dF(CF <sub>3</sub> )ppy) <sub>2</sub> (dtbbpy)] (PF <sub>6</sub> ) (1.0)	427	THF	0.01	96
17	[Ir(dF(CF <sub>3</sub> )ppy) <sub>2</sub> (dtbbpy)] (PF <sub>6</sub> ) (0.5)	427	THF	0.01	98
18	—	427	THF	0.01	—
19 <sup>d</sup>	[Ir(dF(CF <sub>3</sub> )ppy) <sub>2</sub> (dtbbpy)] (PF <sub>6</sub> ) (2.5)	—	THF	0.01	—

Reactions were performed on 0.1 mmol scale under irradiation with blue LED light (427 nm) unless otherwise specified. <sup>a</sup> Yields were determined by quantitative <sup>1</sup>H NMR analysis from the crude mixture using an internal standard. <sup>b</sup> 24 h reaction. <sup>c</sup> 12 h reaction. <sup>d</sup> Run in the dark.

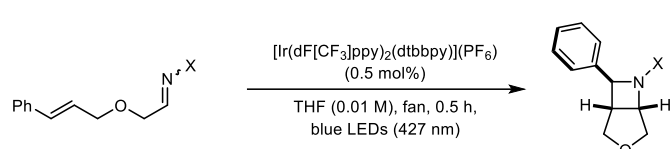
With the goal of developing a mild and general protocol, we next evaluated visible light absorbing photosensitizers using 40 W 427 nm LEDs as the light source. Irradiating oxime **3.73** with visible light in the presence of [Ru(bpy)<sub>3</sub>](PF<sub>6</sub>)<sub>2</sub> (**3.66**) resulted in no formation of the desired product (Table 3.1, entry 3). Switching to higher triplet energy catalysts *fac*-[Ir(ppy)<sub>3</sub>] (**3.64**), *fac*-[Ir(dFppy)<sub>3</sub>], and *fac*-[Ir(Fppy)<sub>3</sub>] proved beneficial, as the desired azetidine product **3.74** was isolated in 39%, 52%, and 30% yield respectively (Table 3.1, entries 4 – 6). Gratifyingly, reacting oxime **3.73** in the presence of 2.5 mol% of Ir[dF(CF<sub>3</sub>)ppy]<sub>2</sub>(dtbbpy)(PF<sub>6</sub>) (**3.63**) produced azetidine **3.74** in 97% yield in >20:1 diastereomeric ratio (d.r.) (Table 3.1, entry 7). The Yoon group has previously demonstrated the capabilities of this catalyst in the synthesis of cyclobutanes.<sup>57,58</sup> Additional optimization identified THF as the ideal solvent and 0.01 M as the

optimal concentration forming **3.74** in 97% yield with a catalyst loading of 2.5 mol% (Table 3.1, entry 7). Additionally, the catalyst loading could be lowered to 0.5 mol% resulting in azetidine **3.74** in 98% yield under optimal reaction conditions (Table 3.1, entry 17). Importantly, control reactions confirmed that both light and photocatalyst were necessary for a successful reaction (Table 3.1, entries 18 & 19).

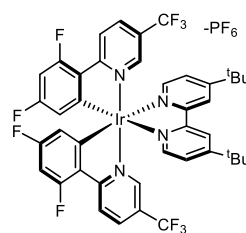
### 3.2.2 Substrate Scope

After establishing the optimal reaction conditions, we focused on exploring the substrate scope of this aza Paternò-Büchi reaction starting by evaluating different oximes and hydrazones (Table 3.2). *O*-Benzyl oxime **3.75** performed comparably well providing 96% of **3.76** in 16:1 d.r. (Table 3.2, entry 2). To demonstrate the scalability of this reaction, substrates **3.73** and **3.75** were reacted on a gram scale with no significant loss in yield or d.r. (Table 3.2, entry 1 & 2). Free hydroxy oxime **3.77** was also tested and provided 54% yield of **3.78** (Table 3.2, entry 3). Hydrazones were also tested for their compatibility with this reaction. *N*-Boc hydrazone **3.79** afforded azetidine **3.80** in 62% yield and 13:1 d.r (Table 3.2, entry 4). The structure of this compound was unambiguously assigned by X-ray crystallography. On the other hand, *N,N*-dimethyl hydrazone **3.81** did not react under these conditions, instead the starting material was fully recovered (Table 3.2, entry 5). We also evaluated *N*-tosyl imines, and although these substrates could successfully undergo a [2+2] reaction, the instability of the products made isolating a sufficiently pure azetidine product impossible. Importantly, all substrates were prepared and used as mixture of *E/Z* isomers, but the high diastereoselectivity of this reaction indicates that the *E/Z* ratio does not influence the outcome of the reaction. Based on these studies, *O*-alkyl oximes were selected as the optimal C=N double bond for this aza Paternò-Büchi reaction. Although this means that all the azetidine products would contain a N-O bond, we hypothesized that this could function as a protecting group and be cleaved if desired.

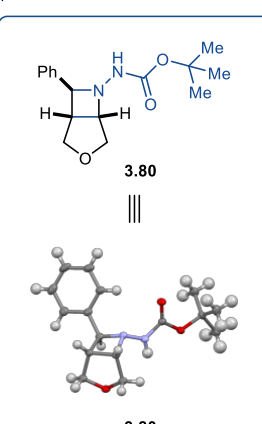
Table 3.2 Oxime and hydrazone scope.



entry	substrate	Z/E ratio	yield	d.r.	
1		3.73	1 : 1.3	96% 91% <sup>b</sup>	3.74 >20:1 >20:1
2		3.75	1 : 1.3	96% 90% <sup>b</sup>	3.76 16:1 20:1
3		3.77	1 : 1.1	54%	3.78 >20:1
4		3.79	1 : 2.6	62%	3.80 13:1
5 <sup>a</sup>		3.81	0 : 1	0%	3.82 -



**3.63**  
[Ir(dF[CF<sub>3</sub>]ppy)<sub>2</sub>(dtbbpy)](PF<sub>6</sub>)

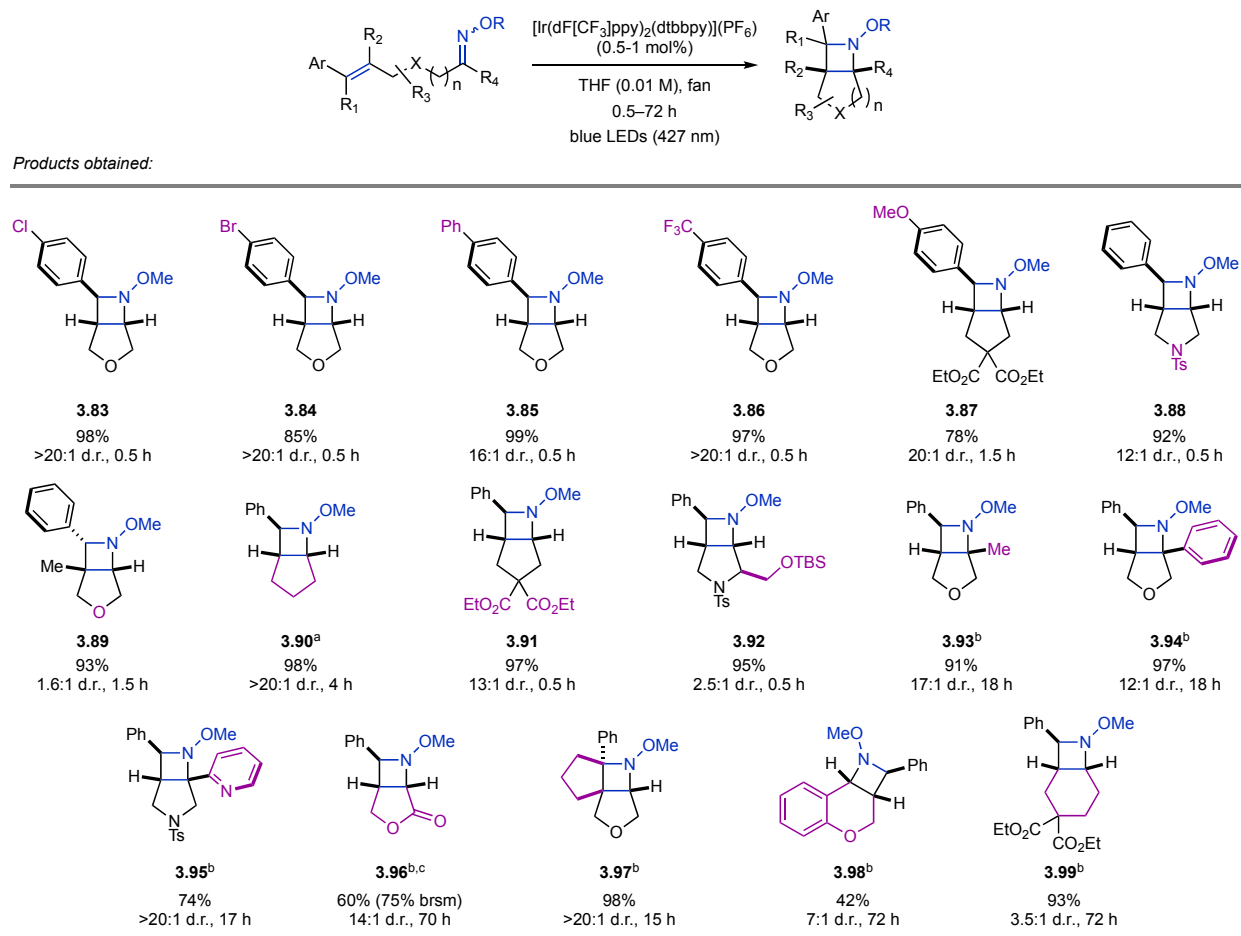


**3.80**

Reactions were performed on a 0.25 mmol scale with 0.5 mol% [Ir(dF[CF<sub>3</sub>]ppy)<sub>2</sub>(dtbbpy)](PF<sub>6</sub>) in THF(0.01 M) at ambient temperature (fan cooling) under blue light irradiation (427 nm). Diastereomeric ratios were determined by <sup>1</sup>H NMR of the crude reaction mixture. Yields refer to the mixture of diastereomers. <sup>a</sup> 16 h reaction. <sup>b</sup> Reaction performed on gram scale.

From there, our focus turned to expanding the scope with an emphasis on exploring the functional group tolerance and synthesizing highly functionalized azetidines (Figure 3.12). This reaction proved tolerant to several electronically differentiated styrenes with all azetidine products being isolated in high yields and d.r. (**3.83-3.87**). A variety of substitution and functional groups could be incorporated into the backbone without diminishing the yield. This includes ester (**3.87**, **3.91**, **3.96**, **3.99**) sulfonamide (**3.88**, **3.92**, **3.95**), and silyl enol ether functional groups (**3.92**). We found that methyl-substituted styrene greatly diminished the d.r. to 1.6:1 (**3.89**). When extended reaction times were required (**3.93 – 3.99**), deoxygenation of the reaction mixture helped mitigate decomposition caused by triplet state oxygen. Ketone derived oximes were also amenable to this transformation providing azetidines **3.93**, **3.94**, and **3.95** in 91%, 97%, and 74% yield respectively all with high d.r. Azetidine **3.95** also demonstrated that pyridine heterocycles were well tolerated. Lactone tethered azetidine **3.96** could be synthesized in 60% yield (75% BRSM) and 14:1 d.r., although it required heating to 80 °C in acetonitrile for 70 hours. Tricyclic azetidine **3.97** was prepared from the corresponding tetrasubstituted styrene in 98% yield and >20:1 d.r. This method

could also be successfully used to form 4/6 fused ring systems as demonstrated by azetidines **3.98** and **3.99**.



Reactions were performed on 0.25 mmol scale with 0.5-1.0 mol%  $[\text{Ir}(\text{dF}[\text{CF}_3]\text{ppy})_2(\text{dtbbpy})](\text{PF}_6)$  in THF (0.01 M) at ambient temperature (fan cooling) under blue LED irradiation (427 nm). Diastereomeric ratios were determined by  $^1\text{H}$  NMR of the crude reaction mixture. Yields refer to the mixture of diastereomers (major is drawn). <sup>a</sup> On a 500 mg scale. <sup>b</sup> Under an  $\text{N}_2$  atmosphere, <sup>c</sup> run at 82 °C.

Figure 3.12 Evaluation of the scope of this [2+2]-cycloaddition reaction.

As a demonstration of utility in late-stage diversification, the agrochemical herbicide safener isoxadefin ethyl was converted to tricyclic azetidine **3.102** in three steps (Figure 3.13).

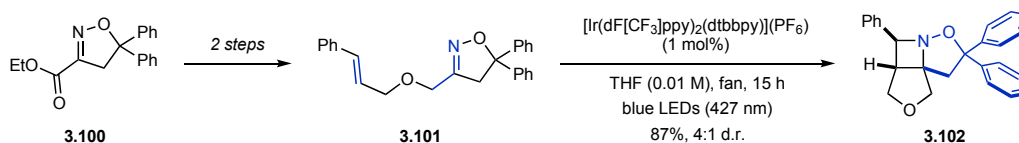


Figure 3.13 Modification of the agrochemical herbicide safener isoxadefin ethyl.

Dienes possess a comparable triplet energy to styrenes, around  $60 \text{ kcal mol}^{-1}$ , and as a result were also evaluated (Figure 3.14).<sup>58</sup> Diene **3.103** underwent the desired [2+2] reaction resulting in the formation of azetidine **3.104** in 99% yield. However, azetidine **3.104** was isolated in lower d.r.

than styrene analogue **3.74**. Additionally, diene substrate **3.105** was subjected to the optimized reaction conditions and successfully provided strained azetidinium **3.106** in 39% yield. Notably, no [4+2] cycloaddition products were observed in either of these cases.

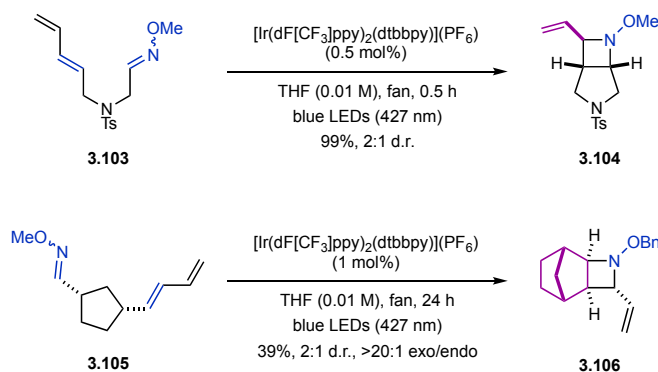


Figure 3.14 Diene substrate evaluations.

### 3.2.3 Mechanistic Studies

Subsequent experiments were dedicated to understanding the underlying mechanism of this aza Paternò-Büchi reaction. Stern-Volmer quenching studies were used to verify that this transformation was proceeding through a triplet energy transfer from the iridium photocatalyst to the styrene (Figure 3.15A). Quenching of the photocatalysts was observed with substrates **3.73**; however, no quenching was observed with substrate **3.107**. This confirms that the styrene moiety is quenching the photocatalyst. Furthermore, the quenching process likely does not occur through a single electron transfer event. The redox capabilities of **3.63** ( $E_{1/2}^{\text{III}^*/\text{II}} = +1.21$  V vs SCE,  $E_{1/2}^{\text{IV}/\text{III}^*} = -0.89$  V vs. SCE) are not powerful enough to oxidize or reduce substrate **3.73** ( $E_{p/2} = +1.82$  V vs. SCE).<sup>59</sup> However, the triplet energy of **3.63** ( $E_T = 60.1$  kcal mol<sup>-1</sup>) is energetically favorable when compared with that of a styrene moiety (about 60 kcal mol<sup>-1</sup>). Additionally, a photocatalyst with a slightly lower triplet energy, *fac*-[Ir(ppy)<sub>3</sub>] ( $E_T = 55.8$  kcal mol<sup>-1</sup>), is less efficient in this transformation, whereas [Ru(bpy)<sub>3</sub>](PF<sub>6</sub>)<sub>2</sub> ( $E_T = 46.5$  kcal mol<sup>-1</sup>) was incapable of catalyzing this reaction (Figure 3.15B). The lack of observed reactivity with substrates containing alkenes with higher triplet energies, such as terminal alkene **3.108** ( $E_T > 76$  kcal mol<sup>-1</sup>), was further evidence of an energy transfer process (Figure 3.15B).<sup>60</sup> Based on our oxime and hydrazone evaluation, it was clear that the oxime geometry did not influence the outcome of the reaction, and we wanted to determine if the same thing was true for the styrene geometry. To test this, **3.110** was prepared and subjected to the reaction conditions. **3.74** was isolated in almost identical yield and d.r. to the

corresponding **3.73** substrate reaction, proving that this reaction is stereoconvergent (Figure 3.15C).

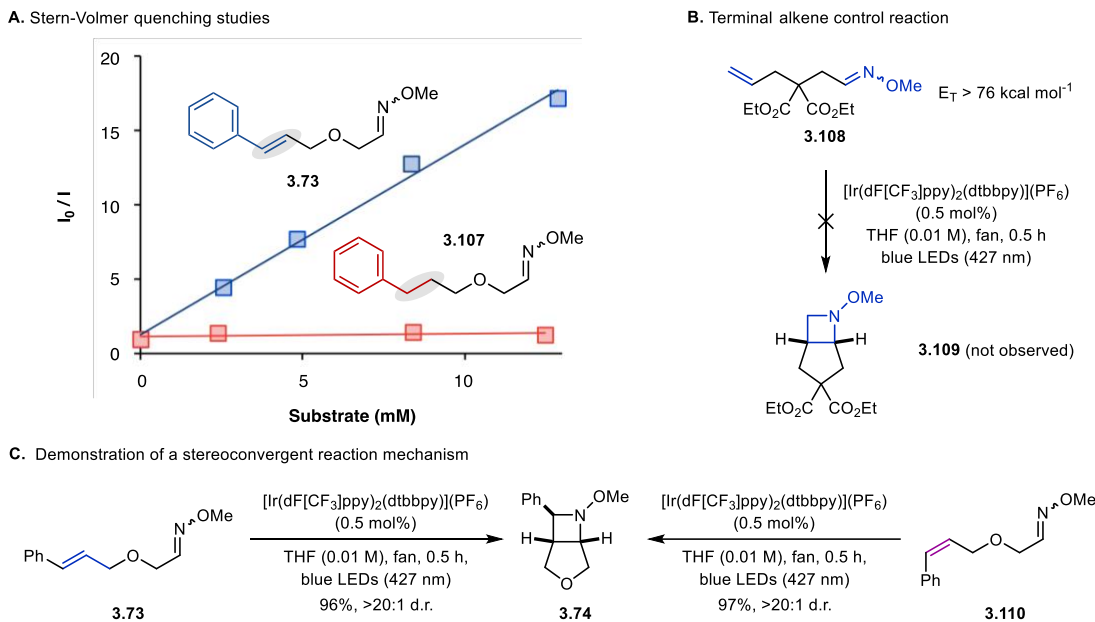


Figure 3.15 (A) Stern-Volmer quenching studies. (B) Terminal alkene control reaction. (C) Styrene stereoconvergence experiments.

$^1\text{H}$  NMR monitoring revealed rapid interconversion between **3.73** and **3.110** as both isomers ultimately converting to product **3.74** (Figure 3.16). E/Z oxime isomer scrambling was also observed as the ratio changed from 1.6:1 to 1:1 within the first two minutes of the reaction (Figure 3.16B). This data suggests the E isomer reacts faster than the Z isomer. Interestingly, there was a brief increase in the overall concentration of the Z isomer, which cannot be explained by different reaction rates. The same study was conducted with substrate **3.107**, lacking a styrene moiety, and no oxime scrambling was observed.

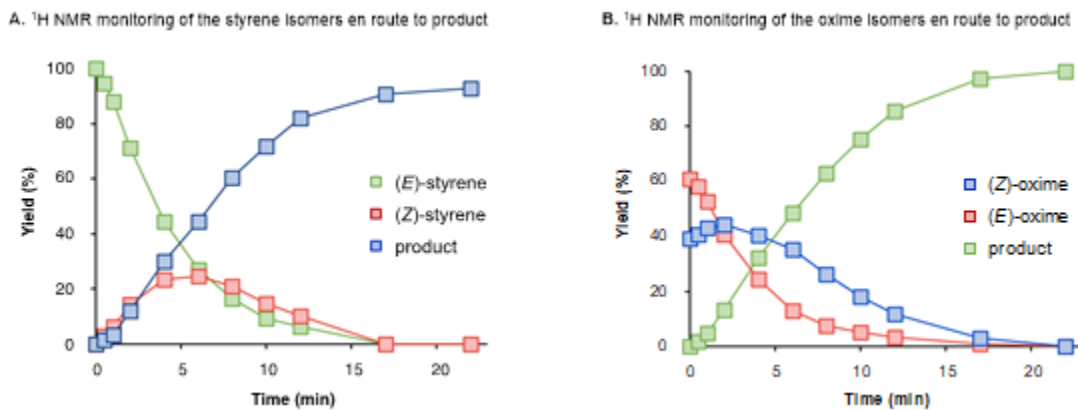


Figure 3.16  $^1\text{H}$  NMR studies of the styrene and oxime isomer consumption and formation of the desired product.

Taken together, these mechanistic experiments point towards a reaction mechanism that begins with photoexcitation of the iridium catalyst (Figure 3.17). A subsequent triplet energy transfer results in a triplet excited state substrate **3.112**. In this biradical state, the substrate is free to rotate around the remaining single bond explaining the observed E/Z styrene isomerization. Alternatively, intermediate **3.112** can undergo a stepwise [2+2]-cycloaddition reaction with the oxime fragment. The first bond that forms likely closes the five membered ring. This step also ablates the stereochemistry of the oxime as there is now freedom of rotation about the C-N bond in **3.113**. We propose that this initial bond forming reaction is reversible, explaining the brief increase in the concentration of the Z oxime isomer. After intersystem crossing (ISC), the singlet state biradical will recombine to form azetidine **3.74**.

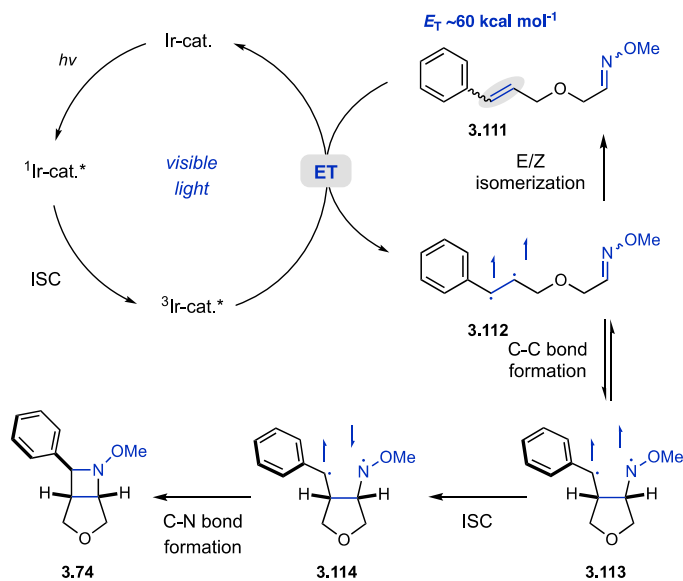


Figure 3.17 Proposed mechanism for the aza Paternò-Büchi reaction.

### 3.2.4 Synthetic Applications

Our efforts turned to diversifying the azetidine products to illustrate the synthetic utility of this aza Paternò-Büchi reaction. Firstly, the N-O bond was cleaved using zinc metal in HCl providing free azetidine **3.115**, which validates the notion that the N-O bond can function as a cleavable protecting group (Figure 3.18A). While studying the N-O bond cleavage reaction, we discovered that, under palladium-mediated hydrogenolysis conditions, both the N-O bond and the benzylic C-N bond could be reduced providing tetrahydrofuran **3.116** in 98% after tosylation. Additionally, 2-phenylazetidine **3.117** was converted to the corresponding azetidine-2-carboxylic acid **3.118** in 38% yield using  $\text{RuCl}_3/\text{H}_5\text{IO}_6$  (Figure 3.18B).<sup>61</sup> This product represents an analog of



the non-proteinogenic amino acid Aze (**3.119**). Furthermore, lactone bearing substrate **3.96** was fully reduced to the diol using  $\text{LiAlH}_4$  providing monocyclic azetidine **3.120** in 84% yield (Figure 3.18C).

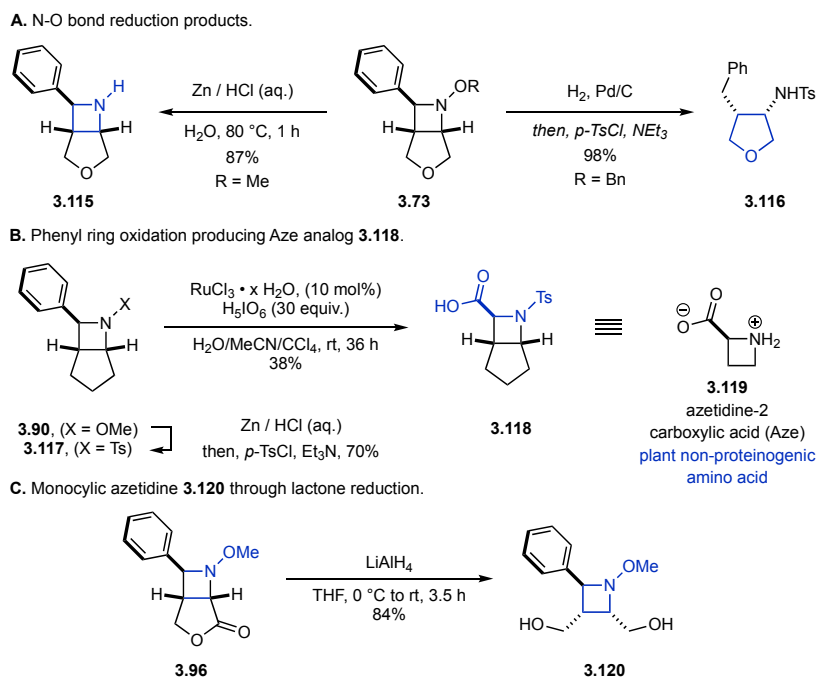


Figure 3.18 Synthetic modifications of the azetidine products prepared through this method.

### 3.3 Conclusion

In summary, we have developed a mild, visible light mediated approach to the aza Paternò-Büchi reaction between alkenes and oximes that relies on alkene activation using an iridium-based photosensitizer. This strategy overcomes the previous limitation associated with excited state imines. Mechanistic studies confirmed that the reaction developed herein proceeds through an efficient triplet energy transfer from the photocatalyst to the alkene. The functional group tolerance was broad, and 24 different functionalized azetidines were synthesized in up to 99% yield and >20:1 d.r. Several different diversification strategies were studied including facile reduction of the N-O bond. Overall, we believe this strategy will help enable access to highly functionalized azetidines, as well as facilitate the development of new [2+2] cycloaddition reactions involving C=N double bonds.

### 3.4 Experimental

#### 3.4.1 General Information

All air- or moisture-sensitive reactions were carried out in flame-dried glassware under an atmosphere of nitrogen. Thin-layer chromatography (TLC) was performed on *Merck* silica gel 60 F<sub>254</sub> plates using UV light (254 or 366 nm), KMnO<sub>4</sub> or CAM stain for visualization. Flash chromatography was performed using silica gel Silia Flash<sup>®</sup> 40-63 micron (230-400 mesh) from Silicycle.

All chemicals were purchased from Sigma-Aldrich, Alfa Aesar, Acros Organics, Oakwood, TCI America, Frontier Scientific, Matrix Scientific, Ark Pharm, Strem and Chem Impex International, and were used as received unless otherwise stated. THF, CH<sub>2</sub>Cl<sub>2</sub>, Et<sub>2</sub>O, MeOH, MeCN and DMF were dried by being passed through a column of activated alumina under argon using a JC-Meyer Solvent Systems. Triethylamine was freshly distilled prior to use over CaH. [Ir(dF(CF<sub>3</sub>)ppy)<sub>2</sub>(dtbbpy)]PF<sub>6</sub> (**3.63**) was prepared according to the procedure described by Stephenson.<sup>62</sup> 2-Iodoxybenzoic acid (IBX) was prepared as described by Santagostino.<sup>63</sup> Proton nuclear magnetic resonance (<sup>1</sup>H NMR) spectra were recorded on Varian MR400, Varian vnmrs 500, Varian Inova 500, and Varian vnmrs 700 spectrometers and are referenced to residual protic NMR solvent (CHCl<sub>3</sub>: δ 7.26 ppm, CH<sub>2</sub>Cl<sub>2</sub>: δ 5.32 ppm). Data for <sup>1</sup>H NMR are reported as follows: chemical shift (δ ppm), multiplicity (s = singlet, d = doublet, t = triplet, q = quartet, m = multiplet, b = broad), coupling constant (Hz), integration. Carbon nuclear magnetic resonance (<sup>13</sup>C NMR) spectra were recorded on Varian vnmrs 500 and Varian vnmrs 700 spectrometers and are referenced to the carbon resonances of the NMR solvent (CDCl<sub>3</sub>: δ 77.16 ppm, CD<sub>2</sub>Cl<sub>2</sub>: δ 54.00 ppm). High-resolution mass spectrometry (MS) data was recorded at the Mass Spectrometry Facility at the Department of Chemistry of the University of Michigan in Ann Arbor, MI on an Agilent 6230 TOF HPLC-MS (ESI) or Micromass AutoSpec Ultima Magnetic Sector mass spectrometer (ESI, EI). Infrared (IR) spectra were obtained using a Thermo-Nicolet IS-50 spectrometer. IR data are represented as frequency of absorption (cm<sup>-1</sup>). Stereochemistry indicators with asterisk (*R*\*, *S*\*) were used to indicate relative stereochemistry of diastereomers.

Abbreviations used: AcOH = acetic acid, Ag/AgCl = silver/silver chloride, aq. = aqueous, brsm = based on recovered starting material, CaH = calcium hydride, CAM = cerium ammonium molybdate, CD<sub>2</sub>Cl<sub>2</sub> = deuterated dichloromethane, CCl<sub>4</sub> = carbon tetrachloride, CDCl<sub>3</sub> = deuterated chloroform, CH<sub>2</sub>Cl<sub>2</sub> = dichloromethane, CuBr = copper(I) bromide, DIBAL-H = diisobutylaluminum hydride, d.r. = diastereomeric ratio, DMF = *N,N*-dimethylformamide, DMSO = dimethylsulfoxide, EI = electron ionization, ESI = electrospray ionization, *E*<sub>T</sub> = triplet

energy, Et<sub>2</sub>O = diethyl ether, Et<sub>3</sub>N = triethylamine, EtOAc = ethyl acetate, EtOH = ethanol, HCl = hydrochloric acid, IBX = 2-iodoxybenzoic acid, IR = infrared, K<sub>2</sub>CO<sub>3</sub> = potassium carbonate, KCl = potassium chloride, KI = potassium iodide, KMnO<sub>4</sub> = potassium permanganate, LiAlH<sub>4</sub> = lithium aluminum hydride, MeCN = acetonitrile, MeOH = methanol, MgSO<sub>4</sub> = magnesium sulfate, MS = mass spectrometry, *n*-Bu<sub>4</sub>NPF<sub>6</sub> = tetrabutylammonium hexafluorophosphate, Na<sub>2</sub>SO<sub>4</sub> = sodium sulfate, NaH = sodium hydride, NaHCO<sub>3</sub> = sodium bicarbonate, NaHSO<sub>3</sub> = sodium bisulfite, NaIO<sub>4</sub> = sodium periodate, NaOAc = sodium acetate, NaOH = sodium hydroxide, NH<sub>4</sub>Cl = ammonium chloride, NMR = nuclear magnetic resonance, *p*-TsOH = *p*-toluenesulfonic acid monohydrate, *p*-TsCl = *p*-toluenesulfonyl chloride, rt = room temperature, RuCl<sub>3</sub> = ruthenium(III) chloride, sat. = saturated, SCE = saturated calomel electrode, TBSCl = *tert*-butyldimethylsilyl chloride, THF = tetrahydrofuran, TLC = thin-layer chromatography, UV = ultraviolet.

### 3.4.2 Mechanistic Investigations

#### Electrochemical Measurements

Cyclic voltammetry was performed on a CHI620E electrochemical analyzer (CH instruments) using a 3-mL five-necked electrochemical cell equipped with a carbon working electrode, a platinum counter or auxiliary electrode, an Ag/AgCl (3 M KCl) reference electrode and a scan rate of 100 mV/s. The experimental setup was calibrated using ferrocene (Fc<sup>+</sup>/Fc) prior to each experiment. Samples were prepared with 0.03 mmol substrate in 3 mL *n*-Bu<sub>4</sub>NPF<sub>6</sub> electrolyte (0.1 M in MeCN) and degassed by sparging with argon gas for 10 min prior to use. The potential ( $E_{p/2}$ ) was determined and converted to SCE as described by Nicewicz.<sup>64</sup> The cyclic voltammogram shows an irreversible oxidation process with  $E_{p/2} = +1.82$  V (vs. SCE). [Ir(dF(CF<sub>3</sub>)ppy)<sub>2</sub>(dtbbpy)]PF<sub>6</sub> (**3.63**) ( $E_{1/2}^{III^*/II} = +1.21$  V vs. SCE)<sup>65</sup> does not possess an excited state oxidation potential sufficient to oxidize **3.73**, thus, a photoredox process is unlikely.

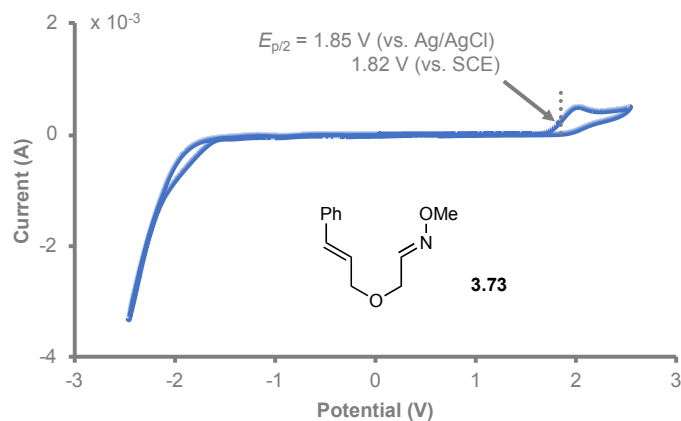


Figure 3.19 Cyclic voltammogram of compound **3.73**.

### UV/Vis Absorption Spectra

UV/Vis absorption spectra were recorded on a Shimadzu UV-1601 UV/Vis spectrometer. Samples were prepared in THF with substrate **3.73** (10 mM) and photocatalyst **3.63** (0.05 mM). The photocatalyst is the only species absorbing at 427 nm.

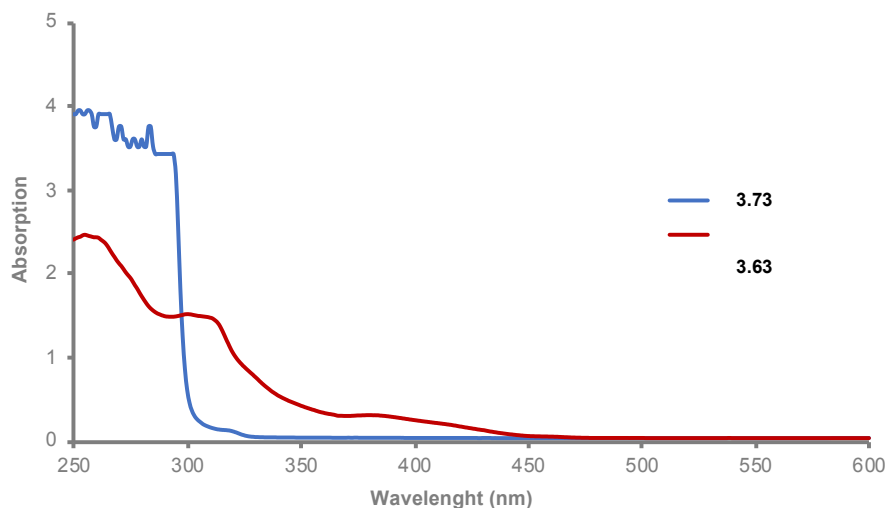


Figure 3.20 UV/Vis spectra of **3.73** (blue) and **3.63** (red).

### Stern-Volmer-Quenching Studies

All samples were prepared using stock solutions of **3.63** (0.11 mM), **3.73** (102.9 mM), or **3.107** (102.4 mM) in dry MeCN. To a volumetric flask was added **17**•PF<sub>6</sub> (190 μL) and the respective amount of quencher and the volume adjusted to 4 mL with dry MeCN. The solution was transferred to a 1-cm quartz cuvette and degassed by sparging with nitrogen gas for 15 min. Emission spectra were recorded using a PTI QuantaMaster fluorimeter (Horiba) with an excitation wavelength of

420 nm. The emission intensities for the Stern-Volmer analysis were observed at 471 nm. The ratio of  $I_0/I$  was plotted as a function of the quencher concentration ( $I_0$ : emission intensity of **3.63** without quencher;  $I$ : emission intensity of **3.63** in the presence of quencher). The Stern-Volmer analysis shows that **3.63** is only efficiently quenched by the styrene moiety in **3.73**, while the oxime moiety (**3.107**) does not quench the photocatalyst.

Table 3.3 Data from the Stern-Volmer quenching study.

	0.0 mM	2.5 mM	5.0 mM	8.5 mM	12.5 mM
$I_0/I$ ( <b>3.73</b> )	1.0	8.7	16.4	27.7	37.8
$I_0/I$ ( <b>3.107</b> )	1.0	1.1	1.0	1.0	1.1

### NMR Time Studies

A 1-dram vial was charged with **3.73** (6.2 mg, 0.03 mmol, 1.0 equiv.), **3.63** (0.2 mg, 0.5 mol%), dimethyl terephthalate (4.7 mg) and  $d_3$ -MeCN (3 mL). 1 mL of the resulting solution was transferred to a NMR tube, which was placed in front of a 40 W PR160-427 nm Kessil light (~5 cm distance; 50% intensity) and the solution irradiated under ambient atmosphere. Conversion and yield were determined at several time points by quantitative  $^1\text{H}$  NMR using dimethyl terephthalate as internal standard. The time study shows that styrene  $E/Z$  isomerization occurs at a similar rate as productive formation of **3.74**, however, both ( $E$ )- and ( $Z$ )-**3.73** eventually are converted to **3.74** (Fig. 4A). Additionally, the observed oxime  $E/Z$  isomerization at low conversion indicates reversible  $C-C$  bond formation from the triplet styrene, which generates a 1,4-biradical that can freely rotate around the  $C-N$  bond. In contrast, no oxime  $E/Z$  isomerization was observed for compound **3.107** lacking the styrene moiety.

Table 3.4 Data from the NMR time study.

t (min)	% of <b>3.73</b> ( <i>E</i> -oxime)	% of <b>3.73</b> ( <i>Z</i> -oxime)	% of <b>3.73</b> ( <i>E</i> -styrene)	% of <b>3.73</b> ( <i>Z</i> -styrene)	% of <b>2.74</b>
0.0	61	39	100	0	0
0.5	58	41	95	3	1
1.0	53	43	88	6	3
2.0	41	44	71	14	12
4.0	24	40	44	23	30
6.0	13	35	27	25	44
8.0	8	26	17	21	60
10.0	5	18	9	15	72
12.0	3	12	6	10	82
17.0	1	3	0	0	91
22.0	0	0	0	0	93

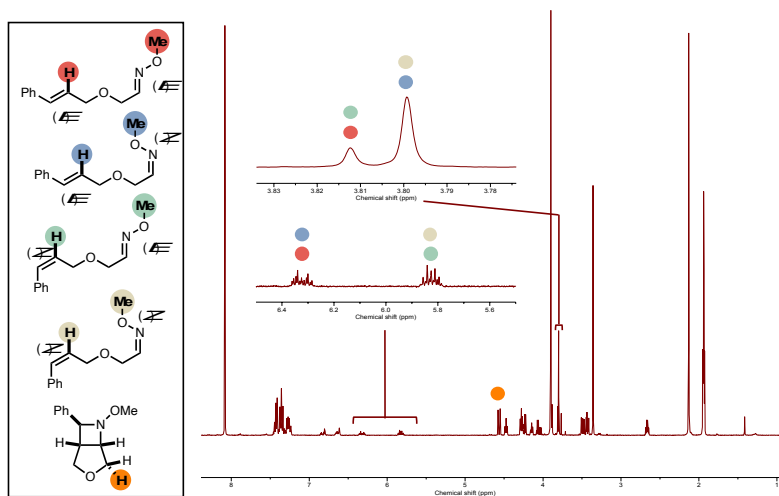
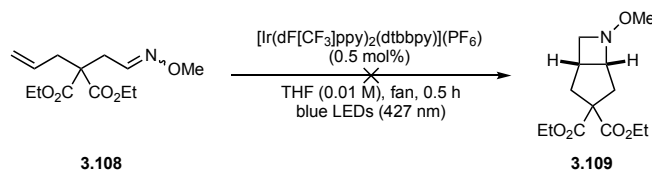


Figure 3.21 NMR spectra at t = 8 min. The signals that were used to obtain the data in table 2.4 have been highlighted.

## Control Experiments



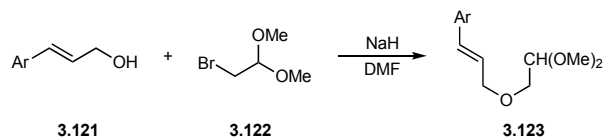
Reaction was carried out according to GP-6a on 0.25 mmol scale. No formation of azetidine **3.109** was observed, and only unreacted starting material (**3.108**) was isolated from the reaction mixture.

### 3.4.3 Experimental Procedures

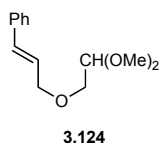
#### Reaction Optimization

A test tube was charged with **3.73** (21 mg, 0.1 mmol, 1.0 equiv.), photocatalyst and solvent, then sealed with a rubber septum and placed in front of a 40 W PR160-427 nm Kessil light at a distance of approximately 5 cm, which was set to 100% intensity (reactions involving UV light were carried out in a Luzchem LZG-ORG photoreactor). After stirring for 0.5 h, the reaction mixture was transferred to a 50-mL round-bottom flask and the solvent removed *in vacuo*. The crude reaction mixture was analyzed by <sup>1</sup>H NMR to determine the yield of **3.74** using mesitylene as internal standard.

#### General Procedure for Alkylation of Cinnamyl Alcohols (GP-1)

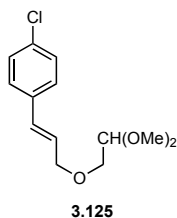


A round-bottom flask equipped with a magnetic stir bar was charged with NaH (60% dispersion in mineral oil; 1.5 equiv.) and dry DMF (0.5 M). The mixture was cooled to 0 °C and the corresponding cinnamyl alcohol was added slowly and the solution stirred for 1 h. Next, 2-bromo-1,1-dimethoxyethane (2.0 equiv.) was added and the reaction heated at 110°C for 24 h. NH<sub>4</sub>Cl (aq., sat.) and water were sequentially added, the organic layer was separated and the aqueous layer extracted with EtOAc (3x). The combined organic layers were washed with water (2x) and brine (2x), dried over Na<sub>2</sub>SO<sub>4</sub>, filtered and concentrated *in vacuo*. The crude product was purified by flash column chromatography (EtOAc/hexanes) to afford the corresponding pure alkylated cinnamyl alcohol.

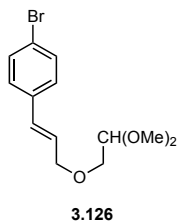


**(E)-(3-(2,2-Dimethoxyethoxy)prop-1-en-1-yl)benzene (3.124):** Prepared according to GP-1 from (*E*)-cinnamyl alcohol (37.3 mmol). Purification by flash column chromatography (5-15% EtOAc/hexanes) afforded the pure title compound as yellow oil (2.90 g, 35%). <sup>1</sup>H NMR

(700 MHz, CDCl<sub>3</sub>):  $\delta$  7.39 (d,  $J$  = 7.4 Hz, 2H), 7.32 (t,  $J$  = 7.6 Hz, 2H), 7.24 (t,  $J$  = 7.3 Hz, 1H), 6.61 (d,  $J$  = 15.9 Hz, 1H), 6.29 (dt,  $J$  = 15.9, 6.2 Hz, 1H), 4.56 (t,  $J$  = 5.2 Hz, 1H), 4.21 (dd,  $J$  = 6.2, 1.2 Hz, 2H), 3.54 (d,  $J$  = 5.2 Hz, 2H), 3.41 (s, 6H); <sup>13</sup>C NMR (176 MHz, CDCl<sub>3</sub>):  $\delta$  136.7, 133.0, 128.7, 127.9, 126.7, 125.9, 102.9, 72.3, 69.8, 54.1; IR (cm<sup>-1</sup>): 2936, 2834, 1724, 1450, 1366, 1312, 1194, 1111, 1067, 966, 841, 750, 697; HRMS:  $m/z$  calculated for C<sub>13</sub>H<sub>18</sub>O<sub>3</sub>Na<sup>+</sup> [M+Na]<sup>+</sup>: 245.1148; found: 245.1163.



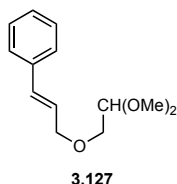
**(E)-1-Chloro-4-(3-(2,2-dimethoxyethoxy)prop-1-en-1-yl)benzene (3.125):** Prepared according to GP-1 from (*E*)-4-chlorocinnamyl alcohol<sup>66</sup> (5.7 mmol). Purification by flash column chromatography (5-20% EtOAc/hexanes) afforded the pure title compound as yellow oil (482 mg, 33%). <sup>1</sup>H NMR (500 MHz, CDCl<sub>3</sub>):  $\delta$  7.31 (d,  $J$  = 8.7 Hz, 2H), 7.28 (d,  $J$  = 8.8 Hz, 2H), 6.56 (d,  $J$  = 15.9 Hz, 1H), 6.26 (dt,  $J$  = 15.9, 6.0 Hz, 1H), 4.55 (t,  $J$  = 5.2 Hz, 1H), 4.19 (dd,  $J$  = 6.0, 1.3 Hz, 2H), 3.54 (d,  $J$  = 5.2 Hz, 2H), 3.41 (s, 6H); <sup>13</sup>C NMR (126 MHz, CDCl<sub>3</sub>):  $\delta$  135.3, 133.5, 131.6, 128.9, 127.8, 126.6, 102.9, 72.1, 70.0, 54.1; IR (cm<sup>-1</sup>): 2909, 2831, 1491, 1447, 1193, 1112, 1090, 1012, 967, 849, 797; HRMS:  $m/z$  calculated for C<sub>13</sub>H<sub>17</sub>ClO<sub>3</sub>Na<sup>+</sup> [M+Na]<sup>+</sup>: 279.0758; found: 279.0760.



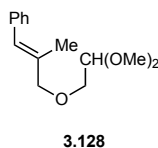
**(E)-1-Bromo-4-(3-(2,2-dimethoxyethoxy)prop-1-en-1-yl)benzene (3.126):** Prepared according to GP-1 from (*E*)-4-bromocinnamyl alcohol<sup>67</sup> (4.7 mmol). Purification by flash column chromatography (5-20% EtOAc/hexanes) afforded the pure title compound as yellow oil (433 mg, 31%). <sup>1</sup>H NMR (400 MHz, CDCl<sub>3</sub>):  $\delta$  7.43 (d,  $J$  = 8.4 Hz, 2H), 7.24 (d,  $J$  = 8.5 Hz, 2H), 6.55 (d,  $J$  = 15.9 Hz, 1H), 6.28 (dt,  $J$  = 15.9, 6.0 Hz, 1H), 4.55 (t,  $J$  = 5.2 Hz, 1H), 4.19 (dd,  $J$  = 6.0, 1.2 Hz, 2H), 3.54 (d,  $J$  = 5.2 Hz, 2H), 3.41 (s, 6H); <sup>13</sup>C NMR (176 MHz, CDCl<sub>3</sub>):  $\delta$  135.7, 131.8, 131.7, 128.2, 126.8, 121.7, 102.9, 72.1, 70.0, 54.1; IR (cm<sup>-1</sup>): 2928, 2831, 1488, 1401, 1323, 1201,



1114, 1072, 1009, 969, 848; **HRMS**:  $m/z$  calculated for  $C_{13}H_{17}BrO_3Na^+$   $[M+Na]^+$ : 323.0253; found: 323.0252.

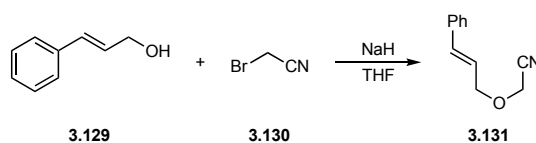


**(E)-4-(3-(2,2-Dimethoxyethoxy)prop-1-en-1-yl)-1,1'-biphenyl (3.127)**: Prepared according to GP-1 from (*E*)-4-phenylcinnamyl alcohol<sup>67</sup> (5.6 mmol). Purification by flash column chromatography (5-20% EtOAc/hexanes) afforded the pure title compound as pale-yellow foam (624 mg, 38%). **<sup>1</sup>H NMR** (700 MHz, CDCl<sub>3</sub>): δ 7.60 (d,  $J$  = 7.3 Hz, 2H), 7.56 (d,  $J$  = 8.2 Hz, 2H), 7.48 – 7.42 (m, 4H), 7.34 (t,  $J$  = 7.4 Hz, 1H), 6.65 (d,  $J$  = 15.9 Hz, 1H), 6.34 (dt,  $J$  = 15.9, 6.2 Hz, 1H), 4.57 (t,  $J$  = 5.2 Hz, 1H), 4.23 (dd,  $J$  = 6.1, 1.0 Hz, 2H), 3.56 (d,  $J$  = 5.2 Hz, 2H), 3.42 (s, 6H); **<sup>13</sup>C NMR** (176 MHz, CDCl<sub>3</sub>): δ 140.7, 140.6, 135.7, 132.5, 128.9, 127.4, 127.4, 127.1, 127.0, 125.9, 102.9, 72.3, 69.8, 54.1; **IR** (cm<sup>-1</sup>): 2915, 2832, 1487, 1449, 1408, 1364, 1193, 1109, 1077, 971, 911, 853, 756, 731, 695; **HRMS**:  $m/z$  calculated for  $C_{19}H_{22}O_3Na^+$   $[M+Na]^+$ : 321.1461; found: 321.1466.

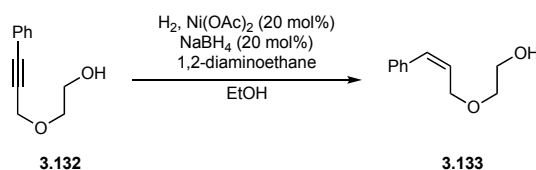


**(E)-3-(2,2-dimethoxyethoxy)-2-methylprop-1-en-1-ylbenzene (3.128)**: Prepared according to GP-1 from (*E*)-2-methyl-3-phenylprop-2-en-1-ol (6.8 mmol). Purification by flash column chromatography (5-20% EtOAc/hexanes) afforded the pure title compound as yellow oil (530 mg, 33%). **<sup>1</sup>H NMR** (500 MHz, CDCl<sub>3</sub>): δ 7.33 (t,  $J$  = 7.6 Hz, 2H), 7.28 (d,  $J$  = 7.5 Hz, 2H), 7.22 (t,  $J$  = 7.2 Hz, 1H), 6.50 (s, 1H), 4.56 (t,  $J$  = 5.2 Hz, 1H), 4.09 (s, 2H), 3.52 (d,  $J$  = 5.2 Hz, 2H), 3.42 (s, 6H), 1.90 (s, 3H); **<sup>13</sup>C NMR** (126 MHz, CDCl<sub>3</sub>): δ 137.6, 135.0, 129.0, 128.2, 127.5, 126.6, 103.0, 77.8, 69.5, 54.0, 15.5; **IR** (cm<sup>-1</sup>): 2911, 2831, 1445, 1358, 1110, 1072, 964, 918, 855, 746, 699; **HRMS**:  $m/z$  calculated for  $C_{14}H_{20}O_3Na^+$   $[M+Na]^+$ : 259.1305; found: 259.1308.

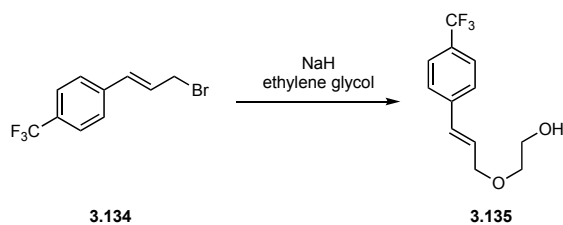
### Miscellaneous Procedure



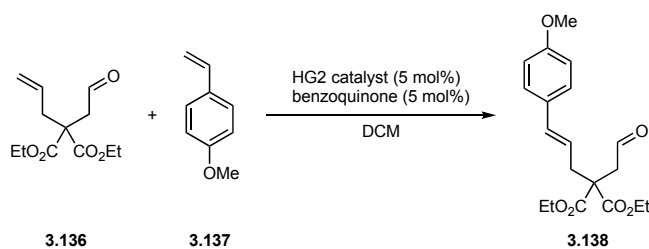
**2-(Cinnamyloxy)acetonitrile (3.131):** A 100-mL round-bottom flask equipped with a stir bar was charged with NaH (60% dispersion in mineral oil; 1.79 g, 44.7 mmol, 1.2 equiv.) and THF (35 mL). The mixture was cooled to 0 °C and a solution of cinnamyl alcohol (5.00 g, 37.3 mmol, 1.0 equiv.) in THF (5 mL) was added dropwise. After stirring for 30 min at 0 °C, bromoacetonitrile (3.1 mL, 44.7 mmol, 1.2 equiv.) was added and the reaction mixture allowed to warm up to rt and stirred overnight. Then, NH<sub>4</sub>Cl (aq., sat.) was added and the biphasic mixture partitioned between water and EtOAc. The organic layer was separated and the aqueous layer extracted with EtOAc (3x). The combined organic layers were washed with brine, dried over Na<sub>2</sub>SO<sub>4</sub> filtered and concentrated *in vacuo*. Purification by flash column chromatography (5-10% EtOAc/hexanes) afforded the pure title compound as pale-yellow oil (3.23 g, 50%). **<sup>1</sup>H NMR** (700 MHz, CDCl<sub>3</sub>): δ 7.41 (d, *J* = 7.4 Hz, 2H), 7.34 (t, *J* = 7.6 Hz, 2H), 7.28 (t, *J* = 7.3 Hz, 1H), 6.70 (d, *J* = 15.9 Hz, 1H), 6.23 (dt, *J* = 15.9, 6.4 Hz, 1H), 4.31 (dd, *J* = 6.5, 1.2 Hz, 2H), 4.29 (s, 2H); **<sup>13</sup>C NMR** (176 MHz, CDCl<sub>3</sub>): δ 136.0, 135.4, 128.8, 128.4, 126.8, 123.2, 116.1, 71.8, 54.8; **IR** (cm<sup>-1</sup>): 3027, 2861, 1494, 1450, 1352, 1091, 967, 883, 744, 692; **HRMS**: *m/z* calculated for C<sub>11</sub>H<sub>11</sub>NONa<sup>+</sup> [M+Na]<sup>+</sup>: 196.0733; found: 196.0730.



**(Z)-2-((3-Phenylallyl)oxy)ethan-1-ol (3.133):** A 25-mL round-bottom flask equipped with a stir bar was charged with nickel(II) acetate tetrahydrate (71 mg, 0.28 mmol, 0.2 equiv.), sodium borohydride (11 mg, 0.28 mmol, 0.2 equiv.) and EtOH (4 mL). The mixture was sparged with hydrogen gas from a balloon and stirred for 1 h at rt. A solution of 2-((3-phenylprop-2-yn-1-yl)oxy)ethan-1-ol<sup>68</sup> (250 mg, 1.4 mmol, 1.0 equiv.) and 1,2-diaminoethane (38 μL, 0.57 mmol, 0.4 equiv.) in EtOH (1 mL) was added and the reaction stirred for 5.5 h at rt under an atmosphere of hydrogen. The mixture was filtered through celite and the filtrate concentrated *in vacuo*. Purification by flash column chromatography (30% EtOAc/hexanes) afforded the pure title compound as clear oil (207 mg, 82%). Spectroscopic data were consistent with those reported in the literature.<sup>69</sup>

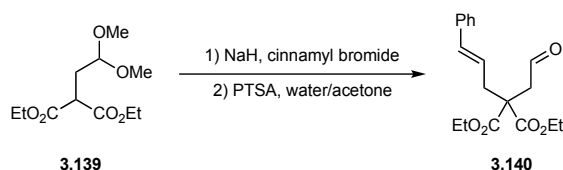


**(E)-2-((3-(4-(Trifluoromethyl)phenyl)allyl)oxy)ethan-1-ol (3.135):** In a 25-mL round-bottom flask equipped with a magnetic stir bar, NaH (60% dispersion in mineral oil; 148 mg, 3.7 mmol, 1.2 equiv.) was added to a solution of ethylene glycol (0.31 mL, 5.6 mmol, 1.9 equiv.) in THF (8 mL) at 0 °C and the mixture stirred for 0.5 h at that temperature, before adding 4-(trifluoromethyl)cinnamyl bromide<sup>70</sup> (800 mg, 3.0 mmol, 1.0 equiv.) as solution in THF (2 mL) dropwise. Then, the reaction mixture was allowed to warm up to rt and heated at reflux overnight. After cooling down to rt, NH<sub>4</sub>Cl (aq., sat.) was added and the biphasic mixture partitioned between water and EtOAc. The organic layer was separated and the aqueous layer extracted with EtOAc (3x). The combined organic layers were washed with brine, dried over Na<sub>2</sub>SO<sub>4</sub>, filtered and concentrated *in vacuo*. Purification by flash column chromatography (5-50% EtOAc/hexanes) afforded the pure title compound as clear oil (470 mg, 64%). <sup>1</sup>H NMR (700 MHz, CDCl<sub>3</sub>): δ 7.57 (d, *J* = 8.2 Hz, 2H), 7.48 (d, *J* = 8.2 Hz, 2H), 6.66 (d, *J* = 16.0 Hz, 1H), 6.39 (dt, *J* = 16.0, 5.8 Hz, 1H), 4.23 (dd, *J* = 5.8, 1.4 Hz, 2H), 3.80 (t, *J* = 4.6 Hz, 2H), 3.64 (t, *J* = 4.6 Hz, 2H); <sup>13</sup>C NMR (176 MHz, CDCl<sub>3</sub>): δ 140.2, 131.0, 129.7 (q, *J* = 32.4 Hz), 128.7, 126.8, 125.7 (q, *J* = 3.8 Hz), 124.3 (q, *J* = 271.4 Hz), 71.7, 71.6, 62.0; IR (cm<sup>-1</sup>): 3396, 2860, 1615, 1322, 1162, 1106, 1065, 1016, 968, 852, 730; HRMS: *m/z* calculated for C<sub>12</sub>H<sub>13</sub>F<sub>3</sub>O<sub>2</sub>Na<sup>+</sup> [M+Na]<sup>+</sup>: 269.0760; found: 269.0762.



**Diethyl (E)-2-(3-(4-methoxyphenyl)allyl)-2-(2-oxoethyl)malonate (3.138):** A 25-mL round-bottom flask equipped with a magnetic stir bar was charged with diethyl 2-allyl-2-(2-oxoethyl)malonate<sup>71</sup> (300 mg, 1.2 mmol, 1.0 equiv.) and CH<sub>2</sub>Cl<sub>2</sub> (2.5 mL). Hoveyda-Grubbs catalyst (2<sup>nd</sup> generation) (39 mg, 0.06 mmol, 5 mol%), 4-methoxystyrene (332 mg, 2.5 mmol, 2.0 eq.), and benzoquinone (7 mg, 0.06 mmol, 5 mol%) were added sequentially and the reaction

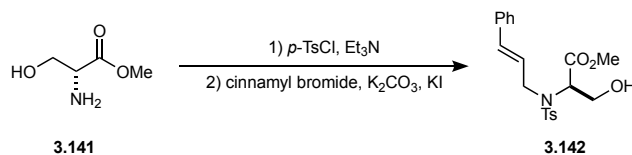
was heated at reflux for 16 h. After cooling to room temperature, the solvent was removed *in vacuo* and the crude product purified by flash column chromatography (2-30% EtOAc/hexanes) to afford the pure title compound as a yellow oil (220 mg, 55%). **<sup>1</sup>H NMR** (500 MHz, CD<sub>2</sub>Cl<sub>2</sub>): δ 9.70 (s, 1H), 7.26 (d, *J* = 8.6 Hz, 2H), 6.83 (d, *J* = 8.7 Hz, 2H), 6.37 (d, *J* = 15.7 Hz, 1H), 5.90 (dt, *J* = 15.5, 7.6 Hz, 1H), 4.27 – 4.12 (m, 4H), 3.78 (s, 3H), 2.96 (s, 2H), 2.86 (d, *J* = 7.6 Hz, 2H), 1.25 (t, *J* = 7.1 Hz, 6H); **<sup>13</sup>C NMR** (126 MHz, CD<sub>2</sub>Cl<sub>2</sub>): δ 199.6, 170.8, 159.9, 134.6, 130.2, 127.9, 121.8, 114.4, 62.5, 55.8, 55.7, 46.8, 38.2, 14.4; **IR** (cm<sup>-1</sup>): 2981, 2839, 1723, 1607, 1511, 1247, 1190, 1176, 1094, 1031, 972, 843; **HRMS**: *m/z* calculated for C<sub>19</sub>H<sub>24</sub>O<sub>6</sub>Na<sup>+</sup> [M+Na]<sup>+</sup>: 371.1465; found: 371.1465.



**Diethyl 2-cinnamyl-2-(2-oxoethyl)malonate (3.140)**: A 25-mL round-bottom flask equipped with a magnetic stir bar was charged with NaH (60% dispersion in mineral oil; 193 mg, 4.8 mmol, 1.2 equiv.) and THF (13 mL). After cooling the mixture to 0 °C, diethyl 2-(2,2-dimethoxyethyl)malonate<sup>72</sup> (1.00 g, 4.0 mmol, 1.0 equiv.) was added dropwise and the solution allowed to warm up to rt and stirred for 1 h. The solution was cooled to 0 °C, cinnamyl bromide (1.19 g, 6.0 mmol, 1.5 equiv.) was added subsequently and the solution allowed to warm up to rt and stirred overnight. Then, NH<sub>4</sub>Cl (aq., sat.) was added and the biphasic mixture partitioned between water and Et<sub>2</sub>O. The organic layer was separated and the aqueous layer extracted with Et<sub>2</sub>O (3x). The combined organic layers were dried over MgSO<sub>4</sub>, filtered, concentrated *in vacuo* and dried using high-vac.

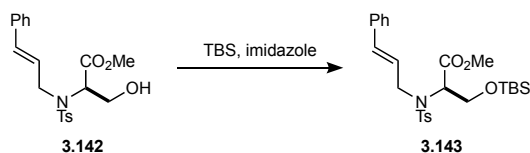
The crude acetal was dissolved in a 1:1 mixture (*v/v*) of water/acetone (40 mL). *p*-TsOH (153 mg, 0.8 mmol, 0.2 equiv.) was added and the reaction heated at 85 °C for 2 h. After cooling down to rt, NaHCO<sub>3</sub> (aq., sat.) was added and the mixture extracted with EtOAc (3x). The combined organic layers were dried over Na<sub>2</sub>SO<sub>4</sub>, filtered and concentrated *in vacuo*. Purification by flash column chromatography (20% EtOAc/hexanes) afforded the pure title compound as colorless oil (950 mg, 74%). **<sup>1</sup>H NMR** (500 MHz, CDCl<sub>3</sub>): δ 9.73 (s, 1H), 7.34 – 7.27 (m, 4H), 7.25 – 7.21 (m, 1H), 6.43 (d, *J* = 15.7 Hz, 1H), 6.05 (dt, *J* = 15.5, 7.6 Hz, 1H), 4.24 (q, *J* = 7.1 Hz, 4H), 3.01 (s, 2H), 2.92 (d, *J* = 7.6 Hz, 2H), 1.27 (t, *J* = 7.1 Hz, 6H); **<sup>13</sup>C NMR** (176 MHz, CDCl<sub>3</sub>): δ 199.0, 170.1, 136.8, 134.9, 128.7, 127.8, 126.4, 123.6, 62.1, 55.2, 46.4, 37.7, 14.1; **IR** (cm<sup>-1</sup>): 2982, 1721,

1446, 1367, 1188, 1093, 1020, 969, 860, 741, 693; **HRMS**:  $m/z$  calculated for  $C_{18}H_{22}O_5Na^+$   $[M+Na]^+$ : 341.1359; found: 341.1362.



**Methyl *N*-cinnamyl-*N*-tosyl-*D*-serinate (3.142)**: A 100-mL round-bottom flask equipped with a magnetic stir bar was charged with *D*-serine methyl ester hydrochloride (1.00 g, 6.43 mmol, 1.0 equiv.) and  $CH_2Cl_2$  (30 mL), before adding tosyl chloride (1.76 g, 9.23 mmol, 1.4 equiv.) and triethylamine (2.93 mL, 21.0 mmol, 3.3 equiv.). After stirring at rt for 16 h,  $NaHCO_3$  (aq., sat.) was added, the organic layer separated, and the aqueous layer extracted with  $CH_2Cl_2$  (3x). The combined organic layers were washed with brine, dried over  $Na_2SO_4$ , filtered and concentrated *in vacuo*, then dried using high-vac.

The crude *N*-tosyl amine was dissolved in acetone (30 mL), before adding  $K_2CO_3$  (1.74 g, 12.6 mmol, 2.0 equiv.), cinnamyl bromide (2.49 g, 12.6 mmol, 2.0 equiv.), and KI (140 mg, 0.84 mmol, 0.1 equiv.). The resulting mixture was stirred at 60 °C for 3 h.  $NaHCO_3$  (aq., sat.) was added, the organic layer separated, and the aqueous layer extracted with  $Et_2O$  (3x). The combined organic layers were washed with brine, dried over  $MgSO_4$ , filtered and concentrated *in vacuo*. Purification by flash column chromatography (5-65%  $EtOAc$ /hexanes) afforded the pure title compound as pale-yellow oil (1.17 g, 47%).  **$^1H$  NMR** (700 MHz,  $CDCl_3$ ):  $\delta$  7.73 (d,  $J$  = 8.2 Hz, 2H), 7.26 (m, 6H), 7.21 (m, 1H), 6.48 – 6.43 (m, 1H), 6.10 (dt,  $J$  = 15.9, 6.7 Hz, 1H), 4.62 (t,  $J$  = 6.4 Hz, 1H), 4.10 (dd,  $J$  = 16.1, 6.2 Hz, 1H), 4.06 (dd,  $J$  = 11.8, 6.1 Hz, 1H), 3.94 (dd,  $J$  = 16.0, 7.2 Hz, 1H), 3.86 (dd,  $J$  = 11.8, 6.8 Hz, 1H), 3.55 (s, 3H), 2.39 (s, 3H);  **$^{13}C$  NMR** (176 MHz,  $CDCl_3$ ):  $\delta$  170.4, 143.8, 137.1, 136.1, 133.8, 129.7, 128.7, 128.2, 127.7, 126.6, 125.2, 61.5, 60.9, 52.5, 49.1, 21.7; **IR** ( $cm^{-1}$ ): 3522, 2953, 1739, 1336, 1290, 1246, 1155, 1089, 1038, 970, 731, 660; **HRMS**:  $m/z$  calculated for  $C_{20}H_{23}NO_5SNH_4^+$   $[M+NH_4]^+$ : 407.1635; found: 407.1635.



**Methyl *O*-(*tert*-butyldimethylsilyl)-*N*-cinnamyl-*N*-tosyl-*D*-serinate (3.143)**: A 100-mL round-bottom flask equipped with a magnetic stir bar was charged with **3.142** (1.17 g, 3.00 mmol, 1.0 equiv.), imidazole (205 mg, 3.00 mmol, 1.0 equiv.),  $TBSCl$  (543 mg, 3.60 mmol, 1.2 equiv.)

and CH<sub>2</sub>Cl<sub>2</sub> (30.0 mL). After stirring for 16 h at rt, the NaHCO<sub>3</sub> (aq., sat.) was added and the organic layer separated. Then, the aqueous layer was extracted with CH<sub>2</sub>Cl<sub>2</sub> (3x) and the combined organic layers washed with brine, dried over Na<sub>2</sub>SO<sub>4</sub>, filtered and concentrated *in vacuo*. Purification by flash chromatography (2-20% EtOAc/hexanes) afforded the pure title compound as clear oil (1.30 g, 86%). **<sup>1</sup>H NMR** (400 MHz, CDCl<sub>3</sub>): δ 7.72 (d, *J* = 8.2 Hz, 2H), 7.31 – 7.18 (m, 7H), 6.46 (d, *J* = 15.9 Hz, 1H), 6.22 – 6.07 (m, 1H), 4.71 (t, *J* = 5.5 Hz, 1H), 4.23 – 4.08 (m, 2H), 4.04 (d, *J* = 5.5 Hz, 2H), 3.57 (s, 3H), 2.37 (s, 3H), 0.82 (s, 9H), 0.00 (d, *J* = 3.9 Hz, 6H); **<sup>13</sup>C NMR** (100 MHz, CD<sub>2</sub>Cl<sub>2</sub>): δ 170.3, 144.1, 138.2, 137.3, 132.6, 130.0, 129.0, 128.1, 128.0, 127.5, 126.9, 63.2, 61.9, 52.5, 49.1, 26.0, 21.8, 18.6, –5.3, –5.5; **IR** (cm<sup>-1</sup>): 2952, 2929, 2884, 2856, 1743, 1342, 1254, 1157, 1093, 837, 813, 779, 753, 693, 657; **HRMS**: *m/z* calculated for C<sub>26</sub>H<sub>37</sub>NO<sub>5</sub>SSiNH<sub>4</sub><sup>+</sup> [M+NH<sub>4</sub>]<sup>+</sup>: 521.2500; found: 521.2501.

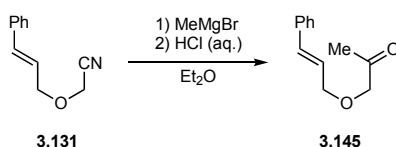


**(R)-N-(1-((*tert*-butyldimethylsilyl)oxy)-3-oxopropan-2-yl)-N-cinnamyl-4-**

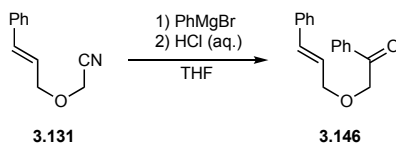
**methylbenzenesulfonamide (3.144)**: A 100-mL round-bottom flask equipped with a magnetic stir bar was charged with **3.143** (1.17 g, 2.32 mmol, 1.0 equiv.) and CH<sub>2</sub>Cl<sub>2</sub> (25 mL). After cooling the solution to –78 °C, a freshly prepared 1 M solution of DIBAL-H (0.91 mL, 5.11 mmol, 2.2 equiv.) in CH<sub>2</sub>Cl<sub>2</sub> was added slowly over 12 min. After stirring for 0.5 h at –78 °C, the flask was transferred to an ice bath and allowed to warm to 0 °C. The mixture was diluted with diethyl ether (25 mL), then, water (0.2 mL) was added dropwise, followed by the sequential addition of 15% NaOH (aq., 0.2 mL) and water (0.5 mL). The mixture was allowed to warm to rt and stirred for 15 min. MgSO<sub>4</sub> was added and the mixture stirred for an additional 15 min. Solids were filtered off and the filtrate concentrated *in vacuo* to afford the corresponding crude alcohol.

The crude alcohol was dissolved in DMSO (20 mL), before adding IBX (971 mg, 3.47 mmol, 1.5 equiv.). The mixture was stirred at rt for 12 h, after which Et<sub>2</sub>O (20 mL) and water (20 mL) were added. The mixture was filtered through celite, and the organic layer was separated from the biphasic filtrate. The aqueous layer was extracted with Et<sub>2</sub>O (3x), and the combined organic layers were washed with brine, dried over MgSO<sub>4</sub>, filtered and concentrated *in vacuo*. Purification by flash chromatography (2-20% EtOAc/hexanes) afforded the pure title compound as clear oil (343 mg, 31%). **<sup>1</sup>H NMR** (500 MHz, CDCl<sub>3</sub>): δ 9.68 (s, 1H), 7.77 (d, *J* = 8.3 Hz, 2H), 7.34 – 7.21

(m, 7H), 6.47 (d,  $J = 15.9$  Hz, 1H), 6.12 (dt,  $J = 15.8, 6.8$  Hz, 1H), 4.34 (dd,  $J = 7.3, 5.0$  Hz, 1H), 4.20 – 4.05 (m, 3H), 4.02 (dd,  $J = 11.0, 7.4$  Hz, 1H), 2.41 (s, 3H), 0.82 (s, 9H), 0.00 (d,  $J = 10.6$  Hz, 6H);  $^{13}\text{C NMR}$  (100 MHz,  $\text{CDCl}_3$ ):  $\delta$  198.8, 143.7, 137.5, 136.1, 134.4, 129.8, 128.7, 128.2, 127.6, 126.6, 125.0, 67.5, 61.0, 49.7, 25.8, 21.6, 18.2,  $-5.5, -5.6$ ; **IR** ( $\text{cm}^{-1}$ ): 2954, 2928, 2856, 1734, 1471, 1338, 1256, 1157, 1092, 837, 781, 751; **HRMS**:  $m/z$  calculated for  $\text{C}_{25}\text{H}_{35}\text{NO}_4\text{SSiNH}_4^+ [\text{M}+\text{NH}_4]^+$ : 491.2394; found: 491.2400.

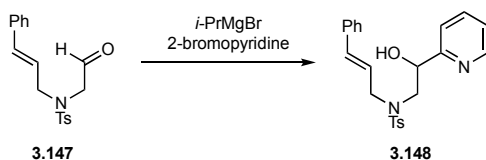


**1-(Cinnamyloxy)propan-2-one (3.145)**: A 25-mL round-bottom flask equipped with a magnetic stir bar was charged with **3.131** (500 mg, 2.9 mmol, 1.0 equiv.) and THF (10 mL). After cooling to  $0^\circ\text{C}$ , methylmagnesium bromide (3 M solution in  $\text{Et}_2\text{O}$ , 1.2 mL, 3.6 mmol, 1.2 equiv.) was added dropwise and the reaction mixture allowed to warm up to rt and stirred for 2 h. Then, a 2 M aqueous solution of HCl (5 mL) was added at  $0^\circ\text{C}$ , the mixture allowed to warm up to rt and stirred vigorously for 0.5 h. The biphasic mixture was diluted with water and EtOAc, the organic layer separated and the aqueous layer extracted with EtOAc (3x). The combined organic layers were washed with  $\text{NaHCO}_3$  (aq., sat.), brine, dried over  $\text{MgSO}_4$ , filtered and concentrated *in vacuo*. Purification by flash column chromatography (5-15% EtOAc/hexanes) afforded the pure title compound as clear oil (328 mg, 60%).  $^1\text{H NMR}$  (700 MHz,  $\text{CDCl}_3$ ):  $\delta$  7.39 (d,  $J = 7.5$  Hz, 2H), 7.33 (t,  $J = 7.6$  Hz, 2H), 7.26 (t,  $J = 7.8$  Hz, 1H), 6.63 (d,  $J = 15.9$  Hz, 1H), 6.29 (dt,  $J = 15.9, 6.2$  Hz, 1H), 4.23 (dd,  $J = 6.2, 1.1$  Hz, 2H), 4.11 (s, 2H), 2.18 (s, 3H);  $^{13}\text{C NMR}$  (176 MHz,  $\text{CDCl}_3$ ):  $\delta$  206.8, 136.5, 133.7, 128.8, 128.1, 126.7, 125.1, 75.4, 72.1, 26.6; **IR** ( $\text{cm}^{-1}$ ): 3027, 2852, 1729, 1716, 1495, 1449, 1354, 1119, 966, 733, 692; **HRMS**:  $m/z$  calculated for  $\text{C}_{12}\text{H}_{14}\text{O}_2\text{Na}^+ [\text{M}+\text{Na}]^+$ : 213.0886; found: 213.0893.



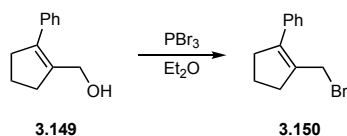
**2-(Cinnamyloxy)-1-phenylethan-1-one (3.146)**: A 50-mL round-bottom flask equipped with a magnetic stir bar was charged with freshly grinded magnesium turnings (105 mg, 4.3 mmol, 1.5 equiv.). THF (4 mL) and bromobenzene (0.48 mL, 4.6 mmol, 1.6 equiv.) were added sequentially and the mixture brought to reflux with a heat gun, then allowed to stir at rt for 2 h.

After diluting the solution with THF (4 mL), CuBr (8 mg, 0.06 mmol, 0.02 equiv.) and **3.131** (500 mg, 2.9 mmol, 1.0 equiv.) were added and the reaction heated at reflux for 0.5 h. Then, the mixture was cooled to 0 °C and 2 M aqueous HCl (5 mL) was added followed by vigorous stirring for 0.5 h. The biphasic mixture was partitioned between water and Et<sub>2</sub>O, the organic layer separated and the aqueous layer extracted with Et<sub>2</sub>O (3x). The combined organic layers were washed with NaHCO<sub>3</sub> (aq., sat.) and brine, dried over MgSO<sub>4</sub>, filtered and concentrated *in vacuo*, then dried using high-vac. The crude phenyl ketone was used for the synthesis of **S31** without further purification.

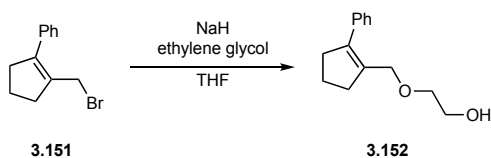


***N*-Cinnamyl-*N*-(2-hydroxy-2-(pyridin-2-yl)ethyl)-4-methylbenzenesulfonamide (3.148):** A 25-mL round-bottom flask with a magnetic stir bar was charged with 2-bromopyridine (0.16 mL, 1.61 mmol, 1.0 equiv.) and THF (1 mL), and a 1 M solution of isopropylmagnesium bromide in THF (1.6 mL, 1.0 equiv.) was added over 5 minutes. After stirring for 2 h at rt, a solution of *N*-cinnamyl-*N*-(2-hydroxyethyl)-4-methylbenzenesulfonamide<sup>73</sup> (530 mg, 1.61 mmol, 1.0 equiv.) in THF (1 mL) was added dropwise. The mixture was stirred for 12 h at rt followed by addition of NH<sub>4</sub>Cl (aq., sat.). The organic layer was separated, and the aqueous layer extracted with diethyl ether (3x). The combined organic layers were washed with brine, dried over MgSO<sub>4</sub>, filtered and concentrated *in vacuo*. Purification by flash column chromatography (10-70% EtOAc/hexanes) afforded the pure title compound as yellow oil (225 mg, 34%). **<sup>1</sup>H NMR** (500 MHz, CDCl<sub>3</sub>): δ 8.47 (d, *J* = 4.7 Hz, 1H), 7.74 (d, *J* = 8.3 Hz, 2H), 7.70 (td, *J* = 7.7, 1.7 Hz, 1H), 7.48 (d, *J* = 7.8 Hz, 1H), 7.32 – 7.27 (m, 4H), 7.25 – 7.13 (m, 4H), 6.37 (d, *J* = 15.9 Hz, 1H), 5.80 (dt, *J* = 15.8, 6.8 Hz, 1H), 5.02 (q, *J* = 5.0 Hz, 1H), 4.27 (d, *J* = 5.4 Hz, 1H), 4.03 (dd, *J* = 15.5, 5.8 Hz, 1H), 3.92 (dd, *J* = 15.5, 7.3 Hz, 1H), 3.51 (dd, *J* = 14.7, 4.5 Hz, 1H), 3.44 (dd, *J* = 14.8, 7.4 Hz, 1H), 2.41 (s, 3H); **<sup>13</sup>C NMR** (126 MHz, CDCl<sub>3</sub>): δ 159.5, 148.6, 143.7, 136.9, 136.8, 136.3, 134.4, 129.9, 128.6, 128.0, 127.6, 126.6, 123.7, 123.0, 121.7, 72.4, 54.2, 52.0, 21.6; **IR** (cm<sup>-1</sup>): 3026, 2924, 1596, 1438, 1335, 1305, 1155, 1089, 969, 925, 815, 732, 693, 662; **HRMS**: *m/z* calculated for C<sub>23</sub>H<sub>24</sub>N<sub>2</sub>O<sub>4</sub>SH<sup>+</sup> [M+H]<sup>+</sup>: 409.1580; found: 409.1578.

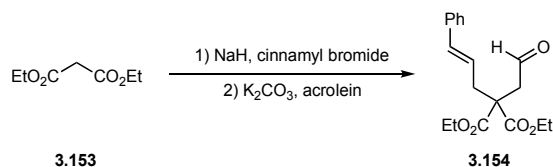




**(2-(Bromomethyl)cyclopent-1-en-1-yl)benzene (3.150):** A 25-mL round-bottom flask equipped with a magnetic stir bar was charged with (2-phenylcyclopent-1-en-1-yl)methanol<sup>74</sup> (940 mg, 5.4 mmol, 1.0 equiv.) and Et<sub>2</sub>O (6 mL). PBr<sub>3</sub> (0.21 mL, 2.2 mmol, 0.4 equiv.) was added dropwise at 0 °C and the reaction stirred for 1 h at that temperature. Then, brine (1 mL) was added and the aqueous layer separated. The organic layer was washed sequentially with NaHCO<sub>3</sub> (aq., sat., 3x) and brine, dried over MgSO<sub>4</sub>, filtered and concentrated *in vacuo* and dried using high-vac to afford the crude title compound as clear oil (1.18 g, 92%), which was directly used for the next step without further purification.

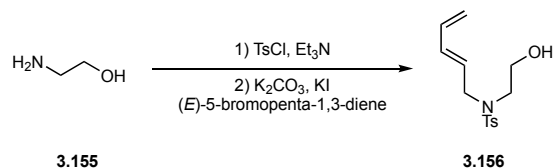


**2-((2-Phenylcyclopent-1-en-1-yl)methoxy)ethan-1-ol (3.152):** NaH (60% dispersion in mineral oil; 498 mg, 12.4 mmol, 2.5 equiv.) was carefully added to a solution of ethylene glycol (2.8 mL, 49.8 mmol, 10.0 equiv.) in THF (10 mL) at 0 °C. After stirring for 15 min, the mixture was transferred to a 50-mL round-bottom flask equipped with a magnetic stir bar containing a solution of **A1-34** (1.18 g, 5.0 mmol, 1.0 equiv.) in THF (10 mL) and the resulting mixture refluxed for 4 h. After cooling down to rt, NH<sub>4</sub>Cl (aq., sat.) was added and the biphasic mixture extracted with EtOAc (3x). The combined organic layers were washed with brine, dried over Na<sub>2</sub>SO<sub>4</sub>, filtered and concentrated *in vacuo*. Purification by flash column chromatography (5-50% EtOAc/hexanes) afforded the pure title compound as clear oil (869 mg, 80%). <sup>1</sup>H NMR (700 MHz, CDCl<sub>3</sub>): δ 7.34 (t, *J* = 7.6 Hz, 2H), 7.27 – 7.25 (m, 1H), 7.25 – 7.22 (m, 2H), 4.17 (s, 2H), 3.74 – 3.70 (m, 2H), 3.52 – 3.48 (m, 2H), 2.79 (t, *J* = 7.5 Hz, 2H), 2.65 (t, *J* = 7.5 Hz, 2H), 1.97 (p, *J* = 7.5 Hz, 2H), 1.91 (t, *J* = 6.2 Hz, 1H); <sup>13</sup>C NMR (176 MHz, CDCl<sub>3</sub>): δ 140.9, 137.8, 135.51, 128.3, 127.9, 127.1, 71.4, 68.1, 62.1, 37.9, 36.0, 22.1; IR (cm<sup>-1</sup>): 3386, 2843, 1493, 1442, 1355, 1253, 1207, 1105, 1054, 1035, 1005, 889, 760, 732, 698, 655; HRMS: *m/z* calculated for C<sub>14</sub>H<sub>18</sub>O<sub>2</sub><sup>+</sup> [M]<sup>+</sup>: 218.1307; found: 218.1312.



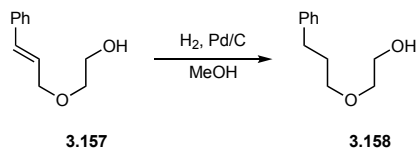
**Diethyl 2-cinnamyl-2-(3-oxopropyl)malonate (3.154):** A round-bottom flask equipped with a magnetic stir bar was charged with NaH (60% dispersion in mineral oil; 457 mg, 11.4 mmol, 1.5 equiv.) and THF (15 mL). After cooling to 0 °C, diethyl malonate (1.7 mL, 11.4 mmol, 1.5 equiv.) was added dropwise and the reaction mixture stirred for 1 h at that temperature. Next, a solution of cinnamyl bromide (1.50 g, 7.6 mmol, 1.0 equiv.) in THF (2 mL) was added and the reaction mixture allowed to warm up to rt and stirred overnight. NH<sub>4</sub>Cl (aq., sat.) and water were sequentially added, the organic layer separated and the aqueous layer extracted with EtOAc (3x). The combined organic layers were dried over Na<sub>2</sub>SO<sub>4</sub>, filtered and concentrated *in vacuo*. Excess diethyl malonate was removed under high-vac at 70 °C and the crude product was taken to the next step without further purification.

A 100-mL round-bottom flask equipped with a magnetic stir bar was charged with crude diethyl 2-cinnamylmalonate, K<sub>2</sub>CO<sub>3</sub> (1.16 g, 8.4 mmol, 1.1 equiv.), acrolein (0.85 mL, 11.4 mmol, 1.5 equiv.) and CH<sub>2</sub>Cl<sub>2</sub> (20 mL) and the mixture stirred at rt overnight. Water and EtOAc were added, the organic layer separated and the aqueous layer extracted with EtOAc (3x). The combined organic layers were washed with brine, dried over Na<sub>2</sub>SO<sub>4</sub>, filtered and concentrated *in vacuo*. Purification by flash column chromatography (20% EtOAc/hexanes) afforded the pure title compound as pale-yellow oil (914 mg, 36%). <sup>1</sup>H NMR (500 MHz, CDCl<sub>3</sub>): δ 9.74 (s, 1H), 7.33 – 7.27 (m, 4H), 7.24 – 7.20 (m, 1H), 6.45 (d, *J* = 15.7 Hz, 1H), 6.04 (dt, *J* = 15.5, 7.5 Hz, 1H), 4.26 – 4.15 (m, 4H), 2.80 (d, *J* = 7.5 Hz, 2H), 2.53 (t, *J* = 7.8 Hz, 2H), 2.24 (t, *J* = 8.1 Hz, 2H), 1.26 (t, *J* = 7.1 Hz, 6H); <sup>13</sup>C NMR (176 MHz, CDCl<sub>3</sub>): δ 200.9, 170.9, 137.0, 134.3, 128.6, 127.6, 126.3, 123.6, 61.6, 57.0, 39.3, 37.5, 25.4, 14.2; IR (cm<sup>-1</sup>): 2981, 1721, 1446, 1367, 1233, 1184, 1095, 1025, 968, 858, 739, 693; HRMS: *m/z* calculated for C<sub>19</sub>H<sub>24</sub>O<sub>5</sub>Na<sup>+</sup> [M+Na]<sup>+</sup>: 355.1516; found: 355.1518.



**(E)-N-(2-Hydroxyethyl)-4-methyl-N-(penta-2,4-dien-1-yl)benzenesulfonamide (3.156):**

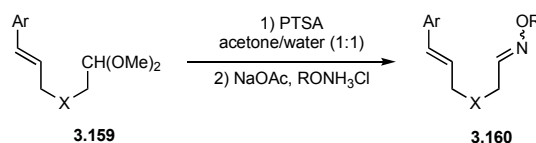
Ethanolamine (0.25 mL, 4.1 mmol, 1.0 equiv.) was converted to *N*-(2-hydroxyethyl)-4-toluenesulfonamide following a literature procedure<sup>73</sup> and the crude product used for the next step without further purification. A 25-mL round-bottom flask equipped with a magnetic stir bar was charged with crude *N*-(2-hydroxyethyl)-4-toluenesulfonamide and acetone (10 mL), followed by the sequential addition of K<sub>2</sub>CO<sub>3</sub> (859 mg, 6.2 mmol, 1.5 equiv.), KI (69 mg, 0.41 mmol, 0.1 equiv.) and freshly prepared (*E*)-5-bromopenta-1,3-diene<sup>75</sup> (913 mg, 6.2 mmol, 1.5 equiv.). The reaction was set to reflux and stirred overnight. Then, the reaction mixture was diluted with water and EtOAc, the organic layer separated and the aqueous layer extracted with EtOAc (3x). The combined organic layers were washed with brine, dried over Na<sub>2</sub>SO<sub>4</sub>, filtered and concentrated *in vacuo*. Purification by flash column chromatography (30-50% EtOAc/hexanes) afforded the pure title compound as pale-yellow oil (994 mg, 85%; *E/Z* (diene) = 15:1). <sup>1</sup>H NMR (700 MHz, CDCl<sub>3</sub>): δ 7.71 (d, *J* = 8.3 Hz, 2H), 7.32 (d, *J* = 7.9 Hz, 2H), 6.25 (dt, *J* = 17.0, 10.3 Hz, 1H), 6.11 (dd, *J* = 15.2, 10.5 Hz, 1H), 5.51 (dt, *J* = 15.0, 6.8 Hz, 1H), 5.18 (d, *J* = 17.0 Hz, 1H), 5.11 (d, *J* = 10.1 Hz, 1H), 3.89 (d, *J* = 6.8 Hz, 2H), 3.73 (t, *J* = 5.3 Hz, 2H), 3.24 (t, *J* = 5.3 Hz, 2H), 2.44 (s, 3H); <sup>13</sup>C NMR (176 MHz, CDCl<sub>3</sub>): δ 143.7, 136.4, 135.7, 135.1, 129.9, 127.9, 127.4, 118.6, 61.2, 51.3, 49.8, 21.6; IR (cm<sup>-1</sup>): 3510, 2925, 1598, 1447, 1329, 1152, 1047, 1003, 950, 909, 814, 752, 726, 657; HRMS: *m/z* calculated for C<sub>14</sub>H<sub>19</sub>NO<sub>3</sub>SNa<sup>+</sup> [M+Na]<sup>+</sup>: 304.0978; found: 304.0982.



**2-(3-Phenylpropoxy)ethan-1-ol (3.158):** A 100-mL round-bottom flask equipped with a magnetic stir bar was charged with 2-(cinnamyloxy)ethan-1-ol<sup>76</sup> (1.00 g, 5.6 mmol, 1.0 equiv.), palladium on activated carbon (10 wt%; 299 mg, 5 mol%) and MeOH (30 mL). The mixture was sparged for 20 min with hydrogen gas and stirred at rt for 2 h under a hydrogen atmosphere. Then, the reaction mixture was passed through a pad of celite. After washing the pad with EtOAc, the filtrate was concentrated *in vacuo* and dried using high-vac to obtain the pure title compound as clear oil (1.00 g, 99%). <sup>1</sup>H NMR (700 MHz, CDCl<sub>3</sub>): δ 7.29 (t, *J* = 7.6 Hz, 2H), 7.21 – 7.18 (m, 3H), 3.73 (q, *J* = 5.4 Hz, 2H), 3.53 (t, *J* = 4.5 Hz, 2H), 3.49 (t, *J* = 6.4 Hz, 2H), 2.70 (t, *J* = 7.8 Hz, 2H), 1.96 – 1.90 (m, 3H); <sup>13</sup>C NMR (176 MHz, CDCl<sub>3</sub>): δ 141.9, 128.54, 128.46, 125.9,

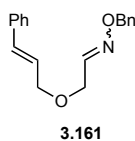
71.9, 70.5, 62.0, 32.4, 31.3; **IR** (cm<sup>-1</sup>): 3418, 2927, 2862, 1496, 1453, 1361, 1118, 1044, 891, 745, 698; **HRMS**: *m/z* calculated for C<sub>11</sub>H<sub>16</sub>O<sub>2</sub>Na<sup>+</sup> [M+Na]<sup>+</sup>: 203.1043; found: 203.1037.

### General Procedure for Oxime Synthesis from Acetals (GP-2)



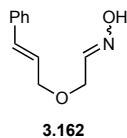
A 100-mL round-bottom flask equipped with a magnetic stir bar was charged with the corresponding acetal (1.0 equiv.) and a 1:1 mixture (v/v) of water/acetone (0.1 M). *p*-TsOH (0.2 equiv.) was added and the reaction heated at 85 °C until complete as determined by TLC analysis (4-8 h). After cooling down to rt, NaHCO<sub>3</sub> (aq., sat.) was added and the mixture extracted with EtOAc (3x). The combined organic layers were dried over Na<sub>2</sub>SO<sub>4</sub>, filtered, concentrated *in vacuo* and dried using high-vac.

The crude aldehyde was dissolved in CH<sub>2</sub>Cl<sub>2</sub> (0.1 M), before adding NaOAc (4.0 equiv.) and the corresponding hydroxylamine hydrochloride (2.0 equiv.). The mixture was stirred at rt until complete as judged by TLC analysis (4-18 h). NaHCO<sub>3</sub> (aq., sat.) was added, the organic layer separated and the aqueous layer extracted with EtOAc (3x). The combined organic layers were washed with brine, dried over Na<sub>2</sub>SO<sub>4</sub>, filtered and concentrated *in vacuo*. Purification by flash column chromatography (EtOAc/hexanes) afforded the corresponding pure oxime as mixture of *E/Z* oxime isomers.

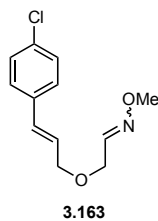


**2-(Cinnamyloxy)acetaldehyde *O*-benzyl oxime (3.161)**: Prepared according to GP-2 from **3.124** (500 mg, 2.3 mmol, 1.0 equiv.) and *O*-benzylhydroxylamine hydrochloride (718 mg, 4.5 mmol, 2.0 equiv.). Purification by flash column chromatography (5-10% EtOAc/hexanes) afforded the pure title compound as pale yellow oil (444 mg, 70%; *E/Z* (oxime) = 1.3:1). **<sup>1</sup>H NMR** (700 MHz, CDCl<sub>3</sub>): δ 7.56 (t, *J* = 5.7 Hz, 1.3H; major), 7.41 – 7.30 (m, 20.7H; major+minor), 7.28 – 7.24 (m, 2.3H; major+minor), 6.94 (t, *J* = 3.6 Hz, 1H; minor), 6.61 (dd, *J* = 18.9, 16.1 Hz, 2.3H; major+minor), 6.27 (dq, *J* = 15.9, 6.1 Hz, 2.3H; major+minor), 5.12 (d, *J* = 3.3 Hz, 4.6H; major+minor), 4.37 (d, *J* = 3.6 Hz, 2H; minor), 4.17 (ddd, *J* = 12.0, 6.1, 1.3 Hz, 4.6H; major+minor), 4.14 (d, *J* = 5.7 Hz, 2.6H; major); **<sup>13</sup>C NMR** (176 MHz, CDCl<sub>3</sub>): δ 150.9, 147.7,

137.7, 137.5, 136.7, 136.6, 133.4, 133.3, 128.72, 128.70, 128.57, 128.56, 128.4, 128.2, 128.10, 128.08, 127.99, 127.95, 126.68, 126.67, 125.3, 125.2, 76.4, 76.2, 71.9, 71.2, 66.8, 64.6; **IR** (cm<sup>-1</sup>): 3028, 2851, 1495, 1453, 1365, 1107, 1013, 966, 914, 842, 733, 691; **HRMS**: *m/z* calculated for C<sub>18</sub>H<sub>19</sub>NO<sub>2</sub>Na<sup>+</sup> [M+Na]<sup>+</sup>: 304.1308; found: 304.1312.

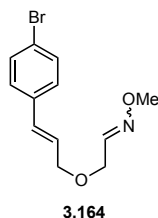


**2-((E)-3-(benzyloxy)allyloxy)acetaldehyde oxime (3.162)**: Prepared according to GP-2 from **3.124** (500 mg, 2.3 mmol, 1.0 equiv.) and hydroxylamine hydrochloride (313 mg, 4.5 mmol, 2.0 equiv.). Purification by flash column chromatography (10-30% EtOAc/hexanes) afforded the pure title compound as pale-yellow oil (287 mg, 67%; *E/Z* (oxime) = 1.1:1). **<sup>1</sup>H NMR** (700 MHz, CDCl<sub>3</sub>): δ 8.13 (b, 1H; minor), 7.85 (b, 1.1H; major), 7.54 (t, *J* = 5.6 Hz, 1.1H; major), 7.41 – 7.38 (m, 4.2H; major+minor), 7.34 – 7.30 (m, 4.2H; major+minor), 7.27 – 7.23 (m, 2.1H; major+minor), 6.96 (t, *J* = 3.7 Hz, 1H; minor), 6.63 (dd, *J* = 15.9, 9.8 Hz, 2.1H; major+minor), 6.28 (dq, *J* = 15.9, 6.2 Hz, 2.1H; major+minor), 4.40 (d, *J* = 3.7 Hz, 2H; minor), 4.19 (ddd, *J* = 9.7, 6.1, 1.3 Hz, 4.2H; major+minor), 4.15 (d, *J* = 5.6 Hz, 2.2H; major); **<sup>13</sup>C NMR** (176 MHz, CDCl<sub>3</sub>): δ 151.5, 148.7, 136.61, 136.57, 133.5, 133.4, 128.73, 128.71, 128.02, 127.99, 126.69, 126.68, 125.24, 125.15, 72.0, 71.3, 66.7, 64.0; **IR** (cm<sup>-1</sup>): 3203, 3027, 2868, 1448, 1395, 1348, 1284, 1116, 967, 920, 829, 731, 689; **HRMS**: *m/z* calculated for C<sub>11</sub>H<sub>13</sub>NO<sub>2</sub>H<sup>+</sup> [M+H]<sup>+</sup>: 192.1019; found: 192.1026.

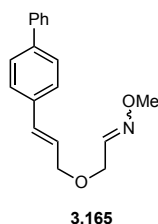


**2-(((E)-3-(4-chlorophenyl)allyloxy)acetaldehyde O-methyl oxime (3.163)**: Prepared according to GP-2 from **3.125** (438 mg, 1.7 mmol, 1.0 equiv.) and *O*-methylhydroxylamine hydrochloride (285 mg, 3.4 mmol, 2.0 equiv.). Purification by flash column chromatography (5-10% EtOAc/hexanes) afforded the pure title compound as clear oil (312 mg, 76%; *E/Z* (oxime) = 1.5:1). **<sup>1</sup>H NMR** (500 MHz, CDCl<sub>3</sub>): δ 7.46 (t, *J* = 5.7 Hz, 1.5H; major), 7.33 – 7.27 (m, 10H; major+minor), 6.86 (t, *J* = 3.9 Hz, 1H; minor), 6.58 (d, *J* = 15.9 Hz, 2.5H; major+minor), 6.25 (dt, *J* = 15.9, 6.0 Hz, 2.5H; major+minor), 4.31 (d, *J* = 3.7 Hz, 2H; minor), 4.16 (d, *J* = 6.0 Hz, 5H; major+minor), 4.12 (d, *J* = 5.7 Hz, 3H; major), 3.89 – 3.86 (m, 7.5H; major+minor); **<sup>13</sup>C NMR**

(126 MHz, CDCl<sub>3</sub>):  $\delta$  150.0, 146.9, 135.13, 135.07, 133.6, 133.5, 131.82, 131.80, 128.9, 128.8, 127.82, 127.81, 126.1, 126.0, 71.6, 71.0, 66.9, 64.5, 62.2, 61.8; **IR** (cm<sup>-1</sup>): 2938, 2899, 1491, 1464, 1359, 1089, 1040, 1012, 967, 846, 796; **HRMS**:  $m/z$  calculated for C<sub>12</sub>H<sub>14</sub>ClNO<sub>2</sub>Na<sup>+</sup> [M+Na]<sup>+</sup>: 262.0605; found: 262.0603.

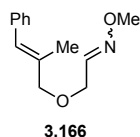


**2-(((E)-3-(4-Bromophenyl)allyl)oxy)acetaldehyde O-methyl oxime (3.164)**: Prepared according to GP-2 from **3.126** (434 mg, 1.4 mmol, 1.0 equiv.) and *O*-methylhydroxylamine hydrochloride (241 mg, 2.9 mmol, 2.0 equiv.). Purification by flash column chromatography (5-10% EtOAc/hexanes) afforded the pure title compound as colorless foam (308 mg, 75%; *E/Z* (oxime) = 1.3:1). **<sup>1</sup>H NMR** (700 MHz, CDCl<sub>3</sub>):  $\delta$  7.46 (t,  $J$  = 5.7 Hz, 1.3H; major), 7.45 – 7.42 (m, 4.6H; major+minor), 7.27 – 7.23 (m, 4.6H; major+minor), 6.86 (t,  $J$  = 3.7 Hz, 1H; minor), 6.56 (dd,  $J$  = 15.9, 3.8 Hz, 2.3H; major+minor), 6.26 (dt,  $J$  = 15.9, 6.0 Hz, 2.3H; major+minor), 4.31 (d,  $J$  = 3.7 Hz, 2H; minor), 4.17 – 4.15 (m, 4.6H; major+minor), 4.12 (d,  $J$  = 5.7 Hz, 2.6H; major), 3.87 (d,  $J$  = 0.7 Hz, 6.9H; major+minor); **<sup>13</sup>C NMR** (176 MHz, CDCl<sub>3</sub>):  $\delta$  150.0, 146.9, 135.6, 135.5, 131.9, 131.83, 131.80, 131.79, 128.14, 128.13, 126.2, 126.1, 121.74, 121.70, 71.6, 71.0, 66.9, 64.5, 62.2, 61.8; **IR** (cm<sup>-1</sup>): 2937, 2851, 1487, 1401, 1358, 1109, 1072, 1040, 1008, 966, 844, 793; **HRMS**:  $m/z$  calculated for C<sub>12</sub>H<sub>14</sub>BrNO<sub>2</sub>Na<sup>+</sup> [M+Na]<sup>+</sup>: 306.0100; found: 306.0107.



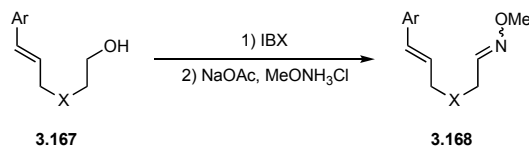
**2-(((E)-3-([1,1'-Biphenyl]-4-yl)allyl)oxy)acetaldehyde O-methyl oxime (3.165)**: Prepared according to GP-2 from **3.127** (497 mg, 1.7 mmol, 1.0 equiv.) and *O*-methylhydroxylamine hydrochloride (278 mg, 3.3 mmol, 2.0 equiv.). Purification by flash column chromatography (5-10% EtOAc/hexanes) afforded the pure title compound as colorless solid (364 mg, 78%; *E/Z* (oxime) = 1.1:1). **<sup>1</sup>H NMR** (700 MHz, CDCl<sub>3</sub>):  $\delta$  7.60 (d,  $J$  = 7.4 Hz, 4.2H; major+minor), 7.57 (dd,  $J$  = 8.3, 2.8 Hz, 4.2H; major+minor), 7.50 – 7.42 (m, 9.5H; major+minor), 7.36 – 7.33

(m, 2.1H; major+minor), 6.88 (t,  $J = 3.7$  Hz, 1H; minor), 6.69 – 6.64 (m, 2.1H; major+minor), 6.32 (dtd,  $J = 15.9, 6.1, 1.4$  Hz, 2.1H; major+minor), 4.33 (d,  $J = 3.7$  Hz, 2H; minor), 4.22 – 4.19 (m, 4.2H; major+minor), 4.14 (d,  $J = 5.7$  Hz, 2.2H; major), 3.88 (d,  $J = 1.0$  Hz, 6.3H; major+minor);  $^{13}\text{C}$  NMR (176 MHz,  $\text{CDCl}_3$ ):  $\delta$  150.2, 147.0, 140.74 (2C), 140.72, 140.69, 135.7, 135.6, 132.84, 132.82, 128.9 (2C), 127.48, 127.46, 127.39, 127.37, 127.09, 127.08, 127.05 (2C), 125.4, 125.3, 71.9, 71.3, 66.8, 64.4, 62.2, 61.9; IR ( $\text{cm}^{-1}$ ): 2940, 2848, 1486, 1448, 1349, 1264, 1104, 1042, 967, 851, 754, 689; HRMS:  $m/z$  calculated for  $\text{C}_{18}\text{H}_{19}\text{NO}_2\text{Na}^+$   $[\text{M}+\text{Na}]^+$ : 304.1308; found: 304.1301.



**2-(((*E*)-2-Methyl-3-phenylallyl)oxy)acetaldehyde *O*-methyl oxime (3.166):** Prepared according to GP-2 from **3.128** (499 mg, 2.1 mmol, 1.0 equiv.) and *O*-methylhydroxylamine hydrochloride (353 mg, 4.2 mmol, 2.0 equiv.). Purification by flash column chromatography (5-10% EtOAc/hexanes) afforded the pure title compound as pale-yellow oil (407 mg, 88%; *E/Z* (oxime) = 1.4:1).  $^1\text{H}$  NMR (500 MHz,  $\text{CDCl}_3$ ):  $\delta$  7.48 (t,  $J = 5.7$  Hz, 1.4H; major), 7.34 (td,  $J = 7.7, 2.0$  Hz, 4.8H; major+minor), 7.28 (dd,  $J = 6.7, 3.8$  Hz, 4.8H; major+minor), 7.23 (dt,  $J = 8.7, 3.8$  Hz, 2.4H, major+minor), 6.88 (t,  $J = 3.6$  Hz, 1H; minor), 6.52 (s, 2.4H; major+minor), 4.29 (d,  $J = 3.7$  Hz, 2H; minor), 4.11 (d,  $J = 5.7$  Hz, 2.8H; major), 4.06 (s, 4.8H; major+minor), 3.88 (d,  $J = 1.6$  Hz, 7.2H; major+minor), 1.92 – 1.87 (m, 7.2H; major+minor);  $^{13}\text{C}$  NMR (176 MHz,  $\text{CDCl}_3$ ):  $\delta$  150.2, 147.1, 137.42, 137.36, 134.5, 134.4, 129.00, 128.99, 128.22, 128.20, 127.8, 127.7, 126.70, 126.65, 77.4, 76.9, 66.6, 64.1, 62.1, 61.8, 15.6, 15.5; IR ( $\text{cm}^{-1}$ ): 2938, 2900, 144, 1351, 1091, 1039, 918, 848, 744, 697; HRMS:  $m/z$  calculated for  $\text{C}_{13}\text{H}_{17}\text{NO}_2\text{H}^+$   $[\text{M}+\text{H}]^+$ : 220.1332; found: 220.1333.

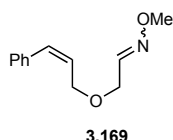
### General Procedure for Oxime Synthesis from Alcohols (GP-3)



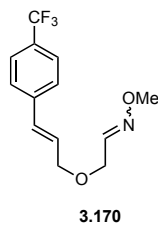
A 25-mL round-bottom flask equipped with a magnetic stir bar was charged with the corresponding alcohol (1.0 equiv.) and DMSO (0.3 M). IBX (1.5 equiv.) was added and the mixture stirred at rt until complete as judged by TLC analysis (4-18 h). Water was added to the reaction and the mixture filtered through a pad of celite. After washing the pad with  $\text{Et}_2\text{O}$ , the

filtrate was collected, the organic layer separated and the aqueous layer extracted with Et<sub>2</sub>O (3x). The combined organic layers were washed with water (2x) and brine (2x), dried over MgSO<sub>4</sub>, filtered, concentrated *in vacuo* and dried using high-vac.

The crude aldehyde was dissolved in CH<sub>2</sub>Cl<sub>2</sub> (0.1 M), before adding NaOAc (4.0 equiv.) and the respective hydroxylamine hydrochloride (2.0 equiv.). The mixture was stirred at rt until complete as judged by TLC analysis (4-18 h). NaHCO<sub>3</sub> (aq., sat.) was added, the organic layer separated and the aqueous layer extracted with EtOAc (3x). The combined organic layers were washed with brine, dried over Na<sub>2</sub>SO<sub>4</sub>, filtered and concentrated *in vacuo*. Purification by flash column chromatography (EtOAc/hexanes) afforded the corresponding pure oxime as mixture of *E/Z* oxime isomers.



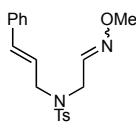
**2-(((*Z*)-3-Phenylallyl)oxy)acetaldehyde *O*-methyl oxime (3.169):** Prepared according to GP-3 from **3.133** (207 mg, 1.2 mmol, 1.0 equiv.) and *O*-methylhydroxylamine hydrochloride (194 mg, 2.3 mmol, 2.0 equiv.). Purification by flash column chromatography (20-30% EtOAc/hexanes) afforded the pure title compound as clear oil (84 mg, 35%; *E/Z* (oxime) = 1.3:1). **<sup>1</sup>H NMR** (700 MHz, CDCl<sub>3</sub>): δ 7.43 (t, *J* = 5.7 Hz, 1.3H; major), 7.35 (t, *J* = 7.6 Hz, 4.6H; major+minor), 7.29 – 7.26 (m, 2.3H; major+minor), 7.20 (d, *J* = 7.4 Hz, 4.6H; major+minor), 6.84 (t, *J* = 3.7 Hz, 1H; minor), 6.64 (dd, *J* = 11.8, 4.9 Hz, 2.3H; major+minor), 5.86 – 5.81 (m, 2.3H; major+minor), 4.29 – 4.27 (m, 6.6H; major+minor), 4.09 (d, *J* = 5.7 Hz, 2.6H; major), 3.86 (s, 3H; minor), 3.84 (s, 3.9H; major); **<sup>13</sup>C NMR** (176 MHz, CDCl<sub>3</sub>): δ 150.2, 147.0, 136.59, 136.55, 132.5, 132.4, 128.89, 128.87, 128.41, 128.40, 128.3, 128.2, 127.5, 127.4, 68.0, 67.4, 67.1, 64.7, 62.2, 61.8; **IR** (cm<sup>-1</sup>): 2938, 1494, 1447, 1340, 1098, 1041, 866, 851, 772, 698; **HRMS**: *m/z* calculated for C<sub>12</sub>H<sub>15</sub>NO<sub>2</sub>Na<sup>+</sup> [M+Na]<sup>+</sup>: 228.0995; found: 228.0995.



**2-(((*E*)-3-(4-(Trifluoromethyl)phenyl)allyl)oxy)acetaldehyde *O*-methyl oxime (3.170):** Prepared according to GP-3 from **1.135** (437 mg, 1.8 mmol, 1.0 equiv.) and *O*-

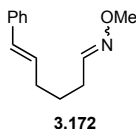


methylhydroxylamine hydrochloride (296 mg, 3.6 mmol, 2.0 equiv.). Purification by flash column chromatography (5-10% EtOAc/hexanes) afforded the pure title compound as clear solid (343 mg, 71%; *E/Z* (oxime) = 1.4:1). **<sup>1</sup>H NMR** (700 MHz, CDCl<sub>3</sub>): δ 7.57 (dd, *J* = 8.2, 2.8 Hz, 4.8H; major+minor), 7.49 – 7.45 (m, 6.2H; major+minor), 6.87 (t, *J* = 3.7 Hz, 1H; minor), 6.66 (dd, *J* = 16.0, 4.1 Hz, 2.4H; major+minor), 6.36 (dt, *J* = 16.0, 5.8 Hz, 2.4H; major+minor), 4.32 (d, *J* = 3.7 Hz, 2H; minor), 4.20 (d, *J* = 5.8 Hz, 4.8H; major+minor), 4.14 (d, *J* = 5.7 Hz, 2.8H; major), 3.88 (s, 7.2H; major+minor); **<sup>13</sup>C NMR** (176 MHz, CDCl<sub>3</sub>): δ 149.9, 146.8, 140.2, 140.1, 131.3, 131.2, 129.7 (q, *J* = 32.4 Hz), 129.6 (q, *J* = 32.4 Hz), 128.3, 128.1, 126.73, 126.72, 125.7 – 125.5 (m, 2C), 124.3 (q, *J* = 271.9 Hz, 2C), 71.4, 70.8, 67.0, 64.6, 62.1, 61.8; **IR** (cm<sup>-1</sup>): 2943, 1615, 1323, 1106, 1066, 1040, 1016, 967, 854, 821, 728, 651; **HRMS**: *m/z* calculated for C<sub>13</sub>H<sub>14</sub>F<sub>3</sub>NO<sub>2</sub>H<sup>+</sup> [M+H]<sup>+</sup>: 274.1049; found: 274.1044.

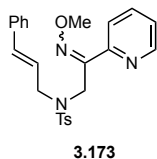


3.171

***N*-Cinnamyl-*N*-(2-(methoxyimino)ethyl)-4-methylbenzenesulfonamide (3.171)**: Prepared according to GP-3 from *N*-cinnamyl-*N*-(2-hydroxyethyl)-4-methylbenzenesulfonamide<sup>73</sup> (700 mg, 2.1 mmol, 1.0 equiv.) and *O*-methylhydroxylamine hydrochloride (353 mg, 4.2 mmol, 2.0 equiv.). Purification by flash column chromatography (10-30% EtOAc/hexanes) afforded the pure title compound as clear oil (371 mg, 49%; *E/Z* (oxime) = 1.2:1). **<sup>1</sup>H NMR** (700 MHz, CDCl<sub>3</sub>): δ 7.73 (d, *J* = 7.6 Hz, 4.4H; major+minor), 7.34 – 7.28 (m, 8.8H; major+minor), 7.27 (d, *J* = 7.4 Hz, 4.4H; major+minor), 7.26 – 7.23 (m, 2.2H; major+minor), 7.21 (t, *J* = 5.9 Hz, 1.2H; major), 6.65 (t, *J* = 4.3 Hz, 1H; minor), 6.45 (d, *J* = 15.7 Hz, 2.2H; major+minor), 6.01 – 5.93 (m, 2.2H; major+minor), 4.04 (d, *J* = 4.3 Hz, 2H; minor), 3.96 (dd, *J* = 9.6, 7.0 Hz, 4.4H; major+minor), 3.93 (d, *J* = 5.9 Hz, 2.4H; major), 3.79 (s, 3H; minor), 3.77 (s, 3.6H; major), 2.44 (s, 3H; minor), 2.43 (s, 3.6H; major); **<sup>13</sup>C NMR** (176 MHz, CDCl<sub>3</sub>): δ 147.9, 145.6, 143.9, 143.8, 137.0, 136.5, 136.3, 136.1, 135.0, 134.9, 130.1, 130.0, 128.74, 128.69, 128.2, 128.1, 127.43, 127.43, 126.7, 126.6, 123.3, 123.0, 62.2, 61.9, 51.5, 50.0, 45.9, 42.9, 21.7, 21.6; **IR** (cm<sup>-1</sup>): 2937, 1597, 1495, 1448, 1337, 1156, 1089, 1030, 968, 897, 814, 731, 654; **HRMS**: *m/z* calculated for C<sub>19</sub>H<sub>22</sub>N<sub>2</sub>O<sub>3</sub>SNa<sup>+</sup> [M+Na]<sup>+</sup>: 381.1243; found: 381.1245.

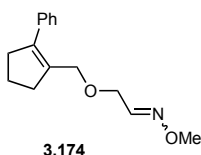


**(5E)-6-Phenylhex-5-enal O-methyl oxime (3.172):** Prepared according to GP-3 from 6-phenylhex-5-en-1-ol<sup>69</sup> (763 mg, 4.3 mmol, 1.0 equiv.; *E/Z* = 2.6:1) and *O*-methylhydroxylamine hydrochloride (723 mg, 8.7 mmol, 2.0 equiv.) Purification by flash column chromatography (2-10% EtOAc/hexanes) afforded the pure title compound as clear oil (797 mg, 91%; *E/Z* (styrene) = 2.6:1; *E/Z* (oxime) = 1.5:1). Characterization data is provided for the two major (*E*)-styrene isomers: <sup>1</sup>H NMR (700 MHz, CDCl<sub>3</sub>): δ 7.39 (t, *J* = 6.2 Hz, 1.5H; major), 7.36 – 7.30 (m, 5H; major+minor), 7.31 – 7.27 (m, 5H; major+minor), 7.24 – 7.18 (m, 2.5H; major+minor), 6.66 (t, *J* = 5.5 Hz, 1H; minor), 6.40 (d, *J* = 15.8 Hz, 2.5H; major+minor), 6.19 (dtd, *J* = 15.6, 6.9, 1.5 Hz, 2.5H; major+minor), 3.87 (s, 3H; minor), 3.82 (s, 4.5H; major), 2.41 – 2.32 (m, 4H; minor), 2.29 – 2.19 (m, 6H; major), 1.71 – 1.60 (m, 5H; major+minor)<sup>17</sup>; <sup>13</sup>C NMR (176 MHz, CDCl<sub>3</sub>): δ 151.5, 151.4, 150.6, 150.5, 137.74, 137.73, 137.6 (2C), 131.9 (2C), 130.80, 130.79, 129.84 (2C), 129.81, 129.76, 128.8 (2C), 128.62, 128.62, 128.3 (2C), 127.1 (2C), 126.74, 126.73, 126.1 (2C), 61.71, 61.69, 61.4, 61.3, 32.7, 32.5, 29.2, 29.1, 28.4, 28.1, 27.1, 26.64, 26.56, 26.1, 25.4, 25.2; IR (cm<sup>-1</sup>): 3024, 2936, 1493, 1448, 1047, 964, 917, 883, 847, 803, 741, 692; HRMS: *m/z* calculated for C<sub>13</sub>H<sub>17</sub>NOH<sup>+</sup> [M+H]<sup>+</sup>: 204.1383; found: 204.1376.

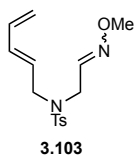


***N*-Cinnamyl-*N*-((*Z*)-2-(methoxyimino)-2-(pyridin-2-yl)ethyl)-4-methylbenzenesulfonamide (3.173):** Prepared according to GP-3 from **3.148** (225 mg, 0.55 mmol, 1.0 equiv.) and *O*-methylhydroxylamine hydrochloride (92 mg, 1.1 mmol, 2.0 equiv.). The oxime formation was carried out in methanol (5 mL) at reflux for 16 h. Purification by flash column chromatography (10-60% EtOAc/hexanes) afforded the pure title compound as clear oil (602 mg, 64%; 1:1.3 mixture of oxime isomers). <sup>1</sup>H NMR (500 MHz, CDCl<sub>3</sub>): δ 8.58 (d, *J* = 4.8 Hz, 1H; minor), 8.54 (d, *J* = 4.3 Hz, 1.3H; major), 7.74 – 7.60 (m, 8.2H; major+minor), 7.57 (d, *J* = 7.9 Hz, 1H; minor), 7.32 – 7.14 (m, 18.4H; major+minor), 6.43 (d, *J* = 15.8 Hz, 1H; minor), 6.32 (d, *J* = 15.9 Hz, 1.3H; major), 5.94 (ddt, *J* = 15.9, 11.2, 6.7 Hz, 2.3H; major+minor), 4.62 (s, 2.6H; major), 4.47 (s, 2H; minor), 3.99 – 3.96 (m, 8.5H; major+minor), 3.83 (s, 3H; minor), 2.41 (s, 6.9H; major+minor);

$^{13}\text{C}$  NMR (176 MHz,  $\text{CDCl}_3$ ):  $\delta$  154.2, 152.9, 151.7, 149.7, 149.2, 148.8, 143.3, 143.1, 137.05, 137.03, 136.53, 136.46, 136.4, 135.7, 134.2, 133.7, 129.52, 129.51, 128.6, 128.5, 127.9, 127.8, 127.6, 127.5, 126.51, 126.45, 126.21, 124.2, 124.1, 123.9, 123.8, 122.0, 62.7, 62.5, 51.4, 50.4, 49.1, 40.4, 21.6, 21.5; IR ( $\text{cm}^{-1}$ ): 2936, 2821, 1598, 1566, 1582, 1495, 1435, 1339, 1156, 1091, 1044, 994, 997, 906, 814, 729, 692, 667, 650; HRMS:  $m/z$  calculated for  $\text{C}_{24}\text{H}_{25}\text{N}_3\text{O}_3\text{SH}^+$   $[\text{M}+\text{H}]^+$ : 436.1689; found: 436.1687.

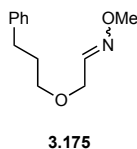


**(2-((2-Phenylcyclopent-1-en-1-yl)methoxy)acetaldehyde O-methyl oxime (3.174):** Prepared according to GP-3 from **3.152** (834 mg, 3.8 mmol, 1.0 equiv.) and *O*-methylhydroxylamine hydrochloride (638 mg, 7.6 mmol, 2.0 equiv.) Purification by flash column chromatography (0-10% EtOAc/hexanes) afforded the pure title compound as clear oil (602 mg, 64%; *E/Z* (oxime) = 1:1.6).  $^1\text{H}$  NMR (700 MHz,  $\text{CDCl}_3$ ):  $\delta$  7.42 (t,  $J = 5.8$  Hz, 1H; minor), 7.34 (t,  $J = 7.6$  Hz, 5.2H; major+minor), 7.27 – 7.25 (m, 2.6H; major+minor), 7.24 – 7.21 (m, 5.2H; major+minor), 6.83 (t,  $J = 3.6$  Hz, 1.6H; major), 4.22 (d,  $J = 3.6$  Hz, 3.2H; major), 4.14 (d,  $J = 5.2$  Hz, 5.2H; major+minor), 4.02 (d,  $J = 5.8$  Hz, 2H; minor), 3.85 (s, 4.8H; major), 3.83 (s, 3H; minor), 2.81 – 2.77 (m, 5.2H; major+minor), 2.66 – 2.61 (m, 5.2H; major+minor), 2.00 – 1.94 (m, 5.2H; major+minor);  $^{13}\text{C}$  NMR (176 MHz,  $\text{CDCl}_3$ ):  $\delta$  150.5, 147.2, 141.51, 141.49, 137.64, 137.60, 135.03, 134.96, 128.31, 128.29, 127.88, 127.86, 127.14, 127.09, 68.2, 67.6, 67.0, 64.6, 62.2, 61.8, 37.9 (2C), 35.9 (2C), 22.12, 22.10; IR ( $\text{cm}^{-1}$ ): 2937, 2843, 1493, 1442, 1341, 1250, 1100, 1042, 850, 761, 698, 655; HRMS:  $m/z$  calculated for  $\text{C}_{15}\text{H}_{19}\text{NO}_2\text{Na}^+$   $[\text{M}+\text{Na}]^+$ : 268.1308; found: 268.1307.



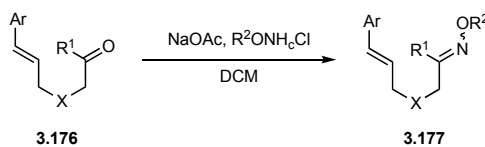
***N*-(2-(Methoxyimino)ethyl)-4-methyl-*N*-((*E*)-penta-2,4-dien-1-yl)benzenesulfonamide (3.103):** Prepared according to GP-3 from **3.156** (500 mg, 1.8 mmol, 1.0 equiv.) and *O*-methylhydroxylamine hydrochloride (297 mg, 3.6 mmol, 2.0 equiv.). Purification by flash column chromatography (20% EtOAc/hexanes) afforded the pure title compound as clear oil (337 mg, 62%; *E/Z* (oxime) = 1.3:1; *E/Z* (diene) = 8:1).  $^1\text{H}$  NMR (700 MHz,  $\text{CDCl}_3$ ):  $\delta$  7.69 (dd,  $J = 8.3$ ,

2.2 Hz, 4.6H; major+minor), 7.31 (t,  $J = 8.4$  Hz, 4.6H; major+minor), 7.17 (t,  $J = 5.9$  Hz, 1.3H; major), 6.61 (t,  $J = 4.3$  Hz, 1H; minor), 6.29 – 6.22 (m, 2.3H; major+minor), 6.10 (dd,  $J = 15.2, 10.7$  Hz, 2.3H; major+minor), 5.54 – 5.43 (m, 2.3H; major+minor), 5.18 (d,  $J = 17.0$  Hz, 2.3H; major+minor), 5.11 (dd,  $J = 10.0, 7.8$  Hz, 2.3H; major+minor), 3.98 (d,  $J = 4.3$  Hz, 2H; minor), 3.88 (d,  $J = 5.9$  Hz, 2.6H; major), 3.84 – 3.81 (m, 7.6H; major+minor), 3.79 (s, 3.9H; major+minor), 2.43 (d,  $J = 2.2$  Hz, 6.9H; major+minor);  $^{13}\text{C NMR}$  (176 MHz,  $\text{CDCl}_3$ ):  $\delta$  147.9, 145.5, 143.9, 143.7, 136.8, 136.3, 135.8, 135.7, 135.64, 135.56, 130.0, 129.9, 127.38, 127.37, 127.2, 127.0, 118.6, 118.4, 62.2, 61.9, 51.0, 49.9, 45.9, 42.8, 21.64, 21.63; **IR** ( $\text{cm}^{-1}$ ): 2938, 1598, 1441, 1337, 1156, 1090, 1030, 1005, 911, 854, 814, 743, 658; **HRMS**:  $m/z$  calculated for  $\text{C}_{15}\text{H}_{20}\text{N}_2\text{O}_3\text{SNa}^+ [\text{M}+\text{Na}]^+$ : 331.1087; found: 331.1088.



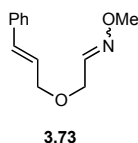
**2-(3-Phenylpropoxy)acetaldehyde *O*-methyl oxime (3.175)**: Prepared according to GP-3 from **3.158** (926 mg, 5.1 mmol, 1.0 equiv.) and *O*-methylhydroxylamine hydrochloride (858 mg, 10.3 mmol, 2.0 equiv.). Purification by flash column chromatography (2-10% EtOAc/hexanes) afforded the pure title compound as clear oil (338 mg, 32%; *E/Z* (oxime) = 1:1.1).  $^1\text{H NMR}$  (700 MHz,  $\text{CDCl}_3$ ):  $\delta$  7.44 (t,  $J = 5.8$  Hz, 1H; minor), 7.28 (td,  $J = 7.9, 2.2$  Hz, 4.2H; major+minor), 7.21 – 7.17 (m, 6.3H; major+minor), 6.83 (t,  $J = 3.7$  Hz, 1.1H; major), 4.24 (d,  $J = 3.7$  Hz, 2.2H; major), 4.06 (d,  $J = 5.8$  Hz, 2H; minor), 3.87 (s, 3.3H; major), 3.86 (s, 3H; minor), 3.46 (q,  $J = 6.2$  Hz, 4.2H; major+minor), 2.70 (q,  $J = 7.7$  Hz, 4.2H; major+minor), 1.95 – 1.88 (m, 4.2H; major+minor);  $^{13}\text{C NMR}$  (176 MHz,  $\text{CDCl}_3$ ):  $\delta$  150.6, 147.3, 141.9, 141.8, 128.6 (2C), 128.49, 128.47, 125.99, 125.96, 70.6, 70.0, 67.5, 65.1, 62.2, 61.8, 32.34, 32.33, 31.3, 31.2; **IR** ( $\text{cm}^{-1}$ ): 2938, 2861, 1496, 1454, 1114, 1040, 911, 850, 744, 698; **HRMS**:  $m/z$  calculated for  $\text{C}_{12}\text{H}_{17}\text{NO}_2\text{H}^+ [\text{M}+\text{H}]^+$ : 208.1332; found: 208.1328.

#### General Procedure for Oxime Synthesis from Carbonyl Compounds (GP-4)

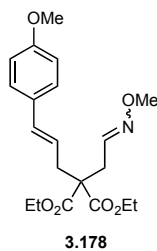


A 50-mL round-bottom flask equipped with a magnetic stir bar was charged with the corresponding aldehyde (1.0 equiv.) and  $\text{CH}_2\text{Cl}_2$  (0.1 M). Next, NaOAc (4.0 equiv.) and the

corresponding hydroxylamine hydrochloride (2.0 equiv.) were added sequentially and the mixture stirred at rt until complete as judged by TLC analysis (4-18 h). NaHCO<sub>3</sub> (aq., sat.) was added and the organic layer separated. Then, the aqueous layer was extracted with EtOAc (3x) and the combined organic layers washed with brine, dried over Na<sub>2</sub>SO<sub>4</sub>, filtered and concentrated in vacuo. Purification by flash column chromatography (EtOAc/hexanes) afforded the pure oxime as mixture of *E/Z* oxime isomers.

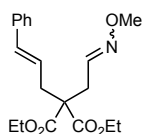


**2-(Cinnamyloxy)acetaldehyde *O*-methyl oxime (3.73):** Prepared according to GP-4 from 2-(cinnamyloxy)acetaldehyde<sup>78</sup> (1.33 g, 7.6 mmol, 1.0 equiv.) and *O*-methylhydroxylamine hydrochloride (1.26 g, 15.1 mmol, 2.0 equiv.). Purification by flash column chromatography (10-20% EtOAc/hexanes) afforded the pure title compound as clear oil (1.05 g, 68%; *E/Z* (oxime) = 1.4:1). **<sup>1</sup>H NMR** (700 MHz, CDCl<sub>3</sub>): δ 7.47 (t, *J* = 5.7 Hz, 1.4H; major), 7.41 – 7.37 (m, 4.8H; major+minor), 7.34 – 7.30 (m, 4.8H; major+minor), 7.27 – 7.23 (m, 2.4H; major+minor), 6.87 (t, *J* = 3.6 Hz, 1H; minor), 6.62 (d, *J* = 15.9 Hz, 2.4H; major+minor), 6.27 (dtd, *J* = 15.9, 6.1, 1.0 Hz, 2.4H; major+minor), 4.31 (d, *J* = 3.7 Hz, 2H; minor), 4.20 – 4.16 (m, 4.8H; major+minor), 4.13 (d, *J* = 5.7 Hz, 2.8H; major), 3.87 (s, 7.2H; major+minor); **<sup>13</sup>C NMR** (176 MHz, CDCl<sub>3</sub>): δ 150.2, 147.0, 136.7, 136.6, 133.37, 133.35, 128.73, 128.71, 128.01, 127.97, 126.69, 126.68, 125.4, 125.3, 71.9, 71.3, 66.8, 64.4, 62.2, 61.9; **IR** (cm<sup>-1</sup>): 2938, 2850, 1449, 1358, 1108, 1040, 965, 851, 735, 691; **HRMS**: *m/z* calculated for C<sub>12</sub>H<sub>15</sub>NO<sub>2</sub>Na<sup>+</sup> [*M*+Na]<sup>+</sup>: 228.0995; found: 228.0999.



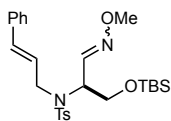
**Diethyl 2-(2-(methoxyimino)ethyl)-2-((*E*)-3-(4-methoxyphenyl)allyl)malonate (3.178):** Prepared according to GP-4 from **3.138** (190 mg, 0.6 mmol, 1.0 equiv.) and *O*-methylhydroxylamine hydrochloride (91 mg, 1.1 mmol, 2.0 equiv.). Purification by flash column chromatography (2-20% EtOAc/hexanes) afforded the pure title compound as yellow oil (150 mg, 73%; *E/Z* (oxime) = 2:1). **<sup>1</sup>H NMR** (500 MHz, CD<sub>2</sub>Cl<sub>2</sub>): δ 7.38 – 7.31 (m, 2H; major), 7.26 (dd,

$J = 8.8, 3.0$  Hz, 6H), 6.85 – 6.81 (m, 6H), 6.70 (t,  $J = 5.4$  Hz, 1H), 6.40 (dd,  $J = 15.7, 7.3$  Hz, 3H), 5.91 (dt,  $J = 15.5, 7.6$  Hz, 3H), 4.19 (q,  $J = 7.1$  Hz, 12H), 3.83 (s, 3H), 3.78 (s, 15H), 2.87 (d,  $J = 5.4$  Hz, 2H), 2.77 (dd,  $J = 7.5, 3.8$  Hz, 6H), 2.73 (d,  $J = 6.4$  Hz, 4H), 1.24 (t,  $J = 7.1$  Hz, 18H);  $^{13}\text{C}$  NMR (126 MHz,  $\text{CD}_2\text{Cl}_2$ ):  $\delta$  170.9, 170.7, 159.8 (2C), 147.1, 147.0, 134.44 (2C), 134.3 (2C), 130.3, 127.9 (2C), 121.62, 121.60, 114.4, 62.22, 62.15, 62.1, 61.9, 57.4, 56.5, 55.8 (2C), 38.0, 37.5, 33.4, 29.6, 14.5, 14.4; IR ( $\text{cm}^{-1}$ ): 2980, 2936, 1729, 1608, 1512, 1301, 1250, 1205, 1032, 971, 841; HRMS:  $m/z$  calculated for  $\text{C}_{20}\text{H}_{27}\text{NO}_6\text{H}^+$   $[\text{M}+\text{H}]^+$ : 378.1911; found: 378.1910.



3.179

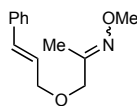
**Diethyl 2-cinnamyl-2-(2-(methoxyimino)ethyl)malonate (3.180):** Prepared according to GP-4 from **3.140** (350 mg, 1.1 mmol, 1.0 equiv.) and *O*-methylhydroxylamine hydrochloride (184 mg, 2.2 mmol, 2.0 equiv.). Purification by flash column chromatography (20% EtOAc/hexanes) afforded the pure title compound as pale-yellow oil (366 mg, 96%; *E/Z* (oxime) = 1.3:1).  $^1\text{H}$  NMR (500 MHz,  $\text{CDCl}_3$ ):  $\delta$  7.37 (t,  $J = 6.4$  Hz, 1.3H; major), 7.33 – 7.27 (m, 9.2H; major+minor), 7.22 (t,  $J = 6.5$  Hz, 2.3H; major+minor), 6.73 (t,  $J = 5.4$  Hz, 1H; minor), 6.46 (dd,  $J = 15.7, 5.2$  Hz, 2.3H; major+minor), 6.10 – 6.02 (m, 2.3H; major+minor), 4.22 (q,  $J = 7.1$  Hz, 9.2H; major+minor), 3.86 (s, 3H; minor), 3.81 (s, 3.9H; major), 2.93 (d,  $J = 5.4$  Hz, 2H; minor), 2.86 – 2.80 (m, 4.6H; major+minor), 2.78 (d,  $J = 6.4$  Hz, 2.6H; major), 1.26 (t,  $J = 7.1$  Hz, 13.8H; major+minor);  $^{13}\text{C}$  NMR (176 MHz,  $\text{CDCl}_3$ ):  $\delta$  170.5, 170.3, 146.62, 146.57, 137.1 (2C), 134.74, 134.73, 128.6 (2C), 127.6 (2C), 126.4 (2C), 123.5, 123.4, 61.84, 61.83, 61.76, 61.6, 56.9, 56.1, 37.7, 37.3, 33.2, 29.4, 14.22, 14.21; IR ( $\text{cm}^{-1}$ ): 2981, 2938, 1727, 1445, 1367, 1185, 1095, 1041, 968, 851, 741, 693; HRMS:  $m/z$  calculated for  $\text{C}_{19}\text{H}_{25}\text{NO}_5\text{Na}^+$   $[\text{M}+\text{Na}]^+$ : 370.1625; found: 370.1630.



3.180

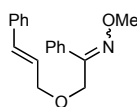
***N*-Cinnamyl-4-methyl-*N*-((*S,E*)-8,8,9,9-tetramethyl-2,7-dioxa-3-aza-8-siladec-3-en-5-yl)benzenesulfonamide (3.180):** Prepared according to GP-4 from crude **3.144** (343 mg, 0.72 mmol, 1.0 equiv.) and *O*-methylhydroxylamine hydrochloride (121 mg, 1.45 mmol,

2.0 equiv.). Purification by flash column chromatography (2-18% EtOAc/hexanes) afforded the pure title compound as clear oil (326 mg, 90%; *E/Z* (oxime) = 1.1:1). **<sup>1</sup>H NMR** (500 MHz, CDCl<sub>3</sub>): δ 7.73 (dd, *J* = 10.2, 8.3 Hz, 4.2H; major+minor), 7.36 – 7.18 (m, 15.8H; major+minor), 6.75 (d, *J* = 5.6 Hz, 1H; minor), 6.46 (dd, *J* = 20.2, 15.9 Hz, 2.1H; major+minor), 6.09 (ddt, *J* = 32.6, 15.9, 6.7 Hz, 2.1H; major+minor), 4.83 (q, *J* = 6.1 Hz, 1H; minor), 4.61 (q, *J* = 6.3 Hz, 1.1H; major), 4.17 – 3.91 (m, 6.3H; major+minor), 3.88 (ddd, *J* = 10.6, 6.7, 1.7 Hz, 2.1H; major+minor), 3.74 (s, 3.3H; major), 3.67 (s, 3H; minor), 2.40 (s, 3H; minor), 2.39 (s, 3.3H; major), 0.87 – 0.78 (m, 18.9H; major+minor), 0.00 (d, *J* = 3.2 Hz, 12.6H; major+minor); **<sup>13</sup>C NMR** (176 MHz, CDCl<sub>3</sub>): δ 147.5, 147.0, 143.32, 143.26, 138.1, 137.7, 136.5, 136.4, 133.5, 133.0, 129.6, 129.5, 128.7, 128.6, 128.0, 127.9, 127.68, 127.65, 126.59, 126.57, 126.3, 126.0, 63.4, 62.7, 62.0, 61.9, 58.6, 54.8, 49.3, 48.1, 25.9 (2C), 21.6 (2C), 18.34, 18.30, -5.35 (3C), -5.41; **IR** (cm<sup>-1</sup>): 2928.4, 2855.9, 1462.9, 13339.7, 1253.1, 1156.5, 1090.2, 1043.9, 967.1, 900.1, 834.0, 813.1, 776.5, 727.4, 691.6, 657.8.; **HRMS**: *m/z* calculated C<sub>26</sub>H<sub>38</sub>N<sub>2</sub>O<sub>4</sub>SSiH<sup>+</sup> for [M+H]<sup>+</sup>: 503.2394; found: 503.2393.



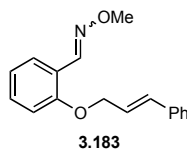
3.181

**1-(Cinnamyloxy)propan-2-one *O*-methyl oxime (3.181)**: Prepared according to GP-4 from **3.145** (295 mg, 1.6 mmol, 1.0 equiv.) and *O*-methylhydroxylamine hydrochloride (259 mg, 3.1 mmol, 2.0 equiv.). Purification by flash column chromatography (5-15% EtOAc/hexanes) afforded the pure title compound as clear oil (316 mg, 93%; *E/Z* (oxime) = 1:3.3). **<sup>1</sup>H NMR** (700 MHz, CDCl<sub>3</sub>): δ 7.41 – 7.37 (m, 8.6H; major+minor), 7.34 – 7.29 (m, 8.6H; major+minor), 7.24 (t, *J* = 7.3 Hz, 4.3H; major+minor), 6.62 (dd, *J* = 15.7, 3.7 Hz, 4.3H; major+minor), 6.31 – 6.25 (m, 4.3H; major+minor), 4.32 (s, 2H; minor), 4.14 (td, *J* = 6.5, 1.4 Hz, 8.6H; major+minor), 4.04 (s, 6.6H; major), 3.88 (s, 9.9H; major), 3.81 (s, 3H; minor), 1.97 (s, 3H; minor), 1.91 (s, 9.9H; major); **<sup>13</sup>C NMR** (176 MHz, CDCl<sub>3</sub>): δ 157.2, 154.9, 136.72, 136.67, 133.0, 132.9, 128.69, 128.67, 127.90, 127.86, 126.6 (2C), 125.59, 125.55, 71.9, 71.5, 70.9, 65.6, 61.7, 61.6, 16.7, 12.2; **IR** (cm<sup>-1</sup>): 2937, 2852, 1495, 1448, 1366, 1115, 1045, 965, 888, 831, 735, 691; **HRMS**: *m/z* calculated for C<sub>13</sub>H<sub>17</sub>NO<sub>2</sub>Na<sup>+</sup> [M+Na]<sup>+</sup>: 242.1151; found: 242.1155.

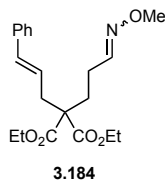


3.182

**(Z)-2-(Cinnamyloxy)-1-phenylethan-1-one O-methyl oxime (3.182):** Prepared according to GP-4 from crude **3.146** (stoichiometry based on 2.9 mmol **3.146**) and *O*-methylhydroxylamine hydrochloride (482 mg, 5.8 mmol, 2.0 equiv.). Purification by flash column chromatography (5-15% EtOAc/hexanes) afforded the pure title compound as clear oil (255 mg, 31%; *Z* only). **<sup>1</sup>H NMR** (700 MHz, CDCl<sub>3</sub>): δ 7.71 (dd, *J* = 6.5, 2.9 Hz, 2H), 7.39 – 7.34 (m, 5H), 7.31 (t, *J* = 7.6 Hz, 2H), 7.24 (t, *J* = 7.3 Hz, 1H), 6.55 (d, *J* = 15.9 Hz, 1H), 6.22 (dt, *J* = 15.9, 6.1 Hz, 1H), 4.69 (s, 2H), 4.13 (d, *J* = 6.1 Hz, 2H), 4.00 (s, 3H); **<sup>13</sup>C NMR** (176 MHz, CDCl<sub>3</sub>): δ 155.5, 136.7, 134.4, 133.1, 129.3, 128.7, 128.4, 127.9, 127.2, 126.6, 125.6, 71.5, 62.4, 62.0; **IR** (cm<sup>-1</sup>): 2936, 1724, 1494, 1445, 1327, 1184, 1115, 1041, 965, 885, 763, 743, 690; **HRMS**: *m/z* calculated for C<sub>18</sub>H<sub>19</sub>NO<sub>2</sub>H<sup>+</sup> [M+H]<sup>+</sup>: 282.1489; found: 282.1494.



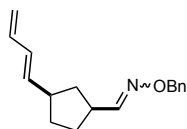
**(E)-2-(Cinnamyloxy)benzaldehyde O-methyl oxime (3.183):** Prepared according to GP-4 from 2-(cinnamyloxy)benzaldehyde<sup>79</sup> (508 mg, 2.1 mmol, 1.0 equiv.) and *O*-methylhydroxylamine hydrochloride (356 mg, 4.3 mmol, 2.0 equiv.). Purification by flash column chromatography (10% EtOAc/hexanes) afforded the pure title compound as clear oil (459 mg, 81%; *E* only). **<sup>1</sup>H NMR** (700 MHz, CDCl<sub>3</sub>): δ 8.53 (s, 1H), 7.81 (dd, *J* = 7.7, 1.6 Hz, 1H), 7.41 (d, *J* = 7.6 Hz, 2H), 7.34 (t, *J* = 7.6 Hz, 3H), 7.29 – 7.26 (m, 1H), 6.96 (t, *J* = 7.5 Hz, 1H), 6.94 (d, *J* = 8.3 Hz, 1H), 6.72 (d, *J* = 16.0 Hz, 1H), 6.40 (dt, *J* = 16.0, 5.7 Hz, 1H), 4.73 (dd, *J* = 5.7, 1.4 Hz, 2H), 3.98 (s, 3H); **<sup>13</sup>C NMR** (176 MHz, CDCl<sub>3</sub>): δ 156.8, 145.0, 136.5, 133.2, 131.2, 128.8, 128.1, 126.7, 126.6, 124.2, 121.3, 121.2, 112.7, 69.3, 62.0; **IR** (cm<sup>-1</sup>): 2934, 1598, 1486, 1449, 1340, 1241, 1108, 1051, 1005, 963, 917, 743, 690; **HRMS**: *m/z* calculated for C<sub>17</sub>H<sub>17</sub>NO<sub>2</sub>Na<sup>+</sup> [M+Na]<sup>+</sup>: 290.1151; found: 290.1147.



**Diethyl 2-cinnamyl-2-(3-(methoxyimino)propyl)malonate (3.185):** Prepared according to GP-4 from **3.154** (500 mg, 1.5 mmol, 1.0 equiv.) and *O*-methylhydroxylamine hydrochloride (251 mg, 3.0, 2.0 equiv.). Purification by flash column chromatography (20% EtOAc/hexanes) afforded the

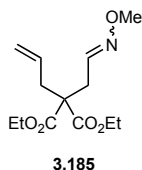


pure title compound as pale-yellow oil (476 mg, 88%; *E/Z* (oxime) = 1.2:1). **<sup>1</sup>H NMR** (500 MHz, CDCl<sub>3</sub>): δ 7.35 – 7.27 (m, 10H; major+minor), 7.21 (t, *J* = 6.8 Hz, 2.2H; major+minor), 6.62 (t, *J* = 5.3 Hz, 1H; minor), 6.45 (d, *J* = 15.7 Hz, 2.2H; major+minor), 6.03 (dtd, *J* = 15.4, 7.5, 2.6 Hz, 2.2H; major+minor), 4.25 – 4.17 (m, 8.8H; major+minor), 3.84 (s, 3H; minor), 3.80 (s, 3.6H; major), 2.82 (d, *J* = 7.5 Hz, 4.4H; major+minor), 2.34 – 2.27 (m, 2H; minor), 2.24 – 2.17 (m, 2.4H; major), 2.14 – 2.06 (m, 4.4H; major+minor), 1.25 (t, *J* = 7.1 Hz, 13.2H; major+minor); **<sup>13</sup>C NMR** (176 MHz, CDCl<sub>3</sub>): δ 170.9 (2C), 150.2, 149.5, 137.12, 137.10, 134.2 (2C), 128.6 (2C), 127.6 (2C), 126.34, 126.33, 123.81, 123.79, 61.8, 61.6 (2C), 61.4, 57.5, 57.4, 36.8, 36.4, 29.7, 29.1, 24.8, 20.8, 14.2 (2C); **IR** (cm<sup>-1</sup>): 2980, 1725, 1446, 1367, 1263, 1180, 1094, 1049, 1028, 967, 858, 741, 693; **HRMS**: *m/z* calculated for C<sub>20</sub>H<sub>27</sub>NO<sub>5</sub>Na<sup>+</sup> [M+Na]<sup>+</sup>: 384.1781; found: 384.1783.



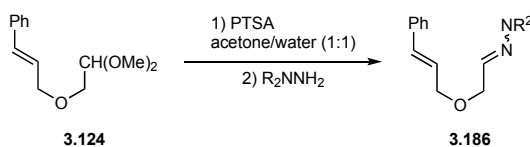
3.105

**3-(Buta-1,3-dien-1-yl)cyclopentane-1-carbaldehyde *O*-benzyl oxime (3.105)**: Prepared according to GP-4 from (1*S*\*,3*R*\*)-3-(buta-1,3-dien-1-yl)cyclopentane-1-carbaldehyde<sup>80</sup> (172 mg, 1.2 mmol, 1.0 equiv.; *E/Z* (diene) = 4:1) and *O*-benzylhydroxylamine hydrochloride (366 mg, 2.3 mmol, 2.0 equiv.). Purification by flash column chromatography (0-10% EtOAc/hexanes) afforded the pure title compound as clear oil (205 mg, 70%; *E/Z* (oxime) = 2:1; *E/Z* (diene) = 10:1). Characterization data is provided for the two major (*E*)-diene isomers: **<sup>1</sup>H NMR** (700 MHz, CDCl<sub>3</sub>): δ 7.38 (d, *J* = 7.4 Hz, 2H; major), 7.37 – 7.33 (m, 12H; major+minor), 7.31 – 7.28 (m, 3H; major+minor), 6.65 (d, *J* = 6.9 Hz, 1H, minor), 6.29 (dt, *J* = 17.2, 10.3 Hz, 3H; major+minor), 6.05 (dd, *J* = 15.2, 10.6 Hz, 3H; major+minor), 5.69 – 5.63 (m, 3H; major+minor), 5.10 (d, *J* = 18.0 Hz, 5H; major+minor), 5.04 (s, 4H; major), 4.98 (d, *J* = 10.1 Hz, 3H; major+minor), 3.38 – 3.31 (m, 1H; minor), 2.80 – 2.71 (m, 2H; major), 2.66 – 2.52 (m, 3H; major+minor), 2.17 – 2.10 (m, 1H; minor), 2.06 – 2.00 (m, 2H; major), 1.99 – 1.83 (m, 6H; major+minor), 1.69 – 1.60 (m, 3H; major+minor), 1.49 – 1.41 (m, 3H; major+minor), 1.33 (dt, *J* = 12.6, 10.3 Hz, 2H; major), 1.21 (dt, *J* = 12.5, 10.3 Hz, 1H; minor); **<sup>13</sup>C NMR** (176 MHz, CDCl<sub>3</sub>): δ 156.9, 156.5, 154.9, 154.8, 138.7, 138.6, 137.24, 137.22, 129.89, 129.86, 128.53, 128.50, 128.44, 128.43, 127.98, 127.98, 115.41, 115.39, 75.8, 75.7, 43.34, 43.33, 39.90, 39.90, 38.28, 38.26, 32.3, 32.1, 30.0, 29.8; **IR** (cm<sup>-1</sup>): 2950, 2866, 1496, 1453, 1366, 1040, 1003, 899, 732, 696; **HRMS**: *m/z* calculated for C<sub>17</sub>H<sub>21</sub>NOH<sup>+</sup> [M+H]<sup>+</sup>: 256.1696; found: 256.1701.



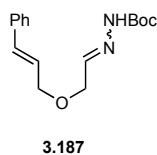
**Diethyl 2-allyl-2-(2-(methoxyimino)ethyl)malonate (3.185):** Prepared according to GP-4 from diethyl 2-allyl-2-(2-oxoethyl)malonate<sup>71</sup> (271 mg, 1.0 mmol, 1.0 equiv.) and *O*-methylhydroxylamine hydrochloride (167 mg, 2.0 mmol, 2.0 equiv.). Purification by flash column chromatography (10% EtOAc/hexanes) afforded the pure title compound as clear oil (233 mg, 86%; *E/Z* (oxime) = 1.3:1). Spectroscopic data were consistent with those reported in the literature.<sup>81</sup>

### General Procedure for Hydrazone Synthesis (GP-5)



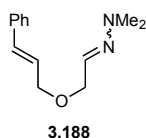
A 100-mL round-bottom flask equipped with a magnetic stir bar was charged with acetal (1.0 equiv.) and a 1:1 mixture (*v/v*) of water/acetone (0.1 M). *p*-TsOH (0.2 equiv.) was added and the reaction heated at 85 °C until complete as determined by TLC analysis (4-8 h). After cooling down to rt, NaHCO<sub>3</sub> (aq., sat.) was added and the mixture extracted with EtOAc (3x). The combined organic layers were dried over Na<sub>2</sub>SO<sub>4</sub>, filtered, concentrated *in vacuo* and dried using high-vac.

The crude aldehyde was dissolved in MeOH (0.1 M), the corresponding hydrazide/hydrazine (1.5 equiv.) added and the reaction stirred overnight at rt. Solvent was removed *in vacuo* and the crude product purified by flash column chromatography (EtOAc/hexanes) to afford the corresponding pure hydrazone.



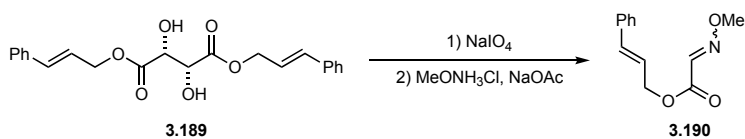
**Tert-butyl 2-(2-(cinnamyloxy)ethylidene)hydrazine-1-carboxylate (3.187):** Prepared according to GP-5 from 3.124 (500 mg, 2.3 mmol, 1.0 equiv.) and *tert*-butyl carbazate (446 mg, 3.4 mmol, 1.5 equiv.). Purification by flash column chromatography (20-40% EtOAc/hexanes) afforded the pure title compound as pale-yellow solid (402 mg, 62%; *E/Z* (hydrazone) = 3.9:1). <sup>1</sup>H NMR (700 MHz, CDCl<sub>3</sub>): δ 7.86 (s, 3.9H; major), 7.41 – 7.36 (m, 9.8H; major+minor), 7.35

– 7.29 (m, 9.8H; major+minor), 7.24 (t,  $J = 7.3$  Hz, 5.9H; major+minor), 6.65 (d,  $J = 7.8$  Hz, 1H; minor), 6.61 (d,  $J = 15.8$  Hz, 3.9H; major), 6.26 (dt,  $J = 15.9$ , 6.1 Hz, 4.9H; major+minor), 4.24 – 4.19 (m, 9.8H; major+minor), 4.19 – 4.15 (m, 9.8H; major+minor), 1.50 (s, 44.1H; major+minor);  $^{13}\text{C}$  NMR (176 MHz,  $\text{CDCl}_3$ ):  $\delta$  152.8, 152.5, 143.1, 139.4, 136.6, 136.2, 134.2, 133.1, 128.7, 128.6, 128.2, 127.8, 126.7, 126.6, 125.4, 124.2, 81.4, 81.2, 71.8, 71.3, 69.3, 66.7, 28.3 (2C); IR ( $\text{cm}^{-1}$ ): 3232, 2978, 2931, 1706, 1533, 1449, 1366, 1269, 1247, 1164, 1133, 1042, 1015, 966, 859, 723, 691; HRMS:  $m/z$  calculated for  $\text{C}_{16}\text{H}_{22}\text{N}_2\text{O}_3\text{Na}^+$   $[\text{M}+\text{Na}]^+$ : 313.1523; found: 313.1530.



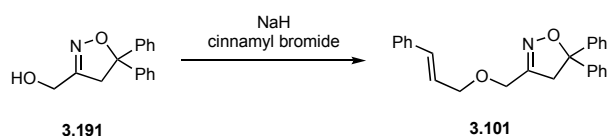
**(*E*)-2-(2-(Cinnamyloxy)ethylidene)-1,1-dimethylhydrazine (3.188):** Prepared according to GP-5 from **3.124** (300 mg, 1.4 mmol, 1.0 equiv.) and *N,N*-dimethylhydrazine (0.15 mL, 2.0 mmol, 1.5 equiv.). Purification by flash column chromatography (5-10% EtOAc/hexanes) afforded the pure title compound as pale-yellow oil (116 mg, 39%; *E* only).  $^1\text{H}$  NMR (700 MHz,  $\text{CDCl}_3$ ):  $\delta$  7.38 (d,  $J = 8.0$  Hz, 2H), 7.31 (t,  $J = 7.2$  Hz, 2H), 7.23 (t,  $J = 7.3$  Hz, 1H), 6.65 – 6.59 (m, 2H), 6.31 (dt,  $J = 15.9$ , 6.1 Hz, 1H), 4.18 (d,  $J = 6.1$  Hz, 2H), 4.15 (d,  $J = 5.3$  Hz, 2H), 2.83 (s, 6H);  $^{13}\text{C}$  NMR (176 MHz,  $\text{CDCl}_3$ ):  $\delta$  136.9, 132.9, 131.8, 128.7, 127.8, 126.6, 126.1, 71.0, 70.7, 42.8; IR ( $\text{cm}^{-1}$ ): 2854, 1598, 1496, 1447, 1262, 1116, 1036, 968, 817, 745, 693; HRMS:  $m/z$  calculated for  $\text{C}_{13}\text{H}_{18}\text{N}_2\text{OH}^+$   $[\text{M}+\text{H}]^+$ : 219.1492; found: 219.1498.

### Miscellaneous Procedure



**Cinnamyl 2-(methoxyimino)acetate (3.190):** A 25-mL round-bottom flask equipped with a magnetic stir bar was charged with dicinnamyl (*2R,3R*)-2,3-dihydroxysuccinate<sup>82</sup> (1.00 g, 2.6 mmol, 1.0 equiv.) and a 2:1 THF/water mixture.  $\text{NaIO}_4$  (1.12 g, 5.2 mmol, 2.0 equiv.) was added and the reaction stirred overnight at rt. Then, solids were removed by filtration through a pad of celite and  $\text{NaHSO}_3$  (aq., sat.) was added to the filtrate. The resulting mixture was extracted with  $\text{Et}_2\text{O}$  (3x) and the combined organic layers washed with brine, dried over  $\text{MgSO}_4$ , filtered and concentrated *in vacuo* and dried using high-vac. The crude oxoacetate was used for the next step without further purification.

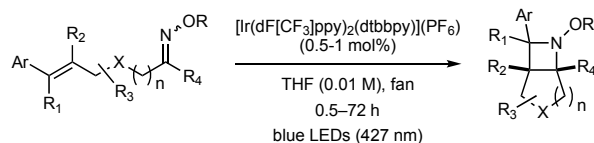
To a 50-mL round-bottom flask equipped with magnetic stir bar containing crude oxoacetate and CH<sub>2</sub>Cl<sub>2</sub> (25 mL) was sequentially added NaOAc (1.72 g, 20.9 mmol, 8.0 equiv.) and *O*-methylhydroxylamine hydrochloride (874 mg, 10.5 mmol, 4.0 equiv.). After stirring the resulting mixture overnight at rt, NaHCO<sub>3</sub> (aq., sat.) was added, the organic layer separated and the aqueous layer extracted with EtOAc (3x). The combined organic layers were washed with brine, dried over Na<sub>2</sub>SO<sub>4</sub>, filtered and concentrated *in vacuo*. Purification by flash column chromatography (5-10% EtOAc/hexanes) afforded the pure title compound as clear oil (453 mg, 40%; *E/Z* (oxime) = 6.7:1). **<sup>1</sup>H NMR** (500 MHz, CDCl<sub>3</sub>): δ 7.52 (s, 6.7H; major), 7.40 (d, *J* = 7.3 Hz, 15.4H; major+minor), 7.33 (t, *J* = 7.4 Hz, 15.4H; major+minor), 7.29 – 7.25 (m, 7.7H; major+minor), 6.99 (s, 1H; minor), 6.71 (d, *J* = 15.9 Hz, 7.7H; major+minor), 6.39 – 6.26 (m, 7.7H; major+minor), 4.92 (dd, *J* = 6.6, 1.3 Hz, 13.4H; major), 4.86 (dd, *J* = 6.6, 1.3 Hz, 2H; minor), 4.07 (s, 20.1H; major), 4.05 (s, 3H; minor); **<sup>13</sup>C NMR** (176 MHz, CDCl<sub>3</sub>): δ 161.9, 158.8, 140.7, 136.9, 136.1 (2C), 135.5, 135.3, 128.77, 128.75, 128.40, 128.39, 126.84, 126.82, 122.3, 122.2, 66.3, 65.9, 64.0, 63.7; **IR** (cm<sup>-1</sup>): 2941, 1719, 1598, 1494, 1449, 1382, 1318, 1265, 1198, 1171, 1047, 962, 917, 735, 691; **HRMS**: *m/z* calculated for C<sub>12</sub>H<sub>13</sub>NO<sub>3</sub>Na<sup>+</sup> [M+Na]<sup>+</sup>: 242.0788; found: 242.0794.



**3-((Cinnamyloxy)methyl)-5,5-diphenyl-4,5-dihydroisoxazole (3.101)**: A 25-mL round-bottom flask equipped with a magnetic stir bar was charged with NaH (60% dispersion in mineral oil; 71 mg, 1.8 mmol, 1.5 equiv.) and THF (10 mL). Next, a solution of (5,5-diphenyl-4,5-dihydroisoxazol-3-yl)methanol<sup>83</sup> (300 mg, 1.2 mmol, 1.0 equiv.) in THF (2 mL) was added dropwise at 0 °C and then, after stirring for 15 min, a solution of cinnamyl bromide (257 mg, 1.3 mmol, 1.1 equiv.) in THF (2 mL) and the reaction allowed to warm up to rt and stirred overnight. NH<sub>4</sub>Cl (aq., sat.) was added and the mixture extracted with EtOAc (3x). The combined organic layers were washed with brine, dried over Na<sub>2</sub>SO<sub>4</sub>, filtered and concentrated *in vacuo*. Purification by flash column chromatography (2-10% EtOAc/hexanes) afforded the pure title compound as pale-yellow oil (384 mg, 88%). **<sup>1</sup>H NMR** (700 MHz, CDCl<sub>3</sub>): δ 7.44 – 7.41 (m, 4H), 7.36 – 7.30 (m, 8H), 7.29 – 7.26 (m, 2H), 7.27 – 7.23 (m, 1H), 6.50 (d, *J* = 15.9 Hz, 1H), 6.18 (dt, *J* = 15.9, 6.2 Hz, 1H), 4.32 (s, 2H), 4.03 (dd, *J* = 6.2, 1.4 Hz, 2H), 3.70 (s, 2H); **<sup>13</sup>C NMR** (176 MHz, CDCl<sub>3</sub>): δ 156.7, 144.0, 136.5, 133.6, 128.7, 128.5, 128.00, 127.8, 126.7, 126.2, 124.9,

91.8, 71.0, 64.7, 48.4; **IR** (cm<sup>-1</sup>): 3025, 2852, 1598, 1492, 1447, 1363, 1328, 1221, 1109, 1058, 966, 894, 865, 747, 692; **HRMS**: *m/z* calculated for C<sub>25</sub>H<sub>23</sub>NO<sub>2</sub>Na<sup>+</sup> [M+Na]<sup>+</sup>: 392.1621; found: 392.1619.

### [2+2]-Cycloaddition



**General Procedure (GP-6a)** An oven-dried test tube (25x150 mm) equipped with a magnetic stir bar was charged with substrate (0.25 mmol, 1.0 equiv.), [Ir(dF(CF<sub>3</sub>)ppy)<sub>2</sub>(dtbbpy)](PF<sub>6</sub>) (**3.63**) (1.4 mg or 2.8 mg, 0.5 or 1 mol%) and THF (25 mL). When a substrate required extended reaction time (>2 h), the reaction mixture was degassed by sparging with nitrogen gas for 30 min prior to irradiation and the reaction conducted under a nitrogen atmosphere. The test tube was sealed with a rubber septum and placed in front of a 40 W PR160-427 nm Kessil light at a distance of approximately 5 cm. The light was set to 100% intensity and the reaction stirred until complete as judged by TLC analysis (0.5-72 h). The internal temperature of the photoreactor was maintained below 45 °C by a fan. Upon completion, the reaction mixture was transferred to a 100-mL round-bottom flask and the solvent removed *in vacuo*. The diastereomeric ratio was determined by <sup>1</sup>H NMR analysis from the crude mixture, before purifying the crude product by flash column chromatography (EtOAc/hexanes) to afford the corresponding pure azetidine.

**Note:** The reaction can be alternatively run utilizing a 23W CFL lamp, although extended reaction times are necessary (~24 h for (*E*)-**15**).

**General Procedure for Gram-Scale Reaction (GP-6b):** A 500-mL round-bottom flask equipped with a magnetic stir bar was charged with substrate (1.0 equiv.), [Ir(dF(CF<sub>3</sub>)ppy)<sub>2</sub>(dtbbpy)](PF<sub>6</sub>) (**3.63**) (0.5 mol%) and THF (0.025 M). The flask was placed in between a 40 W PR160-427 nm Kessil light (100% intensity) and a 34 W H150-BLUE Kessil light at a distance of approximately 5 cm and the reaction stirred under ambient atmosphere until complete as judged by TLC analysis. Solvent was removed *in vacuo* and the diastereomeric ratio determined by <sup>1</sup>H NMR analysis from the crude mixture. Purification of the crude product by flash column chromatography (EtOAc/hexanes) afforded the corresponding pure azetidine.

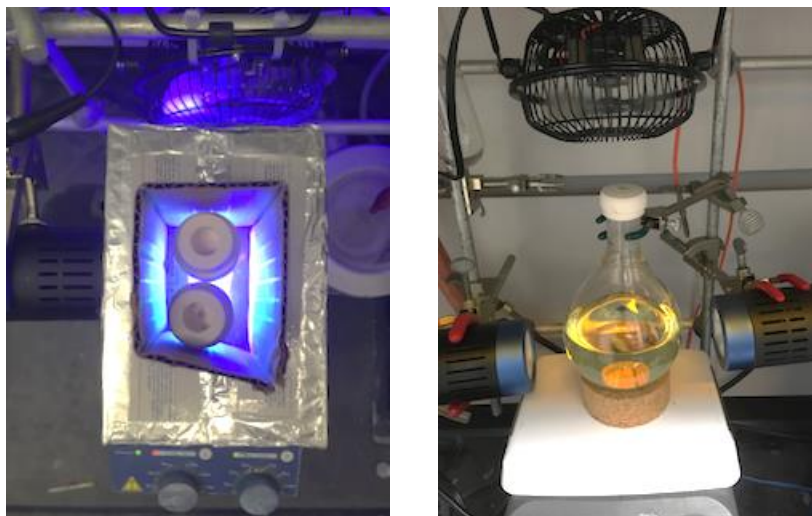
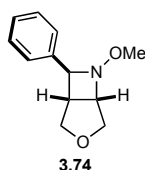
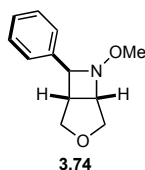


Figure 3.22 Reaction set up for small and large scale [2+2]-photocycloadditions.

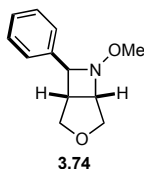


**(1*R*\*,5*S*\*,7*S*\*)-6-Methoxy-7-phenyl-3-oxa-6-azabicyclo[3.2.0]heptane (3.74):** Prepared according to GP-6a using **3.73** (51 mg, 0.25 mmol, 1.0 equiv.), **3.63** (1.4 mg, 0.5 mol%) and THF (25 mL) with a reaction time of 0.5 h. The diastereomeric ratio was determined to be >20:1 by <sup>1</sup>H NMR analysis of the crude mixture. Purification by flash column chromatography (10-20% EtOAc/hexanes) afforded the pure title compound as clear oil (49 mg, 96%; combined yield). **<sup>1</sup>H NMR** (500 MHz, CDCl<sub>3</sub>): δ 7.43 (d, *J* = 7.5 Hz, 2H), 7.37 (t, *J* = 7.6 Hz, 2H), 7.29 (t, *J* = 7.2 Hz, 1H), 4.76 (d, *J* = 10.6 Hz, 1H), 4.54 (t, *J* = 5.5 Hz, 1H), 4.42 (d, *J* = 5.8 Hz, 1H), 3.98 (d, *J* = 9.4 Hz, 1H), 3.58 (dd, *J* = 10.6, 5.3 Hz, 1H), 3.52 (dd, *J* = 9.4, 3.6 Hz, 1H), 3.45 (s, 3H), 2.72 (td, *J* = 5.8, 3.9 Hz, 1H); **<sup>13</sup>C NMR** (126 MHz, CDCl<sub>3</sub>): δ 141.9, 128.6, 127.6, 126.4, 73.9, 70.8, 67.5, 67.2, 60.6, 42.1; **IR** (cm<sup>-1</sup>): 2949, 2852, 1466, 1162, 1084, 1059, 1019, 909, 730, 697; **HRMS**: *m/z* calculated for C<sub>12</sub>H<sub>15</sub>NO<sub>2</sub>H<sup>+</sup> [M+H]<sup>+</sup>: 206.1176; found: 206.1175.

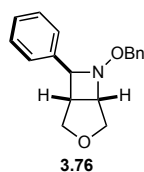


**(1*R*\*,5*S*\*,7*S*\*)-6-Methoxy-7-phenyl-3-oxa-6-azabicyclo[3.2.0]heptane (3.74):** Prepared according to GP-6a using **3.73** (51 mg, 0.25 mmol, 1.0 equiv.), **3.63** (1.4 mg, 0.5 mol%) and THF (25 mL) with a reaction time of 0.5 h. The diastereomeric ratio was determined to be >20:1 by <sup>1</sup>H

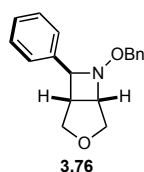
NMR analysis of the crude mixture. Purification by flash column chromatography (10-20% EtOAc/hexanes) afforded the pure title compound as clear oil (50 mg, 97%; combined yield). Spectroscopic data was found consistent with those obtained when (*E*)-**13** was used.



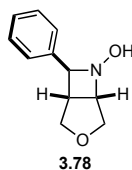
**(1*R*\*,5*S*\*,7*S*\*)-6-Methoxy-7-phenyl-3-oxa-6-azabicyclo[3.2.0]heptane (3.74):** Prepared according to GP-6b using **3.73** (1.40 g, 6.8 mmol, 1.0 equiv.), **3.63** (38 mg, 0.5 mol%) and THF (300 mL) with a reaction time of 1 h. The diastereomeric ratio was determined to be >20:1 by <sup>1</sup>H NMR analysis of the crude mixture. Purification by flash column chromatography (5-20% EtOAc/hexanes) afforded the pure title compound as clear oil (1.27 g, 91%; combined yield). Spectroscopic data was found consistent with those obtained when the reaction was conducted on 0.25 mmol scale.



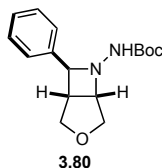
**(1*R*\*,5*S*\*,7*S*\*)-6-(Benzyloxy)-7-phenyl-3-oxa-6-azabicyclo[3.2.0]heptane (3.76):** Prepared according to GP-6a using **3.75** (70 mg, 0.25 mmol, 1.0 equiv.), **3.63** (1.4 mg, 0.5 mol%) and THF (25 mL) with a reaction time of 0.5 h. The diastereomeric ratio was determined to be 16:1 by <sup>1</sup>H NMR analysis of the crude mixture. Purification by flash column chromatography (5-10% EtOAc/hexanes) afforded the pure title compound as clear oil (67 mg, 96%; combined yield). <sup>1</sup>H NMR (700 MHz, CDCl<sub>3</sub>): δ 7.37 – 7.35 (m, 2H), 7.33 (t, *J* = 7.6 Hz, 2H), 7.29 – 7.23 (m, 6H), 4.76 (d, *J* = 10.5 Hz, 1H), 4.62 (s, 2H), 4.48 (d, *J* = 5.8 Hz, 1H), 4.30 (t, *J* = 5.6 Hz, 1H), 3.95 (d, *J* = 9.4 Hz, 1H), 3.50 – 3.45 (m, 2H), 2.65 (td, *J* = 5.9, 3.6 Hz, 1H) <sup>13</sup>C NMR (176 MHz, CDCl<sub>3</sub>): δ 141.9, 138.4, 128.6, 128.5, 128.3, 127.7, 127.5, 126.5, 75.6, 74.1, 70.8, 68.5, 67.6, 42.6; IR (cm<sup>-1</sup>): 2850, 1495, 1453, 1366, 1204, 1084, 1061, 977, 909, 742, 695; HRMS: *m/z* calculated for C<sub>18</sub>H<sub>19</sub>NO<sub>2</sub>H<sup>+</sup> [M+H]<sup>+</sup>: 282.1489; found: 282.1491.



**(1*R*\*,5*S*\*,7*S*\*)-6-(Benzyloxy)-7-phenyl-3-oxa-6-azabicyclo[3.2.0]heptane (3.76):** Prepared according to GP-6b using **3.75** (1.20 g, 4.3 mmol, 1.0 equiv.), **3.63** (24 mg, 0.5 mol%) and THF (300 mL) with a reaction time of 1 h. The diastereomeric ratio was determined to be 20:1 by <sup>1</sup>H NMR analysis of the crude mixture. Purification by flash column chromatography (5-20% EtOAc/hexanes) afforded the pure title compound as clear oil (1.08 g, 90%; combined yield). Spectroscopic data was found consistent with those obtained when the reaction was conducted on 0.25 mmol scale.



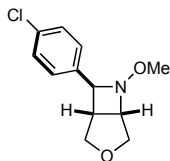
**(1*R*\*,5*S*\*,7*S*\*)-7-Phenyl-3-oxa-6-azabicyclo[3.2.0]heptan-6-ol (3.78):** Prepared according to GP-6a using **3.77** (48 mg, 0.25 mmol, 1.0 equiv.), **3.63** (1.4 mg, 0.5 mol%) and THF (25 mL) with a reaction time of 0.5 h. The diastereomeric ratio was determined to be >20:1 by <sup>1</sup>H NMR analysis of the crude mixture. Purification by flash column chromatography (20-40% EtOAc/hexanes) afforded the pure title compound as off-white solid (48 mg, 54%; combined yield). <sup>1</sup>H NMR (700 MHz, CDCl<sub>3</sub>): δ 7.35 – 7.30 (m, 4H), 7.29 – 7.26 (m, 1H), 4.79 (d, *J* = 10.7 Hz, 1H), 4.36 (d, *J* = 5.9 Hz, 1H), 4.32 (t, *J* = 5.6 Hz, 1H), 3.92 (d, *J* = 9.4 Hz, 1H), 3.51 – 3.45 (m, 2H), 2.74 (td, *J* = 5.9, 3.6 Hz, 1H); <sup>13</sup>C NMR (176 MHz, CDCl<sub>3</sub>): δ 140.8, 128.6, 127.9, 126.9, 75.5, 70.7, 69.1, 66.8, 41.8; IR (cm<sup>-1</sup>): 3243, 2853, 1454, 1353, 1266, 1162, 1084, 1055, 954, 815, 741, 697; HRMS: *m/z* calculated for C<sub>11</sub>H<sub>13</sub>NO<sub>2</sub>Na<sup>+</sup> [M+Na]<sup>+</sup>: 214.0838; found: 214.0838.



**Tert-butyl ((1*R*\*,5*S*\*,7*S*\*)-7-phenyl-3-oxa-6-azabicyclo[3.2.0]heptan-6-yl)carbamate (3.80):** Prepared according to GP-6a using **3.79** (73 mg, 0.25 mmol, 1.0 equiv.), **3.63** (1.4 mg, 0.5 mol%) and THF (25 mL) with a reaction time of 0.5 h. The diastereomeric ratio was determined to be 13:1 by <sup>1</sup>H NMR analysis of the crude mixture. Purification by flash column chromatography (30-40% EtOAc/hexanes) afforded the pure title compound as pale-yellow solid (45 mg, 62%; combined yield). <sup>1</sup>H NMR (700 MHz, CDCl<sub>3</sub>): δ 7.50 (d, *J* = 7.4 Hz, 2H), 7.36 (t, *J* = 7.7 Hz, 2H), 7.26 (t, *J* = 7.4 Hz, 1H), 5.91 (b, 1H), 4.60 (t, *J* = 4.8 Hz, 1H), 4.49 (d, *J* = 11.5 Hz, 1H), 4.22 (d,



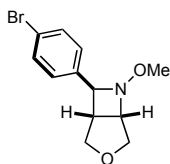
$J = 4.8$  Hz, 1H), 4.03 (d,  $J = 9.5$  Hz, 1H), 3.50 (dd,  $J = 9.5, 3.9$  Hz, 1H), 3.47 (dd,  $J = 11.5, 4.1$  Hz, 1H), 2.75 (q,  $J = 4.9$  Hz, 1H), 1.41 (s, 9H);  $^{13}\text{C}$  NMR (176 MHz,  $\text{CDCl}_3$ ):  $\delta$  154.9, 141.6, 128.6, 127.5, 126.0, 80.3, 77.2, 71.9, 68.7, 67.5, 43.2, 28.4; IR ( $\text{cm}^{-1}$ ): 3262, 2975, 2857, 1734, 1695, 1522, 1455, 1366, 1247, 1161, 1049, 993, 906, 743, 670; HRMS:  $m/z$  calculated for  $\text{C}_{16}\text{H}_{22}\text{N}_2\text{O}_3\text{Na}^+$   $[\text{M}+\text{Na}]^+$ : 313.1523; found: 313.1528.



3.83

**(1R\*,5S\*,7S\*)-7-(4-Chlorophenyl)-6-methoxy-3-oxa-6-azabicyclo[3.2.0]heptane (3.83):**

Prepared according to GP-6a using **3.163** (62 mg, 0.26 mmol, 1.0 equiv.), **3.63** (1.4 mg, 0.5 mol%) and THF (25 mL) with a reaction time of 0.5 h. The diastereomeric ratio was determined to be >20:1 by  $^1\text{H}$  NMR analysis of the crude mixture. Purification by flash column chromatography (20-20% EtOAc/hexanes) afforded the pure title compound as clear oil (61 mg, 98%; combined yield).  $^1\text{H}$  NMR (500 MHz,  $\text{CDCl}_3$ ):  $\delta$  7.35 (d,  $J = 8.6$  Hz, 2H), 7.32 (d,  $J = 8.6$  Hz, 2H), 4.73 (d,  $J = 10.7$  Hz, 1H), 4.52 (t,  $J = 5.6$  Hz, 1H), 4.36 (d,  $J = 5.8$  Hz, 1H), 3.94 (d,  $J = 9.5$  Hz, 1H), 3.55 (dd,  $J = 10.7, 5.3$  Hz, 1H), 3.49 (dd,  $J = 9.5, 3.6$  Hz, 1H), 3.42 (s, 3H), 2.66 (td,  $J = 5.9, 3.5$  Hz, 1H);  $^{13}\text{C}$  NMR (100 MHz,  $\text{CDCl}_3$ ):  $\delta$  140.4, 133.3, 128.7, 127.8, 73.1, 70.7, 67.5, 67.1, 60.6, 42.2; IR ( $\text{cm}^{-1}$ ): 2951, 2895, 2852, 1491, 1466, 1081, 1064, 1050, 1023, 1014, 979, 913, 820, 803, 725; HRMS:  $m/z$  calculated for  $\text{C}_{12}\text{H}_{14}\text{ClNO}_2\text{H}^+$   $[\text{M}+\text{H}]^+$ : 240.0786; found: 240.0786.

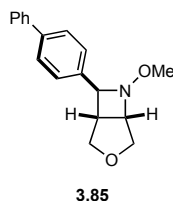


3.84

**(1R\*,5S\*,7S\*)-7-(4-Bromophenyl)-6-methoxy-3-oxa-6-azabicyclo[3.2.0]heptane (3.84):**

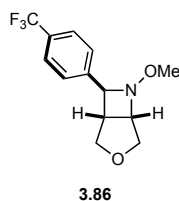
Prepared according to GP-6a using **3.164** (71 mg, 0.25 mmol, 1.0 equiv.), **3.63** (1.4 mg, 0.5 mol%) and THF (25 mL) with a reaction time of 0.5 h. The diastereomeric ratio was determined to be >20:1 by  $^1\text{H}$  NMR analysis of the crude mixture. Purification by flash column chromatography (10-20% EtOAc/hexanes) afforded the pure title compound as white solid (60 mg, 85%; combined yield).  $^1\text{H}$  NMR (500 MHz,  $\text{CDCl}_3$ ):  $\delta$  7.48 (d,  $J = 8.3$  Hz, 2H), 7.29 (d,  $J = 8.3$  Hz, 2H), 4.73 (d,  $J = 10.7$  Hz, 1H), 4.51 (t,  $J = 5.5$  Hz, 1H), 4.34 (d,  $J = 5.8$  Hz, 1H), 3.94 (d,  $J = 9.5$  Hz, 1H), 3.55

(dd,  $J = 10.7, 5.3$  Hz, 1H), 3.49 (dd,  $J = 9.5, 3.6$  Hz, 1H), 3.41 (s, 3H), 2.65 (td,  $J = 5.8, 3.7$  Hz, 1H);  $^{13}\text{C NMR}$  (126 MHz,  $\text{CDCl}_3$ ):  $\delta$  141.0, 131.7, 128.2, 121.4, 73.2, 70.7, 67.5, 67.1, 60.7, 42.2; **IR** ( $\text{cm}^{-1}$ ): 2929, 2843, 1485, 1161, 1059, 1007, 937, 903, 858, 814, 792, 718; **HRMS**:  $m/z$  calculated for  $\text{C}_{12}\text{H}_{14}\text{BrNO}_2\text{H}^+$   $[\text{M}+\text{H}]^+$ : 284.0281; found: 284.0279.



**(1R\*,5S\*,7S\*)-7-([1,1'-Biphenyl]-4-yl)-6-methoxy-3-oxa-6-azabicyclo[3.2.0]heptane (3.85):**

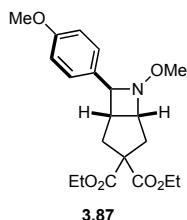
Prepared according to GP-6a using **3.165** (70 mg, 0.25 mmol, 1.0 equiv.), **3.63** (1.4 mg, 0.5 mol%) and THF (25 mL) with a reaction time of 0.5 h. The diastereomeric ratio was determined to be 16:1 by  $^1\text{H NMR}$  analysis of the crude mixture. Purification by flash column chromatography (10-20% EtOAc/hexanes) afforded the pure title compound as clear oil (70 mg, 99%; combined yield).  $^1\text{H NMR}$  (500 MHz,  $\text{CDCl}_3$ ):  $\delta$  7.60 (d,  $J = 8.1$  Hz, 4H), 7.49 (d,  $J = 8.1$  Hz, 2H), 7.44 (t,  $J = 7.6$  Hz, 2H), 7.35 (t,  $J = 7.4$  Hz, 1H), 4.77 (d,  $J = 10.6$  Hz, 1H), 4.56 (t,  $J = 5.5$  Hz, 1H), 4.45 (d,  $J = 5.8$  Hz, 1H), 3.99 (d,  $J = 9.4$  Hz, 1H), 3.58 (dd,  $J = 10.6, 5.3$  Hz, 1H), 3.53 (dd,  $J = 9.3, 3.6$  Hz, 1H), 3.46 (s, 3H), 2.75 (td,  $J = 5.8, 3.8$  Hz, 1H);  $^{13}\text{C NMR}$  (126 MHz,  $\text{CDCl}_3$ ):  $\delta$  141.1, 141.0, 140.6, 128.9, 127.4 (2C), 127.2, 126.9, 73.7, 70.8, 67.5, 67.2, 60.7, 42.2; **IR** ( $\text{cm}^{-1}$ ): 2930, 2849, 1486, 1098, 1079, 1008, 978, 911, 832, 760, 734, 695; **HRMS**:  $m/z$  calculated for  $\text{C}_{18}\text{H}_{19}\text{NO}_2\text{Na}^+$   $[\text{M}+\text{Na}]^+$ : 304.1308; found: 304.1311.



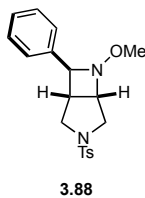
**(1R\*,5S\*,7S\*)-6-Methoxy-7-(4-(trifluoromethyl)phenyl)-3-oxa-6-azabicyclo[3.2.0]heptane**

**(3.86):** Prepared according to GP-6a using **3.170** (68 mg, 0.25 mmol, 1.0 equiv.), **3.63** (1.4 mg, 0.5 mol%) and THF (25 mL) with a reaction time of 0.5 h. The diastereomeric ratio was determined to be >20:1 by  $^1\text{H NMR}$  analysis of the crude mixture. Purification by flash column chromatography (5-20% EtOAc/hexanes) afforded the pure title compound as clear oil (66 mg, 97%; combined yield).  $^1\text{H NMR}$  (700 MHz,  $\text{CDCl}_3$ ):  $\delta$  7.61 (d,  $J = 8.1$  Hz, 2H), 7.53 (d,  $J = 8.1$  Hz, 2H), 4.75 (d,  $J = 10.6$  Hz, 1H), 4.54 (t,  $J = 5.5$  Hz, 1H), 4.45 (d,  $J = 5.7$  Hz, 1H), 3.97 (d,

$J = 9.5$  Hz, 1H), 3.57 (dd,  $J = 10.6, 5.2$  Hz, 1H), 3.52 (dd,  $J = 9.5, 3.5$  Hz, 1H), 3.44 (s, 3H), 2.68 (td,  $J = 5.8, 3.6$  Hz, 1H);  $^{13}\text{C}$  NMR (176 MHz,  $\text{CDCl}_3$ ):  $\delta$  145.9, 129.8 (q,  $J = 32.3$  Hz), 126.6, 125.5 (q,  $J = 3.8$  Hz), 124.3 (q,  $J = 272$  Hz), 73.1, 70.7, 67.6, 67.1, 60.6, 42.2; IR ( $\text{cm}^{-1}$ ): 2940, 2854, 1620, 1417, 1322, 1161, 1118, 1064, 1017, 913, 832, 807, 712, 639; HRMS:  $m/z$  calculated for  $\text{C}_{13}\text{H}_{14}\text{F}_3\text{NO}_2\text{H}^+$   $[\text{M}+\text{H}]^+$ : 274.1049; found: 274.1044.

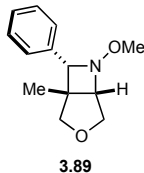


**Diethyl (1*S*\*,5*R*\*,7*S*\*)-6-methoxy-7-(4-methoxyphenyl)-6-azabicyclo[3.2.0]heptane-3,3-dicarboxylate (3.87):** Prepared according to GP-6a using **3.179** (94 mg, 0.25 mmol, 1.0 equiv.), **17**•PF<sub>6</sub> (1.4 mg, 0.5 mol%) and THF (25 mL) with a reaction time of 1.5 h. The diastereomeric ratio was determined to be 20:1 by  $^1\text{H}$  NMR analysis of the crude mixture. Purification by flash column chromatography (2-30% EtOAc/hexanes) afforded the pure title compound as clear oil (68 mg, 72%; combined yield).  $^1\text{H}$  NMR (400 MHz,  $\text{C}_6\text{D}_6$ ):  $\delta$  7.37 (d,  $J = 8.6$  Hz, 2H), 6.83 (d,  $J = 8.6$  Hz, 2H), 4.57 (d,  $J = 6.0$  Hz, 1H), 4.52 (q,  $J = 6.9$  Hz, 1H), 4.13 – 4.02 (m, 2H), 3.98 – 3.87 (m, 2H), 3.41 (dd,  $J = 14.7, 4.6$  Hz, 1H), 3.32 (s, 3H), 3.31 (s, 3H), 2.89 – 2.79 (m, 2H), 2.39 (qd,  $J = 7.1, 6.2, 1.8$  Hz, 1H), 2.29 (dd,  $J = 14.0, 7.9$  Hz, 1H), 0.99 (t,  $J = 7.1$  Hz, 3H), 0.89 (t,  $J = 7.1$  Hz, 3H);  $^{13}\text{C}$  NMR (126 MHz,  $\text{C}_6\text{D}_6$ ):  $\delta$  172.3, 171.7, 159.8, 134.2, 128.5, 114.2, 76.6, 69.9, 63.9, 61.52, 61.49, 60.5, 54.8, 42.6, 38.5, 34.7, 14.1, 14.0; IR ( $\text{cm}^{-1}$ ): 2937, 1725, 1611, 1513, 1464, 1443, 1300, 1244, 1206, 1178, 1094, 1062, 1034, 859, 809; HRMS:  $m/z$  calculated for  $\text{C}_{20}\text{H}_{27}\text{NO}_6\text{H}^+$   $[\text{M}+\text{H}]^+$ : 378.1911; found: 378.1917.



**(1*R*\*,5*S*\*,7*S*\*)-6-Methoxy-7-phenyl-3-tosyl-3,6-diazabicyclo[3.2.0]heptane (3.88):** Prepared according to GP-6a using **3.171** (90 mg, 0.25 mmol, 1.0 equiv.), **3.63** (1.4 mg, 0.5 mol%) and THF (25 mL) with a reaction time of 0.5 h. The diastereomeric ratio was determined to be 12:1 by  $^1\text{H}$  NMR analysis of the crude mixture. Purification by flash column chromatography (10-30% EtOAc/hexanes) afforded the pure title compound as white solid (83 mg, 92%; combined yield).

**<sup>1</sup>H NMR** (700 MHz, CDCl<sub>3</sub>): δ 7.77 (d, *J* = 8.2 Hz, 2H), 7.39 – 7.32 (m, 6H), 7.30 – 7.26 (m, 1H), 4.51 (d, *J* = 6.0 Hz, 1H), 4.40 – 4.33 (m, 2H), 3.61 (d, *J* = 10.0 Hz, 1H), 3.40 (s, 3H), 2.82 – 2.75 (m, 2H), 2.57 (q, *J* = 5.8 Hz, 1H), 2.45 (s, 3H); **<sup>13</sup>C NMR** (176 MHz, CDCl<sub>3</sub>): δ 143.9, 141.3, 132.5, 129.8, 128.6, 128.1, 127.8, 126.5, 73.8, 66.2, 60.8, 51.5, 46.4, 40.5, 21.7; **IR** (cm<sup>-1</sup>): 2936, 1597, 1466, 1343, 1158, 1093, 1055, 1023, 813, 735, 699, 665; **HRMS**: *m/z* calculated for C<sub>19</sub>H<sub>22</sub>N<sub>2</sub>O<sub>3</sub>SNa<sup>+</sup> [M+Na]<sup>+</sup>: 381.1243; found: 381.1245.

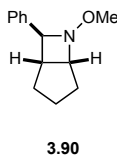


**(1R\*,5S\*,7S\*)-6-Methoxy-1-methyl-7-phenyl-3-oxa-6-azabicyclo[3.2.0]heptane (3.89):**

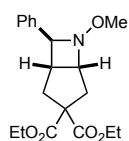
Prepared according to GP-6a using **3.166** (55 mg, 0.25 mmol, 1.0 equiv.), **3.63** (1.4 mg, 0.5 mol%) and THF (25 mL) with a reaction time of 1.5 h. The diastereomeric ratio was determined to be 1.6:1 by <sup>1</sup>H NMR analysis of the crude mixture. Purification by flash column chromatography (1-5% EtOAc/hexanes) afforded the pure title compound as clear oil (51 mg, 93%; combined yield).

**(1R\*,5S\*,7S\*) Diastereomer (major):** **<sup>1</sup>H NMR** (700 MHz, CDCl<sub>3</sub>): δ 7.41 (d, *J* = 7.5 Hz, 2H), 7.36 (t, *J* = 7.6 Hz, 2H), 7.27 (t, *J* = 7.4 Hz, 1H), 4.48 (s, 1H), 4.12 (d, *J* = 9.8 Hz, 1H), 3.83 (d, *J* = 2.8 Hz, 1H), 3.54 – 3.50 (m, 5H), 2.98 (d, *J* = 9.8 Hz, 1H), 1.44 (s, 3H); **<sup>13</sup>C NMR** (176 MHz, CDCl<sub>3</sub>): δ 138.7, 128.5, 127.5, 126.8, 77.6, 77.2, 73.0, 72.5, 61.8, 45.0, 22.7; **IR** (cm<sup>-1</sup>): 2952, 2894, 2844, 1495, 1466, 1452, 1062, 1032, 1023, 911, 744, 721; **HRMS**: *m/z* calculated for C<sub>13</sub>H<sub>17</sub>NO<sub>2</sub>H<sup>+</sup> [M+H]<sup>+</sup>: 220.1332; found: 220.1333; **(1R\*,5S\*,7R\*) Diastereomer (minor):**

**<sup>1</sup>H NMR** (500 MHz, CDCl<sub>3</sub>): δ 7.39 (d, *J* = 7.1 Hz, 2H), 7.35 (t, *J* = 7.6 Hz, 2H), 7.27 (t, *J* = 7.1 Hz, 1H), 4.72 (d, *J* = 10.7 Hz, 1H), 4.58 (s, 1H), 4.05 (d, *J* = 5.1 Hz, 1H), 3.83 (d, *J* = 9.1 Hz, 1H), 3.68 (dd, *J* = 10.7, 5.1 Hz, 1H), 3.48 (s, 3H), 3.29 (d, *J* = 9.1 Hz, 1H), 0.86 (s, 3H); **<sup>13</sup>C NMR** (176 MHz, CDCl<sub>3</sub>): δ 139.5, 128.3, 127.3, 126.8, 76.8, 75.3, 72.3, 67.8, 60.8, 46.2, 14.3; **IR** (cm<sup>-1</sup>): 2935, 2849, 1495, 1467, 1451, 1056, 1032, 1008, 943, 911, 734, 701; **HRMS**: *m/z* calculated for C<sub>13</sub>H<sub>17</sub>NO<sub>2</sub>H<sup>+</sup> [M+H]<sup>+</sup>: 220.1332; found: 220.1331.

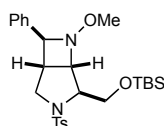


**(1*S*\*,5*R*\*,7*S*\*)-6-Methoxy-7-phenyl-6-azabicyclo[3.2.0]heptane (3.90):** Prepared according to GP-6b using **3.172** (0.50 g, 2.50 mmol, 1.0 equiv.), **3.63** (14 mg, 0.5 mol%) and THF (250 mL) with a reaction time of 4 h. The diastereomeric ratio was determined to be >20:1 by <sup>1</sup>H NMR analysis of the crude mixture. Purification by flash column chromatography (1-5% EtOAc/hexanes) afforded the pure title compound as pale-yellow oil (0.49 g, 98%; combined yield). <sup>1</sup>H NMR (700 MHz, CDCl<sub>3</sub>): δ 7.39 (d, *J* = 7.3 Hz, 2H), 7.34 (t, *J* = 7.7 Hz, 2H), 7.25 (t, *J* = 7.3 Hz, 1H), 4.40 (t, *J* = 6.5 Hz, 1H), 4.15 (d, *J* = 5.8 Hz, 1H), 3.44 (s, 3H), 2.54 (q, *J* = 5.8 Hz, 1H), 2.48 – 2.43 (m, 1H), 2.00 – 1.93 (m, 2H), 1.82 – 1.77 (m, 1H), 1.62 – 1.50 (m, 2H); <sup>13</sup>C NMR (176 MHz, CDCl<sub>3</sub>): δ 143.1, 128.4, 127.1, 126.2, 74.0, 68.4, 60.5, 42.5, 30.8, 25.99, 25.95; IR (cm<sup>-1</sup>): 2934, 1853, 1494, 1465, 1451, 1325, 1267, 1179, 1058, 1022, 970, 944, 907, 833, 751, 734, 697; HRMS: *m/z* calculated for C<sub>13</sub>H<sub>17</sub>NOH<sup>+</sup> [M+H]<sup>+</sup>: 204.1383; found: 204.1376.



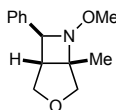
3.91

**Diethyl (1*S*\*,5*R*\*,7*S*\*)-6-Methoxy-7-phenyl-6-azabicyclo[3.2.0]heptane-3,3-dicarboxylate (3.91):** Prepared according to GP-6a using **3.180** (87 mg, 0.25 mmol, 1.0 equiv.), **3.63** (1.4 mg, 0.5 mol%) and THF (25 mL) with a reaction time of 0.5 h. The diastereomeric ratio was determined to be 13:1 by <sup>1</sup>H NMR analysis of the crude mixture. Purification by flash column chromatography (5-10% EtOAc/hexanes) afforded the pure title compound as clear oil (84 mg, 97%; combined yield). <sup>1</sup>H NMR (500 MHz, CDCl<sub>3</sub>): δ 7.39 (d, *J* = 7.5 Hz, 2H), 7.34 (t, *J* = 7.5 Hz, 2H), 7.29 – 7.24 (m, 1H), 4.50 (q, *J* = 6.6 Hz, 1H), 4.34 (d, *J* = 6.0 Hz, 1H), 4.30 – 4.23 (m, 2H), 4.23 – 4.14 (m, 2H), 3.38 (s, 3H), 3.04 (dd, *J* = 14.7, 4.8 Hz, 1H), 2.62 (d, *J* = 14.4 Hz, 1H), 2.55 (q, *J* = 7.4 Hz, 2H), 2.33 (dd, *J* = 14.2, 7.9 Hz, 1H), 1.30 (t, *J* = 7.1 Hz, 3H), 1.25 (t, *J* = 7.1 Hz, 3H); <sup>13</sup>C NMR (126 MHz, CDCl<sub>3</sub>): δ 172.5, 171.7, 141.3, 128.5, 127.6, 126.7, 76.6, 69.5, 63.6, 61.9, 61.8, 60.5, 41.5, 38.8, 34.2, 14.3, 14.2; IR (cm<sup>-1</sup>): 2980, 2938, 1726, 1445, 1366, 1252, 1180, 1094, 1061, 1039, 934, 746, 698; HRMS: *m/z* calculated for C<sub>19</sub>H<sub>25</sub>NO<sub>5</sub>Na<sup>+</sup> [M+Na]<sup>+</sup>: 370.1625; found: 370.1629.



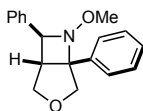
3.92

**(1*R*\*,4*S*\*,5*S*\*,7*S*\*)-4-(((*Tert*-butyldimethylsilyl)oxy)methyl)-6-methoxy-7-phenyl-3-tosyl-3,6-diazabicyclo[3.2.0]heptane (3.92):** Prepared according to GP-6a using **3.181** (126 mg, 0.25 mmol, 1.0 equiv.), **3.63** (1.4 mg, 0.5 mol%) and THF (25 mL) with a reaction time of 0.5 h. The diastereomeric ratio was determined to be 2.5:1 by <sup>1</sup>H NMR analysis of the crude mixture. Purification by flash column chromatography (2-20% diethyl ether/pentane) afforded the pure title compound as clear oil (120 mg, 95%; combined yield). <sup>1</sup>H NMR (500 MHz, CDCl<sub>3</sub>): δ 7.87 (d, *J* = 8.2 Hz, 2H), 7.35 (d, *J* = 8.2 Hz, 2H), 7.28 (m, 2H), 7.24 (m, 1H), 7.06 (d, *J* = 7.0 Hz, 2H), 4.79 (t, *J* = 4.0 Hz, 1H), 4.46 (d, *J* = 6.1 Hz, 1H), 3.85 (d, *J* = 4.0 Hz, 2H), 3.53 – 3.44 (m, 3H), 3.33 (s, 3H), 2.50 (tt, *J* = 6.0, 2.4 Hz, 1H), 2.43 (s, 3H), 0.86 (s, 9H), 0.06 (d, *J* = 15.9 Hz, 6H); <sup>13</sup>C NMR (176 MHz, CDCl<sub>3</sub>): δ 143.5, 140.8, 137.5, 129.9, 128.5, 127.8, 127.6, 126.5, 73.1, 71.2, 66.2, 60.4, 58.8, 51.8, 41.2, 25.9, 21.7, 18.2, -5.36, -5.43; IR (cm<sup>-1</sup>): 2929, 2883, 2856, 1463, 1345, 1251, 1187, 1156, 1091, 1033, 1005, 956, 869, 831, 813, 776, 751, 699, 666; HRMS: *m/z* calculated for C<sub>26</sub>H<sub>38</sub>N<sub>2</sub>O<sub>4</sub>SSiH<sup>+</sup> [M+H]<sup>+</sup>: 503.2394; found: 503.2394.



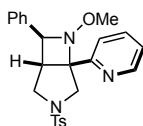
3.93

**(1*R*\*,5*S*\*,7*S*\*)-6-Methoxy-5-methyl-7-phenyl-3-oxa-6-azabicyclo[3.2.0]heptane (3.93):** Prepared according to GP-6a using **3.182** (55 mg, 0.25 mmol, 1.0 equiv.), **3.63** (2.8 mg, 1 mol%) and degassed THF (25 mL) with a reaction time of 18 h. The diastereomeric ratio was determined to be 17:1 by <sup>1</sup>H NMR analysis of the crude mixture. Purification by flash column chromatography (5-15% EtOAc/hexanes) afforded the pure title compound as clear oil (50 mg, 91%; combined yield). <sup>1</sup>H NMR (700 MHz, CDCl<sub>3</sub>): δ 7.43 (d, *J* = 7.3 Hz, 2H), 7.36 (t, *J* = 7.6 Hz, 2H), 7.28 (t, *J* = 7.3 Hz, 1H), 4.73 (d, *J* = 10.1 Hz, 1H), 4.28 (d, *J* = 5.8 Hz, 1H), 3.93 (d, *J* = 9.4 Hz, 1H), 3.63 (dd, *J* = 9.4, 3.5 Hz, 1H), 3.49 (s, 3H), 3.37 (d, *J* = 10.1 Hz, 1H), 2.23 (dd, *J* = 5.7, 3.5 Hz, 1H), 1.51 (s, 3H); <sup>13</sup>C NMR (126 MHz, CDCl<sub>3</sub>): δ 142.4, 128.5, 127.4, 126.6, 74.3, 71.8, 70.9, 70.7, 62.2, 48.4, 23.5; IR (cm<sup>-1</sup>): 2935, 2851, 1452, 1375, 1192, 1130, 1061, 1045, 939, 913, 792, 746, 697; HRMS: *m/z* calculated for C<sub>13</sub>H<sub>17</sub>NO<sub>2</sub>H<sup>+</sup> [M+H]<sup>+</sup>: 220.1332; found: 220.1329.



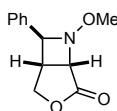
3.94

**(1*R*\*,5*R*\*,7*S*\*)-6-Methoxy-5,7-diphenyl-3-oxa-6-azabicyclo[3.2.0]heptane (3.94):** Prepared according to GP-6a using **3.183** (70 mg, 0.25 mmol, 1.0 equiv.), **3.63** (2.8 mg, 1 mol%) and degassed THF (25 mL) with a reaction time of 18 h. The diastereomeric ratio was determined to be 12:1 by <sup>1</sup>H NMR analysis of the crude mixture. Purification by flash column chromatography (1-10% EtOAc/hexanes) afforded the pure title compound as clear oil (68 mg, 97%; combined yield). <sup>1</sup>H NMR (700 MHz, CDCl<sub>3</sub>): δ 7.51 (d, *J* = 7.1 Hz, 2H), 7.42 – 7.38 (m, 4H), 7.33 (t, *J* = 7.6 Hz, 2H), 7.29 (t, *J* = 7.4 Hz, 1H), 7.28 – 7.24 (m, 1H), 5.03 (d, *J* = 10.5 Hz, 1H), 4.47 (d, *J* = 5.7 Hz, 1H), 4.12 (d, *J* = 9.6 Hz, 1H), 3.91 (dd, *J* = 9.6, 3.5 Hz, 1H), 3.79 (d, *J* = 10.5 Hz, 1H), 3.59 (s, 3H), 2.60 (dd, *J* = 5.6, 3.5 Hz, 1H); <sup>13</sup>C NMR (176 MHz, CDCl<sub>3</sub>): δ 143.0, 142.2, 128.56, 128.55, 127.6, 127.1, 126.9, 125.5, 79.3, 73.6, 71.9, 71.6, 61.6, 51.0; IR (cm<sup>-1</sup>): 2933, 2851, 1602, 1492, 1446, 1262, 1059, 1043, 1022, 964, 914, 840, 748, 696; HRMS: *m/z* calculated for C<sub>18</sub>H<sub>19</sub>NO<sub>2</sub>H<sup>+</sup> [M+H]<sup>+</sup>: 282.1489; found: 282.1491.



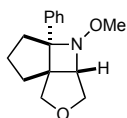
3.95

**(1*R*\*,5*S*\*,7*S*\*)-6-Methoxy-7-phenyl-5-(pyridin-2-yl)-3-tosyl-3,6-diazabicyclo[3.2.0]heptane (3.95):** Prepared according to GP-6a using **3.173** (109 mg, 0.25 mmol, 1.0 equiv.), **3.63** (1.4 mg, 0.5 mol%) and degassed THF (25 mL) with a reaction time of 17 h. The diastereomeric ratio was determined to be >20:1 by <sup>1</sup>H NMR analysis of the crude mixture. Purification by flash column chromatography (10-60% EtOAc/hexanes) afforded the pure title compound as clear oil (80 mg, 74%; combined yield). <sup>1</sup>H NMR (500 MHz, CDCl<sub>3</sub>): δ 8.39 (d, *J* = 4.7 Hz, 1H), 7.81 (d, *J* = 7.9 Hz, 3H), 7.70 (t, *J* = 7.7 Hz, 1H), 7.35 (dt, *J* = 15.5, 7.5 Hz, 6H), 7.31 – 7.23 (m, 1H), 7.17 – 7.10 (m, 1H), 4.61 (d, *J* = 10.8 Hz, 1H), 4.56 (d, *J* = 6.0 Hz, 1H), 3.73 (d, *J* = 10.0 Hz, 1H), 3.58 (d, *J* = 10.8 Hz, 1H), 3.54 (s, 3H), 3.20 (dd, *J* = 10.0, 4.5 Hz, 1H), 2.55 – 2.49 (m, 1H), 2.46 (s, 3H); <sup>13</sup>C NMR (176 MHz, CDCl<sub>3</sub>): δ 161.6, 149.2, 143.7, 141.5, 136.7, 133.4, 129.8, 128.6, 128.1, 127.8, 126.9, 122.2, 120.8, 79.3, 71.2, 61.8, 52.0, 50.9, 48.4, 21.7; IR (cm<sup>-1</sup>): 2934, 1590, 1465, 1161, 1091, 1027, 1012, 911, 815, 784, 749, 731, 698, 666; HRMS: *m/z* calculated for C<sub>24</sub>H<sub>25</sub>N<sub>3</sub>O<sub>3</sub>SN<sup>+</sup> [M+Na]<sup>+</sup>: 458.1509; found: 458.1507.



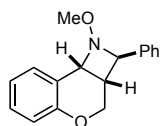
3.96

**(1*R*\*,5*S*\*,7*S*\*)-6-methoxy-7-phenyl-3-oxa-6-azabicyclo[3.2.0]heptan-4-one (3.96):** Prepared according to GP6-a, the reaction was conducted in a sealed 30-mL microwave vial using **3.192** (55 mg, 0.25 mmol, 1.0 equiv.), **3.63** (2.8 mg, 1 mol%) and degassed MeCN (25 mL) at 82 °C with a reaction time of 70 h. The diastereomeric ratio was determined to be 14:1 by <sup>1</sup>H NMR analysis of the crude mixture. Purification by flash column chromatography (5-40% EtOAc/hexanes) afforded the pure title compound as yellow oil (33 mg, 60%; combined yield; 75% brsm). <sup>1</sup>H NMR (500 MHz, CDCl<sub>3</sub>): δ 7.43 – 7.37 (m, 4H), 7.36 – 7.32 (m, 1H), 4.57 (ddd, *J* = 12.8, 6.1, 1.2 Hz, 2H), 4.40 (d, *J* = 9.7 Hz, 1H), 4.34 (dd, *J* = 9.8, 5.0 Hz, 1H), 3.54 (s, 3H), 2.87 (q, *J* = 5.7 Hz, 1H); <sup>13</sup>C NMR (126 MHz, CDCl<sub>3</sub>): δ 171.9, 139.3, 128.9, 128.6, 126.7, 75.6, 70.5, 63.2, 61.2, 37.1; IR (cm<sup>-1</sup>): 2934, 1774, 1456, 1371, 1266, 1160, 1046, 993, 974, 943, 731, 698; HRMS: *m/z* calculated for C<sub>12</sub>H<sub>13</sub>NO<sub>3</sub>Na<sup>+</sup> [M+Na]<sup>+</sup>: 242.0788; found: 242.0787.



3.97

**(3*aS*\*,4*aS*\*,7*aS*\*)-4-methoxy-4a-phenylhexahydro-1*H*,3*H*-cyclopenta[*b*]furo[3,4-*c*]azete (3.97):** Prepared according to GP-6a using **3.174** (61 mg, 0.25 mmol, 1.0 equiv.), **3.63** (2.8 mg, 1 mol%) and degassed THF (25 mL) with a reaction time of 15 h. The diastereomeric ratio was determined to be >20:1 by <sup>1</sup>H NMR analysis of the crude mixture. Purification by flash column chromatography (2-10% EtOAc/hexanes) afforded the pure title compound as white solid (60 mg, 98%; combined yield). <sup>1</sup>H NMR (700 MHz, CDCl<sub>3</sub>): δ 7.43 (dd, *J* = 8.2, 1.1 Hz, 2H), 7.35 (t, *J* = 7.8 Hz, 2H), 7.20 (tt, *J* = 7.2, 1.3 Hz, 1H), 4.02 (d, *J* = 10.0 Hz, 1H), 3.76 (d, *J* = 3.7 Hz, 1H), 3.61 (s, 3H), 3.48 (d, *J* = 10.0 Hz, 1H), 3.36 (dd, *J* = 10.0, 3.7 Hz, 1H), 3.18 (d, *J* = 10.0 Hz, 1H), 2.82 (dd, *J* = 14.8, 6.8 Hz, 1H), 2.11 – 2.02 (m, 2H), 1.94 – 1.87 (m, 1H), 1.87 – 1.81 (m, 2H); <sup>13</sup>C NMR (176 MHz, CDCl<sub>3</sub>): δ 144.2, 128.2, 126.3, 126.2, 80.9, 73.5, 72.8, 69.3, 61.4, 59.0, 35.6, 32.6, 25.7; IR (cm<sup>-1</sup>): 2959, 2941, 2841, 1492, 1461, 1446, 1061, 1043, 992, 902, 786, 757, 736, 717, 704, 653; HRMS: *m/z* calculated for C<sub>15</sub>H<sub>19</sub>NO<sub>2</sub>Na<sup>+</sup> [M+Na]<sup>+</sup>: 268.1308; found: 268.1314.

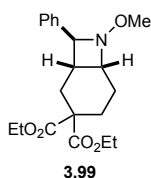


3.98



**(2*R*\*,2*aS*\*,8*bR*\*)-1-Methoxy-2-phenyl-1,2*a*,3,8*b*-tetrahydro-2*H*-chromeno[4,3-*b*]azete**

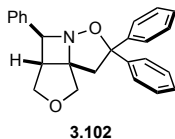
**(3.98):** Prepared according to GP-6a using **3.184** (67 mg, 0.25 mmol, 1.0 equiv.), **3.63** (2.8 mg, 1 mol%) and degassed THF (25 mL) with a reaction time of 72 h. The diastereomeric ratio was determined to be 7:1 by <sup>1</sup>H NMR analysis of the crude mixture. Purification by flash column chromatography (1-10% EtOAc/hexanes) afforded the pure title compound as clear oil (28 mg, 42%). <sup>1</sup>H NMR (700 MHz, CDCl<sub>3</sub>): δ 7.51 (d, *J* = 7.3 Hz, 2H), 7.39 (t, *J* = 7.6 Hz, 2H), 7.34 – 7.27 (m, 2H), 7.24 (dd, *J* = 7.8, 1.4 Hz, 1H), 7.06 – 7.02 (m, 2H), 4.97 (d, *J* = 7.6 Hz, 1H), 4.61 (d, *J* = 8.4 Hz, 1H), 4.17 (dd, *J* = 11.9, 1.5 Hz, 1H), 3.90 (dd, *J* = 11.9, 1.9 Hz, 1H), 3.48 (s, 3H), 2.68 – 2.63 (m, 1H); <sup>13</sup>C NMR (176 MHz, CDCl<sub>3</sub>): δ 155.4, 141.0, 133.4, 129.4, 128.6, 127.8, 126.9, 121.2, 118.9, 117.8, 70.5, 63.4, 61.2, 59.9, 36.8; IR (cm<sup>-1</sup>): 2823, 1581, 1486, 1447, 1220, 1209, 1079, 1051, 1030, 1001, 940, 929, 747, 699; HRMS: *m/z* calculated for C<sub>17</sub>H<sub>17</sub>NO<sub>2</sub>Na<sup>+</sup> [M+Na]<sup>+</sup>: 290.1151; found: 290.1150.



**Diethyl (1*S*\*,6*R*\*,8*S*\*)-7-Methoxy-8-phenyl-7-azabicyclo[4.2.0]octane-3,3-dicarboxylate**

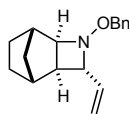
**(3.99):** Prepared according to GP-6a using **3.185** (90 mg, 0.25 mmol, 1.0 equiv.), **3.63** (2.8 mg, 1 mol%) and degassed THF (25 mL) with a reaction time of 72 h. The diastereomeric ratio was determined to be 3.5:1 by <sup>1</sup>H NMR analysis of the crude mixture. Purification by flash column chromatography (5-10% EtOAc/hexanes) afforded the pure title compound as clear oil (84 mg, 93%; combined yield). Characterization data was obtained for a 5:1 mixture of (1*S*\*,6*R*\*,8*S*\*) diastereomer (major) and (1*S*\*,6*R*\*,8*R*\*) diastereomer (minor). <sup>1</sup>H NMR (700 MHz, CDCl<sub>3</sub>): δ 7.48 (d, *J* = 6.1 Hz, 9H; major+minor), 7.39 – 7.31 (m, 15H; major+minor), 7.29 – 7.24 (m, 6H; major+minor), 4.47 (d, *J* = 8.0 Hz, 5H; major), 4.29 (q, *J* = 7.2 Hz, 10H; major), 4.21 – 4.11 (m, 15H; major), 4.04 (d, *J* = 9.4 Hz, 1H; minor), 3.98 (q, *J* = 7.6 Hz, 5H; minor), 3.49 (s, 3H; minor), 3.44 (s, 15H; major), 2.80 (td, *J* = 11.2, 3.2 Hz, 1H; minor), 2.64 (dd, *J* = 12.5, 3.1 Hz, 1H; minor), 2.59 – 2.54 (m, 1H; minor), 2.52 – 2.34 (m, 10H; major+minor), 2.21 – 2.01 (m, 13H; major+minor), 1.97 – 1.73 (m, 15H; major+minor), 1.44 – 1.36 (m, 1H; minor), 1.30 (t, *J* = 7.1 Hz, 16H; major+minor), 1.23 (td, *J* = 7.1, 1.6 Hz, 20H; major+minor); <sup>13</sup>C NMR (176 MHz, CDCl<sub>3</sub>): δ 172.5, 172.0, 171.7, 170.9, 141.6, 140.1, 128.5, 128.4, 127.7, 127.4, 126.9, 126.5, 78.8, 74.0,

72.8, 61.73, 61.66, 61.59, 61.56, 60.9, 60.8 (2C), 56.0, 53.4, 36.5, 34.9, 32.9, 30.7, 28.6, 27.6, 26.2, 17.8, 14.21, 14.15, 14.13, 14.11; **IR** (cm<sup>-1</sup>): 2938, 1726, 1449, 1367, 1228, 1175, 1111, 1024, 952, 860, 733, 699; **HRMS**: *m/z* calculated for C<sub>20</sub>H<sub>27</sub>NO<sub>5</sub>Na<sup>+</sup> [M+Na]<sup>+</sup>: 384.1781; found: 384.1784.



**(3aR\*,4S\*,8aS\*)-4,7,7-Triphenyltetrahydro-1H,3H-furo[3',4':2,3]azeto[1,2-b]isoxazole**

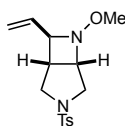
**(3.102)**: Prepared according to GP-6a using **3.101** (94 mg, 0.25 mmol, 1.0 equiv.), **3.63** (2.8 mg, 1 mol%) and degassed THF (25 mL) with a reaction time of 14.5 h. The diastereomeric ratio was determined to be 4:1 by <sup>1</sup>H NMR analysis of the crude mixture. Purification by flash column chromatography (10-60% EtOAc/hexanes) afforded the pure title compound as off-white solid (82 mg, 87%; combined yield). **<sup>1</sup>H NMR** (700 MHz, CDCl<sub>3</sub>): δ 7.45 – 7.42 (m, 4H), 7.39 – 7.33 (m, 3H), 7.30 (t, *J* = 7.8 Hz, 2H), 7.21 (t, *J* = 7.3 Hz, 1H), 7.14 – 7.10 (m, 3H), 7.02 – 6.99 (m, 2H), 4.84 (d, *J* = 6.4 Hz, 1H), 4.04 (d, *J* = 9.8 Hz, 1H), 3.71 (dd, *J* = 9.9, 5.1 Hz, 1H), 3.69 (d, *J* = 10.2 Hz, 1H), 3.54 (t, *J* = 5.6 Hz, 1H), 3.37 (d, *J* = 10.2 Hz, 1H), 3.18 (s, 2H); **<sup>13</sup>C NMR** (176 MHz, CDCl<sub>3</sub>): δ 144.3, 143.2, 135.7, 129.6, 128.5, 128.14, 128.10, 127.9, 127.3, 127.2, 126.06, 126.06, 89.4, 78.3, 74.7, 71.5, 68.2, 48.0, 47.8; **IR** (cm<sup>-1</sup>): 3058, 2968, 2850, 1598, 1492, 1448, 1265, 1189, 1125, 1043, 1032, 985, 912, 866, 731, 694; **HRMS**: *m/z* calculated for C<sub>25</sub>H<sub>23</sub>NO<sub>2</sub>H<sup>+</sup> [M+H]<sup>+</sup>: 370.1802; found: 370.1799.



**(1S\*,2R\*,4R\*,5R\*,6R\*)-3-(Benzyloxy)-4-vinyl-3-azatricyclo[4.2.1.0<sup>2,5</sup>]nonane** **(3.106)**:

Prepared according to GP-6a using **3.105** (64 mg, 0.25 mmol, 1.0 equiv.), **17•PF<sub>6</sub>** (2.8 mg, 1 mol%) and degassed THF (25 mL) with a reaction time of 24 h. The diastereomeric ratio was determined to be 4:1 (exo/endo >20:1) by <sup>1</sup>H NMR analysis of the crude mixture. Purification by flash column chromatography (0-10% EtOAc/hexanes) afforded the pure title compound as clear oil (25 mg, 39%; combined yield). Characterization data was obtained for the (1S\*,2R\*,4R\*,5R\*,6R\*) diastereomer (major). **<sup>1</sup>H NMR** (700 MHz, CDCl<sub>3</sub>): δ 7.34 – 7.30 (m, 4H), 7.28 – 7.24 (m, 1H), 5.96 (ddd, *J* = 17.1, 10.2, 6.8 Hz, 1H), 5.11 (d, *J* = 17.1 Hz, 1H), 5.01

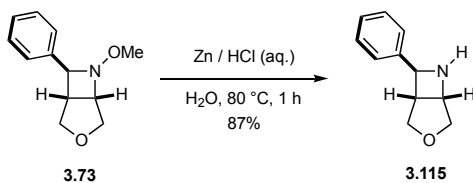
(d,  $J = 10.3$  Hz, 1H), 4.60 (d,  $J = 11.7$  Hz, 1H), 4.56 (d,  $J = 11.7$  Hz, 1H), 3.90 (t,  $J = 5.4$  Hz, 1H), 3.70 (d,  $J = 5.6$  Hz, 1H), 2.46 (s, 1H), 2.17 (d,  $J = 10.6$  Hz, 2H), 1.98 (t,  $J = 4.9$  Hz, 1H), 1.49 – 1.42 (m, 2H), 1.30 (d,  $J = 10.5$  Hz, 1H), 1.02 – 0.91 (m, 2H);  $^{13}\text{C}$  NMR (176 MHz,  $\text{CDCl}_3$ ):  $\delta$  139.1, 138.8, 128.4, 128.3, 127.6, 114.6, 75.8, 73.4, 71.5, 43.2, 37.9, 37.8, 34.1, 27.6, 25.2; IR ( $\text{cm}^{-1}$ ): 2952, 1871, 1453, 1364, 1023, 987, 916, 846, 733, 695; HRMS:  $m/z$  calculated for  $\text{C}_{17}\text{H}_{21}\text{NOH}^+ [\text{M}+\text{H}]^+$ : 256.1696; found: 256.1700.



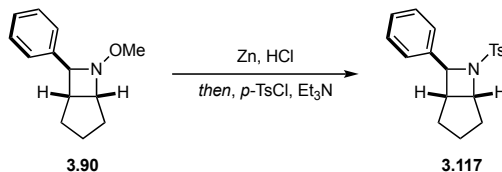
3.104

**(1R\*,5S\*,7R\*)-6-Methoxy-3-tosyl-7-vinyl-3,6-diazabicyclo[3.2.0]heptane (3.104):** Prepared according to GP-6a using **3.103** (77 mg, 0.25 mmol, 1.0 equiv.), **17**•PF<sub>6</sub> (1.4 mg, 0.5 mol%) and THF (25 mL) with a reaction time of 0.5 h. The diastereomeric ratio was determined to be 2:1 by  $^1\text{H}$  NMR analysis of the crude mixture. Purification by flash column chromatography (25% EtOAc/hexanes) afforded the pure title compound as pale-yellow solid (76 mg, 99%; combined yield). **(1R\*,5S\*,7R\*) Diastereomer (major):**  $^1\text{H}$  NMR (500 MHz,  $\text{CDCl}_3$ ):  $\delta$  7.73 (d,  $J = 8.2$  Hz, 2H), 7.34 (d,  $J = 8.0$  Hz, 2H), 5.94 (ddd,  $J = 17.3, 10.3, 7.0$  Hz, 1H), 5.23 (d,  $J = 17.2$  Hz, 1H), 5.12 (d,  $J = 10.3$  Hz, 1H), 4.29 – 4.21 (m, 2H), 3.97 (t,  $J = 6.4$  Hz, 1H), 3.49 (d,  $J = 10.0$  Hz, 1H), 3.42 (s, 3H), 2.72 (td,  $J = 11.6, 10.6, 5.8$  Hz, 2H), 2.48 (q,  $J = 5.7$  Hz, 1H), 2.44 (s, 3H);  $^{13}\text{C}$  NMR (126 MHz,  $\text{CDCl}_3$ ):  $\delta$  143.9, 137.8, 132.6, 129.8, 128.1, 116.8, 73.2, 66.7, 60.8, 51.2, 46.6, 38.2, 21.7; IR ( $\text{cm}^{-1}$ ): 2936, 2890, 1598, 1472, 1338, 1156, 1125, 1053, 1013, 928, 809, 708, 667; HRMS:  $m/z$  calculated for  $\text{C}_{15}\text{H}_{20}\text{N}_2\text{O}_3\text{SNa}^+ [\text{M}+\text{Na}]^+$ : 331.1087; found: 331.1089; **(1R\*,5S\*,7S\*) Diastereomer (minor):**  $^1\text{H}$  NMR (500 MHz,  $\text{CDCl}_3$ ):  $\delta$  7.73 (d,  $J = 8.2$  Hz, 2H), 7.32 (d,  $J = 8.0$  Hz, 2H), 5.76 (ddd,  $J = 16.9, 10.5, 6.1$  Hz, 1H), 5.31 (d,  $J = 17.2$  Hz, 1H), 5.23 (d,  $J = 10.5$  Hz, 1H), 4.02 – 3.93 (m, 2H), 3.66 (d,  $J = 10.6$  Hz, 1H), 3.51 (dd,  $J = 10.6, 2.5$  Hz, 1H), 3.43 (s, 3H), 2.99 (qd,  $J = 8.7, 2.3$  Hz, 1H), 2.89 – 2.82 (m, 2H), 2.43 (s, 3H);  $^{13}\text{C}$  NMR (126 MHz,  $\text{CDCl}_3$ ):  $\delta$  143.6, 133.9, 133.6, 129.6, 128.0, 118.8, 70.1, 69.0, 61.9, 53.8, 46.9, 35.6, 21.8; IR ( $\text{cm}^{-1}$ ): 2939, 2889, 1464, 1334, 1176, 1155, 1093, 1045, 1030, 988, 923, 812, 737, 665; HRMS:  $m/z$  calculated for  $\text{C}_{15}\text{H}_{20}\text{N}_2\text{O}_3\text{SNa}^+ [\text{M}+\text{Na}]^+$ : 331.1087; found: 331.1090.

### Synthetic Modifications of Azetidine Products

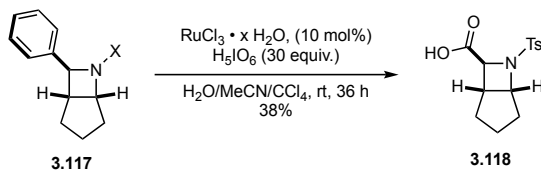


**(1R\*,5S\*,7S\*)-7-Phenyl-3-oxa-6-azabicyclo[3.2.0]heptane (3.115):** A 25-mL round-bottom flask equipped with a magnetic stir bar was charged with azetidine **3.73** (51 mg, 0.25 mmol, 1.0 equiv.). Then, 2 M aqueous HCl (5 mL) and zinc powder (82 mg, 1.25 mmol, 5 equiv.) were added sequentially and the resulting mixture stirred at 80 °C for 1 h. The reaction was cooled to 0 °C and 2 M aqueous NaOH was added dropwise until pH 10-12 was reached. The mixture was subsequently extracted with CH<sub>2</sub>Cl<sub>2</sub> (3x) and the combined organic layers dried over Na<sub>2</sub>SO<sub>4</sub>, filtered and concentrated *in vacuo*. Purification by flash column chromatography (1-10% MeOH/CH<sub>2</sub>Cl<sub>2</sub>) afforded the pure title compound as yellow oil (38 mg, 87%). <sup>1</sup>H NMR (500 MHz, CDCl<sub>3</sub>): δ 7.43 (d, *J* = 7.3 Hz, 2H), 7.37 (t, *J* = 7.6 Hz, 2H), 7.28 – 7.24 (m, 1H), 4.60 (d, *J* = 4.5 Hz, 1H), 4.38 (dd, *J* = 6.3, 3.6 Hz, 1H), 4.16 (d, *J* = 9.7 Hz, 1H), 4.08 (d, *J* = 10.4 Hz, 1H), 3.57 (dd, *J* = 10.4, 3.6 Hz, 1H), 3.54 (dd, *J* = 9.7, 4.6 Hz, 1H), 3.07 (dt, *J* = 6.3, 4.6 Hz, 1H); <sup>13</sup>C NMR (126 MHz, CDCl<sub>3</sub>): δ 145.1, 128.7, 127.2, 125.9, 76.0, 72.9, 64.0, 60.4, 48.1; IR (cm<sup>-1</sup>): 3314, 3025, 2929, 2844, 1603, 1491, 1452, 1338, 1165, 1094, 1070, 977, 909, 881, 735, 697; HRMS: *m/z* calculated for C<sub>11</sub>H<sub>13</sub>NOH<sup>+</sup> [M+H]<sup>+</sup>: 176.1070; found: 176.1067.



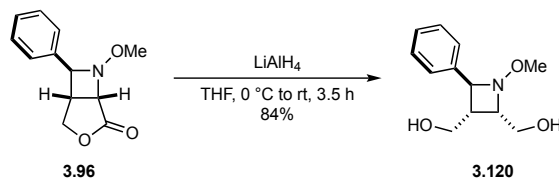
**(1S\*,5R\*,7S\*)-7-Phenyl-6-tosyl-6-azabicyclo[3.2.0]heptane (3.117):** A 100-mL round-bottom flask equipped with a magnetic stir bar was charged with **3.90** (178 mg, 0.88 mmol, 1.0 equiv.) and a 9:1 mixture (*v/v*) of 2 M HCl (aq.) and THF (20 mL). The mixture was heated to reflux until the substrate completely dissolved, then, Zn (286 mg, 4.38 mmol, 5.0 equiv.) was added and the mixture continued to reflux for 1.5 h. After cooling to 0 °C, 2 M NaOH (aq.) was added until pH 12 and the mixture subsequently extracted with CH<sub>2</sub>Cl<sub>2</sub> (3x) and EtOAc (3x). The combined organic layers were dried over Na<sub>2</sub>SO<sub>4</sub>, filtered and concentrated *in vacuo*, then dried using high-vac to afford the crude azetidine (quant. yield), which was used in the next step without further purification. The crude azetidine was dissolved in CH<sub>2</sub>Cl<sub>2</sub> (10 mL) and the solution cooled to 0 °C. Et<sub>3</sub>N (0.13 mL, 0.96 mmol, 1.1 equiv.) and *p*-TsCl (184 mg, 0.96 mmol, 1.1 equiv.) were added

sequentially and the solution allowed to warm up to rt and stirred for 1.5 h. Then, water was added, the organic layer separated and the aqueous layer extracted with CH<sub>2</sub>Cl<sub>2</sub> (3x). The combined organic layers were dried over Na<sub>2</sub>SO<sub>4</sub>, filtered and concentrated *in vacuo*. Purification by flash column chromatography (5-15% EtOAc/hexanes) afforded the pure title compound as white solid (200 mg, 70%). **<sup>1</sup>H NMR** (700 MHz, CDCl<sub>3</sub>): δ 7.43 (d, *J* = 8.2 Hz, 2H), 7.22 (s, 5H), 7.10 (d, *J* = 8.0 Hz, 2H), 4.85 (t, *J* = 5.5 Hz, 1H), 4.65 (d, *J* = 4.1 Hz, 1H), 2.76 (q, *J* = 6.3 Hz, 1H), 2.57 (dd, *J* = 14.1, 5.6 Hz, 1H), 2.36 (s, 3H), 1.89 – 1.79 (m, 2H), 1.80 – 1.71 (m, 1H), 1.52 – 1.39 (m, 2H); **<sup>13</sup>C NMR** (176 MHz, CDCl<sub>3</sub>): δ 142.8, 140.2, 137.9, 129.3, 128.5, 127.9, 127.2, 126.9, 70.9, 68.9, 44.6, 32.2, 30.7, 24.1, 21.6; **IR** (cm<sup>-1</sup>): 3030, 2952, 1598, 1495, 1455, 1338, 1186, 1152, 1121, 1090, 1059, 1028, 997, 951, 815, 754, 698, 665; **HRMS**: *m/z* calculated for C<sub>19</sub>H<sub>21</sub>NO<sub>2</sub>SNa<sup>+</sup> [M+Na]<sup>+</sup>: 350.1185; found: 350.1185.



**(1*S*\*,5*R*\*,7*S*\*)-6-Tosyl-6-azabicyclo[3.2.0]heptane-7-carboxylic acid (3.117)**: According to a procedure by Enders with minor modifications.<sup>84</sup> A 10-mL microwave vial equipped with a magnetic stir bar was charged with **3.118** (100 mg, 0.31 mmol, 1.0 equiv.). CCl<sub>4</sub> (0.7 mL), MeCN (0.7 mL) and water (1.0 mL) were added and the mixture stirred until all solids were dissolved. Next, periodic acid (879 mg, 4.6 mmol, 15.0 equiv.) and RuCl<sub>3</sub> hydrate (3.4 mg, 0.015 mmol, 0.05 equiv.) were added sequentially and the vial sealed with a rubber septa pierced with a needle to maintain an open atmosphere. The biphasic mixture was vigorously stirred for 24 h, before adding additional periodic acid (879 mg, 4.6 mmol, 15.0 equiv.) and RuCl<sub>3</sub> hydrate (3.4 mg, 0.015 mmol, 0.05 equiv.), and the reaction was continued to stir for 12 h. Et<sub>2</sub>O was added and the mixture stirred for 0.5 h, before the addition of water. The organic layer was separated and the aqueous layer extracted with Et<sub>2</sub>O (3x) and EtOAc (3x). The combined organic layers were dried over MgSO<sub>4</sub>, filtered and concentrated *in vacuo*. Purification by flash column chromatography (94:5:1 CH<sub>2</sub>Cl<sub>2</sub>/MeOH/AcOH) afforded the pure title compound as pale-yellow oil (34 mg, 38%). **<sup>1</sup>H NMR** (700 MHz, CDCl<sub>3</sub>): δ 7.75 (d, *J* = 8.0 Hz, 2H), 7.35 (d, *J* = 7.9 Hz, 2H), 4.74 (t, *J* = 5.4 Hz, 1H), 4.19 (d, *J* = 4.1 Hz, 1H), 3.06 (q, *J* = 5.6 Hz, 1H), 2.46 (s, 3H), 2.31 (dd, *J* = 14.7, 5.9 Hz, 1H), 1.81 (dd, *J* = 13.7, 6.3 Hz, 1H), 1.71 (dt, *J* = 13.1, 6.6 Hz, 1H), 1.50 (h, *J* = 13.5, 6.8 Hz, 1H), 1.33 (h, *J* = 19.6, 12.5, 5.7 Hz, 1H), 1.20 – 1.11 (m, 1H); **<sup>13</sup>C NMR** (176 MHz,

CDCl<sub>3</sub>):  $\delta$  174.2, 144.2, 136.5, 129.9, 127.5, 69.5, 65.7, 39.9, 31.2, 30.6, 23.6, 21.8; **IR** (cm<sup>-1</sup>): 2960, 1716, 1598, 1434, 1335, 1289, 1241, 1150, 1090, 1060, 1001, 907, 815, 727, 708, 674, 648; **HRMS**:  $m/z$  calculated for C<sub>14</sub>H<sub>17</sub>NO<sub>4</sub>SNa<sup>+</sup> [M+Na]<sup>+</sup>: 318.0770; found: 318.0769.



**((2*S*\*,3*R*\*,4*S*\*)-1-Methoxy-4-phenylazetidine-2,3-diyl)dimethanol (3.120)**: A 10-mL round-bottom flask equipped with a magnetic stir bar was charged with LiAlH<sub>4</sub> (12 mg, 0.32 mmol, 2.6 equiv.) and THF (1.5 mL). After cooling to 0 °C, a solution of **3.96** (27 mg, 0.12 mmol, 1.0 equiv.) in THF (0.5 mL) was added dropwise. Then, the reaction mixture was allowed to warm up to rt and stirred for 3.5 h. Water was carefully added at 0 °C, followed by Rochelle salt solution (aq., sat.) and the resulting mixture allowed to gradually warm up to rt and stirred for 3 h. The resulting biphasic mixture was extracted with Et<sub>2</sub>O (3x) and the combined organic layers dried over MgSO<sub>4</sub>, filtered and concentrated *in vacuo*. Purification by flash column chromatography (30-95% EtOAc/hexanes) afforded the pure title compound as white solid (23 mg, 84%). **<sup>1</sup>H NMR** (700 MHz, CDCl<sub>3</sub>):  $\delta$  7.43 (d,  $J$  = 7.3 Hz, 2H), 7.36 (t,  $J$  = 7.6 Hz, 2H), 7.28 (t,  $J$  = 7.3 Hz, 1H), 4.76 (d,  $J$  = 9.0 Hz, 1H), 4.31 – 4.24 (m, 1H), 4.17 – 4.10 (m, 2H), 3.91 – 3.83 (m, 2H), 3.52 (s, 3H), 3.03 (t,  $J$  = 5.2 Hz, 1H), 2.90 (dd,  $J$  = 7.6, 4.4 Hz, 1H), 2.50 (bs, 1H); **<sup>13</sup>C NMR** (176 MHz, CDCl<sub>3</sub>):  $\delta$  141.2, 128.6, 127.7, 126.6, 73.4, 66.6, 62.1, 59.8, 59.6, 40.7; **IR** (cm<sup>-1</sup>): 3319, 2935, 1596, 1495, 1453, 1370, 1266, 1155, 1091, 1020, 736, 698; **HRMS**:  $m/z$  calculated for C<sub>12</sub>H<sub>17</sub>NO<sub>3</sub>Na<sup>+</sup> [M+Na]<sup>+</sup>: 246.1101; found: 246.1105.

### Rationale for Observed Diastereoselectivity

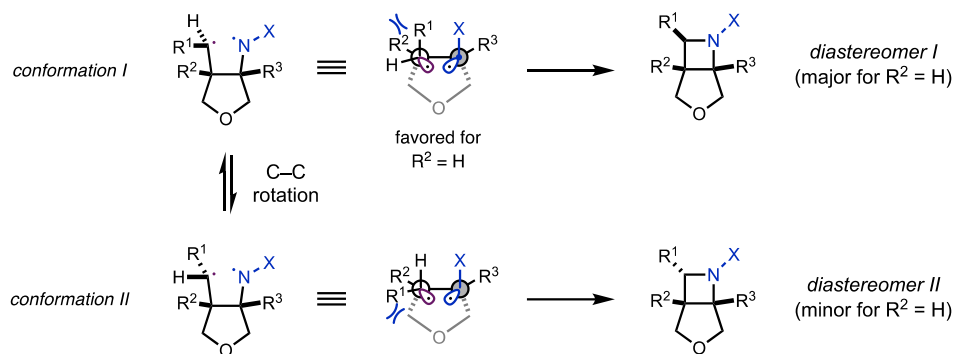


Figure 3.23 Rationale for the observed diastereoselectivity.

The observed relative stereoselectivity in the developed aza Paternò-Büchi reaction can be rationalized through analysis of the conformation of the biradical intermediate prior final C–C bond formation. Generally, the conformation leading to the major diastereomer (conformation I) avoids steric interactions between the alkene residue ( $R^1$ ) and cyclic backbone of the substrate. In particular, small substituents on the alkene moiety ( $R^2 = H$ ) achieve excellent diastereoselectivity, while larger substituents ( $R^2 = Me$ ) lead to an erosion of selectivity due to additional steric interactions between  $R^1$  and  $R^2$ . This effect is smaller for remote substituents ( $R^3$ ), for which we observed a correlation between the selectivity and size of the substituent ( $R^3 = H > Me > Ph$ ). Finally, larger alkene residues ( $R^1 = Ph$ ) provide greater levels of stereoselectivity, which can be rationalized through increased steric interactions between  $R^1$  and the backbone of the substrate, further disfavoring conformation II. In contrast, substrates bearing a diene ( $R^2 = vinyl$ ) proceed with lower diastereoselectivity as a result of the smaller size of the vinyl group.

## Representative NOE Data

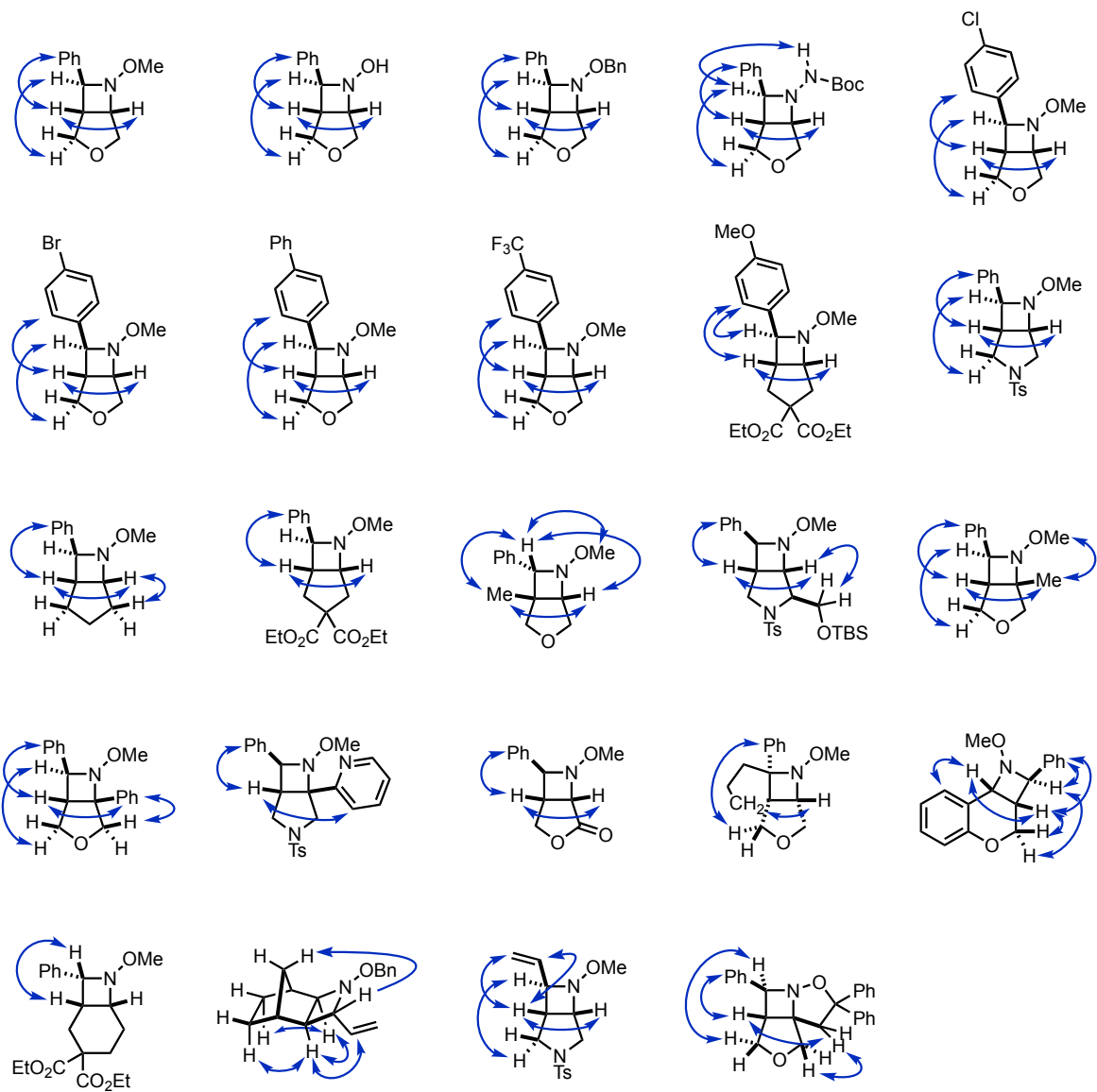


Figure 3.24 Selected NOE data for the azetidines synthesized herein



### 3.4.4 X-Ray Crystallographic Data

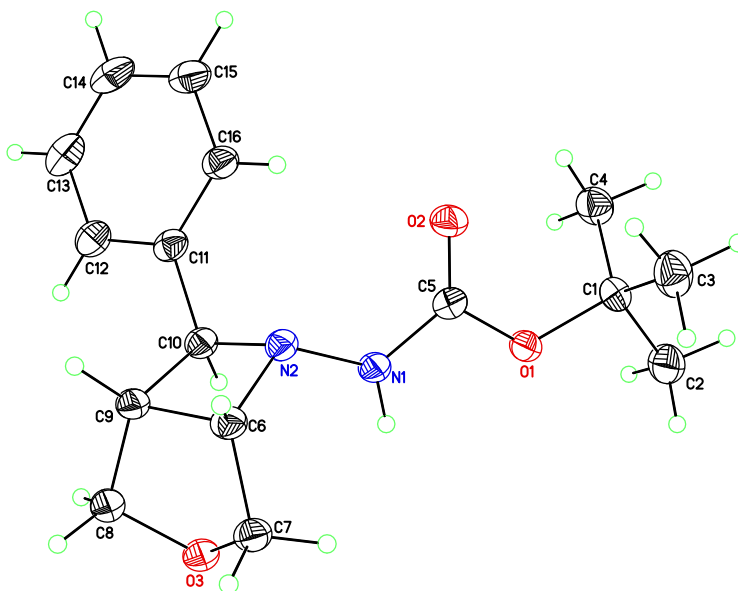


Figure 3.25 ORTEP diagram of **3.80**.

Colorless blocks of *tert*-butyl ((1*R*\*,5*S*\*,7*S*\*)-7-phenyl-3-oxa-6-azabicyclo[3.2.0]heptan-6-yl)carbamate (**3.80**) were grown via vapor diffusion (pentane/ethyl acetate) of the compound at ambient temperature. A crystal of dimensions 0.18 x 0.14 x 0.10 mm was mounted on a Rigaku AFC10K Saturn 944+ CCD-based X-ray diffractometer equipped with a low temperature device and Micromax-007HF Cu-target micro-focus rotating anode ( $\lambda = 1.54187 \text{ \AA}$ ) operated at 1.2 kW power (40 kV, 30 mA). The X-ray intensities were measured at 85(1) K with the detector placed at a distance 42.00 mm from the crystal. A total of 2028 images were collected with an oscillation width of  $1.0^\circ$  in  $\omega$ . The exposure times were 1 sec. for the low angle images, 2 sec. for high angle. Rigaku d\*trek images were exported to CrysAlisPro for processing and corrected for absorption. The integration of the data yielded a total of 23789 reflections to a maximum  $2\theta$  value of  $138.67^\circ$  of which 2901 were independent and 2802 were greater than  $2\sigma(I)$ . The final cell constants (Table 3.5) were based on the xyz centroids of 17770 reflections above  $10\sigma(I)$ . Analysis of the data showed negligible decay during data collection. The structure was solved and refined with the Bruker SHELXTL (version 2016/6) software package, using the space group P2(1)/c with  $Z = 4$  for the formula  $C_{16}H_{22}N_2O_3$ . All non-hydrogen atoms were refined anisotropically with the hydrogen atoms placed in a combination of idealized and refined positions. Full matrix least-

squares refinement based on  $F^2$  converged at  $R1 = 0.0505$  and  $wR2 = 0.1183$  [based on  $I > 2\sigma(I)$ ],  $R1 = 0.0512$  and  $wR2 = 0.1191$  for all data. Additional details are presented in Table 3.5 and are given as Supporting Information in a CIF file. Acknowledgement is made for funding from NSF grant CHE-0840456 for X-ray instrumentation.

G.M. Sheldrick (2015) "Crystal structure refinement with SHELXL", *Acta Cryst.*, C71, 3-8 (Open Access).

CrystalClear Expert 2.0 r16, Rigaku Americas and Rigaku Corporation (2014), Rigaku Americas, 9009, TX, USA 77381-5209, Rigaku Tokyo, 196-8666, Japan.

CrysAlisPro 1.171.38.41 (Rigaku Oxford Diffraction, 2015).

Table 3.5 Crystallographic parameters and structure refinement for compound **3.80**.

Identification code	<i>tert</i> -butyl ((1 <i>R</i> *,5 <i>S</i> *,7 <i>S</i> *)-7-phenyl-3-oxa-6-azabicyclo[3.2.0]heptan-6-yl)carbamate
Empirical formula	C <sub>16</sub> H <sub>22</sub> N <sub>2</sub> O <sub>3</sub>
Formula weight	290.35
Temperature	85(2) K
Wavelength	1.54184 Å
Crystal system, space group	Monoclinic, P2(1)/c
Unit cell dimensions	a = 9.81308(10) Å    alpha = 90 deg.
	b = 16.02162(18) Å    beta = 96.5969(9) deg.
	c = 10.02249(9) Å    gamma = 90 deg.
Volume	1565.32(3) Å <sup>3</sup>
Z, Calculated density	4, 1.232 Mg/m <sup>3</sup>
Absorption coefficient	0.693 mm <sup>-1</sup>
F(000)	624

Crystal size	0.180 x 0.140 x 0.100 mm
Theta range for data collection	4.536 to 69.335 deg.
Limiting indices	-11<=h<=11, -19<=k<=18, -11<=l<=12
Reflections collected / unique	23789 / 2901 [R(int) = 0.0747]
Completeness to theta = 67.684	99.70%
Absorption correction	Semi-empirical from equivalents
Max. and min. transmission	1.00000 and 0.76509
Refinement method	Full-matrix least-squares on F <sup>2</sup>
Data / restraints / parameters	2901 / 0 / 198
Goodness-of-fit on F <sup>2</sup>	1.105
Final R indices [I>2sigma(I)]	R1 = 0.0505, wR2 = 0.1183
R indices (all data)	R1 = 0.0512, wR2 = 0.1191
Extinction coefficient	0.041(2)
Largest diff. peak and hole	0.283 and -0.352 e.A <sup>-3</sup>

### 3.5 References

- (1) Becker, M. R.; Richardson, A. D.; Schindler, C. S. Functionalized Azetidines via Visible Light-Enabled Aza Paternò-Büchi Reactions. *Nat. Commun.* **2019**, *10*, 5095. <https://doi.org/10.1038/s41467-019-13072-x>.
- (2) Richardson, A. D.; Becker, M. R.; Schindler, C. S. Synthesis of Azetidines by Aza Paternò-Büchi Reactions. *Chem. Sci.* **2020**, *11*, 7553–7561.
- (3) Vitaku, E.; Smith, D. T.; Njardarson, J. T. Analysis of the Structural Diversity, Substitution Patterns, and Frequency of Nitrogen Heterocycles among U.S. FDA Approved Pharmaceuticals: Miniperspective. *J. Med. Chem.* **2014**, *57*, 10257–10274.
- (4) Cotellic (cobimetinib) [https://www.accessdata.fda.gov/drugsatfda\\_docs/nda/2015/206192Orig1s000TOC.cfm](https://www.accessdata.fda.gov/drugsatfda_docs/nda/2015/206192Orig1s000TOC.cfm).
- (5) Baxdela (delafloxacin) <https://www.accessdata.fda.gov/scripts/cder/daf/index.cfm?event=overview.process&varApplNo=208610>.
- (6) Olumiant (baricitinib) [https://www.accessdata.fda.gov/drugsatfda\\_docs/nda/2018/207924Orig1s000TOC.cfm](https://www.accessdata.fda.gov/drugsatfda_docs/nda/2018/207924Orig1s000TOC.cfm).
- (7) St. Jean, D. J.; Fotsch, C. Mitigating Heterocycle Metabolism in Drug Discovery. *J. Med. Chem.* **2012**, *55*, 6002–6020.
- (8) Lovering, F.; Bikker, J.; Humblet, C. Escape from Flatland: Increasing Saturation as an Approach to Improving Clinical Success. *J. Med. Chem.* **2009**, *52*, 6752–6756.
- (9) Brown, A.; Brown, T. B.; Calabrese, A.; Ellis, D.; Puhalo, N.; Ralph, M.; Watson, L. Triazole Oxytocin Antagonists: Identification of an Aryloxyazetidone Replacement for a Biaryl Substituent. *Bioorg. Med. Chem. Lett.* **2010**, *20*, 516–520.
- (10) Fish, P. V.; Brown, A. D.; Evrard, E.; Roberts, L. R. 7-Sulfonamido-3-Benzazepines as Potent and Selective 5-HT<sub>2C</sub> Receptor Agonists: Hit-to-Lead Optimization. *Bioorg. Med. Chem. Lett.* **2009**, *19*, 1871–1875.
- (11) Brandi, A.; Cicchi, S.; Cordero, F. M. Novel Syntheses of Azetidines and Azetidinones. *Chem. Rev.* **2008**, *108*, 3988–4035.
- (12) Antermite, D.; Degennaro, L.; Luisi, R. Recent Advances in the Chemistry of Metallated Azetidines. *Org. Biomol. Chem.* **2017**, *15* (1), 34–50.
- (13) Yoda, H.; Takahashi, M.; Sengoku, T. Azetidine and Its Derivatives. In *Heterocycles in Natural Product Synthesis*; Wiley-VCH, 2011.
- (14) Clayden, J.; Greeves, N.; Warren, S. *Organic Chemistry*, 2nd ed.; Oxford Univ. Press, 2012.
- (15) Warren, S.; Wyatt, P. *Organic Synthesis: The Disconnection Approach*, 2nd ed.; Wiley, 2008.
- (16) Alcaide, B.; Almendros, P.; Aragoncillo, C.  $\beta$ -Lactams: Versatile Building Blocks for the Stereoselective Synthesis of Non- $\beta$ -Lactam Products. *Chem. Rev.* **2007**, *107*, 4437–4492.
- (17) Pitts, C. R.; Lectka, T. Chemical Synthesis of  $\beta$ -Lactams: Asymmetric Catalysis and Other Recent Advances. *Chem. Rev.* **2014**, *114*, 7930–7953.
- (18) Hosseyni, S.; Jarrahpour, A. Recent Advances in  $\beta$ -Lactam Synthesis. *Org. Biomol. Chem.* **2018**, *16*, 6840–6852.
- (19) Gianatassio, R.; Lopchuk, J. M.; Wang, J.; Pan, C.-M.; Malins, L. R.; Prieto, L.; Brandt, T. A.; Collins, M. R.; Gallego, G. M.; Sach, N. W.; Spangler, J. E.; Zhu, H.; Zhu, J.; Baran, P. S. Strain-Release Amination. *Science* **2016**, *351*, 241–246.
- (20) Lopchuk, J. M.; Fjelbye, K.; Kawamata, Y.; Malins, L. R.; Pan, C.-M.; Gianatassio, R.; Wang, J.; Prieto, L.; Bradow, J.; Brandt, T. A.; Collins, M. R.; Elleraas, J.; Ewanicki, J.;

- Farrell, W.; Fadeyi, O. O.; Gallego, G. M.; Mousseau, J. J.; Oliver, R.; Sach, N. W.; Smith, J. K.; Spangler, J. E.; Zhu, H.; Zhu, J.; Baran, P. S. Strain-Release Heteroatom Functionalization: Development, Scope, and Stereospecificity. *J. Am. Chem. Soc.* **2017**, *139*, 3209–3226.
- (21) Gianatassio, R.; Kadish, D. Direct Alkylation of 1-Azabicyclo[1.1.0]Butanes. *Org. Lett.* **2019**, *21*, 2060–2063.
- (22) Fawcett, A.; Murtaza, A.; Gregson, C. H. U.; Aggarwal, V. K. Strain-Release-Driven Homologation of Boronic Esters: Application to the Modular Synthesis of Azetidines. *J. Am. Chem. Soc.* **2019**, *141*, 4573–4578.
- (23) Poplata, S.; Tröster, A.; Zou, Y.-Q.; Bach, T. Recent Advances in the Synthesis of Cyclobutanes by Olefin [2 + 2] Photocycloaddition Reactions. *Chem. Rev.* **2016**, *116*, 9748–9815.
- (24) D'Auria, M. The Paternò–Büchi Reaction – A Comprehensive Review. *Photochem. Photobiol. Sci.* **2019**, *18*, 2297–2362.
- (25) Padwa, A. Photochemistry of the Carbon-Nitrogen Double Bond. *Chem. Rev.* **1977**, *77*, 37–68.
- (26) Pratt, A. C. The Photochemistry of Imines. *Chem. Soc. Rev.* **1977**, *6*, 63–81.
- (27) Padwa, A.; Albrecht, F. Photoisomerization About the Carbon-Nitrogen Double Bond of an Oxime Ether. *J. Am. Chem. Soc.* **1972**, *94*, 1000–1002.
- (28) Anderson, D. R.; Keute, J. S.; Koch, T. H.; Moseley, R. H. Di-Tert-Butyl Nitroxide Quenching of the Photoaddition of Olefins to the Carbon-Nitrogen Double Bond of 3-Ethoxyisoindolenone. *J. Am. Chem. Soc.* **1977**, *99*, 6332–6340.
- (29) Tsuge, O.; Tashiro, M.; Oe, K. Photochemical Reaction of 2,5-Diphenyl-1,3,4-Oxadiazole with Indene. *Tetrahedron Lett.* **1968**, *9*, 3971–3974.
- (30) Rodehorst, R. M.; Koch, T. H. Photochemical Reactivity of Keto Imino Ethers. VI. Type I Rearrangement and (2 + 2) Photocycloaddition to the Carbon-Nitrogen Double Bond of 2-Oxazolin-4-Ones. *J. Am. Chem. Soc.* **1975**, *97*, 7298–7304.
- (31) Koch, T. H.; Rodehorst, R. M. 2+2 Photocycloaddition to a Carbon Nitrogen Double Bond II. 2-Phenyl-2-Oxazolin-4-One. *Tetrahedron Lett.* **1972**, *13*, 4039–4042.
- (32) Howard, K. A.; Koch, T. H. Photochemical Reactivity of Keto Imino Ethers. V. (2 + 2) Photocycloaddition to the Carbon-Nitrogen Double Bond of 3-Ethoxyisoindolone. *J. Am. Chem. Soc.* **1975**, *97*, 7288–7298.
- (33) Koch, T. H.; Howard, K. A. 2+2 Photocycloaddition to a Carbon Nitrogen Double Bond I. 3-Ethoxyisoindolone. *Tetrahedron Lett.* **1972**, *13*, 4035–4038.
- (34) Swenton, J. S.; Balchunis, R. J. Photochemical Functionalization of 6-Azaauracils to 5-Substituted-6-Azaauracils. *J. Heterocycl. Chem.* **1974**, *11*, 917–920.
- (35) Swenton, J. S.; Hyatt, J. A. Photosensitized Cycloadditions to 1,3-Dimethyl-6-Azaauracil and 1,3-Dimethyl-6-Azathymine. Imine Linkage Unusually Reactive Toward Photocycloaddition. *J. Am. Chem. Soc.* **1974**, *96*, 4879–4885.
- (36) Hyatt, J. A.; Swenton, J. S. Photochemical Reactivity of 2,4-Dimethyl-1,2,4-Triazine-3,5(2H)-Dione (1,3-Dimethyl-6-Azaauracil). *J. Chem. Soc., Chem. Commun.* **1972**, *20*, 1144–1145.
- (37) Futamura, S.; Ohta, H.; Kamiya, Y. Photocycloaddition of 6-Cyanophenanthridine to Electron-Rich Olefins. *Chem. Lett.* **1980**, *9*, 655–658.
- (38) Futamura, S.; Ohta, H.; Kamiya, Y. The Photocycloaddition of 6-Substituted Phenanthridines to Electron-Rich Olefins. *Bull. Chem. Soc. Jpn.* **1982**, *55*, 2190–2194.

- (39) Nishio, T.; Kondo, M.; Omote, Y. Photochemical Reaction of Tetrahydroquinoxalin-2(1H)-Ones and Related Compounds. *Helv. Chim. Acta.* **1991**, *74*, 225–231.
- (40) Nishio, T.; Nishiyama, T.; Omote, Y. Photochemical [2+2] Cycloaddition of the C-N Bond of Pteridine-2,4,7-Triones to Alkenes. *Liebigs Ann. Chem.* **1988**, *1988*, 441–443.
- (41) Nishio, T.; Omote, Y. Photocycloaddition Reactions of 1,4-Benzoxazin-2-Ones and Electron-Poor Olefins. *J. Org. Chem.* **1985**, *50*, 1370–1373.
- (42) Kawamura, Y.; Kumagai, T.; Mukai, T. Photocycloaddition Reaction of 3-Aryl-2-Isoxazolines with Indene. Generation of [2+2] Cycloadduct Stereoisomers. *Chem. Lett.* **1985**, *14*, 1937–1940.
- (43) Kumagai, T.; Kawamura, Y.; Mukai, T. Photocycloaddition of 3-Aryl-2-Isoxazolines with Five-Membered Heterocycles. *Chem. Lett.* **1983**, *12*, 1357–1360.
- (44) Kumagai, T.; Shimizu, K.; Kawamura, Y.; Mukai, T. Photochemistry of 3-Aryl-2-Isoxazoline. *Tetrahedron* **1981**, *37*, 3365–3376.
- (45) Sampedro, D.; Soldevilla, A.; Campos, P. J.; Ruiz, R.; Rodríguez, M. Regio- and Stereochemistry of [2+2] Photocycloadditions of Imines to Alkenes: A Computational and Experimental Study. *J. Org. Chem.* **2008**, *73*, 8331–8336.
- (46) Sampedro, D. Computational Exploration of the Photocycloaddition of Imines to Alkenes. *ChemPhysChem* **2006**, *7*, 2456–2459.
- (47) Fischer, G.; Fritz, H.; Prinzbach, H. An Intramolecular Imine/Ene - Photo-[2+2]-Cycloaddition Reaction. *Tetrahedron Lett.* **1986**, *27*, 1269–1272.
- (48) Sakamoto, R.; Inada, T.; Sakurai, S.; Maruoka, K. [2 + 2] Photocycloadditions between the Carbon–Nitrogen Double Bonds of Imines and Carbon–Carbon Double Bonds. *Organic Letters* **2016**, *18*, 6252–6255.
- (49) Becker, M. R.; Wearing, E. R.; Schindler, C. S. Synthesis of Azetidines via Visible-Light-Mediated Intermolecular [2+2] Photocycloadditions. *Nat. Chem.* **2020**, *12*, 898–905.
- (50) Wearing, E. R.; Blackmun, D. E.; Becker, M. R.; Schindler, C. S. 1- and 2-Azetines via Visible Light-Mediated [2 + 2]-Cycloadditions of Alkynes and Oximes. *J. Am. Chem. Soc.* **2021**, *143*, 16235–16242.
- (51) Rykaczewski, K. A.; Schindler, C. S. Visible-Light-Enabled Paternò–Büchi Reaction via Triplet Energy Transfer for the Synthesis of Oxetanes. *Org. Lett.* **2020**, *22*, 6516–6519.
- (52) Li, X.; Großkopf, J.; Jandl, C.; Bach, T. Enantioselective, Visible Light Mediated Aza Paternò–Büchi Reactions of Quinoxalinones. *Angew. Chem. Int. Ed.* **2021**, *60*, 2684–2688.
- (53) Kumarasamy, E.; Kandappa, S. K.; Raghunathan, R.; Jockusch, S.; Sivaguru, J. Realizing an Aza Paternò–Büchi Reaction. *Angew. Chem. Int. Ed.* **2017**, *56*, 7056–7061.
- (54) Zhu, M.; Zhang, X.; Zheng, C.; You, S.-L. Visible-Light-Induced Dearomatization via [2+2] Cycloaddition or 1,5-Hydrogen Atom Transfer: Divergent Reaction Pathways of Transient Diradicals. *ACS Catal.* **2020**, *10*, 12618–12626.
- (55) Strieth-Kalthoff, F.; James, M. J.; Teders, M.; Pitzer, L.; Glorius, F. Energy Transfer Catalysis Mediated by Visible Light: Principles, Applications, Directions. *Chem. Soc. Rev.* **2018**, *47*, 7190–7202.
- (56) Zhou, Q.-Q.; Zou, Y.-Q.; Lu, L.-Q.; Xiao, W.-J. Visible-Light-Induced Organic Photochemical Reactions through Energy-Transfer Pathways. *Angew. Chem. Int. Ed.* **2019**, *58*, 1586–1604.
- (57) Lu, Z.; Yoon, T. P. Visible Light Photocatalysis of [2+2] Styrene Cycloadditions by Energy Transfer. *Angew. Chem. Int. Ed.* **2012**, *51*, 10329–10332.

- (58) Hurlley, A. E.; Lu, Z.; Yoon, T. P. [2+2] Cycloaddition of 1,3-Dienes by Visible Light Photocatalysis. *Angew. Chem. Int. Ed.* **2014**, *53*, 8991–8994.
- (59) Teegardin, K.; Day, J. I.; Chan, J.; Weaver, J. Advances in Photocatalysis: A Microreview of Visible Light Mediated Ruthenium and Iridium Catalyzed Organic Transformations. *Org. Process Res. Dev.* **2016**, *20*, 1156–1163.
- (60) Ni, T.; Caldwell, R. A.; Melton, L. A. The Relaxed and Spectroscopic Energies of Olefin Triplets. *J. Am. Chem. Soc.* **1989**, *111*, 457–464.
- (61) Enders, Ad.; Gries, J. Asymmetric Synthesis of Substituted Azetidine Type A- and b-Amino Acids. *New York* **2005**, No. 20, 9.
- (62) Monos, T. M.; Sun, A. C.; McAtee, R. C.; Devery, J. J.; Stephenson, C. R. J. Microwave-Assisted Synthesis of Heteroleptic Ir(III) <sup>+</sup> Polypyridyl Complexes. *J. Org. Chem.* **2016**, *81*, 6988–6994.
- (63) Frigerio, M.; Santagostino, M.; Sputore, S. A User-Friendly Entry to 2-Iodoxybenzoic Acid (IBX). *J. Org. Chem.* **1999**, *64*, 4537–4538.
- (64) Roth, H.; Romero, N.; Nicewicz, D. Experimental and Calculated Electrochemical Potentials of Common Organic Molecules for Applications to Single-Electron Redox Chemistry. *Synlett.* **2015**, *27*, 714–723.
- (65) Prier, C. K.; Rankic, D. A.; MacMillan, D. W. C. Visible Light Photoredox Catalysis with Transition Metal Complexes: Applications in Organic Synthesis. *Chem. Rev.* **2013**, *113*, 5322–5363.
- (66) Huo, X.; He, R.; Fu, J.; Zhang, J.; Yang, G.; Zhang, W. Stereoselective and Site-Specific Allylic Alkylation of Amino Acids and Small Peptides via a Pd/Cu Dual Catalysis. *J. Am. Chem. Soc.* **2017**, *139*, 9819–9822.
- (67) Guo, R.; Yang, H.; Tang, P. Silver-Catalyzed Meerwein Arylation: Intermolecular and Intramolecular Fluoroarylation of Styrenes. *Chem. Commun.* **2015**, *51*, 8829–8832.
- (68) Yu, Z.; Liu, L.; Zhang, J. Triflic Acid-Catalyzed Enynes Cyclization: A New Strategy beyond Electrophilic  $\pi$ -Activation. *Chem. Eur. J.* **2016**, *22*, 8488–8492.
- (69) Tamura, O.; Mitsuya, T.; Huang, X.; Tsutsumi, Y.; Hattori, S.; Ishibashi, H. Intramolecular Cycloaddition of *O* - *Tert* -Butyldimethylsilyloximes in the Presence of  $\text{BF}_3 \cdot \text{OEt}_2$ . *J. Org. Chem.* **2005**, *70*, 10720–10725.
- (70) West, T. H.; Daniels, D. S. B.; Slawin, A. M. Z.; Smith, A. D. An Isothiourea-Catalyzed Asymmetric [2,3]-Rearrangement of Allylic Ammonium Ylides. *J. Am. Chem. Soc.* **2014**, *136*, 4476–4479.
- (71) Kablaoui, N. M.; Buchwald, S. L. Development of a Method for the Reductive Cyclization of Enones by a Titanium Catalyst. *J. Am. Chem. Soc.* **1996**, *118*, 3182–3191.
- (72) Chen, Z.; Sun, J. Enantio- and Diastereoselective Assembly of Tetrahydrofuran and Tetrahydropyran Skeletons with All-Carbon-Substituted Quaternary Stereocenters. *Angewandte Chemie* **2013**, *125*, 13838–13841.
- (73) Venning, A. R. O.; Kwiatkowski, M. R.; Roque Peña, J. E.; Lainhart, B. C.; Guruparan, A. A.; Alexanian, E. J. Palladium-Catalyzed Carbocyclizations of Unactivated Alkyl Bromides with Alkenes Involving Auto-Tandem Catalysis. *J. Am. Chem. Soc.* **2017**, *139*, 11595–11600.
- (74) Logan, A. W. J.; Parker, J. S.; Hallside, M. S.; Burton, J. W. Manganese(III) Acetate Mediated Oxidative Radical Cyclizations. Toward Vicinal All-Carbon Quaternary Stereocenters. *Org. Lett.* **2012**, *14*, 2940–2943.
- (75) Bosque, I.; Bagdatli, E.; Foubelo, F.; Gonzalez-Gomez, J. C. Regio- and Stereoselective Aminopentadienylation of Carbonyl Compounds. *J. Org. Chem.* **2014**, *79*, 1796–1804.

- (76) Li, G.-Y.; Che, C.-M. Highly Selective Intra- and Intermolecular Coupling Reactions of Diazo Compounds to Form *Cis* -Alkenes Using a Ruthenium Porphyrin Catalyst. *Org. Lett.* **2004**, *6*, 1621–1623.
- (77) Mahesh, M.; Murphy, J. A.; Wessel, H. P. Novel Deoxygenation Reaction of Epoxides by Indium. *J. Org. Chem.* **2005**, *70*, 4118–4123.
- (78) Musacchio, A. J.; Nguyen, L. Q.; Beard, G. H.; Knowles, R. R. Catalytic Olefin Hydroamination with Aminium Radical Cations: A Photoredox Method for Direct C–N Bond Formation. *J. Am. Chem. Soc.* **2014**, *136*, 12217–12220.
- (79) Miege, F.; Meyer, C.; Cossy, J. Rhodium-Catalyzed Cycloisomerization Involving Cyclopropenes: Efficient Stereoselective Synthesis of Medium-Sized Heterocyclic Scaffolds. *Angew. Chem. Int. Ed.* **2011**, *50*, 5932–5937.
- (80) Kimura, M.; Mori, M.; Tamaru, Y. Palladium-Catalyzed 1,3-Diol Fragmentation: Synthesis of  $\omega$ -Dienyl Aldehydes. *Chem. Commun.* **2007**, *2007*, 4504–4506.
- (81) Miyata, O.; Muroya, K.; Kobayashi, T.; Yamanaka, R.; Kajisa, S.; Koide, J.; Naito, T. Sulfanyl Radical Addition-Cyclization of Oxime Ethers and Hydrazones Connected with Alkenes for Synthesis of Cyclic  $\beta$ -Amino Acids. *Tetrahedron* **2002**, *58*, 4459–4479.
- (82) Desrat, S.; van de Weghe, P. Intramolecular Imino Diels–Alder Reaction: Progress toward the Synthesis of Uncialamycin. *J. Org. Chem.* **2009**, *74*, 6728–6734.
- (83) Cremonesi, G.; Croce, P. D.; Fontana, F.; Fiorelli, C.; La Rosa, C. Stereoselective Synthesis of  $\beta,\epsilon$ -Dihydroxy- $\alpha$ -Amino Acids by Ring Opening of 4,5-Dihydroisoxazolyl Derivatives. *Tetrahedron Asymmetry* **2008**, *19*, 2850–2855.
- (84) Enders, D.; Gries, J. Asymmetric Synthesis of Substituted Azetidine Type  $\alpha$ - and  $\beta$ -Amino Acids. *Synthesis* **2005**, *2005*, 3508–3516.



## Chapter 4 Total Synthesis of Cochlearol B

Portions of this chapter have been published in: Richardson, A. D.; Vogel, T. R.; Trafficante, E. F.; Glover, K. J.; Schindler, C. S. Total Synthesis of (+)-Cochlearol B by an Approach Based on a Catellani Reaction and Visible-Light-Enabled [2+2] Cycloaddition. *Angew. Chem. Int. Ed.* **2022**, *Accepted*, DOI: 10.1002/anie.202201213.

### 4.1 Introduction

Fungi within the *Ganoderma* genus have been used in traditional Asian medicines for the prevention and treatment of many diseases for over 2,000 years.<sup>1</sup> Chapter 1 provided an in-depth discussion of the *Ganoderma* genus, as well as the species *Ganoderma lucidum*, the origin of the meroterpenoid natural product lingzhiol. Including *Ganoderma lucidum*, there are 219 different species of fungi within the *Ganoderma* genus with each species being a rich source of structurally diverse meroterpenoid natural products.<sup>1</sup> Interestingly, several simple meroterpenoids, such as fornicin A (**4.5**), can be found in many species of *Ganoderma*, whereas individual species seem to produce unique, structurally complex meroterpenoids.<sup>2</sup> The extracts from *Ganoderma cochlear* have been studied for the pharmacological effects as well as their chemical composition. Numerous meroterpenoid natural products with various biological activities have been isolated. Although the less complex, more ubiquitous compounds do possess interesting biological activity (fornicin A, antioxidant), this discussion will focus on meroterpenoids exclusive to *Ganoderma cochlear* (Figure 4.1A). In 2014, ganocins A-D were isolated as pairs of enantiomers and tested as inhibitors of acetylcholinesterase (AChE),<sup>3</sup> an enzyme responsible for the hydrolysis of acetyl choline to choline.<sup>4</sup> AChE has been linked with chronic diseases such as Alzheimer's and epilepsy,<sup>4,5</sup> and was chosen as a target it has been shown that *Ganoderma* extracts can inhibit this enzyme.<sup>6</sup> Of these compounds ganocin D (**4.3**) was the only one with some anti-AChE activity, demonstrating an inhibition of 32% at 50  $\mu$ M.

(+)- and (-)- Cochlearol A (**4.2**) were isolated together with (+)- and (-)-cochlearol B (**4.1**) from the fruiting bodies of *Ganoderma cochlear* in 2014.<sup>7</sup> All four compounds were tested for antifibrotic effects in the treatment of renal fibrosis.<sup>8</sup> Both enantiomers of cochlearol A (**4.2**)

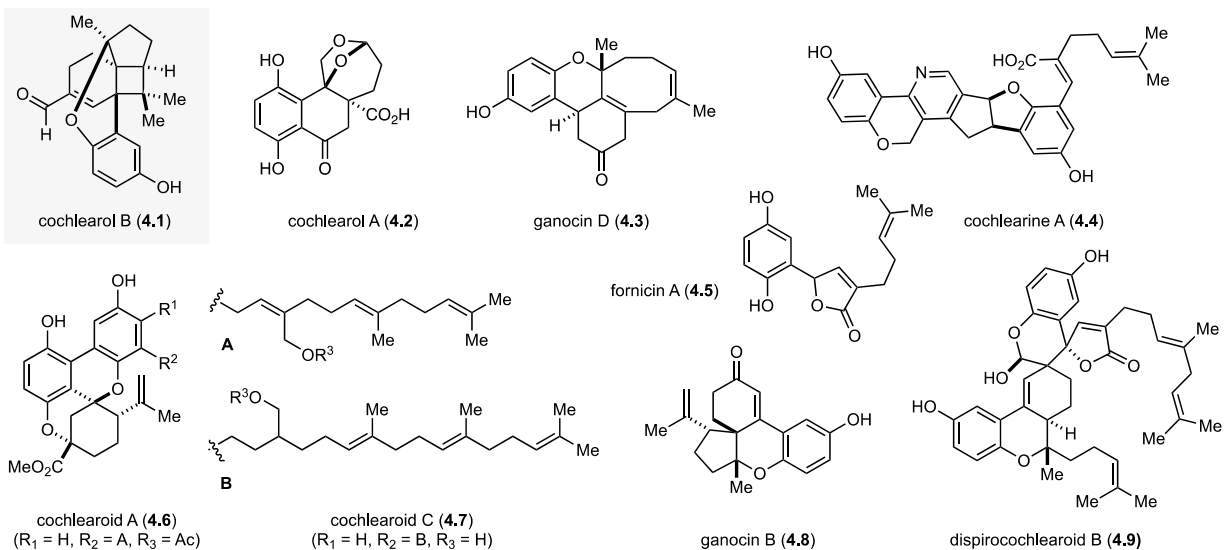
showed no apparent inhibition, and also damaged cell viability. However, (–)-cochlearol B (**4.1**) showed potent, dose dependent antifibrotic efficacy, whereas (+)-**4.1** was inactive. A more in-depth analysis revealed that (–)-cochlearol B disrupts activation of Smad2 and Smad3, signal transducing proteins that have been implicated in renal fibrosis.<sup>8 9 10 11</sup> The role of Smad proteins in renal fibrosis was discussed at length in Chapter 1. In 2015, five pairs of dimeric enantiomers (cochlearoids A-E) as well as two additional meroterpenoids (cochlearines A and B) were reported.<sup>12</sup> All compounds were tested as inhibitors of T-type calcium channels (TTCCs), neural regulatory channels that are implicated in central nervous system (CNS) diseases such as epilepsy, insomnia, neuropathic pain, and Parkinson’s disease.<sup>13</sup> In this capacity, (+)-cochlearoid A (**4.6**), (–)-cochlearoid C (**4.7**) and (±)-cochlearine A (**4.4**) proved the most effective. This study provides support that these natural products, as well as *Ganoderma cochlear* as a whole, can be used for the treatment of neurological disorders. Recently, dispirocochlearoids A-C were reported and tested as cyclooxygenase (COX) pathway inhibitors.<sup>14</sup> COX has become a popular target for the development of nonsteroidal anti-inflammatory drugs (NSAIDs) because of its role in modulating inflammation.<sup>15</sup> This study demonstrated that (–)-dispirocochlearoids B (**4.9**) is a selective COX2 inhibitor with an IC<sub>50</sub> value of 386 nm. In addition, (–)-**4.9** inhibited COX2 expression in lung tissue and reduced lung injury in ALI (acute lung injury) mice.

In summary, meroterpenoids natural products isolated from the extracts of *Ganoderma cochlear* exhibit a wide range of biological activity and show strong efficacy in these areas. Moreover, the structures of these compounds are quite diverse supporting the notion that these individual compounds may possess different biological activities and the history of *Ganoderma cochlear* being used to treat many diseases.

Cochlearol B (**4.1**) is unique among all these compounds because contains a cyclobutane ring in its 4/5/6/6/6 core structure.<sup>7</sup> Although the biosynthesis is not known some inferences can be made from related studies. All *Ganoderma* meroterpenoids consist of substitution 1,2,4-triubstitued phenyl groups, with additional substitution in some cases, a common scaffold found in lignin.<sup>2</sup> The hypothesis that the phenolic component comes from lignin is supported by the fact that the genome sequence of *Ganoderma lucidum* contains coding for ligninolytic enzymes.<sup>16</sup> The terpene fragment of these meroterpenoids is likely incorporated via a prenyltransferase enzyme, an enzyme involved in the biosynthesis of other meroterpenoids.<sup>17</sup> It’s probable that one of the less complex meroterpenoids acts as an intermediate in the biosynthesis of cochlearol B, although the

exact route is not known. Interestingly, the structure of the terpene fragment of cochlearol B can also be found in the natural product italicene (**4.10**) which comes from *Lantana* and *Helichrysum* oil.<sup>18</sup> Unfortunately, the biosynthesis of this compound is also not known. The most structurally intriguing part of cochlearol B is the hepta-substituted cyclobutane ring containing three stereocenters. Despite their high ring strain and inherent instability, cyclobutanes are featured in many biological active natural products (Figure 4.1B).<sup>19</sup> Examples include cannabiorecycloic acid (**4.11**), paesslerin A (**4.12**), astellatene (**4.13**), and nigramide R (**4.14**) among many others. The proposed biosynthetic origin of these fragments typically involves an intramolecular polar, or single electron, cyclization to close the four membered ring.<sup>20</sup> A directed [2+2] cycloaddition is rarely implicated.

A. Biologically active meroterpenoids isolated from *Ganoderma cochlear*.



B. Biologically active cyclobutane containing natural products.

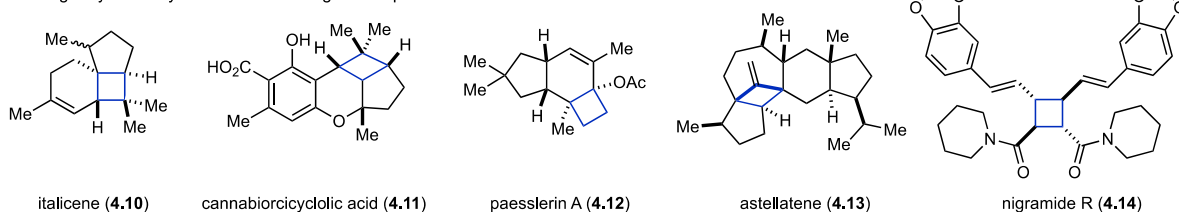


Figure 4.1 (A) Biologically active meroterpenoids isolated from *Ganoderma cochlear*. (B) Biologically active cyclobutane containing natural products.

Cochlearol B (**4.1**) stands out with a more highly substituted cyclobutane than most other natural products. Although increasing substitution does not always correlate with higher ring strain,<sup>19</sup> cochlearol B is a formidable target in large part due to the unique cyclobutane ring. Cochlearol B also has low natural abundance as 100 kg of *Ganoderma cochlear* was needed to isolate

1.8 mg of racemic material.<sup>7</sup> The combination of promising biological activity, complex structure, and low natural abundance makes cochlearol B a perfect target for total synthesis.

That being said, because of the challenges presented by this molecule, the first total synthesis of cochlearol B (**4.1**) was not reported until 2021. The Sugita group reported a 16-step synthesis of (±)-cochlearol B in 9% overall yield (Figure 4.2).<sup>21</sup> In their synthesis, starting materials **4.15**, **4.16**, and **4.17** were taken through an 8 step sequence to arrive at intermediate **4.18**. A subsequent dearomative oxidative cyclization formed intermediate **4.19** and closed the third 6 membered ring of cochlearol B. The next step was a UV light mediated [2+2] cycloaddition between the enone and trisubstituted olefin. This cyclization closed the remaining 4 and 5 membered rings and formed the core structure of cochlearol B (**4.20**) in 10 total steps. The remaining six steps were dedicated to restoring the aromatic ring and converting the ketone to the α,β-unsaturated aldehyde completing the first total synthesis of cochlearol B (**4.1**).

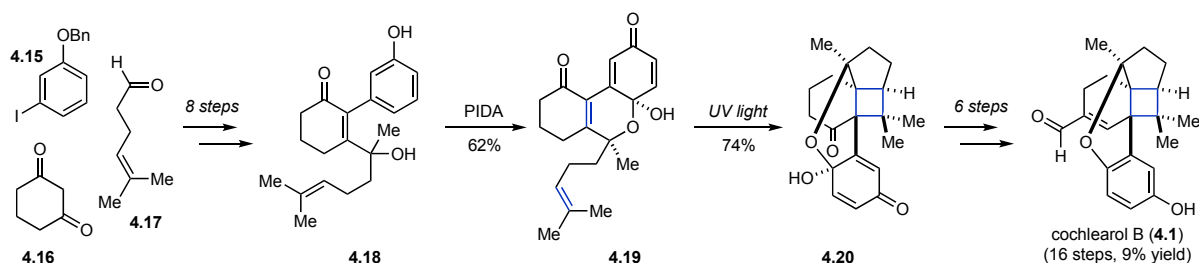


Figure 4.2 Sugita's synthesis of cochlearol B.

Simultaneous efforts in our lab were focused on a markedly different approach to cochlearol B. Herein we report a 12-step synthesis of cochlearol B. Our strategy employs three key carbon-carbon bond forming reactions to rapidly assemble to core structure of cochlearol B in just 4 steps. These key steps are an organocatalytic Kabbe condensation, a palladium catalyzed Catellani reaction, and a visible light mediated [2+2] cycloaddition. A thorough understanding of each transformation proved crucial in overcoming the early challenges in this project. Later, a 14-step synthesis of (+)-cochlearol B was developed using a chiral resolution. This is the first synthesis of (+)-cochlearol B.

## 4.2 Retrosynthesis

Our retrosynthetic analysis commenced with late-stage oxidation state manipulations to arrive at the α,β-unsaturated aldehyde and protecting group manipulations to reveal the phenol (Figure 4.3). We proposed that an Aldol condensation could be used to form the final six membered ring and the enone (**4.21**). The corresponding aldehyde could arise from an ozonolysis reaction

(4.22). Then, we envisioned constructing the 4 and 5 membered rings (4.23) simultaneously through an intramolecular, visible light mediated [2+2]-cycloaddition from 4.24.<sup>22 23</sup> Introduction of the two methyl ester fragments could occur concomitantly using a Catellani reaction from the corresponding vinyl triflate 4.25.<sup>24</sup> In turn, triflate 4.25 could come from triflation of chromanone 4.26. We concluded that there were several routes to chromanone 4.26, and we intended to thoroughly study those options.

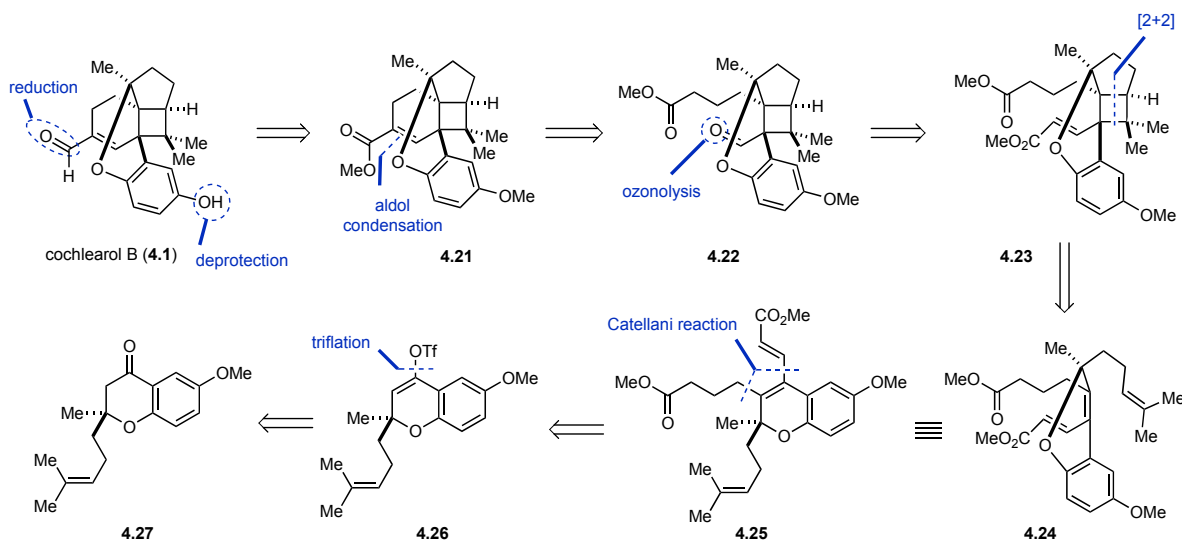


Figure 4.3 Retrosynthetic analysis of cochlearol B.

The key steps of this proposed synthesis were a visible light mediated [2+2]-cycloaddition and a Catellani reactions. The [2+2]-cycloaddition has been well established in the total synthesis of biologically active cyclobutane containing molecules,<sup>19</sup> however, our proposed [2+2]-cycloaddition would be between a tri-substituted olefin and a tetra-substituted olefin adding additional steric challenges that are not always present. Since a thermal [2+2] reaction is ‘forbidden’ photochemical methods are typically used. Traditionally, high energy UV light is required to excite the olefins and accomplish this transformation, but, the tools of modern visible light photocatalysis have greatly enhanced the scope of transformations accessible using visible light.<sup>25</sup> In 2012, the Yoon group developed an intramolecular visible light mediated [2+2]-cycloaddition between styrenes and alkenes through a process called triplet energy transfer,<sup>22</sup> which is discussed in detail in Chapter 3. Conjugated alkenes, like styrenes, possess low lying triplet energies ( $\sim 60 \text{ kcal mol}^{-1}$ ) that are accessible using visible light absorbing photosensitizers. Triplet energy transfer is discussed in detail in Chapter 3.<sup>26</sup> As a demonstration of the power of this method, they completed a 3-step synthesis of ( $\pm$ )-cannabiorcicyclic acid (**4.11**) (Figure

4.4).<sup>22</sup> In 2014, Yoon and coworkers extended the scope of this transformation from to dienes.<sup>23</sup> Dienes have comparable triplet energies to styrenes and thus could be sensitized using the same photocatalysts. Based on our proposed retrosynthesis, we designed our visible light mediated [2+2]-cycloaddition around this report from the Yoon group.

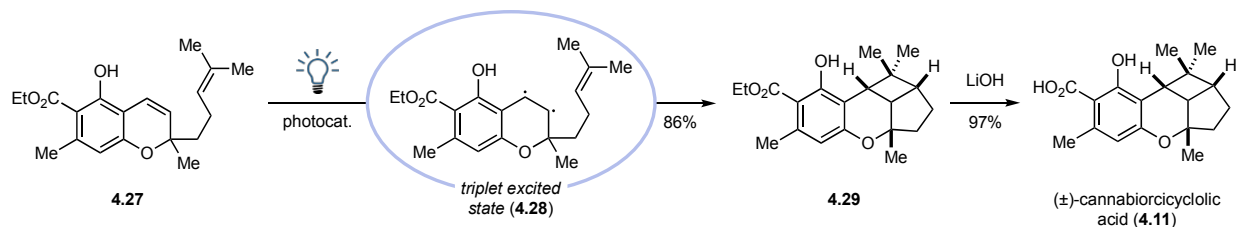


Figure 4.4 Yoon's synthesis of (±)-cannabiorcycloic acid enabled by a visible light mediated [2+2]-cycloaddition.

Arriving at the substrate **4.24** for the [2+2]-cycloaddition presented its own set of challenges. Particularly the formation of an appropriately functionalized tetrasubstituted olefin. To address this challenge, we drew inspiration from the Dong groups work on the Catellani reaction.<sup>24</sup> Discovered by Marta Catellani in 1997,<sup>27</sup> the Catellani reaction is defined as the palladium/norbornene catalyzed ortho-ipso-difunctionalization of aryl iodides (Figure 4.5A).<sup>28</sup> Under this reaction paradigm, the ortho and ipso positions have different reactivity allowing for differential selective functionalization. Specifically, the “electrophilic” coupling partner ends up on the ortho position and the “nucleophilic” coupling partner ends up on the ipso position. Since its discovery, this method has been greatly expanded by Catellani,<sup>29</sup> Lautens,<sup>30</sup> Dong<sup>28</sup> and others. Currently, protocols have allowed for ortho alkylation, arylation, amination, acylation and more. Additionally, the ipso position can be functionalized through Heck, Suzuki, and Sonogashira reactions as well as through borylation, hydrogenation, thiolation, cyanation and others. In 2019, Dong and coworkers reported an alkenyl Catellani reaction for the synthesis of tetrasubstituted olefins using vinyl triflates (Figure 4.5B).<sup>24</sup> This protocol could accomplish ortho alkylation and arylation, as well as ipso Heck, Suzuki, and hydrogenation reactions. The choice of norbornene cocatalyst proved crucial to this reaction. Since this report, the Dong group has continued to develop innovative modifications to the traditional Catellani reaction.<sup>31 32</sup>

Despite being a powerful method for forming carbon-carbon bonds, the Catellani reaction is not broadly utilized in total synthesis.<sup>28</sup> For our purposes, the alkenyl Catellani reaction represented an ideal strategy for the synthesis of **4.24**. For this synthesis, vinyl triflate **4.26** would be used in combination with coupling partners methyl acrylate (**4.36**) and methyl 4-iodobutyrate

(4.37) (Figure 4.5C). After conducting a thorough retrosynthetic analysis, focus shifted towards the total synthesis of cochlearol B.

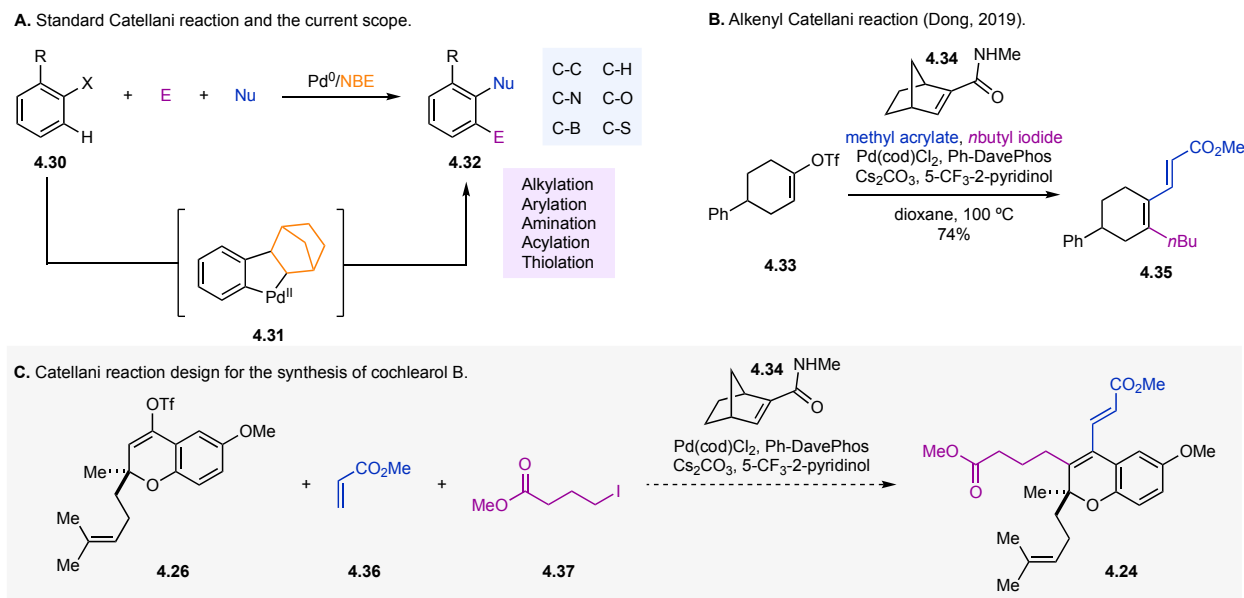


Figure 4.5 (A) Overview of the Catellani reaction. (B) Alkenyl Catellani reaction for the synthesis of all-carbon tetrasubstituted olefins. (C) Catellani reaction design for the synthesis of cochlearol B.

## 4.3 Results and Discussion

### 4.3.1 Chromanone Synthesis

In initial studies towards cochlearol B, chromanone **4.26** was prepared through a two-step process from **4.38** (Figure 4.6A). The first step was a one pot acylation, Baker-Venkataraman rearrangement<sup>33 34 35</sup> and condensation following a protocol developed by Brown and coworkers.<sup>36</sup> With **4.39** in hand, the homoprenyl chain was introduced via a copper catalyzed conjugate addition reaction using homoprenyl magnesium bromide (**4.40**).<sup>37</sup> A number of copper(I) sources were evaluated, and CuBr•(SMe<sub>2</sub>) proved to be the best catalyst for this transformation. However, this reaction was inconsistent and low yielding, providing chromanone **4.26** only in up to 34% yield. A dramatic improvement in yield and reliability was realized by adding stoichiometric amounts of TMSCl to this reaction. This dramatic improvement can be explained by the formation of pyrylium chloride ion **4.41**, which likely forms *in situ* in the presence of TMSCl.<sup>38</sup> This renders the 4 position of the enone even more electrophilic, which promotes addition of the organocuprate. This protocol could be performed on >10g and easily provided the material necessary for preliminary studies. Alternatively, a Kabbe condensation<sup>39</sup> between **4.38** and **4.42** was employed to access chromanone

**4.26** in one less step (Figure 4.6B). This reaction utilized pyrrolidine as an organocatalyst and butyric acid as an additive. Low conversion was observed with 50 mol% of both pyrrolidine and butyric acid. Maintaining a 1:1 ratio but increasing the equivalents to super stoichiometric quantities did not result in complete conversion. Ultimately, a 3 eq.:1 eq. ratio of pyrrolidine:butyric acid proved to be the ideal conditions, providing **4.26** in 76% yield.

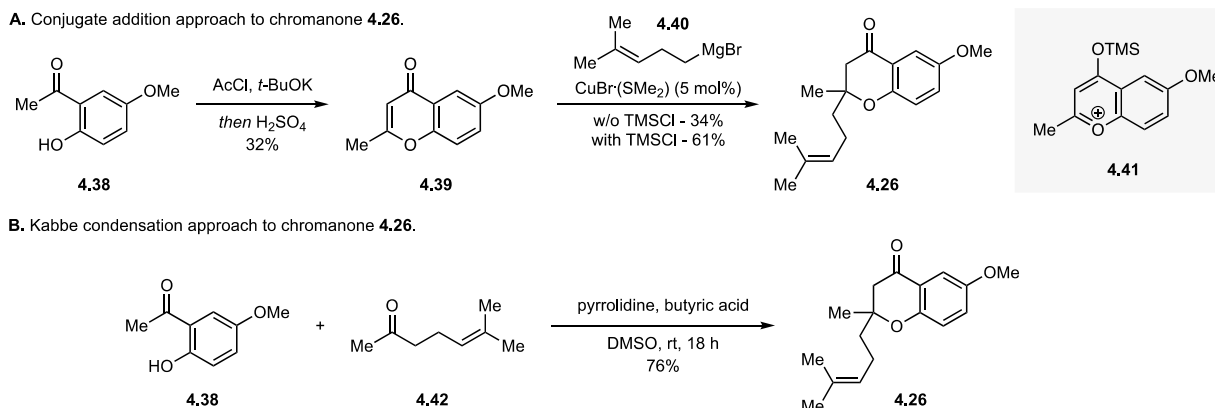


Figure 4.6 (A) Conjugate addition approach to chromanone **4.26**. (B) Kabbe condensation approach to chromanone **4.26**.

### 4.3.2 Investigations towards enantioenriched chromanone

With multiple strategies to access racemic chromanone **4.26** in hand, we investigated enantioselective approaches to enable an asymmetric synthesis of either (+) or (–)-cochlearol B. The stereocenter in chromanone **4.26** is the only stereocenter in the molecule that isn't a part of the cyclobutane ring. Since we proposed forming the cyclobutane via a [2+2] cycloaddition, the cyclobutane stereocenters will be set according to the enantiomer of **4.26** that we start with. As such, the stereoselectivity of any asymmetric reaction that forms **4.26** will determine what enantiomer of cochlearol B we make and in what level of enantiopurity.

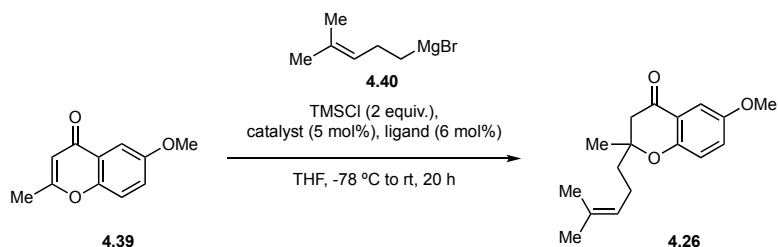
Our initial efforts towards enantioenriched **4.26** were focused on developing an asymmetric version of the methods we already established for the synthesis of racemic **4.26**. Enantioselective conjugate addition of alkyl cuprates is a well-established transformation<sup>40</sup> with many applications in natural product synthesis,<sup>41</sup> and as such we sought to apply it to our system. Specifically, we envisioned using Grignard **4.40** in combination with a copper catalyst and chiral ligand. An asymmetric copper catalyzed conjugate addition using Grignard **4.40** has been reported lending credibility to this proposal.<sup>42</sup> Drawing inspiration from the literature, we evaluated a number of chiral ligands including phosphine ligands,<sup>41</sup> an amine ligand,<sup>43</sup> and a thiourea<sup>44</sup> (Table 4.1A).



However, treating **4.39** with TMSCl and homoprenylmagnesium bromide in the presence of Cu(I) and a chiral ligand (**4.43-4.47**) only provided racemic **4.26** (Table 4.1A, entries 1-6).

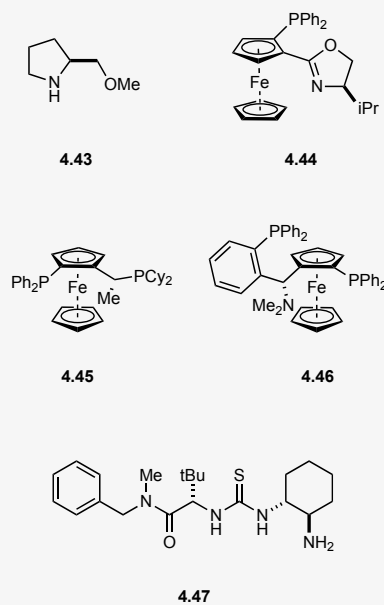
Table 4.1 (A) Conditions evaluated for an asymmetric copper-catalyzed conjugate addition. (B) Background reactivity responsible for racemic product observation.

A. Conditions evaluated for an asymmetric copper-catalyzed conjugate addition



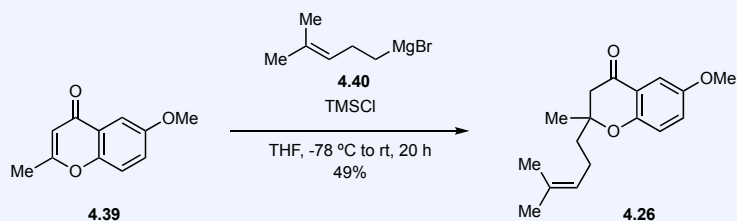
Entry	Catalyst	Ligand	ee (%)
1	CuBr(SMe <sub>2</sub> )	<b>4.43</b>	0
2	CuI	<b>4.43</b>	0
3	CuBr(SMe <sub>2</sub> )	<b>4.44</b>	0
4	CuBr(SMe <sub>2</sub> )	<b>4.45</b>	0
5	CuI	<b>4.46</b>	0
6	CuBr(SMe <sub>2</sub> )	<b>4.47</b>	0
7 <sup>a</sup>	CuBr(SMe <sub>2</sub> )	<b>4.43</b>	0
8 <sup>a</sup>	CuI	<b>4.43</b>	0
9 <sup>a</sup>	CuBr(SMe <sub>2</sub> )	<b>4.44</b>	0
10 <sup>a</sup>	CuI	<b>4.44</b>	0
11 <sup>a</sup>	CuBr(SMe <sub>2</sub> )	<b>4.45</b>	0
12 <sup>a</sup>	CuI	<b>4.45</b>	0
13 <sup>a</sup>	CuBr(SMe <sub>2</sub> )	<b>4.46</b>	0
14 <sup>a</sup>	CuI	<b>4.46</b>	0

Ligands:



<sup>a</sup> Reaction performed without TMSCl

B. Background reactivity responsible for racemic product observed

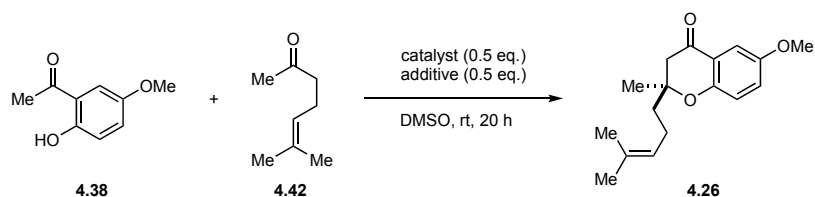


To verify that the copper catalyst was participating, a control reaction was run without copper and ligand (Table 4.1B). Interestingly, this reaction performed comparably well suggesting that the chiral copper catalyst is not playing a role in this reaction (Table 4.1B). This outcome can

be explained by simple Grignard addition into the pyrilium chloride species **4.41** that forms *in situ*. This is evidence that a background, achiral addition reaction readily occurs and diminishes the possibility of accomplishing an asymmetric transformation using Grignard **4.40**. In an attempt to overcome this achiral addition, TMSCl was omitted from the reaction. However, the yields dramatically decreased, and the product was still isolated with 0% ee (Table 4.1A, entries 7-14). Organozinc species are also known to participate in enantioselective conjugate addition reactions. To test this, **4.43** was prepared according to the literature.<sup>45</sup> Unfortunately, subjecting **4.39** to **4.43** in the presence of CuBr•(SMe<sub>2</sub>) and TMSCl only provided **4.26X** in <5% yield. Despite the precedent, an asymmetric conjugate addition did not seem like a viable strategy to enable an enantioselective synthesis of **4.26** and ultimately cochlearol B (**4.1**).

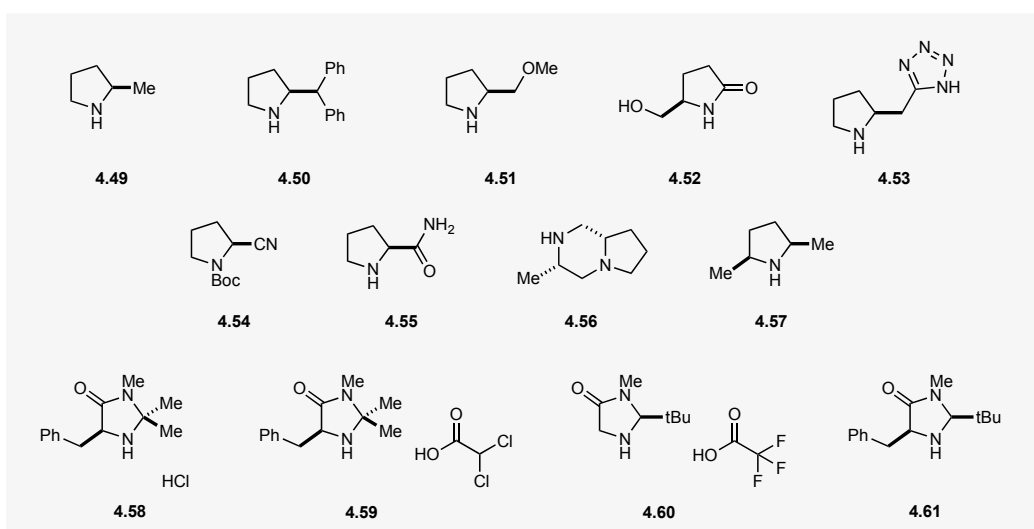
There has been a growing interest in organocatalysis and asymmetric organocatalysis,<sup>46 47</sup> culminating in the Nobel Prize in 2021.<sup>48</sup> For this reason, an asymmetric Kabbe condensation, using a chiral amine as a promoter, was also evaluated as a route to enantioenriched **4.26** (Table 4.2). The use of a chiral pyrrolidine mimics most closely the racemic reaction and thus served as a logical starting point. Switching from a super stoichiometric amount of pyrrolidine to 50 mol% (*R*)-2-methylpyrrolidine (**4.49**) decreased the yield of the reaction to 5% (Table 4.2, entry 1). However, some enantioselectivity was observed, as **4.26** was isolated in 23% ee. Next, **4.50** was evaluated to determine if a sterically bulkier ligand would increase the enantioselectivity (Table 4.2, entry 2). Unfortunately, this completely shut down the reactivity. Several other chiral pyrrolidine catalysts were evaluated (Table 4.2, entries 3-9). The only one that provided any amount of **4.26** was **4.55**. Under these conditions, **4.26** was isolated in 7% yield and 7% ee (Table 4.2, entry 7). In addition to pyrrolidines, chiral imidazolidinones were evaluated,<sup>49</sup> however, none of these catalyst promoted the reaction (Table 4.2, entries 10-13). In an effort to increase the reactivity, **4.49** was evaluated at elevated temperatures (50 °C). While this did improve the yield from 5% to 19%, the ee dropped to 0% (Table 4.2, entry 14). Select pyrrolidines were also evaluated at super stoichiometric quantities to mimic the racemic conditions (Table 4.2, entries 15-17). However, **4.26** was only isolated in up to 30% yield or 16% ee. With low yield and enantiomeric excess, as well as high catalyst loading, this strategy would not be practical for the enantioselective total synthesis of cochlearol B.

Table 4.2 Conditions evaluated for an asymmetric Kabbe condensation.



Entry	Catalyst	Additive	Yield (%)	ee (%)
1	(R)-2-methylpyrrolidine ( <b>4.49</b> )	butyric acid	5	23
2	(S)-2-diphenylmethylpyrrolidine ( <b>4.50</b> )	butyric acid	NR	-
3	(S)-2-(methoxymethyl)pyrrolidine ( <b>4.51</b> )	butyric acid	NR	-
4	(R)-5-(hydroxymethyl)-2-pyrrolidine ( <b>4.52</b> )	butyric acid	NR	-
5	(S)-5-(2-pyrrolidinyl)-1H-tetrazole ( <b>4.53</b> )	butyric acid	NR	-
6	(S)-1-boc-2-pyrrolidinecarbonitrile ( <b>4.54</b> )	butyric acid	NR	-
7	L-prolinamide ( <b>4.55</b> )	butyric acid	7	7
8	(3 <i>S</i> ,8 <i>aS</i> )-3-methyloctahydropyrrolo[1,2- <i>a</i> ]pyrazine ( <b>4.56</b> )	butyric acid	NR	-
9	(2 <i>S</i> ,5 <i>R</i> )-2,5-dimethylpyrrolidine ( <b>4.57</b> )	butyric acid	NR	-
10	(S)-5-benzyl-2,2,3-trimethylimidazolidin-4-one monohydrochloride ( <b>4.58</b> )	-	NR	-
11	(S)-5-benzyl-2,2,3-trimethylimidazolidin-4-one dichloroacetic acid ( <b>4.59</b> )	-	NR	-
12	(S)-2-(tertbutyl)-3-methylimidazolidin-4-one trifluoroacetic acid ( <b>4.60</b> )	-	NR	-
13	(2 <i>S</i> ,5 <i>S</i> )-5-benzyl-2-(tertbutyl)-3-methylimidazolidin-4-one ( <b>4.61</b> )	butyric acid	NR	-
14 <sup>a</sup>	(R)-2-methylpyrrolidine ( <b>4.49</b> )	butyric acid	19	0
15 <sup>b</sup>	(S)-2-(methoxymethyl)pyrrolidine ( <b>4.51</b> )	butyric acid	26	12
16 <sup>b</sup>	(R)-2-methylpyrrolidine ( <b>4.49</b> )	butyric acid	30	9
17 <sup>b</sup>	(S)-2-diphenylmethylpyrrolidine ( <b>4.50</b> )	butyric acid	3	16

<sup>a</sup> Reaction performed at 50 °C. <sup>b</sup> 3 eq. of the catalyst and 1 eq. of the additive were used. NR = no reaction.



Based on the proposed mechanism for the Kabbe condensation,<sup>39</sup> there are several potential explanations for why low ee was observed (Figure 4.7). First, the distance between the new stereocenter and the chiral catalyst may diminish the catalysts impact. Secondly, the steric difference between the methyl and alkyl chain is small and may not provide enough influence on the enantioselectivity. This is supported by the insignificant difference between the A-value of a methyl (1.7) and ethyl chain (1.75).<sup>50</sup> Thirdly, based on the reversible nature of the steps in these reactions, it is possible that some amount of product initially forms in high enantiomeric excess then racemizes over time via a ring opening/ring closing process.

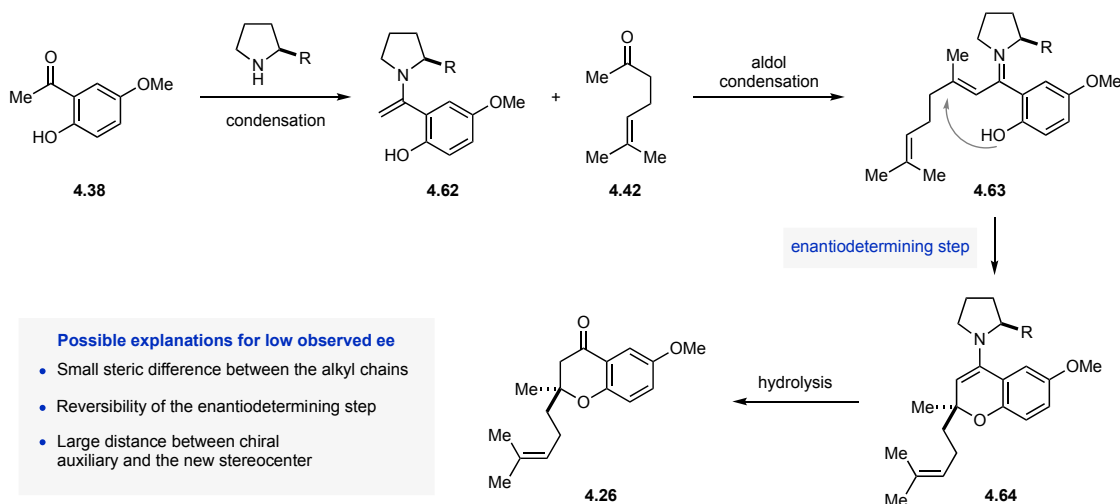


Figure 4.7 Proposed mechanism for the Kabbe condensation.

Although there are theoretically other methods that could be utilized to synthesize **4.26** enantioselectively, they could potentially add several steps to this synthesis. As a result, we elected to evaluate resolution strategies. With such a negligible steric difference between the methyl and alkyl groups, we felt that kinetic resolutions strategies that rely on sterics, such as enantioselective deprotonation or kinetic resolution via asymmetric hydrogenation, would not be effective. As a result, we turned to a classical resolution by using a chiral auxiliary to ideally generate a separable mixture of diastereomers. Towards this goal, **4.26** was treated with  $\text{Ti}(\text{OEt})_4$  and (*R*)-*tert*-butanesulfinamide (**4.65**) (Ellman's sulfinamide)<sup>51</sup> to provide a mixture of diastereomers **4.66** and **4.67** (Figure 4.8). After separation, **4.67** was hydrolyzed returning chromanone (–)-**4.26** in 95% ee. Knowing we now had a viable protocol to synthesize (–)-**4.26** in high ee, we moved on to testing the rest of the route using racemic **4.26** in order to conserve the valuable enantioenriched material.

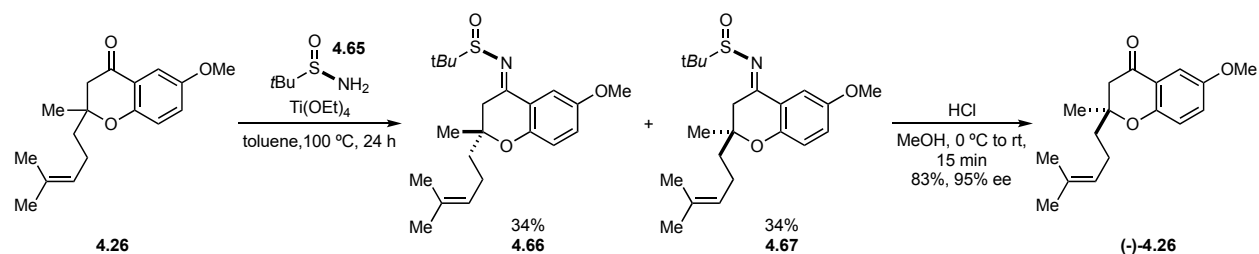


Figure 4.8 Chiral resolution using Ellman's sulfonamide enables synthesis of (-)-**4.26**.

### 4.3.3 Preliminary Investigations of the Key Steps

Using racemic chromanone **4.26**, our focus turned towards testing the key Catellani and [2+2] cycloaddition reactions. First, the synthesis of vinyl triflate **4.25** was investigated. Upon treatment with NaHMDS and phenyltriflimide, **4.26** was converted to **4.25** in 59% yield (Figure 4.9). Interestingly, cyclopentenylchromene **4.68** was also isolated in 35% yield. The structure of this byproduct was verified through X-ray crystallographic analysis of derivative **4.70**. This was prepared through an initial hydroboration/oxidation, followed by guanidinium sulfate formation and crystallization according to the procedure developed by Whitehead and coworkers.<sup>52</sup> The structure of **4.68** is also found within ganocins B (**4.8**) and C, meroterpenoid natural products that were also isolated from *Ganoderma cochlear* (Figure 4.1).<sup>3</sup> Investigation into the mechanism leading to the formation of **4.68** are ongoing.

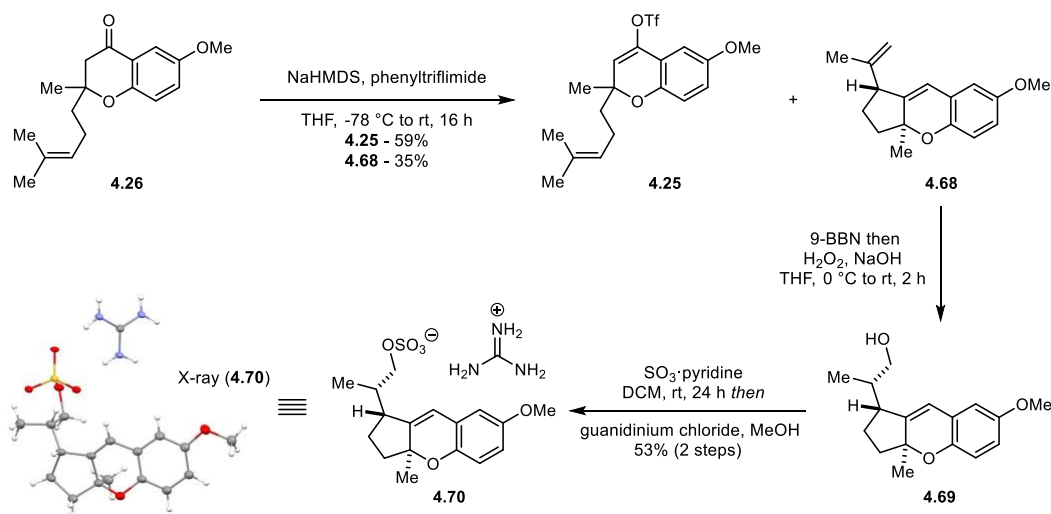


Figure 4.9 Synthesis of vinyl triflate **4.25** and the unexpected formation of **4.68**, a structure found within ganocins B and C.

The competing formation of byproduct **4.68** could be eliminated by switching from phenyltriflimide to Comins' reagent.<sup>53</sup> This more reactive triflating reagent enabled the reaction to

be run at cryogenic temperatures in shorter reaction times, and ultimately provided an 86% yield of **4.25** as the sole product (Figure 4.10).

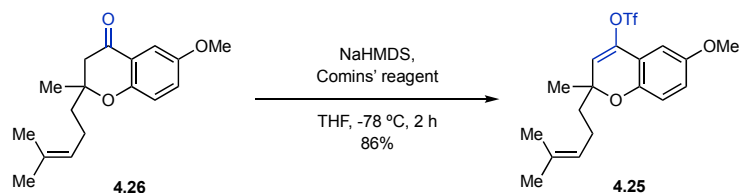


Figure 4.10 Triflation using Comins' reagent.

Vinyl triflate **4.25** was then subjected to Catellani conditions using norbornene **4.34** as well methyl acrylate and methyl 4-iodobutyrate as coupling partners.<sup>24</sup> Gratifyingly, tetrasubstituted olefin **4.24** was isolated in 31% yield (Figure 4.11). In addition, byproduct **4.71** was isolated in 11% yield. This product likely forms through an intramolecular [4+2] cycloaddition from the *in situ* generated Heck product (**4.72**) of methyl acrylate and **4.25**.<sup>54</sup> To test this hypothesis, **4.72** was independently prepared and heated to 100 °C in dioxane, and **4.71** was isolated as the sole product confirming its origin. Literature on the Catellani reaction suggests that increasing the amount of norbornene co-catalyst can prevent the formation of direct Heck products. However, in light of subsequent results, this hypothesis was not tested.

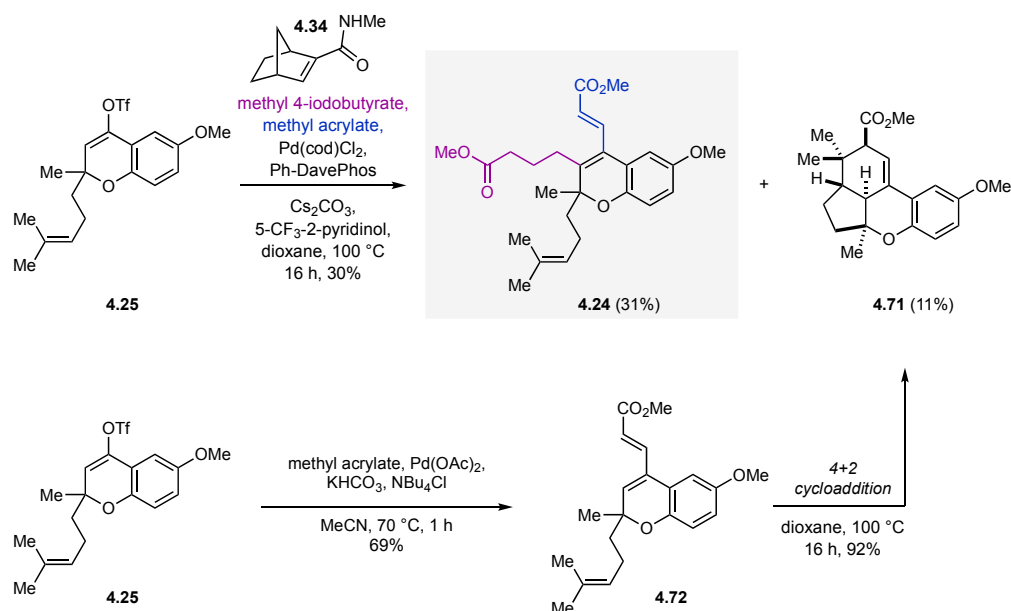


Figure 4.11 Initial investigations into the alkenyl Catellani reaction.

Tetrasubstituted alkene **4.24** was carried forward to the [2+2] reaction. Unfortunately, when **4.24** was irradiated with visible light, in the presence of photocatalyst

$[\text{Ir}(\text{dF}(\text{CF}_3)\text{ppy})_2(\text{dtbbpy})](\text{PF}_6)$  (**4.73**),<sup>22,23</sup> none of the desired cyclobutane **4.23** was formed. Instead, cyclopropane **4.74** was isolated as the sole product in 85% yield (Figure 4.12). The structure of this product was confirmed by X-ray crystallography (see Experimental section for details). We hypothesize that this product arises through an initial triplet energy transfer event from the excited state photocatalyst to the substrate generating **4.75**.<sup>26</sup> The resulting biradical then cyclizes onto the prenyl olefin forming the first five-membered ring (**4.76**). Then, instead of radical recombination to form the desired cyclobutane (**4.23**), a second radical addition occurs at the  $\beta$  position of the methyl acrylate fragment forming the second five membered ring (**4.77**). Finally, radical recombination closes the cyclopropane and forms the isolated product **4.74**. Other photocatalysts with different triplet energies (e.g.  $[\text{Ru}(\text{bpy})_3](\text{PF}_6)_2$ ),<sup>55</sup> as well direct excitation using UV light, also exclusively yielded **4.74** and none of **4.23**.

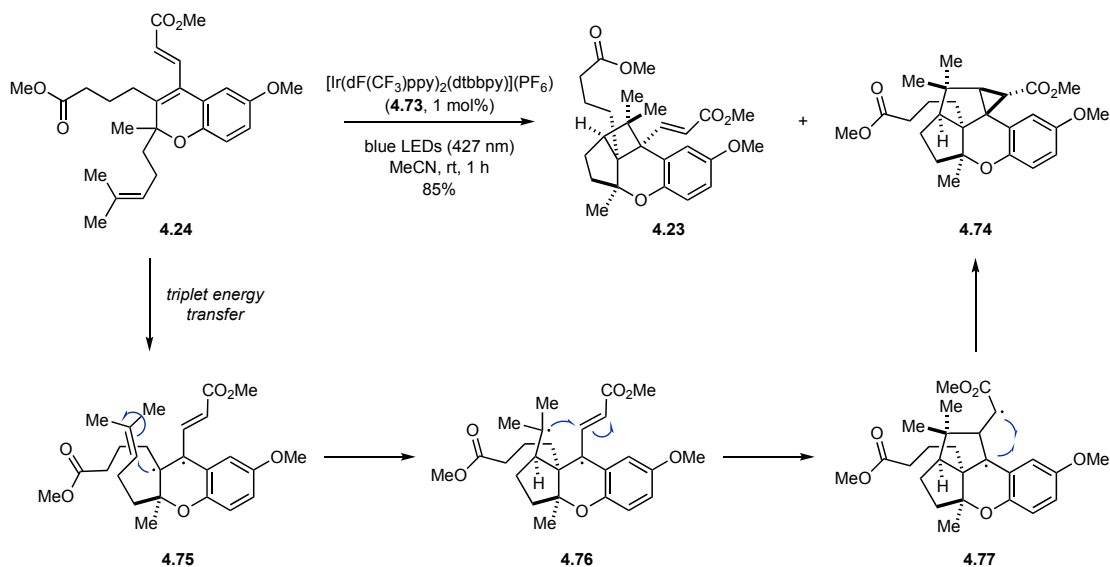
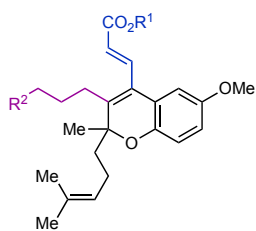


Figure 4.12 Photochemical excitation of **4.24** using a visible light absorbing photosensitizer leads to unexpected formation of cyclopropane **4.74**.

Substrates **4.78** and **4.79** were also prepared and tested in the [2+2] cycloaddition reaction, however they also only formed the analogous cyclopropane products (Figure 4.13A). In an effort to overcome this undesired reactivity, other ipso coupling partners with tested in the Catellani reaction, specifically Suzuki<sup>24</sup> and cyanation reaction,<sup>56</sup> however they failed to provide any of the Catellani product (Figure 4.13B).

A. Additional unsuccessful [2+2] substrates.



B. Failed ipso coupling partners in the Catellani reaction.

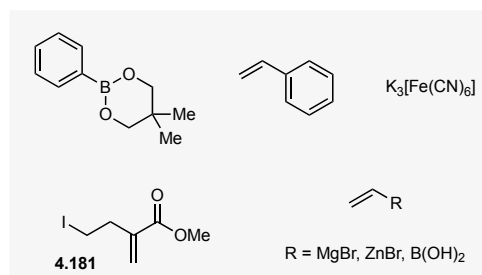
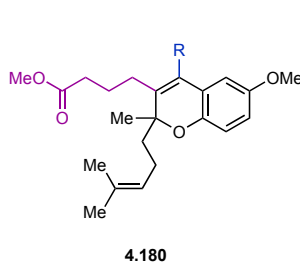
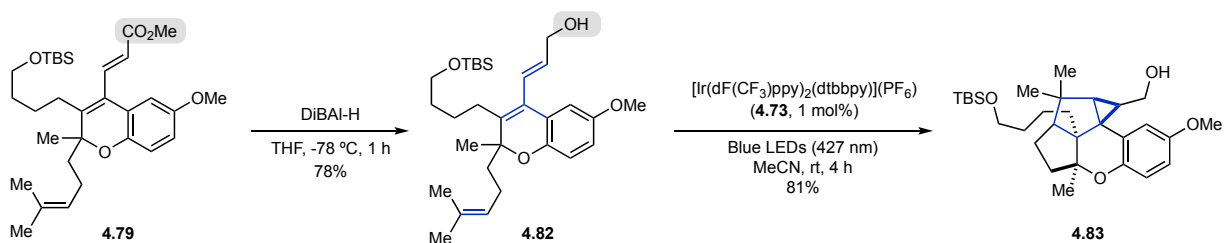


Figure 4.13 Alternative, failed substrates in the [2+2]-cycloaddition and Catellani reactions.

To try and overcome this undesired reactivity, we tested the role of sterics and electronics in this reaction. To test the electronics, ester **4.79** was reduced to the corresponding alcohol **4.82** (Figure 4.14A) in an attempt to destabilize the intermediate analogous to **4.77** in route to cyclopropane **4.74** (Figure 4.12). Although this reaction is slower, the corresponding cyclopropane **4.83** still formed as the sole product (Figure 4.14A). To study the sterics, electronically comparable substrate **4.72** was subjected to the same [2+2] cycloaddition reaction conditions and none of the anticipated cyclopropane product (**4.84**) was observed (Figure 4.14B). Instead, a mixture of [2+2] product (**4.85**) and [4+2] products (**4.71** and **4.86**) were isolated in 29% and 32% yield, respectively. Interestingly, the major [4+2] product isomer is different than that from the thermal [4+2] cycloaddition pointing to a different reaction mechanism. Overall, this result suggests that the steric constraints of the methyl butyrate and methyl acrylate chains favor the formation of cyclopropane **4.74** over cyclobutane **4.23**. This is consistent with **4.74** being isolated as a single diastereomer with the methyl butyrate chain and cyclopropane on opposite faces of the molecule. In addition, we hypothesize that the electrophilic nature of the acrylate moiety in **4.76**, in combination with the high stability of enol radical **4.77**, favors formation of **4.74**. These initial studies into the key steps, the Catellani reaction and [2+2] cycloaddition, gave us insights into the issues that we would need to overcome. Namely, in the Catellani reaction, highly reactive Heck coupling partners like methyl acrylate promote competing reactions from Heck adducts. Additionally, the sterics of tetrasubstituted olefin make the desired [2+2] reaction challenging, especially when there is another viable reaction pathway such as the one leading to **4.74**.



A. Testing the role of electronics in the undesired cyclopropanation reaction.



B. Testing the role of sterics in the undesired cyclopropanation reaction.

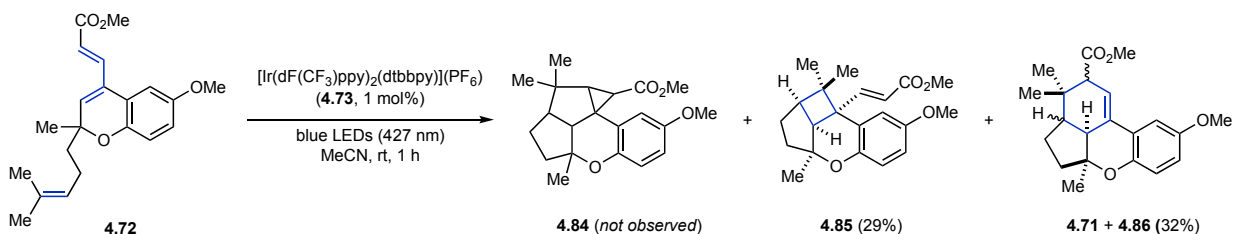


Figure 4.14 Model systems to test the role of sterics and electronics in cyclopropane formation.

#### 4.3.4 Revised Approach to the Core of Cochlearol B

With this in mind, a revised approach towards cochlearol B (**4.1**) was developed. Specifically, we postulated that a less electron deficient alkene could reduce the viability of the simple Heck reaction in the Catellani process. Additionally, a diene locked in the *s*-trans confirmation could prevent any undesired [4+2] cycloaddition reaction. Furthermore, to alleviate the steric constraints in the [2+2] reaction, the order of ring formation was reconsidered. We hypothesized that a tricyclic substrate with the third six membered ring already formed would be more likely to undergo the desired [2+2] cycloaddition. Finally, we aimed to destabilize the intermediates on the route to cyclopropane **4.74** in order to prevent this reaction pathway from occurring. Towards this end, vinyl triflate **4.25** was subjected to Catellani reaction conditions with 5-iodo-1-pentene,<sup>24</sup> which functions as both the nucleophilic and electrophilic coupling partner (Figure 4.15). The product of this Catellani reaction, **4.87**, would exhibit several of the distinct advantages highlighted above when compared to chromene **4.24**: 1) a locked *S*-trans diene confirmation to prevent [4+2] reaction, 2) the absence of the methyl acrylate moiety to potentially disfavor cyclopropane formation, and 3) the third six membered ring is now formed prior to the [2+2] reaction. Gratifyingly, **4.87** was isolated as the sole product in 11% yield, supporting our ideas regarding the problems encountered earlier (Figure 4.15). Reaction optimization revealed that increasing the amount of norbornene had no effect on the reaction, whereas increasing the equivalents of iodide could improve the yield from 11% to 65%. Remarkably, this Catellani

reaction could be performed on a one-gram scale, providing **4.87** in 81% yield. With a viable and scalable route to **4.87** established, this compound was then tested in the [2+2] cycloaddition reaction. Irradiating **4.87** with visible light, in the presence of 1 mol%  $[\text{Ir}(\text{dF}(\text{CF}_3)\text{ppy})_2(\text{dtbbpy})](\text{PF}_6)$  (**4.73**), resulted in the exclusive formation of desired cyclobutane **4.88** in 94% yield. Alternatively, irradiation of **4.87** with UV light and no photocatalyst resulted in no reaction. Through this route, the core polycyclic structure of cochlearol B was synthesized in 4 steps with 50% overall yield.

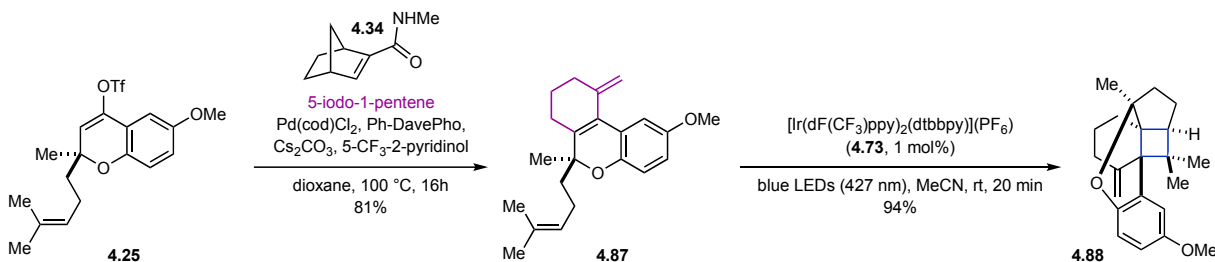


Figure 4.15 Revised Catellani reaction using 5-iodo-1-pentene subsequently enables a successful [2+2]-photocycloaddition.

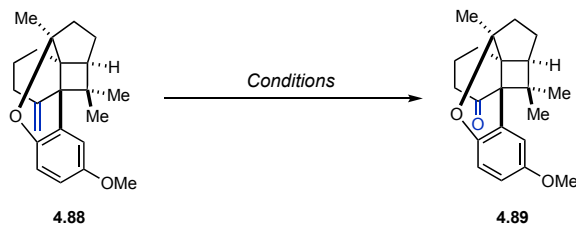
#### 4.3.5 Strategies Towards the $\alpha,\beta$ -Unsaturated Aldehyde

The remaining challenges in our synthesis of cochlearol B (**4.1**) were deprotection of the phenolic methyl ether, and formation of the  $\alpha,\beta$ -unsaturated aldehyde. Because of the reactivity of unprotected phenols in the presence of oxidants and electrophiles, we elected to address formation of the  $\alpha,\beta$ -unsaturated aldehyde first and leave the deprotection until the end. Our strategy commenced with oxidative cleavage of the 2,2-disubstituted alkene to both remove the extra carbon and incorporate a functional handle to enable formation of the desired  $\alpha,\beta$ -unsaturated aldehyde (Table 4.3A). Initially, ozonolysis of the alkene was attempted. However, exposure to ozone at  $-78$  C, even for as little as 30 seconds, resulted in decomposition of **4.88** (Table 4.3A, entries 1 & 2). Pyridine is known to attenuate the reactivity of ozone,<sup>57</sup> however, it did not help prevent decomposition in this substrate (Table 4.3A, entry 3).  $\text{RuCl}_3/\text{NaIO}_4$  based oxidative cleavage conditions were also evaluated (Table 4.3A, entry 4 & 5).<sup>58-59</sup> Interestingly, these conditions promoted a retro-[2+2] reaction to provide **4.87** in some cases. Conditions relying on  $\text{KMnO}_4/\text{NaIO}_4$  also resulted in decomposition (Table 4.3A, entry 6).<sup>60</sup> Some success was realized using osmium(VIII) based conditions, with a mixture of potassium osmate,  $\text{NaIO}_4$ , and lutidine giving 5% of ketone **4.89** (Table 4.3A, entries 7 & 8).<sup>61</sup> Ultimately, a two-step protocol was developed starting with dihydroxylation of **4.88** using  $\text{OsO}_4$  in the presence of citric acid providing

diol **4.90** in 48% yield (Table 4.3B).<sup>62 63</sup> A subsequent oxidative cleavage of the diol using NaIO<sub>4</sub> furnished the desired ketone **4.89** in 83% yield.<sup>64</sup>

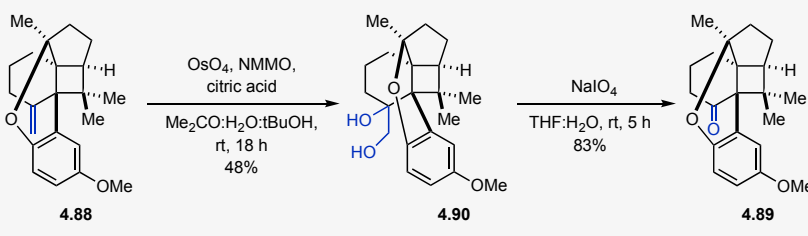
Table 4.3 (A) Conditions evaluated for oxidative cleavage of **4.88** to provide **4.89**. (B) Two step protocol to **4.89** through dihydroxylation followed by oxidative cleavage.

A. Conditions evaluated for oxidative cleavage of **4.88** to provide **4.89**.



Entry	Oxidant	Solvent	Temp. (°C)	Time	Product
1	O <sub>3</sub>	DCM	-78	10 min	decomp.
2	O <sub>3</sub>	DCM	-78	30 s	decomp.
3	O <sub>3</sub> , pyridine	DCM	-78	30 s	decomp.
4	RuCl <sub>3</sub> , NaIO <sub>4</sub>	DCM:MeCN:H <sub>2</sub> O	rt	1 h	SM
5	RuCl <sub>3</sub> , NaIO <sub>4</sub>	MeCN:H <sub>2</sub> O	rt	1.5 h	retro [2+2]
6	KMnO <sub>4</sub> , NaIO <sub>4</sub>	dioxane:water	rt	72 h	SM + decomp.
7	K <sub>2</sub> [OsO <sub>2</sub> (OH) <sub>4</sub> ], NaIO <sub>4</sub>	Me <sub>2</sub> CO:H <sub>2</sub> O	rt	120 h	trace
8	K <sub>2</sub> [OsO <sub>2</sub> (OH) <sub>4</sub> ], NaIO <sub>4</sub> , lutidine	Me <sub>2</sub> CO:H <sub>2</sub> O: tBuOH	rt	72 h	5%

B. Two step protocol to **4.89** through dihydroxylation followed by oxidative cleavage.



The next objective became converting ketone **4.89** into  $\alpha,\beta$ -unsaturated aldehyde **4.92**. To accomplish this, we envisioned a multi-step approach whereby a carbonyl group was first incorporated  $\alpha$  to the ketone followed by conversion to the  $\alpha,\beta$ -unsaturated aldehyde (Figure 4.16).

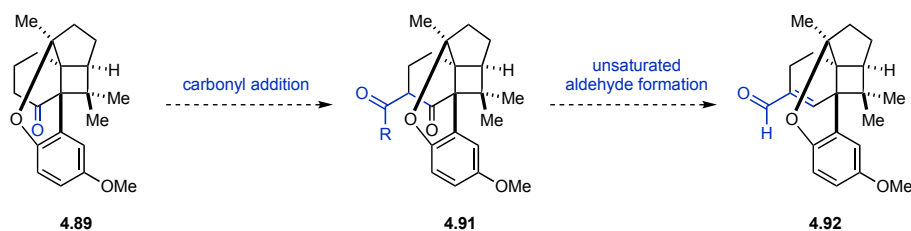


Figure 4.16 Strategy for  $\alpha,\beta$ -unsaturated aldehyde formation.

Initially,  $\beta$ -keto ester **4.93** was selected as the ideal intermediate (Figure 4.17). Treatment of **4.89** with LiHMDS and Mander's reagent<sup>65</sup> successfully formed  $\beta$ -keto ester **4.93** in 86% yield.<sup>66</sup> In order to convert **4.93** to **4.92**, the ketone would first need to be converted to the enoate.

Several strategies to achieve this were evaluated, the first being a two-step triflation, reduction approach.<sup>66</sup> First **4.93** was subjected to different triflation conditions in an effort to make vinyl triflate **4.96**,<sup>66 67</sup> however no reaction was observed. Alternatively, ketone reduction followed by elimination was evaluated.<sup>68</sup> With NaBH<sub>4</sub> no reaction was observed and surprisingly, when switching to a harsher reductant (LiAlH<sub>4</sub>) ester reduction product **4.94** was isolated. This unexpected result makes a successful reduction/elimination approach unlikely. Extensive experimentation revealed that enol phosphate **4.97** could be synthesized as the sole example of a successful manipulation of the ketone in this system.<sup>66</sup> There are selected examples in the literature of these types of enol phosphates undergoing reduction to the alkene in the presence of different alkyl-Cu(I) species.<sup>69 70</sup> However, after treatment with **4.97** the only products that were observed were hydrolysis back to **4.93** and addition of an alkyl group to give **4.98**, this being a known alternative reaction pathway in these systems.<sup>71</sup> After limited success with β-keto ester substrate **4.93**, we elected to move on.

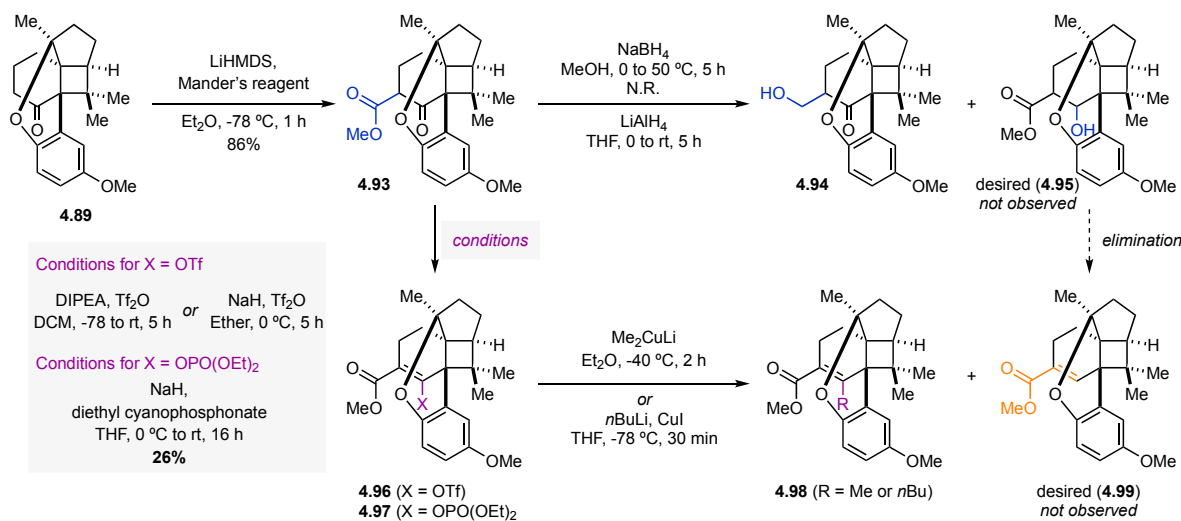


Figure 4.17 First approach to the α,β-unsaturated aldehyde.

Formylation of **4.89** using ethyl formate under basic conditions smoothly provided **4.100** in 52% yield (Figure 4.18).<sup>72</sup> **4.100** could then be protected as either the corresponding methyl ether **4.101** (R = Me) or ethoxyethyl ether **4.102** (R = EE).<sup>73</sup> Per the literature,<sup>73</sup> these compounds were treated with hydride reductants in an effort to accomplish ketone reduction that would be followed by a one-pot deprotection/elimination reaction. Under NaBH<sub>4</sub> reduction conditions, **4.102** formed a complex mixture; however, when substrate **4.101** was treated with LiAlH<sub>4</sub>, conjugate reduction product **4.103** was isolated instead of the desired 1,2-reduction product **4.104**.

In an effort to adapt the triflation/reduction approach to this system, **4.101** was treated with triflic anhydride. Unfortunately, none of the desired triflate was observed.

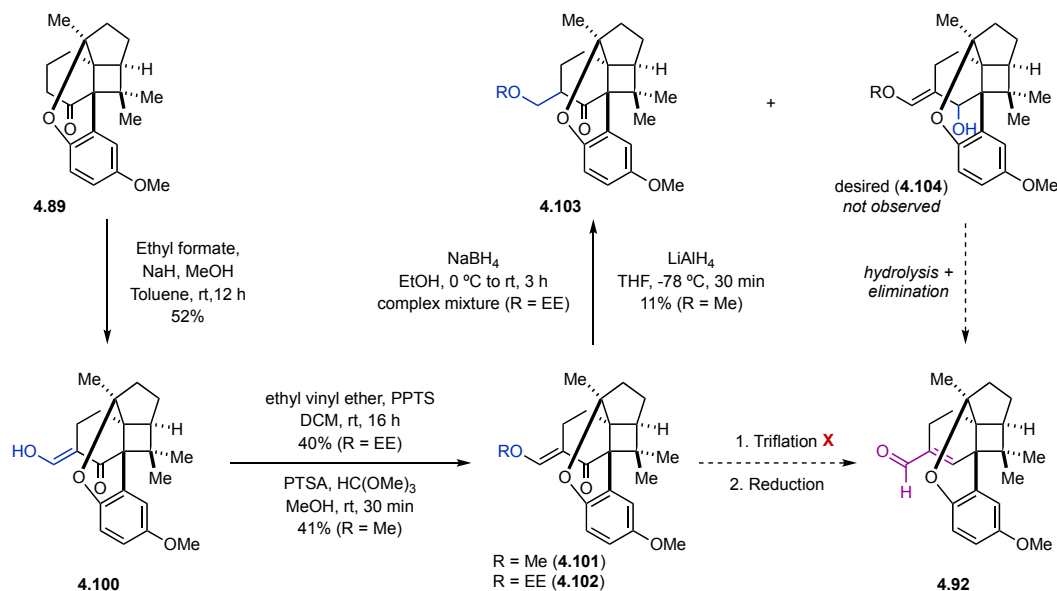


Figure 4.18 Second approach to the  $\alpha,\beta$ -unsaturated aldehyde.

In a slightly different approach, **4.89** was converted in 39% yield to **4.105** using Eschenmoser's salt<sup>74</sup> in 39% yield (Figure 4.19).<sup>75</sup> As with the previous strategies, we envisioned reducing the ketone to the corresponding alcohol. A subsequent rearrangement or Sn2' reaction would move the exocyclic alkene to the desired internal position and install a functional handle at the primary carbon.<sup>76</sup> Then, depending on the identity of the functional group, the necessary steps would be taken to form the desired aldehyde. However, under Luche reduction conditions,<sup>77</sup> **4.105** underwent a conjugate reduction to give **4.106**. In addition, when **4.105** was treated with LiAlH<sub>4</sub>

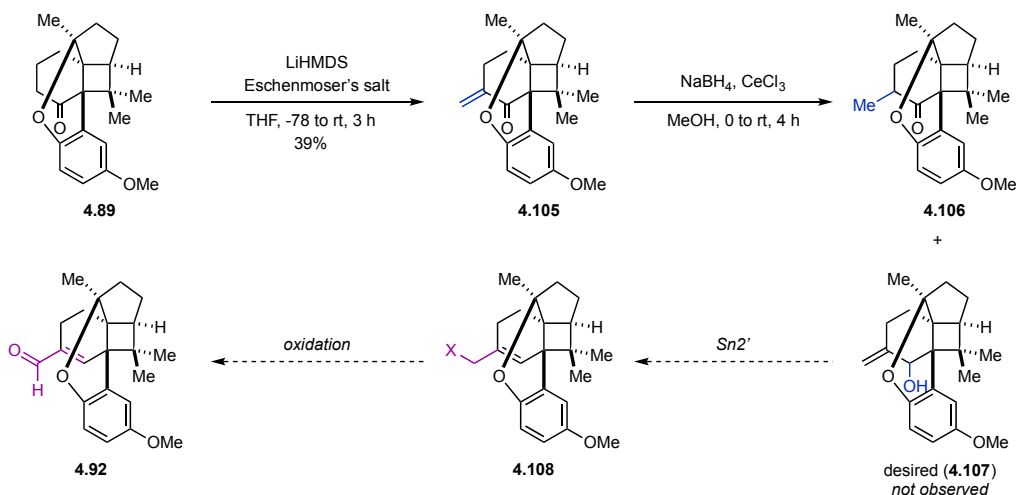


Figure 4.19 Third approach to the  $\alpha,\beta$ -unsaturated aldehyde.

decomposition was observed. This result is in line with our previous experiments that all show that hydride reductants preferentially react at the exocyclic carbon. We concluded that a strategy relying on ketone reduction would not be viable.

The experiments up until this point proved that  $\alpha$ -functionalization of ketone **4.89** was possible using a variety of different conditions. The unsolved challenge of further manipulating the ketone remained. As such, we turned to methods that could accomplish multi-site functionalization. It has been shown that ketones can be converted to the corresponding formyl vinyl bromides using the Vilsmeier-Haack reagent. In accordance with the literature,<sup>78</sup> ketone **4.89** was treated with a pre-stirred mixture of  $\text{PBr}_3$  and DMF. However, the desired product **4.109** was not observed (Figure 4.20).

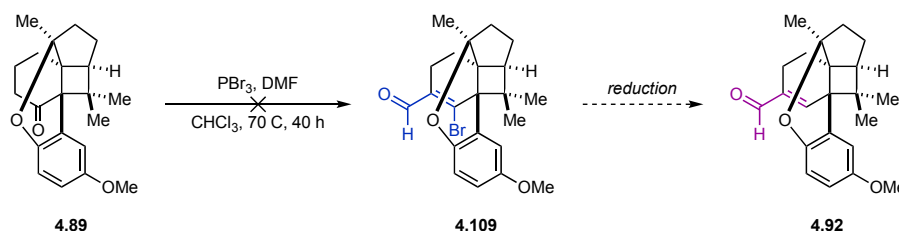


Figure 4.20 Fourth approach to the  $\alpha,\beta$ -unsaturated aldehyde.

Since a reduction/elimination strategy did not seem viable, we returned to a triflation/reduction approach. Since triflation of **4.93** and **4.101** was unsuccessful, an alternative substrate was investigated. It is known in the literature that ketone derived enaminones can be converted to the corresponding formyl vinyl triflates.<sup>79 80</sup> In order to test this on our system, **4.89** was treated with DMF-DMA at elevated temperatures and the desired product **4.110** was isolated in 86% yield (Figure 4.21).<sup>81</sup> Under triflation conditions, **4.110** was successfully converted to the desired vinyl triflate **4.111** in 83% yield.<sup>79 80</sup> The vinyl triflate was then reduced to the corresponding alkene **4.92** under palladium catalyzed reduction conditions in 92% yield.<sup>82</sup> With that, we arrived at desired intermediate **4.92** with the  $\alpha,\beta$ -unsaturated aldehyde intact. A similar approach was taken by the Sugita group in their total synthesis of cochlearol B.<sup>21</sup>

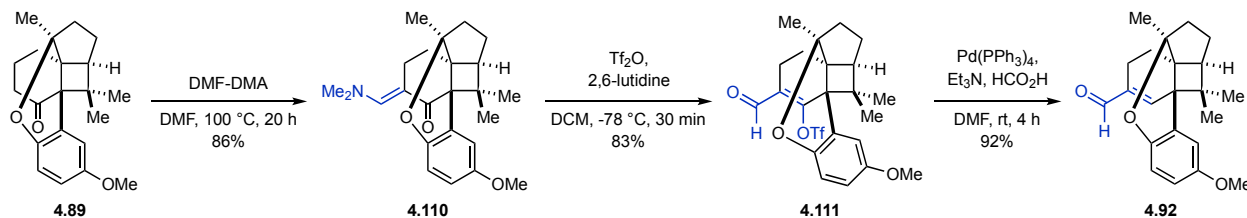
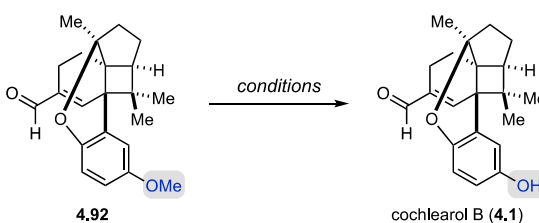


Figure 4.21 3-step synthesis of  $\alpha,\beta$ -unsaturated aldehyde **4.92** from ketone **4.89**.

### 4.3.6 Completion of the Total Synthesis of Cochlearol B

The final obstacle in our synthesis of cochlearol B (**4.1**) was deprotection of the phenolic methyl ether. Aryl methyl ether deprotection is typically accomplished under strongly Lewis acidic conditions, in the presence of strong nucleophiles, or a combination of both.<sup>83</sup> Treating **4.92** with  $\text{BBr}_3$  at  $-78\text{ }^\circ\text{C}$  led to rapid decomposition (Table 4.4, entry 1). As a result, we switched to a milder Lewis acid,  $\text{TMSCl}$ , and added a strong nucleophile,  $\text{NaI}$ , to try and accomplish deprotection. Unfortunately, this also led to decomposition of **4.92** (Table 4.4, entry 2). It's possible that the decomposition is promoted by Lewis acid coordination to the aldehyde or the tertiary phenolic ether. With this in mind, we switched to evaluating nucleophilic deprotection conditions. Several different nucleophiles were evaluated ( $\text{MePhSLi}$ ,<sup>84</sup>  $\text{LiPPh}_2$ ,<sup>85</sup>  $\text{KPPh}_2$ ,<sup>86</sup>  $\text{LiI}$ ,  $\text{MgI}_2$ <sup>87</sup>) however the desired product was never observed with decomposition being the main outcome (Table 4.4, entries 3-7). This strategy for demethylation typically requires harsh temperatures which may also explain the decomposition. In addition, there are multiple electrophilic sites that could react under these nucleophilic conditions.

Table 4.4 Conditions evaluated for phenol demethylation.



Entry	Reagents	Solvent	Temp. ( $^\circ\text{C}$ )	Time (h)	Product
1	$\text{BBr}_3$	DCM	$-78$	0.5	decomp.
2	$\text{TMSCl}$ , $\text{NaI}$	MeCN	0	0.5	decomp.
3	$\text{MePhSLi}$	HMPA:toluene	130	16	decomp.
4	$n\text{BuLi}$ , $\text{HPPPh}_2$	THF	rt	16	SM
5	$t\text{BuOK}$ , $\text{HPPPh}_2$	DMF	80	16	decomp.
6	$\text{LiI}$	collidine	150	16	decomp.
7	$\text{MgI}_2$	$\text{BMIMBF}_4$	50	4 h	decomp.

With no evidence of a feasible demethylation, an alternative pathway was devised. Following reduction of aldehyde **4.92** using  $\text{NaBH}_4$  to provide **4.112** in 96% yield, demethylation was achieved using neat  $\text{MeMgI}$  at  $160\text{ }^\circ\text{C}$  in 34% yield (Figure 4.22).<sup>88</sup> To complete the synthesis, the primary alcohol was oxidized back to the aldehyde using Swern conditions in 77% yield. This completed our 12-step synthesis of cochlearol B (**4.1**) in 3.3% overall yield.<sup>89</sup> Importantly, the spectroscopic data matched the reported data from Cheng<sup>7</sup> and Sugita.<sup>21</sup>

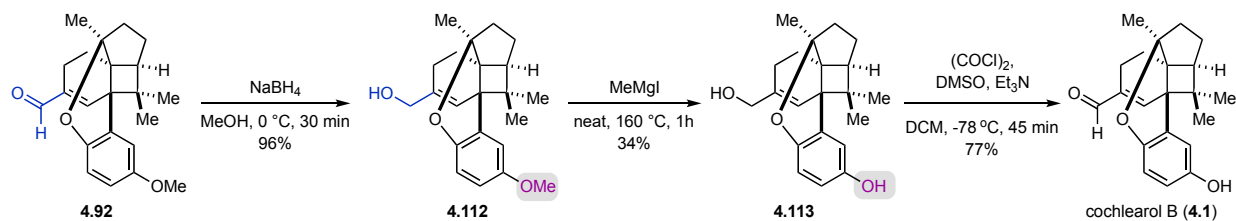


Figure 4.22 Completion of the synthesis of cochlearol B.

### 4.3.7 Total Synthesis of (+)-Cochlearol B

Using our modified route to (–)-**4.26** via sulfinimine **4.67**, the same sequence used in our racemic preparation of cochlearol B were used to complete a 14-step synthesis of (+)-cochlearol B in 1.8% overall yield (Figure 4.23).<sup>89</sup> Alternatively, sulfinimine **4.66** could theoretically be used to synthesize (–)-cochlearol B.

## 4.4 Conclusion

Our lab's interest in cochlearol B stemmed from our previous work on the total synthesis of lingzhiol (Chapter 1). Both are complex meroterpenoid natural products isolated from mushrooms within the *Ganoderma* genus. These fungi have a long history of use in traditional medicines, and studies have shown that the meroterpenoid compounds isolated from *Ganoderma cochlear* possess potent and unique biological activity. For example, cochlearol B, isolated from *Ganoderma cochlear* in 2014, shows promise as a treatment for renal fibrosis. However, further studies are limited by low natural abundance. Initially, 100 kg of *Ganoderma cochlear* was used to isolate 1.5 mg of cochlearol B. As such, cochlearol B is an ideal candidate for total synthesis. Our proposed synthesis of cochlearol B involved a few key carbon-carbon bond forming reactions including a Kabbe condensation, a vinyl Catellani reaction, and a visible light mediated [2+2]-cycloaddition. Initial studies on these key steps provided crucial insights into the underlying issues and potential solutions. Ultimately, these reactions enabled a 4-step synthesis of the core of cochlearol B. An additional 8 steps were used to complete our 12-step synthesis of cochlearol B in 3.3% yield. Additionally, a 14-step synthesis of (+)-cochlearol B was developed in 1.8% yield. Ultimately, a chiral resolution was utilized to provide the enantioenriched material necessary for this synthesis. This is the first synthesis of (+)-cochlearol B.



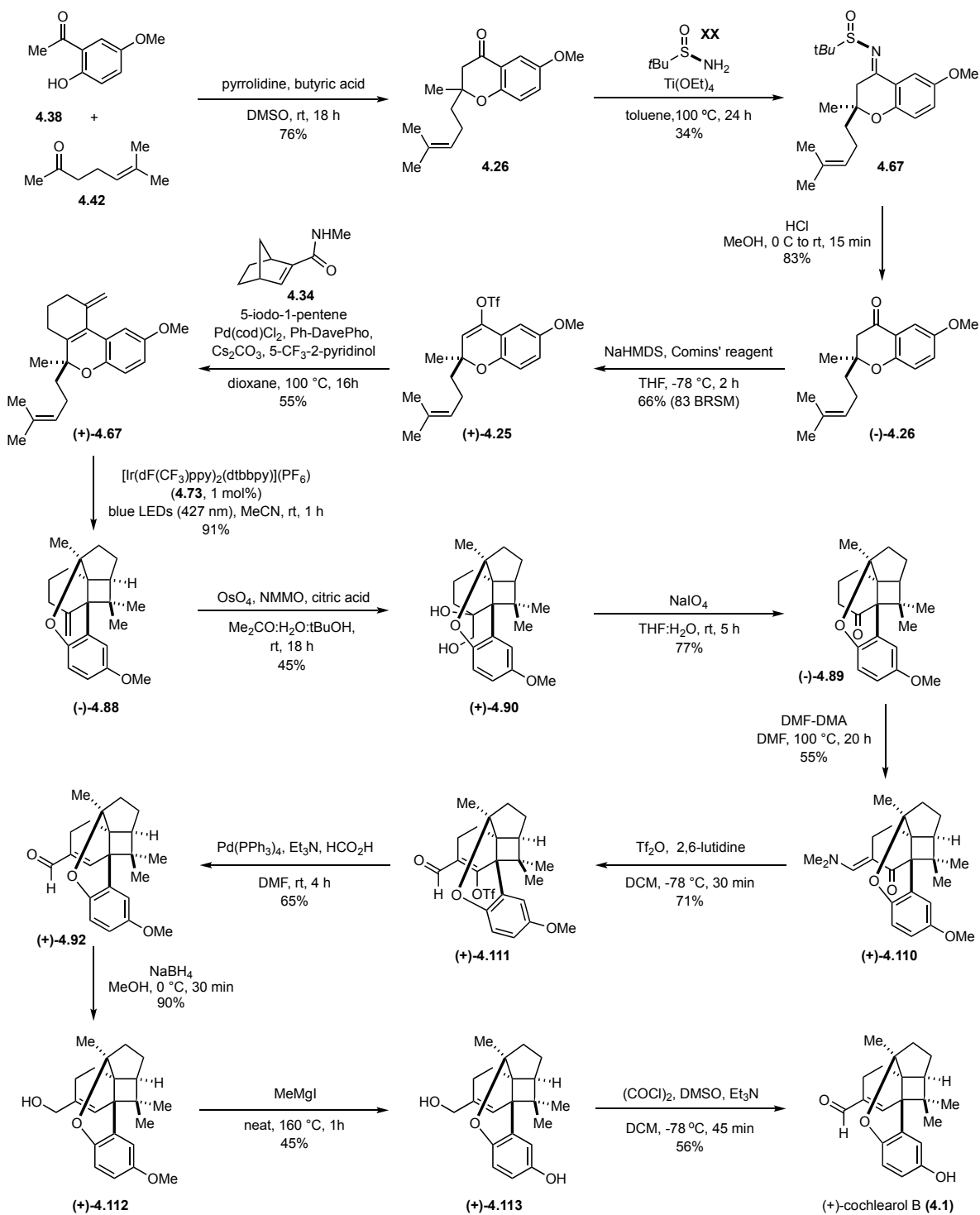


Figure 4.23 Total synthesis of (+)-cochlearol B.

## 4.5 Experimental

### 4.5.1 General Information

All air- or moisture-sensitive reaction were carried out in flame-dried glassware under an atmosphere of nitrogen. Thin-layer chromatography (TLC) was performed on *Merck* silica gel 60 F<sub>254</sub> plates using UV light (254 or 366 nm), KMnO<sub>4</sub> or CAM stain for visualization. Flash chromatography was performed using silica gel Silia Flash<sup>®</sup> 40-63 micron (230-400 mesh) from Silicycle unless otherwise noted.

### Materials and Instrumentation

All chemicals were purchased from Sigma-Aldrich, Alfa Aesar, Acros Organics, Oakwood, TCI America, Frontier Scientific, Matrix Scientific, and Strem were used as received unless otherwise stated. THF, DCM, Et<sub>2</sub>O, MeOH, MeCN, DMF, DMSO were dried by being passed through a column of activated alumina under argon using a JC- Meyer Solvent Systems. [Ir(dF(CF<sub>3</sub>)ppy)<sub>2</sub>(dtbbpy)]PF<sub>6</sub> was prepared according to the procedure described by Stephenson.<sup>90</sup> Proton nuclear magnetic resonance (<sup>1</sup>H NMR) spectra were recorded on Varian MR400, Bruker Avance Neo 500, Varian Vnmrs 500, Varian Vnmrs 600, and Varian Vnmrs 700 spectrometers and are referenced to the residual NMR solvent signal (CHCl<sub>3</sub>: δ 7.26 ppm; C<sub>6</sub>H<sub>6</sub>: δ 7.16 ppm; (CH<sub>3</sub>)<sub>2</sub>SO: δ 2.50 ppm; (CH<sub>3</sub>)<sub>2</sub>CO: δ 2.05 ppm). Data for <sup>1</sup>H NMR are reported as follows: chemical shift (δ ppm), multiplicity (s = singlet, d = doublet, t = triplet, q = quartet, m = multiplet, b = broad), coupling constant (Hz), integration. Carbon nuclear magnetic resonance (<sup>13</sup>C NMR) spectra were recorded on Bruker Avance Neo 500, Varian Vnmrs 500, Varian Vnmrs 600, and Varian Vnmrs 700 spectrometers and are referenced to the carbon resonances of the NMR solvent (CDCl<sub>3</sub>: δ 77.16 ppm; C<sub>6</sub>D<sub>6</sub>: δ 128.06 ppm; (CD<sub>3</sub>)<sub>2</sub>S<sub>2</sub>O: δ 39.52 ppm; (CD<sub>3</sub>)<sub>2</sub>CO: δ 29.84 ppm). High-resolution mass spectrometry (HRMS) data was recorded at the Mass Spectrometry Facility at the Department of Chemistry of the University of Michigan in Ann Arbor, MI on an Agilent 6230 TOF HPLC-MS (ESI) or Micromass AutoSpec Ultima Magnetic Sector mass spectrometer (ESI, EI). Infrared (IR) spectra were obtained using a PerkinElmer Frontier FT-IR spectrometer. IR data are represented as frequency of absorption (cm<sup>-1</sup>). Chiral HPLC analysis was performed on a Agilent Infinity 1260 equipped with a Daicel Chiralpak OJ-H column (5 μm, 4.6 mm x 250 mm) or a Daicel Chiralpak IC column (5 μm, 4.6 mm x 250 mm). Optical rotations

were acquired on a Jasco P-2000 digital polarimeter and reported as  $c = \text{g}/100 \text{ mL}$  at 589 nm (sodium D line) at room temperature and 10 cm path length. Stereochemistry indicators with asterisk ( $R^*$ ,  $S^*$ ) were used to indicate relative stereochemistry of diastereomers.

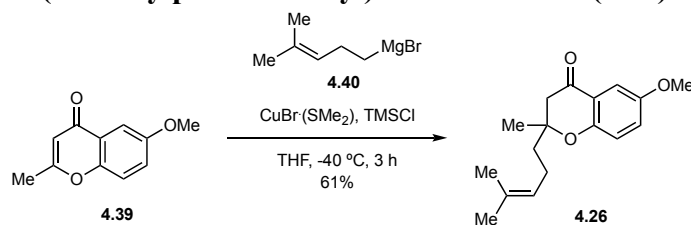
### Abbreviations

CAM = ceric ammonium molybdate, THF = tetrahydrofuran, DCM = dichloromethane, Et<sub>2</sub>O = diethyl ether, MeOH = methanol, MeCN = acetonitrile, DMF = *N,N*-dimethylformamide, DMSO = dimethylsulfoxide, EtOAc = ethyl acetate, ESI = electrospray ionization, EI = electron ionization, h = hours, min = minutes, rt = room temperature, TMSCl = trimethylsilyl chloride, NaHMDS = sodium bis(trimethylsilyl)amide, 9-BBN = 9-borabicyclo[3.3.1]nonane, Py·SO<sub>3</sub> = pyridine sulfur trioxide complex, NMMO = *N*-Methylmorpholine *N*-oxide, DMF-DMA = *N,N*-dimethylformamide dimethyl acetal, Tf<sub>2</sub>O = triflic anhydride.

### 4.5.2 Experimental Procedures

#### Synthesis of Chromanone 4.26

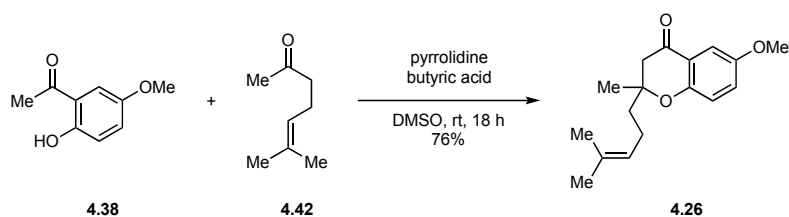
#### 6-methoxy-2-methyl-2-(4-methylpent-3-en-1-yl)chroman-4-one (4.26)



*General Procedure A (GP-A)*: Preparation of homoprenyl magnesium bromide (**4.40**): A flask was charged with acid washed magnesium (2.18 g, 89.6 mmol, 1.00 equiv) turnings and flame dried under vacuum. To the flask was added THF (128 mL) and a small crystal of iodine. Then 5-bromo-2-methylpent-2-ene (12.80 mL, 95.56 mmol, 1.07 equiv) was added slowly while stirring. The reaction mixture was left to react at room temperature for 1.5 h.

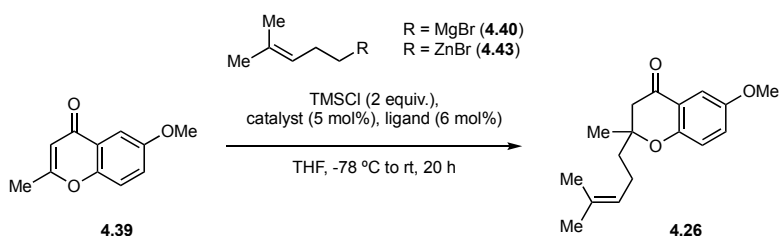
Conjugate Addition: A flame dried flask was charged with CuBr(SMe<sub>2</sub>) (1.228 g, 5.97 mmol, 0.10 equiv) and THF (200 mL). The mixture was cooled to -40 °C, the solution of **4.40** was added, and the mixture was left to stir for 30 min. TMS-Cl (12.98 g, 15.2 mL, 2.0 Eq, 119.5 mmol) was added to the reaction mixture followed by a solution of 6-methoxy-2-methyl-4H-chromen-4-one<sup>36</sup> (**4.39**) (11.36 g, 1 Eq, 59.7 mmol) in THF (50 mL). The mixture was left to react at -40 °C for 3 h. While the reaction was still cold, quenched with water. Diluted in diethyl ether and NH<sub>4</sub>Cl (aq., sat.). Stirred for 30 min while warming to room temperature. Then, the organic layer was separated, and

the aqueous layer was extracted with diethyl ether (x3). The combined organic layers were washed with brine, dried over MgSO<sub>4</sub>, filtered, and concentrated *in vacuo*. Purification by flash column chromatography over silica (hexanes:EtOAc, 99:1 to 9:1) afforded **4.26** as a yellow oil (10.00 g, 36.45 mmol, 61%). *R<sub>f</sub>* = 0.29 (hexanes:EtOAc, 9:1); <sup>1</sup>H NMR (400 MHz, CDCl<sub>3</sub>): δ 7.28 (d, J = 3.2 Hz, 1H), 7.08 (dd, J = 9.0, 3.2 Hz, 1H), 6.86 (d, J = 9.0 Hz, 1H), 5.06 (t, J = 7.0 Hz, 1H), 3.80 (s, 3H), 2.77 (d, J = 16.5 Hz, 1H), 2.65 (d, J = 16.5 Hz, 1H), 2.17 – 2.05 (m, 2H), 1.85 – 1.74 (m, 1H), 1.71 – 1.60 (m, 4H), 1.57 (s, 3H), 1.40 (s, 3H); <sup>13</sup>C NMR (151 MHz, CDCl<sub>3</sub>) δ 192.8, 154.6, 153.7, 132.4, 125.4, 123.5, 120.2, 119.8, 107.1, 81.0, 55.9, 47.6, 39.2, 25.8, 24.0, 22.4, 17.7.; IR (neat) 2971, 2933, 2915, 2859, 2836, 1686, 1619, 1485, 1430, 1282, 1218, 1052, 1034, 802, 701; HRMS (ESI) *m/z* calculated for C<sub>17</sub>H<sub>22</sub>O<sub>3</sub>H<sup>+</sup> ([M+H]<sup>+</sup>) 275.1642, found 275.1637.



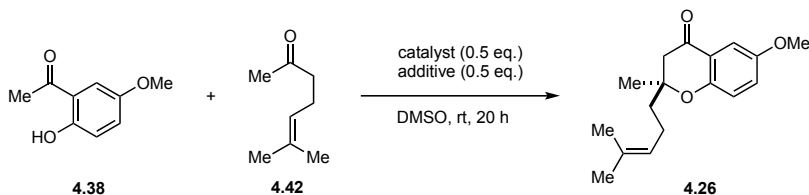
*General Procedure B (GP-B)*:<sup>39</sup> Charged a flame dried flask with pyrrolidine (1.50 mL, 18.13 mmol, 3.00 equiv), DMSO (12.0 mL), and butyric acid (0.55 mL, 6.05 mmol, 1.00 equiv). After the mixture was stirred for 10 min, ketone **4.42** (984 μL, 6.65 mmol, 1.10 equiv) was added dropwise. After stirring for an additional 15 min, acetophenone **4.38** (1.005 g, 6.05 mmol, 1.00 equiv) was added in one portion. The resulting reaction mixture was stirred at room temperature for 18 hours. Then, the reaction mixture was diluted with water (600 mL) and EtOAc (300 mL). The organic layer was separated, and the aqueous layer was extracted with EtOAc (2 x 300 mL). The combined organic layers were washed with 1 N HCl (300 mL) and brine (300 mL), dried over MgSO<sub>4</sub>, filtered, and concentrated *in vacuo*. Purification by flash column chromatography over silica (hexanes:DCM, 19:1 to 3:2) afforded **4.26** as a yellow oil (1.261 g, 4.60 mmol, 76%).

### Investigations into the Asymmetric Synthesis of **4.26**

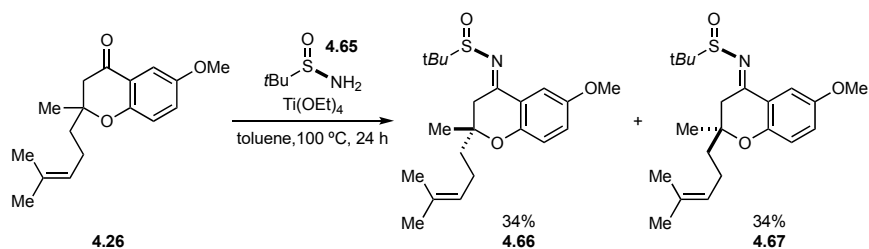


An asymmetric copper-catalyzed conjugate addition between **4.26** and **4.40/4.43** was explored using chiral ligands **4.44-4.48**. The results are tabulated in Table 4.1. The catalyst and ligand were

pre-stirred in THF at rt for 30 min, then cooled to -78 °C. Each reaction was subsequently completed according to *GP-A*, with any modifications indicated in Table 4.1.

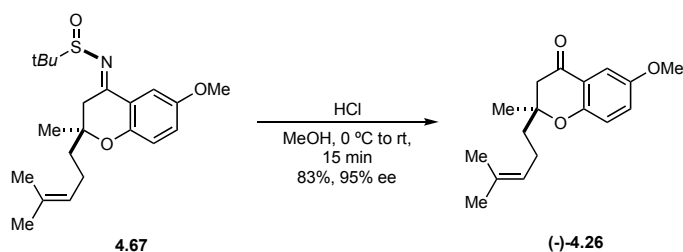


In addition, an asymmetric Kabbe condensation between **4.38** and **4.42** was explored using chiral catalysts **4.49-4.61**. The results are tabulated in Table 4.2. Each reaction was completed according to *GP-B*, with any modifications indicated in Table 4.2.



**(R)-N-((S,E)-6-methoxy-2-methyl-2-(4-methylpent-3-en-1-yl)chroman-4-ylidene)-2-methylpropane-2-sulfinamide (4.67)** and **(R)-N-((R,E)-6-methoxy-2-methyl-2-(4-methylpent-3-en-1-yl)chroman-4-ylidene)-2-methylpropane-2-sulfinamide (4.66)** Charged a flame dried flask with chromanone **4.26** (2.28 g, 8.31 mmol, 1.00 equiv), toluene (16.6 mL), titaniummethoxide (3.79 g, 16.6 mmol, 2.00 equiv), and (R)-(+)-2-methylpropane-2-sulphinamide (**4.65**) (1.01 g, 8.31 mmol, 1.00 equiv). The resulting mixture was stirred at 100 °C for 24 hours. Then, the reaction mixture was diluted in THF and quenched with 24% NaCl (aq.). The mixture was filtered through celite and the filtrate was washed with brine. The organic layer was separated, dried over MgSO<sub>4</sub>, filtered, and concentrated *in vacuo*. Purification by flash column chromatography over silica (hexanes:EtOAc, 99:1 to 4:1) afforded **4.66** as a yellow oil (1.06 g, 2.81 mmol, 34%) followed by **4.67** as a yellow oil (1.05 g, 2.78 mmol, 34%). (**4.66**) *R<sub>f</sub>* = 0.48 (hexanes:EtOAc, 7:3); [ $\alpha$ ]<sub>D</sub><sup>24</sup> = +15.6 (c = 0.10, MeOH); <sup>1</sup>H NMR (600 MHz, CDCl<sub>3</sub>) δ 7.42 (d, *J* = 3.2 Hz, 1H), 7.00 (dd, *J* = 9.0, 3.2 Hz, 1H), 6.81 (d, *J* = 9.0 Hz, 1H), 5.07 – 5.02 (m, 1H), 3.78 (s, 3H), 3.42 (d, *J* = 16.7 Hz, 1H), 3.09 (d, *J* = 16.7 Hz, 1H), 2.19 – 2.02 (m, 2H), 1.79 – 1.70 (m, 1H), 1.67 – 1.61 (m, 4H), 1.57 (s, 3H), 1.35 (s, 3H), 1.32 (s, 9H).; <sup>13</sup>C NMR (151 MHz, CDCl<sub>3</sub>) δ 170.30, 153.46, 151.78, 132.23, 123.60, 122.87, 120.22, 119.54, 108.19, 78.62, 57.93, 55.81, 39.86, 38.94, 25.78, 23.96, 22.76, 22.29, 17.76; IR (neat) 2967, 2913, 2870, 2834, 1740, 1622,

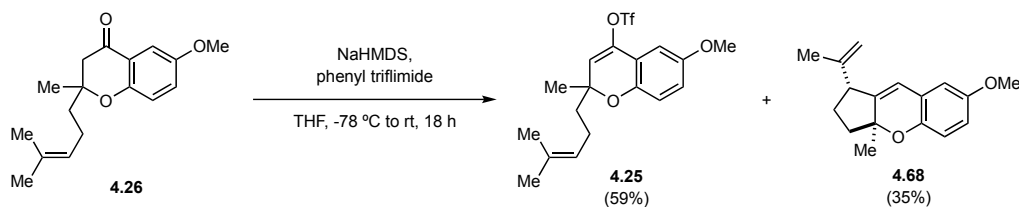
1594, 1487, 1426, 1285, 1220, 1199, 1068, 1032, 895, 688; **HRMS** (ESI)  $m/z$  calculated for  $C_{21}H_{31}NO_3S^+H$  ( $[M+H]^+$ ) 378.2098, found 378.2094. (**4.67**)  $R_f = 0.43$  (hexanes:EtOAc, 7:3);  $[\alpha]_D^{24} = -139.6$  ( $c = 0.10$ , MeOH);  **$^1H$  NMR** (500 MHz,  $CDCl_3$ )  $\delta$  7.41 (d,  $J = 3.1$  Hz, 1H), 7.00 (dd,  $J = 9.0, 3.2$  Hz, 1H), 6.81 (d,  $J = 9.0$  Hz, 1H), 5.05 (t,  $J = 7.1$  Hz, 1H), 3.78 (s, 3H), 3.35 (d,  $J = 16.6$  Hz, 1H), 3.19 (d,  $J = 16.6$  Hz, 1H), 2.16 – 2.01 (m, 2H), 1.75 – 1.69 (m, 1H), 1.66 (s, 3H), 1.64 – 1.58 (m, 1H), 1.57 (s, 3H), 1.38 (s, 3H), 1.32 (s, 9H).;  **$^{13}C$  NMR** (126 MHz,  $CDCl_3$ )  $\delta$  170.24, 153.47, 151.73, 132.32, 123.59, 122.80, 120.30, 119.55, 108.22, 78.70, 58.00, 55.83, 39.74, 38.63, 25.80, 24.22, 22.79, 22.48, 17.74.; **IR** (neat) 2975, 2924, 2865, 2835, 1740, 1590, 1485, 1427, 1284, 1214, 1086, 1037, 890, 823, 735, 694; **HRMS** (ESI)  $m/z$  calculated for  $C_{21}H_{31}NO_3S^+H$  ( $[M+H]^+$ ) 378.2098, found 378.2092.



**(S)-6-methoxy-2-methyl-2-(4-methylpent-3-en-1-yl)chroman-4-one [(-)-4.26]** Charged a flask with **4.67** (1.44 g, 3.81 mmol, 1.00 equiv) and methanol (8.80 mL). The resulting mixture was cooled to 0 °C in an ice bath, then a solution of HCl (aq.) (556 mg, 1.27 mL, 12 molar, 15.3 mmol, 4.00 equiv) was added dropwise while stirring. The mixture was removed from the cold bath and allowed to warm to room temp. for 15 minutes. The reaction was quenched with  $NaHCO_3$  (sat. aq.) and diluted with DCM. The organic layer was separated, and the aqueous layer was extracted with DCM (x3). The combined organic layers were washed with brine, dried over  $Na_2SO_4$ , filtered, and concentrated *in vacuo*. Purification by flash column chromatography over silica (hexanes:EtOAc, 99:1 to 17:3) afforded **(-)-4.26** as a yellow oil (866 mg, 3.16 mmol, 83%).  $R_f = 0.29$  (hexanes:EtOAc, 9:1);  $[\alpha]_D^{24} = -43.6$  ( $c = 0.10$ , MeOH); **HPLC** (Daicel Chiralpak OJ-H, hexanes:isopropanol 99.9:0.1 to 99.7:0.3) 13.3 min (minor), 23.2 min (major);  **$^1H$  NMR** (401 MHz,  $CDCl_3$ ):  $\delta$  7.28 (d,  $J = 3.2$  Hz, 1H), 7.08 (dd,  $J = 9.0, 3.2$  Hz, 1H), 6.86 (d,  $J = 9.0$  Hz, 1H), 5.06 (t,  $J = 7.0$  Hz, 1H), 3.80 (s, 3H), 2.77 (d,  $J = 16.5$  Hz, 1H), 2.65 (d,  $J = 16.5$  Hz, 1H), 2.17 – 2.05 (m, 2H), 1.85 – 1.74 (m, 1H), 1.71 – 1.60 (m, 4H), 1.57 (s, 3H), 1.40 (s, 3H);  **$^{13}C$  NMR** (151 MHz,  $CDCl_3$ )  $\delta$  192.8, 154.6, 153.7, 132.4, 125.4, 123.5, 120.2, 119.8, 107.1, 81.0, 55.9, 47.6, 39.2, 25.8, 24.0, 22.4, 17.7.; **IR** (neat) 2971, 2933, 2915, 2859, 2836, 1686, 1619, 1485, 1430,

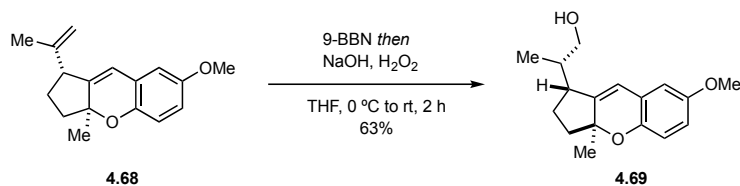
1282, 1218, 1052, 1034, 802, 701; **HRMS** (ESI)  $m/z$  calculated for  $C_{17}H_{22}O_3H^+$  ( $[M+H]^+$ ) 275.1642, found 275.1637.

### Model Systems and Initial Route

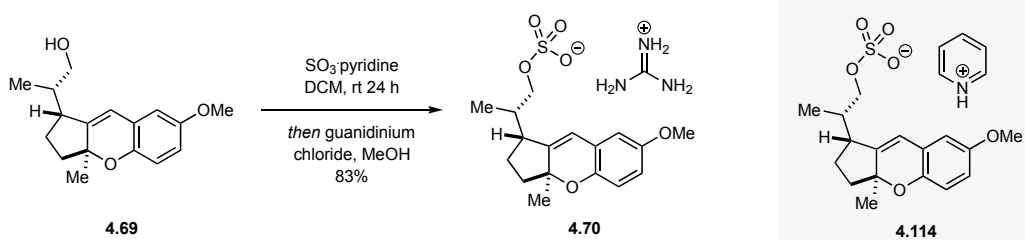


**6-methoxy-2-methyl-2-(4-methylpent-3-en-1-yl)-2H-chromen-4-yl trifluoromethanesulfonate (4.25) and (1*R*\*,3*aS*\*)-7-methoxy-3*a*-methyl-1-(prop-1-en-2-yl)-1,2,3,3*a*-tetrahydrocyclopenta[*b*]chromene (4.68)** Charged a flame dried flask with **4.26** (1.092 g, 3.98 mmol, 1.00 equiv) and THF (15 mL) and cooled to -78 °C. In a separate flame dried flask, NaHMDS (1.094 g, 5.97 mmol, 1.50 equiv) was dissolved in THF (5 mL). This mixture was then added dropwise to the solution chromanone **4.26** at -78 °C. After stirring at -78 °C for 1 hour, phenyl triflimide (1.706 g, 4.78 mmol, 1.20 equiv) was added in one portion. The reaction mixture was allowed to warm to room temperature and stirred for 18 h. Then, the reaction mixture was quenched with water and diluted with EtOAc. The organic layer was separated, and the aqueous layer was extracted with EtOAc (x3). The combined organic layers were washed with  $NH_4Cl$  (aq. sat.), brine, dried over  $MgSO_4$ , filtered, and concentrated *in vacuo*. Purification by flash column chromatography over silica (hexanes:DCM, 19:1 to 3:2) afforded **4.25** as a colorless oil (956 mg, 2.35 mmol, 59%) and **4.68** as a yellow oil (359 mg, 1.40 mmol, 35%). (**4.26**)  $R_f$  = 0.38 (hexanes:DCM, 3:2);  $^1H$  NMR (700 MHz,  $CDCl_3$ )  $\delta$  6.83 – 6.74 (m, 3H), 5.61 (s, 1H), 5.08 (t,  $J$  = 7.0 Hz, 1H), 3.77 (s, 3H), 2.19 – 2.06 (m, 2H), 1.84 – 1.77 (m, 1H), 1.73 – 1.68 (m, 1H), 1.67 (s, 3H), 1.58 (s, 3H), 1.45 (s, 3H);  $^{13}C$  NMR (176 MHz,  $CDCl_3$ )  $\delta$  154.0, 147.7, 142.6, 132.5, 123.5, 118.7 (q,  $J$  = 320 Hz), 118.6, 117.7, 117.3, 116.6, 106.4, 80.0, 55.9, 41.0, 26.1, 25.8, 22.8, 17.7; **IR** (neat) 2972, 2929, 2859, 2837, 1661, 1615, 1579, 1488, 1424, 1207, 1139, 1040, 1020, 1010, 868, 848, 815, 784, 760, 706; **HRMS** (ESI)  $m/z$  calculated for  $C_{18}H_{21}F_3O_5S^+$  ( $[M]^+$ ) 406.1062, found 406.1059. (**4.68**)  $R_f$  = 0.26 (hexanes:DCM, 3:2);  $^1H$  NMR (700 MHz,  $CDCl_3$ )  $\delta$  6.78 (d,  $J$  = 8.7 Hz, 1H), 6.65 (dd,  $J$  = 8.7, 2.9 Hz, 1H), 6.60 (d,  $J$  = 2.9 Hz, 1H), 6.13 (d,  $J$  = 1.84 Hz, 1H), 4.85 (d,  $J$  = 56.0 Hz, 2H), 3.76 (s, 3H), 3.45 (t,  $J$  = 8.7 Hz, 1H), 2.11 – 2.02 (m, 3H), 1.75 (s, 3H), 1.67 – 1.58 (m, 1H), 1.30 (s, 3H);  $^{13}C$  NMR (176 MHz,  $CDCl_3$ )  $\delta$  154.2, 146.2, 146.2, 146.0, 124.4, 117.7, 117.0, 113.3, 111.7, 111.2, 82.9, 55.8, 48.8, 38.8, 28.3, 22.1, 20.2.; **IR** (neat)

2965, 2871, 2832, 1645, 1610, 1578, 1484, 1268, 1212, 1178, 1159, 1038, 882, 798, 762, 692;  
**HRMS** (ESI)  $m/z$  calculated for  $C_{17}H_{20}O_2H^+$  ( $[M+H]^+$ ) 257.1536, found 257.1533.



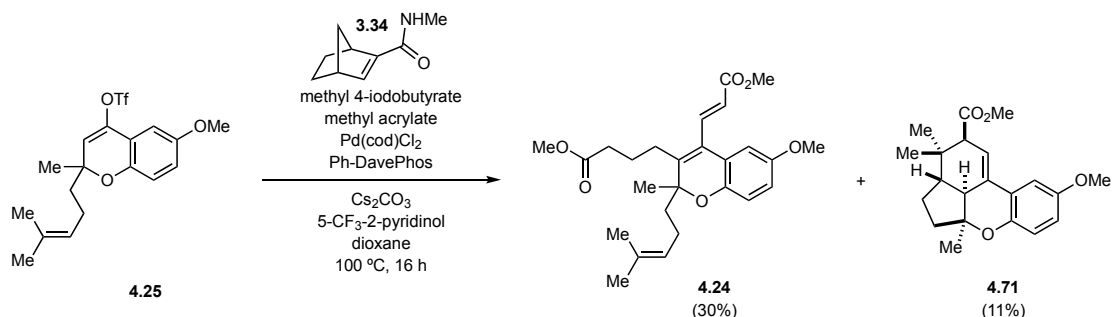
**(*S*<sup>\*</sup>)-2-((1*R*<sup>\*</sup>,3*aS*<sup>\*</sup>)-7-methoxy-3*a*-methyl-1,2,3,3*a*-tetrahydrocyclopenta[*b*]chromen-1-yl)propan-1-ol (4.69)** Charged flame dried flask with **4.68** (133 mg, 519  $\mu$ mol, 1.00 equiv) and THF (3.00 mL), then cooled this solution to 0 °C. Added 9-BBN (1.04 mL, 0.5 M in THF, 519  $\mu$ mol, 1.00 equiv) and stirred the reaction mixture at room temperature for 1 h. Returned the reaction to 0 °C then added NaOH (0.5 mL, 2 M) followed by H<sub>2</sub>O<sub>2</sub> (53  $\mu$ L, 30% w/w in water, 519  $\mu$ mol, 1.00 equiv). Stirred this mixture at room temperature for 1 h. Then, diluted the reaction with water and Et<sub>2</sub>O. The organic layer was separated, and the aqueous layer was extracted with Et<sub>2</sub>O (x3). The combined organic layers were washed with brine, dried over MgSO<sub>4</sub>, filtered, and concentrated *in vacuo*. Purification by flash chromatography over silica (hexanes:EtOAc, 9:1 to 1:1) afforded **4.69** as a colorless oil (90 mg, 328  $\mu$ mol, 63%). **R<sub>f</sub>** = 0.42 (hexanes:EtOAc, 1:1); **<sup>1</sup>H NMR** (500 MHz, CDCl<sub>3</sub>)  $\delta$  6.75 (d,  $J$  = 8.6 Hz, 1H), 6.64 (dd,  $J$  = 8.7, 2.8 Hz, 1H), 6.58 (d,  $J$  = 2.8 Hz, 1H), 6.24 – 6.13 (d,  $J$  = 1.5 Hz, 1H), 3.76 (m, 4H), 3.58 – 3.51 (m, 1H), 2.84 (q,  $J$  = 7.4 Hz, 1H), 2.07 – 1.93 (m, 3H), 1.85 (dt,  $J$  = 13.4, 6.8 Hz, 1H), 1.54 (m, 1H), 1.34 (t,  $J$  = 5.1 Hz, 1H), 1.27 (s, 3H), 1.09 (d,  $J$  = 6.8 Hz, 3H); **<sup>13</sup>C NMR** (126 MHz, CDCl<sub>3</sub>)  $\delta$  154.2, 146.6, 146.1, 124.3, 117.4, 116.9, 113.3, 111.6, 83.1, 66.3, 55.8, 43.4, 39.7, 38.7, 26.1, 22.2, 15.4; **IR** (neat) 3434, 2960, 2875, 2834, 1733, 1485, 1465, 1269, 1214, 1183, 1159, 1036, 971, 877, 813, 756; **HRMS** (ESI)  $m/z$  calculated for  $C_{17}H_{22}O_3^+$  ( $[M]^+$ ) 274.1569, found 274.1561.



**Guanidinium (*S*<sup>\*</sup>)-2-((1*R*<sup>\*</sup>,3*aS*<sup>\*</sup>)-7-methoxy-3*a*-methyl-1,2,3,3*a*-tetrahydrocyclopenta[*b*]chromen-1-yl)propyl sulfate (4.70)** A flame dried flask was charged with Py·SO<sub>3</sub> (26 mg, 166  $\mu$ mol, 1.3 equiv). Added a solution of **4.69** (35 mg, 128  $\mu$ mol, 1.00 equiv) in DCM (0.6 mL) and

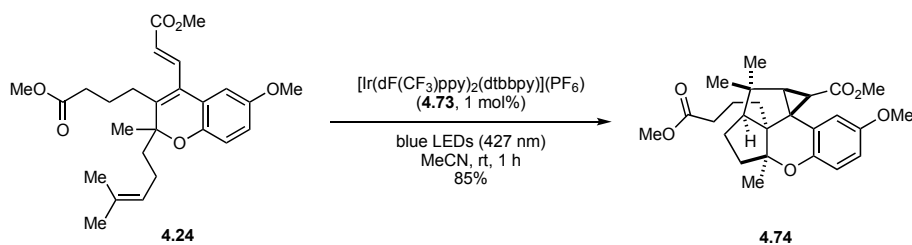


stirred this mixture at room temperature for 18 hours. Then, the reaction mixture was filtered, and the filtrate was concentrated *in vacuo*. To this residue was added guanidinium chloride (12 mg, 128  $\mu\text{mol}$ , 1.00 equiv) and methanol (2.0 mL). Slow evaporation of this homogeneous solution afforded **4.70** as a yellow crystalline solid (44 mg, 106  $\mu\text{mol}$ , 83%). In accordance with the literature,<sup>3</sup>  $^1\text{H}$ ,  $^{13}\text{C}$ , and IR data is provided for the intermediate pyridinium sulfate **4.114**.<sup>52</sup>  $^1\text{H}$  NMR (500 MHz,  $(\text{CD}_3)_2\text{SO}$ )  $\delta$  9.29 (d,  $J = 5.8$  Hz, 6H), 8.89 (d,  $J = 4.3$  Hz, 5H), 8.66 (t,  $J = 7.6$  Hz, 3H), 8.51 (s, 2H), 8.14 (t,  $J = 6.7$  Hz, 6H), 8.00 (s, 5H), 6.73 – 6.66 (m, 1H), 6.61 (dd,  $J = 8.7$ , 2.8 Hz, 1H), 6.24 (s, 1H), 3.77 (dd,  $J = 9.5$ , 5.0 Hz, 1H), 3.68 (m, 4H), 2.78 (q,  $J = 7.8$  Hz, 1H), 2.00 – 1.79 (m, 4H), 1.56 – 1.42 (m, 1H), 1.15 (s, 3H), 0.96 (d,  $J = 6.8$  Hz, 3H);  $^{13}\text{C}$  NMR (500 MHz,  $(\text{CD}_3)_2\text{SO}$ )  $\delta$  153.59, 146.98, 146.18, 145.41, 144.92, 143.21, 140.15, 127.98, 126.80, 123.90, 116.77, 116.37, 113.25, 111.19, 82.43, 68.70, 55.27, 42.48, 38.03, 36.45, 25.54, 21.81, 15.09; IR (neat) 3455, 3074, 2964, 2889, 1620, 1545, 1488, 1216, 1156, 1023, 971, 848, 750, 680; HRMS (ESI)  $m/z$  calculated for  $\text{C}_{17}\text{H}_{21}\text{O}_6\text{S}^-$  (M-H) $^-$  353.1064, found 353.1068.



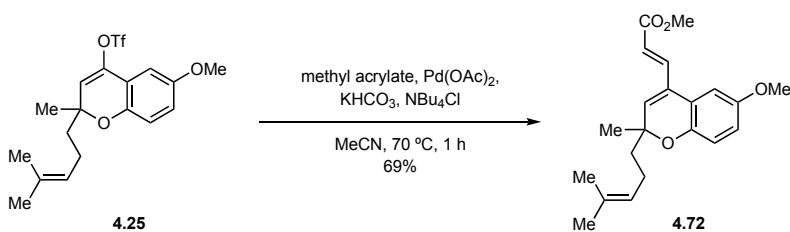
**Methyl (E)-4-(6-methoxy-4-(3-methoxy-3-oxoprop-1-en-1-yl)-2-methyl-2-(4-methylpent-3-en-1-yl)-2H-chromen-3-yl)butanoate (4.24) and methyl (2S\*,3aS\*,3a1S\*,5aS\*)-9-methoxy-3,3,5a-trimethyl-3,3a,3a1,4,5,5a-hexahydro-2H-indeno[1,7-bc]chromene-2-carboxylate (4.71)** In a glovebox, Pd(cod)Cl<sub>2</sub> (8.4 mg, 29.5  $\mu\text{mol}$ , 0.10 equiv) and Ph-DavePhos (11.3 mg, 29.5  $\mu\text{mol}$ , 0.10 equiv) were dissolved in a vial in 1,4-dioxane (1 mL). This mixture was stirred for 1 min. Vinyl triflate **4.25** (120 mg, 295  $\mu\text{mol}$ , 1.00 equiv), methyl 4-iodobutanoate (120  $\mu\text{L}$ , 886  $\mu\text{mol}$ , 3.00 equiv), methyl acrylate (40  $\mu\text{L}$ , 443  $\mu\text{mol}$ , 1.50 equiv), N-methylbicyclo[2.2.1]hept-2-ene-2-carboxamide<sup>24</sup> (22.3 mg, 148  $\mu\text{mol}$ , 0.50 equiv), 5-(trifluoromethyl)-2-pyridinol (9.6 mg, 59.1  $\mu\text{mol}$ , 0.20 equiv), Cs<sub>2</sub>CO<sub>3</sub> (289 mg, 886  $\mu\text{mol}$ , 3.00 equiv), and additional 1,4-dioxane (5 mL) were added to the reaction mixture. The vial was sealed, removed from the glovebox, and stirred at 100 °C for 16 h. Then, the mixture was filtered through a thin pad of silica eluting with EtOAc. The combined filtrate was concentrated *in vacuo*. Purification by flash column

chromatography over silica (hexanes:EtOAc, 99:1 to 4:1) afforded **4.24** as a colorless oil (40 mg, 91  $\mu\text{mol}$ , 31%) and **4.71** as a colorless oil (11 mg, 32  $\mu\text{mol}$ , 11%). (**4.24**)  $R_f = 0.23$  (hexanes:EtOAc, 4:1);  $^1\text{H NMR}$  (500 MHz,  $\text{CDCl}_3$ ) 7.61 (d,  $J = 16.2$  Hz, 1H), 6.80 (d,  $J = 8.6$  Hz, 1H), 6.74 (d,  $J = 2.8$  Hz, 1H), 6.70 (dd,  $J = 8.6, 2.8$  Hz, 1H), 6.15 (d,  $J = 16.2$  Hz, 1H), 4.99 (t,  $J = 6.9$  Hz, 1H), 3.81 (s, 3H), 3.75 (s, 3H), 3.70 (s, 3H), 2.45 – 2.35 (m, 3H), 2.29 – 2.17 (m, 1H), 2.13 – 2.02 (m, 2H), 1.85 – 1.76 (m, 2H), 1.75 – 1.68 (m, 1H), 1.63 (s, 3H), 1.52 (s, 3H), 1.51 – 1.46 (m, 4H);  $^{13}\text{C NMR}$  (126 MHz,  $\text{CDCl}_3$ )  $\delta$  173.5, 167.3, 153.8, 146.3, 143.6, 140.3, 132.0, 126.4, 123.9, 123.8, 123.1, 117.5, 113.8, 111.1, 80.0, 55.9, 51.9, 51.8, 37.4, 34.1, 29.4, 25.8, 25.4, 23.0, 22.3, 17.7; **IR** (neat) 2951, 2880, 1735, 1721, 1631, 1491, 1435, 1271, 1194, 1168, 1040, 987, 870, 816, 775, 722; **HRMS** (ESI)  $m/z$  calculated for  $\text{C}_{26}\text{H}_{34}\text{O}_6\text{Na}^+$  ( $[\text{M}+\text{Na}]^+$ ) 465.2247; found 465.2243. (**4.71**)  $R_f = 0.26$  (hexanes:EtOAc, 9:1);  $^1\text{H NMR}$  (600 MHz,  $\text{CDCl}_3$ )  $\delta$  6.89 (d,  $J = 3.0$  Hz, 1H), 6.80 (d,  $J = 8.7$  Hz, 1H), 6.72 (dd,  $J = 8.7, 3.0$  Hz, 1H), 6.05 (t,  $J = 2.9$  Hz, 1H), 3.78 (s, 3H), 3.74 (s, 3H), 2.96 (t,  $J = 2.5$  Hz, 1H), 2.19 – 2.15 (m, 2H), 1.96 (dt,  $J = 12.3, 2.1$  Hz, 1H), 1.79 – 1.68 (m, 2H), 1.49 – 1.38 (m, 1H), 1.29 (s, 3H), 1.15 (s, 3H), 0.92 (s, 3H);  $^{13}\text{C NMR}$  (151 MHz,  $\text{CDCl}_3$ )  $\delta$  174.08, 154.75, 147.64, 137.39, 125.42, 119.46, 114.99, 108.16, 82.93, 55.84, 54.84, 53.84, 51.69, 51.08, 42.19, 35.10, 27.15, 26.95, 24.86, 24.31; **IR** (neat) 2959, 2874, 2835, 1732, 1483, 1432, 1258, 1208, 1156, 1038, 923, 868, 847, 820, 791, 736; **HRMS** (ESI)  $m/z$  calculated for  $\text{C}_{21}\text{H}_{26}\text{O}_4\text{H}^+$  ( $[\text{M}+\text{H}]^+$ ) 343.1904; found 343.1898.

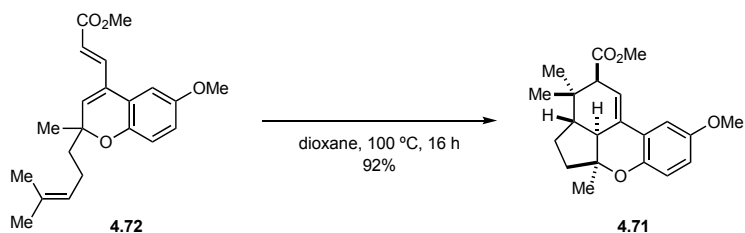


**Methyl (1*R*\*,1*aR*\*,2*a*<sup>1</sup>*S*\*,4*aS*\*,9*bS*\*)-8-methoxy-2*a*<sup>1</sup>-(4-methoxy-4-oxobutyl)-2,2,4*a*-trimethyl-1,1*a*,2,2*a*,2*a*<sup>1</sup>,3,4,4*a*-octahydrocyclopropa[5,6]pentaleno[1,6-*bc*]chromene-1-carboxylate (**4.74**)** Charged a flame dried flask with **4.24** (15 mg, 34  $\mu\text{mol}$ , 1.00 equiv), MeCN (0.400 mL) and  $\text{Ir}[(\text{dF}(\text{CF}_3)\text{ppy})_2\text{dtbbpy}]\text{PF}_6$  (0.3 mg, 0.34  $\mu\text{mol}$ , 0.01 equiv). The reaction mixture was degassed by sparging with nitrogen gas for 30 min. The flask was placed approximately 5 cm in front of two 40 W PR160-427 nm Kessil lights. The lights were set to 100% intensity, a fan was used for cooling, and the reaction was stirred for 1 h. Then, the reaction mixture was concentrated *in vacuo* and purification by flash column chromatography over silica (hexanes:EtOAc, 99:1 to 9:1) afforded **4.74** as a colorless solid (13 mg, 29  $\mu\text{mol}$ , 85%).  $R_f = 0.23$  (hexanes:EtOAc, 4:1);

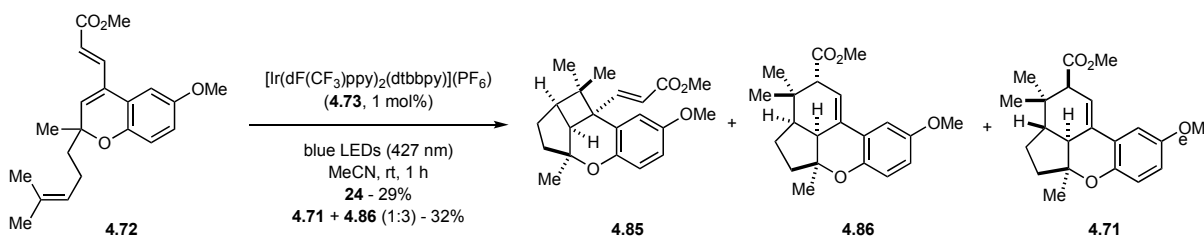
**<sup>1</sup>H NMR** (600 MHz, CDCl<sub>3</sub>) δ 6.69 (d, J = 8.7 Hz, 1H), 6.62 (dd, J = 8.7, 3.0 Hz, 1H), 6.51 (d, J = 3.0 Hz, 1H), 3.74 (s, 3H), 3.60 (s, 3H), 3.31 (s, 3H), 2.60 (q, J = 11.1 Hz, 1H), 2.43 (d, J = 2.6 Hz, 1H), 2.26 – 2.18 (m, 2H), 2.17 – 2.06 (m, 2H), 2.00 (dd, J = 13.7, 8.6 Hz, 1H), 1.83 – 1.72 (m, 1H), 1.71 – 1.62 (m, 2H), 1.50 – 1.38 (m, 1H), 1.35 (s, 3H), 1.28 (s, 3H), 1.22 (td, J = 14.2, 13.4, 5.6 Hz, 1H), 1.16 (s, 3H), 1.10 (m, 1H); **<sup>13</sup>C NMR** (126 MHz, CDCl<sub>3</sub>) δ 173.8, 170.2, 152.5, 151.0, 125.3, 115.8, 112.8, 112.5, 92.7, 59.0, 55.8, 51.6, 51.5, 48.5, 48.5, 45.9, 40.9, 36.9, 35.8, 34.1, 33.0, 30.7, 26.8, 24.2, 24.2, 22.8; **IR** (neat) 2958, 1728, 1464, 1429, 1269, 1209, 1159, 1140, 1032, 927, 888, 874, 848, 814, 783; **HRMS** (ESI) *m/z* calculated for C<sub>26</sub>H<sub>34</sub>O<sub>6</sub>H<sup>+</sup> ([M+H]<sup>+</sup>) 443.2438, found 443.2424.



**Methyl (E)-3-(6-methoxy-2-methyl-2-(4-methylpent-3-en-1-yl)-2H-chromen-4-yl)acrylate (4.72)** Charged a flamed dried flask with potassium bicarbonate (185 mg, 1.85 mmol, 3.00 equiv), palladium(II) acetate (2.07 mg, 9.23 μmol, 0.015 equiv) and tetrabutylammonium chloride (205 mg, 738 μmol, 1.20 equiv). A solution of **4.25** (250 mg, 615 μmol, 1.00 equiv) in MeCN (5.00 mL) was then added, followed by methyl acrylate (223 μL, 2.46 mmol, 4.00 equiv). The reaction mixture was stirred at 70 °C for 1 h. The mixture was concentrated *in vacuo*, re-dissolved in DCM, and diluted with water. The organic layer was separated, and the aqueous layer was extracted with DCM (x3). The combined organic layers were washed with brine, dried over Na<sub>2</sub>SO<sub>4</sub>, filtered, and concentrated *in vacuo*. Purification by flash column chromatography over silica (hexanes:EtOAc, 99:1 to 17:3) afforded **4.72** as a colorless oil (145 mg, 423 μmol, 69%). **R<sub>f</sub>** = 0.27 (hexanes:EtOAc, 9:1); **<sup>1</sup>H NMR** (600 MHz, CDCl<sub>3</sub>) δ 7.57 (d, J = 15.9 Hz, 1H), 6.83 (d, J = 2.9 Hz, 1H), 6.79 (d, J = 8.7 Hz, 1H), 6.74 (dd, J = 8.7, 2.9 Hz, 1H), 6.29 (d, J = 15.9 Hz, 1H), 5.94 (s, 1H), 5.07 (t, J = 7.1 Hz, 1H), 3.80 (s, 3H), 3.77 (s, 3H), 2.15 – 2.05 (m, 2H), 1.76 – 1.67 (m, 2H), 1.66 (s, 3H), 1.56 (s, 3H), 1.38 (s, 3H); **<sup>13</sup>C NMR** (151 MHz, CDCl<sub>3</sub>) δ 167.2, 154.0, 147.0, 141.3, 132.6, 132.1, 129.7, 124.0, 121.3, 120.9, 117.7, 114.9, 109.8, 77.7, 56.0, 51.9, 40.2, 25.8, 25.2, 22.8, 17.8; **IR** (neat) 2969, 2949, 2925, 2857, 2845, 2838, 1719, 1486, 1429, 1308, 1262, 1168, 1039, 979, 821, 737; **HRMS** (ESI) *m/z* calculated for C<sub>21</sub>H<sub>26</sub>O<sub>4</sub>H<sup>+</sup> ([M+H]<sup>+</sup>) 343.1904, found 343.1903.



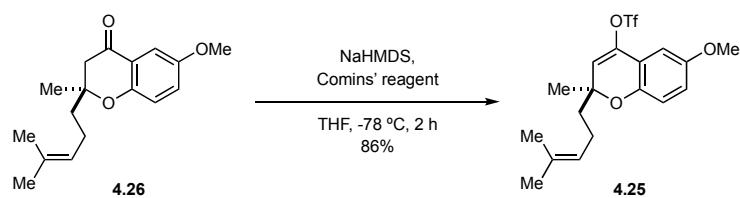
**Methyl (2*S*\*,3*aS*\*,3*a*<sup>1</sup>*S*\*,5*aS*\*)-9-methoxy-3,3,5*a*-trimethyl-3,3*a*,3*a*<sup>1</sup>,4,5,5*a*-hexahydro-2*H*-indeno[1,7-*bc*]chromene-2-carboxylate (4.71)** Charged a flame dried flask with **4.72** (34 mg, 99  $\mu$ mol, 1.00 equiv) and dioxane (3.0 mL). The reaction mixture was degassed by sparging with nitrogen gas for 15 mins. The reaction mixture was stirred at 100 °C for 16 h. Then, the reaction mixture was concentrated *in vacuo* and purification by flash column chromatography over silica (hexanes:EtOAc, 99:1 to 9:1) afforded **4.71** as a colorless oil (31 mg, 91  $\mu$ mol, 92%).  $R_f$  = 0.26 (hexanes:EtOAc, 9:1);  $^1\text{H NMR}$  (600 MHz,  $\text{CDCl}_3$ )  $\delta$  6.89 (d,  $J$  = 3.0 Hz, 1H), 6.80 (d,  $J$  = 8.7 Hz, 1H), 6.72 (dd,  $J$  = 8.7, 3.0 Hz, 1H), 6.05 (t,  $J$  = 2.9 Hz, 1H), 3.78 (s, 3H), 3.74 (s, 3H), 2.96 (t,  $J$  = 2.5 Hz, 1H), 2.19 – 2.15 (m, 2H), 1.96 (dt,  $J$  = 12.3, 2.1 Hz, 1H), 1.79 – 1.68 (m, 2H), 1.49 – 1.38 (m, 1H), 1.29 (s, 3H), 1.15 (s, 3H), 0.92 (s, 3H);  $^{13}\text{C NMR}$  (151 MHz,  $\text{CDCl}_3$ )  $\delta$  174.1, 154.8, 147.6, 137.4, 125.4, 119.5 (2C), 115.0, 108.2, 82.9, 55.8, 54.8, 53.8, 51.7, 51.1, 42.2, 35.1, 27.1, 26.95, 24.86, 24.31; **IR** (neat) 2959, 2874, 2835, 1732, 1483, 1432, 1258, 1208, 1156, 1038, 923, 868, 847, 820, 791, 736; **HRMS** (ESI)  $m/z$  calculated for  $\text{C}_{21}\text{H}_{26}\text{O}_4\text{H}^+$  ( $[\text{M}+\text{H}]^+$ ) 343.1904; found 343.1898.



**methyl (E)-3-((1*aR*\*,1*a*<sup>1</sup>*S*\*,3*aS*\*,8*bS*\*)-7-methoxy-1,1,3*a*-trimethyl-1,1*a*,1*a*<sup>1</sup>,2,3,3*a*-hexahydro-8*bH*-4-oxabenzof[*f*]cyclobuta[*cd*]inden-8*b*-yl)acrylate (4.85)** and **methyl (2*S*\*,3*aS*\*,3*a*<sup>1</sup>*S*\*,5*aS*\*)-9-methoxy-3,3,5*a*-trimethyl-3,3*a*,3*a*<sup>1</sup>,4,5,5*a*-hexahydro-2*H*-indeno[1,7-*bc*]chromene-2-carboxylate (4.71)** and **methyl (2*R*\*,3*aR*\*,3*a*<sup>1</sup>*S*\*,5*aS*\*)-9-methoxy-3,3,5*a*-trimethyl-3,3*a*,3*a*<sup>1</sup>,4,5,5*a*-hexahydro-2*H*-indeno[1,7-*bc*]chromene-2-carboxylate (4.86)** Charged a flame dried flask with **4.72** (97 mg, 283  $\mu$ mol, 1.00 equiv), MeCN (90 mL) and  $\text{Ir}[(\text{dF}(\text{CF}_3)\text{ppy})_2\text{dtbbpy}]\text{PF}_6$  (3.2 mg, 2.83  $\mu$ mol, 0.01 equiv). The reaction mixture was degassed by sparging with nitrogen gas for 30 min. The flask was placed approximately 5 cm in front of two

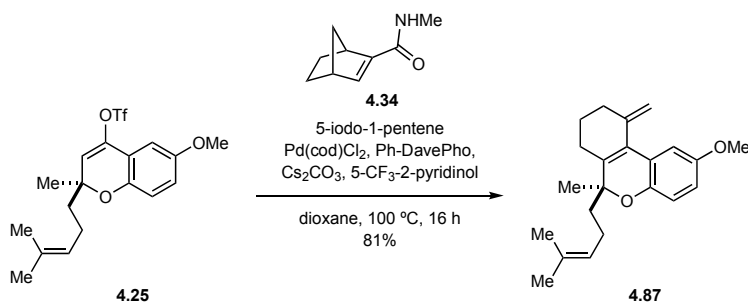
40 W PR160-427 nm Kessil lights. The lights were set to 100% intensity, a fan was used for cooling, and the reaction was stirred for 1 h. Then, the reaction mixture was concentrated *in vacuo* and purification by flash column chromatography over silica (hexanes:EtOAc, 99:1 to 9:1) afforded **4.85** as a colorless oil (28 mg, 82  $\mu$ mol, 29%) and **4.71** + **4.86** as a colorless oil (1:3, 31 mg, 91  $\mu$ mol, 32%). (**4.85**) **R<sub>f</sub>** = 0.23 (hexanes:EtOAc, 9:1); **<sup>1</sup>H NMR** (500 MHz, CDCl<sub>3</sub>)  $\delta$  7.36 (d, *J* = 15.6 Hz, 1H), 6.78 (d, *J* = 8.8 Hz, 1H), 6.69 (dd, *J* = 8.8, 3.0 Hz, 1H), 6.46 (d, *J* = 2.9 Hz, 1H), 5.68 (d, *J* = 15.6 Hz, 1H), 3.75 (s, 3H), 3.69 (s, 3H), 2.76 (d, *J* = 8.2 Hz, 1H), 2.31 (t, *J* = 8.0 Hz, 1H), 2.04 – 1.94 (m, 1H), 1.75 – 1.68 (m, 1H), 1.66 – 1.47 (m, 2H), 1.43 (s, 3H), 1.24 (s, 3H), 0.87 (s, 3H); **<sup>13</sup>C NMR** (126 MHz, CDCl<sub>3</sub>)  $\delta$  167.5, 154.1, 153.4, 147.2, 126.7, 119.4, 118.4, 114.8, 113.1, 84.7, 55.8, 51.6, 46.0, 46.0, 45.1, 43.5, 36.8, 29.7, 27.8, 25.5, 22.1; **IR** (neat) 2952, 2866, 2835, 1721, 1640, 1492, 1463, 1436, 1376, 1297, 1267, 1176, 1129, 1040, 809, 771; **HRMS** (ESI) *m/z* calculated for C<sub>21</sub>H<sub>26</sub>O<sub>4</sub>H<sup>+</sup> ([M+H]<sup>+</sup>) 343.1904, found 343.1903. (**4.71** + **4.86**) **R<sub>f</sub>** = 0.26 (hexanes:EtOAc, 9:1); **<sup>1</sup>H NMR** (700 MHz, CDCl<sub>3</sub>)  $\delta$  6.90 – 6.87 (m, 1.3H), 6.81 – 6.71 (m, 2.6H), 6.05 (s, 0.3H), 6.02 (s, 1H), 3.77 (s, 3.9H), 3.74 (s, 0.9H), 3.68 (s, 3H), 3.07 (s, 1H), 2.96 (s, 0.3H), 2.35 (s, 1H), 2.19 – 2.15 (m, 0.6H), 2.05 (d, *J* = 7.5 Hz, 1H), 2.00 – 1.9 (m, 2.3H), 1.77 – 1.70 (m, 0.6H), 1.66 – 1.57 (m, 1H), 1.55 – 1.49 (m, 1H), 1.49 – 1.41 (m, 3.3H), 1.30 (s, 0.9H), 1.20 – 1.15 (m, 3.9H), 1.06 (s, 3H), 0.92 (s, 0.9H); **<sup>13</sup>C NMR** (176 MHz, CDCl<sub>3</sub>)  $\delta$  174.2, 174.1, 154.7, 153.5, 147.6, 146.9, 137.4, 129.7, 125.4, 121.8, 119.5 (2C), 119.0, 117.8, 116.1, 115.0, 108.6, 108.1, 84.3, 82.9, 56.0, 55.8, 54.8, 53.8, 51.7, 51.7, 51.4, 51.0, 46.8, 42.5, 42.2, 35.2, 35.1, 33.9, 32.9, 27.1 (2C), 27.0, 25.5, 24.9, 24.3, 20.8; **IR** (neat) 2959, 2874, 2835, 1732, 1483, 1432, 1258, 1208, 1156, 1038, 923, 868, 847, 820, 791, 736; **HRMS** (ESI) *m/z* calculated for C<sub>21</sub>H<sub>26</sub>O<sub>4</sub>H<sup>+</sup> ([M+H]<sup>+</sup>) 343.1904; found 343.1898.

### Total Synthesis of Cochlearol B



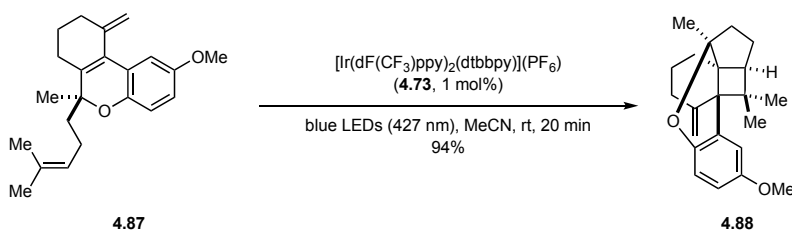
**(S)-6-methoxy-2-methyl-2-(4-methylpent-3-en-1-yl)-2H-chromen-4-yl trifluoromethanesulfonate [4.25]** Charged a flame dried flask with NaHMDS (2.16 g, 11.8 mmol, 1.10 equiv) and THF (24 mL), then cooled this mixture to -78 °C. A solution of **4.26** (2.94 g, 10.7 mmol, 1.00 equiv) in THF (8 mL) was then added. After stirring for 1 h at -78 °C, a solution of Comins' reagent

(4.63 g, 11.8 mmol, 1.10 equiv) in THF (8 mL) was added and the mixture was stirred at -78 °C for 2 h. Then, the reaction mixture was quenched with water and diluted with diethyl ether and NaHCO<sub>3</sub> (aq. sat.). The organic layer was separated, and the aqueous layer was extracted with diethyl ether (x3). The combined organic layers were washed with brine, dried over MgSO<sub>4</sub>, filtered, and concentrated *in vacuo*. Purification by flash column chromatography over silica (hexanes:DCM, 19:1 to 3:2) afforded **4.25** as a yellow oil (3.75 g, 9.23 mmol, 86%). *R<sub>f</sub>* = 0.54 (hexanes:EtOAc, 9:1); [ $\alpha$ ]<sub>D</sub><sup>23</sup> = +109.7 (c = 0.10, MeOH); <sup>1</sup>H NMR (700 MHz, CDCl<sub>3</sub>) δ 6.83 – 6.74 (m, 3H), 5.61 (s, 1H), 5.08 (t, J = 7.0 Hz, 1H), 3.77 (s, 3H), 2.19 – 2.06 (m, 2H), 1.84 – 1.77 (m, 1H), 1.73 – 1.68 (m, 1H), 1.67 (s, 3H), 1.58 (s, 3H), 1.45 (s, 3H); <sup>13</sup>C NMR (176 MHz, CDCl<sub>3</sub>) δ 154.0, 147.7, 142.6, 132.5, 123.5, 118.7 (q, J = 320 Hz), 118.6, 117.7, 117.3, 116.6, 106.4, 80.0, 55.9, 41.0, 26.1, 25.8, 22.8, 17.7; IR (neat) 2972, 2929, 2859, 2837, 1661, 1615, 1579, 1488, 1424, 1207, 1139, 1040, 1020, 1010, 868, 848, 815, 784, 760, 706; HRMS (ESI) *m/z* calculated for C<sub>18</sub>H<sub>21</sub>F<sub>3</sub>O<sub>5</sub>S<sup>+</sup> ([M]<sup>+</sup>) 406.1062, found 406.1059.

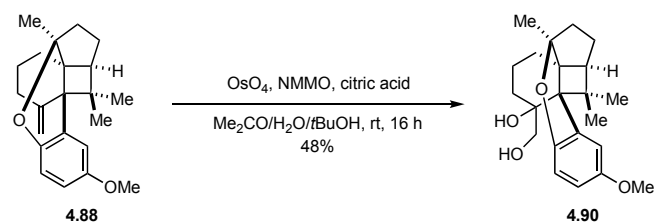


**(S)-2-methoxy-6-methyl-10-methylene-6-(4-methylpent-3-en-1-yl)-7,8,9,10-tetrahydro-6H-benzo-[c]chromene (4.87)** In a glovebox, Pd(cod)Cl<sub>2</sub> (70 mg, 246 μmol, 0.10 equiv) and Ph-DavePhos (94 mg, 246 μmol, 0.10 equiv) were dissolved in 1,4-dioxane (10 mL). This mixture was stirred for 1 min. Vinyl triflate **4.25** (1.00 g, 2.46 mmol, 1.00 equiv), 5-iodopent-1-ene (923 μL, 7.38 mmol, 3.00 equiv), N-methylbicyclo[2.2.1]hept-2-ene-2-carboxamide<sup>24</sup> (186 mg, 1.23 mmol, 0.50 equiv), 5-(trifluoromethyl)-2-pyridinol (80 mg, 492 μmol, 0.20 equiv), Cs<sub>2</sub>CO<sub>3</sub> (2.41 g, 7.38 mmol, 3.00 equiv), and additional 1,4-dioxane (36 mL) were added to the reaction mixture. The flask was sealed with a rubber septum, removed from the glovebox, and stirred at 100 °C for 16 h. Then, the mixture was filtered through a thin pad of silica eluting with EtOAc. The combined filtrate was concentrated *in vacuo*. Purification by flash column chromatography over silica gel (hexanes:EtOAc, 49:1 to 4:1) followed by purification by flash chromatography over C-18 silica (Water:MeCN, 1:4 to 0:1) afforded **4.87** as a colorless oil (647 mg, 1.99 mmol, 81%). *R<sub>f</sub>* = 0.57

(hexanes:EtOAc, 9:1) and on C-18 silica  $R_f = 0.19$  (Water/MeCN, 1:4);  $[\alpha]_D^{23} = +65.8$  ( $c = 0.10$ , MeOH);  $^1\text{H NMR}$  (500 MHz,  $\text{CDCl}_3$ )  $\delta$  7.07 (d,  $J = 3.0$  Hz, 1H), 6.81 (d,  $J = 8.6$  Hz, 1H), 6.67 (dd,  $J = 8.7, 3.0$  Hz, 1H), 5.18 (d,  $J = 53.8$  Hz, 2H), 5.03 (t,  $J = 7.8$  Hz, 1H), 3.76 (s, 3H), 2.45 – 2.34 (m, 2H), 2.25 (qt,  $J = 18.5, 6.3$  Hz, 2H), 2.16 – 1.99 (m, 2H), 1.92 – 1.80 (m, 2H), 1.71 – 1.59 (m, 4H), 1.56 – 1.48 (m, 4H), 1.35 (s, 3H).;  $^{13}\text{C NMR}$  (126 MHz,  $\text{CDCl}_3$ )  $\delta$  153.2, 151.8, 148.3, 130.6, 118.3, 115.9, 112.3, 110.9, 86.1, 55.7, 53.6, 50.6, 47.4, 42.3, 38.8, 33.8, 30.1, 29.8, 23.8, 23.7, 23.5, 19.9.; **IR** (neat) 2987, 2966, 2930, 2856, 2831, 1632, 1610, 1574, 1486, 1454, 1424, 1375, 1272, 1226, 1166, 1045, 882, 849, 765, 740; **HRMS** (ESI)  $m/z$  calculated for  $\text{C}_{22}\text{H}_{28}\text{O}_2\text{H}^+$  ( $[\text{M}+\text{H}]^+$ ) 325.2162; found 325.2160.

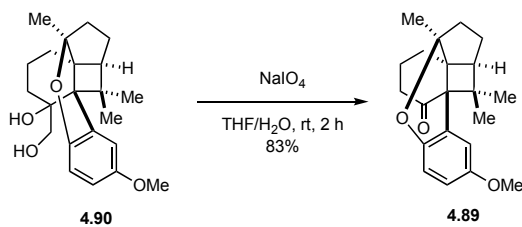


**(4a*S*,5*S*,7a*S*,12b*S*)-11-methoxy-7a,13,13-trimethyl-1-methylene-1,2,3,4,5,6,7,7a-octahydro-5,12b-methanobenzo[*c*]cyclopenta[*b*]chromene (4.88)** Charged a flame dried flask with **4.87** (300 mg, 925  $\mu\text{mol}$ , 1.00 equiv), MeCN (90 mL) and  $\text{Ir}[(\text{dF}(\text{CF}_3)\text{ppy})_2\text{dtbbpy}]\text{PF}_6$  (10.4 mg, 9.25  $\mu\text{mol}$ , 0.01 equiv). The reaction mixture was degassed by sparging with nitrogen gas for 20 min. The flask was placed approximately 5 cm in front of two 40 W PR160-427 nm Kessil lights. The lights were set to 100% intensity, a fan was used for cooling, and the reaction was stirred for 1 h. Then, the reaction mixture was concentrated *in vacuo* and purification by flash column chromatography over silica (hexanes:EtOAc, 99:1 to 9:1) afforded **4.88** as a colorless oil (283 mg, 872  $\mu\text{mol}$ , 94%).  $R_f = 0.48$  (hexanes:EtOAc, 9:1);  $[\alpha]_D^{23} = -117.7$  ( $c = 0.10$ , MeOH);  $^1\text{H NMR}$  (700 MHz,  $\text{CDCl}_3$ )  $\delta$  6.72 – 6.68 (m, 2H), 6.65 (dd,  $J = 8.7, 2.6$  Hz, 1H), 4.86 (d,  $J = 35.7$  Hz, 2H), 3.73 (s, 3H), 2.13 – 2.06 (m, 1H), 2.05 – 1.99 (m, 1H), 1.95 – 1.86 (m, 1H), 1.86 – 1.80 (m, 2H), 1.73 – 1.64 (m, 3H), 1.60 – 1.45 (m, 3H), 1.40 (s, 3H), 1.37 (s, 3H), 0.93 (s, 3H).;  $^{13}\text{C NMR}$  (126 MHz,  $\text{CDCl}_3$ )  $\delta$  153.5, 147.0, 140.8, 139.5, 131.8, 126.7, 124.3, 123.4, 117.7, 112.9, 112.2, 111.5, 79.6, 55.8, 37.0, 33.6, 26.0, 25.8, 23.9, 23.0, 22.4, 17.7.; **IR** (neat) 2945, 2865, 2831, 1489, 1455, 1374, 1267, 1229, 1210, 1137, 1043, 848, 802, 784, 773, 722; **HRMS** (ESI)  $m/z$  calculated for  $\text{C}_{22}\text{H}_{28}\text{O}_2\text{H}^+$  ( $[\text{M}+\text{H}]^+$ ) 325.2162, found 325.2157.



**(4a*S*,5*S*,7a*S*,12b*R*)-1-(hydroxymethyl)-11-methoxy-7a,13,13-trimethyl-1,2,3,4,5,6,7,7a-octahydro-5,12b-methanobenzo[*c*]cyclopenta[*b*]chromen-1-ol (4.90)**

Charged a flask with **4.88** (485 mg, 1.49 mmol, 1.00 equiv) and acetone:water (3:1, 16 mL). To this mixture was added osmium tetroxide (3.04 g, 3.8 mL, 2.5% wt in tBuOH, 299  $\mu$ mol, 0.20 equiv), citric acid (574 mg, 2.99 mmol, 2.00 equiv), and N-Methylmorpholine N-oxide (350 mg, 2.99 mmol, 2.00 equiv). This solution was stirred at room temperature for 16 h. Then, the reaction mixture was diluted with Na<sub>2</sub>SO<sub>4</sub> (aq. sat.) and EtOAc. The organic layer was separated, and the aqueous layer was extracted with EtOAc (x3). The combined organic layers were washed with brine, dried over MgSO<sub>4</sub>, filtered, and concentrated *in vacuo*. Purification by flash column chromatography over silica (hexanes:EtOAc, 9:1 to 2:3) afforded **4.90** as an off-white foam (247 g, 715  $\mu$ mol, 48%). **R<sub>f</sub>** = 0.18 (hexanes:EtOAc, 1:1);  $[\alpha]_{\text{D}}^{23} = +72.1$  (c = 0.10, MeOH); **<sup>1</sup>H NMR** (700 MHz, CDCl<sub>3</sub>)  $\delta$  6.81 (d, J = 8.5 Hz, 1H), 6.76 – 6.73 (m, 1H), 6.53 (s, 1H), 3.78 – 3.73 (m, 4H), 3.51 (d, J = 10.9 Hz, 1H), 2.20 – 2.13 (m, 2H), 2.09 – 2.00 (m, 2H), 2.00 – 1.85 (m, 3H), 1.59 (dd, J = 13.9, 7.6 Hz, 1H), 1.50 – 1.42 (m, 1H), 1.41 (s, 3H), 1.38 (dd, J = 13.0, 6.2 Hz, 1H), 1.34 (s, 3H), 0.95 (s, 3H); **<sup>13</sup>C NMR** (126 MHz, CDCl<sub>3</sub>)  $\delta$  152.3, 150.1, 127.1, 119.5, 118.1, 113.7, 87.2, 77.2, 69.7, 55.8, 52.0, 48.8, 47.7, 39.1, 37.3, 29.9, 29.3, 26.3, 24.8, 24.4, 24.1, 17.8; **IR** (neat) 3473, 3468, 2950, 2881, 2834, 1489, 1414, 1376, 1265, 1219, 1137, 1039, 860, 807, 784, 733, 703; **HRMS** (ESI) m/z calculated for C<sub>22</sub>H<sub>30</sub>O<sub>4</sub>Na<sup>+</sup> ([M+Na]<sup>+</sup>) 381.2036; Found: 381.2034.

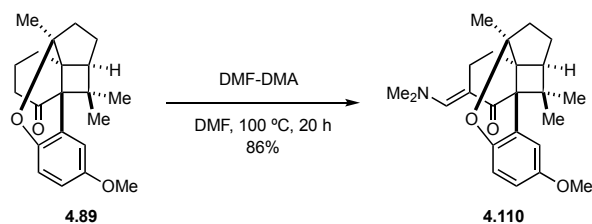


**(4a*S*,5*S*,7a*S*,12b*R*)-11-methoxy-7a,13,13-trimethyl-3,4,5,6,7,7a-hexahydro-5,12b-methanobenzo[*c*]cyclopenta[*b*]chromen-1(2*H*)-one (4.89)**

Charged a flask with **4.90** (586 mg, 1.63 mmol, 1.00 equiv) and THF:water (1:1, 8.5 mL). Added sodium periodate (699 mg, 3.27 mmol, 2.00 equiv) to this solution and stirred at room temperature for 2 h. Then, the reaction



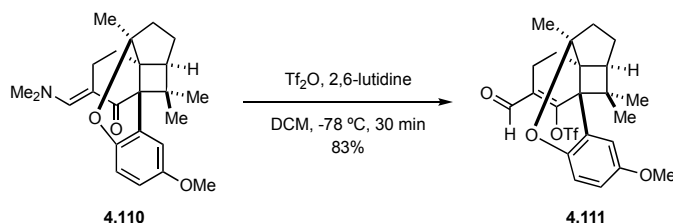
mixture diluted with Na<sub>2</sub>SO<sub>4</sub> (aq. sat.) and EtOAc. The organic layer was separated, and the aqueous layer was extracted with EtOAc (x3). The combined organic layers were washed with brine, dried over MgSO<sub>4</sub>, filtered, and concentrated *in vacuo*. Purification by flash column chromatography over silica (hexanes:EtOAc, 99:1 to 9:1) afforded **4.89** as a white powder (440 mg, 1.35 mmol, 83%). *R*<sub>f</sub> = 0.31 (hexanes:EtOAc, 9:1); [ $\alpha$ ]<sub>D</sub><sup>23</sup> = -53.1 (c = 0.10, MeOH); <sup>1</sup>H NMR (500 MHz, C<sub>6</sub>D<sub>6</sub>)  $\delta$  7.31 (d, J = 3.0 Hz, 1H), 6.92 (d, J = 8.8 Hz, 1H), 6.71 (dd, J = 8.8, 3.0 Hz, 1H), 3.39 (s, 3H), 2.18 – 2.02 (m, 2H), 1.90 (dt, J = 17.7, 6.6 Hz, 1H), 1.76 – 1.67 (m, 2H), 1.65 (d, J = 7.9 Hz, 1H), 1.41 – 1.33 (m, 3H), 1.31 (s, 3H), 1.27 – 1.17 (m, 5H), 0.86 (s, 3H); <sup>13</sup>C NMR (126 MHz, C<sub>6</sub>D<sub>6</sub>)  $\delta$  210.5, 154.3, 148.4, 123.5, 119.2, 115.3, 115.2, 86.0, 55.8, 55.2, 51.9, 48.4, 42.6, 39.0, 38.1, 32.5, 31.0, 24.0 (2C), 22.1, 19.7; IR (neat) 2990, 2975, 2952, 2937, 2873, 2831, 1691, 1609, 1493, 1271, 1227, 1134, 1038, 858, 815, 810, 744, 711, 688; HRMS (ESI) *m/z* calculated for C<sub>21</sub>H<sub>26</sub>O<sub>3</sub>H<sup>+</sup> ([M+H]<sup>+</sup>) 327.1955, found 327.1955.



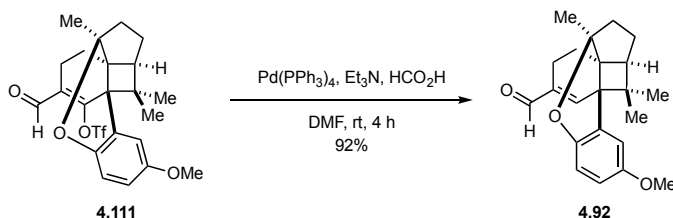
**(4a*S*,5*S*,7a*S*,12b*R*,*E*)-2-((dimethylamino)methylene)-11-methoxy-7a,13,13-trimethyl-3,4,5,6,7,7a-hexahydro-5,12b-methanobenzo[*c*]cyclopenta[*b*]chromen-1(2*H*)-one** (**4.110**)

Charged oven dried vial with **4.89** (200 mg, 613  $\mu$ mol, 1.00 equiv), DMF-DMA (730 mg, 814  $\mu$ L, 6.13 mmol, 10 equiv.), and DMF (1.20 mL). The vial was sealed, and the reaction mixture was stirred at 100 °C for 20 h. Then, the reaction was diluted with water and EtOAc. The organic layer was separated, and the aqueous layer was extracted with EtOAc (x3). The combined organic layers were washed with brine, dried over MgSO<sub>4</sub>, filtered, and concentrated *in vacuo*. Purification by flash column chromatography over silica (hexanes:EtOAc, 9:1 to 2:3) afforded **4.110** as a yellow solid (201 mg, 527  $\mu$ mol, 86%). *R*<sub>f</sub> = 0.17 (hexanes:EtOAc, 1:1); [ $\alpha$ ]<sub>D</sub><sup>23</sup> = +23.3 (c = 0.10, MeOH); <sup>1</sup>H NMR (700 MHz, CDCl<sub>3</sub>)  $\delta$  7.24 (s, 1H), 7.08 (d, J = 2.6 Hz, 1H), 6.69 – 6.61 (m, 2H), 3.74 (s, 3H), 2.95 (s, 6H), 2.65 (dt, J = 13.7, 3.6 Hz, 1H), 2.59 (t, J = 13.3 Hz, 1H), 2.33 (dt, J = 14.0, 3.5 Hz, 1H), 2.12 – 2.05 (m, 1H), 1.88 (d, J = 7.3 Hz, 1H), 1.81 (td, J = 13.5, 3.1 Hz, 1H), 1.58 – 1.49 (m, 2H), 1.49 – 1.44 (m, 1H), 1.43 (s, 3H), 1.38 (s, 3H), 0.92 (s, 3H); <sup>13</sup>C NMR (176 MHz, CDCl<sub>3</sub>)  $\delta$  198.9, 153.1, 148.5, 147.8, 126.4, 118.1, 115.2, 113.7, 105.3, 85.9, 55.6, 53.4, 52.2, 47.6, 43.2, 41.9, 38.1, 32.3, 32.3, 24.4, 23.6, 22.5, 22.5; IR (neat) 2975, 2952, 2914,

2861, 1648, 1550, 1488, 1429, 1230, 1198, 1130, 1088, 1041 922, 870, 806, 780, 703; **HRMS** (ESI)  $m/z$  calculated for  $C_{24}H_{31}NO_3H^+$  ( $[M+H]^+$ ) 382.2377, found 382.2373.

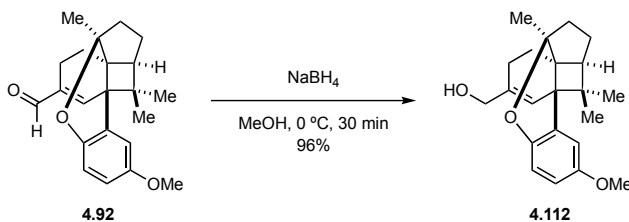


**(4a*S*,5*S*,7a*S*,12b*R*)-2-formyl-11-methoxy-7a,13,13-trimethyl-3,4,5,6,7,7a-hexahydro-5,12b-methanobenzo[*c*]cyclopenta[*b*]chromen-1-yl trifluoromethanesulfonate (4.111)** Charged a flame dried flask with **4.110** (183 mg, 480  $\mu$ mol, 1.00 equiv) and DCM (15 mL) and cooled this solution to  $-78$   $^{\circ}C$ . To this flask was added 2,6-lutidine (514  $\mu$ L, 4.80 mmol, 10.00 equiv) then triflicanhydride (405  $\mu$ L, 2.40 mmol, 5.00 equiv). The mixture was stirred at  $-78$   $^{\circ}C$  for 30 min. Then, the reaction quenched with  $NaHCO_3$  (aq. sat.). The organic layer was separated, and the aqueous layer was extracted with DCM (x3). The combined organic layers were washed with brine, dried over  $MgSO_4$ , filtered, and concentrated *in vacuo*. Purification by flash column chromatography over silica (hexanes:EtOAc, 99:1 to 17:3) afforded **4.111** as a pale yellow powder (193 mg, 397  $\mu$ mol, 83%).  $R_f = 0.30$  (hexanes:EtOAc, 9:1);  $[\alpha]_D^{24} = +9.0$  ( $c = 0.10$ , MeOH);  $^1H$  NMR (500 MHz,  $CDCl_3$ )  $\delta$  9.87 (s, 1H), 6.91 (s, 1H), 6.85 – 6.71 (m, 2H), 3.78 (s, 3H), 3.02 (dt,  $J = 16.9, 4.2$  Hz, 1H), 2.29 (ddd,  $J = 16.7, 11.7, 4.7$  Hz, 1H), 2.05 (td,  $J = 13.4, 7.6$  Hz, 1H), 1.97 (d,  $J = 7.3$  Hz, 1H), 1.76 (dt,  $J = 13.6, 4.1$  Hz, 1H), 1.72 – 1.56 (m, 3H), 1.45 (dd,  $J = 12.9, 7.2$  Hz, 1H), 1.38 (s, 3H), 1.27 (s, 3H), 1.06 (s, 3H);  $^{13}C$  NMR (126 MHz,  $CDCl_3$ )  $\delta$  187.2, 159.9, 153.2, 148.3, 133.6, 122.1, 119.4, 118.7 (q,  $J = 320$  Hz), 117.8, 115.2, 87.6, 55.7, 51.1, 50.4, 49.6, 45.4, 36.1, 28.7, 25.2, 24.9, 24.4, 22.8, 22.0; **IR** (neat) 2995, 2966, 2924, 2873, 1688, 1496, 1395, 1382, 1213, 1135, 1037, 951, 888, 816, 766, 748, 701, 673; **HRMS** (ESI)  $m/z$  calculated for  $C_{23}H_{25}F_3O_6S^+$  ( $[M]^+$ ) 486.1324, found 486.1336.



**(4a*S*\*,5*S*\*,7a*S*\*,12b*S*\*)-11-methoxy-7a,13,13-trimethyl-3,4,5,6,7,7a-hexahydro-5,12b-methanobenzo[*c*]cyclopenta[*b*]chromene-2-carbaldehyde (4.92)** Charged a flame dried flask with **4.111** (180 mg, 370  $\mu$ mol, 1.00 equiv), THF (8.0 mL), triethylamine (464  $\mu$ L, 3.33 mmol,

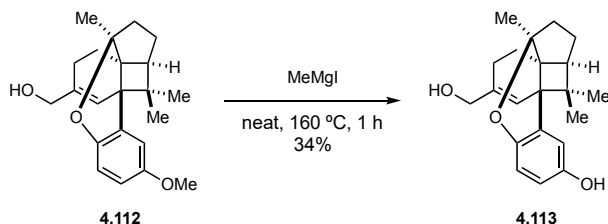
9.00 equiv), and formic acid (84  $\mu\text{L}$ , 2.22 mmol, 6.00 equiv). This solution was then degassed by sparging with nitrogen gas for 10 mins. This mixture was then added to a separate flask containing  $\text{Pd}(\text{PPh}_3)_4$  (43 mg, 37.0  $\mu\text{mol}$ , 0.10 equiv). The reaction was stirred at room temperature for 4 h. Then, the reaction mixture was diluted with  $\text{NaHCO}_3$  (aq. sat.) and EtOAc. The organic layer was separated, and the aqueous layer was extracted with EtOAc (x3). The combined organic layers were washed with brine, dried over  $\text{MgSO}_4$ , filtered, and concentrated *in vacuo*. Purification by flash column chromatography over silica (hexanes:EtOAc, 99:1 to 17:3) afforded **4.92** as a colorless, viscous oil (116 mg, 341  $\mu\text{mol}$ , 92%).  $R_f = 0.19$  (hexanes:EtOAc, 9:1);  $[\alpha]_{\text{D}}^{23} = +23.9$  ( $c = 0.10$ , MeOH);  $^1\text{H NMR}$  (600 MHz,  $\text{CDCl}_3$ )  $\delta$  9.48 (s, 1H), 6.88 (d,  $J = 2.3$  Hz, 1H), 6.80 (d,  $J = 8.7$  Hz, 1H), 6.72 (dd,  $J = 8.7, 2.9$  Hz, 1H), 6.68 (d,  $J = 2.9$  Hz, 1H), 3.80 (s, 3H), 2.73 (dt,  $J = 16.6, 4.2$  Hz, 1H), 2.19 – 2.10 (m, 1H), 2.08 – 1.97 (m, 2H), 1.77 – 1.70 (m, 1H), 1.66 – 1.56 (m, 3H), 1.41 (ddd,  $J = 13.3, 11.8, 4.7$  Hz, 1H), 1.31 (s, 3H), 0.98 (s, 3H), 0.88 (s, 3H);  $^{13}\text{C NMR}$  (151 MHz,  $\text{CDCl}_3$ )  $\delta$  193.3, 156.5, 154.0, 147.5, 141.5, 128.3, 119.4, 113.6, 112.6, 87.0, 55.9, 49.6, 47.4, 45.7, 44.9, 38.4, 29.0, 26.0, 24.3, 23.8, 21.8, 19.1; **IR** (neat) 2947, 2912, 2864, 2851, 2834, 1737, 1679, 1636, 1493, 1460, 1375, 1267, 1210, 1182, 1134, 1041, 874, 812, 775, 723; **HRMS** (ESI)  $m/z$  calculated for  $\text{C}_{22}\text{H}_{26}\text{O}_3\text{H}^+$  ( $[\text{M}+\text{H}]^+$ ) 339.1955, found 339.1955.



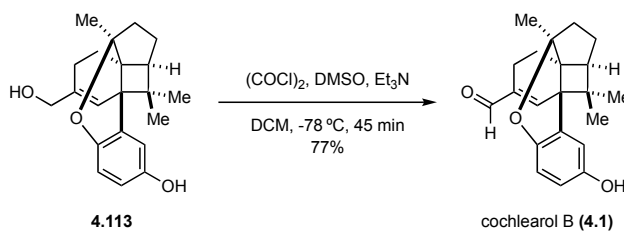
**((4a*S*,5*S*,7a*S*,12b*S*)-11-methoxy-7a,13,13-trimethyl-3,4,5,6,7,7a-hexahydro-5,12b-methanobenzo[*c*]cyclopenta[*b*]chromen-2-yl)methanol (**4.112**)**

Charged a flask with **4.92** (114 mg, 337  $\mu\text{mol}$ , 1.00 equiv) and methanol (3.00 mL). Cooled this solution to 0  $^\circ\text{C}$  then added  $\text{NaBH}_4$  (12.7 mg, 337  $\mu\text{mol}$ , 1.00 equiv). This mixture was stirred at room temperature for 30 min. Then, the reaction was quenched with  $\text{NH}_4\text{Cl}$  (aq. sat.) and diluted with EtOAc. The organic layer was separated, and the aqueous layer was extracted with EtOAc (x3). The combined organic layers were washed with brine, dried over  $\text{MgSO}_4$ , filtered, and concentrated *in vacuo*. Purification by flash column chromatography (hexanes:EtOAc, 19:1 to 7:3) afforded **4.112** as a pale yellow solid (110 mg, 320  $\mu\text{mol}$ , 96%).  $R_f = 0.32$  (hexanes:EtOAc, 1:1);  $[\alpha]_{\text{D}}^{25} = +71.5$  ( $c = 0.10$ , MeOH);  $^1\text{H NMR}$  (700 MHz,  $\text{CDCl}_3$ )  $\delta$  6.76 (d,  $J = 8.7$  Hz, 1H), 6.66 (dd,  $J = 8.7, 2.9$  Hz, 1H), 6.64 (d,  $J$

= 2.9 Hz, 1H), 5.81 (s, 1H), 4.12 (d,  $J = 13.2$  Hz, 1H), 4.09 (d,  $J = 13.1$  Hz, 1H) 3.77 (s, 3H), 2.25 (dt,  $J = 16.1, 4.0$  Hz, 1H), 2.14 – 2.02 (m, 2H), 1.95 (d,  $J = 6.2$  Hz, 1H), 1.74 – 1.66 (m, 1H), 1.62 – 1.51 (m, 3H), 1.45 (td,  $J = 12.5, 4.7$ , 1H), 1.29 (s, 3H), 0.98 (s, 3H), 0.81 (s, 3H);  $^{13}\text{C NMR}$  (176 MHz,  $\text{CDCl}_3$ )  $\delta$  153.8, 147.2, 138.7, 130.8, 129.0, 118.9, 113.7, 112.0, 86.8, 67.5, 55.8, 49.4, 46.4, 43.6, 43.5, 38.4, 29.2, 26.8, 24.2, 23.9, 23.7, 21.8; **IR** (neat) 3411, 3402, 2944, 2924, 2910, 2863, 2845, 1491, 1459, 1265, 1221, 1206, 1135, 1042, 952, 867, 811, 783, 774; **HRMS** (ESI)  $m/z$  calculated for  $\text{C}_{22}\text{H}_{28}\text{O}_3\text{H}^+$  ( $[\text{M}+\text{H}]^+$ ) 341.2111, found 341.2110.



**(4a*S*,5*S*,7a*S*,12b*S*)-2-(hydroxymethyl)-7a,13,13-trimethyl-3,4,5,6,7,7a-hexahydro-5,12b-methanobenzo[*c*]cyclopenta[*b*]chromen-11-ol (4.113)** Charged a flame dried flask with **4.112** (93 mg, 0.27 mmol, 1.00 equiv) and diethyl ether (5.00 mL). Cooled this solution to 0 °C then added MeMgI (2.7 mL, 3.0 molar in  $\text{Et}_2\text{O}$ , 8.2 mmol, 30.0 equiv). After gently removing diethyl ether under vacuum, the resulting residue was heated to 160 °C under vacuum for 1 h. After cooling to room temperature, then back to 0 °C, the residue was diluted in diethyl ether. Then, the reaction mixture was carefully quenched with water then  $\text{NH}_4\text{Cl}$  (aq. sat.). The organic layer was separated, and the aqueous layer was extracted with EtOAc (x3). The combined organic layers were washed with brine, dried over  $\text{MgSO}_4$ , filtered, and concentrated *in vacuo*. Purification by flash column chromatography over silica (hexanes:EtOAc, 9:1 to 2:3) afforded **4.113** as a pale yellow powder (30 mg, 92  $\mu\text{mol}$ , 34%).  $R_f = 0.18$  (hexanes:EtOAc, 1:1);  $[\alpha]_{\text{D}}^{23} = +17.9$  ( $c = 0.10$ , MeOH);  $^1\text{H NMR}$  (700 MHz,  $(\text{CD}_3)_2\text{CO}$ )  $\delta$  7.73 (s, 1H), 6.64 (d,  $J = 2.7$  Hz, 1H), 6.60 (d,  $J = 8.5$  Hz, 1H), 6.57 (dd,  $J = 8.5, 2.7$  Hz, 1H), 5.81 (s, 1H), 4.09 – 3.98 (m, 2H), 3.77 (t,  $J = 5.8$  Hz, 1H), 2.21 (dt,  $J = 16.1, 4.0$  Hz, 1H), 2.11 – 2.06 (m, 1H), 2.04 – 1.99 (m, 1H), 1.97 (dd,  $J = 8.5, 2.2$  Hz, 1H), 1.72 – 1.66 (m, 1H), 1.65 – 1.58 (m, 1H), 1.58 – 1.50 (m, 2H), 1.36 (td,  $J = 12.5, 4.8$  Hz, 1H), 1.23 (s, 3H), 0.96 (s, 3H), 0.79 (s, 3H);  $^{13}\text{C NMR}$  (151 MHz,  $(\text{CD}_3)_2\text{CO}$ )  $\delta$  151.9, 146.6, 139.6, 131.5, 128.0, 119.2, 114.9, 114.3, 86.9, 66.3, 49.8, 47.1, 43.8, 43.8, 38.9, 29.3, 27.2, 24.4, 24.1, 23.7, 21.8; **IR** (neat) 3429, 3212, 3212, 2988, 2967, 2924, 2879, 2846, 2540, 2400, 1494, 1442, 1377, 1210, 1182, 1143, 1131, 997, 952, 944, 869, 810, 758, 740; **HRMS** (ESI)  $m/z$  calculated for  $\text{C}_{21}\text{H}_{26}\text{O}_3\text{Na}^+$  ( $[\text{M}+\text{Na}]^+$ ) 349.1774, found 349.1778.



**Cochlearol B (4.1)** Charged a flame dried flask with oxalyl chloride (2.36  $\mu\text{L}$ , 27.0  $\mu\text{mol}$ , 1.10 equiv) and DCM (0.3 mL), then cooled to  $-78\text{ }^\circ\text{C}$ . To this solution was added DMSO (3.83  $\mu\text{L}$ , 53.9  $\mu\text{mol}$ , 2.20 equiv). The resulting mixture was stirred at  $-78\text{ }^\circ\text{C}$  for 15 mins. Next, a solution of **4.113** (0.008 g, 24.5  $\mu\text{mol}$ , 1.00 eq.) in DCM:DMSO (10:1, 0.33 mL) was added. After stirring for 15 min at  $-78\text{ }^\circ\text{C}$ , triethylamine (17.1  $\mu\text{L}$ , 123  $\mu\text{mol}$ , 5.0 equiv) was added. Following an additional 15 min of stirring, the reaction mixture was quenched with water and diluted in EtOAc. The organic layer was separated, and the aqueous layer was extracted with EtOAc (x3). The combined organic layers were washed with brine, dried over  $\text{MgSO}_4$ , filtered, and concentrated *in vacuo*. Purification by flash column chromatography (hexanes:EtOAc, 19:1 to 7:3) afforded cochlearol B (**4.1**) as a pale yellow solid (6.1 mg, 19  $\mu\text{mol}$ , 77%).  $R_f = 0.17$  (hexanes:EtOAc, 4:1);  $[\alpha]_D^{25} = +112.8$  ( $c = 0.10$ , MeOH); **HPLC** (Daicel Chiralpak IC, hexanes:ethanol 75:25) 4.6 min (minor), 6.9 min (major).  **$^1\text{H NMR}$**  (700 MHz,  $(\text{CD}_3)_2\text{CO}$ )  $\delta$  9.54 (s, 1H), 7.89 (s, 1H), 7.06 (d,  $J = 2.3$  Hz, 1H), 6.79 (d,  $J = 2.1$  Hz, 1H), 6.71 – 6.58 (m, 2H), 2.64 (ddd,  $J = 16.5, 4.6, 3.7$  Hz, 1H), 2.15 – 2.10 (m, 1H), 2.07 (d,  $J = 1.9$  Hz, 1H), 2.04 – 1.98 (m, 1H), 1.76 – 1.71 (m, 1H), 1.70 – 1.58 (m, 3H), 1.37 (ddd,  $J = 13.4, 11.6, 4.7$  Hz, 1H), 1.28 (s, 3H), 1.00 (s, 3H), 0.88 (s, 3H);  **$^{13}\text{C NMR}$**  (176 MHz,  $(\text{CD}_3)_2\text{CO}$ )  $\delta$  193.4, 156.5, 152.3, 147.3, 142.0, 129.1, 119.9, 115.3, 115.0, 87.2, 50.2, 48.1, 46.1, 45.1, 39.0, 29.1, 26.7, 24.6, 23.9, 21.8, 19.5; **IR** (neat) 3375, 2951, 2928, 2859, 1679, 1663, 1492, 1445, 1209, 1182, 1134, 952, 882, 815, 789, 679; **HRMS** (ESI)  $m/z$  calculated for  $\text{C}_{21}\text{H}_{24}\text{O}_3\text{H}^+$  ( $[\text{M}+\text{H}]^+$ ) 325.1798, found 325.1794.

Isolated Cochlearol B NMR Data.<sup>7</sup>  **$^1\text{H NMR}$**  (600 MHz,  $(\text{CD}_3)_2\text{CO}$ )  $\delta$  9.55 (s, 1H), 7.08 (d,  $J = 2.0$  Hz, 1H), 6.80 (d,  $J = 2.2$  Hz, 1H), 6.68 (d,  $J = 8.5$  Hz, 1H), 6.65 (dd,  $J = 8.5, 2.2$  Hz, 1H), 2.65 (m, 1H), 2.15 (m, 1H), 2.09 (m, 1H), 2.03 (m, 1H), 1.75 (m, 1H), 1.69 (m, 1H), 1.66 (m, 1H), 1.63 (m, 1H), 1.39 (m, 1H), 1.30 (s, 3H), 1.01 (s, 3H), 0.90 (s, 3H);  **$^{13}\text{C NMR}$**  (150 MHz,  $(\text{CD}_3)_2\text{CO}$ )  $\delta$  193.4, 156.4, 152.2, 147.2, 142.0, 129.0, 119.8, 115.2, 114.9, 87.2, 50.2, 48.1, 46.1, 45.1, 38.9, 29.0, 26.7, 24.5, 23.8, 21.8, 19.5.

Previously Synthesized Cochlearol B NMR Data.<sup>21</sup> **<sup>1</sup>H NMR** (600 MHz, (CD<sub>3</sub>)<sub>2</sub>CO) δ 9.53 (s, 1H), 7.83 (s, 1H), 7.05 (d, *J* = 3.0 Hz, 1H), 6.78 (d, *J* = 2.4 Hz, 1H), 6.65 (d, *J* = 7.8 Hz, 1H), 6.63 (dd, *J* = 7.8, 2.4 Hz, 1H), 2.65 – 2.61 (m, 1H), 2.15 – 2.10 (m, 1H), 2.06 (m, 1H), 2.02 – 1.98 (m, 1H), 1.75 – 1.70 (m, 1H), 1.69 – 1.65 (m, 1H), 1.64 – 1.62 (m, 1H), 1.62 – 1.58 (m, 1H), 1.39 – 1.34 (m, 1H), 1.27 (s, 3H), 0.99 (s, 3H), 0.87 (s, 3H); **<sup>13</sup>C NMR** (150 MHz, (CD<sub>3</sub>)<sub>2</sub>CO) δ 193.4, 156.4, 152.3, 147.3, 142.0, 129.1, 119.8, 115.3, 115.0, 87.2, 50.3, 48.1, 46.1, 45.1, 39.0, 29.0, 26.7, 24.5, 23.8, 21.8, 19.5.

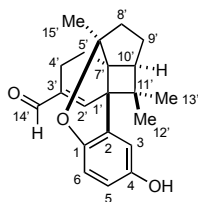


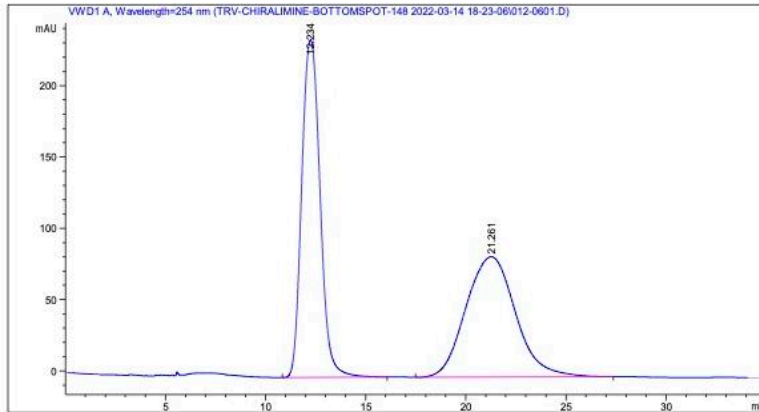
Table 4.5 Comparing  $^1\text{H}$  and  $^{13}\text{C}$  NMR data for natural and synthetic cochlearol B.

Position	Synthetic (Schindler, 2022)		Isolated (Cheng, 2014)		Synthetic (Sugita, 2021)	
	$\delta_{\text{C}}$	$\delta_{\text{H}}$ (mult., $J$ in Hz)	$\delta_{\text{C}}$	$\delta_{\text{H}}$ (mult., $J$ in Hz)	$\delta_{\text{C}}$	$\delta_{\text{H}}$ (mult., $J$ in Hz)
OH		7.89 (s)				7.83 (s)
1	156.5		156.4		156.4	
2	129.1		129.0		129.1	
3	115.0	6.79 (d, 2.1)	114.9	6.80 (d, 2.2)	115.0	6.78 (d, 2.4)
4	147.3		147.2		147.3	
5	115.3	6.71 – 6.58 (m)	115.2	6.65 (dd, 8.5, 2.2)	115.0	6.63 (dd, 7.8, 2.4)
6	119.9	6.71 – 6.58 (m)	119.8	6.68 (d, 8.5)	119.8	6.65 (d, 7.8)
1'	46.1		46.1		46.1	
2'	152.2	7.06 (d, 2.3)	152.2	7.08 (d, 2.0)	152.3	7.05 (d, 3.0)
3'	142.0		142.0		142.0	
4'a	19.5	2.64 (ddd, 16.5, 4.6, 3.7)	19.5	2.65 (m)	19.5	2.65 – 2.61 (m)
4'b		2.04 – 1.98 (m)		2.03 (m)		2.02 – 1.98 (m)
5'a	26.7	1.70 – 1.58 (m)	26.7	1.66 (m)	26.7	
5'b		1.37 (ddd, 13.4, 11.6, 4.7)		1.39 (m)		
6'	45.1		45.1		45.1	
7'	87.2		87.2		87.2	
8'a	39.0	2.15 – 2.10 (m)	38.9	2.15 (m)	39.0	2.15 – 2.10 (m)
8'b		1.70 – 1.58 (m)		1.63 (m)		1.64 – 1.62 (m)
9'a	24.6	1.76 – 1.71 (m)	24.5	1.75 (m)	24.5	1.75 – 1.70 (m)
9'b		1.70 – 1.58 (m)		1.69 (m)		1.69 – 1.65 (m)
10'	50.2	2.07 (d, 1.9)	50.2	2.09 (m)	50.3	2.06 (m)

11'	48.1		48.1		48.1	
12'	21.8	0.88 (s)	21.8	0.90 (s)	21.8	0.87 (s)
13'	29.1	1.00 (s)	29.0	1.01 (s)	29.0	0.99 (s)
14'	193.4	9.54 (s)	193.4	9.55 (s)	193.4	9.53 (s)
15'	23.9		23.8		23.8	



### 4.5.3 HPCL Spectra



=====  
 Area Percent Report  
 =====

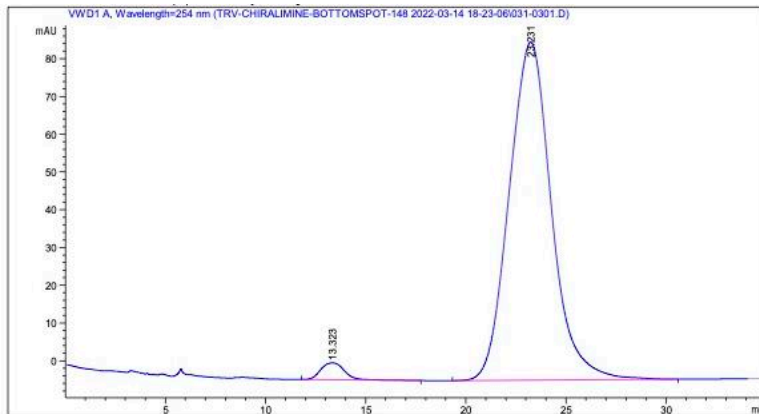
Sorted By : Signal  
 Multiplier : 1.0000  
 Dilution : 1.0000  
 Use Multiplier & Dilution Factor with ISTDs

Signal 1: VWD1 A, Wavelength=254 nm

Peak #	RetTime [min]	Type	Width [min]	Area [mAU*s]	Height [mAU]	Area %
1	12.234	BB	1.0143	1.50214e4	236.71468	50.7720
2	21.261	BB	2.7131	1.45645e4	84.36419	49.2280

Totals : 2.95859e4 321.07887

Figure 4.24 HPLC traces of racemic (above) and enantioenriched (below) **4.26**.



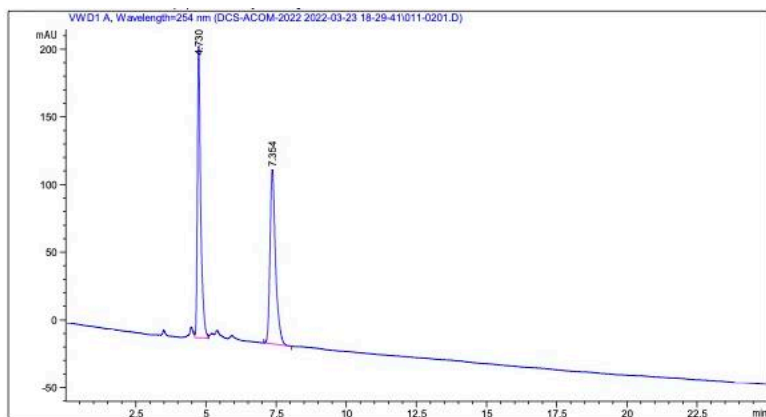
=====  
 Area Percent Report  
 =====

Sorted By : Signal  
 Multiplier : 1.0000  
 Dilution : 1.0000  
 Use Multiplier & Dilution Factor with ISTDs

Signal 1: VWD1 A, Wavelength=254 nm

Peak #	RetTime [min]	Type	Width [min]	Area [mAU*s]	Height [mAU]	Area %
1	13.323	BB	0.9890	370.70453	4.46791	2.7525
2	23.231	BB	2.2520	1.30971e4	89.51569	97.2475

Totals : 1.34678e4 93.98360



=====  
 Area Percent Report  
 =====

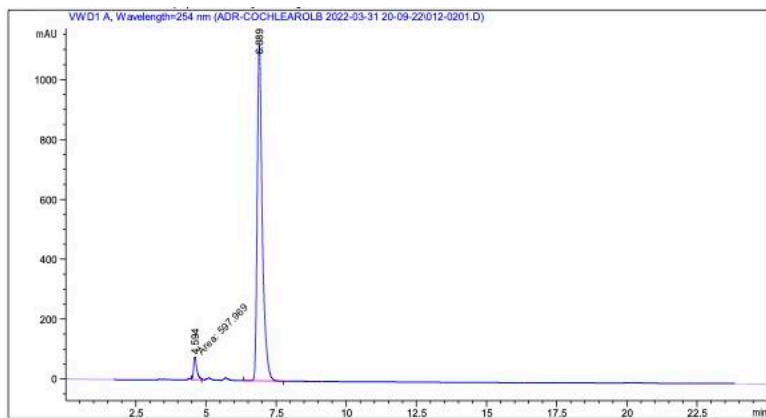
Sorted By : Signal  
 Multiplier : 1.0000  
 Dilution : 1.0000  
 Use Multiplier & Dilution Factor with ISTDs

Signal 1: VWD1 A, Wavelength=254 nm

Peak #	RetTime [min]	Type	Width [min]	Area [mAU*s]	Height [mAU]	Area %
1	4.730	VV	0.1205	1764.70984	215.51315	50.1599
2	7.354	BB	0.2039	1753.46082	128.76698	49.8401

Totals : 3518.17065 344.28014

Figure 4.25 HPLC traces of racemic (above) and enantioenriched (below) cochlearol B.



=====  
 Area Percent Report  
 =====

Sorted By : Signal  
 Multiplier : 1.0000  
 Dilution : 1.0000  
 Use Multiplier & Dilution Factor with ISTDs

Signal 1: VWD1 A, Wavelength=254 nm

Peak #	RetTime [min]	Type	Width [min]	Area [mAU*s]	Height [mAU]	Area %
1	4.594	MM	0.1296	597.96875	76.89019	4.0682
2	6.889	BB	0.1868	1.41008e4	1120.88000	95.9318

Totals : 1.46988e4 1197.77020

#### 4.5.4 X-Ray Crystallographic Data

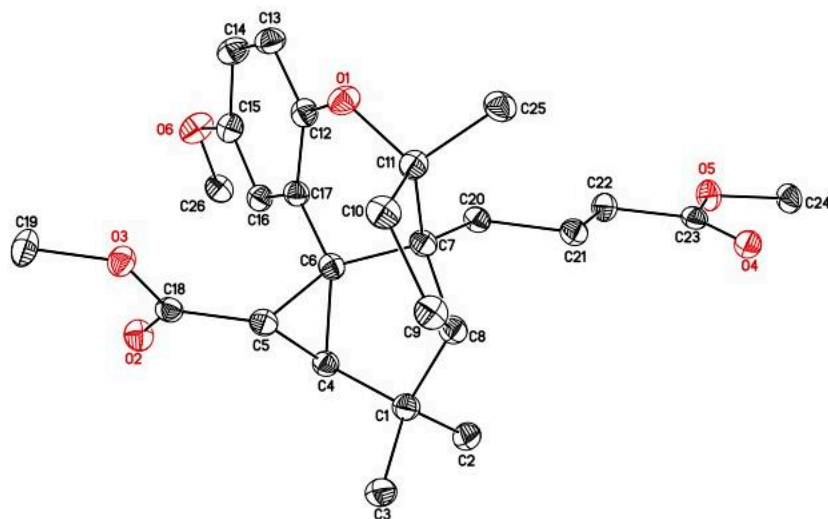


Figure 4.26 ORTEP diagram of **4.74**.

Crystal structure of **4.74**. X-ray crystallographic coordinates have been deposited at the Cambridge Crystallographic Data Centre (CCDC) with the deposit number 2142344.

Colorless blocks of **4.74** were grown from an ethyl acetate solution of the compound at 20 deg. C. A crystal of dimensions 0.14 x 0.12 x 0.08 mm was mounted on a Rigaku AFC10K Saturn 944+ CCD-based X-ray diffractometer equipped with a low temperature device and Micromax-007HF Cu-target micro-focus rotating anode ( $\lambda = 1.54187 \text{ \AA}$ ) operated at 1.2 kW power (40 kV, 30 mA). The X-ray intensities were measured at 85(1) K with the detector placed at a distance 42.00 mm from the crystal. A total of 2028 images were collected with an oscillation width of  $1.0^\circ$  in  $\omega$ . The exposure times were 1 sec. for the low angle images, 2 sec. for high angle. Rigaku d\*trek images were exported to CrysAlisPro for processing and corrected for absorption. The integration of the data yielded a total of 32993 reflections to a maximum  $2\theta$  value of  $138.76^\circ$  of which 4189 were independent and 4068 were greater than  $2\sigma(I)$ . The final cell constants (Table 1) were based on the xyz centroids of 18434 reflections above  $10\sigma(I)$ . Analysis of the data showed negligible decay during data collection. The structure was solved and refined with the Bruker SHELXTL (version 2018/3) software package, using the space group  $P2(1)/c$  with  $Z = 4$  for the formula  $C_{26}H_{34}O_6$ . All non-hydrogen atoms were refined anisotropically with the hydrogen atoms placed in idealized positions. Full matrix least-squares refinement based on  $F^2$  converged at  $R1 = 0.0433$  and  $wR2 = 0.1154$  [based on  $I > 2\sigma(I)$ ],  $R1 = 0.0448$  and  $wR2 = 0.1178$  for all data. Additional details are presented in Table S3 and are given as Supporting Information in a CIF file. Acknowledgement is made for funding from NSF grant CHE-0840456 for X-ray instrumentation. Table 4.6 Crystal data and structure refinement for **4.74**.

Empirical formula	$C_{26}H_{34}O_6$
Formula weight	442.53
Temperature	85(2) K

Wavelength	1.54184 Å
Crystal system, space group	Monoclinic, P2(1)/c
Unit cell dimensions	a = 17.6211(3) Å    alpha = 90 deg. b = 8.05114(8) Å    beta = 118.0448(19) deg. c = 17.9615(3) Å    gamma = 90 deg.
Volume	2248.98(6) Å <sup>3</sup>
Z, Calculated density	4, 1.307 Mg/m <sup>3</sup>
Absorption coefficient	0.744 mm <sup>-1</sup>
F(000)	952
Crystal size	0.140 x 0.120 x 0.080 mm
Theta range for data collection	2.841 to 69.387 deg.
Limiting indices	-21 ≤ h ≤ 21, -9 ≤ k ≤ 9, -21 ≤ l ≤ 21
Reflections collected / unique	32993 / 4189 [R(int) = 0.0664]
Completeness to theta = 67.684	100.0 %
Absorption correction	Semi-empirical from equivalents
Max. and min. transmission	1.00000 and 0.81148
Refinement method	Full-matrix least-squares on F <sup>2</sup>
Data / restraints / parameters	4189 / 0 / 296
Goodness-of-fit on F <sup>2</sup>	1.094
Final R indices [I > 2σ(I)]	R1 = 0.0433, wR2 = 0.1154
R indices (all data)	R1 = 0.0448, wR2 = 0.1178
Extinction coefficient	0.0064(4)
Largest diff. peak and hole	0.311 and -0.298 e.Å <sup>-3</sup>

G.M. Sheldrick (2015) "Crystal structure refinement with SHELXL", Acta Cryst., C71, 3-8 (Open Access).

CrystalClear Expert 2.0 r16, Rigaku Americas and Rigaku Corporation (2014), Rigaku Americas, 9009, TX, USA 77381-5209, Rigaku Tokyo, 196-8666, Japan.

CrysAlisPro 1.171.40.53 (Rigaku Oxford Diffraction, 2019).

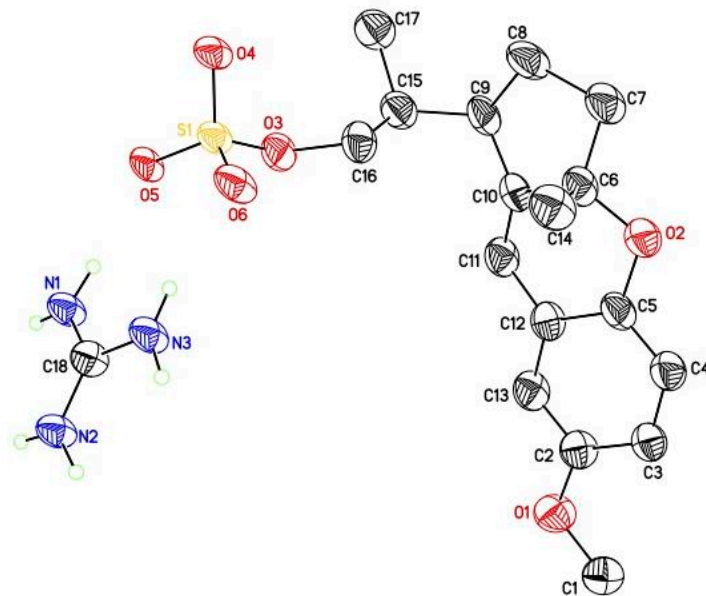


Figure 4.27 ORTEP diagram of **4.70**.

Crystal structure of **4.70**. X-ray crystallographic coordinates have been deposited at the Cambridge Crystallographic Data Centre (CCDC) with the deposit number 2142345.

Colorless plates of **4.70** were grown from a methanol solution of the compound at 25 deg. C. A crystal of dimensions 0.07 x 0.06 x 0.02 mm was mounted on a Rigaku AFC10K Saturn 944+ CCD-based X-ray diffractometer equipped with a low temperature device and Micromax-007HF Cu-target micro-focus rotating anode ( $\lambda = 1.54187 \text{ \AA}$ ) operated at 1.2 kW power (40 kV, 30 mA). The X-ray intensities were measured at 85(1) K with the detector placed at a distance 42.00 mm from the crystal. A total of 2028 images were collected with an oscillation width of  $1.0^\circ$  in  $\omega$ . The exposure times were 1 sec. for the low angle images, 4 sec. for high angle. Rigaku d\*trek images were exported to CrysAlisPro for processing and corrected for absorption. The integration of the data yielded a total of 29002 reflections to a maximum  $2\theta$  value of  $139.36^\circ$  of which 3765 were independent and 2703 were greater than  $2\sigma(I)$ . The final cell constants (Table 1) were based on the xyz centroids of 3313 reflections above  $10\sigma(I)$ . Analysis of the data showed negligible decay during data collection. The structure was solved and refined with the Bruker SHELXTL (version 2018/3) software package, using the space group P2(1)/c with  $Z = 4$  for the formula  $C_{18}H_{27}N_3O_6S$ . All non-hydrogen atoms were refined anisotropically with the hydrogen atoms placed in a combination of refined and idealized positions. Full matrix least-squares refinement based on  $F^2$  converged at  $R1 = 0.0851$  and  $wR2 = 0.2275$  [based on  $I > 2\sigma(I)$ ],  $R1 = 0.1118$  and  $wR2 = 0.2448$  for all data. Additional details are presented in Table S4 and are given as Supporting Information in a CIF file. Acknowledgement is made for funding from NSF grant CHE-0840456 for X-ray instrumentation.

Table 4.7 Crystal data and structure refinement for **4.70**.

Empirical formula

$C_{18}H_{27}N_3O_6S$

Formula weight	413.48
Temperature	85(2) K
Wavelength	1.54184 Å
Crystal system, space group	Monoclinic, P2(1)/c
Unit cell dimensions	a = 22.2228(16) Å    alpha = 90 deg. b = 7.1175(4) Å    beta = 100.377(5) deg. c = 12.9942(5) Å    gamma = 90 deg.
Volume	2021.7(2) Å <sup>3</sup>
Z, Calculated density	4, 1.358 Mg/m <sup>3</sup>
Absorption coefficient	1.771 mm <sup>-1</sup>
F(000)	880
Crystal size	0.070 x 0.060 x 0.020 mm
Theta range for data collection	4.045 to 69.679 deg.
Limiting indices	-26<=h<=25, -8<=k<=8, -15<=l<=15
Reflections collected / unique	29002 / 3765 [R(int) = 0.1067]
Completeness to theta = 67.684	99.7 %
Absorption correction	Semi-empirical from equivalents
Max. and min. transmission	1.00000 and 0.63671
Refinement method	Full-matrix least-squares on F <sup>2</sup>
Data / restraints / parameters	3765 / 15 / 280
Goodness-of-fit on F <sup>2</sup>	1.115
Final R indices [I>2sigma(I)]	R1 = 0.0851, wR2 = 0.2275
R indices (all data)	R1 = 0.1118, wR2 = 0.2448
Extinction coefficient	n/a
Largest diff. peak and hole	0.500 and -0.381 e.Å <sup>-3</sup>

G.M. Sheldrick (2015) "Crystal structure refinement with SHELXL", Acta Cryst., C71, 3-8 (Open Access).

CrystalClear Expert 2.0 r16, Rigaku Americas and Rigaku Corporation (2014), Rigaku Americas, 9009, TX, USA 77381-5209, Rigaku Tokyo, 196-8666, Japan.

CrysAlisPro 1.171.40.53 (Rigaku Oxford Diffraction, 2019).

## 4.6 References

- (1) Wachtel-Galor, S.; Yuen, J.; Buswell, J. A.; Benzie, I. F. F. *Ganoderma Lucidum* (Lingzhi or Reishi): A Medicinal Mushroom. In *Herbal Medicine: Biomolecular and Clinical Aspects*; Benzie, I. F. F., Wachtel-Galor, S., Eds.; CRC Press/Taylor & Francis: Boca Raton (FL), 2011.
- (2) Peng, X.; Qiu, M. Meroterpenoids from *Ganoderma* Species: A Review of Last Five Years. *Nat. Prod. Bioprospect.* **2018**, *8*, 137–149.
- (3) Peng, X.-R.; Liu, J.-Q.; Wan, L.-S.; Li, X.-N.; Yan, Y.-X.; Qiu, M.-H. Four New Polycyclic Meroterpenoids from *Ganoderma Cochlear*. *Org. Lett.* **2014**, *16*, 5262–5265.
- (4) Williams, P.; Sorribas, A.; Howes, M.-J. R. Natural Products as a Source of Alzheimer's Drug Leads. *Nat. Prod. Rep.* **2011**, *28*, 48–77.
- (5) Mishra, A.; Goel, R. K. Psychoneurochemical Investigations to Reveal Neurobiology of Memory Deficit in Epilepsy. *Neurochem Res* **2013**, *38*, 2503–2515.
- (6) Jiang, Y.; Gao, H.; Turdu, G. Traditional Chinese Medicinal Herbs as Potential AChE Inhibitors for Anti-Alzheimer's Disease: A Review. *Bioorg. Chem.* **2017**, *75*, 50–61.
- (7) Dou, M.; Di, L.; Zhou, L.-L.; Yan, Y.-M.; Wang, X.-L.; Zhou, F.-J.; Yang, Z.-L.; Li, R.-T.; Hou, F.-F.; Cheng, Y.-X. Cochlearols A and B, Polycyclic Meroterpenoids from the Fungus *Ganoderma Cochlear* That Have Renoprotective Activities. *Org. Lett.* **2014**, *16*, 6064–6067.
- (8) Liu, Y. Renal Fibrosis: New Insights into the Pathogenesis and Therapeutics. *Kidney Int.* **2006**, *69*, 213–217.
- (9) Derynck, R.; Zhang, Y.; Feng, X.-H. Smads: Transcriptional Activators of TGF- $\beta$  Responses. *Cell* **1998**, *95*, 737–740.
- (10) Zhang, Y.; Feng, X.-H.; Wu, R.-Y.; Derynck, R. Receptor-Associated Mad Homologues Synergize as Effectors of the TGF- $\beta$  Response. *Nature* **1996**, *383*, 168–172.
- (11) Meng, X. M.; Huang, X. R.; Chung, A. C. K.; Qin, W.; Shao, X.; Igarashi, P.; Ju, W.; Bottinger, E. P.; Lan, H. Y. Smad2 Protects against TGF- $\beta$ /Smad3-Mediated Renal Fibrosis. *J. Am. Soc. Nephrol.* **2010**, *21*, 1477–1487.
- (12) Zhou, F.-J.; Nian, Y.; Yan, Y.; Gong, Y.; Luo, Q.; Zhang, Y.; Hou, B.; Zuo, Z.-L.; Wang, S.-M.; Jiang, H.-H.; Yang, J.; Cheng, Y.-X. Two New Classes of T-Type Calcium Channel Inhibitors with New Chemical Scaffolds from *Ganoderma Cochlear*. *Org. Lett.* **2015**, *17*, 3082–3085.
- (13) Cheong, E.; Shin, H.-S. T-Type Ca<sup>2+</sup> Channels in Normal and Abnormal Brain Functions. *Physiol. Rev.* **2013**, *93*, 961–992.
- (14) Qin, F.-Y.; Zhang, H.-X.; Di, Q.-Q.; Wang, Y.; Yan, Y.-M.; Chen, W.-L.; Cheng, Y.-X. *Ganoderma Cochlear* Metabolites as Probes to Identify a COX-2 Active Site and as in Vitro and in Vivo Anti-Inflammatory Agents. *Org. Lett.* **2020**, *22*, 2574–2578.
- (15) Jacob, J. P.; Manju, S. L.; Ethiraj, K. R.; Elias, G. Safer Anti-Inflammatory Therapy Through Dual COX-2/5-LOX Inhibitors: A Structure-Based Approach. *Eur. J. Pharm. Sci.* **2018**, *121*, 356–381.
- (16) Liu, D.; Gong, J.; Dai, W.; Kang, X.; Huang, Z.; Zhang, H.-M.; Liu, W.; Liu, L.; Ma, J.; Xia, Z.; Chen, Y.; Chen, Y.; Wang, D.; Ni, P.; Guo, A.-Y.; Xiong, X. The Genome of *Ganoderma Lucidum* Provide Insights into Triterpenes Biosynthesis and Wood Degradation. *PLoS ONE* **2012**, *7*, e36146.

- (17) Saleh, O.; Haagen, Y.; Seeger, K.; Heide, L. Prenyl Transfer to Aromatic Substrates in the Biosynthesis of Aminocoumarins, Meroterpenoids and Phenazines: The ABBA Prenyltransferase Family. *Phytochem.* **2009**, *70*, 1728–1738.
- (18) Weyerstahl, P.; Marschall, H.; Christiansen, C.; Seelmann, I. On Some Italicene Derivatives. *Liebigs Ann.* **1996**, *1996*, 1641–1644.
- (19) Li, J.; Gao, K.; Bian, M.; Ding, H. Recent Advances in the Total Synthesis of Cyclobutane-Containing Natural Products. *Org. Chem. Front.* **2020**, *7*, 136–154.
- (20) Dembitsky, V. M. Bioactive Cyclobutane-Containing Alkaloids. *J. Nat. Med.* **2007**, *62*, 1–33.
- (21) Mashiko, T.; Shingai, Y.; Sakai, J.; Kamo, S.; Adachi, S.; Matsuzawa, A.; Sugita, K. Total Synthesis of Cochlearol B via Intramolecular [2+2] Photocycloaddition. *Angew. Chem. Int. Ed.* **2021**, *60*, 24484–24487.
- (22) Lu, Z.; Yoon, T. P. Visible Light Photocatalysis of [2+2] Styrene Cycloadditions by Energy Transfer. *Angew. Chem. Int. Ed.* **2012**, *51*, 10329–10332.
- (23) Hurtley, A. E.; Lu, Z.; Yoon, T. P. [2+2] Cycloaddition of 1,3-Dienes by Visible Light Photocatalysis. *Angew. Chem. Int. Ed.* **2014**, *53*, 8991–8994.
- (24) Wang, J.; Dong, Z.; Yang, C.; Dong, G. Modular and Regioselective Synthesis of All-Carbon Tetrasubstituted Olefins Enabled by an Alkenyl Catellani Reaction. *Nat. Chem.* **2019**, *11*, 1106–1112.
- (25) Poplata, S.; Tröster, A.; Zou, Y.-Q.; Bach, T. Recent Advances in the Synthesis of Cyclobutanes by Olefin [2 + 2] Photocycloaddition Reactions. *Chem. Rev.* **2016**, *116*, 9748–9815.
- (26) Strieth-Kalthoff, F.; James, M. J.; Teders, M.; Pitzer, L.; Glorius, F. Energy Transfer Catalysis Mediated by Visible Light: Principles, Applications, Directions. *Chemical Society Reviews* **2018**, *47*, 7190–7202.
- (27) Catellani, M.; Frignani, F.; Rangoni, A. A Complex Catalytic Cycle Leading to a Regioselective Synthesis of *o,O'*-Disubstituted Vinylarenes. *Angew. Chem. Int. Ed.* **1997**, *36*, 119–122.
- (28) Wang, J.; Dong, G. Palladium/Norbornene Cooperative Catalysis. *Chem. Rev.* **2019**, *119*, 7478–7528.
- (29) Della Ca', N.; Fontana, M.; Motti, E.; Catellani, M. Pd/Norbornene: A Winning Combination for Selective Aromatic Functionalization via C–H Bond Activation. *Acc. Chem. Res.* **2016**, *49*, 1389–1400.
- (30) Ye, J.; Lautens, M. Palladium-Catalysed Norbornene-Mediated C–H Functionalization of Arenes. *Nat. Chem.* **2015**, *7*, 863–870.
- (31) Wu, Z.; Fatuzzo, N.; Dong, G. Distal Alkenyl C–H Functionalization via the Palladium/Norbornene Cooperative Catalysis. *J. Am. Chem. Soc.* **2020**, *142*, 2715–2720.
- (32) Wu, Z.; Xu, X.; Wang, J.; Dong, G. Carbonyl 1,2-Transposition Through Triflate-Mediated  $\alpha$ -Amination. *Science* **2021**, *374*, 734–740.
- (33) Baker, W. Molecular Rearrangement of Some O-Acyloxyacetophenones and the Mechanism of the Production of 3-Acylchromones. *J. Chem. Soc.* *1933*, 1381–1389.
- (34) Mahal, H. S.; Venkataraman, K. Synthetic Experiments in the Chromone Group. Part XIV. The Action of Sodamide on 1-Acyloxy-2-Acetonaphthones. *J. Chem. Soc.* *1934*, 1767–1769.
- (35) Ameen, D.; Snape, T. Mechanism and Application of Baker–Venkataraman O→C Acyl Migration Reactions. *Synthesis* **2014**, *47*, 141–158.



- (36) Abdel Ghani, S. B.; Mugisha, P. J.; Wilcox, J. C.; Gado, E. A. M.; Medu, E. O.; Lamb, A. J.; Brown, R. C. D. Convenient One-Pot Synthesis of Chromone Derivatives and Their Antifungal and Antibacterial Evaluation. *Synth. Commun.* **2013**, *43*, 1549–1556.
- (37) Diethelm, S.; Carreira, E. M. Total Synthesis of Gelsemoxonine through a Spirocyclopropane Isoxazolidine Ring Contraction. *J. Am. Chem. Soc.* **2015**, *137*, 6084–6096.
- (38) Jeong, Y.; Moon, Y.; Hong, S. Tandem Dehydrogenation/Oxidation/Oxidative Cyclization Approach to Wrightiadione and Its Derivatives. *Org. Lett.* **2015**, *17*, 3252–3255.
- (39) Kapuriya, N. P.; Bhalodia, J. J.; Ambasana, M. A.; Patel, R. B.; Bapodra, A. H. Organocatalyzed Kabbe Condensation Reaction for Mild and Expedient Synthesis of 2,2-Dialkyl and 2-Spiro-4-Chromanones. *J. Heterocycl. Chem.* **2020**, *57*, 3369–3374.
- (40) Harutyunyan, S. R.; den Hartog, T.; Geurts, K.; Minnaard, A. J.; Feringa, B. L. Catalytic Asymmetric Conjugate Addition and Allylic Alkylation with Grignard Reagents. *Chem. Rev.* **2008**, *108*, 2824–2852.
- (41) Vargová, D.; Némethová, I.; Šebesta, R. Asymmetric Copper-Catalyzed Conjugate Additions of Organometallic Reagents in the Syntheses of Natural Compounds and Pharmaceuticals. *Org. Biomol. Chem.* **2020**, *18*, 3780–3796.
- (42) Godfrey, N. A.; Schatz, D. J.; Pronin, S. V. Twelve-Step Asymmetric Synthesis of (–)-Nodulisporic Acid C. *J. Am. Chem. Soc.* **2018**, *140*, 12770–12774.
- (43) Chesnokov, G. A.; Gademann, K. Concise Total Synthesis of Peyssonoside A. *J. Am. Chem. Soc.* **2021**, *143* (35), 14083–14088.
- (44) Hollmann, K.; Oppermann, A.; Witte, M.; Li, S.; Amen, M.; Flörke, U.; Egold, H.; Henkel, G.; Herres-Pawlis, S. Copper(I) Complexes with Thiourea Derivatives as Ligands: Revealing Secrets of Their Bonding Scheme. *Eur. J. Inorg. Chem.* **2017**, *2017*, 1266–1279.
- (45) Fulton, T. J.; Alley, P. L.; Rensch, H. R.; Ackerman, A. M.; Berlin, C. B.; Krout, M. R. Access to Functionalized Quaternary Stereocenters via the Copper-Catalyzed Conjugate Addition of Monoorganozinc Bromide Reagents Enabled by *N*, *N*-Dimethylacetamide. *J. Org. Chem.* **2018**, *83*, 14723–14732.
- (46) List, B. Introduction: Organocatalysis. *Chem. Rev.* **2007**, *107*, 5413–5415.
- (47) MacMillan, D. W. C. The Advent and Development of Organocatalysis. *Nature* **2008**, *455*, 304–308.
- (48) The Nobel Prize in Chemistry 2021 <https://www.nobelprize.org/prizes/chemistry/2021/summary/> (accessed 2022 -04 -01).
- (49) Lelais, G.; MacMillan, D. W. C. Modern Strategies in Organic Catalysis: The Advent and Development of Iminium Activation. *Aldrichimica Acta* **2006**, *39*, 11.
- (50) Eliel, E. L.; Wilen, S. H.; Doyle, M. P. *Basic Organic Stereochemistry*; Wiley, 2001.
- (51) Robak, M. T.; Herbage, M. A.; Ellman, J. A. Synthesis and Applications of *Tert*-Butanesulfinamide. *Chem. Rev.* **2010**, *110*, 3600–3740.
- (52) Brummel, B. R.; Lee, K. G.; McMillen, C. D.; Kolis, J. W.; Whitehead, D. C. One-Pot Absolute Stereochemical Identification of Alcohols via Guanidinium Sulfate Crystallization. *Org. Lett.* **2019**, *21*, 9622–9627.
- (53) Comins, D. L.; Dehghani, A. Pyridine-Derived Triflating Reagents: An Improved Preparation of Vinyl Triflates from Metallo Enolates. *Tetrahedron Lett.* **1992**, *33*, 6299–6302.
- (54) Reddy, Ch. R.; Srikanth, B.; Rao, N. N.; Shin, D.-S. Solid-Supported Acid-Catalyzed C3-Alkylation of 4-Hydroxycoumarins with Secondary Benzyl Alcohols: Access to 3,4-Disubstituted Coumarins via Pd-Coupling. *Tetrahedron* **2008**, *64*, 11666–11672.

- (55) Teegardin, K.; Day, J. I.; Chan, J.; Weaver, J. Advances in Photocatalysis: A Microreview of Visible Light Mediated Ruthenium and Iridium Catalyzed Organic Transformations. *Org. Process Res. Dev.* **2016**, *20*, 1156–1163.
- (56) Mariampillai, B.; Alliot, J.; Li, M.; Lautens, M. A Convergent Synthesis of Polysubstituted Aromatic Nitriles via Palladium-Catalyzed C–H Functionalization. *J. Am. Chem. Soc.* **2007**, *129*, 15372–15379.
- (57) Willand-Charnley, R.; Fisher, T. J.; Johnson, B. M.; Dussault, P. H. Pyridine Is an Organocatalyst for the Reductive Ozonolysis of Alkenes. *Org. Lett.* **2012**, *14* (9), 2242–2245.
- (58) Yang, D.; Zhang, C. Ruthenium-Catalyzed Oxidative Cleavage of Olefins to Aldehydes. *J. Org. Chem.* **2001**, *66* (14), 4814–4818.
- (59) Watson, D. W.; Gill, M.; Kemmitt, P.; Lamont, S. G.; Popescu, M. V.; Simpson, I. An Investigation Into the Role of 2,6-Lutidine as an Additive for the RuCl<sub>3</sub>-NaIO<sub>4</sub> Mediated Oxidative Cleavage of Olefins to Ketones. *Tetrahedron Lett.* **2018**, *49*, 4479–4482.
- (60) Taylor, J. E.; Janini, T. E.; Elmer, O. C. Aqueous Permanganate Oxidations of Cycloalkenes to *Cis* -Glycols and *Cis* to *Trans* Conversions. *Org. Process Res. Dev.* **1998**, *2*, 147–150.
- (61) Yu, W.; Mei, Y.; Kang, Y.; Hua, Z.; Jin, Z. Improved Procedure for the Oxidative Cleavage of Olefins by OsO<sub>4</sub>–NaIO<sub>4</sub>. *Org. Lett.* **2004**, *6*, 3217–3219.
- (62) Dupau, P.; Epple, R.; Thomas, A. A.; Fokin, V. V.; Sharpless, K. B. Osmium-Catalyzed Dihydroxylation of Olefins in Acidic Media: Old Process, New Tricks. *Adv. Synth. Catal.* **2002**, *344*, 421–433.
- (63) Chu, H.; Smith, J. M.; Felding, J.; Baran, P. S. Scalable Synthesis of (–)-Thapsigargin. *ACS Cent. Sci.* **2017**, *3*, 47–51.
- (64) Sudalai, A.; Khenkin, A.; Neumann, R. Sodium Periodate Mediated Oxidative Transformations in Organic Synthesis. *Org. Biomol. Chem.* **2015**, *13*, 4374–4394.
- (65) Crabtree, S. R.; Alex Chu, W. L.; Mander, L. N. C-Acylation of Enolates by Methyl Cyanofornate: An Examination of Site- and Stereoselectivity. *Synlett.* **1990**, *1990*, 169–170.
- (66) Schwartz, B. D.; Matoušová, E.; White, R.; Banwell, M. G.; Willis, A. C. A Chemoenzymatic Total Synthesis of the Protoilludane Aryl Ester (+)-Armillarivin. *Org. Lett.* **2013**, *15*, 1934–1937.
- (67) Bian, Z.; Marvin, C. C.; Pettersson, M.; Martin, S. F. Enantioselective Total Syntheses of Citrinadins A and B. Stereochemical Revision of Their Assigned Structures. *J. Am. Chem. Soc.* **2014**, *136*, 14184–14192.
- (68) Dietinger, C. E.; Banwell, M. G.; Garson, M. J.; Willis, A. C. Chemoenzymatic and Enantioselective Assembly of the (1 $\alpha$ ,3 $\beta$ ,6 $\alpha$ ,7 $\alpha\beta$ )-Octahydro-1,6-Methano-1H-Indene Framework Associated with 2-Isocyanoallopupukeanane: Validation of a New Synthetic Strategy and the Identification of Enantiomeric Switching Regimes. *Tetrahedron* **2010**, *66*, 5250–5261.
- (69) Ishihara, T.; Maekawa, T.; Yamasaki, Y.; Ando, T. New Organocuprate-Induced Reduction of the Enol Phosphate Moiety in 1-[(Diethoxyphosphinyl)Oxy]-F-1-Alkene-1-Phosphonates: An Efficient Synthesis of (*Z*)-1-Hydro-F-1-Alkene-1-Phosphonates. *J. Org. Chem.* **1987**, *52*, 300–302.
- (70) Paquette, L. A.; Dahnke, K.; Doyon, J.; He, W.; Wyant, K.; Friedrich, D. Regioselective Conversion of Cycloalkanones to Vinyl Bromides with 1,2-Functionality Transposition. A General Stratagem. *J. Org. Chem.* **1991**, *56*, 6199–6205.

- (71) Moorhoff, C. M.; Schneider, D. F. Preparation of Alkyl 3-Methylalka-2,4-Dienoates from Gamma,Delta-Unsaturated Beta-Keto Esters via the Corresponding Conjugated Unsaturated 3-Enol Phosphates. *Tetrahedron* **1998**, *54*, 3279–3290.
- (72) Krawczuk, P. J.; Schöne, N.; Baran, P. S. A Synthesis of the Carbon Skeleton of Maoecrystal V. *Org. Lett.* **2009**, *11*, 4774–4776.
- (73) Zhang, F.; Danishefsky, S. J. An Efficient Stereoselective Total Synthesis of Dl-Sesquicillin, a Glucocorticoid Antagonist. *Angew. Chem. Int. Ed.* **2002**, *41*, 1434–1437.
- (74) Schreiber, J.; Maag, H.; Hashimoto, N.; Eschenmoser, A. Dimethyl(Methylene)Ammonium Iodide. *Angew. Chem. Int. Ed.* **1971**, *10*, 330–331.
- (75) Dudley, G. B.; Tan, D. S.; Kim, G.; Tanski, J. M.; Danishefsky, S. J. Remarkable Stereoselectivity in the Alkylation of a Hydroazulenone: Progress Towards the Total Synthesis of Guanacastepene. *Tetrahedron Lett.* **2001**, *42*, 6789–6791.
- (76) Iwamoto, M.; Miyano, M.; Utsugi, M.; Kawada, H.; Nakada, M. Synthetic Studies on the Seven- and Eight-Membered Rings by the Intramolecular Nozaki-Hiyama Reaction of the Allylic Phosphates. *Tetrahedron Lett.* *45*, 8653–8657.
- (77) Luche, J.-L.; Rodriguez-Hahn, L.; Crabbé, P. Reduction of Natural Enones in the Presence of Cerium Trichloride. *J. Chem. Soc., Chem. Commun.* **1978**, *14*, 601–602.
- (78) Kong, L.; Su, F.; Yu, H.; Jiang, Z.; Lu, Y.; Luo, T. Total Synthesis of (–)-Oridonin: An Interrupted Nazarov Approach. *J. Am. Chem. Soc.* **2019**, *141*, 20048–20052.
- (79) Shiina, Y.; Tomata, Y.; Miyashita, M.; Tanino, K. Asymmetric Total Synthesis of Glycinoeclepin A: Generation of a Novel Bridgehead Anion Species. *Chem. Lett.* **2010**, *39*, 835–837.
- (80) Kotoku, N.; Mizushima, K.; Tamura, S.; Kobayashi, M. Synthetic Studies of Cortistatin A Analogue from the CD-Ring Fragment of Vitamin D<sub>2</sub>. *Chem. Pharm. Bull.* **2013**, *61*, 1024–1029.
- (81) Frolov, A. I.; Ostapchuk, E. N.; Pashenko, A. E.; Chuchvera, Y. O.; Rusanov, E. B.; Volochnyuk, D. M.; Ryabukhin, S. V. Selective  $\alpha$ -Methylation of Ketones. *J. Org. Chem.* **2021**, *86*, 7333–7346.
- (82) Winkler, J. D.; Londregan, A. T.; Hamann, M. T. Antimalarial Activity of a New Family of Analogues of Manzamine A. *Org. Lett.* **2006**, *8*, 2591–2594.
- (83) Wuts, P. G. M.; Theodora, W. G. *Greene's Protective Groups in Organic Synthesis*, 4th ed.; Wiley: Hoboken, New Jersey, 2007.
- (84) Tanaka, T.; Mikamiyama, H.; Maeda, K.; Iwata, C.; In, Y.; Ishida, T. Total Synthesis of (–)-Macrocarpal C. Stereoselective Coupling Reaction with a Novel Hexasubstituted Benzene Cr(CO)<sub>3</sub> Complex as a Biomimetic Chiral Benzyl Cation Equivalent. *J. Org. Chem.* **1998**, *63*, 9782–9793.
- (85) Wipf, P.; Jung, J.-K. Formal Total Synthesis of (+)-Diepoxin  $\sigma$ . *J. Org. Chem.* **2000**, *65*, 6319–6337.
- (86) Pan, W.; Li, C.; Zhu, H.; Li, F.; Li, T.; Zhao, W. A Mild and Practical Method for Deprotection of Aryl Methyl/Benzyl/Allyl Ethers with HPPH<sub>2</sub> and *t*BuOK. *Org. Biomol. Chem.* **2021**, *19*, 7633–7640.
- (87) Lee, Kwan-Soo. A Convenient and Efficient Method for Demethylation of Aryl Methyl Ethers with Magnesium Iodide in Ionic Liquid. *Bull. Korean Chem. Soc.* **2010**, *31*, 3842–3843.

- (88) Hoye, T. R.; Humpal, P. E.; Moon, B. Total Synthesis of (–)-Cylindrocyclophane A via a Double Horner-Emmons Macrocyclic Dimerization Event. *J. Am. Chem. Soc.* **2000**, *122*, 4982–4983.
- (89) Richardson, A. D.; Vogel, T. R.; Traficante, E. F.; Glover, K. J.; Schindler, C. S. Total Synthesis of (+)-Cochlearol B by an Approach Based on a Catellani Reaction and Visible-Light-Enabled [2+2] Cycloaddition. *Angew. Chem. Int. Ed.* **2022**, *Accepted*, DOI: 10.1002/anie.202201213.
- (90) Monos, T. M.; Sun, A. C.; McAtee, R. C.; Devery, J. J.; Stephenson, C. R. J. Microwave-Assisted Synthesis of Heteroleptic Ir(III)<sup>+</sup> Polypyridyl Complexes. *J. Org. Chem.* **2016**, *81*, 6988–6994.

## Chapter 5 Progress Towards the Total Synthesis of Gelsemoxonine

### 5.1 Introduction

*Gelsemium* is a genus of flowering plants in the Gelsemiaceae family. This genus is comprised of three species: *Gelsemium elegans*, *Gelsemium rankinii*, and *Gelsemium sempervirens*. Found across Asia and North America, these plants have a rich history in traditional medicines.<sup>1</sup> Among other things, these plants have been used to treat cancer pain, skin ulcers, rheumatism, influenza, and anxiety. In an effort to identify the compounds responsible for the pharmacological activity, phytochemical studies of *Gelsemium* plants have identified more than 190 different alkaloids, iridoids, and steroids.<sup>1</sup> Bioactivity evaluations have shown that individual compounds possess different therapeutic properties including analgesic, anti-inflammatory, immunomodulating, and antitumor activity.<sup>1</sup> The vast majority of these *Gelsemium* derived products are alkaloids, with over 120 structures identified to date.<sup>2</sup>

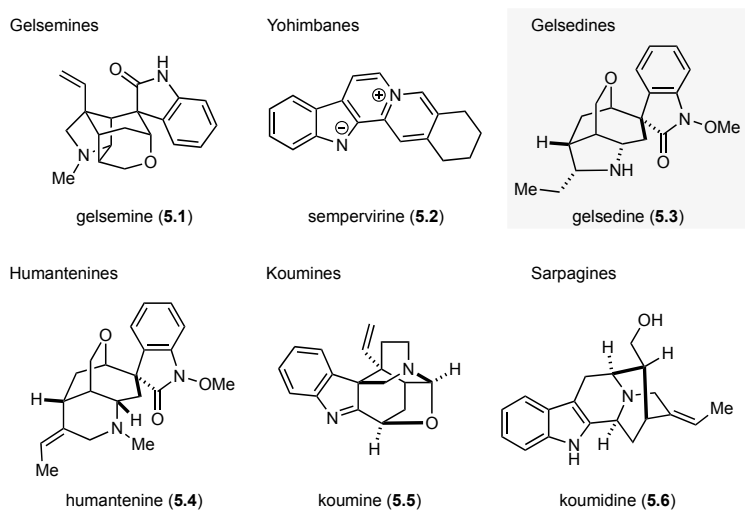


Figure 5.1 Representative member from each of the six families of *Gelsemium* alkaloids.

Referred to broadly as the *Gelsemium* alkaloids, these many diverse and complex natural products have been further classified into six families: gelsemines, yohimbanes, gelsedines, humantenines, koumines, and sarpagines (Figure 5.1). Of these six families, three contain a common spiro-oxindole motif (the gelsemines, humantenines, and gelsedines). Spirocyclic

oxindoles are considered a privileged scaffold in drug discovery because of their presence in some anticancer agents.<sup>3</sup>

Gelsemine (**5.1**), and its analogs, have received considerable attention from the synthetic communities because of its challenging three-dimensional architecture.<sup>4</sup> However, recent bioactivity evaluations have sparked researchers' interest in gelsidine (**5.3**) type alkaloids.<sup>5</sup> These will be the focus of the remainder of this section.

The gelsidine family is composed of around 50 different monoterpenoid indole alkaloids (Figure 5.2). The majority have been isolated from *Gelsemium elegans*, with a handful coming from *Gelsemium sempervirens*.<sup>1</sup> Although structurally different, these natural products all contain a conserved oxabicyclo[3.2.2]nonane core with a pendant spirocyclic oxindole (Figure 5.2A). These alkaloids all differ in the substituents that decorate the core, primarily at C14 and C15, and in the identity and substitution of the *N*-heterocycle substituent (Figure 5.2B). The gelsidine alkaloids have been the subject of numerous biological studies; however, a comprehensive bioactivity analysis remains challenging because of the low natural abundance of these natural products.

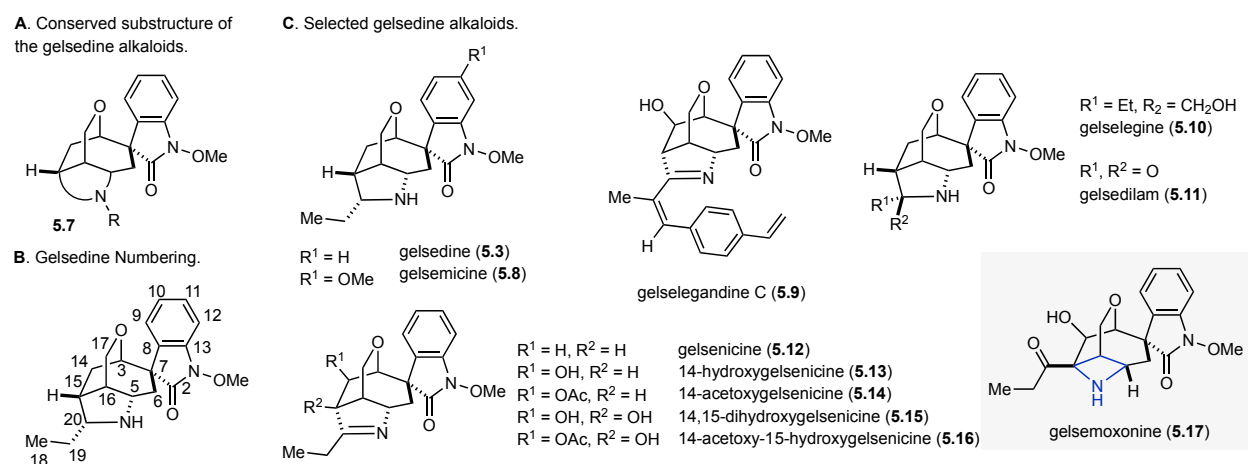


Figure 5.2 (A) Conserved substructures of the gelsidine alkaloids. (B) Carbon numbering scheme of gelsidine. (C) Representative *Gelsemium* alkaloids.

Despite their use in traditional medicine, the leaves, stems, and roots of all three *Gelsemium* species are highly poisonous. Individuals who overdose on *Gelsemium* exhibit symptoms similar to alkaloid poisoning, which is attributed to the high alkaloid concentration of these plants.<sup>1-6</sup> Crude alkaloid extracts from *Gelsemium elegans* have an LD<sub>50</sub> of 1.56 mg/kg in female mice when administered intravenously.<sup>7</sup> Among the monomer alkaloids from *Gelsemium sempervirens*,

gelsemicine was the most toxic, whereas gelsenicine was the most toxic alkaloid from *Gelsemium elegans*.<sup>1</sup>

Extracts from *Gelsemium* plants demonstrate anti-tumor effects *in vivo* and *in vitro*. These extracts have shown activity against hepatic carcinoma cells, ovarian cancer cells and breast cancer cells.<sup>1</sup> However, there have only been a limited number of studies evaluating the pharmacological activities of individual gelsedine type alkaloids. The Takayama group evaluated the cytotoxicity of 14 different *Gelsemium* alkaloids against A431 epidermoid carcinoma cells.<sup>8,9</sup> Of the 14 different alkaloids tested, the six highest performing compounds were all gelsedine type alkaloids (Figure 5.3). Four of those six compounds outperformed the positive control, cisplatin, with the best cytotoxicity coming from 14,15-dihydroxygelsenicine (**5.15**) with an EC<sub>50</sub> of 250 nM (Figure 5.3).

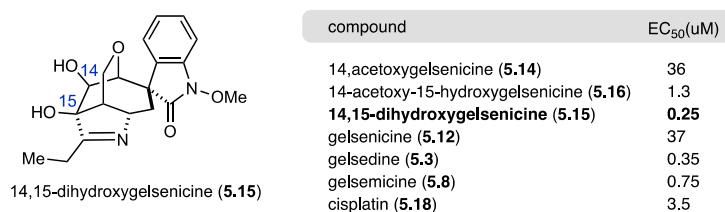


Figure 5.3 EC<sub>50</sub> values for six gelsedine type alkaloids against human A431 epidermoid carcinoma cells.

Chronic neuropathic pain, in both the peripheral and central nervous systems, remains extremely challenging to treat and is particularly unresponsive to currently available drugs. Alkaloid extracts from *Gelsemium elegans* have demonstrated potent analgesic activity measured by the increased pain threshold in rats and mice that have been administered sub lethal doses of the extracts.<sup>1</sup> In an effort to identify gelsenicine's (**5.12**) role in the observed analgesic properties, the Yu group tested its effects on inflammatory and neuropathic pain in mice.<sup>10</sup> A variable dose analysis showed that gelsenicine (**5.12**) exhibits dose dependent analgesic effects on acetic acid-induced writhing. Pretreating mice with 4 or 20 µg/kg of gelsenicine (**5.12**) inhibited writhing by 41-59% with an ED<sub>50</sub> of 10.4 µg/kg. In addition, the Yu group analyzed the effects of gelsenicine (**5.12**) on formalin-induced nociceptive behavior. Hind paw injection of formalin is used to assess intense, short term pain, the effects of which are expressed by hind limb licking and shaking. These effects can be observed in two separate phases, phase I and phase II, separated by a short period of quiescence. Gelsenicine (**5.12**) dose-dependently inhibited nociceptive behavior, or pain induced reflexes, in phase II with an ED<sub>50</sub> of 7.4 µg/kg. Gelsenicine (**5.12**) was also tested for its effects on thermal hyperalgesia, or heightened sensitivity to heat or cold. Mice with chronic

constriction injury induced thermal hyperalgesia were treated with different doses of gelsenicine (**5.12**). It attenuated the thermal hypersensitivity with an ED<sub>50</sub> of 9.8 μg/kg. This study demonstrates that gelsenicine (**5.12**) has dose-dependent analgesic effects on both inflammatory and neuropathic pain.

Totalling around 2000 different compounds, terpene indole alkaloids are a diverse and complex class of natural products. Given the many structural differences, and the inherent challenges associated with studying plant metabolite biosynthesis, the biosynthetic relationship between these compounds has remained unclear.<sup>11</sup> It is known that monoterpene indole alkaloids, like the gelsedine type alkaloids, are derived from tryptamine (**5.19**) and the iridoid terpene secologanin (**5.20**) (Figure 5.4). In fact, it has been shown that these two precursors combine to form strictosidine (**5.21**) which lies along the route to *Gelsemium* oxindole alkaloids.<sup>12</sup> In 2019, the O'Connor group discovered three genes encoding the enzymes responsible for converting tryptophan and secologanin (**5.20**) to strictosidine (**5.21**) and then strictosidine aglycone (**5.22**).<sup>13</sup> Specifically, tryptophan decarboxylase converts tryptophan to tryptamine (**5.19**). Then, strictosidine synthase (STR) catalyzes a stereoselective Pictet-Spengler condensation between tryptamine (**5.19**) and secologanin (**5.20**), yielding strictosidine (**5.21**) (Figure 5.4). Following that, strictosidine glucosidase (SGD) converts strictosidine (**5.21**) into strictosidine aglycone (**5.22**). This structure is believed to be a common intermediate along the pathway to many of these alkaloids.

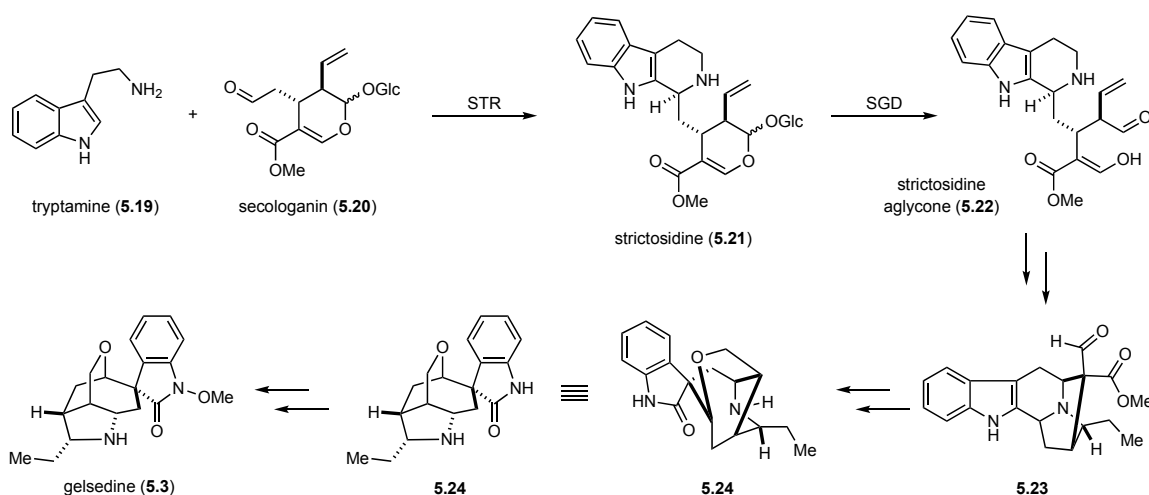


Figure 5.4 Proposed biosynthesis of gelsedine.

In regard to how **5.22** converts to the gelsedine alkaloids, the Sakai group proposed that **5.22** is first converted to norsarpagine type compound **5.23**. **5.23** was then proposed to convert to



**5.24** through a key oxidative-ring opening-rearrangement cascade. Final oxidation of the indole to the *N*-methoxyindole would furnish gelsedine.<sup>14</sup> In support of this biosynthetic proposal, the Sakai group disclosed their efforts to mimic it using chemical synthesis. Using their biomimetic approach, the Sakai group completed semi-syntheses of several gelsedine type alkaloids, including gelsemicine,<sup>15</sup> gelselegine, gelsenicine, and gelsedine.<sup>16</sup>

In response to their potent biological activity, low natural abundance, and interesting structural features, the gelsedine type alkaloids have become popular targets for synthetic organic chemists.<sup>5</sup> A number of total syntheses, formal syntheses, semi-syntheses, and synthetic efforts towards these natural products have been reported. The first came in 1979 when the Baldwin group disclosed their synthesis of the core of gelsedine (**5.3**) and gelsemicine (**5.8**).<sup>17</sup> In 1990 two additional studies toward gelsedine (**5.3**) and gelsemicine (**5.8**) were reported.<sup>18</sup> <sup>19</sup> In 1994 Sakai and coworkers published a 17-step semi-synthesis of gelsemicine (**5.8**) starting from the natural product gardnerine.<sup>15</sup> They claimed that their route represented a biomimetic approach. Later that year, they also published the semi-syntheses of gelselegine (**5.10**), gelsenicine (**5.12**), and gelsedine (**5.3**) relying on a similar strategy.<sup>16</sup> The first total synthesis of a gelsidine alkaloid came in 1999 when Hiemstra and coworkers reported their synthesis of the non-natural enantiomer of gelsedine (**5.3**), (+)-gelsedine.<sup>20</sup> Since then, total syntheses of gelsedine (**5.3**), gelsenicine (**5.12**), gelsedilam (**5.11**), gelsemoxonine (**5.17**) and more have been published by groups including those of Fukuyama,<sup>21,22</sup> Carreira,<sup>23,24</sup> Ma,<sup>25</sup> Ferreira,<sup>26</sup> Zhao,<sup>27</sup> Takayama,<sup>28</sup> and others (Figure 5.5).



Figure 5.5 Previously used disconnections to access the oxacyclic[3.2.2]nonane core of the gelsedine type alkaloids.

Originally structurally misassigned upon isolation in 1991,<sup>29</sup> gelsemoxonine (**5.17**) is a unique among the gelsedine type because it features a densely substituted azetidine ring.<sup>30</sup> Although gelsemoxonine (**5.17**) has no reported potent biological activity, there have only been a limited number of studies thus far and further analysis is needed to fully elucidate gelsemoxonine's pharmacological properties. The structural similarities between gelsemoxonine (**5.17**) and other bioactive gelsedine type alkaloids is a promising indication that unrealized potential is present. Total synthesis represents one solution to providing enough material to conduct these studies and

overcome the low natural abundance of gelsemoxonine (**5.17**). Due in part to this fact, and its unique structural features, gelsemoxonine (**5.17**) has become a popular target for synthetic organic chemists.

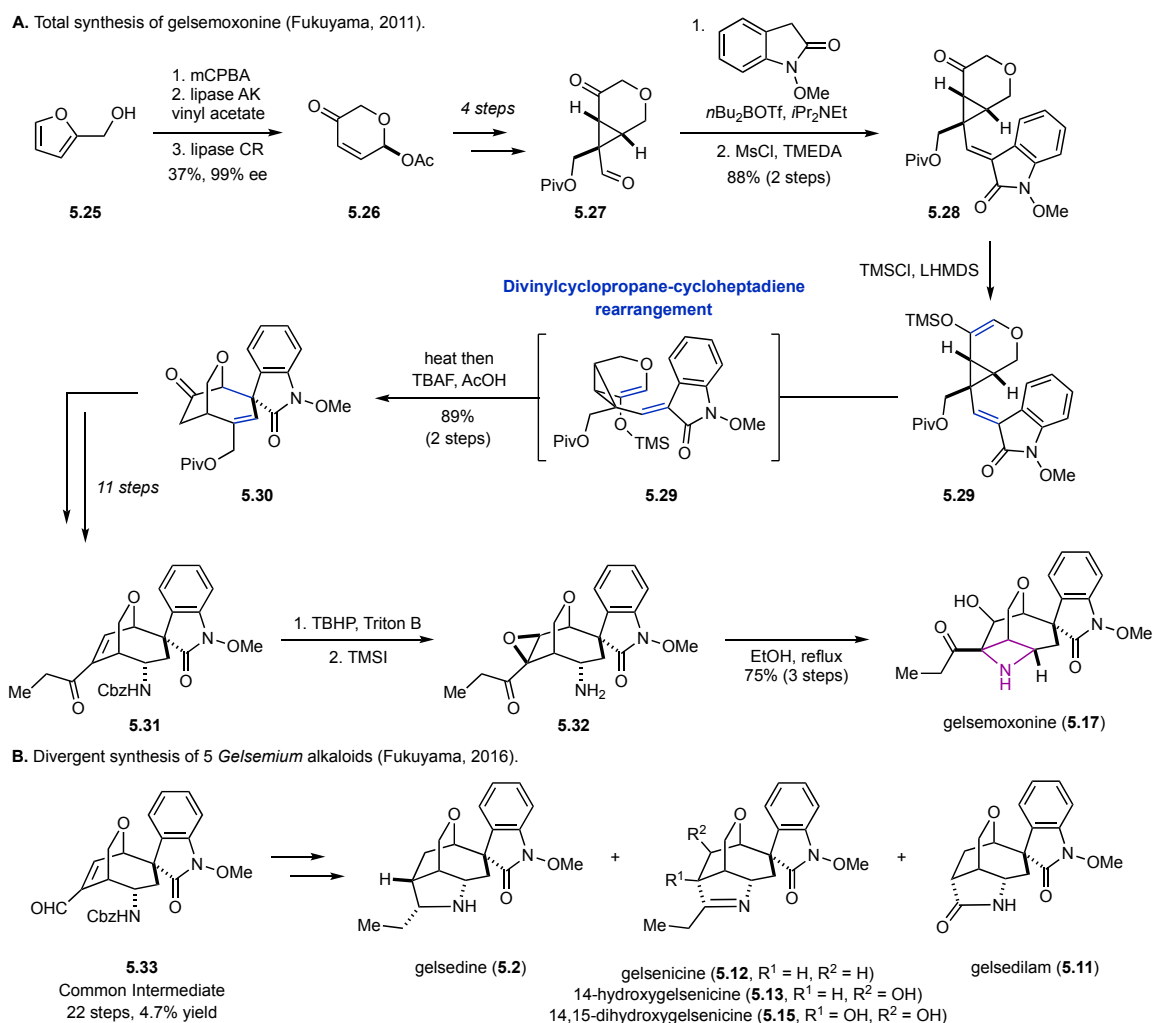


Figure 5.6 (A) Fukuyama's asymmetric total synthesis of gelsemoxonine. (B) Divergent synthesis of gelsidine, gelsenicine, 14-hydroxygelsenicine, 14,15-dihydroxygelsenicine, and gelsedilam.

The first total synthesis of gelsemoxonine (**5.17**) was reported by the Fukuyama group in 2011 (Figure 5.6A).<sup>21</sup> Starting from furfuryl alcohol (**5.25**), enantiomerically enriched **5.26** was prepared using an Achmatowicz reaction followed by two sequential enzymatic kinetic resolutions. An additional 4 steps brought **5.27** to cyclopropane-containing, keto aldehyde **5.28**. Following an aldol condensation with *N*-methoxyoxindole, the ketone was converted to the corresponding TMS enol ether **5.29** setting up the key divinylcyclopropane rearrangement. **5.29** successfully underwent the desired rearrangement upon treatment with TBAF and AcOH, forming the oxabicyclo[3.2.2]-nonane core and the spirocyclic oxindole (**5.30**). An additional 11 steps were needed to install the

C5 amine and the  $\alpha,\beta$ -unsaturated ethyl ketone (**5.31**). Following epoxidation and deprotection, the azetidine ring was closed through an intramolecular epoxide opening reaction (**5.17**). This was the final step in Fukuyama and coworkers 24 step enantioselective total synthesis of gelsemoxonine (**5.17**). In 2016, the Fukuyama group published a divergent approach to five different gelsedine type alcohols relying on a common intermediate from their synthesis of gelsemoxonine (**5.17**) (Figure 5.6B).<sup>22</sup>

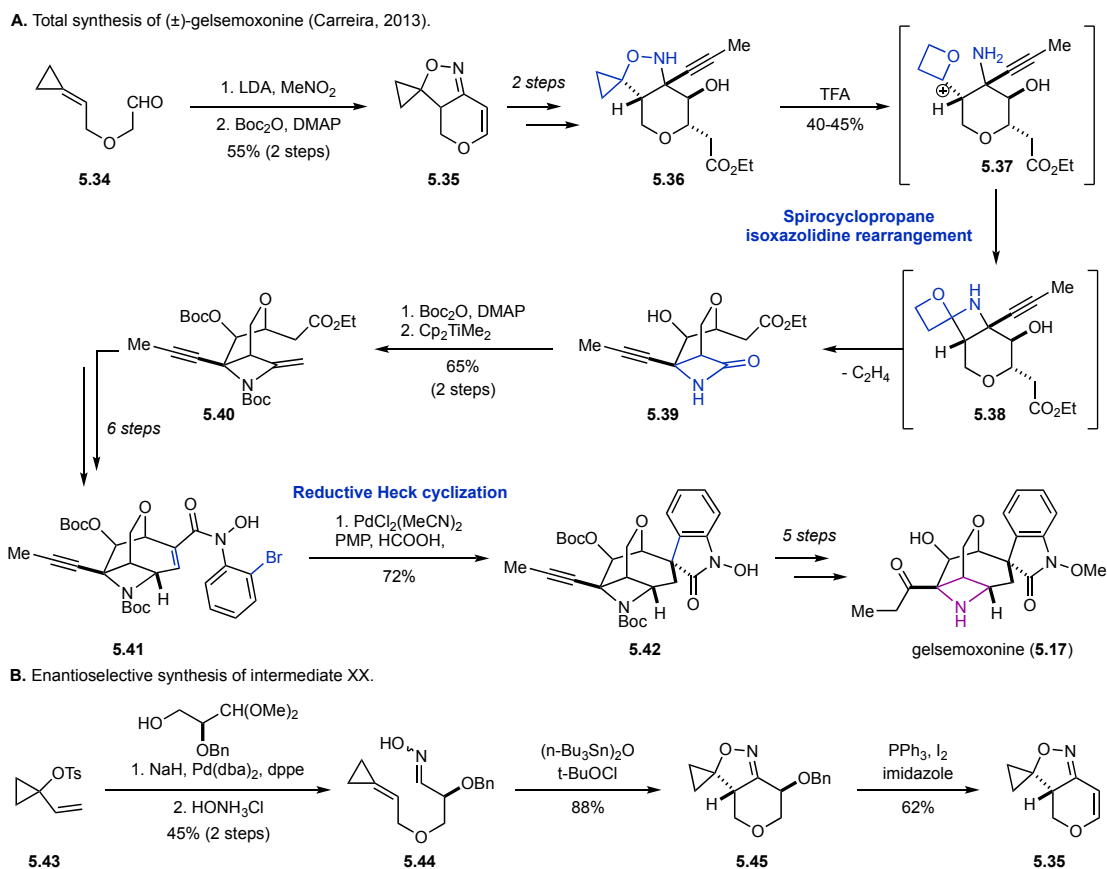


Figure 5.7 (A) Carreira's total synthesis of ( $\pm$ )-gelsemoxonine. (B) Enantioselective approach to intermediate **5.35**.

In 2013, the Carreira group reported a 26 steps synthesis of ( $\pm$ )-gelsemoxonine (**5.17**),<sup>23</sup> 21 steps from known aldehyde **5.34** (Figure 5.7A).<sup>31</sup> Starting from aldehyde **5.34**, spirocyclopropane isoxazolidine **5.35** was prepared in 2 steps. **5.36** was then elaborated prior to undergoing a desired acid mediated rearrangement to lactam **5.39**. Following a Boc protection, the lactam was methenylated according to a protocol developed by Howell and coworkers (**5.40**).<sup>32</sup> An additional 6-steps takes intermediate **5.40** through to **5.41**. The final hurdle was the formation of the spirocyclic oxindole, which was done using a reductive Heck cyclization (**5.42**). This is a common strategy in the synthesis of *Gelsemium* alkaloids and was initially applied by the Overman group

in their total synthesis of ( $\pm$ )-gelsemine.<sup>33</sup> Minor protecting group and oxidation state manipulations completed the synthesis of ( $\pm$ )-gelsemoxonine (**5.17**). In 2015, Carreira and coworkers reported an enantioselective synthesis of intermediate **3.35** that could enable an asymmetric total synthesis of gelsemoxonine (Figure 5.7B).<sup>24</sup>

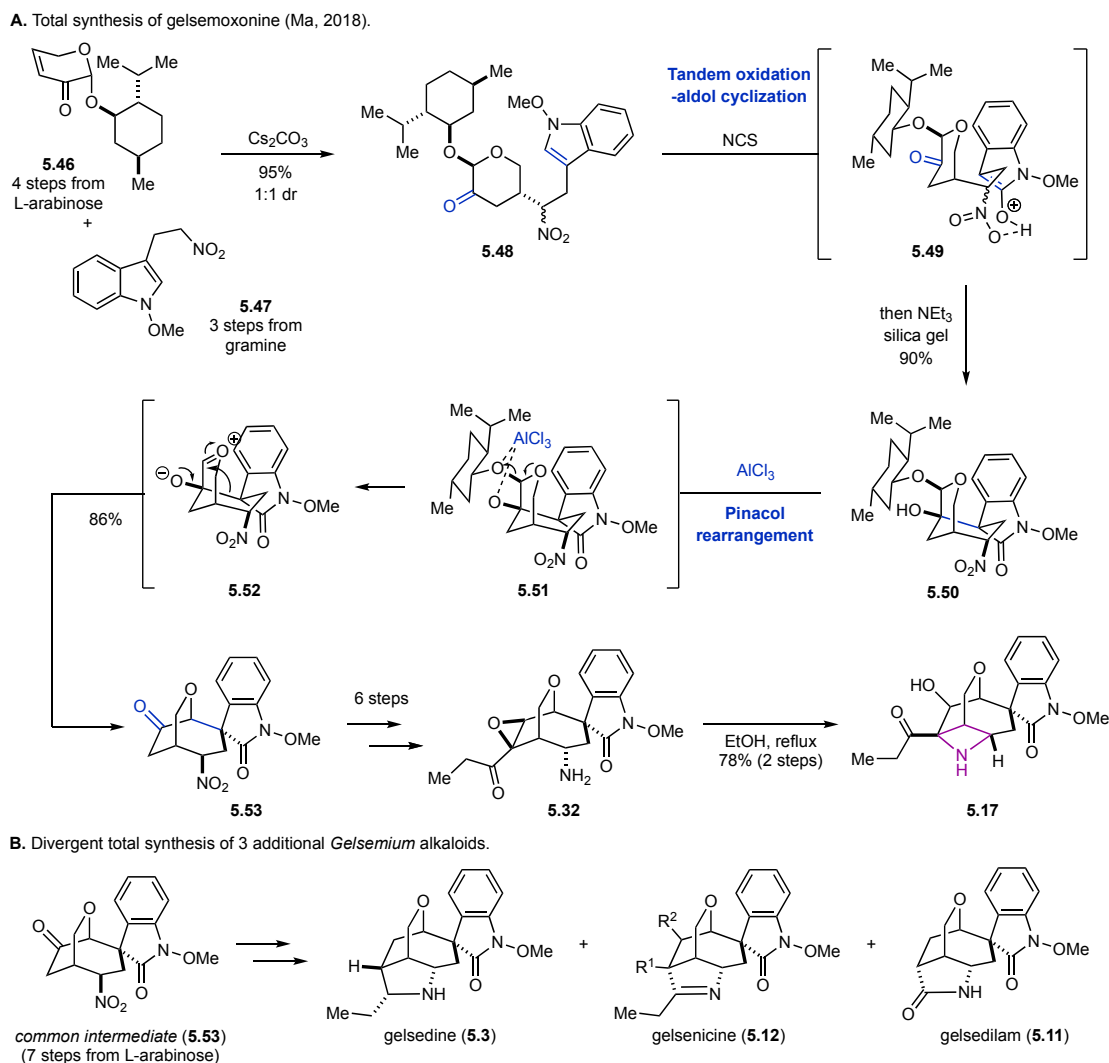


Figure 5.8 (A) Ma's asymmetric total synthesis of gelsemoxonine. (B) Divergent total synthesis of gelsedine, gelsenicine, gelsedilam.

The most recent synthesis of gelsemoxonine came from Ma and coworkers in 2018 as part of their divergent entry to four different *Gelsemium* alkaloids (Figure 5.8A).<sup>25</sup> Their synthesis started from known indole **5.47** and menthol derived enone **5.46**. Following a Michael addition between these two, a one pot oxidation/aldol addition formed the spirocyclic oxindole ring (**5.50**). A subsequent pinacol rearrangement formed the oxabicyclo[3.2.2]nonane core of gelsemoxonine (**5.17**). The menthol group acted as a chiral auxiliary through these first three steps and was cleaved

during the pinacol rearrangement step to provide enantiopure **5.53**. An additional 6 steps were needed to arrive at intermediate **5.32**, the same final intermediate as in Fukuyama's synthesis of gelsemoxonine (**5.17**). Intramolecular epoxide opening completes their 13-step asymmetric synthesis of gelsemoxonine (**5.17**). The Ma group postulated that an intramolecular cyclization is likely the way the azetidine ring is formed biosynthetically. They also diversified intermediate **5.53** to three other gelsedine type natural products (Figure 5.8B).

Apart from the azetidine ring of gelsemoxonine, arguably the most synthetically challenging feature of these natural products is the stereogenic spirocyclic oxindole. Broadly speaking, C3-stereogenic oxindoles exist in a number of different forms in natural products<sup>2</sup> and pharmaceuticals.<sup>34</sup> However, this discussion will focus on spirocyclic oxindoles. This scaffold is common to many natural products and pharmaceuticals outside of just the *Gelsemium* alkaloids (Figure 5.9A). Additionally, spirocyclic oxindoles are also considered a privileged scaffold in drug discovery because of their presence in anticancer agents.<sup>3</sup> As such, oxindoles have received a lot of attention from the synthetic community. However, differentially C3-disubstituted oxindoles are difficult to synthesize using traditional enolate chemistry because of the high stability of the enolate and tendency towards over reactivity (over alkylation, aldol condensation, etc.). As a result a number of alternative methods have been developed to overcome this limitation.<sup>35,36,37</sup> Isatin (**5.58**) is an alternative feedstock chemical that is often used to synthesize C3-quaternary oxindoles (Figure 5.9C).<sup>38</sup> However, it is generally used for the synthesis C3-hydroxy oxindoles. One common method to synthesize spirocyclic oxindoles is an oxidative rearrangement from the corresponding indole (Figure 5.9D). This strategy has been utilized in the synthesis of some gelsedine type alkaloids.<sup>15,16</sup> That said, one drawback of this strategy is that competing formation of the indoxyl isomer (**5.63**) can occur. It also typically requires harsh reaction conditions. There has also been significant research into the synthesis of oxindoles using transition metal catalysis (Figure 5.9E and 5.9F).<sup>39</sup> These methods can be used to form either the C3-C4 bond or the C2-C3 bond. As mentioned above, metal catalyzed approaches to the oxindole have a history of use in the *Gelsemium* alkaloids starting with Overman and coworkers synthesis of (±)-gelsemine (**5.1**) in 2005.<sup>33</sup> In their synthesis, they utilized a Heck reaction to form the spirocyclic oxindole. Additionally, a number of enantioselective variations have been developed enabling the synthesis of chiral oxindoles. Very recently, the Hyster group reported an enzymatic approach to enantioenriched oxindoles through the asymmetric formation of the C3-C4 bond.<sup>40</sup> Alternatively,

there is one example of *N*-C9 bond formation being used to close the oxindole ring. This example comes from the Ferreira group in their total synthesis of gelsenicine (**5.12**).<sup>26</sup>

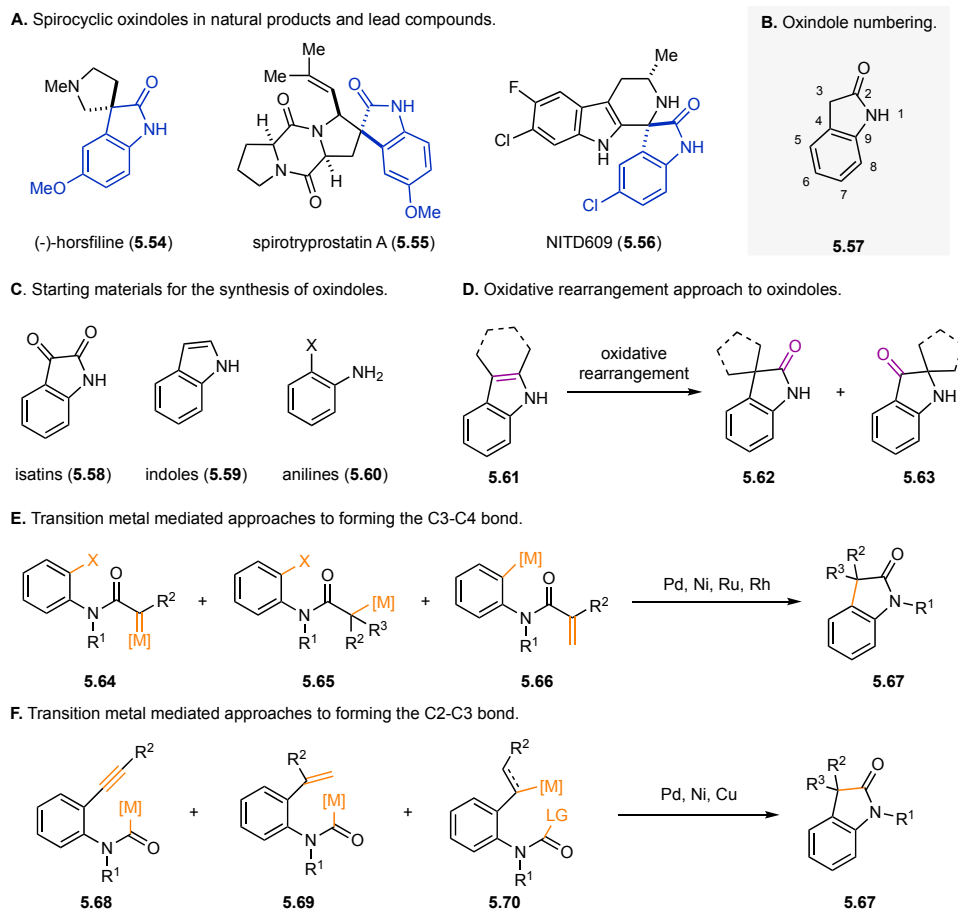


Figure 5.9 (A) Spirocyclic oxindoles in natural products and lead compounds. (B) Numbered oxindole. (C) Common starting materials for the synthesis of oxindoles. (D) Oxidative rearrangement approach to oxindoles. (E) Transition metal mediated approach to forming the C3-C4 bond. (F) Transition metal mediated approach to forming the C2-C3 bond.

Chapter 3 focused on our group's development of a visible light mediated aza Paternò-Büchi reaction for the synthesis of azetidines.<sup>41</sup> Historically, the aza Paternò-Büchi has been limited by competing reactivity and, as a result, has not been frequently used in total synthesis.<sup>42</sup> For example, the previous syntheses of gelsemoxonine (**5.17**) used more established methods, such as intramolecular substitution and  $\beta$ -lactam reduction, to form the azetidines. We hypothesized that our novel approach to azetidines could enable facile access to gelsemoxonine (**5.17**) and help realize new disconnections. Herein, we report our efforts towards the total synthesis of gelsemoxonine (**5.17**) centered around an aza Paternò-Büchi approach.

## 5.2 Results and Discussion

### 5.2.1 First Generation: Aldol/Enyne Metathesis Approach

Central to our proposal was the idea that the azetidine ring could be formed using an aza Paternò-Büchi reaction. To accomplish this, we envisioned using the method we developed for selective alkene excitation using triplet energy transfer from a visible light absorbing photosensitizer (Chapter 3).<sup>43,44</sup> This transformation relies on conjugated alkenes (dienes and styrenes) because of their low-lying triplet energies. This requirement was factored into our retrosynthetic analysis (Figure 5.20), and as a result [2+2], cycloaddition precursor **5.72** was proposed. We believed that after the aza Paternò-Büchi reaction, intermediate **5.71** could be carried forward to gelsemoxonine (**5.17**) through three simple functional group manipulations. The challenge then became accessing **5.72** in an efficient manner. We envisioned that an enyne metathesis reaction could close the dihydropyran and form the diene.<sup>45</sup> We proposed forming oxime intermediate **5.72** after attempting an enyne metathesis because of Grubbs catalyst's ability to engage in metathesis reaction between alkenes and oximes.<sup>46</sup> Our focus then shifted to arriving at key enyne metathesis precursor **5.74**. Much of this chapter will be dedicated to our efforts towards this goal.

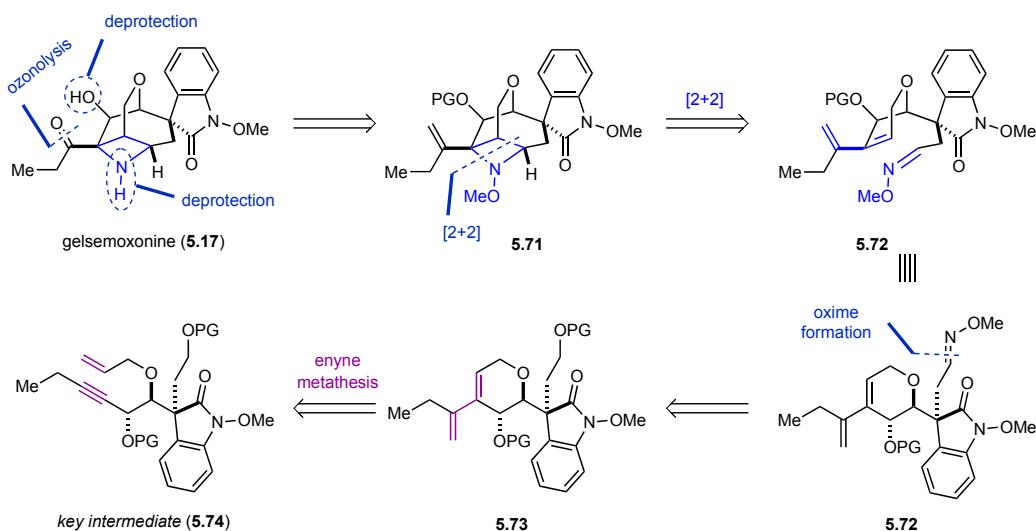


Figure 5.10 Retrosynthetic analysis of gelsemoxonine featuring a key visible light mediated [2+2]-cycloaddition as well as an enyne metathesis reaction.

Initially, an aldol addition reaction between a 3-substituted oxindole **3.76** and aldehyde **3.75** was proposed (Figure 5.11A). Aldehyde **5.48** was prepared in a 5-step sequence (Figure 5.11B) starting with the addition of butynyllithium to diethyl oxalate (**5.77**) to form keto ester **5.78**.

Subsequent treatment of **5.78** with alpine borane produced **5.79** in high enantioselectivity.<sup>47</sup> Following PMB protection under acidic conditions, the ester was converted to the desired aldehyde in a two-step sequence. With **5.82** in hand, our efforts turned to an aldol addition between **5.82** and known 3-substituted oxindole **5.83**.<sup>27</sup>

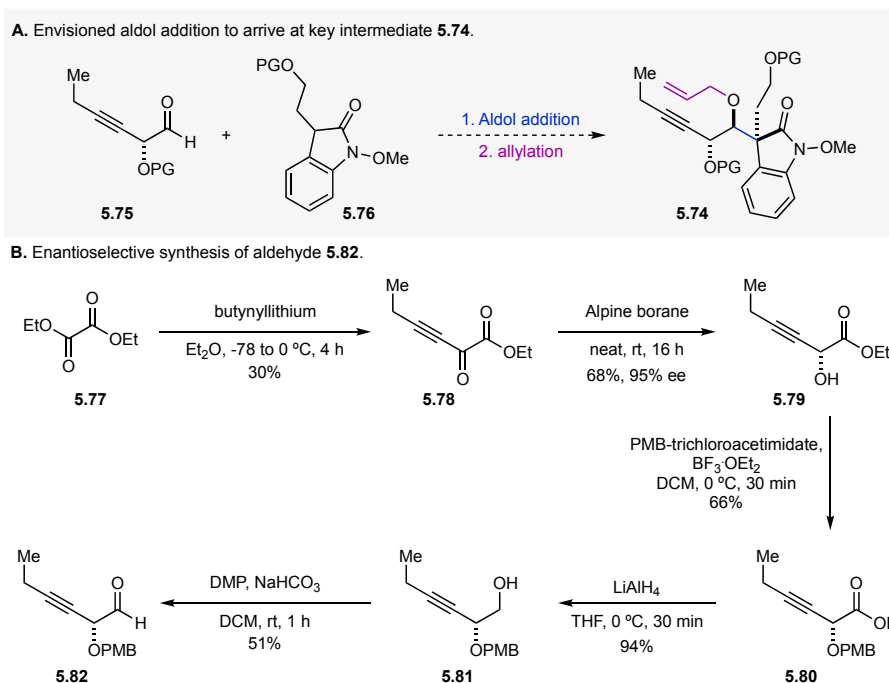


Figure 5.11 A) Envisioned aldol approach to key intermediate **5.74**. B) Enantioselective synthesis of aldehyde **5.82**.

Unfortunately, under a variety of conditions, none of the aldol product was observed (Figure 5.12A). Mukaiyama-Aldol conditions using the corresponding TMS enol ether **5.84** were also evaluated;<sup>48</sup> however, none was successful (Figure 5.12A). It is known that aldol addition to form C3-quaternary oxindoles is challenging. This is due in large part to the reversible nature of the aldol reaction<sup>27</sup> and the entropic and thermodynamic favorability of the starting materials (Figure 5.12B). Current methods for the formation of C3 quaternary oxindoles through an aldol reaction have a limited scope and are very sensitive to the protecting group on the nitrogen.<sup>49,50</sup> Typically, an electron withdrawing carbamate group is needed to lower the pKa of the oxindole so that mild bases can be used. For example, *N*-methyl oxindole (**5.89**) has a pKa of 18.5 whereas *N*-acetyl oxindole (**5.90**) has a pKa of 13.7 (Figure 5.12C).<sup>51</sup>



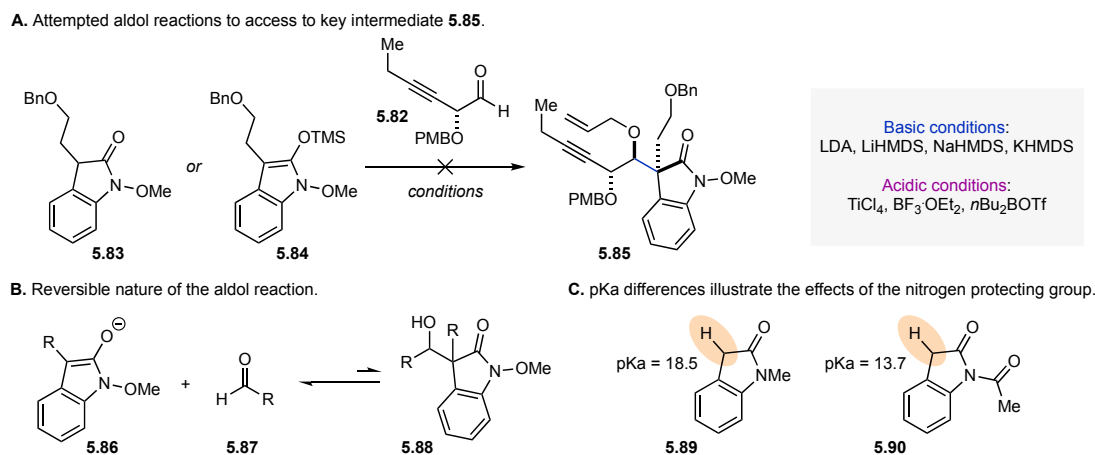


Figure 5.12. (A) Attempted Aldol and Mukaiyama-Aldol reactions to access key intermediate **5.85**. (B) Retro-aldol reaction scheme. (C) Evidence for the influence of the nitrogen protecting group on pKa.

To overcome this obstacle, we envisioned switching the order of steps by first accomplishing an aldol addition using an unsubstituted oxindole, then forming the quaternary center at a later stage. In order to conserve material, initial experiments were conducted using known aldehyde hex-3-ynal.<sup>52</sup> Treating oxindole **5.91** with LDA followed by hex-3-ynal resulted in the formation of aldol product **5.93** in 40% yield (Figure 5.13A). The yield of the aldol addition step could be improved to 58% by first forming TMS enol ether **5.92** then subjecting it to Mukaiyama-Aldol conditions using  $\text{TiCl}_4$  (Figure 5.13A). Prior to forming the C3 quaternary oxindole, methods for incorporating the *O*-allyl fragment necessary for the enyne metathesis reaction were explored (Figure 5.13B). Unfortunately, treatment of **5.93** with a variety of different bases, followed by the addition of allyl bromide, led to exclusive formation of retro-Aldol products (Figure 5.13B, entries 1-3). Alternatively, acidic mediated alkylation reactions, using *O*-allyl trichloroacetimidate, resulted in mostly recovered starting material with small amounts of elimination product **5.95** (Figure 5.13B, entries 5 & 6). Silver mediated alkylation conditions were also unsuccessful (Figure 5.13B, entry 4). Interestingly, treatment of **5.93** with allyl carbonate and a palladium catalyst led to the formation of C3 disubstituted oxindole **5.94** as the sole product. This product arises through palladium catalyzed allylation of the oxindole rather than the alcohol.<sup>53</sup> Before investing more time into evaluating alkylation conditions, we investigated the feasibility of this aldol reaction with aldehyde **5.82**. Although desired product **5.97** could be isolated, it formed in a mixture of 4 diastereomers calling into question the feasibility of a selective aldol addition, as well as this strategy as a whole (Figure 5.13C).

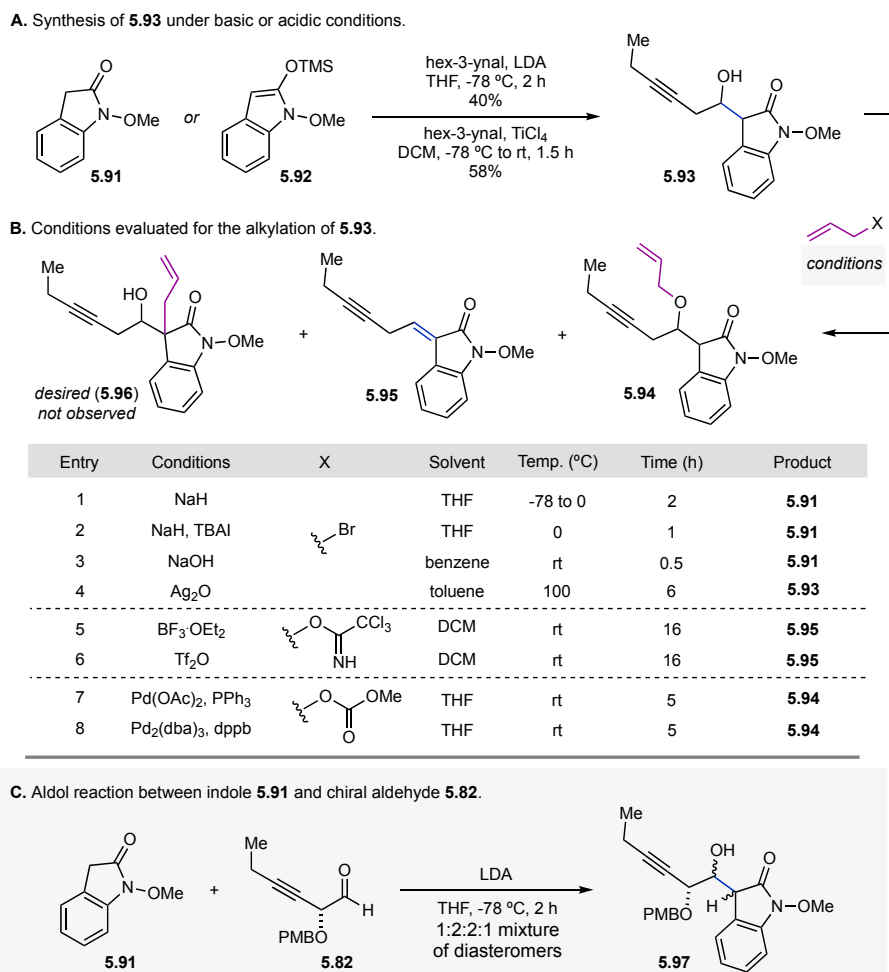


Figure 5.13 (A) Synthesis of **5.93** under acidic or basic conditions. (B) Evaluation of different alkylation conditions. (C) Aldol reaction between indole **5.91** and chiral aldehyde **5.82**.

The challenges associated with working with oxindoles and their propensity for retro-aldol reaction caused us to reevaluate our strategy. Specifically, we hypothesized that the oxindole could be formed at a later stage in the synthesis, which is a common strategy in this family of natural products.<sup>33,23,26</sup> In order to conserve most other aspects of our route, methyl phenylacetate (**5.98**) was used in place of oxindole **5.91** (Figure 5.14). Our studies to this point brought to light the challenges in alkylating alcohols  $\beta$  to a carbonyl group. With this as our main concern, model system **5.99** was prepared and subjected to a variety of alkylation conditions. Both basic and acidic conditions were unsuccessful; however, Ag<sub>2</sub>O mediated alkylation using allyl bromide provided the desired *O*-allyl product **5.100** in 50% yield. **5.100** was then treated with Grubbs second generation catalyst and gratifyingly, the desired enyne metathesis product **5.101** was isolated in 61% yield.<sup>54</sup> Despite this successful demonstration of the feasibility of the enyne metathesis

reaction, serious questions remained about the viability of using an aldol approach to arrive at our proposed advanced intermediates.

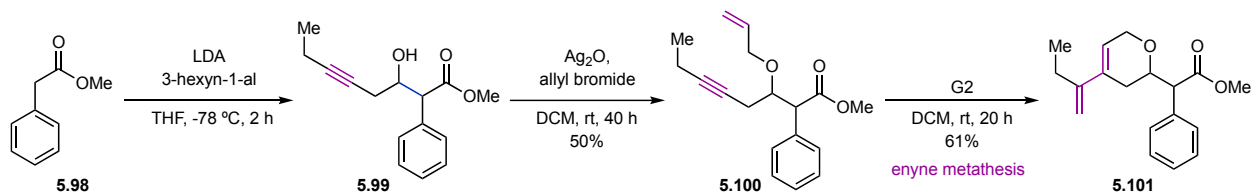


Figure 5.14 Model systems studies on the enyne metathesis reaction.

### 5.2.2 Second Generation: Aldol/Achmatowicz Approach

Concurrent studies were focused on a slightly different approach to the key diene intermediate **5.73**. This strategy centered around using an Achmatowicz reaction to form the dihydropyran ring (Figure 5.15).<sup>55</sup> This approach offered the distinct advantage of incorporating the required oxidation at C14, an aldol reaction without an aldehyde containing an  $\alpha$ -stereocenter, and a potentially shorter route overall. However, there are some also some disadvantages compared to the enyne metathesis approach. For instance, there is now extra oxidation at C17 that would need to be removed, and furthermore, a challenging cross coupling reaction would be needed to form the diene.

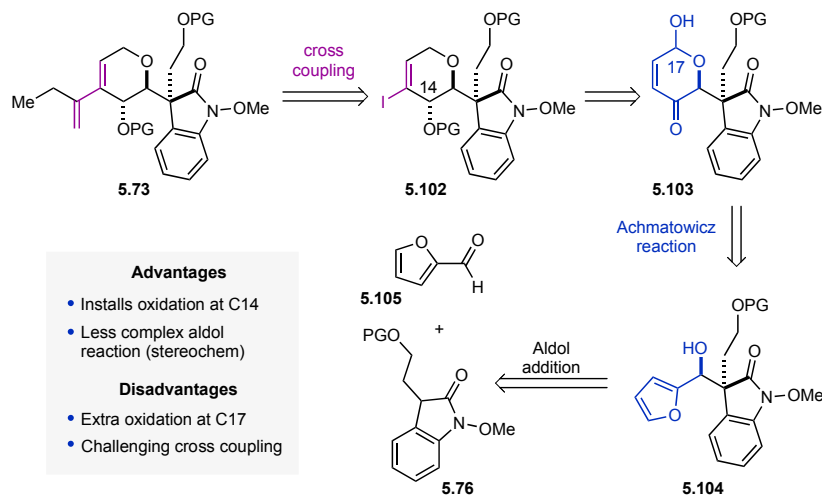


Figure 5.15 Retrosynthetic analysis utilizing an alternative Achmatowicz reaction approach.

Initial base mediated aldol reaction between furfural and N-OMe oxindole resulted in exclusively the aldol condensation products. We quickly switched to using methyl phenylacetate (**5.98**) instead of oxindole **5.91** because of the problems we were experiencing in related aldol reactions (Chapter 5, Section 5.2.1). Known, substituted methyl phenylacetate **5.106**<sup>56</sup> was treated

with LDA and CuI, followed by furfural (**5.105**), and the desired aldol addition product **5.107** was isolated in 33% yield as an equal mixture of two diastereomers (Figure 5.16). Upon treatment with *m*CPBA, the furfuryl alcohol underwent the desired Achmatowicz reaction providing **5.108** as a mixture of 4 isomers in 75% yield. The lactol was subsequently protected using TBSCl to give **5.109** in 79% yield. Treatment of **5.109** with iodine resulted in the formation of  $\alpha$ -iodo-enone **5.110** in 95% yield. As a proof of concept, **5.110** was subjected to Suzuki reaction conditions using phenylboronic acid as a coupling partner. The desired product **5.112** could be isolated in low yields. Our goal was to test ideal coupling partner boronic acid **5.111**, in addition to other coupling partners, at a later stage. In order to arrive at key intermediate **5.73**, the lactol would also have to be reduced. Prior to that, deprotection of TBS was necessary to convert the lactol into a better leaving group. Unfortunately, treating **5.112** with a variety of deprotection conditions resulted in the formation of complex mixtures. We hypothesized that this was likely due to the instability of the dimethyl acetal.

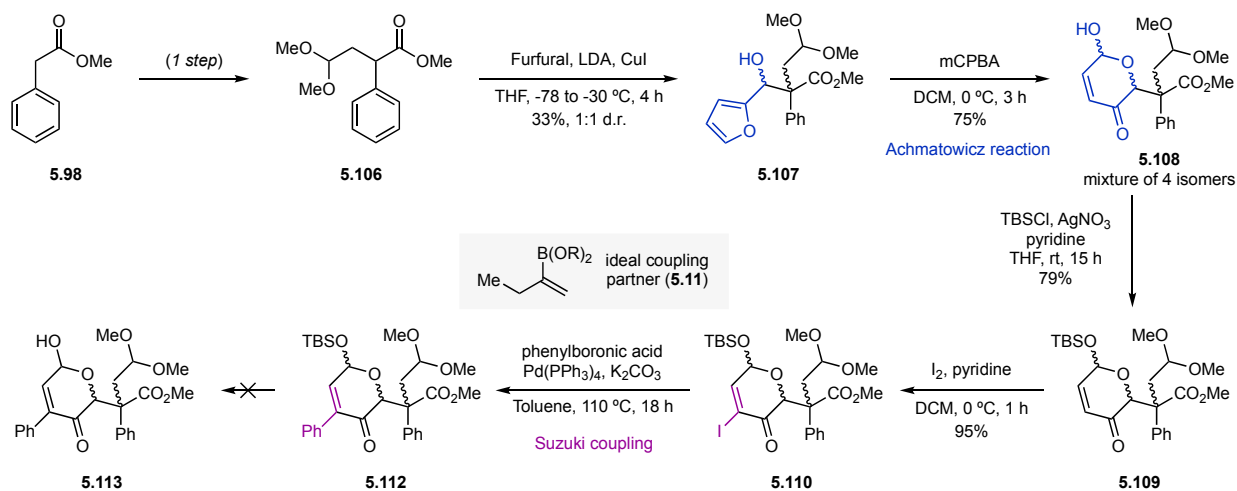


Figure 5.16 Initial studies verifying the feasibility of the Achmatowicz reaction and the challenges that arise in the subsequent steps.

To overcome this, alternative substrate **5.116** was prepared in a similar three step sequence (Figure 5.17). First methyl phenylacetate (**5.98**) was alkylated with allyl bromide to provide **5.114** in 70% yield. Then **5.114** underwent the desired aldol addition reaction to form **5.115** in a 3:1 mixture of diastereomers in 66% yield. Upon treatment with *m*CPBA, the Achmatowicz rearrangement successfully provided **5.116** in 58% yield. Instead of protecting the lactol with a TBS group, **5.116** was treated with acetic anhydride to form the corresponding acetate **5.117**. We elected to work with the acetate because it is a better leaving group and is known to enable lactol

reduction.<sup>57</sup> Unfortunately, selectivity was a major issue in this reaction, as we observed competing 1,4-reduction of the enone. In an effort to mitigate this undesired reactivity, **5.117** was treated with NaBH<sub>4</sub> in an attempt to accomplish a 1,2-reduction, a step that would already be necessary at some point in the synthesis. However, exclusive 1,4-reduction (**5.120**) was observed under those conditions. A successful strategy that relies on an Achmotowicz reaction may still be realized. However, the selectivity issues suggest substrate modification would be necessary, which calls into question the efficiency of this route. This led us to explore other avenues to accessing key later state intermediates.

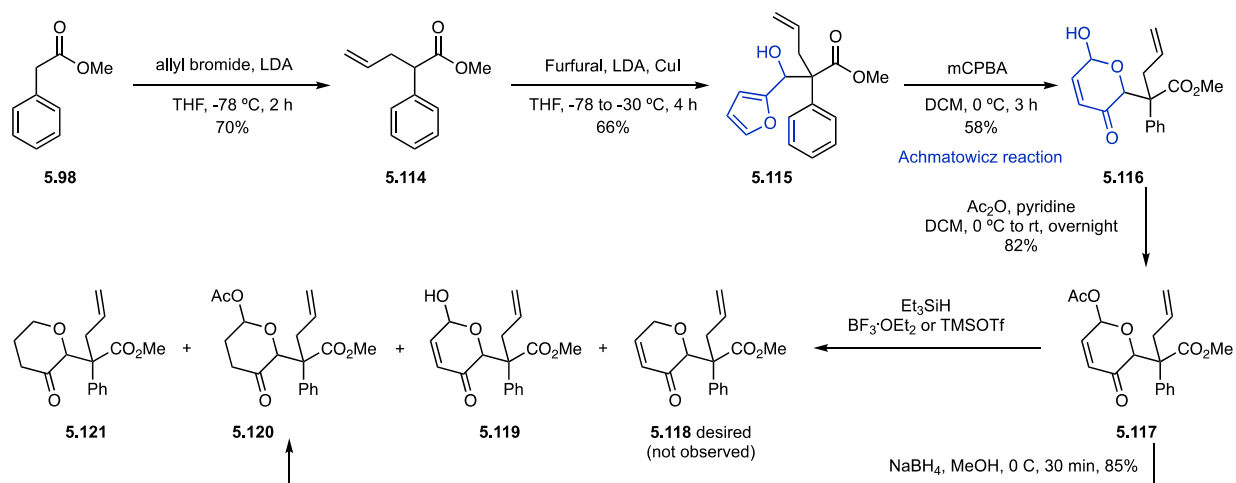


Figure 5.17 Progress towards an Achmatowicz product capable of undergoing selective lactol reduction.

### 5.2.3 Third Generation: Oxidative Rearrangement Approach

In response to the challenges we encountered in constructing C3 quaternary oxindoles using an aldol reaction, we explored other strategies for assembling this subunit. One alternative that has been used previously in the *Gelsemium* alkaloid literature is an oxidative rearrangement that forms oxindoles from the corresponding indoles (Figure 5.9D).<sup>36</sup> For example early work on this strategy came from the Sakai group in their total synthesis of gelsemicine (**5.8**), gelscencicine (**5.12**), gelsedine (**5.3**), and gelselegine (**5.8**).<sup>15,16</sup> It is also postulated to be how this scaffold is formed biosynthetically.<sup>16</sup> There are several advantages to this strategy. First, the amount of literature on functionalizing indoles is much greater than oxindoles.<sup>58</sup> Secondly, this could enable forming the oxindole at a stage in which a retro-aldol is no longer possible, which would solve the major problem we had been experiencing with manipulating oxindoles. With this in mind we altered our retrosynthetic analysis to include the oxidative rearrangement reaction (Figure 5.18).

However, the later state disconnections, including the [2+2] reaction and the enyne metathesis reaction remained the same. The oxidative rearrangement would instead be used in route to enyne precursor **5.74**. To test this strategy, oxidative rearrangement precursor **5.123** was selected as our initial target.

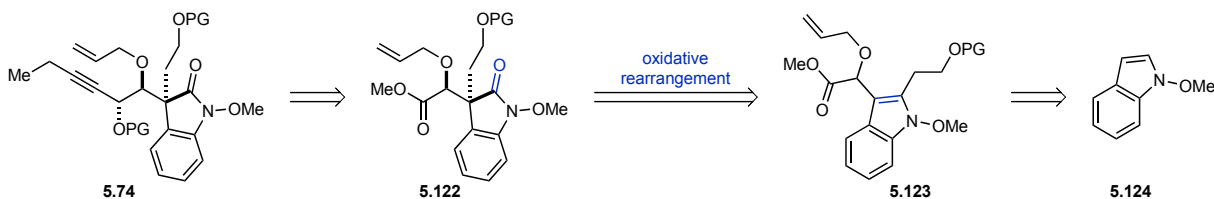


Figure 5.18 Third generation retrosynthetic analysis relying on an oxidative rearrangement approach to the oxindole.

Starting from **5.124**, formylation at C2 was accomplished using *n*BuLi and DMF (Figure 5.19). A subsequent homologation reaction yielded compound **5.126**, which was then hydrolyzed and reduced to the corresponding alcohol **5.127** in 73% yield over those three steps. Following a TBS protection, C3 acylation was achieved using oxalyl chloride. The remaining acid chloride was quenched with methanol, providing **5.128** in 56% yield over two steps. The ketone was reduced to the alcohol using NaBH<sub>4</sub> producing **5.129** in 73% yield. A final Ag<sub>2</sub>O mediated alkylation<sup>59</sup> with allyl bromide provided the desired oxidative rearrangement precursor **5.130** in 45% yield.

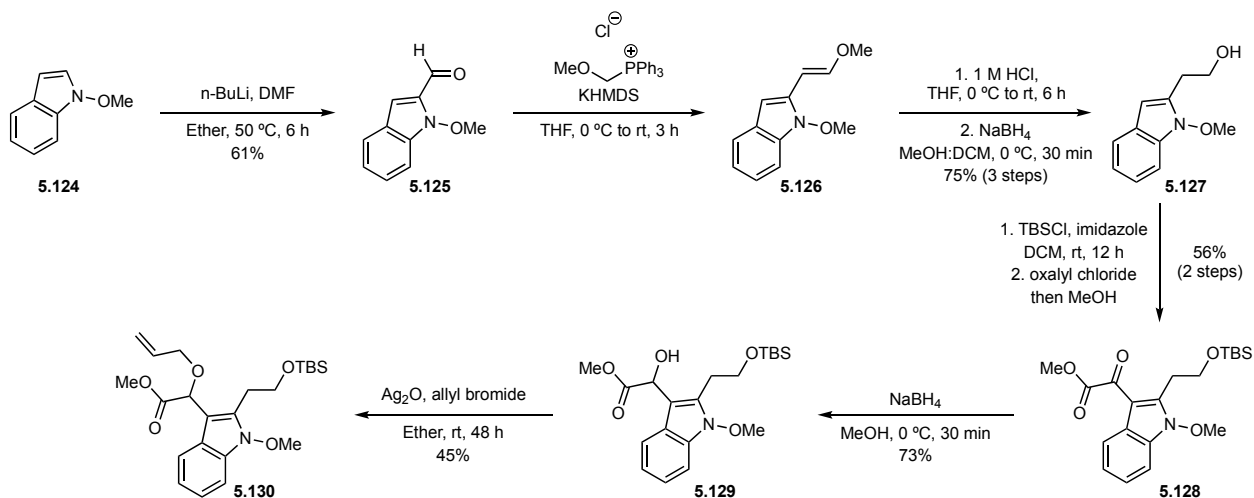
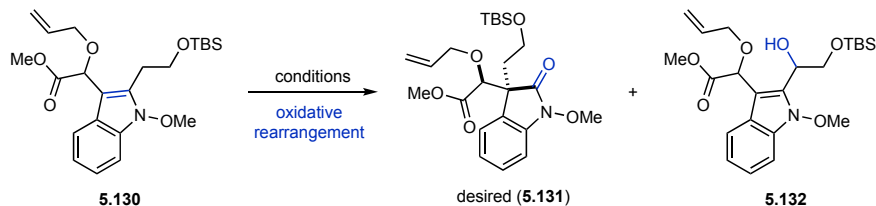


Figure 5.19 Synthesis of oxidative rearrangement substrate **5.130**.

We tested several different oxidants, and the results are summarized in Table 5.1. Functional group intolerance was a concern as **5.130** contains other functionality that may undergo oxidation. Indeed, over oxidation was observed when *m*CPBA<sup>60</sup> and osmium tetroxide<sup>16</sup> were used (Table 1.1, entries 7-9). Treatment with Selectfluor<sup>TM</sup> led to an inscrutable mixture (Table 1.1, entry 4),<sup>61</sup> likely due to additional TBS deprotection. No reaction was observed when using

lead(IV) acetate (Table 1.1, entry 10).<sup>62</sup> With all other oxidants<sup>25,63,64</sup> the only product that was observed was **5.132** in varying amounts.

Table 5.1 Conditions evaluated for the oxidative rearrangement reaction.



Entry	Oxidant	Solvent	Temp. (°C)	Time (h)	Product
1	NCS, H <sub>2</sub> O	THF	-20 to 0	2	<b>5.132</b>
2	NBS, H <sub>2</sub> O	THF	-20	1	<b>5.132</b>
3	NIS, H <sub>2</sub> O	THF	0	1	SM
4	Selectfluor	MeCN	rt	10 min	decomp.
5	Oxone	Me <sub>2</sub> CO:H <sub>2</sub> O	0	2	SM + <b>5.132</b>
6	tBuOCl	DCM	0	5	<b>5.132</b>
7	mCPBA (3 eq.)	DCM	rt	1	over ox.
8	mCPBA (1 eq.)	DCM	0	2	SM + over ox.
9	K <sub>2</sub> [OsO <sub>2</sub> (OH) <sub>4</sub> ], NMO	Me <sub>2</sub> CO:H <sub>2</sub> O	rt	8	over ox.
10	Pb(OAc) <sub>4</sub>	DCM	rt	2	N.R.

We hypothesize that **5.130** forms through the following mechanism. First, the desired oxidation occurs at the C3 position of the indole (**5.133**). The unstable iminium ion that forms then isomerizes to the corresponding enamine (**5.134**). A subsequent rearrangement restores aromaticity to the indole and transfers the oxidation to the benzylic position. After an aqueous workup, **5.132** is then isolated as the product.

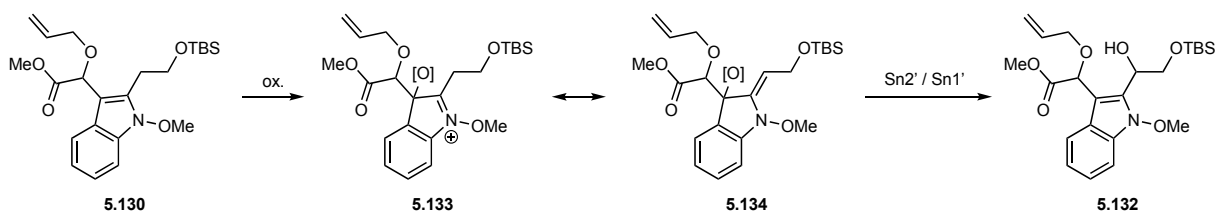


Figure 5.20 Hypothesized mechanism for the formation of unexpected byproduct **5.132**.

The majority of examples of oxidative rearrangements in the literature are on free NH indoles, or indoles bearing no substitution on the C2 position.<sup>36</sup> In these cases, the intermediates are either 1) an imine which is much more stable than the corresponding iminium ion or 2) an iminium ions that is unable to isomerize to the enamine. We hypothesize that the unstable alkoxyiminium in our system is driven to isomerize and directs this undesired reaction. The logical solution to this would be to try the oxidative rearrangement with the corresponding NH indole. However, this would necessitate oxidizing the NH bond to an N-OMe bond at a later stage. The

only reported method for converting NH oxindoles to N-OMe oxindoles uses a three-step sequence that involves first reducing them the corresponding indolene, followed by oxidizing it back to the N-OH oxindole, then alkylation with diazomethane.<sup>15</sup> This sequence is lengthy, low yielding, and involves dangerous and costly reagents such a diazomethane. As a result, we didn't feel this was a practical strategy. This realization concluded our efforts into utilizing an oxidative rearrangement strategy for the synthesis of gelsemoxonine.

### 5.3 Conclusion and Outlook

*Gelsemium* is a genus of flowering plants that has a long history of use in traditional medicines.<sup>1</sup> Gelsemoxonine is a structurally interesting natural product that is part of a large diverse family of alkaloids known as the *Gelsemium* alkaloids.<sup>2</sup> The low natural abundance has limited the biological activity analysis of many of these alkaloids, gelsemoxonine included. As a result, an efficient and scalable synthesis of gelsemoxonine is desirable. However, this remains a challenge in large part to the densely substituted azetidine ring featured in gelsemoxonines structure. Our interest in gelsemoxonine started with our labs work in the area of the aza Paternò-Büchi reaction.<sup>41</sup> Chapter 3 discusses the development of a visible light mediated [2+2]-cycloaddition reaction for the synthesis of azetidines. Although gelsemoxonine has been synthesized previously, a reliable and mild [2+2]-cycloaddition method towards azetidines had not been developed. As a result, the previous syntheses were confined to more traditional methods for azetidine formation (substitution and  $\beta$ -lactam reduction). We felt that our novel method could enable more facile access to gelsemoxonine and help realize new disconnections that were not accessible from the existing methods for azetidine synthesis. Furthermore, gelsemoxonine is an ideal target because the structure can be easily adapted to the requirements for the aforementioned visible light enabled [2+2]-cycloaddition reaction. We proposed multiple routes to access the key [2+2]-cycloaddition precursors. In one route, an enyne metathesis reaction was explored as a way to close the pyran ring and form the diene. In another, an Achmatowicz reaction was implemented to form the pyran ring with the desired oxygenation in place. Unfortunately, early efforts to test these key steps were hampered by difficulties with manipulating oxindoles using an aldol reaction. Switching to methyl phenylacetate alleviated some of these difficulties; however, significant challenges remained. An approach markedly different to the aldol reaction, an oxidative



rearrangement from the corresponding indole, was explored. Despite the precedence in the synthesis of related natural products, this strategy also proved unsuccessful.

The challenges we faced herein highlight the difficulties of making complex 3,3-disubstituted N-OMe oxindoles, and illustrate the need for continued improvement in the available methods. The immediate future of this project will focus on constructing the oxindole fragment of gelsemoxonine. There are number of elegant transition metal catalyzed methods for the synthesis of oxindoles that could provide a solution.<sup>39</sup> Regardless of the method we select, the challenge will be designing an ideal strategy to take advantage of it. Attention can then shift to testing the key disconnections of our proposed synthesis, the [2+2] and enyne metathesis reactions. Importantly, we have demonstrated that enyne metathesis can be used to form the desired pyran ring. Additionally, we have evidence that the [2+2] reaction can successfully form strained polycyclic azetidines. These facts make us cautiously optimistic that, once the problems are solved in early steps of our synthesis, we can complete the total synthesis of gelsemoxonine.

## 5.4 References

- (1) Jin, G.-L.; Su, Y.-P.; Liu, M.; Xu, Y.; Yang, J.; Liao, K.-J.; Yu, C.-X. Medicinal Plants of the Genus *Gelsemium* (Gelsemiaceae, Gentianales)—A Review of Their Phytochemistry, Pharmacology, Toxicology and Traditional Use. *J. Ethnopharmacol.* **2014**, *152*, 33–52.
- (2) Takayama, H.; Sakai, S. *Alkaloids*; Academic Press: San Diego, 1997; Vol. 49.
- (3) Yu, B.; Yu, D.-Q.; Liu, H.-M. Spirooxindoles: Promising Scaffolds for Anticancer Agents. *Eur. J. Med. Chem.* **2015**, *97*, 673–698.
- (4) Lin, H.; Danishefsky, S. J. Gelsemine: A Thought-Provoking Target for Total Synthesis. *Angew. Chem. Int. Ed.* **2003**, *42*, 36–51.
- (5) Ghosh, A.; Carter, R. G. Recent Syntheses and Strategies toward Polycyclic Gelsemium Alkaloids. *Angew. Chem. Int. Ed.* **2019**, *58*, 681–694.
- (6) Dutt, V.; Thakur, S.; Dhar, V. J.; Sharma, A. The Genus *Gelsemium*: An Update. *Pharmacogn Rev* **2010**, *4*, 185–194.
- (7) Tan, J. Q.; Qui, C. Z.; Zheng, L. Z. Analgesic Effect and No Physical Dependence of *Gelsemium Elegans* Benth. *Pharmacol. Clin. Chin. Mater. Med.* **1988**, *4*, 24–28.
- (8) Kitajima, M.; Nakamura, T.; Kogure, N.; Ogawa, M.; Mitsuno, Y.; Ono, K.; Yano, S.; Aimi, N.; Takayama, H. Isolation of Gelsedine-Type Indole Alkaloids from *Gelsemium Elegans* and Evaluation of the Cytotoxic Activity of Gelsemium Alkaloids for A431 Epidermoid Carcinoma Cells. *J. Nat. Prod.* **2006**, *69*, 715–718.
- (9) Kitajima, M.; Nakamura, T.; Kogure, N.; Ogawa, M.; Mitsuno, Y.; Ono, K.; Yano, S.; Aimi, N.; Takayama, H. Isolation of Gelsedine-Type Indole Alkaloids from *Gelsemium Elegans* and Evaluation of the Cytotoxic Activity of Gelsemium Alkaloids for A431 Epidermoid Carcinoma Cells. *J. Nat. Prod.* **2007**, *70*, 142–142.
- (10) Liu, M.; Shen, J.; Liu, H.; Xu, Y.; Su, Y.-P.; Yang, J.; Yu, C.-X. Gelsenicine from *Gelsemium Elegans* Attenuates Neuropathic and Inflammatory Pain in Mice. *Biol. Pharm. Bull.* **2011**, *34*, 1877–1880.
- (11) O'Connor, S. E.; Maresh, J. J. Chemistry and Biology of Monoterpene Indole Alkaloid Biosynthesis. *Nat. Prod. Rep.* **2006**, *23*, 532–547.
- (12) Nagakura, N.; Rüffer, M.; H. Zenk, M. The Biosynthesis of Monoterpenoid Indole Alkaloids from Strictosidine. *J. Chem. Soc., Perkin Trans. I* **1979**, *1979*, 2308–2312.
- (13) Franke, J.; Kim, J.; Hamilton, J. P.; Zhao, D.; Pham, G. M.; Wiegert-Rininger, K.; Crisovan, E.; Newton, L.; Vaillancourt, B.; Tatsis, E.; Buell, C. R.; O'Connor, S. E. Gene Discovery in *Gelsemium* Highlights Conserved Gene Clusters in Monoterpene Indole Alkaloid Biosynthesis. *ChemBioChem* **2019**, *20*, 83–87.
- (14) Ponglux, D.; Wongseripipatana, S.; Subhadhirsakul, S.; Takayama, H.; Yokota, M.; Ogata, K.; Phisalaphong, C.; Aimi, N.; Sakai, S. Studies on the Indole Alkaloids of *Gelsemium Elegans* (Thailand): Structure Elucidation and Proposal of Biogenetic Route. *Tetrahedron* **1988**, *44*, 5075–5094.
- (15) Kitajima, M.; Takayama, H.; Sakai, S. Synthesis of a Novel Gelsedine-Type Gelsemium Alkaloid, Gelsemicine. *J. Chem. Soc., Perkin Trans. I* **1994**, *1994*, 1573–1578.
- (16) Takayama, H.; Tominaga, Y.; Kitajima, M.; Aimi, N.; Sakai, S. First Synthesis of the Novel Gelsemium Alkaloids, Gelselegine, Gelsenicine, and Gelsedine Using a Biomimetic Approach. *J. Org. Chem.* **1994**, *59*, 4381–4385.
- (17) Baldwin, S. W.; Doll, R. J. Synthesis of the 2-Aza-7-Oxatricyclo[4.3.2.0<sup>4,8</sup>]Undecane Nucleus of Some Gelsemium Alkaloids. *Tetrahedron Lett.* **1979**, *20*, 3275–3278.

- (18) Kende, A. S.; Luzzio, M. J.; Mendoza, J. S. Total Synthesis of (±)-7-Epi-20-Desethylgelsemine. *J. Org. Chem.* **1990**, *55*, 918–924.
- (19) Hamer, N. K. A Synthetic Approach to Gelsemine. *J. Chem. Soc., Chem. Commun.* **1990**, *2*, 102–103.
- (20) Henegouwen, W. G. B. van; Fieseler, R. M.; Rutjes, F. P. J. T.; Hiemstra, H. Total Synthesis of (+)-Gelsemine. *Angew. Chem. Int. Ed.* **1999**, *38*, 2214–2217.
- (21) Shimokawa, J.; Harada, T.; Yokoshima, S.; Fukuyama, T. Total Synthesis of Gelsemoxonine. *J. Am. Chem. Soc.* **2011**, *133*, 17634–17637.
- (22) Harada, T.; Shimokawa, J.; Fukuyama, T. Unified Total Synthesis of Five Gelsemine-Type Alkaloids: (–)-Gelsenicine, (–)-Gelsemine, (–)-Gelsedilam, (–)-14-Hydroxygelsemine, and (–)-14,15-Dihydroxygelsemine. *Org. Lett.* **2016**, *18*, 4622–4625.
- (23) Diethelm, S.; Carreira, E. M. Total Synthesis of (±)-Gelsemoxonine. *J. Am. Chem. Soc.* **2013**, *135*, 8500–8503.
- (24) Diethelm, S.; Carreira, E. M. Total Synthesis of Gelsemoxonine through a Spirocyclopropane Isoxazolidine Ring Contraction. *J. Am. Chem. Soc.* **2015**, *137*, 6084–6096.
- (25) Wang, P.; Gao, Y.; Ma, D. Divergent Entry to Gelsemine-Type Alkaloids: Total Syntheses of (–)-Gelsedilam, (–)-Gelsenicine, (–)-Gelsemine, and (–)-Gelsemoxonine. *J. Am. Chem. Soc.* **2018**, *140*, 11608–11612.
- (26) Newcomb, E. T.; Knutson, P. C.; Pedersen, B. A.; Ferreira, E. M. Total Synthesis of Gelsenicine via a Catalyzed Cycloisomerization Strategy. *J. Am. Chem. Soc.* **2016**, *138*, 108–111.
- (27) Huang, Y.-M.; Liu, Y.; Zheng, C.-W.; Jin, Q.-W.; Pan, L.; Pan, R.-M.; Liu, J.; Zhao, G. Total Synthesis of Gelsedilam by Means of a Thiol-Mediated Diastereoselective Conjugate Addition–Aldol Reaction. *Chem. Eur. J.* **2016**, *22*, 18339–18342.
- (28) Saito, A.; Kogure, N.; Kitajima, M.; Takayama, H. Total Synthesis of (–)-14-Hydroxygelsemine and Six Biogenetically Related Gelsemium Alkaloids. *Org. Lett.* **2019**, *21*, 7134–7137.
- (29) Lin, L.-Z.; Cordell, G. A.; Ni, C.-Z.; Clardy, J. Oxindole Alkaloids from Gelsemium Elegans. *Phytochemistry* **1991**, *30*, 1311–1315.
- (30) Kitajima, M.; Kogure, N.; Yamaguchi, K.; Takayama, H.; Aimi, N. Structure Reinvestigation of Gelsemoxonine, a Constituent of Gelsemium Elegans, Reveals a Novel, Azetidene-Containing Indole Alkaloid. *Org. Lett.* **2003**, *5*, 2075–2078.
- (31) Ferrara, M.; Cordero, F. M.; Goti, A.; Brandi, A.; Estieu, K.; Paugam, R.; Ollivier, J.; Salaün, J. Intramolecular Cycloaddition/Rearrangement of Alkylidenecyclopropane Nitrones from Palladium(0)-Catalyzed Alkylation of Amino Acid Derivatives. *European Journal of Organic Chemistry* **1999**, *1999*, 2725–2739.
- (32) Martínez, I.; Howell, A. R. The Reaction of Dimethyltitanocene with N-Substituted-β-Lactam. *Tetrahedron Lett.* **2000**, *41*, 5607–5611.
- (33) Madin, A.; O'Donnell, C. J.; Oh, T.; Old, D. W.; Overman, L. E.; Sharp, M. J. Use of the Intramolecular Heck Reaction for Forming Congested Quaternary Carbon Stereocenters. Stereocontrolled Total Synthesis of (±)-Gelsemine. *J. Am. Chem. Soc.* **2005**, *127*, 18054–18065.
- (34) Galliford, C. V.; Scheidt, K. A. Pyrrolidinyl-Spirooxindole Natural Products as Inspirations for the Development of Potential Therapeutic Agents. *Angew. Chem. Int. Ed.* **2007**, *46*, 8748–8758.

- (35) Marti, C.; Carreira, E. M. Construction of Spiro[Pyrrolidine-3,3'-Oxindoles] – Recent Applications to the Synthesis of Oxindole Alkaloids. *Eur. J. Org. Chem.* **2003**, *2003*, 2209–2219.
- (36) Trost, B.; Brennan, M. Asymmetric Syntheses of Oxindole and Indole Spirocyclic Alkaloid Natural Products. *Synthesis* **2009**, *2009*, 3003–3025.
- (37) Zhou, F.; Liu, Y.-L.; Zhou, J. Catalytic Asymmetric Synthesis of Oxindoles Bearing a Tetrasubstituted Stereocenter at the C-3 Position. *Adv. Synth. Catal.* **2010**, *352*, 1381–1407.
- (38) Liu, Y.; Wang, H.; Wan, J. Recent Advances in Diversity Oriented Synthesis through Isatin-Based Multicomponent Reactions. *Asian J. Org. Chem.* **2013**, *2*, 374–386.
- (39) Marchese, A. D.; Larin, E. M.; Mirabi, B.; Lautens, M. Metal-Catalyzed Approaches toward the Oxindole Core. *Acc. Chem. Res.* **2020**, *53*, 1605–1619.
- (40) Black, M. J.; Biegasiewicz, K. F.; Meichan, A. J.; Oblinsky, D. G.; Kudisch, B.; Scholes, G. D.; Hyster, T. K. Asymmetric Redox-Neutral Radical Cyclization Catalysed by Flavin-Dependent ‘Ene’-Reductases. *Nat. Chem.* **2020**, *12*, 71–75.
- (41) Becker, M. R.; Richardson, A. D.; Schindler, C. S. Functionalized Azetidines via Visible Light-Enabled Aza Paternò-Büchi Reactions. *Nat. Commun.* **2019**, *10*, 5095. <https://doi.org/10.1038/s41467-019-13072-x>.
- (42) Richardson, A. D.; Becker, M. R.; Schindler, C. S. Synthesis of Azetidines by Aza Paternò-Büchi Reactions. *Chem. Sci.* **2020**, *11*, 7553–7561.
- (43) Lu, Z.; Yoon, T. P. Visible Light Photocatalysis of [2+2] Styrene Cycloadditions by Energy Transfer. *Angew. Chem. Int. Ed.* **2012**, *51*, 10329–10332.
- (44) Hurtley, A. E.; Lu, Z.; Yoon, T. P. [2+2] Cycloaddition of 1,3-Dienes by Visible Light Photocatalysis. *Angew. Chem. Int. Ed.* **2014**, *53*, 8991–8994.
- (45) Imahori, T.; Ojima, H.; Yoshimura, Y.; Takahata, H. Acceleration Effect of an Allylic Hydroxy Group on Ring-Closing Enyne Metathesis of Terminal Alkynes: Scope, Application, and Mechanistic Insights. *Chemistry – A European Journal* **2008**, *14*, 10762–10771.
- (46) Nasrallah, D. J.; Zehnder, T. E.; Ludwig, J. R.; Kiernicki, J. J.; Steigerwald, D. C.; Schindler, C. S.; Szymczak, N. K. Hydrazone and Oxime Olefination via Ruthenium Alkylidenes. *Angew. Chem. Int. Ed.* **2022 Accepted**. <https://doi.org/10.1002/anie.202112101>.
- (47) Qin, X.-L.; Xu, L.-J.; Han, F.-S. Recent Advances in Organocatalyzed Asymmetric Reduction of Prochiral Ketones: An Update. *Synthesis* **2022**, *54*, 1708–1720.
- (48) Matsuo, J.; Murakami, M. The Mukaiyama Aldol Reaction: 40 Years of Continuous Development. *Angew. Chem. Int. Ed.* **2013**, *52*, 9109–9118.
- (49) Ogawa, S.; Shibata, N.; Inagaki, J.; Nakamura, S.; Toru, T.; Shiro, M. Cinchona-Alkaloid-Catalyzed Enantioselective Direct Aldol-Type Reaction of Oxindoles with Ethyl Trifluoropyruvate. *Angew. Chem. Int. Ed.* **2007**, *46*, 8666–8669.
- (50) De, S.; Das, M. K.; Bhunia, S.; Bisai, A. Unified Approach to the Spiro(Pyrrolidinyl-Oxindole) and Hexahydropyrrolo[2,3-*b*]Indole Alkaloids: Total Syntheses of Pseudophrynamines 270 and 272A. *Org. Lett.* **2015**, *17*, 5922–5925.
- (51) Bordwell, F. G.; Fried, H. E. Heterocyclic Aromatic Anions with  $4n + 2 \pi$ -Electrons. *J. Org. Chem.* **1991**, *56*, 4218–4223.
- (52) Nicolaou, K. C.; Pulukuri, K. K.; Yu, R.; Rigol, S.; Heretsch, P.; Grove, C. I.; Hale, C. R. H.; ElMarrouni, A. Total Synthesis of  $\Delta^{12}$ -Prostaglandin J3: Evolution of Synthetic Strategies to a Streamlined Process. *Chem. Eur. J.* **2016**, *22*, 8559–8570.

- (53) Franckevičius, V.; Cuthbertson, J. D.; Pickworth, M.; Pugh, D. S.; Taylor, R. J. K. Asymmetric Decarboxylative Allylation of Oxindoles. *Org. Lett.* **2011**, *13*, 4264–4267.
- (54) Vougioukalakis, G. C.; Grubbs, R. H. Ruthenium-Based Heterocyclic Carbene-Coordinated Olefin Metathesis Catalysts. *Chem. Rev.* **2010**, *110*, 1746–1787.
- (55) Ghosh, A. K.; Brindisi, M. Achmatowicz Reaction and Its Application in the Syntheses of Bioactive Molecules. *RSC Adv.* **2016**, *6*, 111564–111598.
- (56) Yin, Z.; Liu, Z.; Huang, Z.; Chu, Y.; Chu, Z.; Hu, J.; Gao, L.; Song, Z. Synthesis of Functionalized  $\gamma$ -Lactone via Sakurai *Exo*-Cyclization/Rearrangement of 3,3-Bis(Silyl) Enol Ester with a Tethered Acetal. *Org. Lett.* **2015**, *17*, 1553–1556.
- (57) Garcia, A.; Otte, D. A. L.; Salamant, W. A.; Sanzone, J. R.; Woerpel, K. A. Influence of Alkoxy Groups on Rates of Acetal Hydrolysis and Tosylate Solvolysis: Electrostatic Stabilization of Developing Oxocarbenium Ion Intermediates and Neighboring-Group Participation To Form Oxonium Ions. *J. Org. Chem.* **2015**, *80*, 4470–4480.
- (58) Bandini, M.; Eichholzer, A. Catalytic Functionalization of Indoles in a New Dimension. *Angew. Chem. Int. Ed.* **2009**, *48*, 9608–964.
- (59) You, B.; Shen, M.; Xie, G.; Mao, H.; Lv, X.; Wang, X. Alternative Sm(II) Species Mediated Cascade Coupling Cyclizations for the Synthesis of Oxobicyclo[3.1.0]hexane-1-ols. *Org. Lett.* **2018**, *20*, 530–533.
- (60) Tratat C.; Giorgi-Renault S.; Husson H.-P. Oxidative Cleavage of Indole  $\delta$ -Lactones with *m*-Chloroperbenzoic Acid: First Synthesis of Spiroindolin-2-one  $\gamma$ -Lactones. *J. Org. Chem.* **2000**, *65*, 6773–6776.
- (61) Jiang, X.; Yang, J.; Zhang, F.; Yu, P.; Yi, P.; Sun, Y.; Wang, Y. Synthesis of Quaternary 3,3-Disubstituted 2-Oxindoles from 2-Substituted Indole Using Selectfluor. *Org. Lett.* **2016**, *18*, 3154–3157.
- (62) Jossang, A.; Jossang, P.; Hadi, H. A.; Sévenet, T.; Bodo, B. Horsfiline, an Oxindole Alkaloid from *Horsfieldia superba*. *J. Org. Chem.* **1991**, *56*, 6527–6530.
- (63) Chen, P.; Yang, H.; Zhang, H.; Chen, W.; Zhang, Z.; Zhang, J.; Li, H.; Wang, X.; Xie, X.; She, X. Total Synthesis of (–)-Gardmultimine A. *Org. Lett.* **2020**, *22*, 2022–2025.
- (64) Marçal, L. L.; Garden, S. J. Synthesis of Spiro-Pyrrolidinyloxindoles by Oxidative Rearrangement of *N*-Acyltetrahydro- $\beta$ -carbolines Using an Oxone/Aqueous Acetone Mixture. *J. Braz. Chem. Soc.* **2019**, *30*, 19–32.